Towards an effective control of the electronic properties in Au(I)-complexes. From basic principles to asymmetric catalysis

vorgelegt von

Elisa González Fernández

aus Terrassa, Spanien

Göttingen, 2017

I hereby declare that this dissertation has been written independently and with no other sources and aids than quoted. I have indicated the parts which were performed by project collaborators.

....

Elisa González Fernández

Acknowledgements

To my family and Javi

Contents

Subject overview

Throughout the last century, many methods based on homogeneous transition metal catalysis have been developed; these now constitute powerful and widely adopted tools, enabling the construction of complex molecules from simple building blocks, often under mild conditions, with high atom economy and functional group tolerance. Unlike many of the other transition metals, gold was perceived as a scarce, expensive and chemically inert metal, precluding for decades the application of gold chemistry in the field of homogeneous catalysis.

It was not until the 1990's that the potential of gold(I) in homogeneous catalysis was recognised with the seminal work by the groups of Teles[1] and Tanaka.[2] They reported that cationic Au(I) complexes (LAu$^+$ obtained *in situ* by acid addition to the corresponding LAuCH$_3$) were excellent catalysts for the hydroalkoxylation and hydration of alkynes (***Scheme 1***).
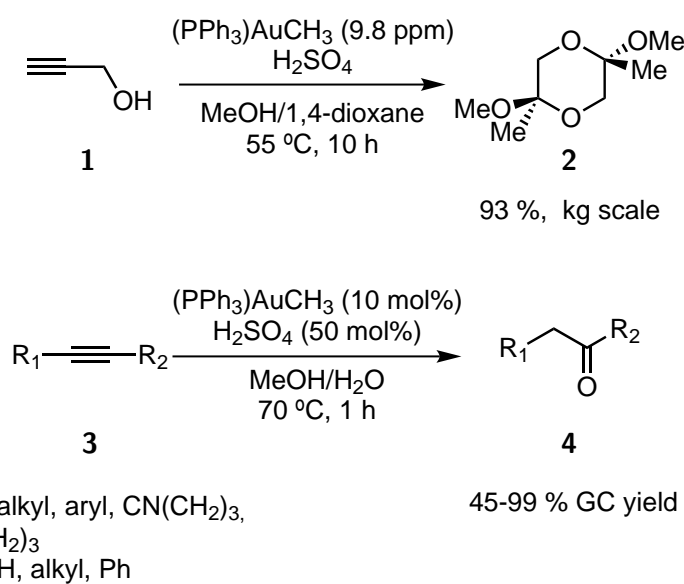
Scheme 1. Representative examples of a hydroalkoxylation reported by Teles and co-workers (above) and hydration of alkynes reported by Tanaka group (below).

Based on these initial results, a wide variety of new gold-catalysed transformations were discovered involving the activation of alkynes, allenes and alkenes towards nucleophilic attack. Moreover, it was found that these processes proceed under mild conditions, have excellent selectivity for the activation of the unsaturated C-C bond and, therefore, exhibit a large functional group tolerance.[3]

The gold(I)-catalysed activation of C-C multiple bonds towards nucleophilic attack is based on the "soft" Lewis acid character of Au(I), which is able to deplete electron density from unsaturated C-C bonds, promoting the attack of the nucleophile. A schematic catalytic cycle for the gold(I)-catalysed nucleophilic addition to an alkyne is depicted in *Scheme 2*. After catalyst activation (**A**), LAu$^+$ coordinates the alkyne, depleting its electron density (**B**). The nucleophile then attacks the activated alkyne in an *anti*- fashion, through an outer-sphere mechanism, with concomitant π-slippage of the LAu$^+$ fragment yielding a vinyl- gold complex (**C**). Finally, the catalyst is regenerated by protodeauration (**D**), releasing the desired product.[3a]
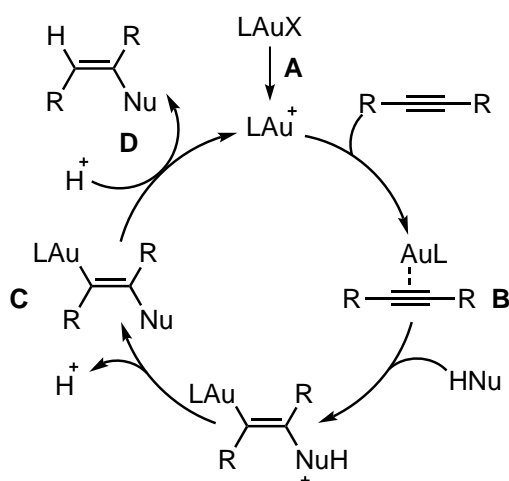
Scheme 2. Schematic catalytic cycle for the activation of an alkyne by Au(I) to nucleophilic attack.

The strong Lewis acidity of Au(I) and, therefore, its ability to trigger the catalytic cycle depicted in *Scheme 2*, can be explained through relativistic effects. Gold and other heavy elements are subject to relativistic effects — a consequence of the high velocity reached by the electrons under the influence of a high nuclear charge. As the velocity of the electrons approaches the speed of light, they have to be treated according to the theory of relativity, which results in an increase in the "relativistic" mass of the electron and, subsequently, in the energetic stabilisation and radial contraction of the s and p orbitals of the metal. This effect is more pronounced for the s-electrons due to their higher probability of being nearer to the nucleus. The contraction results in a

stronger shielding of the d and f orbitals from the nuclear attraction, which become more diffuse and relatively destabilised.[4] Due to its high atomic number and electronic configuration, the relativistic contraction of the valence 6s-orbital of gold is the highest of the sixth period,[5] explaining the unique properties of gold: its unusually high electronegativity (2.54), electron affinity (222.7 kJ/mol) and first ionisation potential (9.23 eV).

The relativistic contraction of the s-orbitals also explains the Lewis acidity of gold(I), since the lowest unoccupied orbital in Au$^+$ is the stabilised 6s-orbital, which is lower in energy than in other transition metals. Thus, despite being a lighter element of the same group, silver(I) 5s-orbital has been calculated in AgH to be higher in energy (-0.2982 a.u.) than the 6s-orbital of gold(I) in AuH (-0.3509 a.u.).[6] Consequently, gold(I) is more Lewis acidic than silver(I) and therefore, is more effective in the activation of C-C multiple bonds towards nucleophilic attack. An interesting example of this is the Conia-ene reaction of β-ketoester **5** leading to cyclopentane **6** (***Scheme 3***). The addition of 10 mol% of AgOTf led to only 50 % conversion after 18 h, whereas the inclusion of 10 mol% of PPh$_3$ resulted in catalysis inhibition. Conversely, 10 mol% of PPh$_3$AuOTf cleanly converted **5** into **6** in less than 15 min.[7]

A)	50 % conversion
A) + 10 mol% PPh$_3$	no conversion
B)	>95 % conversion
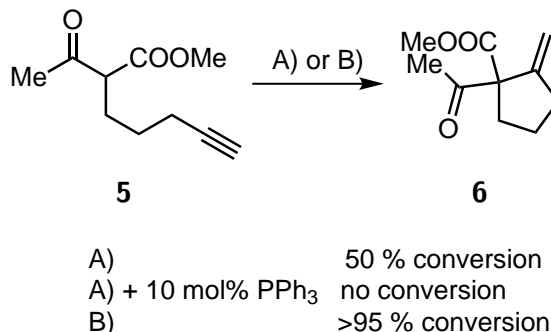
Scheme 3. Coinage metal-catalysed Conia-ene reaction. Conditions A) 10 %mol AgOTf, DCE, rt, 18 h. Conditions B) 10 %mol AgOTf, 10%mol PPh$_3$, DCE, rt, 18 h. Conditions B: 10 %mol PPh$_3$AuOTf, DCE, rt, < 15 min.

Another consequence of the relativistic effects in gold(I) is its preference for linear geometry, which can be explained using the hybridisation theory.[8] Relativistic effects decrease the energy difference between the filled 5d_{z^2}-orbital and the empty 6s-orbital, allowing their combination and the formation of two sd_{z^2} hybrid orbitals Ψ_1 and Ψ_2 (***Figure 1***). The electron pair of 5d_{z^2} is located in Ψ_1, whereas Ψ_2 combines further with 6p_z. The decreased relativistic stabilisation of the 6p-orbitals compared to the 6s, favours the hybridisation of Ψ_2 with just one 6p to form two empty hybrid orbitals oriented in opposite directions σ_{Au1} and σ_{Au2}, with predominant s-character and σ-

symmetry.[9] Thus, coordination of two ligands in a linear fashion can occur through σ-donation of the ligand's lone pair, located in an orbital with σ-symmetry (σ_L), to the aforementioned low-lying hybrid σ_{Au1} and σ_{Au2} orbitals of gold(I), constituting the major contribution to the Au-L bond (***Figure 2***, left). Since its $5d$-orbitals are energetically destabilised, gold(I) is able to backdonate electron density from its filled $5d_{xz}$ in-plane orbital to an empty orbital of the ligand with π-symmetry (π_L, ***Figure 2***, right). The importance of π-backdonation in the Au-L bond depends largely on the energy of π_L and the electronic properties of the second ligand.[10,11]
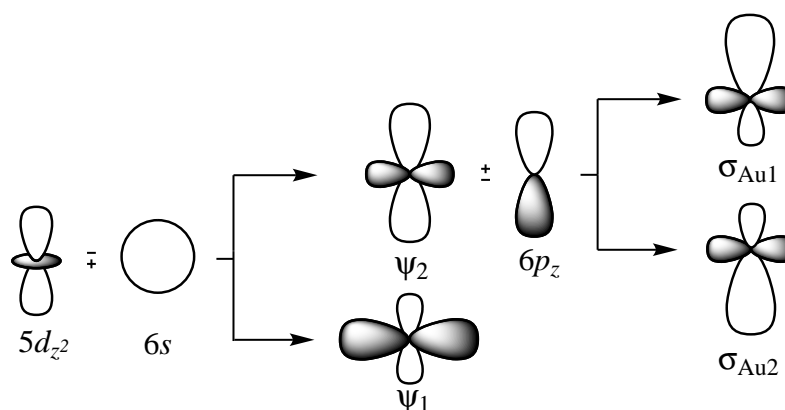
Figure 1. Schematic representation of the hybridisation of the valence orbitals of gold(I).
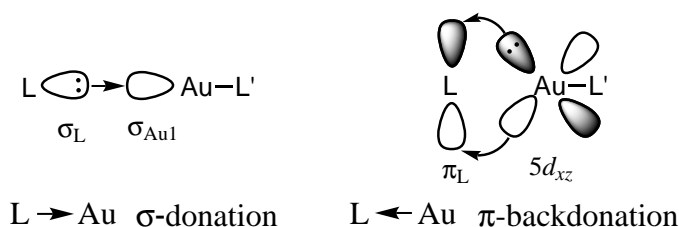
Figure 2. Model of a L-Au-L' coordination complex, the page plane is considered as the xz plane.

Gold(I) has a preference to coordinate C-C multiple bonds, which are "soft" Lewis bases, due to the diffuse nature of its valence orbitals that confers gold(I) a "soft" Lewis acid character. Gold(I) forms side-on η^2-alkyne and -alkene complexes,[12] whose bonding situation explains the activation of C-C multiple bonds towards nucleophilic attack. The bond between gold(I) and an alkyne can be defined within the Dewar-Chatt-Duncanson model,[13] considering two major contributions, σ-donation and π-backdonation (***Figure 3***).[14] Due to the relativistic orbital contraction, the energy of the metal hybrid orbital σ_{Au1} is low and the σ-donation from the alkyne's in-plane π-orbital to the metal centre is energetically favoured, constituting the major contribution to the bond. On the contrary, π-backdonation from the occupied $5d$-orbitals to the high-lying

π^*-C≡C orbital represents a minor contribution, resulting in an overall depletion of electron density on the alkyne that promotes the attack of a nucleophile.[3,11]

This interpretation has been supported by calculations[14] and by the study of η^2-alkyne complexes such as **7**. Complex **7** could be investigated by X-ray diffraction studies, displaying small elongation (0.01 Å) and bending (7.6°) of the C≡C bond compared to the free cyclododecyne. These changes evidence a slight weakening of the C≡C bond, caused by the small population of the π^*-orbital of the alkyne through a weak π-backdonation from the metal. Additionally, DFT calculations on **7** and related compounds showed that the orbital interaction energies for the σ-donation are 3 to 4 times larger than those for π-backdonation, resulting in a net electron donation from the alkyne to the gold centre.[15]
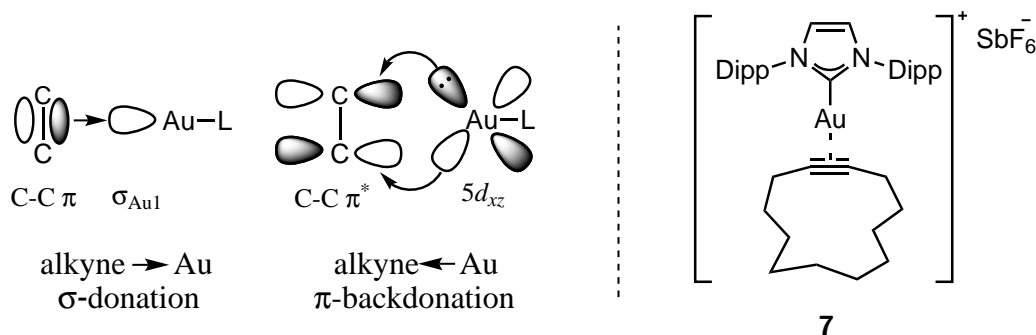
Figure 3. Dewar-Chatt-Duncanson model for η^2-alkyne gold complex (left). NHC-Au-cyclododecyne complex studied by Fürstner and co-workers (right).

Nevertheless, according to theoretical studies, the contribution of the σ and π components to the LAu-(HCCH) bond might be altered significantly depending on the electronic properties of the ancillary ligand L.[16] If L is a poor σ-donor and a good π-acceptor ligand, the gold(I) centre will be more electron poor and therefore, the removal of electron density from the alkyne will be more pronounced, facilitating the attack of the nucleophile to the more electrophilic C-C multiple bond. In consequence, the activity of the catalyst bearing an electron-withdrawing ligand will be enhanced if the nucleophilic attack to the C-C multiple bond is the rate-determining step of the reaction.

The opposite effect will be observed with good σ-donor and poor π-acceptor ligands, which increase the electron density at the gold(I) atom and diminish the rate of the nucleophilic attack. Despite of this, the performance of the catalyst will be better with an electron-donating ancillary ligand if the protodeauration of the vinyl-gold(I) species is the rate-determining step.[17] Protodeauration is facilitated by electron-releasing ligands because they weaken the Au-C bond through a decrease in the electrostatic interaction between the more electron rich $L-Au^+$ and anionic substrate fragments.[18] Finally, the

steric properties of the auxiliary ligand can play also an important role: bulky ligands improve the kinetic stability of the catalyst and diminish catalyst deactivation.[17]

Besides its impact on the catalysis rate, the properties of the ancillary ligand can also influence the reaction outcome due to the variation of the electron density on the gold(I) centre, modifying its ability to stabilise different reaction intermediates.[11,19] A representative example is the cycloaddition of allene-tethered 1,3-diene **8** depicted in **Scheme 4**, which affords the bicyclic compounds **10** and **11** in different ratios depending on the electronic properties of the ligand. Under the same conditions, the use of good σ-donors like NHCs led preferentially to **10**, whereas the employment of π-acceptor ligands like $(PhO)_3P$ promoted the selective formation of **11**.[20]

These results can be explained using the following proposed mechanism: initially a concerted $[4+2]$ process generates the common intermediate **9**, which can be stabilised by π-backdonation from an electron-rich Au^+ centre attached to an electron-donating ligand. This confers to the intermediate **9** a greater "carbene" character and lowers the activation barrier for the 1,2-H migration (in blue), which after catalyst regeneration leads to **10**. Contrarily, π-acceptor ligands remove more electron density from the cationic centre of the intermediate, facilitating a ring contraction by a 1,2-alkyl shift (in green), affording **11**.
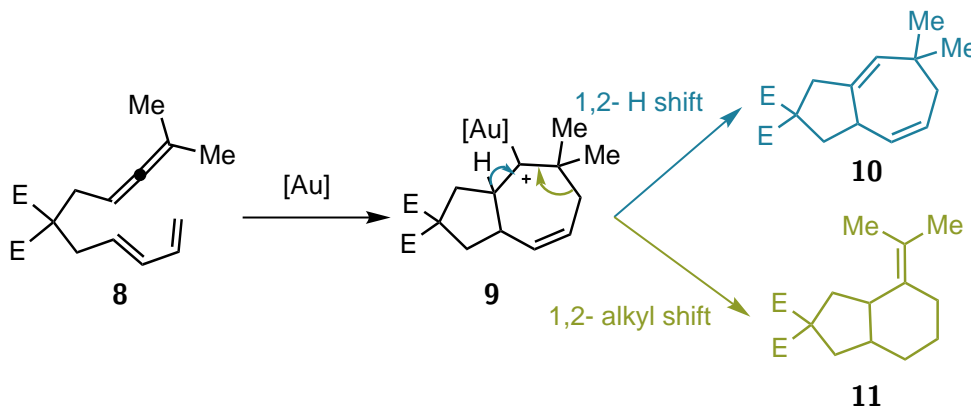
Scheme 4. Cycloaddition of allene-tethered 1,3-diene **8**. E = COOEt.

The careful design of new ligands with distinct electronic properties is thus relevant in order to find new reaction pathways. In the first part of this dissertation, a new class of gold(I)-carbene complexes, the acyclic (amino)-(ylide)carbene (AAYC) gold(I) chlorides **13**, are presented together with a study of their reactivity. Their cyclic counterparts, (amino)-(ylide)carbenes, have been already reported as ligands to transition metals and present interesting properties, including an excellent σ-donor ability, keeping moderate π-acceptor attributes. Acyclic carbenes have significant stereoelectronic differences compared with cyclic scaffolds, together with the advantage of being easily

accessible from the nucleophilic attack to certain metal-isonitrile complexes. Based on the synthesis of acyclic (diamino)carbene-gold(I) chlorides, we have developed a modular strategy for obtaining the AAYC-gold(I) chlorides **13** through the nucleophilic attack of ylides **14** to isonitrile-gold(I) chlorides **12** (***Scheme 5***). Moreover, the presence of additional functional groups on the AAYC-complexes side arm (R_2) allowed their easy derivatisation, leading to the synthesis of heterobinuclear — bearing Rh(I) and Au(I) centres — and cationic AAYC-gold(I) complexes, together with an unprecedented Au(I)→Rh(III) and Au(I)→Ru(II) carbene transmetalation.
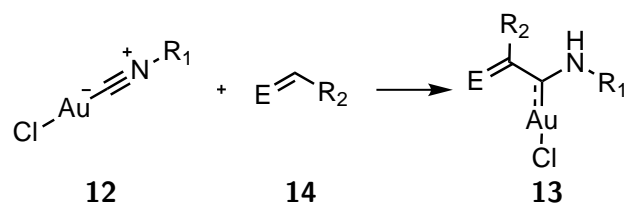
Scheme 5. General synthesis of acyclic (amino)-(ylide)carbene-gold(I) complexes.
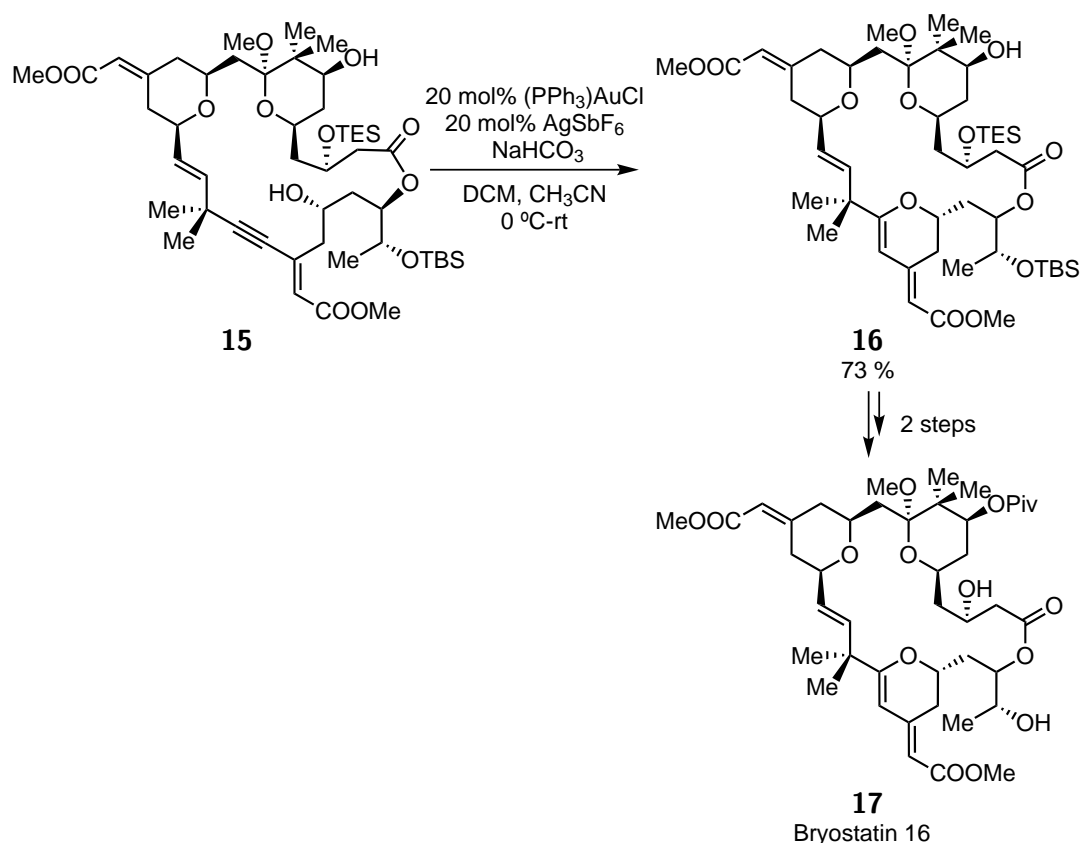
Scheme 6. Gold(I)-catalysed intramolecular hydroalkoxylation in the total synthesis of Bryostatin 16.

In addition to the development of new catalysts, it is also important to apply them to the synthesis of relevant compounds. Due to their selectivity, functional group tolerance and the possibility to promote cascade reactions, gold(I)-catalysed transformations have been elegantly applied, frequently at a late synthetic stage, towards the synthesis of natural products and materials.[21] A remarkable example of this is the gold(I)-promoted intramolecular hydroalkoxylation of the highly functionalised macrocycle **15**, leading to compound **16** at a late-stage in the total synthesis of Bryostatin 16 (**17**), a natural product with anticancer activity, that was obtained in a 28 steps linear sequence (**Scheme 6**).[22]

The development of enantioselective gold(I)-catalysis has additionally broadened the applicability of gold(I)-catalysed transformations to the synthesis of chiral building blocks, natural products and biologically active compounds.

Enantioselective gold(I) catalysis is more challenging compared with many other metal-catalysed transformations, due to the linear coordination of gold(I) that places the chiral ligand (L*, **Figure 4**) 180° away from the substrate, preventing the efficient transfer of chirality to the reaction site. In addition, because the attack of the nucleophile to the C-C multiple bond — which generates the chiral centre — occurs in an *anti*-fashion *via* an outer-sphere mechanism and subsequently at opposite side of the substrate, the efficient transfer of chiral information is further obstructed. Note that due to the coordination mode of gold(I) this problem cannot be solved though the utilisation of chelating ligands. Finally, in gold(I)-alkyne and -alkene complexes the rotational barrier of the gold-alkyne bond is very low, avoiding the adoption of a fixed conformation during the nucleophilic attack.
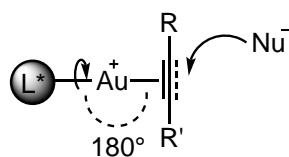
Figure 4. Difficulties faced by enantioselective gold(I)-catalysis, involving the activation of a C-C multiple bond towards nucleophilic attack

Despite these difficulties, Echavarren and co-workers reported the first enantioselective gold(I)-catalysed reaction involving alkynes, consisting in the alkoxycyclisation of enyne **18** to cyclopentane **19** in methanol (**Scheme 7**, above).[23] After their seminal work, several enantioselective gold(I)-catalysed transformations have been published, involving activation of alkynes, alkenes and allenes.[24] One example is the enantioselective synthesis of the antidepressive agent (–)-GSK1360707·HCl **20**, in 5 steps from

propargyl amine **21** with 95 %*ee* and 69 % overall yield, using chiral phosphoramidites as ligands for the cycloisomerisation of the enyne **22** (***Scheme 7***).[25]
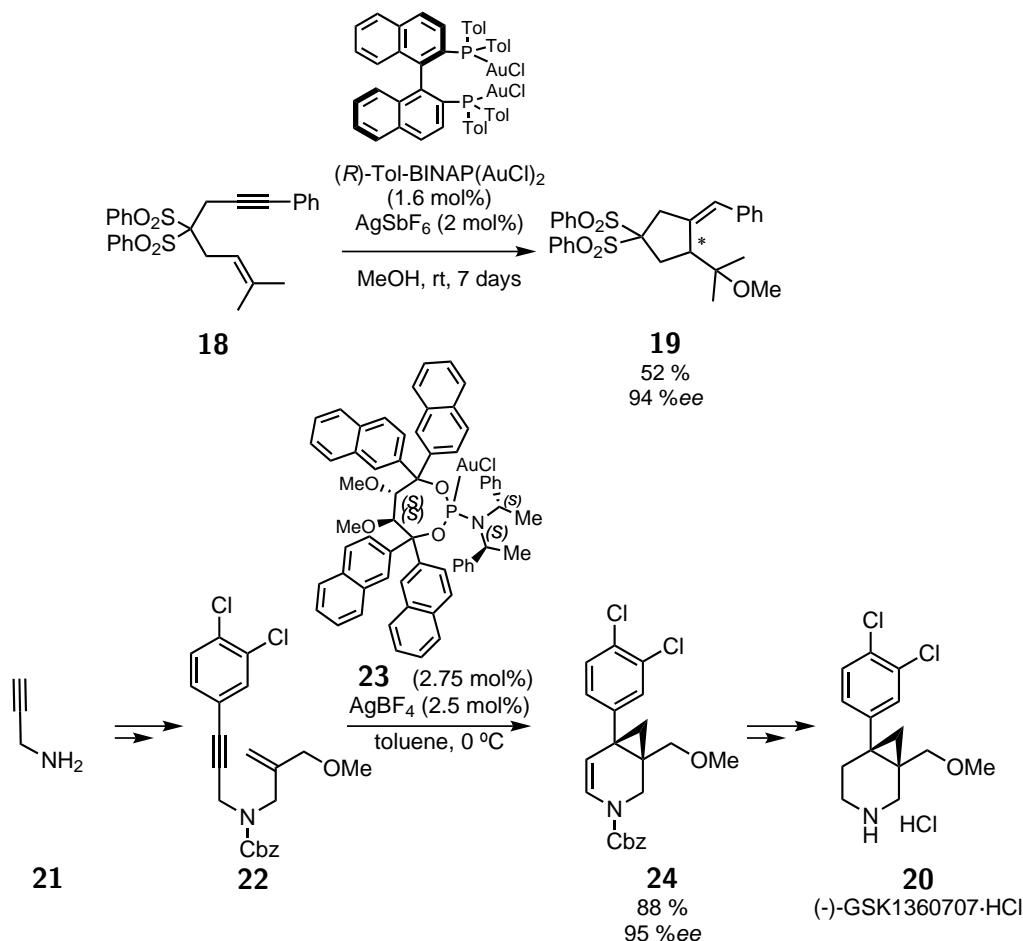
Scheme 7. Enantioselective gold(I)-catalysed alkoxycyclisation of enyne **18** (above). Synthesis of **20** through an enantioselective gold(I)-catalysed cyclisation of enyne **22** (below).

Our research group has recently developed strong π-accepting cationic phosphine ligands,[26] that facilitate the Pt(II)-[27] and Au(I)-[28] catalysed hydroarylations of alkyne-tethered biaryls to obtain highly functionalised phenanthrenes. Gold(I) complex **25** proved to be more efficient in the aforementioned transformation, promoting even the cyclisation of sterically hindered di-*ortho*-substituted biaryls, which generate in the resulting phenanthrene a pronounced steric replusion, twisting the otherwise planar aromatic structure (***Scheme 8***).

In the second part of this thesis, the work of our group in hydroarylation reactions is extended to the development of new chiral, cationic phosphonite ligands and their application to the enantioselective synthesis of hexahelicene derivatives **26**: helical, polyaromatic compounds with potential applications as ligands in asymmetric catalysis,

liquid crystals with non-linear optical responses or molecular switches.[29,30] For this propose, we envisioned an enantioselective gold(I)-catalysed double hydroarylation of achiral alkynes such as **27** leading to hexahelicene derivatives **26** with different substitution patterns, as depicted in *Scheme 9*.
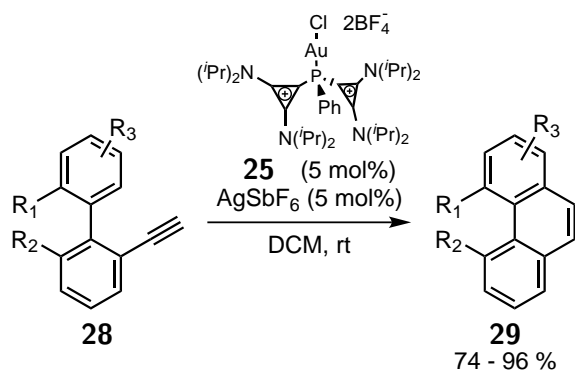
Scheme 8. Hydroarylation of polysubstituted biaryls to form phenanthrenes.
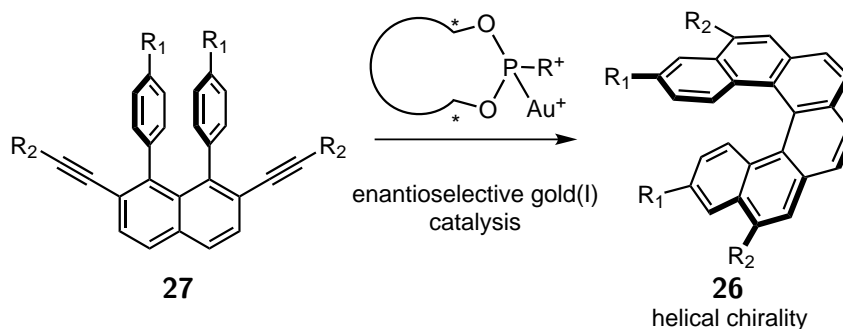
Scheme 9. General enantioselective gold(I)-catalysed transformation leading to hexahelicene derivatives with different substitution patterns.

Part I

Synthesis and reactivity of acyclic (amino)-(ylide)carbene metal complexes

I.1.   Introduction

Carbenes are a class of compounds containing a divalent carbon atom with six electrons in its valence shell. They were first proposed as reaction intermediates in 1862 to explain the alkaline hydrolysis of chloroform[31] and, during the first half of the 20th century they have been invoked as transient species of several organic transformations.[32]

This prompted researchers to pursue the isolation of such an elusive species to determine its structure. Although initial efforts to isolate stable carbenes did not succeed, carbene complexes could be synthesised by Fischer (**30**, ***Figure I.1.1***),[33] Öfele (**31**),[34] Wanzlick[35] (**32**) and Schrock (**33**).[36] However, it was not until the isolation of the first stable carbenes **34** by Bertrand in 1988[37] and **35** by Arduengo in 1991[38] that carbene chemistry became of notable interest for the research community.
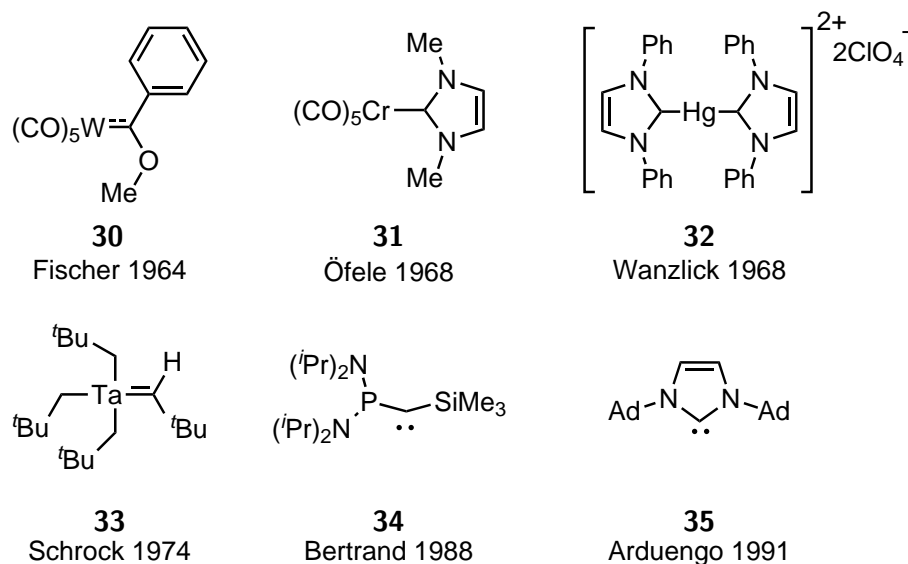
Figure I.1.1. Important compounds in the chemistry of carbenes.

The substituents attached to the carbene centre in **34** and **35** play a decisive role in their stability and reactivity. Depending on the hybridisation at the carbon atom, the geometry of the carbene can be either linear or bent (***Figure I.1.2***). In the former, the carbenic carbon atom displays *sp*-hybridisation and two degenerate non-

bonding p-orbitals, where the two non-bonding electrons will preferentially locate with an open-shell $p_x^1 p_y^1$ configuration. Conversely, in a bent carbene one of the non-bonding p-orbitals is stabilised by combination of atomic orbitals to form the sp^2-hybridised orbital σ, leaving the other p-orbital almost unchanged. In this situation, four possible electronic configurations can be envisaged, resulting in three singlet states: σ^2, $p_{carbene}^2$ and $\sigma^1 p_{carbene}^1$, whereas configuration $\sigma^1 p_{carbene}^1$ with unpaired electrons would lead to a triplet state (**Figure I.1.2**). Singlet configurations $p_{carbene}^2$ and $\sigma^1 p_{carbene}^1$ are excited states and normally the ground states of bent carbenes correspond either to $^1 A_1\ \sigma^2$ or $^3 B_1\ \sigma^1 p_{carbene}^1$.[39]
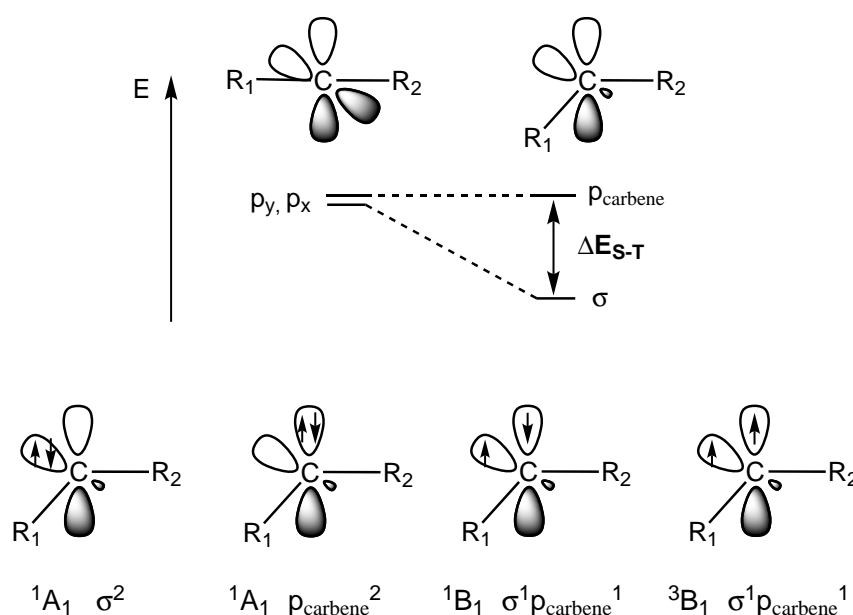
Figure I.1.2. Frontier orbitals in linear and bent carbenes (above). Possible electronic configurations of a bent carbene (below), the page plane is considered as the xz plane.

Most of the carbenes are bent and the difference in energy between the frontier orbitals σ and $p_{carbene}$ (ΔE_{S-T}) determines how the two non-bonding electrons are distributed: if ΔE_{S-T} is large (>2 eV), the repulsion generated between two electrons placed in the same orbital is compensated by the energetic stabilisation of the orbital σ and the singlet configuration will be preferred. The opposite case is observed with a small ΔE_{S-T} gap (<1.5 eV), which would lead to a triplet configuration.[40]

The relative energies of the frontier orbitals are determined by the electronic and steric nature of the substituents R_1 and R_2 attached to the carbene carbon. In general, bulky substituents kinetically stabilise both configurations, but to diminish steric hindrance, they might lead to more linear structures. Wide R_1-C-R_2 angles evidence a decreased s-character of σ and a reduced ΔE_{S-T} gap, whereas the inverse situation

will be observed with acuter R_1-C-R_2 angles.

Concerning the electronic effects, σ-electron-withdrawing groups stabilise the σ-orbital by negative inductive effects and favour the singlet state, whereas the opposite influence is observed with σ-electron-donating substituents. However, mesomeric effects have a greater impact on the relative energy of the orbitals and, depending on their contribution, substituents might be classified in three categories: carbon atoms part of a conjugated π-system, π-electron-acceptor and π-electron-donor substituents. The first category includes double bonds, -COR and aromatic substituents, where combination of the π-orbitals of the substituent with the empty $p_{carbene}$-orbital leads to its stabilisation, thus favouring the triplet state. In fact, the few examples of persistent triplet carbenes reported in the literature bear bulky aromatic substituents.[39b]

Conversely, both π-electron-donor and -acceptor substituents stabilise the singlet ground state of the carbene by increasing ΔE_{S-T} gap. The latter comprises substituents with an empty orbital (*e.g.* -BR$_2$, -SiR$_3$ or -PHR$_2$$^+$) able to stabilise the lone pair of the carbene, whereas π-electron-donor substituents — namely atoms with a lone pair of π-symmetry (*e.g.* N, P, O, S) — destabilise the empty $p_{carbene}$ orbital through delocalisation of electron density. Although stable carbenes with two π-acceptor substituents have been so far not described, several singlet carbenes with one π-donor and one π-acceptor substituent are known to be stable, such as **34**.[37,41]

However, without a doubt, the most prevailing type of singlet stable carbenes are those stabilised by one or two π-donor substituents. N-heterocyclic carbenes (NHCs), defined as cyclic carbenes containing at least one nitrogen atom within a ring structure, are the most relevant class of carbenes, since they have found numerous applications as ligands for transition metals, organocatalysts and stabilising ligands for reactive low-valent species.[42] Although a wide variety of compounds match the description of NHCs, the most employed structures are imidazolylidenes **36**, imidazolidinylidenes **37**, triazolylidenes **38** and cyclic alkyl amino carbenes (CAACs) **39**.
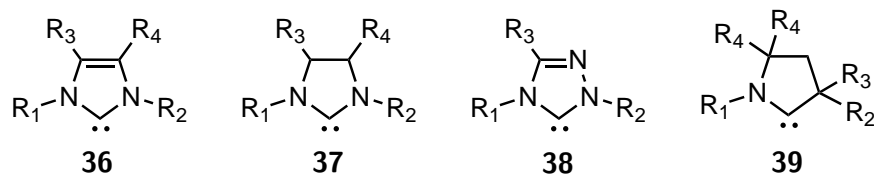
Figure I.1.3. Important scaffolds of NHCs.

Because of the amino substituents and their cyclic structure, imidazolylidene and imidazolidinylidene carbenes are singlet bent species with a large ΔE_{S-T} gap, caused by the inductive stabilisation of the lone pair (***Figure I.1.4***, in blue) and the destabil-

isation of the $p_{carbene}$ empty orbital (***Figure I.1.4***, in green) by π-donation of electron density from the nitrogen atoms. The population of the $p_{carbene}$ by the lone pairs of the amine substituents results in the formation of a four-electron-three-centre π-system, thus conferring the N-C bonds a partial double bond character, schematically represented by the possible resonance structures depicted in ***Figure I.1.4***.
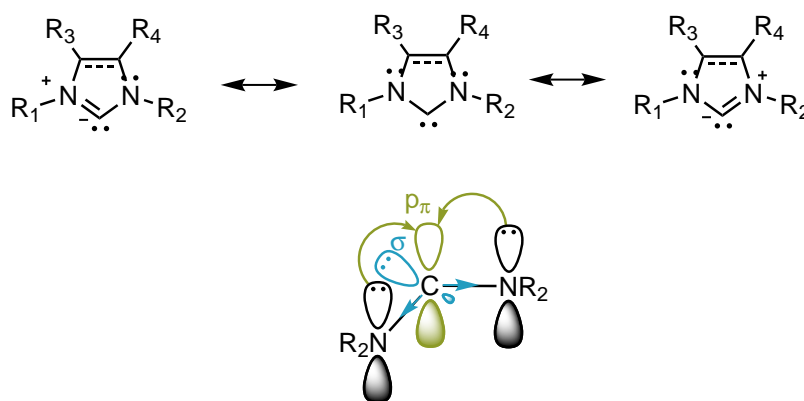
Figure I.1.4. Possible resonance structures of NHCs (above) and electronic effects in (di-amino)carbenes (below).

I.1.1   N-heterocyclic carbene metal complexes

NHC-metal complexes have found applications in many different areas including surface chemistry,[43] organometallic materials,[44] metallopharmaceuticals[45] and, most importantly, in homogeneous catalysis.[46] The metal-carbene bond is stronger than the PR_3-metal bond, preventing ligand dissociation and conferring to carbene complexes a remarkable stability. Moreover, NHC-metal complexes are readily available from the corresponding free carbenes or azolium salts.[46a]

The bonding situation of carbene transition metal complexes can be explained through donor-acceptor interactions between the metal and the ligand. Three different contributions might be considered: the σ-donation from the lone pair of the carbene to an empty orbital of metal with σ-symmetry (d_{z^2}, sd or sp hybrid), π-backdonation from the metal filled d-orbital to the NHC-π^* orbital and π-donation from the carbene to an empty d-orbital of the transition metal (**Figure I.1.5**).[47]
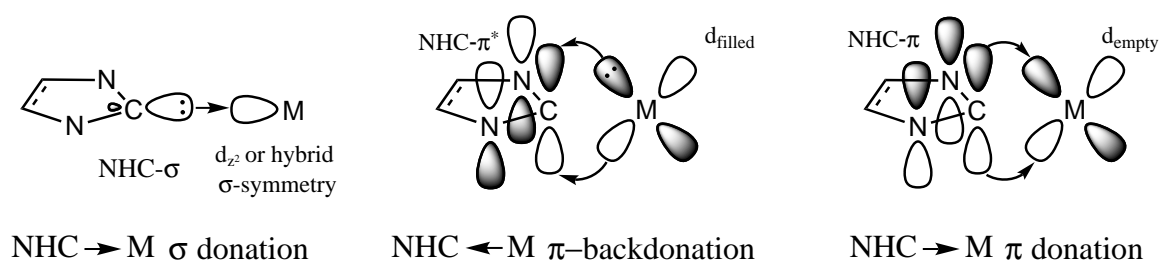
Figure I.1.5. Different contributions to the bond in a metal-NHC complex.

The major contribution to the bond corresponds to the σ-donation and because of this, NHCs behave as two-electron donor ligands, in analogy to phosphines. NHCs are very strong σ-donors, generally stronger than phosphines, whereas they are poorer π-acceptors.[48]

Since the NHC-π^* orbital is high in energy, whereas the orbital NHC-π is highly stabilised, the overall π-contribution to the bond is small, but it must be taken into account to understand the bonding situation according to calculations and experimental results. The π-component varies depending on the d-electron count of the transition metal and the electronic nature of the rest of the ligands attached to it.[49] It has been proven that NHC complexes with electron-deficient metal centres have an important contribution from the NHC π-donation to the metal.[49–51] Inversely, the π^*-backdonation from the metal to the NHC-π^* orbital increases with the number of d-electrons, especially in the group 11 elements, where its contribution could be quantified as 15-30 % of the overall orbital interaction energy, calculated through X-ray supported DFT studies and

SCF and DFT calculations in biscarbene coinage-metal model systems.[52]

Carbene-gold(I) complexes (**40**)AuCl and (**41**)AuCl illustrate the influence of π-backdonation in gold catalysis (***Scheme I.1.1***). DFT calculations revealed that, while the computed energy for the σ-orbital remained similar for both ligands, the interaction of the cyclophane with the benzoimidazolylidene structure in **41** decreased the energy of the NHC-π^*, thus increasing its π-acceptor ability compared with **40**. These differences were translated to distinct results in the cycloaddition of eneallene **8**, previously explained in the Subject overview, favouring **10** for the electron-rich (**40**)AuCl, while **11** constituted the major compound when the better π-acceptor ligand **41** was used.[20d]
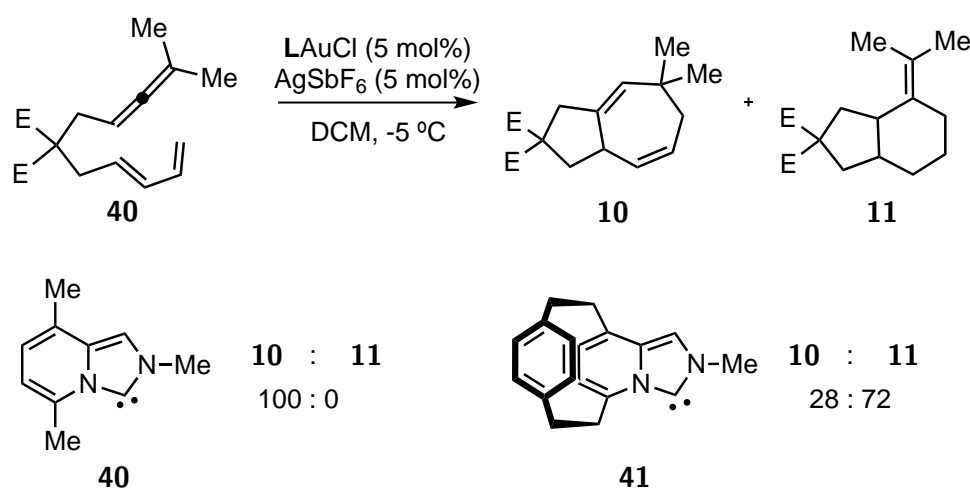
Scheme I.1.1. Results obtained in the gold(I)-catalysed cycloisomerisation of **8**, using as ligands NHCs with different electronic properties. E = COOMe.

These results highlight how important the study of the stereoelectronic properties of carbene ligands is in order to rationalise and predict the outcomes of catalysis. Furthermore, the tuning of the stereoelectronic properties of the carbenes could allow the optimisation of known transformations or the discovery of novel reaction pathways.

I.1.2 Tuning the stereoelectronic properties of carbenes

As previously discussed, the behaviour of a carbene is determined by the energy of the orbital bearing the lone pair, σ, and the empty NHC-π*, both responsible for the σ-donor/π-acceptor properties of the carbene when acting as a ligand to a transition metal. Several modifications are possible in order to alter the steric and electronic properties of a NHC, summarised in **_Figure I.1.6_**,[53] and will be elaborated in the following sections.
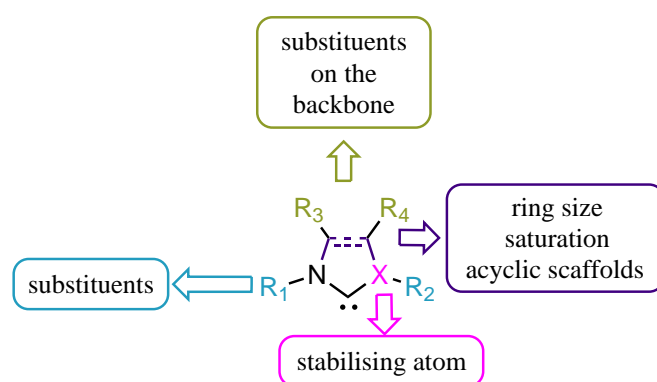
Figure I.1.6. Possible modifications in an NHC in order to tune its stereoelectronic properties.

In order to evaluate the effects of the modifications on the carbene structure, it is useful to quantify the steric and electronic properties of the carbenes as ligands. The most important method to determine the electronic properties of carbene ligands is the Tolman electronic parameter (TEP), which consists in the measurement by IR spectroscopy of the A_1 CO stretching frequency in [NiL(CO)$_3$] complexes.[54] Nowadays, due to the toxicity of nickel-carbonyl complexes, it is more common to measure the CO stretching frequencies in the square-planar and more user-friendly [IrClL(CO)$_2$] and [RhClL(CO)$_2$] complexes — normally given as the average of CO symmetric and asymmetric vibrational frequencies, $\tilde{\nu}_{CO}$(av).

The value of $\tilde{\nu}_{CO}$(av) is determined by the ability of the metal to backdonate electron density to the CO-π* orbital: a more populated CO-π* orbital causes a decrease in the C-O bond strength, which is translated to a diminished $\tilde{\nu}_{CO}$(av) in the IR spectra. Thus, the decrease of $\tilde{\nu}_{CO}$(av) could be related to the total electron density on the metal centre, which is determined by both the σ-donor and π-acceptor properties of the ancillary ligand we wish to analyse. Because of this, if L is a strong electron-releasing ligand, the metal centre has more electron density and the carbonyl metal complex will exhibit low $\tilde{\nu}_{CO}$(av). On the contrary, the decrease in $\tilde{\nu}_{CO}$(av) will be less pronounced

if L is a good π-acceptor ligand (**Figure I.1.7**).[55]
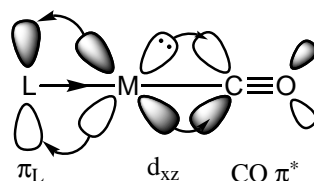
Figure I.1.7. Effect of the electronic density donated by ligand L to the metal in the CO bond in a square-planar metal-carbonyl complex, the page plane is considered as the xz plane.

Because of the simplicity of this measurement, the $\tilde{\nu}_{CO}$(av) provides a convenient system for comparing the electronic properties of ligands. However, it has some limitations and the results should be interpreted with care. Particularly, the steric properties of the ligands can affect the results, since bulky ligands might distort the ideal square-planar geometry of the metal complex, interfering in the optimal overlap between the metal and the carbonyl ligands.

NHCs steric properties can be quantified using the parameter of percentage buried volume ($\%V_{bur}$), introduced by Nolan and co-workers, defined as the fraction of the volume of a 3.5 Å radius sphere centred in the metal occupied by a given ligand.[56]

I.1.2.1 Modification of the amine substituents

Although both steric and electronic properties are entangled, in the case of carbenes is possible to modify the steric properties without a large variation of the electronic descriptors. Thus, it is conceivable to increase $\%V_{bur}$ by replacing R_1, the substituent linked to the amine, by a bulkier residue, and the $\tilde{\nu}_{CO}$ to remain almost unchanged. In general, alkyl substituents on the nitrogen atoms are better electron donors and, in the case of R_1 = aryl, small changes on the $\tilde{\nu}_{CO}$ are observed when varying the electronic nature of the *para*-substituents.[57,58]

I.1.2.2 Modification of the cyclic structure

The steric properties can be modified as well by changing the nature and the size of the carbene backbone (**Figure I.1.8**). Imidazolinylidenes have wider angles than imidazolylidenes,[59] leading to a slight increase in $\%V_{bur}$ of **43** compared to **42** (3 % increase).[56] Modifying the size of the heterocycle to larger six- (**46**), seven- (**47**)[60] or eight-membered rings (**48**)[61] or to smaller four-membered analogues (**45**),[62] dramatically changes the angle of the carbene, locating the substituents closer, in the case of extended ring scaffolds, or further away from the metal centre (see N-C-N angles

in **Figure I.1.8**). Thus, the $\%V_{bur}$ will be smaller for acute N-C-N angles, whereas it will be increased in NHCs with a larger ring size. For example in (**48**)AgCl, whose calculated $\%V_{bur}$ is 48.7, which stays in contrast with the value of 36.1 for (**42**)AgCl.[61]

42
N-C-N = 101.4 º
$\tilde{v}_{CO}$(av) = 2038.5 cm^{-1}

43
N-C-N = 104.7 º
$\tilde{v}_{CO}$(av) = 2040.5 cm^{-1}

44
C-C$_{carbene}$-C = 57.2 º

45
N-C-N = 96.7 º

46
N-C-N = 114.65 º
$\tilde{v}_{CO}$(av) = 2029 cm^{-1}

47
N-C-N = 116.6 º
$\tilde{v}_{CO}$(av) = 2028 cm^{-1}

48
N-C-N = 120.1 º
$\tilde{v}_{CO}$(av) = 2024.5 cm^{-1}

49
N-C-N = 129.6 º
$\tilde{v}_{CO}$(av) = 2026 cm^{-1}
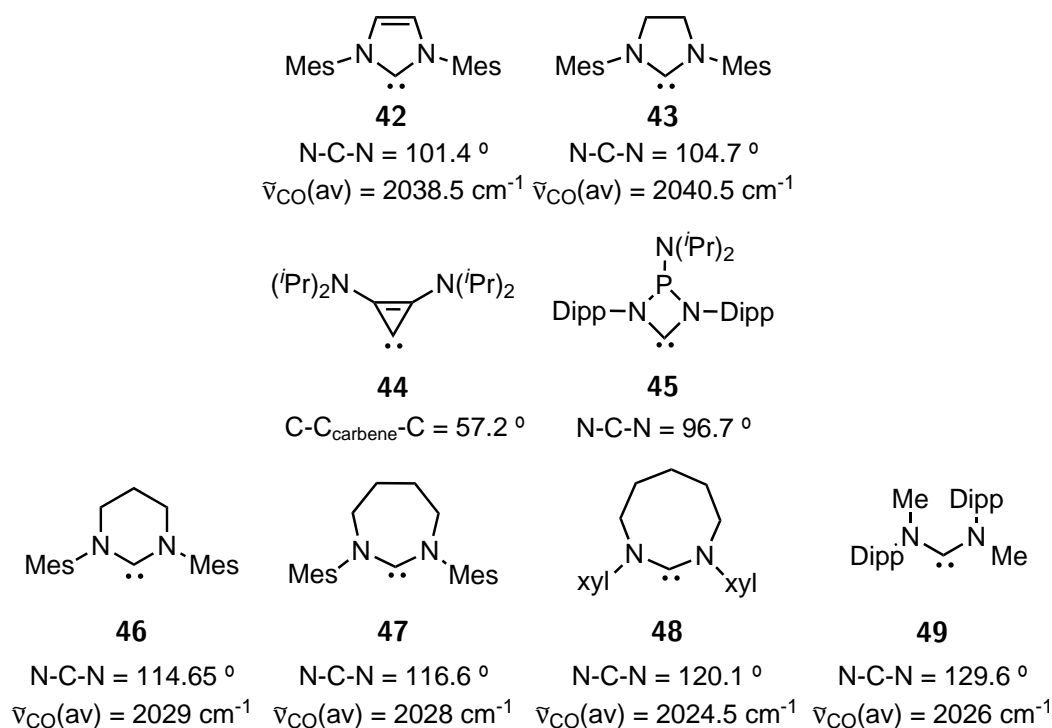
Figure I.1.8. Comparison of stable carbenes with different ring sizes. $\tilde{v}_{CO}$(av) values were calculated from the average of the CO stretching frequencies in [RhClL(CO)$_2$].

An extreme situation can be observed in cyclopropenylidene **44**, the smallest stable cyclic carbene reported to date, with a C-C$_{carbene}$-C angle of 57.2°, which places the substituents in the opposite direction of the carbene's lone pair.[63] On the other hand, the N-C-N angle is maximised with acyclic (diamino)carbenes (ADC) such as **49** (129.6°, **Figure I.1.8**).[64]

The changes in the angle of the carbene have additional implications for its electronic properties, since more linear structures would lead to a decreased s-character of the σ-orbital and an increased σ-donor ability. This is illustrated by the lower $\tilde{v}_{CO}$(av) value of **46**-**49** compared with **42** and **43** (See **Figure I.1.8**).[64,65] Moreover, carbenes **46**-**48**, have more flexible and distorted structures than their five-membered analogues, generating a twist between the nitrogen planes to accommodate ring strain, leading to a less efficient π-donation from the N-lone pairs to the empty $p_{carbene}$-orbital. Flexibility is maximised in ADCs due to the lack of constrain imposed by a cyclic backbone and rotation around the N-C$_{carbene}$ bonds is possible. The result is that carbenes **46**-**49** are

also better electrophiles than imidazolylidene and imidazolinylidene carbenes.[66]

Another modification of the cyclic scaffold that should be considered is the replacement of the carbon atoms of the backbone by other elements. One important example is the triazolylidene **38**, where the more electronegative nitrogen atom leads to a decreased nucleophilicity of the carbene.[67] Alternatively, phosphorus, boron and other elements have been employed to construct NHCs, modifying the electronic properties according to the characteristics of the heteroelement.[62,68]

ADCs[69] are a particularly interesting alternative to NHCs due to their aforementioned flexibility and electronic properties. Regrettably their study is underdeveloped compared with their cyclic analogues, probably because of the higher instability of the free acyclic carbenes and the observation of side reactions upon coordination to metals.[69] To circumvent such problems, one of the most employed strategies to obtain ADC-metal complexes **50** is through the nucleophilic attack of primary or secondary amines **51** to metal isonitriles **52** (*Scheme I.1.2*); a method that can also be applied to the synthesis of NHC complexes.[70]
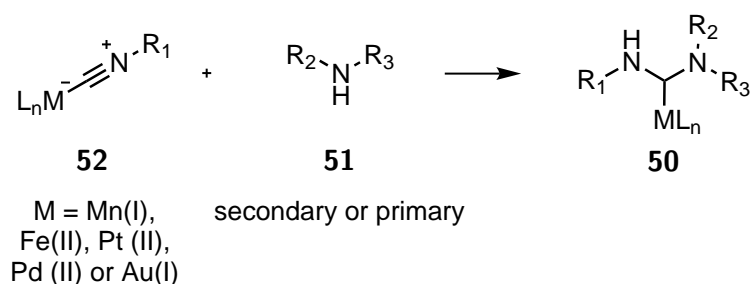
Scheme I.1.2. General synthesis of ADC-metal complexes by the nucleophilic attack of amines to isonitrile complexes.

Although this pathway is restricted to metals which are able to remove enough electronic density from the isonitrile ligand,[70] and only examples using Mn(I),[71] Fe(II),[72] Pt(II), Pd(II) and Au(I)[70d,73] have been reported, it allows an easy access to a broad variety of ADC complexes. Because of this, in the last years interest in ADC-metal complexes has seen a resurgence, especially in their applications to Pd[74] and Au catalysis.[75] In the latter it is important to highlight that, besides presenting comparable or better catalytic activities than traditional NHCs, they have been successfully applied in enantioselective gold(I)-catalysed transformations.[76]

I.1.2.3   Modification of the backbone substituents

An alternative to modify the electronic properties of NHCs is to change the substituents in the backbone R_3 and R_4 (see **Figure I.1.6**), exemplified by compounds **53**-**55** depicted in **Figure I.1.9**. Electron-withdrawing groups, such as chlorine in **53**, lower the energy of the orbitals of the carbene due to inductive effects, translated in slightly higher $\tilde{\nu}_{CO}$(av) than **42**.[77] A stronger impact is seen from π-acceptor substituents able to delocalise electron density, *e.g.* the carbonyl groups in **54**,[78] which significantly increase the carbenes electrophilicity, as demonstrated by higher CO stretching frequencies in [RhClL(CO)$_2$] complexes. Including π-electron donating substituents, such as NMe$_2$ in **55**, has the contrary effect, increasing the σ-donating ability, through an increase in the electron density on the imidazolylidene ring.[79]

$\tilde{\nu}_{CO}$(av) = 2042.5 cm^{-1} $\tilde{\nu}_{CO}$(av) = 2060 cm^{-1} $\tilde{\nu}_{CO}$(av) = 2033.5 cm^{-1}
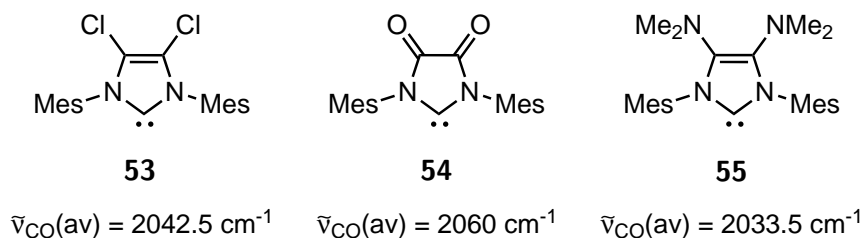
Figure I.1.9. Comparison of NHCs with different backbone substitution patterns. $\tilde{\nu}_{CO}$(av) values were calculated from the average of the CO stretching frequencies in [RhClL(CO)$_2$].

I.1.2.4   Modification of the stabilising atoms of the carbene

Probably, the variation that imposes the greatest influence on the stereoelectronic properties of the carbene is the modification of the stabilising atom attached to the carbene centre. These modifications lead to alternative classes of carbenes that present different reactivity and stability than NHCs and, even though they possess interesting properties, are underdeveloped compared with the ubiquitous (diamino)carbenes.[80]

It is important to consider that just one adjacent nitrogen atom suffices to stabilise free carbenes at room temperature under inert conditions, exemplified by the isolation of free CAAC **56**.[81] Although most of them are not stable enough to be isolated, besides CAACs, other carbene scaffolds with just one adjacent nitrogen atom have been employed as ligands to metals,[82] *e.g.* isoquinolinylidene **57**.[83]

Besides, other chemical entities with the appropriate symmetry and a lone pair might act as nitrogen surrogates, such as P, S or O centres, stabilising singlet carbenes in similar fashion. Examples of stable free carbenes with different stabilising heteroatoms are depicted in **Figure I.1.10**, such as thioazolylidene **58**,[84] acyclic (amino)-(oxy)carbene

**59**[85] and heterocyclic (amino)-(phosphino)carbene **60**.[86]
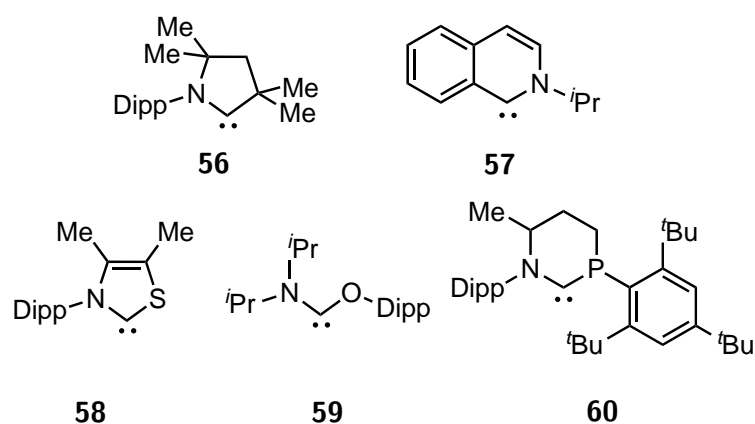
Figure I.1.10. Comparison of carbenes with different stabilising atoms. $\tilde{\nu}_{CO}(\text{av})$ values were calculated from the average of the CO stretching frequencies in $[\text{RhClL(CO)}_2]$.

The replacement of one or two nitrogens in (diamino)carbenes by other atoms modifies their electronic properties: the stabilisation of the σ-orbital increases with the electronegativity of the atom and the empty $p_{carbene}$-orbital energy increases with the ability to donate π-electron density. Thus, carbenes flanked by fewer heteroatoms (**56**-**57**) are better σ-donors and π-acceptors, as evidenced by decreased calculated ΔE_{S-T} values.[87,88] On the other hand, theoretical ΔE_{S-T} values have been calculated to follow the trend $\text{NMe} > O > S > \text{PMe}$, increasing in the reverse order than the σ-donor and π-acceptor ability.[89]

Another chemical entity suitable as nitrogen surrogate is an ylide (***Figure I.1.11***), due to the non-shared electron pair on the formally negatively charged carbon atom, attached to a heteroatom with a formal positive charge. Ylides can be represented in two extreme canonical forms : one "ylene" form with a double bond between the carbon and the heteroatom, and one zwitterionic (ylidic), where the lone pair is located in the carbon atom. The ylidic form is isoelectronic with the amino fragment, and therefore, could stabilise a singlet carbene in a similar fashion. The lower electronegativity of carbon compared with nitrogen decreases the stabilisation of the σ-orbital and increases the σ-donating properties of the carbene. For the same reason, the ylide carbon should populate with more ease the empty $p_{carbene}$-orbital, but the ability of phosphorus of delocalising electron density on the low-lying σ^* P-C bond might prevent a strong π-donation, thus keeping (amino)-(ylide)carbenes (AYCs) as appreciable π-acceptor ligands, in agreement with calculations performed in some complexes that will be commented on below.
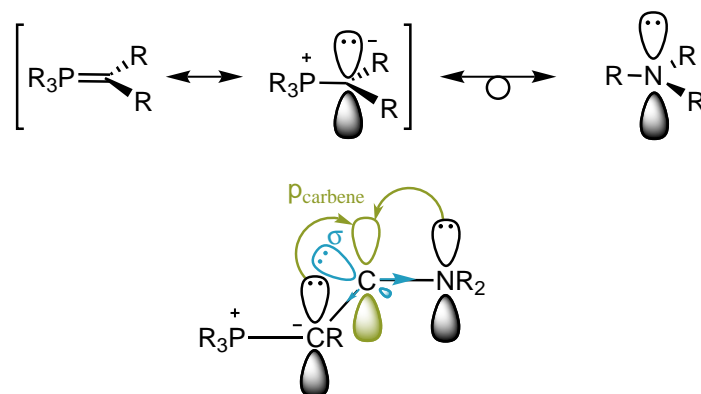
Figure I.1.11. Analogy between phosphorus ylides and nitrogen substituents (above). Stabilisation of a (amino)-(ylide)carbene model (below).

61   **63**   **62**

8 examples
60 - 80 % yield
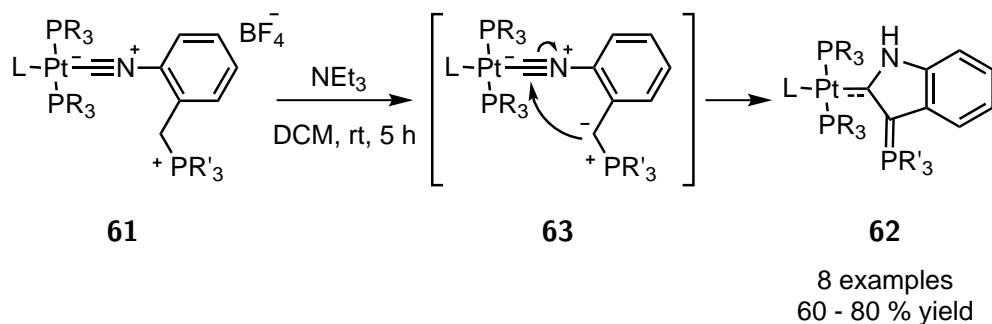
Scheme I.1.3. First examples of AYC-metal complexes.

Cyclic AYC-transition metal complexes have been known since the 1980's. The first reported complexes **62**, were obtained by the intramolecular attack of the ylide moiety in the intermediate **63** — generated *in situ* by deprotonation of phosphonium-tethered isocyanide-Pt(II) complexes **61** with NEt_3 — on the isonitrile carbon atom to afford the corresponding AYC-Pt(II) complexes in good yields (**Scheme I.1.3**).[90]

More recently, it has been proven that free AYCs **64** are stable enough to be generated by deprotonation of the corresponding heterocycles **65** with a strong base before trapping by a metal centre, affording the corresponding AYC-metal complexes **66** as illustrated in **Scheme I.1.4**. Free carbene **67** and AYC lithium adduct **68** have been additionally characterised by NMR spectroscopy, proving the generation in solution of the carbene upon deprotonation. Using this highly versatile methodology, several Rh(I), Pd(II) and Au(I) complexes have been prepared, bearing PR_3 (ligands **67**, **68** and **69**), SR_2 (ligands **70** and **71**) and heterocycles (ligand **72**) as stabilising groups.[91]

65   **64**   **66**

67
$\tilde{\nu}_{CO}$(av) = 2008.5 cm^{-1}

68

69
$\tilde{\nu}_{CO}$(av) = 2012 cm^{-1}

70
$\tilde{\nu}_{CO}$(av) = 2013.5 cm^{-1}

71
$\tilde{\nu}_{CO}$(av) = 2019 cm^{-1}

72
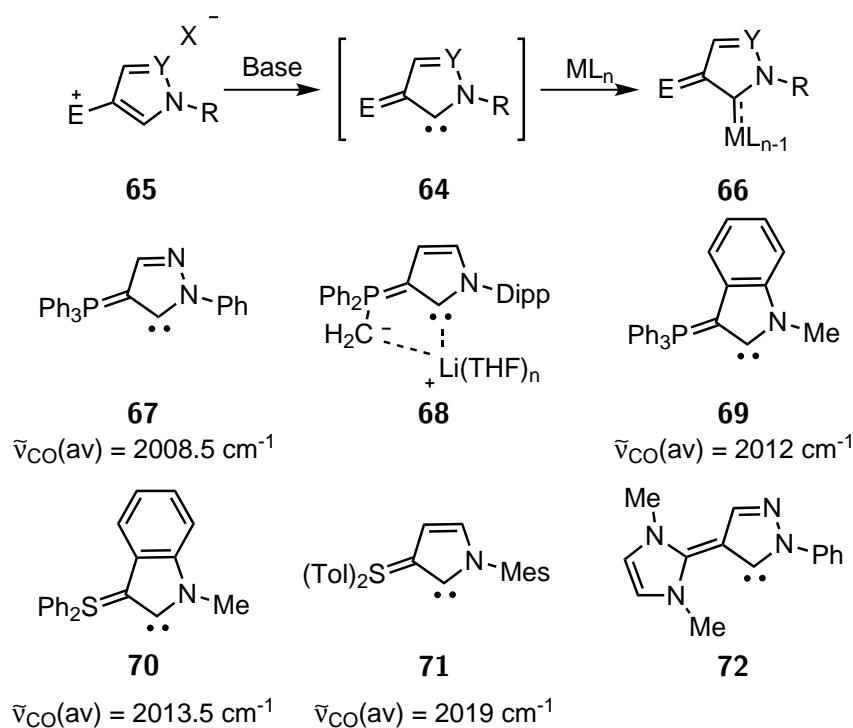
Scheme I.1.4. Synthesis of cyclic AYC metal complexes by trapping of the free carbene with a metal source (above). AYCs ligands prepared through deprotonation (below). $\tilde{\nu}_{CO}$(av) values were calculated from the average of the CO stretching frequencies in [RhClL(CO)$_2$].

69
[{Pd(allyl)Cl}$_2$]
(5 mol%)

DME, 80 ºC, 2 h

75   **76**

77
100 % GC yield

68AuCl (5 mol%)
AgSbF$_6$ (5 mol%)

DCM, -5 ºC

73   **74**
94 %
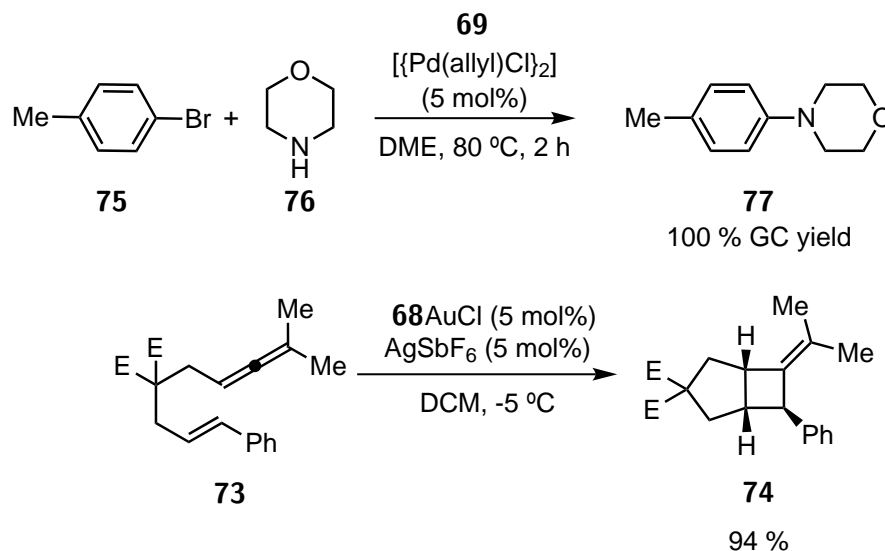
Scheme I.1.5. Applications of AYC ligands in catalysis. E = COOMe.

The analysis of the CO stretching frequencies corresponding to the [RhClL(CO)$_2$] complexes, displayed in ***Scheme I.1.4***, demonstrates that AYCs are among the lowest values reported for a carbene ligand, indicating that they display the expected exceptionally strong σ-donating properties. Moreover, theoretical studies performed in carbenes

67 and **69** revealed that their electronic properties were due to the destabilisation of the σ-orbital of the carbene, whereas the energy of the vacant $p_{carbene}$-orbital remained similar to the parent (diamino)carbenes.[91a]

Despite their interesting electronic properties, the performance of AYC ligands in catalysis is almost unexplored. Preliminary studies showed that 5 mol% of ligand **69** and [{Pd(allyl)Cl}$_2$] are able to catalyse the Buchwald-Hartwig amination of arylbromide **75** with morpholine **76** to afford **77** (***Scheme I.1.5***, above). Furthermore, (**67**)AuCl has been employed successfully as precatalyst in the cycloisomerisation of eneallene **73** to afford selectively the bicycle **74** (***Scheme I.1.5***, below). These results reflect that AYCs are a class of carbenes that deserve further study and might find relevant applications in catalysis.

In summary, since their isolation, NHCs have proved to be useful in a variety of applications, especially as ligands in transition metal catalysis due to their good σ-donor ability and the high stability of their complexes. Usually, carbenes based on imidazolylidene and imidazolinylidene scaffolds are employed, whose electronic properties are not simple to modify and, besides some exceptions, usually fall in a rather narrow range. For this reason, it is important to study alternative carbene ligands with different stereoelectronic properties in order to improve the catalytic performance or discover novel reactivities and further the diversity of the carbene family, which still does not reach the already large variety of phosphines.

18

I.2.   Objective of the project

Cyclic (amino)-(ylide)carbenes are among the strongest σ-donor NHCs known to date, maintaining moderate π-acceptor attributes. Meanwhile, the acyclic analogues of AYCs remained still unknown. Since the stereoelectronic characteristics of the carbenes change upon removing the cyclic backbone, increasing the proximity of the substituents to the metal centre, the σ-donor ability and the flexibility of the ligand, we decided to investigate the synthesis of their acyclic counterparts and study their properties.

Inspired by the synthesis of acyclic (diamino)carbenes and the first cyclic AYC-metal complexes, we envisaged that acyclic (amino)-(ylide)carbenes (AAYCs) **13** could be obtained by the intermolecular nucleophilic attack of an ylide **14** to a suitable isocyanide metal complex **12** (**Scheme I.2.1**). Gold(I) isonitrile complexes **12** were proposed as substrates since they have been successfully employed for the synthesis of ADC complexes using amines as nucleophiles, gold(I)-catalysis also being one of the major application areas of acyclic carbene-metal complexes.
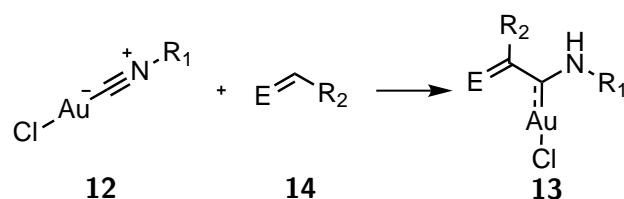
Scheme I.2.1. Proposed synthesis of acyclic (amino)-(ylide)carbene gold(I) complexes.

The proposed strategy is modular, allowing the introduction of a variety of substituents at the nitrogen atom (R_1) and in the ylide (R_2 and E). This would allow the facile study of the effect of the substituents and the exploration of the reactivity of this new class of carbenes.

Interestingly, the presence of additional functional groups on the AAYC-complexes side arm (R_2) allowed their further functionalisation, leading to the synthesis of heterobimetallic complexes, bearing Rh(I) and Au(I) centres, and cationic AAYC-gold(I) complexes. Moreover, an unprecedented Au(I)$\rightarrow$Rh(III) and Au(I)$\rightarrow$Ru(II) carbene

transmetalation is reported, promoted by chelation of the incoming metal to the carbene and the functionalised R_2 substituent.

I.3. Results and discussion

I.3.1 Synthesis of AAYC-gold(I) complexes

As previously discussed, the addition of a nucleophile to isocyanide-metal complexes can be used to synthesise a wide variety of cyclic and acyclic carbenes, allowing the rapid access to carbene-metal complexes without the necessity of using the free carbene. Because of this, we envisaged that ylides could react with isocyanide-metal complexes to yield the novel AAYC-metal complexes. The viability of our proposed strategy was initially tested employing different isocyanide-gold(I) chlorides as electrophiles and phosphorus ylides as nucleophiles. The former are easily accessible in excellent yields through the treatment of $(Me_2S)AuCl$ in DCM solution with the corresponding isocyanides **78** (***Scheme I.3.1***), following already described procedures.[75c]

12a	R_1 = Ph	99 %
12b	$R_1 = Me_2(C_6H_3)$	>99 %
12c	R_1 = 2-pyr	98 %
12d	$R_1 = n\text{-}C_5H_{11}$	>99 %
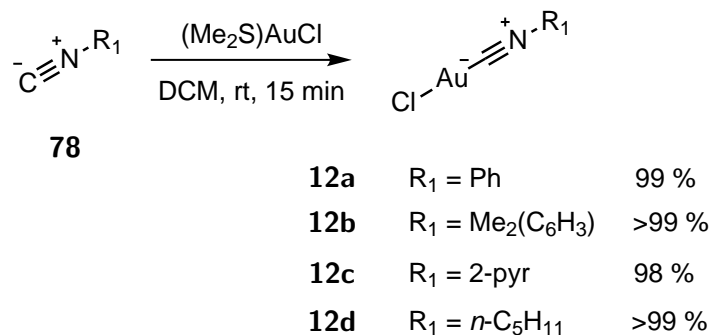
Scheme I.3.1. Synthesis of isocyanide-gold(I) complexes.

Isocyanides are $2e^-$ donor ligands isoelectronic with CO, and they coordinate the metal by σ-donation of a lone pair located on the carbon atom. They also present good π-accepting properties, since they can receive electron density from the metal into the π^* C-N orbital.[55] Isonitrile-gold(I) complexes are suitable for the synthesis of carbenes, as the highly Lewis acidic gold(I) centre enhances the contribution of the σ-donation from the isocyanide to the metal and, consequently, depletes electron density from the isocyanide carbon, thus activating it towards nucleophilic attack. This explains the

success of isocyanide-gold(I) chlorides in the synthesis of cyclic and acylic (diamino)-[73,75] and (amino)-(oxy)carbene complexes,[92] prepared through the nucleophilic attack of amines or alcohols to isonitrile-gold(I) complexes.

Phosphorus ylides were initially tested since a wider variety of structural motifs are known, some stabilised phosphorus ylides being even commercially available.[93] The variation of the substituents attached to the ylidic carbon alters its nucleophilicity and reactivity, depending on their ability to delocalise the negative charge, which could have implications in the synthesis of the AAYC complexes. Furthermore, modifying the electronic properties of the side-arm of the carbene could also have consequences in the attributes of the ligand through the modulation of the energy of the carbene orbitals, allowing the fine-tuning of its electronic properties.

Thus, isocyanide-gold(I) complexes **12a-d** were treated with different phosphorus ylides **79a-f** (***Table I.3.1***), presenting a variety of degrees of stabilisation. Consumption of **12** was observed with the concomitant formation of two different species (***Scheme I.3.2***).
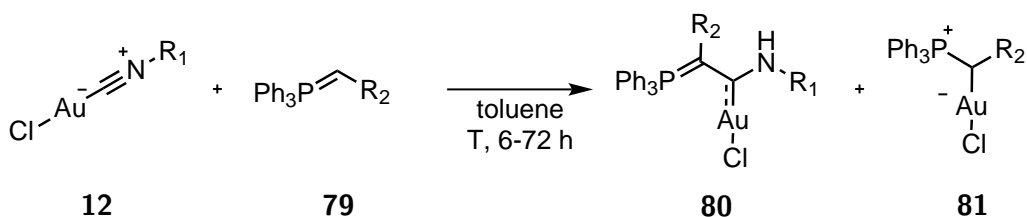
Scheme I.3.2. Synthesis of acyclic (amino)-(ylide)carbene gold(I) complexes.

The major product in most of the cases could be assigned as the desired AAYC-gold(I) complexes **80**, displaying a characteristic ^{31}P-NMR signal at 18–22 ppm, similar to the reported cyclic AYC-metal complexes,[91] and a broad deshielded N-H peak in the ^{1}H-NMR spectra. Furthermore, the carbene nature of the ligand in **80** could be assessed by the characteristic downfield ^{13}C-NMR chemical shift, lying between 187.1–207.0 ppm, similar to the known cyclic AYCs-metal complexes.[91]

Interestingly, even though four different conformers with different arrangements of the substituents are possible, just one set of signals was observed in the NMR, indicating either the presence of only one conformation, or their rapid interconversion at room temperature. The different conformations arise from the distribution of the substituents relative to gold: the two bulkiest substituents on each side, PPh$_3$ and R_1, can arrange both *syn-* to Au, one *syn-* and one *anti-* or both *anti-* as depicted in ***Figure I.3.1***. Some ADC complexes, such as **82** in ***Figure I.3.1***, display an equilibrium between *syn-* and *anti-* rotamers on the NMR time scale, being both observed in the NMR.[75c]

Due to the bulkiness of PPh$_3$, a rapid interconversion in solution is unlikely for the AAYC complexes and the presence of just one rotamer could be attributed to the greater stability of the *syn, syn*-AAYC form, caused by a reduced steric hindrance compared with the other isomers. The presence of an intramolecular hydrogen-bond between the N-H and heteroatoms in R_2 — evidenced by X-ray diffraction studies that will be elaborated in the next section — may also contribute to the stability of the *syn, syn*-conformer.
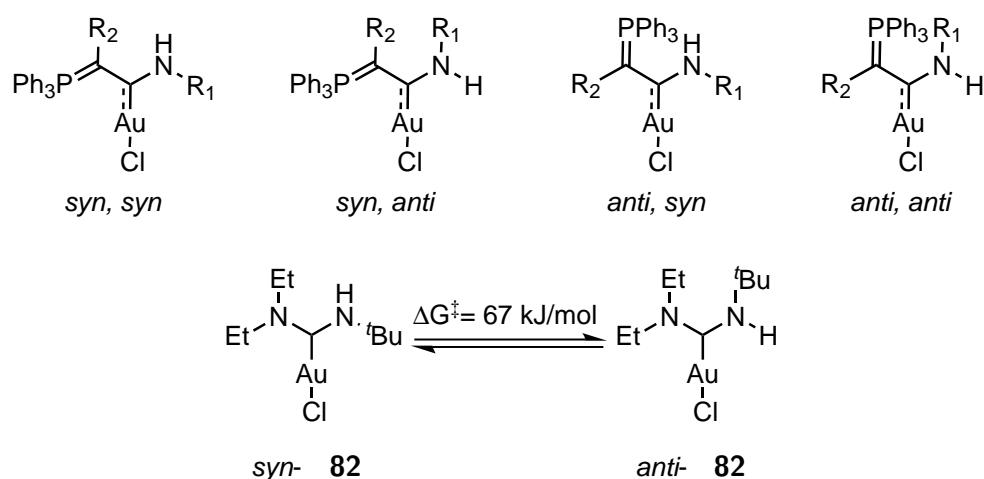
Figure I.3.1. Possible isomers of AAYC complexes **80** (above). Rotamers of **82** in solution (below).

Multinuclear NMR spectroscopy studies revealed that the other by-product, with ^{31}P-NMR shifts between 25–28 ppm, displayed solely NMR signals attributable to the ylide fragment, with a ^{1}H-NMR doublet signal coupled with phosphorus at 3–5 ppm, consistent with a proton attached to the ylidic carbon. These results suggested the formation of an ylide-gold(I) complex **81** through displacement of the isocyanide ligand. Phosphorus ylides are known to be excellent σ-donor ligands, displaying greater ability to coordinate when the ylide is less stabilised, and usually are synthesised through ligand-exchange of a weakly coordinating ligand by the ylide.[94] Comparison of the spectra of ylide-gold(I) complexes **81b**, **81e** and **81f** with those registered in the literature[95] confirmed our proposed connectivity.

In addition, the connectivity of **81e**, illustrated in ***Figure I.3.2***, was confirmed by X-ray crystallography. Compound **81e** consists of a tetrahedral carbon centre, characteristic of monodentate C-bonded ylides, linked to the gold(I) centre. In general, the structural features are comparable to other known ylide-gold(I) complexes.[96] Interestingly, the distance between Au1-H9 of 2.508 Å ($\sum r_{vdW}(\text{Au,H}) = 2.86$ Å).[97] reveals an Au-H agostic interaction.
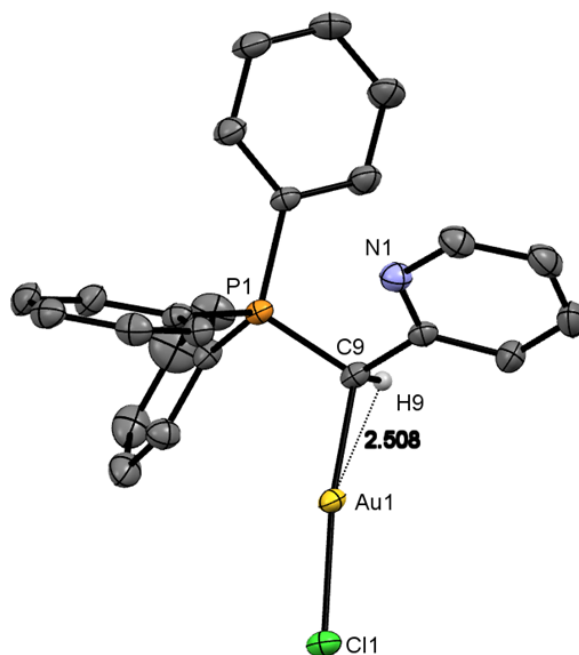
Figure I.3.2. Solid state structure of ylide-gold(I) complex **81e**. Hydrogen atoms, except H9, and solvent molecules have been omitted for clarity. Thermal ellipsoids set at 50 % probability. Selected bond lengths (Å) : Au1-C9 = 2.056, C9-C2 = 1.498 , P1-C9 = 1.780.

The results of the reaction of different gold(I)-isonitriles with phosphorus ylides are summarised in ***Table I.3.1***, revealing that the ratio between the observed products AAYC-gold(I) : ylide-gold(I) complexes (**80**:**81**), determined by ^{31}P-NMR analysis, was highly dependent on three main factors: the ylide substituents, the nature of the isonitrile ligand and the reaction temperature.

The reaction of stabilised ylides bearing electron-withdrawing groups, such as carbonyl- or cyano- substituents in compounds **79a–d**, with isonitrile gold(I) chlorides **12a** and **12b** afforded the AAYC-gold(I) chlorides **80** as the major product (entries 1–5, 9, 11 and 12). Conversely, it could be observed that the formation of the ligand substitution product **81** was increased when more nucleophilic phosphorus ylides were used. Notably, the lesser stabilised phosphorus ylide **79f**, and therefore the most nucleophilic of the tested ylides, favours the formation of **81f** (entry 7). Interestingly, the greater ability of 2-pyridyl substituent to stabilise the adjacent negative charge compared with phenyl residue is enough to favour the formation of the AAYC complexes **80e** and **80k** in excellent yields from unhindered gold-isocyanides **12a** and **12c** respectively (entries 6 and 15).
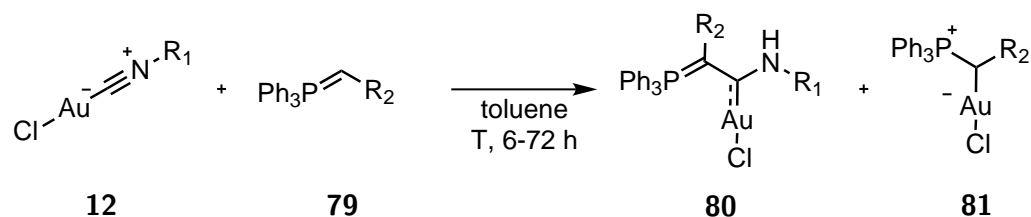
Scheme I.3.3. Synthesis of acyclic (amino)-(ylide)carbene gold(I) complexes.

Entry	12	R$_1$	79	R$_2$	T (°C)	80:81	Yield (%)
1	**12a**	Ph	**79a**	COMe	rt	98 :< 2	85, **80a**
2	**12a**	Ph	**79b**	COOEt	rt	73 : 27	63, **80b**
3	**12a**	Ph	**79b**	COOEt	35	98 :< 2	74, **80b**
4	**12a**	Ph	**79c**	CN	35	98 :< 2	88, **80c**
5	**12a**	Ph	**79d**	CONMe$_2$	35	98 :< 2	81, **80d**
6	**12a**	Ph	**79e**	2-pyr	35	98 : 2	98, **80e**
7	**12a**	Ph	**79f**	Ph	-78 – rt	24 : 76	5, **80f**
8	**12a**	Ph	**79f**	Ph	50	0 : 100	71, **81f**
9	**12b**	2,6-Me$_2$(C$_6$H$_3$)	**79a**	COMe	50	98 :< 2	30, **80g** [a]
10	**12b**	2,6-Me$_2$(C$_6$H$_3$)	**79b**	COOEt	-78 – rt	13 : 87	n.d.
11	**12b**	2,6-Me$_2$(C$_6$H$_3$)	**79b**	COOEt	50	77 : 23	37, **80h**
12	**12b**	2,6-Me$_2$(C$_6$H$_3$)	**79c**	CN	50	74 : 26	25, **80i**
13	**12b**	2,6-Me$_2$(C$_6$H$_3$)	**79d**	CONMe$_2$	-78 – rt	25 : 75	12, **80j**
14	**12b**	2,6-Me$_2$(C$_6$H$_3$)	**79e**	2-pyr	-78 – rt	2 :> 98	83, **81e**
15	**12c**	2-pyr	**79e**	2-pyr	35	98 :< 2	89, **80k**
16	**12d**	n-C$_5$H$_{11}$	**79a**	COMe	rt	n.r.	-
17	**12d**	n-C$_5$H$_{11}$	**79c**	CONMe$_2$	rt	comp. mixt.	-

Table I.3.1: Synthesis of acyclic (amino)-(ylide)carbene gold(I) complexes employing different gold(I) isocyanides and phosphorus ylides. Ratio **80:81** was determined by ^{31}P-NMR. [a] 43 % conversion.

Stabilised ylides bearing electron-withdrawing groups, such as carbonyl- or cyano-substituents, can be described by a third resonance structure that indicates their ability to delocalise the negative charge on their side-arm (**Figure I.3.3**), and in consequence, are less nucleophilic at the ylidic carbon. Their lower nucleophilicity is translated into a decreased donor ability of the ylidic carbon, that will coordinate metals less readily than their non-stabilised analogues and might explain the preferential attack to the

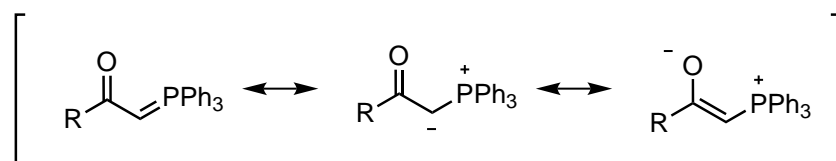isonitrile when employing the stabilised phosphorus ylides **79a–d**.

Figure I.3.3. Mesomeric forms of carbonyl-stabilised phosphorus ylides.

Secondly, the stereoelectronic nature of the substituent attached to the isonitrile (R_1) was decisive for the selectivity towards the AAYC-gold(I) complexes. The steric congestion of the isonitrile yielded more of the ylide-gold(I) complexes **81**, likely due to an increased difficulty of the ylide to attack the electrophilic carbon of the isonitrile. Because of this, the reactions with the less hindered gold(I)-isonitriles **12a** and **12c** led to the corresponding AAYC complexes **80** in good yields (entries 1–6 and 15), whereas for the sterically hindered compound **12b** (entries 9–14), the yields dropped considerably due to the increased amount of the ligand substitution product **81**, which complicated the separation of the desired AAYC complexes by iterative fractional crystallisation.

Moreover, the reaction of the gold(I)-isocyanide **12b** with phosphorus ylides was slower than with the unhindered aromatic isonitriles **12a** and **12c**, highlighted in the reaction of **12b** with the phosphorus ylide **79a**, where just 43 % conversion was achieved after 3 days at 50 °C (entry 9).

Nevertheless, the steric environment of the isonitrile was not the only factor involved, since the reaction of phosphorus ylides with the *n*-pentylisocyanide-gold(I) chloride **12d** did not lead to the desired AAYC complexes. In the case of the less reactive **79a**, no reaction was observed after 24 h, whereas the ylide **79c** led to a complex mixture (entries 16 and 17 respectively). The crude in the latter did not display the characteristic ^{31}P-NMR peak of the AAYC complex, while **81c** could be detected as part of the mixture. These results are likely explained by the higher energy of the LUMO of aliphatic isocyanides compared with the aromatic analogues, where the π^* C-N orbital (LUMO) is stabilised through interaction with the π-system of the aromatic residue, thus favouring the nucleophilic attack.[98]

Finally, the temperature of the reaction was decisive to achieve good yields, favouring the formation of the AAYC-gold(I) complex when the reaction mixture was gently heated, as observed by the improved selectivities of entries 3 and 11 compared with 2 and 10. Nevertheless, this effect was not general, and heating the reaction between **12a** and the more reactive ylide **79f**, shifted the selectivity towards the ligand substitution product **80f**.

It is important to highlight that the AAYC-gold(I) chlorides stabilised by phosphorus are resistant to moisture and air in the solid state, and can be stored in normal vials without noticeable decomposition of the compounds for several months.

In view of the success of our proposal for the synthesis of AAYC-gold(I) complexes from phosphorus ylides, we decided to evaluate whether other ylides could be employed. Hashmi and co-workers have already proven that azomethine ylides are able to react with gold isonitriles by a [3+2] cycloaddition, leading to abnormally bound NHCs.[99] Therefore we decided to investigate the synthesis of AAYCs from arsenic-derived ylides.[100] Thus, phenylisonitrile-gold(I) complex **12a** was treated with the stabilised arsonium ylide **83** to afford the desired AAYC-gold(I) complex **84**, albeit in moderate yield due to the limited stability in solution of compound **84**.
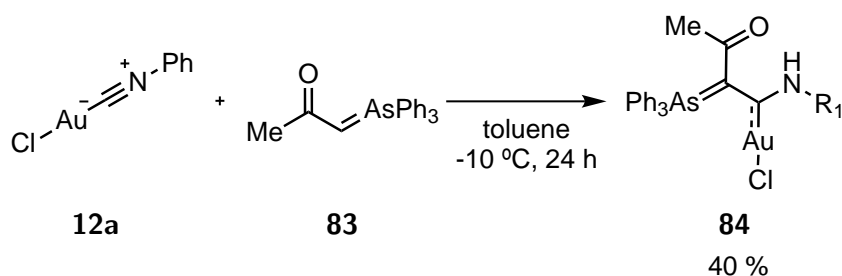
Scheme I.3.4. Synthesis of acyclic (amino)-(ylide)carbene gold(I) complexes from arsenic ylide **83**.

Arsonium ylides, such **83**, are also known to coordinate metals[101] but, probably due to the efficient delocalisation of negative charge on the carbonyl group, the ligand substitution product was not detected in this case.

More interestingly, we tested if polarised C-C bonds could also participate in the stabilisation of AAYCs. It has been proven that some ene-1,1-diamines and enamines hold certain ylidic character, enhanced by the presence of aromatic heterocycles able to stabilise a positive charge and electron-withdrawing groups with the capability of delocalising the negative charge. In analogy with stabilised phosphonium ylides, compounds **85** and **86** can be drawn with two different mesomeric forms, depicted in **Figure I.3.4**: one resonance structure bearing a double bond, and another zwitterionic form, with the positive charge held in the aromatic imidazolium or pyridinum moieties and the negative charge delocalised in the carbonyl substituent.[102]

On treatment of compound **12a** with the diaminoalkene **85** and the enamine **86** under the standard conditions, the desired AAYC complexes **87** and **88** were obtained in excellent yields (**Scheme I.3.5**). Spectroscopic analysis of compounds **84**, **87** and **88** exhibited similar features to their AAYC analogues **80** prepared from phosphonium

ylides. Specifically the broad N-H peak in the ^{1}H-NMR spectra and the characteristic downfield ^{13}C-NMR signal attributable to the carbene carbon. The structure of these compounds could be further confirmed by X-ray analysis that will be discussed in the following section.
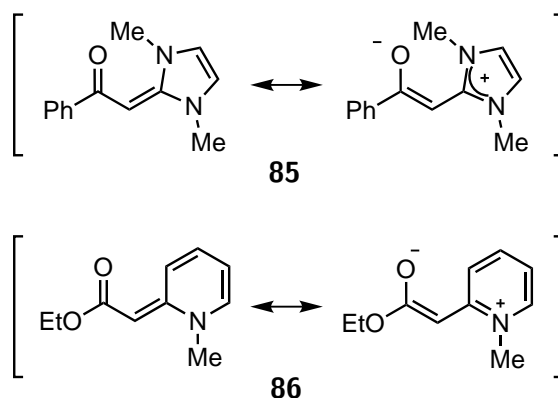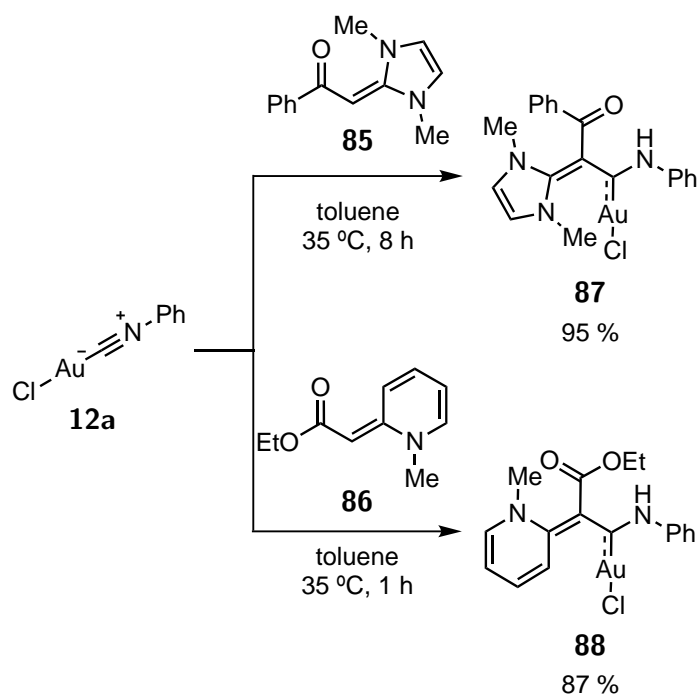

Figure I.3.4. Mesomeric forms of ene-1,1-diamine **85** and enamine **86**.

Scheme I.3.5. Synthesis of acyclic (amino)-(ylide)carbene gold(I) complexes from ene-1,1-diamine **85** and enamine **86**.

I.3.2   Structure of AAYC-gold(I) complexes

Suitable crystals for X-ray diffraction studies could be grown by slow diffusion of
n-pentane into DCM solutions of compounds **80a**, **80d–g**, **80i–k**, **84**, **87** and **88**. The
analysis of the solid state structures confirmed the connectivity of the AAYC-gold(I)
chlorides, illustrated in ***Figure I.3.7*** and ***Figure I.3.8*** for **80a**, **80d**, **80e**, **80f**, **80j**,
80k, **84**, **89** and **88**, whereas compounds **80g** and **80i** can be found in the Appendix
B. The most representative bond lengths are summarised in ***Table I.3.2***.
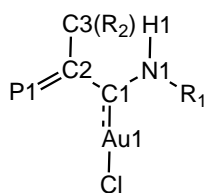
Figure I.3.5. Atom numbering in AAYC-gold(I) chlorides.

Entry	(AAYC)AuCl	C1-Au1	C1-C2	C2-P1	C2-C3	C1-N1	Other
1	**80a**	1.998	1.432	1.778	1.432	1.336	C3-O1 = 1.247
							N1-C5 = 1.430
2	**80d**	2.003	1.409	1.759	1.426	1.345	C3-N2 = 1.151
3	**80e**	2.007	1.413	1.765	1.477	1.352	N1-C8 = 1.418
4	**80f**	2.008	1.391	1.762	1.493	1.372	N1-C9 = 1.408
5	**80g**	2.009	1.441	1.768	1.453	1.325	C3-O1 = 1.247
6	**80i**	2.000	1.421	1.739	1.415	1.330	C3-N2 = 1.152
7	**80j**	2.015	1.390	1.746	1.513	1.355	C3-O1 = 1.228
8	**80k**	2.005	1.388	1.767	1.491	1.376	N1-C26 = 1.395
9	**84**	2.000	1.432	-	1.432	1.341	As1-C2 = 1.898
							C3-O1 = 1.252
10	**87**	2.000	1.430	-	1.435	1.340	C2-C10 = 1.465
							C3-O1 = 1.266
11	**88**	1.986	1.406	-	1.457	1.354	C2-C6 = 1.466
							C3-O1 = 1.238

Table I.3.2: Selected bond lengths of compounds **80a**, **80d–g**, **80i–k**, **84**, **87** and **88**. All the bond
distances are represented in Å.

In general the Au1-C1 distance is almost constant, independently of the substituents on the ylide and the amine, showing the expected linear geometry around the gold(I) centre. Interestingly, in all the AAYC-gold complexes, N1, C1, C2, C3 and P1 are coplanar, indicating the likelihood of charge delocalisation through a conjugated π-system. Because of this and in analogy to AYCs, their acyclic analogues can be described with two different extreme resonance structures, one of carbenic nature (form **I**), and another corresponding to a phosphoniovinyl-gold complex (form **II**), depicted in ***Figure I.3.6***. Additionally, due to the presence of carbonyl- and cyano- substituents able to delocalise electron density in most of the AAYCs reported in the previous section, a third resonance structure is conceivable, corresponding to a (phosphonioenolate)carbene **III**.
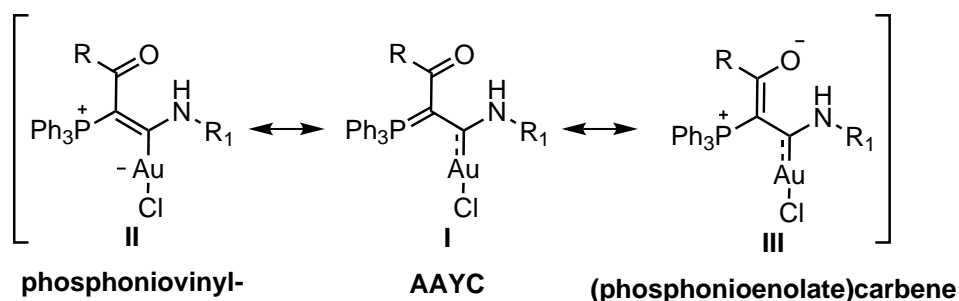

Figure I.3.6. Possible resonance structures of AAYC-gold(I) complexes.

These mesomeric forms are not restricted to AAYCs cointaining the PPh$_3$ fragment, since **84**, **87** and **88** can be described in the same fashion, replacing the phosphonium moiety stabilising the positive charge in forms **II** and **III** and which contributes to the double bond in **I**.

X-ray structures are very informative to determine which resonance structure describes better the ligands and could be employed to evaluate the effects of the structural modifications in the AAYC complexes. It can be observed in ***Figure I.3.7*** that in most of the AAYC complexes bearing a carbonyl or cyano group, these moieties are almost coplanar with the carbene centre, thus allowing the resonance stabilisation of electron density. This is reflected on the bond lengths, since compounds **80a**, **80d**, **80g** and **80i** present a short C2-C3 bond, whereas C3-O1 or C3-N2 distances are longer than model carbonyl or cyano compounds (***Figure I.3.7***, entries 1, 2, 5 and 6 respectively) but shorter than C-O or C-N single bonds,[103] indicating that the (phosphonioenolate)carbene mesomeric form (**III**) likely has a major contribution to the electronic structure.
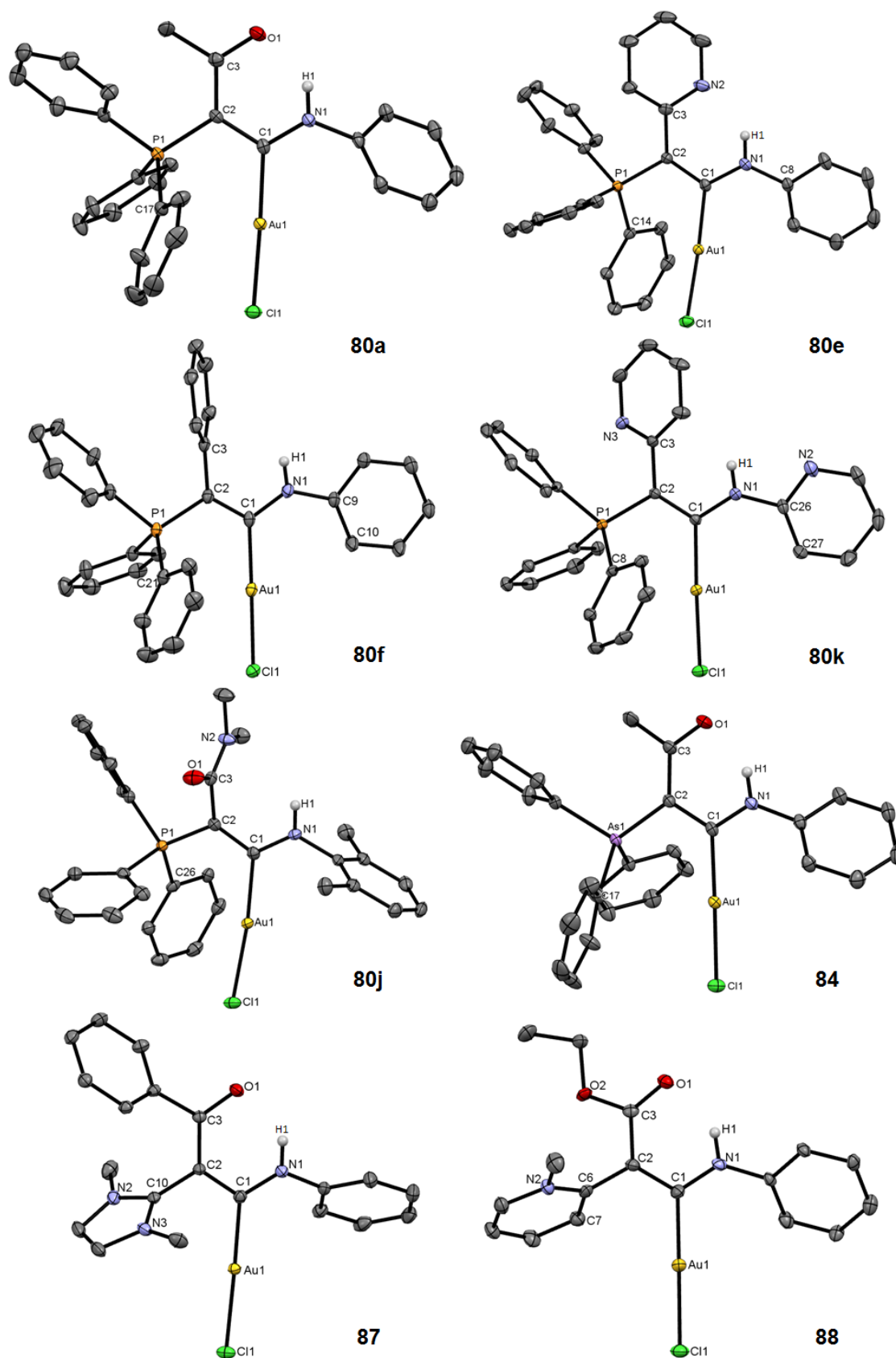
Figure I.3.7. Solid state structure of compounds **80a**, **80e**, **80f**, **80j**, **80k**, **84**, **87** and **88**. Hydrogen atoms, except N-H, and solvent molecules have been omitted for clarity. Thermal ellipsoids set at 50 % probability.
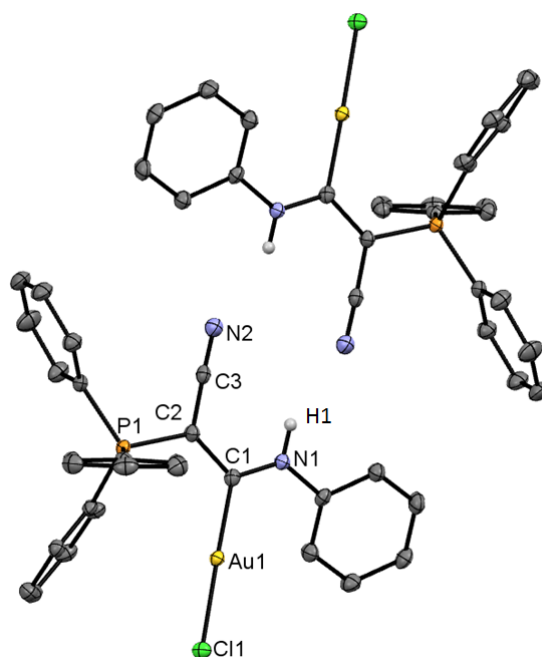
Figure I.3.8. Solid state structure of compound **80d**. Hydrogen atoms, except N-H, and solvent molecules have been omitted for clarity. Thermal ellipsoids set at 50 % probability.

The conjugation of the carbene with the carbonyl group orients the oxygen in proximity to H1, enabling an intramolecular hydrogen-bond in compounds **80a** and **80g** (O3-H1 distances are listed in *Table I.3.4*), which confers rigidity to the ligands and helps to maintain the coplanarity of N1, C1, C2 and C3. In the case of **80d** and **80i**, due to the linear geometry of the CN- groups, intramolecular hydrogen-bonding is not possible, but intermolecular interactions between two molecules of the gold complexes are observed, as illustrated for **80d** in *Figure I.3.8*.

Similar situations are found in **84**, **87** and **88**, where the dipolar (enolate)carbene form **III** is also dominant, bearing the lateral AsPh$_3$, imidazolium or pyridinium moieties a partial positive charge (*Figure I.3.7*, entries 9–11). The former displays very little variation from the parent **80a**, whereas in **87** and **88** the imidazolium and pyridinium cations are tilted away from the carbene plane, with torsion angles of 75.9° (C1-C2-C10-N3) and 60.3° (C1-C2-C6-C7) respectively, preventing the efficient overlap of the aromatic moieties with the π-system of the carbene and thus indicating that the contribution of the carbenic mesomeric form **I** is reduced. Because of the charge delocalisation in the carbonyl group, compounds **84**, **87** and **88** present also an intramolecular hydrogen-bond between the oxygen of the carbonyl group and H1 (see O3-H1 distances in *Table I.3.4*).

Interestingly, even though compound **80j** bears an amide group, its structure differs from **80a** and analogues, since steric clash between the PPh$_3$ and (dimethylamino)-

carbonyl substituent forces a complete twist of the latter out of the C2-C1-N1 plane
(O1-C3-C2-C1 = 90.6°). Hence, the conjugation between the carbonyl and carbene
fragments is largely cancelled and, for this reason, C2-C3 is longer than expected for
a normal C_{sp^2}-C_{sp^2} single bond and falls better within the range for C_{sp^3}-C_{sp^3} bonds
(entry 7).[103] As a result, the donation of electron density from the ylide carbon to the
carbene is maximised and C1-C2 bond length is only 1.390 Å. These structural data
indicate that in compound **80j** mesomeric structure **III** has less contribution and its
electronic structure should be better described as an intermediate between the carbene
I and phosphonio vinyl-**II** resonance structures. The same bonding situation is observed
for compound **80f** (entry 4), bearing a phenyl group that exhibits the lowest ability to
delocalise electron density among the tested ylides.

The case for 2-pyridyl substituted AAYCs is intermediate and depends on the amine
substituents. Thus, in **80e** (entry 3), even though the C2-C3 is longer than in AAYCs
bearing carbonyl- or cyano- groups, the 2-pyridyl moiety is almost coplanar with the
carbene unit and presents an N2-H1 hydrogen-bond, indicating certain importance of
resonance form **III**. Conversely, the 2-pyridyl moiety of the ylide in compound **80k** is
twisted and, therefore, displays a different bonding situation, similar to **80f** and **80j**
(entry 8).

Remarkably, in **80k** the carbene and the 2-pyridyl moiety attached to N1, are almost
coplanar (C1-N1-C26-C27 = 11.02°), displaying longer C1-N1 and shorter N1-C26 bonds
than **80e** that might indicate partial delocalisation of the N1-lone pair into the aromatic
residue. This could explain the different bonding situation, since the N1-lone pair is
less available to release electron density into the $p_{carbene}$-orbital, increasing the donation
from the ylide carbon. A similar situation is also observed in **80f** (C1-N1-C9-C10
= 0.67°) where the phenyl substituent of the amine is also coplanar with C2-C1-N1,
suggesting an increased contribution of resonance form **II**.

In opposition, modification of the amine substituent from phenyl to 2,6-Me$_2$(C$_6$H$_3$)
in **80a** and **80g** does not lead to significant differences in the bond lengths, even though
the 2,6-Me$_2$(C$_6$H$_3$) unit is more twisted out of the carbene plane due to its steric bulk
(see Appendix B).

In view of these results, it can be concluded that the contribution of the different
resonance structures in AAYC-gold(I) complexes is dependent on the stereoelectronic
nature of the ylide substituents (R_2), whereas the amine substituent (R_1) and the
replacement of the PPh$_3$ by other entities have a lesser impact.

Regarding the steric properties of the AAYC-gold(I) chlorides, due to their acyclic
backbone, the angle of the carbene centre in the AAYCs, C2-C1-N1, is larger than in
the cyclic AYC-complex (**67**)AuCl[20d] and in (IMes)AuCl[104] (angle values are depicted

in ***Table I.3.3***), thus placing the substituents closer to the metal centre compared with already described AYC- and NHC-metal complexes.

Additionally, the $\%V_{bur}$ values were calculated from the X-ray structures of the AAYC-gold(I) complexes, except for **80i** because it presents disorder in the solid state structure.[*] In order to compare to other carbene complexes, the $\%V_{bur}$ was also calculated for the AYC and IMes ligands in (**67**)AuCl[20d] and (IMes)AuCl,[104] complexes, whose X-ray structures were obtained from the corresponding references. The results summarised in ***Table I.3.3*** show that **80** have a larger calculated $\%V_{bur}$ compared to AYC **67**, due to their wider carbene angle, while all presented a greater increase compared with (IMes)AuCl, due to the presence of the bulky PPh$_3$ fragment.

Entry	[Au]	C2-C1-N1	$\%\mathbf{V_{bur}}$
1	(IMes)AuCl	109.30[a]	36.9
2	(**67**)AuCl	103.68	40.0
1	**80a**	117.38	49.0
2	**80d**	116.59	46.1
3	**80e**	117.50	47.5
4	**80f**	115.25	47.4
5	**80g**	117.76	52.6
6	**80i**	117.03	-
7	**80j**	118.84	52.4
8	**80k**	116.20	48.9
9	**84**	117.11	48.3
10	**87**	116.38	38.5
11	**88**	116.41	35.7

Table I.3.3: Carbene angles and $\%V_{bur}$ of (IMes)AuCl, (**67**)AuCl, **80a**, **80d**–**g**, **80i**–**k**, **84**, **87** and **88**. All angles are given in °. [a] N1-C1-N2 angle.

Although the $\%V_{bur}$ values obtained for **80a**–**f** and **84** are similar, AAYC complexes with the bulkier 2,5-dimethylphenyl moiety attached to N1 (**80g** and **80j**) present the expected highest values. Contrarily, the heterocycles in **87** and **88** are smaller than PPh$_3$ or AsPh$_3$ fragments, which translates into a lesser steric congestion of the metal

---

[*]Calculated from CIF files r = 3.5 Å, bond radii scaled by 1.17. Hydrogens were not included in the calculations.[105]

environment and, consequently, in even lower $\%V_{bur}$ values than IMes.

These results highlight that the steric properties of the AAYC-gold(I) complexes can be additionally tuned by the modification of the substituents *syn-* to the gold centre, E and R_1, which affect the steric congestion around the metal drastically when replacing the bulky PPh$_3$ or AsPh$_3$ fragments with the smaller imidazolium and pyridinium moeities.

Due to the arrangement of the substituents, the X-ray structures of the AAYC complexes present additional interactions that deserve to be discussed, summarised in *Table I.3.4*.

Entry	(AAYC)AuCl	H-bonds	Arene-Au1	Other
1	**80a**	O1-H1 = 1.851	C17-Au1 = 3.066	
2	**80d**	N2-H1 = 2.317[a]	C22-Au1 = 3.215	
3	**80e**	N2-H1 = 2.027	C14-Au1 = 3.059	
4	**80f**	-	C21-Au1 = 3.171	C3-H1 = 2.386
5	**80g**	O1-H1 = 1.860	C25-Au1 = 2.964	
6	**80i**	N2-H1 = 2.237[a]	C12-Au1 = 3.305	
7	**80j**	N2-H1 = 2.783	C26-Au1 = 3.045	
8	**80k**	-	C8-Au1 = 3.024	C3-H1 = 2.401
9	**84**	O1-H1 = 1.893	C17-Au1 = 3.165	
10	**87**	O1-H1 = 1.893	-	
11	**88**	O1-H1 = 1.923	-	

Table I.3.4: Hydrogen bonds and short intramolecular contacts found in the X-ray structures of compounds **80a**, **80d**–**g**, **80i**–**k**, **84**, **87** and **88**. All distances are given in Å. [a]The hydrogen bonding is intermolecular.

As previously commented, all the complexes except for **80f**, **80j** and **80k** present intramolecular or intermolecular hydrogen bonding. Nevertheless, in compound **80j** (entry 7), the lone pair of the nitrogen of the amide might interact with the N-H proton since the N2-H distance is 2.783 Å, close to the sum of the van der Waals radii ($\sum r_{vdW}$(N,H) = 2.75 Å). Moreover, compounds **80f** and **80k** present a proton-arene interaction between H1 and the *ipso*-carbon of the aromatic substituent in R_2 (entries 4 and 8, $\sum r_{vdW}$(C,H) = 2.90 Å).[97]

Remarkably, in all the AAYC complexes with PPh$_3$ or AsPh$_3$ fragments an η^1-arene-

Au interaction is observed between the metal centre and the *ipso*-carbon of the closest phenyl ring attached to the P or As atoms (entries 1-9, $\sum r_{vdW}(\text{Au,C}) = 3.36$ Å).[97]

In summary, the analysis of the X-ray structures reveals that the steric properties and resonance contributions in AAYC ligands can be modulated by the modification of the E, R_1 and R_2 substituents of the carbene. The steric congestion around the gold centre can be adjusted by the choice of bulky or small substituents, as demonstrated by the changes in $\%V_{bur}$. Furthermore, the structural variations upon the changes on the substituents prove that the contribution of the different resonance structures can be tuned, which might have implications in the electronic properties of the ligands, and, therefore, in the performance of the gold complexes in catalysis.

I.3.3 Reactivity of AAYC-gold(I) complexes

Once the synthesis and structure of the AAYC-gold(I) complexes was established, we decided to investigate their reactivity and whether they could be further functionalised, exploiting the additional functional groups in the carbene side arm present in most of the prepared compounds.

I.3.3.1 Reactivity with other metal sources

Firstly, we envisaged the possibility of preparing heterobinuclear complexes, that could encounter interesting applications in cooperative bimetallic catalysis.[106] The deprotonation of the N-H unit adjacent to the carbene centre would generate an additional lone pair able to coordinate to a second metal centre, fostered by the formation of a chelate through the additional coordination of the carbonyl group in the carbene's side arm. Thus, treatment of compound **80a** with KOMe and 0.5 equivalents of [{RhCl(cod)}$_2$] afforded **90** in good yield (***Scheme I.3.6***). Furthermore, the procedure could be extended to the synthesis of compounds **91** and **92**, from **87** and **88** respectively, with similar yields.
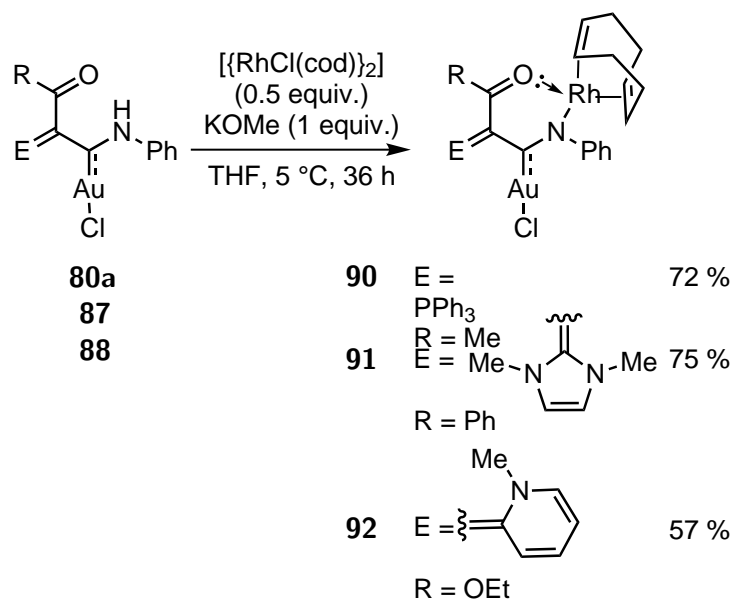
Scheme I.3.6. Synthesis of heterobinuclear complexes from acyclic (amino)-(ylide)carbene gold(I) compounds.

In solution, compounds **90**, **91** and **92** displayed signals in ^{1}H- and ^{13}C-NMR attributable to the cyclooctadiene ligand and to the AAYC fragment, while the distinctive

N-H signal vanished. The connectivity of the bimetallic complex **90** could be further confirmed by X-ray analysis, depicted in **_Figure I.3.9_**, confirming the presence of both Au(I) and Rh(I) centres. The former is linked to the carbene, while the latter is coordinated through the deprotonated nitrogen and the carbonyl group, forming a quasi-planar six membered metallacycle — with torsion angles of (C2-C3-O1-Rh1) = 2.69° and (C2-C1-N1-Rh1) = 1.45° — and causing a widening of the C2-C1-N1 angle. The geometries around both metals are as expected: linear for Au(I) and distorted square-planar for Rh(I). Interestingly, when compared to the starting material **80a**, a shortening of the C2-C3 bond is observed, whereas C2-C1 and C3-O1 bonds are lengthened, indicating that the AAYC fragment in **90** has greater (phosphonioenolate)carbene character.
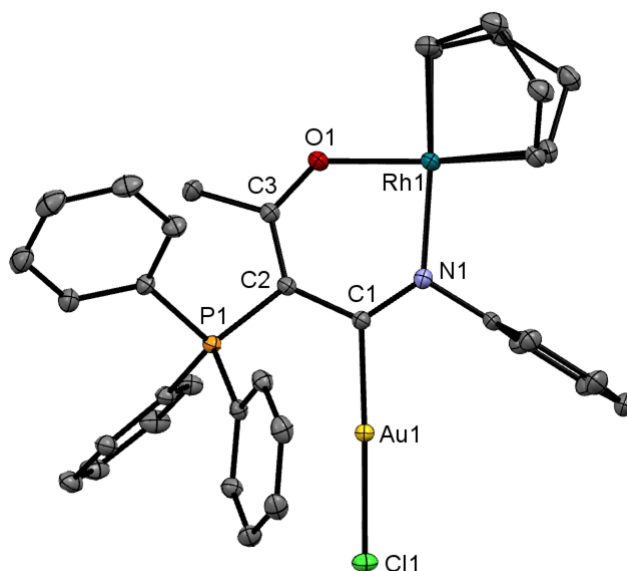

Figure I.3.9. Solid state structure of compound **90**. Hydrogen atoms and solvent molecules have been omitted for clarity. Thermal ellipsoids set at 50 % probability. Selected bond lengths (Å): C1-Au1 = 2.013, Rh1-O1 = 2.051, Rh1-N1 = 2.013, C1-N1 = 1.329, C1-C2 = 1.463, C2-C3 = 1.416, C3-O1 = 1.273, C2-P1 = 1.779. Selected angles (°): C2-C1-N1 = 124.29, N1-Rh1-O1 = 86.82.

Surprisingly, this reaction is strongly influenced by the oxidation state of the metal. Treatment of **80a** with a KOMe and a harder Rh(III) source, $[\{RhCp^*Cl_2\}_2]$, under the same conditions led to an orange solid. Multinuclear NMR analysis again showed the disappearance of the characteristic ^{1}H-NMR N-H signal from **80a**; however, the ^{13}C-NMR resonance attributable to the carbene carbon atom in **80a** was shifted from 200.9 to 185.1 ppm and interestingly, it appeared as a doublet of doublets with $J_{C-Rh} = 3.3$ Hz and $J_{C-P} = 36.2$ Hz. Moreover, MS (ESI) analysis exhibited a molecular ion signal at m/z 694, consistent with the loss of the AuCl fragment. These data suggested a Au(I)→Rh(III) transmetalation and a probable bidentate nature of the carbene ligand

in the product, leading to the formation of compound **93**. The conditions of the reaction could be further optimised, depicted in **Scheme I.3.7**, affording complex **93** in 82 % yield.

Interestingly, under this optimised conditions, similar results were observed upon exposure of **80a** to $[\{Ru(cym)Cl_2\}_2]$, presenting the same ligand-transfer reactivity to afford **94** in 59 % yield.
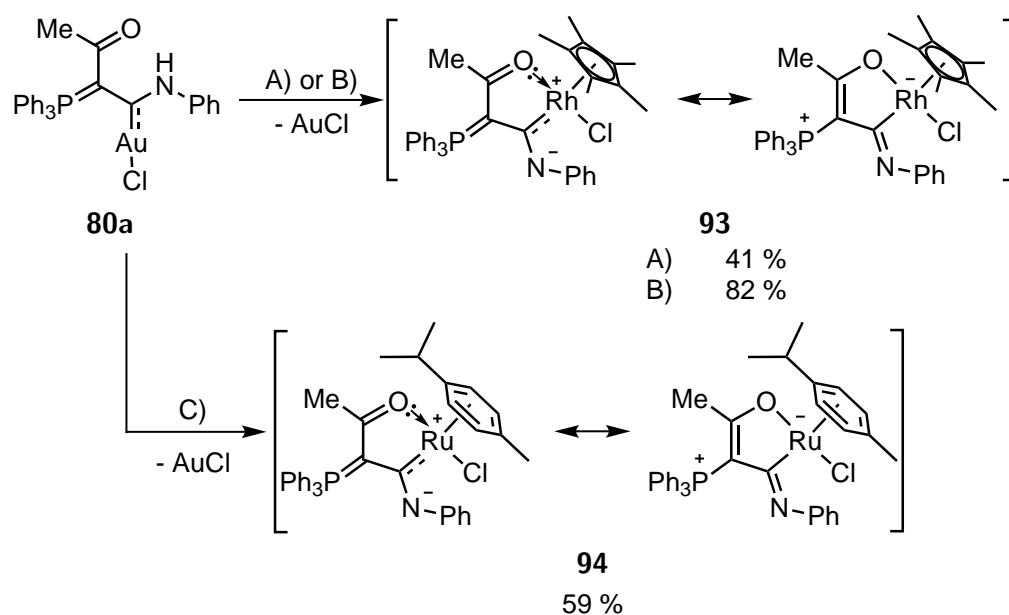
Scheme I.3.7. Synthesis of **93** and **94** by Au(I)→Rh(III) or Au(I)→Ru(II) transmetalation. Conditions A) KOMe (1 equiv.), $[\{RhCp^*Cl_2\}_2]$ (0.5 equiv.), THF, 5 °C, 12 h; Conditions B) $[\{RhCp^*Cl_2\}_2]$ (0.5 equiv.), NEt$_3$ (15 equiv.), DCE, 50 °C, 96 h. Conditions C) $[\{Ru(cym)Cl_2\}_2]$ (0.5 equiv.), NEt$_3$ (15 equiv.), DCE, 50 °C, 96 h.

Crystals suitable for X-ray analysis of **93** and **94** could be grown, confirming their structures, as depicted in **Figure I.3.10** and **Figure I.3.11** respectively. As predicted from the NMR and MS analyses, the AuCl moiety is not present in both complexes. Moreover, the nitrogen atom is deprotonated and the resulting monoanionic ligand coordinates the $[RhCp^*Cl]^+$ or $[Ru(cym)Cl]^+$ fragments in a bidentate fashion through the central carbon atom and the lateral carbonyl group. Both Rh(III) **93** and Ru(II) **94** complexes present the expected piano-stool geometry and, since they are coordinated to four different groups, they are chiral at the metal centre, both enantiomers being observed in the crystal packing. Additionally, the Ru(II)-complex **94** presents two different conformations in the unit cell with similar parameters, depicted in **Figure I.3.11**.
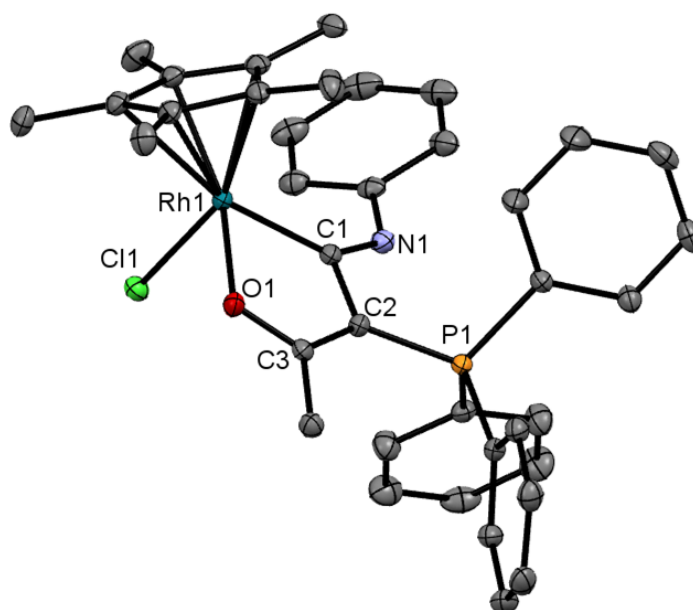
Figure I.3.10. Solid state structure of compound **93**. Hydrogen atoms and solvent molecules have been omitted for clarity. Thermal ellipsoids set at 50 % probability. Selected bond lengths (Å): C1-Rh1 = 2.027, Rh1-O1 = 2.090, C1-N1 = 1.290, C1-C2 = 1.473, C2-C3 = 1.394, C3-O1 = 1.288, C2-P1 = 1.756. Selected angles (°): O1-Rh1-C1 = 80.46.
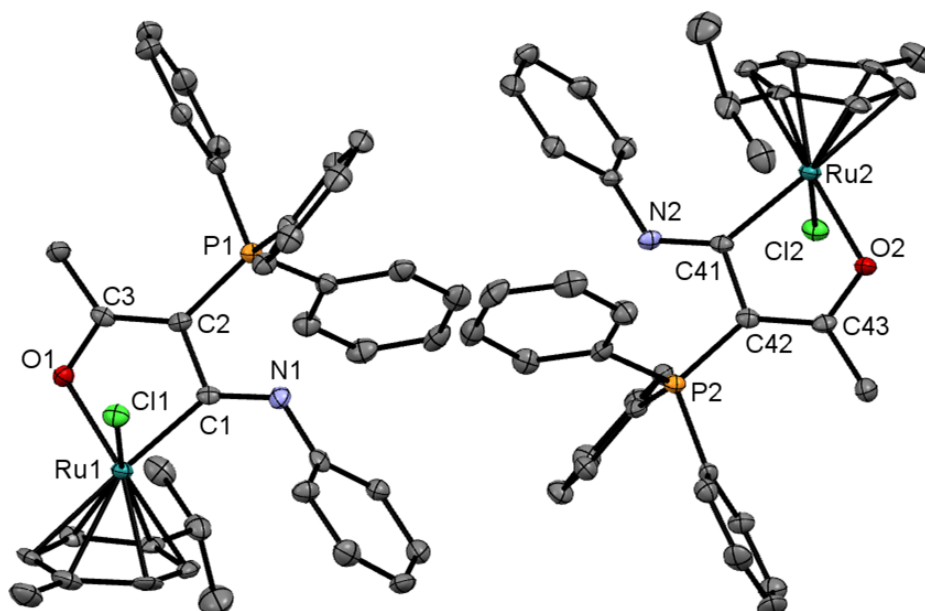

Figure I.3.11. Solid state structure of compound **94**. Hydrogen atoms and solvent molecules have been omitted for clarity. Thermal ellipsoids set at 50 % probability. Selected bond lengths (Å): C1-Ru1 = 2.055, Ru1-O1 = 2.091, C1-N1 = 1.288, C1-C2 = 1.473, C2-C3 = 1.392, C3-O1 = 1.294, C2-P1 = 1.769, Ru2-C41 = 2.047, Ru2-O2 = 2.085, N2-C41 = 1.292, C41-C42 = 1.478, C42-C43 = 1.383, C43-O2 = 1.279, C42-P2 = 1.753. Selected angles (°): O1-Ru1-C1 = 79.13, O2-Ru2-C41 = 78.93.

Similarly to the bimetallic complex **90**, the C2-C3 bond is shorter while C2-C1 and C3-O1 are longer than in **80a**, indicating a greater charge delocalisation on the carbonyl group and more enolate character when the AAYC acts as a bidentate ligand. Although the Rh1-C1 and Ru1-C1 distances fall in the range of metal-carbene bond lengths in related bidentate NHC piano-stool complexes,[107] the C1-N1 bond lengths are very short (1.290 Å and 1.288 Å for **93** and **94** respectively), close to the range of C=N bonds.[103] Because of these structural features, we can describe compounds **93** and **94** as intermediates between two different resonance forms depicted in *Scheme I.3.7*: one bearing an anionic AAYC ligand and another with an (enolate)- η^1-imidoyl structure.

It is important to highlight that examples of Au(I)→Rh(III)[108] and Au(I)→Ru(II)[109] transmetallation are rare in the literature and, due to the stability of the carbene-Au(I) bond, examples of carbene transfer from gold are limited to Au(I)→Pd(II) transmetallation.[110] In our case, the driving force of the transmetallation might be provided by the ability of the deprotonated AAYC ligand to form a chelate with the incoming metal. The difference in reactivity between Rh(I) and Rh(III) and Ru(II) might be explained by the greater electrophilicity of the latter, which prefer to bind to the less electronegative and better electron-donor carbene centre than to the deprotonated nitrogen atom.

Considering that the synthesis of acyclic carbene metal complexes through the classical isocyanide route is limited to Fe(II), Mn(II), Au(I), Pd(II), and Pt(II) isocyanide precursors (see Introduction), the ligand-transfer reactivity would offer access to AAYC complexes with different metals that cannot otherwise be obtained through this developed general synthetic route.

I.3.3.2   Cationic AAYC-gold(I) complexes

As discussed during the Introduction, one strategy to modify the electronic properties of carbene ligands is to install substituents on the carbene backbone. Including electron-withdrawing groups on the carbene decreases the energy of the orbitals involved in the coordination with the metal, σ- and π*-orbitals, reducing the σ-donation ability of the ligand with concomitant increase of the π-acceptor properties. Because positive charges are by definition strong electron-withdrawing groups, introduction of these into the carbene backbone should decrease the overall electron releasing ability of the ligand. This strategy has been rarely applied to modify the properties of NHCs,[111] although some cationic NHC complexes have been prepared, such as **95**[111c] and **96**[111e] in *Figure I.3.12*. Small changes were observed in compound **95** compared to related triazolylidene complexes, however **96** presented increased $\tilde{\nu}_{CO}$(av) values compared with its neutral analogue, indicating the expected decrease in the overall electron-releasing
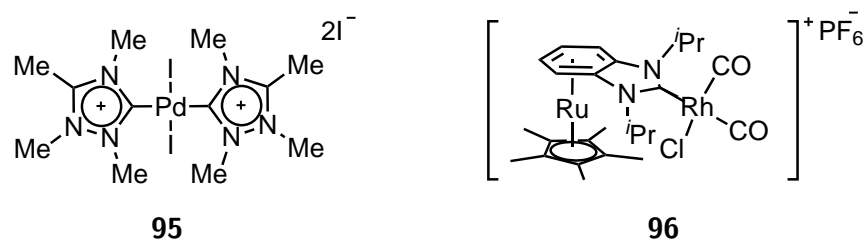
ability of the cationic ligand.

Figure I.3.12. Examples in the literature of cationic NHCs as ligands for transition metal complexes.

Additionally, a positive charge has the effect of increasing the water solubility of the complexes, which could then be applied to catalysis in aqueous or biphasic media, improving the environmental impact, solvent costs and enabling catalyst recycling.[112]

For these reasons, we envisaged the possibility of installing one or two positive charges through methylation of the 2-pyridyl substituted AAYCs **80e** and **80k**. On treatment at low temperature of **80e** with one equivalent of MeOTf, a yellow precipitate was formed, which after purification was identified as the methylated cationic AAYC-gold(I) complex **97**.
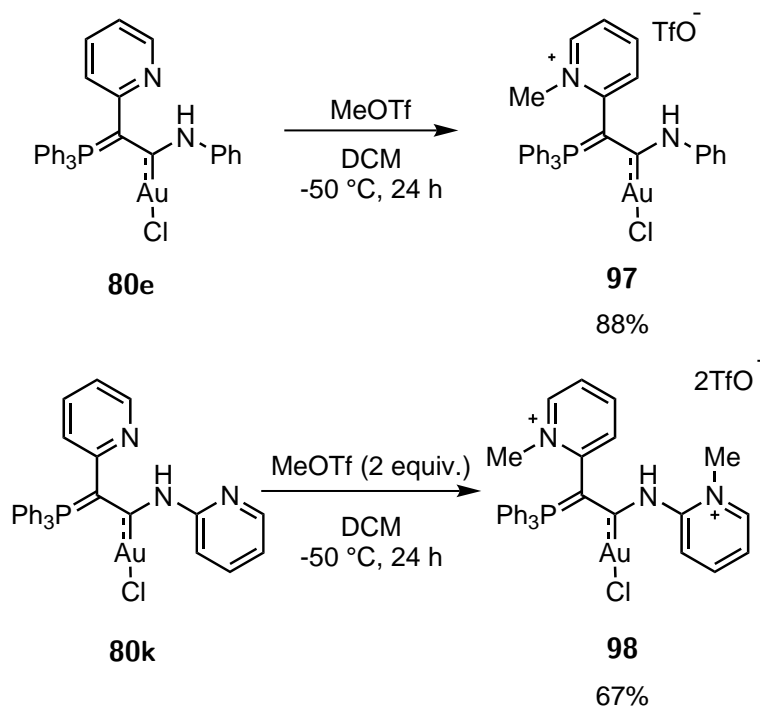
Scheme I.3.8. Synthesis of cationic AAYC gold(I) complexes by methylation of the pyridine moieties.

The methylation product was evidenced by MS (ESI) analysis, displaying a molecular ion signal at m/z 703, and a characteristic singlet in the ^{1}H-NMR spectrum integrating to three protons at 4.28 ppm, consistent with the presence of a methyl group attached to the pyridinium nitrogen. Interestingly, **80k** could be dimethylated under the same conditions employing two equivalents of MeOTf to afford dicationic AAYC complex **98** (***Scheme I.3.8***).

Suitable crystals for X-ray diffraction studies of monocationic compound **97** could be grown, thus confirming the proposed connectivity (***Figure I.3.13***). The geometry around the gold(I) centre is linear, with a slight increase in the C1-Au1 distance compared with the neutral **80e**. Interestingly, the triflate couteranion is located in proximity to the pyridinium and N-H moieties, interacting with the latter through a hydrogen-bond and displaying a short contact, O1-C8 = 3.133 Å, with the methyl group of the pyridinium fragment ($\sum r_{vdW}(O,C) = 3.22$ Å).[97] In the same fashion than all the AAYC-gold complexes with the PPh$_3$ fragment, the solid state structure displays an η^1-arene-Au interaction between the metal centre and one of the *ipso*-carbons of the phenyl rings attached to the phosphorus.
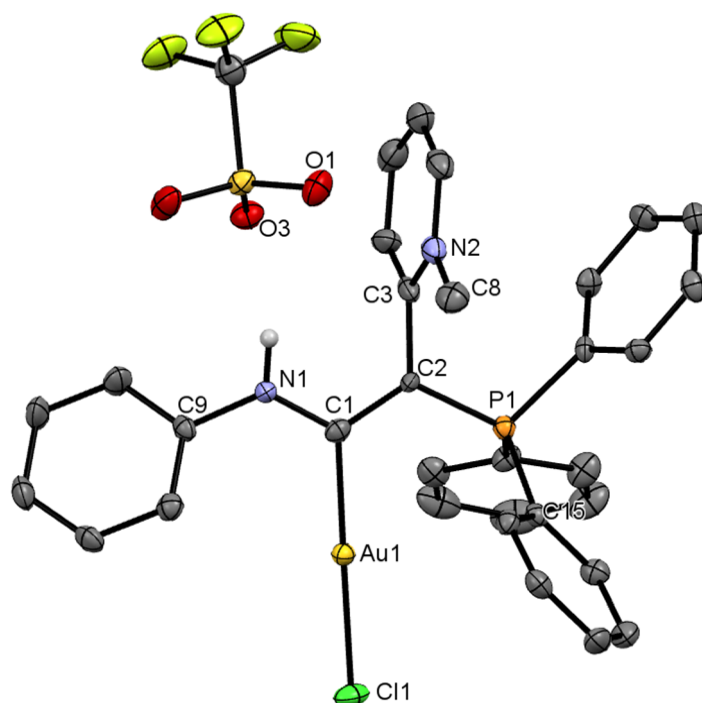

Figure I.3.13. Solid state structure of compound **97**. Hydrogen atoms and solvent molecules have been omitted for clarity. Thermal ellipsoids set at 50 % probability. Selected bond lengths (Å) : C1-Au1 = 2.011, C1-C2 = 1.399, C1-N2 = 1.351, C2-C3 = 1.490, C2-P1 = 1.761. Selected structural features : C2-C1-N2 = 118.20°, H1-C3 = 2.434 Å, Au1-C15 = 3.238 Å, O1-C8 = 3.133 Å, O3-H2 = 2.302 Å.

Compared with the starting material **80e** (***Table I.3.2***, entry 3), the C2-C3 distance is lengthened while the C2-C1 is shortened, indicating a greater donation of electron density from the ylide carbon and less charge delocalisation on the cationic side arm. These differences in the bonding situation between the cationic AAYC **97** and the neutral starting material **80e** are caused by the twist of the 2-pyridinium moiety out from the carbene plane with a torsion angle of (C1-C2-C3-N1) = 103.29°, which could be a consequence of the increased steric hindrance of the methylated substituent. Thus, the bonding situation is similar to the AAYC-gold(I) complexes **80f**, **80j** and **80k**, which display little conjugation with the ylide side arm, indicating that compound **97** is also better described as an intermediate between the carbene **I** and phosphoniovinyl-**II** resonance structures (***Figure I.3.6***). In analogy with compounds **80f** and **80k**, the X-ray structure of **97** presents a proton-arene interaction between C3 and H1.

Unfortunately, the twist of the 2-pyridinium moiety and the subsequent little π-conjugation with the carbene centre, might decrease the effect of the positive charge on the electronic properties of the carbene due to an inefficient overlap between the carbene centre and the cationic residue. Nevertheless, the positive charge still could diminish the energy of the frontier orbitals by inductive effects, conferring to the cationic AAYC complex **97** better π-acceptor and decresead σ-donor properties than its neutral counterpart **80e**.

I.4. Conclusion and Summary

In summary, the synthesis of a new class of carbene-gold(I) complexes has been established, contributing to the large and expanding family of carbene ligands, and their reactivity has been studied.

The synthesis of the unprecedented AAYC-gold(I) complexes was achieved by reaction of gold(I) aromatic isocyanides with stabilised phosphorus or arsenic ylides. In addition, the reaction could be applied with excellent yields to "carbon ylides", such as ene-1,1-diamines and enamines. The synthetic strategy is modular and offers access to a wide variety of gold(I) complexes with different substituents able to modulate the ligand steric properties and resonance contributions, evidenced by the analysis of the solid state structures.

Moreover, the functional groups present on the ligand side arms enabled interesting reactivity, including the formation of bimetallic species and ligand-transfer reactions with appropriate rhodium or ruthenium sources. Additionally, installation of one or two positive charges was also possible by methylation of pyridine substituents.

Whether the mono- and bimetallic complexes described herein will find applications in catalysis would be an exciting topic for future investigation.

Part II

Enantioselective synthesis of hexahelicenes through gold(I)-catalysis employing novel cationic chiral ligands

II.1. Introduction

Helicenes are a class of polycyclic aromatic compounds, defined by consisting of *ortho*-fused benzene or other aromatic rings, forming a non planar screw-shaped structure. Their characteristic shape results from the steric repulsion generated between the overlapping terminal π-systems, leading to a symmetry axis. Because of this, helicenes are inherently chiral, with two possible enantiomers: a (P)-isomer, on which the helix turns counter-clockwise, and an (M)-enantiomer, which turns in the opposite direction (***Figure II.1.1***).

(P) - 99   **(M) - 99**
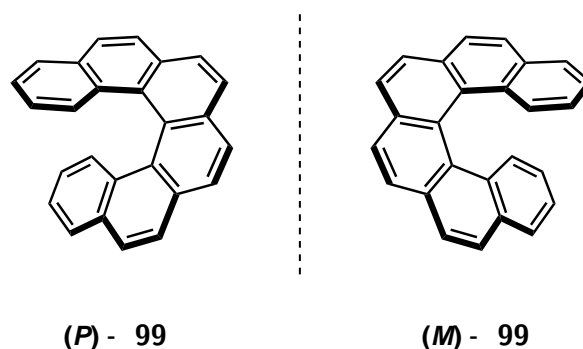
Figure II.1.1. P and M enantiomers of hexahelicene **99**.

In order to simplify the IUPAC nomenclature, the name helicene was introduced by Newman and Lednicer,[113] including a number that indicates the amount of fused aromatic rings. When constructed solely from benzene rings, helicenes are denoted carbohelicenes; when at least one of the constituting rings is a heterocycle, they are defined as heterohelicenes. Other helicene based structures are bihelicenyls, double helicenes and helicenophanes.[29]

Aza-[5]-helicenes **100** and **101** (***Figure II.1.2***) were the first helicenes synthesised by Meisenheimer *et al.* in 1903,[114] followed by tetrahelicene **102** (1913) and pentahelicene **103** (1918). It was not until the late 1940's that interest on helicenes was intensified, with the first reported X-ray structure (tetrahelicene **102**), allowing their distorted structure to be studied for the first time.[115] Furthermore, the crystallisation of salts prepared from tetrahelicenes and pentahelicenes bearing carboxylic acid moieties,

such as **104**, and chiral alkaloids, afforded diasteromeric salts, proving the presence of two different helicene enantiomers. Nevertheless, these initial resolutions failed to isolate the enantiomers due to their low racemisation barrier at room temperature.[116] It was not until 1955 and 1956 that Martin and co-workers were able to synthesise for the first time hexahelicene **99** and resolve the two enantiomers through the formation of a charge-transfer complex with TAPA **105**. (*P*)-**99** crystallised preferentially with (*S*)-TAPA, enabling the isolation of pure (*P*)-**99**, which proved to be stable towards racemisation at room temperature.[113,117] This encouraged other researchers to pursue the synthesis of different helicenes, heterohelicenes and helicene based structures and further study their properties.
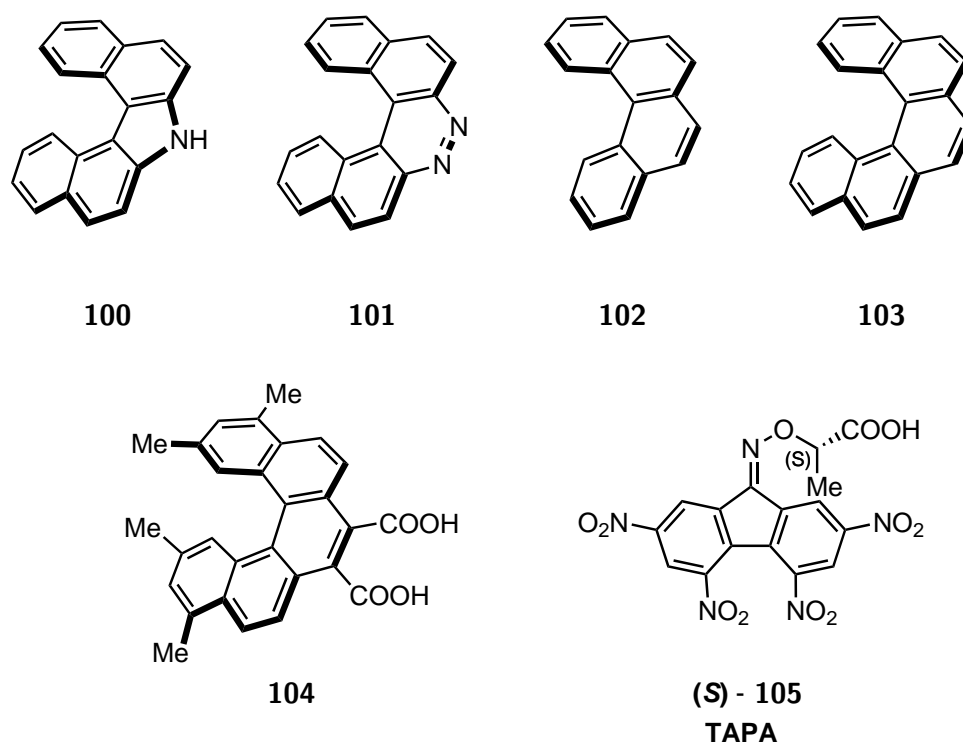

Figure II.1.2. Relevant compounds in the early chemistry of helicenes.

Although the steric hindrance between the two peripheral aromatic rings is large, the backbone of helicenes is rather flexible and the racemisation barrier is lower than expected. Thus, in order for the enantiomers to be stable at room temperature, they should be formed by at least six rings, if based on six-membered rings, and seven, when the monomeric unit is a five-membered ring, although substituents in the internal positions of the helix may alter the racemisation barrier.[118] Even larger helicenes can racemise upon heating, requiring more energy with an increasing number of rings.[119]

Helicenes are fascinating chemical structures, and, since their chirality was proven,

many studies have revealed their compelling properties and have already demonstrated a variety of applications.

II.1.1   Properties and applications of helicenes

In general, the properties of helicenes are a consequence of their distorted conjugated π-system, inherent chirality and ability to interact through non-convalent interactions with themselves and other molecules. This unique combination of properties has led to the application of helicenes in fields as diverse as asymmetric catalysis, molecular recognition, material science, molecular electronics and photonics, supramolecular chemistry and surface chemistry.[30]

Like other polyaromatic hydrocarbons, helicenes are less aromatic than benzene, since not all the aromatic rings can harbour a π-electron sextet. Moreover, calculations have shown that they are just slightly less aromatic than their linear analogues, phenacenes, due to their twist along the helix. In a similar fashion to phenacenes, there is an alternation of the local aromaticity with an overall decrease from the most aromatic terminal rings to the least aromatic inner ones.[120]

Due to their large π-conjugated system, the HOMO-LUMO gap of helicenes is small. Moreover, calculations for carbohelicenes larger than hexahelicene showed that the overlap of parallel rings destabilises the HOMO and stabilises the LUMO, thus leading to a further decreased gap with increasing number of annulated rings.[121] A reduced HOMO-LUMO gap facilitates the electron excitation, rendering some helicenes semiconductors and fluorescent materials. Because of this, helicenes have been employed to manufacture organic transistors,[122] OLEDs[123] and also dye-sensitised solar cells.[124]

(*M*)- 106   **(*M*)- 107**
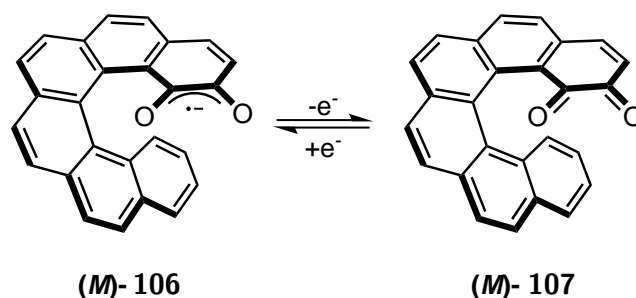
Scheme II.1.1. Chiroptical switch based on a carbohelicene backbone.

Possibly, one of the most interesting properties of helicenes is their optical activity. Enantiomerically pure samples have large specific rotation values and the sign can be used to determine the absolute configuration of the helicene: when irradiated with 589

nm light, (P)-helicenes are consistently dextrorotatory, whereas (M)-enantiomers are levorotatory. Their circular dichroism (CD) spectra show two characteristic bands with very high absorptions, which change upon the number of rings and substituents.[125] Since small changes on the molecule are translated to large effects on the CD spectrum, helicenes have been exploited as chiroptical molecular switches.[126] One recent example is depicted in *Scheme II.1.1*, in which the different oxidation states, semiquinone radical anion **106** and quinone **107**, were found to display large differences in the CD spectra at 357 nm.[127] The potential applications of chiroptical switches include acting as molecular memory elements in data storage, molecular motors, molecular recognition, sensors and asymmetric catalysis with switchable stereoselectivity.[128]

Helicenes contain wide and polarizable π-systems that can interact though non-covalent interactions between themselves or other molecules. In the case of helicenes, more stable charge-transfer complexes can be formed preferentially between one enantiomer of the helicene and another enantiomer of a chiral molecule, leading to chiral recognition. One example of the latter is the charge-transfer complex formed between hexahelicene **99** and TAPA **105**, which helped to resolved for the first time hexahelicene. Furthermore, helicenes have been employed as molecular recognition systems, for instance, in the enantioselective extraction of chiral amines and as fluorescence sensors of chiral amines and amino-alcohols (*Figure II.1.3*, diol **108**).[129] Another relevant example is the ability of thiahelicenes to bind and stabilise Z-DNA[130] (**109**) and G-quadruplex DNA structures, which resulted in the latter case with the inhibition of telomerase with a potential application in cancer therapy (**110**).[131] Other enantiomerically pure (P)-carbohelicenes, such as the amine-tethered tetrahelicene **111**, have also exhibited interactions with DNA, stronger than ethidium bromide, a commonly used fluorescent tag for nucleic acids.[132]

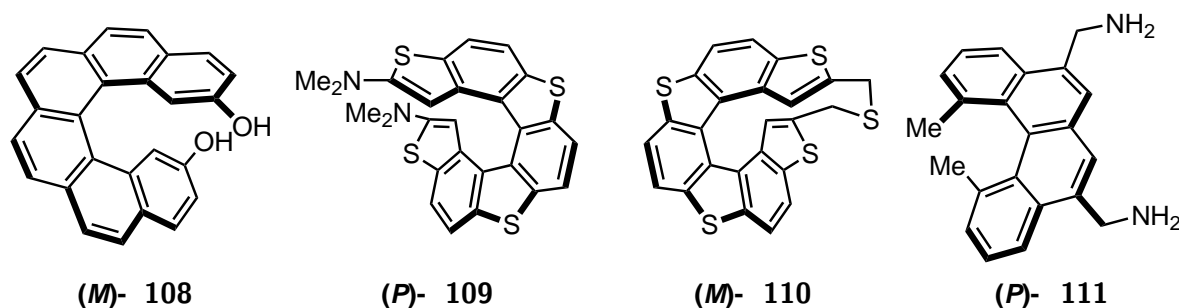**(M)- 108**   **(P)- 109**   **(M)- 110**   **(P)- 111**

Figure II.1.3. Examples of helicenes applied in molecular recognition chemistry.

Their ability to interact with diverse molecules and stabilise certain conformations leading to enantio-induction, renders helicenes as perfect candidates as ligands in enan-

tioselective catalysis. Many transition metal complexes of helicenes have been prepared, either by direct coordination to the π- system or through functional groups pendant to the helix.[133] An early example was published by Reetz and co-workers, who synthesised and resolved the ligand PHelix **112**. Although this ligand afforded low enantioselectivity in Rh(I)-catalysed hydrogenation, it rendered high %*ee* in the kinetic resolution of the Pd-catalysed allylic substitution presented in **Scheme II.1.2**.[134] Since then, more reports of successful enantioselective transition metal-catalysed processes employing helicene-based ligands have been published, using bihelicenyls,[135] oxahelicene,[136] phosphahelicene[137] and helical-cyclopentadiene scaffolds.[138] Moreover, helicenes have been also used as chiral additives,[139] as chiral auxiliaries[140] and as organocatalysts[141] in asymmetric transformations.
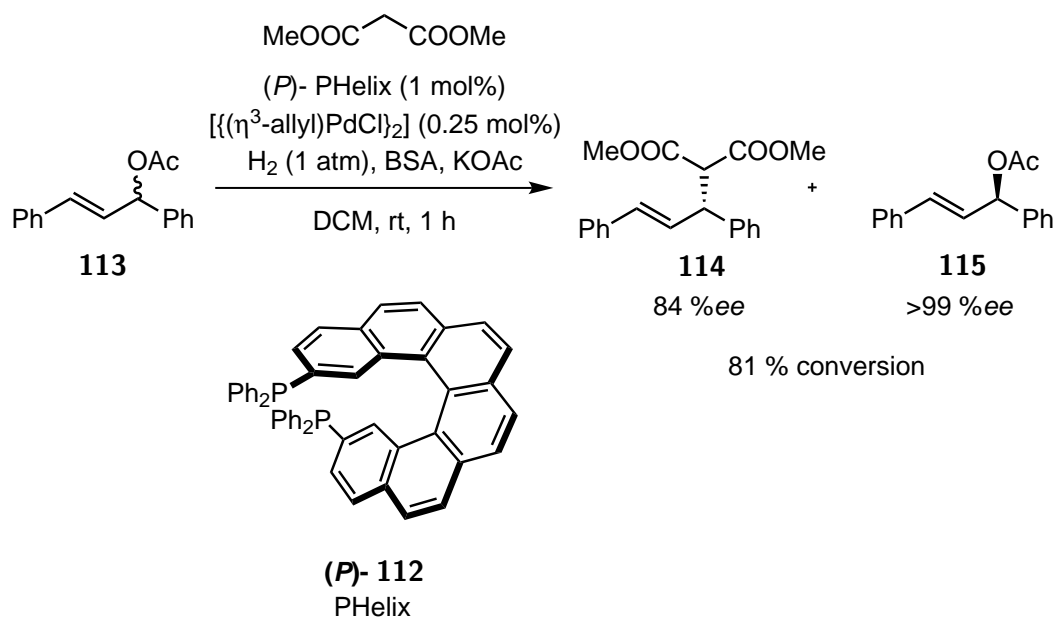
Scheme II.1.2. Kinetic resolution of allyl acetates mediated by Pd and (P)-PHelix ligand.

As previously mentioned, helicenes can interact with themselves through non-covalent interactions, such as π-π interactions and hydrogen-bonding. As a result, in the early chemistry of helicenes, different enantiomers could be separated by crystal picking, due to a strong tendency of some helicenes to crystallise in enantiomerically pure crystals.[142] Additionally, these interactions can stabilise aggregates, in the solid state or in an appropriate solvent, forming molecular assemblies and higher macromolecular structures that could be applied to the synthesis of advanced materials with enhanced electronic and optical properties. The structures thus formed, often depend on the functional groups present on the helicene and its enantiopurity.

Pioneers on this field are Katz and co-workers, who explored thoroughly the properties of enantiopure helicene bisquinone **116** (***Figure II.1.4***). This compound can stack in columnar arrangements, on which all the chiral axes are parallel. These lamellae pack hexagonally, generating aggregates in alkane solutions and large fibrous chiral macrostructures in the case of the enantiopure material (***Figure II.1.5***), both displaying increased optical rotation and more intense responses in the CD spectra.[143,144] Additionally, it was possible to form Langmuir-Blodgett films with similar enhanced properties that, due to their inherent chirality, displayed a large non-linear optical response, indicating a potential application in optical materials.[145]

(P) - **116**   **(P)** - **117**
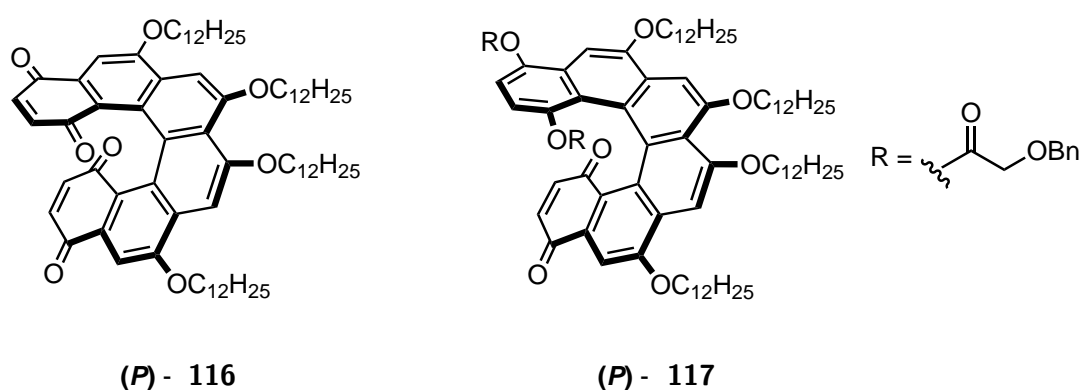
Figure II.1.4. Helicenes reported by Katz and co-workers, which form chiral fibres (**116**) and liquid crystals (**117**).
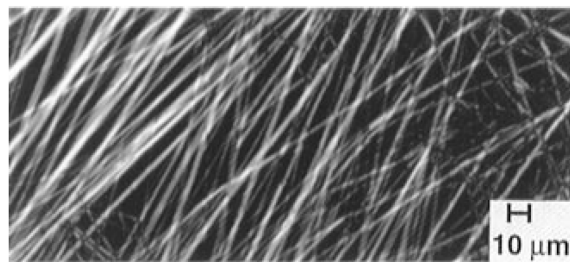
Figure II.1.5. Fibres formed by bisquinone **116** after cooling the isotropically pure liquid helicene from 195 °C to room temperature.[143]

Moreover, the derivative **117** (***Figure II.1.4***) represented the first reported example of chiral helical columnar liquid crystal, showing additionally when mixed with a similar derivative and/or dodecane, an electro-optical and electro-modulated non-linear optical response.[146] Since then, more attention has been paid to helicenes in this field and other helicene-based molecules with self-assembly properties have been reported.[147]

Remarkably, helicenes can self-assemble when interacting with solid surfaces, such as metals or insulators, thus forming ordered layers with a morphology dependant on

the helicene's functional groups and the surface employed.[148]

Enantiopure helicenes are able to transfer their chirality to form chiral surfaces, with potential applications on the study of molecular recognition, asymmetric heterogeneous catalysis and chiral liquid chromatography.[149] Moreover, racemates can arrange forming separated enantiomorphous domains, generated by different spatial interactions between the (M)- and (P)-isomer aggregates, leading to separated chiral domains.[150]

This is the case for the adsorption of heptahelicene on Cu(111) (**Figure II.1.6**), that additionally exhibited a chiral amplification phenomenon, since a small enantiomeric excess (%ee = 0.08) could stabilise preferentially one chiral domain, forming an homogeneous chiral layer.[151] In some cases, upon adsorption on a determined surface, the two-dimensional separation of racemates can be achieved, since the (M)- and (P)-isomers arrange on the surface separately, preferentially forming homochiral domains.[152]
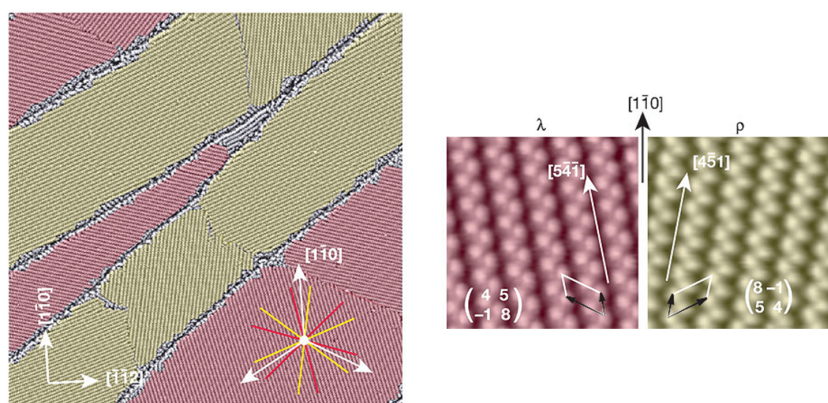
Figure II.1.6. STM images showing the enantiomorphous domains of racemic heptahelicene on Cu(111).[151]

As it might be expected, in order to confer ordered structures and transfer the unique properties of helicenes to materials, many helicene-based oligomers,[153] polymers and copolymers have been synthesised.[154] Although exceptions have been found,[155, 156] the synthesis of the polymers employs the already constructed helicene monomers. Among the interesting obtained results, oligomers which self-assemble,[157] a conducting ladder-thiohelicene polymer,[155] a cobaltocene oligomer with optical activity[158] as well as other polymers with chiroptical properties have been reported.[159]

Although enantiopurity is a prerequisite for most of the applications of helicenes mentioned above, the syntheses of the desired compounds often consists of a sequence towards the racemic helicene and the subsequent resolution of the racemate by chiral HPLC,[122,127,129,134,141,148c, 149] enzymatic resolution,[130,131] formation of dias-

teromeric crystals with a chiral amine,[132,147d 153,157] or with the help of a chiral auxiliary.[135,143,145,146,147a,147c,147e, 159] Few of the examples given in this section rely on a diasteroselective synthesis of the helicene[136,137,158] and just one on an enantioselective transformation,[147f] revealing the scarcity of reliable and versatile enantioselective methods to obtain helicenes. Therefore, it is highly relevant to develop new enantioselective reactions leading to this important class of compounds, to selectively access the desired enantiomer and avoid costly separation methods.

In the next section, a short summary of the reactions leading to helicenes will be given, highlighting the successful enantioselective transformations reported to date.[160]

II.1.2   Synthesis of helicenes

The first reported general method to obtain helicenes was the oxidative photocyclisation/dehydrogenation of stilbenes,[161] introduced in helicene chemistry in 1967 almost simultaneously by the Scholtz[162] and Martin[163] research groups. The latter reported the synthesis of heptahelicene **119** depicted in *Scheme II.1.3* from the stilbene **118** in the presence of light and iodine. Although only the *cis*-isomer leads to the helicene, mixtures of isomers can be employed because *cis-/trans-* isomers are in rapid equilibrium during the irradiation, rendering the necessary substrate easier to prepare.

118   *rac* - **119**

66 %
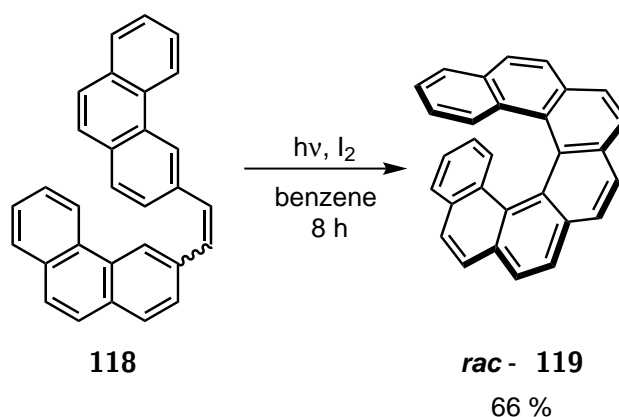
Scheme II.1.3. Synthesis of heptahelicene **119** by oxidative photocyclisation/dehydrogenation.

This reaction has been extensively studied and a wide variety of carbo- and heterohelicenes with different substitution patterns have been successfully prepared with this method.[129–131,134,141d,147b, 164] It is also possible to perform several cyclisations in one pot, thus obtaining longer helicenes; and so far, it is the only route to analogues with more than 11 fused rings, the largest reported to date, [16]-helicene, having been

published recently by Fujita and co-workers.[165]

Although this method is general and convenient, high dilutions are needed in order to prevent dimerisations by [2+2] cycloaddition, making this procedure unpractical for large scale synthesis. Additionally, the reaction requires the appropiate selection of the substrate to avoid side-reactions and few asymmetric photocyclisation/dehydrogenation reactions leading to chiral helicenes have been reported.

Kagan *et al.* proved that it is possible to induce a small enantiomeric excess in the synthesis of hexahelicene **99** when irradiating **120** with left-handed circularly-polarised light (***Scheme II.1.4***). The obtained hexahelicene **99** exhibited a small positive specific rotation value, indicating a slight excess of the (P)-isomer, and the opposite value was observed when irradiating with right-handed circularly-polarised light.[166]

$$\text{120} \qquad \qquad \text{99}$$

25 %, 0.2 %*ee*

$[\alpha]^{23}_{436} = + 30.5 \ (c = 0.77, \text{CHCl}_3)$
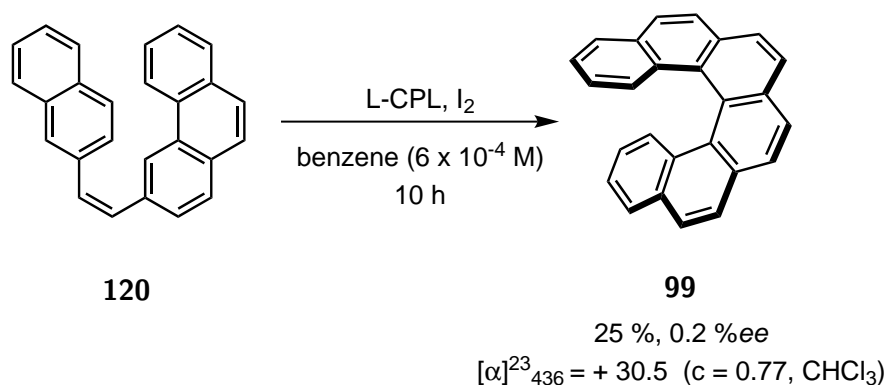
Scheme II.1.4. Synthesis of heptahelicene **119** by oxidative photocyclodehydrogenation.

In that time, the Kagan, Martin and Buchhart research groups found that the observed enantioselectivity was due to the preferential excitation of one enantiomeric conformation of the *cis*-stilbene substrate, affording better results for those substrates with more steric hindrance that partially restricted the rotation of the aryl groups.[167] Although higher specific rotations could be obtained for octahelicene and nonahelicene,[168] all the cases studied afforded poor enantioselectivities, with 2 %*ee* as the best result.

Better results have been obtained by several diasteroselective photocyclodehydrogenations employing stilbenes with chiral substituents on the aromatic fragments[137b, 169] or through the utilisation of substrates with an already enantiopure hexahelicene unit.[170] One representative example is the diasteroselective oxidative photocyclodehydrogenation of **121** with two chiral centres, presented in ***Scheme II.1.5***, introduced through the asymmetric reduction of the corresponding ketone. Employing an enantiopure substrate **121**, just one diastaromer of **122** was obtained.

The observed diasteroselectivity is likely due to the steric hindrance that would be

generated in the (P)-isomer between the -OTBS substituents, which would be pointing to the inner part of the helix. The cyclisation product **122**, after some functional group transformations, afforded nonahelicene (M)-**123** (**Scheme II.1.5**) that could be used to prepare interesting cobaltocene oligomers mentioned in the previous section, by consecutive coordination of the cobalt centres to the cyclopentadiene fragment of two different helicene molecules.[158]
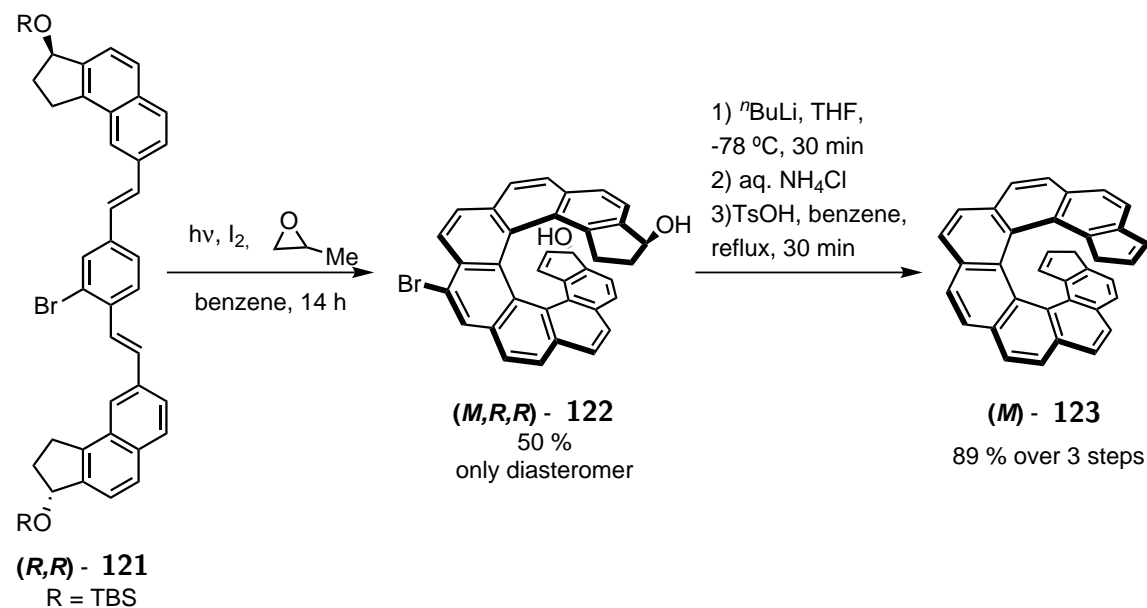

Scheme II.1.5. Synthesis of **123** by asymmetric oxidative photocyclodehydrogenation.

The next breakthrough in helicene synthesis was reported by Katz and co-workers, who were able for the first time to synthesise helicenes in gram-scale through a double Diels-Alder reaction using 1,4-divinylbenzene **124** as the diene and benzoquinone as the dienophile, followed by an oxidation by the excess of bezoquinone to afford helicenebisquinone **125**.[171] As shown in **Scheme II.1.6**, the initially reported yields were poor, but they could be improved by introducing electron-donating substituents in the diene to increase its electron density and promote the cycloaddition, as for example the naphthyl enol ether **126** which afforded **127** in 56 % yield.[172] Bisquinone **127**, after several transformations and resolution, afforded (P)- **116**.[144b]

The possibility of obtaining larger quantities of helicenes provided the Katz group with the opportunity to study their properties in more detail and pursue potential applications. Thus, helicene bisquinone **116**, its derivatives and similar compounds were exhaustively studied culminating in the fascinating results summarised in the previous section.
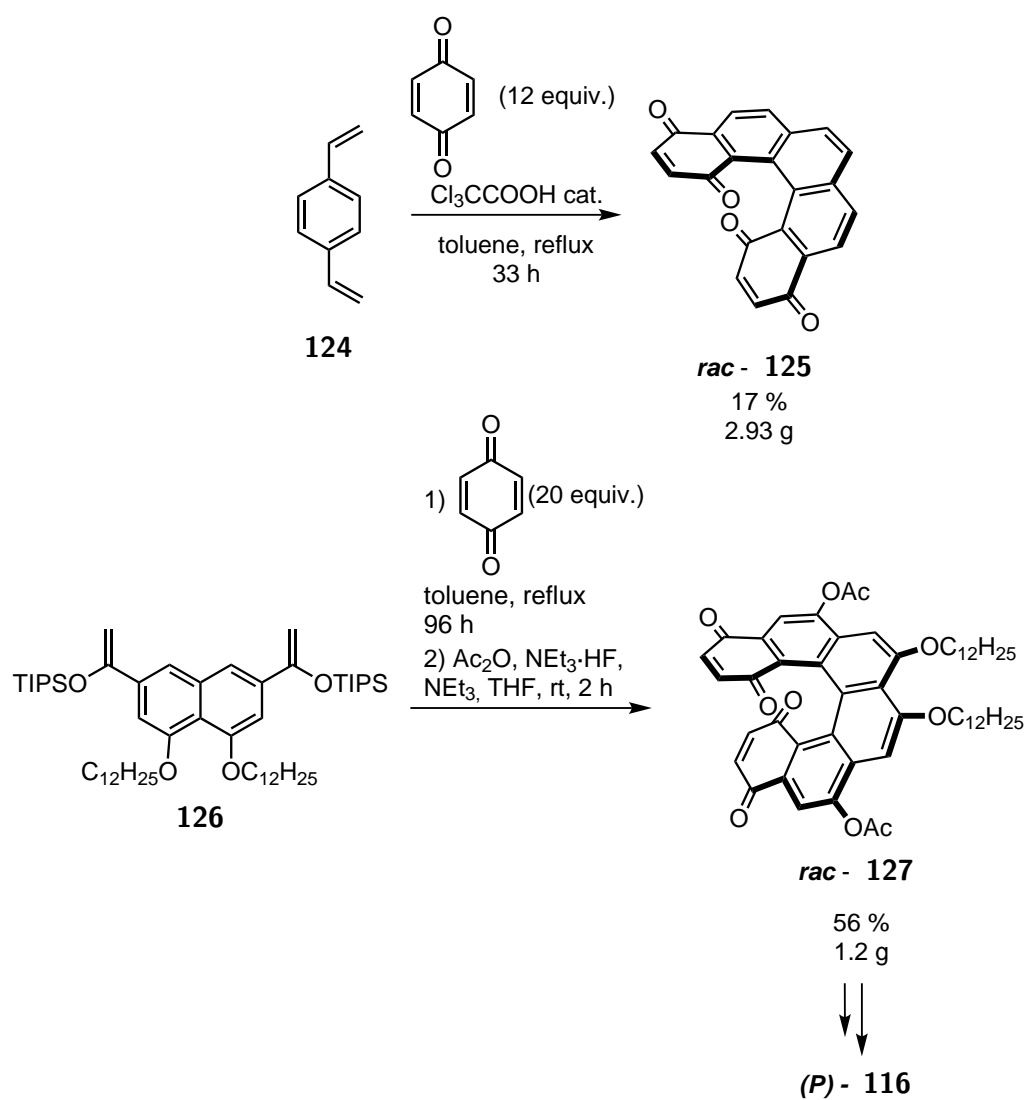
Scheme II.1.6. Diels-Alder reaction leading to helicene bisquinones developed by the Katz group.
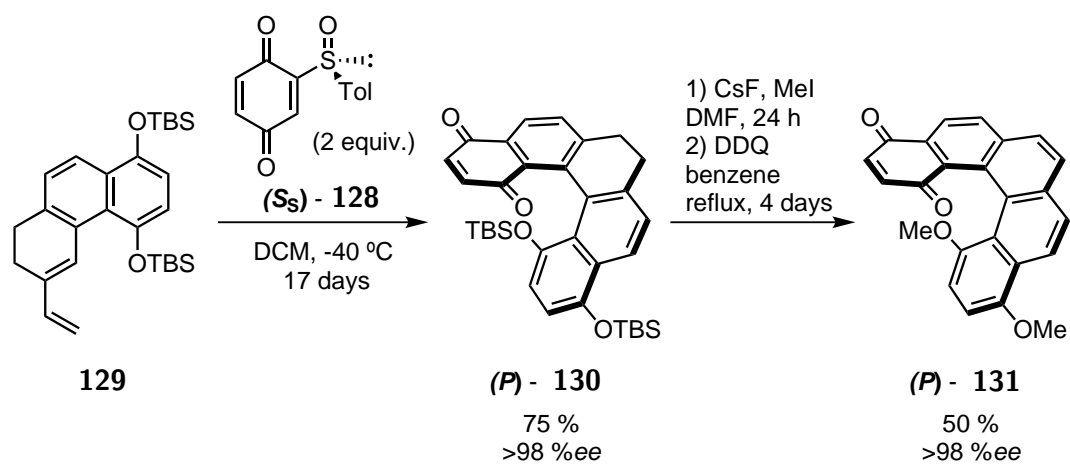
Scheme II.1.7. Enantioselective Diels-Alder strategy developed by Carreño, Urbano and co-workers.

Later, the Carreño and Urbano research groups developed a diasteroselective version of this methodology, employing the enantiopure (S_S)-2-*p*-tolylsulfinylquinone **128**. As presented in ***Scheme II.1.7***, the reaction between the diene **129** and **128** affords the hydropentahelicene quinone (*P*)-**130** under mild conditions with good yield and excellent enantioselecivity, albeit with long reaction times. The transformation consists of a domino Diels-Alder and elimination of *p*-toluenesulfenic acid process followed by the aromatisation of the newly formed 1,4-cyclohexadiene ring by oxidation with the excess of quinone. In the case depicted in ***Scheme II.1.7***, a non-aromatic diene **129** was employed in order to promote the Diels-Alder cycloaddition.[173]

Due to secondary orbital interactions between the diene and the quinone, both reagents aproach in an *endo*- transition state, which controls the enantioselectivity through the steric repulsion between the bulky -OTBS of **129** and tolyl group present on **128**, promoting the approach only through the less hindered side of the chiral sulfoxide, opposite to the tolyl substituent. Additionally, the conformation adopted by the sulfoxide **128** during the cycloaddition, depicted in ***Scheme II.1.7***, is caused by steric repulsion between the oxygen and the inner -OTBS group. Compound (*P*)-**130** could be aromatised with DDQ to the configurationally stable helicenequinone (*P*)-**131** without the loss of enantioselectivity.

Remarkably, this strategy could be extended to the synthesis of a variety of configurationally stable helicene quinones with tetra-, penta- and heptahelicene backbones with good yields and enantioselectivities.[174]

Nevertheless, the variety of chiral helicenes that can be prepared through this methodology is limited, since electron donating substituents are required in order to promote the Diels-Alder reaction and few dienophiles besides benzoquinone have been tested. Moreover, the synthesis of helicenes longer than heptahelicenes using this methodology has not been reported. In addition, two equivalents of a chiral reagent — whose chiral centre is afterwards eliminated — are used to obtain the desired chiral helicenes and an additional oxidation step is necessary afterwards to obtain the conjugated helicenes.

Other reactions have been employed to close six-membered rings to afford helicenes, including Friedel-Crafts type reactions,[116, 113, 175] radical cyclisations[176] and benzylic type couplings,[177] but they are less general and enantioselective versions have not been described.

Heterohelicenes are usually constructed through the formation of one or more benzene rings and, therefore, most of the reactions described during this section can be applied for both carbo- and heterohelicenes, employing heteroatom-containing substrates for the synthesis of the latter.

II.1.2.1   Transition metal catalysed methods

It was not until the late 1990's when transition metal catalysis was applied to the synthesis of helicenes. A general and widely utilised catalytic method, introduced by the Starý and Stará research group, consists in the [2+2+2] cycloisomerisation of triynes catalysed by cobalt(II), rhodium(I) or nickel(0). In their first publications, several substrates similar to **132**, with different substituents on the alkyne and a variety of linkers between the alkyne and the aromatic unit, were studied in the cobalt-catalysed cycloisomerisation, affording the corresponding tetrahydro-[5]-, -[6]- and -[7]-helicenes in yields ranging from poor to excellent, depending on the substitution pattern.[178] Following the reported standard procedure, racemic tetrahydrohexahelicene **133** was obtained from **132** with good yield (***Scheme II.1.8***).

Furthermore, when the cycloisomerisation was carried with [Ni(cod)$_2$] in the presence of the chiral phosphine (*S*)-MOP, a moderate enantiomeric excess was obtained (48 %*ee*), constituting the first example in the literature of a enantioselective catalytic transformation leading to helicenes. More recently optimised conditions for this reaction have been reported, using (*S*)-NAPHEP as ligand instead, but the highest value obtained was 64 %*ee*.[179]
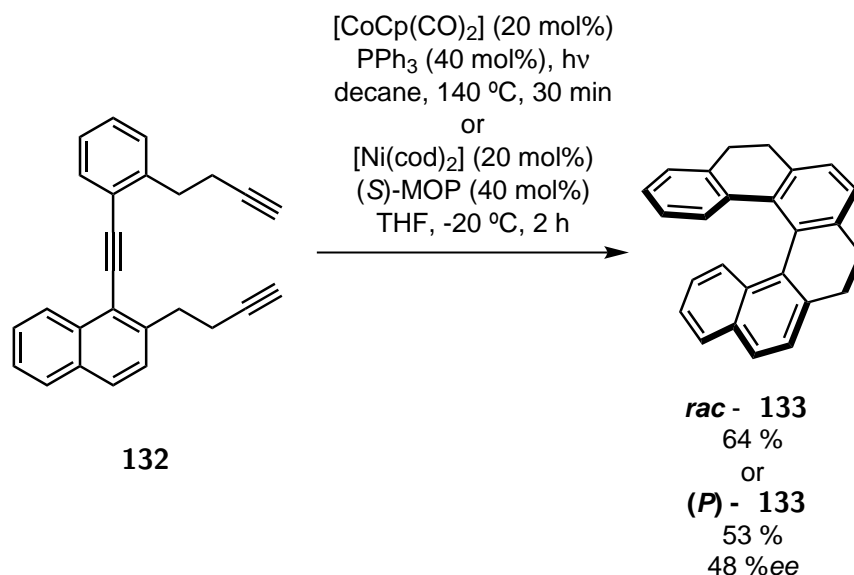
Scheme II.1.8. Ni- or Co-catalysed [2+2+2] cycloisomerisation of triynes leading to tetrahydro-[6]-helicene **133**.

Fully conjugated helicenes could be obtained by oxidation of the corresponding tetrahydrohelicenes or directly through a similar procedure employing aromatic *cis,cis*-dienetriynes as substrates, with nickel exhibiting a better performance in this case for

the cycloisomerisation.[180]

After this seminal work, a wide variety of carbohelicenes and heterohelicenes have been prepared through this route, proving its generality.[127,148b,148c,181] Furthermore, this method enables the synthesis of long helicenes, up to [11]-helicene.[182]

Additionally, central chirality could be transferred efficiently to helical chirality when substrates with one or two chiral centres were used, such as **134**[183] and **136**, facilitating the access to a variety of optically pure non-conjugated helical molecules, such as **135** and **137**, with five to seven fused rings. The latter could then be transformed to the corresponding helicene **138** by acid-promoted elimination of the -OMOM substituents, which had induced the diasteroselectivity of the cyclisation.
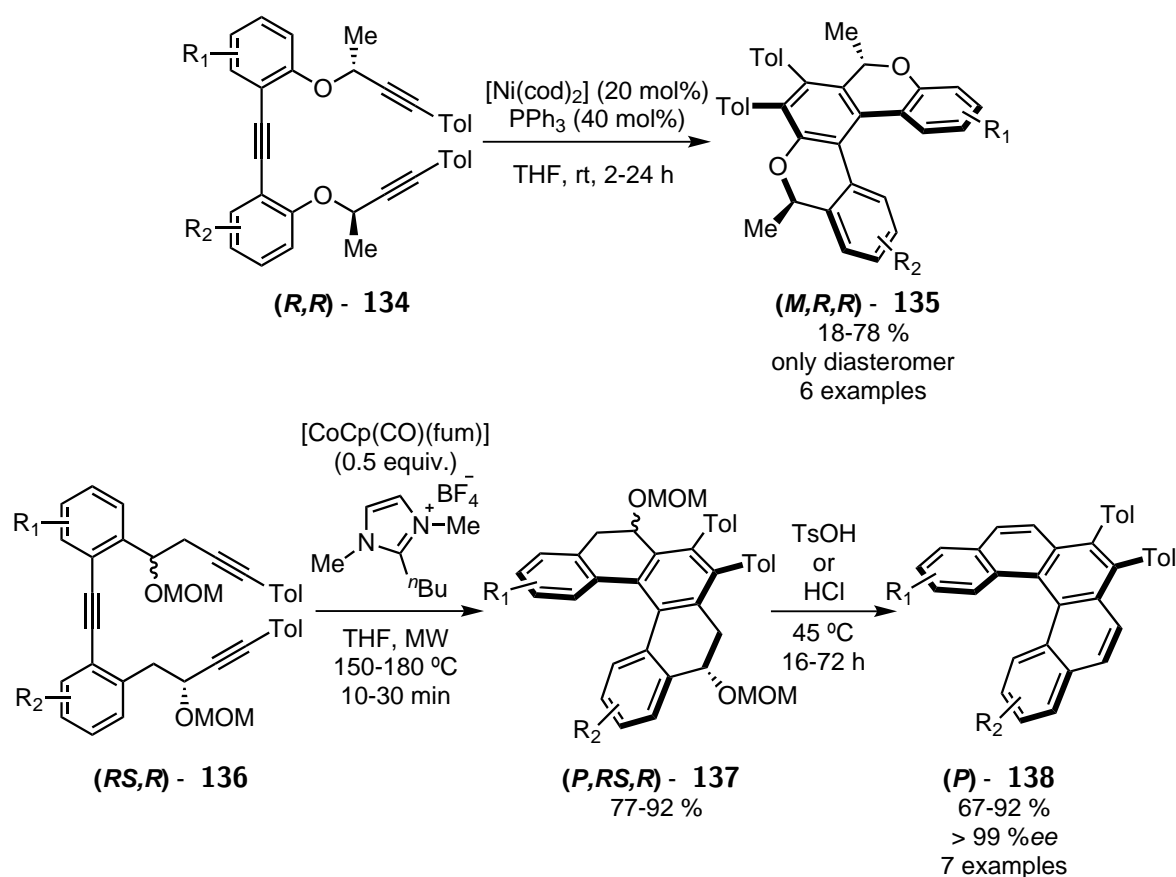
Scheme II.1.9. Diasteroselective synthesis of helicenes by nickel- or cobalt-catalysed [2+2+2] cycloaddition.

Both reactions rely on the greater thermodynamic stability of one diasteromer of **135** and **137**, caused by the steric repulsion between the chiral -Me or -OMOM groups and the tolyl substituents attached to the central aromatic ring. In the case of the nickel-catalysed reaction, probably kinetic stereocontrol favours the more stable

product, however, in the case of the cobalt, high temperatures are needed in order to achieve a post-cyclisation thermodynamic equilibration through racemisation of the helix, favouring the more stable diasteromer.

Besides the examples presented above, other heterohelicenes with different scaffolds could be synthesised diasteroselectively employing a similar strategy.[136,137c,184] Nevertheless, this methodology requires the introduction of a chiral group on the substrate that is not always trivial and, in order to obtain the fully conjugated helicenes, it is necessary to remove it by an additional transformation.

An enantioselective transformation circumvents these problems, but less progress has been made in that direction. In the case of unfunctionalised carbohelicenes, as previously mentioned, moderate enantioselectivities in the synthesis of tetrahydrohexahelicene **133** were achieved. Contrarily, dibenzohexahelicene **140** could be obtained in good yield and good enantiomeric excess through the Ni-catalysed cycloisomerisation of the triyne **139**, employing (R)-QUINAP as ligand (**Scheme II.1.10**).[185]
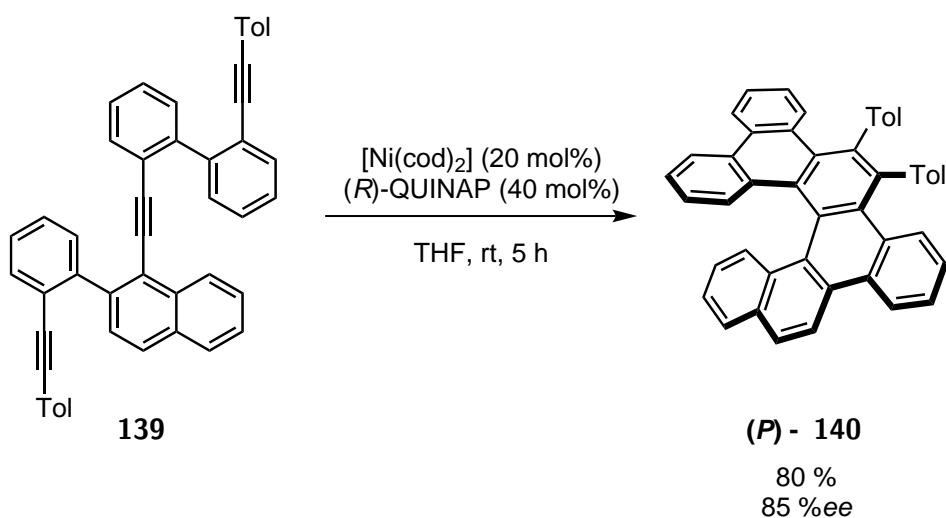
Scheme II.1.10. Enantioselective [2+2+2] cycloisomerisation leading to benzohelicene **140**.

Tanaka and co-workers reported an enantioselective rhodium(I)-catalysed [2+2+2] cycloaddition employing achiral triynes **141**, depicted in **Scheme II.1.11**, as substrates. [Rh(cod)$_2$]BF$_4$ together with (R,R)-Me-DuPhos afforded the corresponding heptaheterohelicenes **142** with moderate to good enantioselectivities and poor to good yields (up to 85 %*ee*, 39-80 % yield) under mild conditions. More recently, the reaction could be applied to the enantioselective synthesis of [9]- and [11]-heterohelicenes, that were obtained with 81 and 91 %*ee* respectively, albeit with low yields (28 % and 22 %, respectively) and high catalyst loadings, since 0.3 equivalents of [Rh(cod)$_2$]BF$_4$ were

required.[147f, 186]

The methodology could be further extended to the enantioselective synthesis of nona- and heptahelicenes with one five-membered ring by a double [2+2+2] cycloaddition.[187] The reaction depicted in **Scheme II.1.12** between aromatic substituted tetraynes **143** and the alkyne-tethered ketones **144** afforded with moderate yields and very good enantioselectivities (49–74 % yield, 53–91 %*ee*) the heptahelicenes (*P*)-**145**, constituting the best %*ee* reported to date for the catalytic synthesis of carbohelicenes.[187b] In separate publications, heptaheterohelicenes containing phosphorous and silicon atoms were also reported with moderate enantioselectivities.[188]
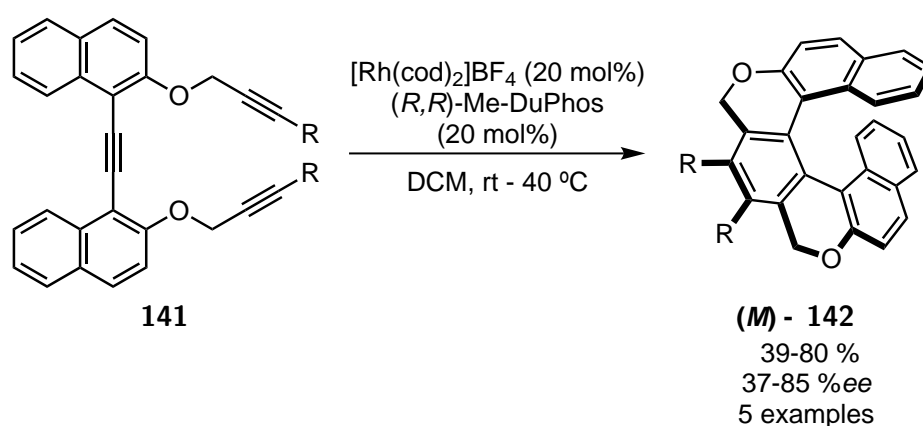
Scheme II.1.11. Enantioselective synthesis of heptaheterohelicenes through an enantioselective Rh(I)-catalysed [2+2+2] cycloaddition.
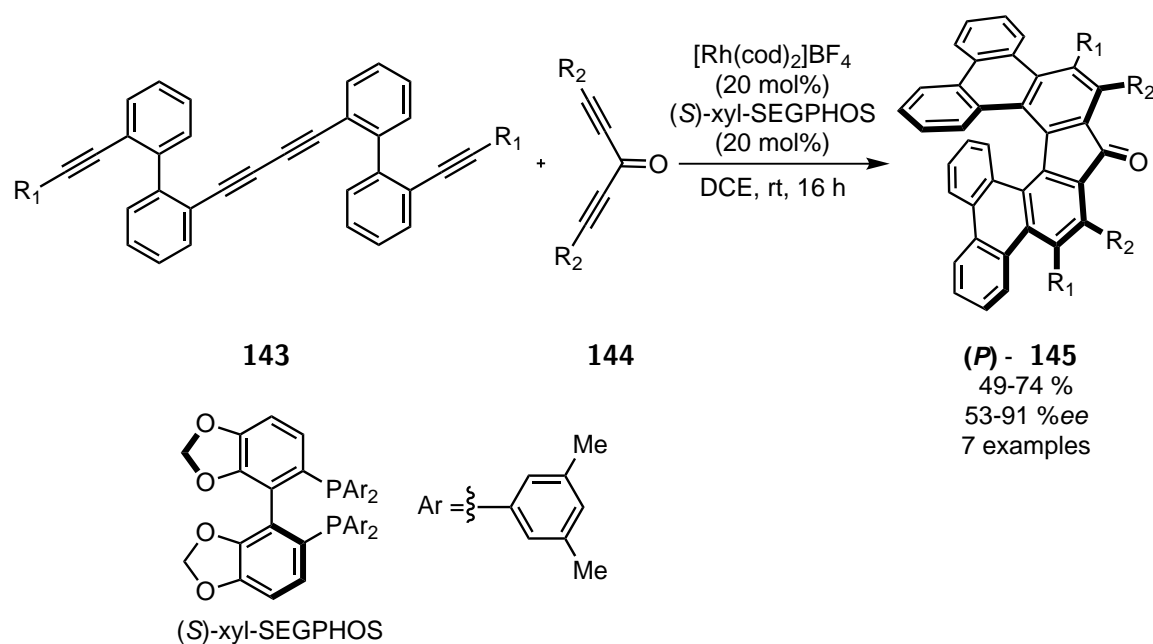
Scheme II.1.12. Enantioselective synthesis of heptahelicenes with a central five-membered ring reported by Tanaka *et al.*

However, the enantioselectivities in these rhodium-catalysed reactions were highly dependant on the substitution pattern of the reagents, thus limiting the reaction scope. Furthermore, this methodology is only applicable to heterohelicenes with embedded hydropyrane rings or to helicenes with one five-membered ring, the latter racemising relatively easily compared to other helicenes.

Other metals have been used for the enantioselective [2+2+2] cycloaddition of alkynes, such as palladium[189] or iridium[190] with chiral phosphines as ligands, but the substrate scope reported in both cases was also narrow, and in the case of the Pd-catalysed system, just moderate enantioselectivities were reached.

Another interesting approach towards the synthesis of carbohelicenes was published by Collins and co-workers using an intramolecular asymmetric ring-closing alkene metathesis of alkene-tethered biaryls.[191] Interestingly, a kinetic resolution was achieved when employing a chiral carbene as ligand for the ruthenium catalyst and heptahelicene could be obtained in 53 % ee and 43 % yield.[192] The concept, although interesting, has not been extended to the synthesis of other helicenes.

The π-acid promoted hydroarylation of aryl-tethered alkynes constitutes a more promising strategy towards the synthesis of racemic helicenes. Fürstner and co-workers reported a versatile synthesis of phenantrenes catalysed by "soft" Lewis acids from readily accessible aryl alkynes. In terms of regioselectivity, efficiency and practicality, $PtCl_2$ performed the best among the π-acids tested, favouring the intramolecular 6-$endo$-dig cyclisation; note however that $AuCl_3$, $GaCl_3$ and other Pt(II) compounds afforded also good results. The substrate scope of the reaction included the synthesis of tetrahelicene **102** and pentahelicene **103** with good yields from the corresponding aryl-tethered alkynes (**146** for **103**, *Scheme II.1.13*).[193]

Our research group demonstrated that the rate of this reaction can be enhanced with the choice of an appropriate ligand.[27,28] Since the aryl group is a poor nucleophile, the rate-limiting step of the π-acid catalysed hydroarylation is the nucleophilic attack to the activated alkyne, supported with experimental results and by theoretical studies by our group and others.[27a, 28,194] Therefore, a catalyst bearing strong π-accepting ligand will increase the reaction rate of such transformations, since it is able to deplete more electron density from the metal, and thus the alkyne, resulting in an enhanced electrophilicity.

One strategy leading to weakly-donating and strong π-acceptor ligands, consists on the introduction of positive charges to the ligand scaffold, as in the case of the cationic phosphines in complexes **147** and **148**.[26–28] The utilisation of **147** and **148** in the hydroarylation of **146** outperformed $PtCl_2$, reducing the reaction time significantly. Other Pt(II) complexes bearing π-acceptor ligands, such as $P(OPh)_3$ and $P(C_6F_5)_3$, also

afforded pentahelicene **103**, but they were less efficient than **147** and **148**, highlighting the effectiveness of this strategy.
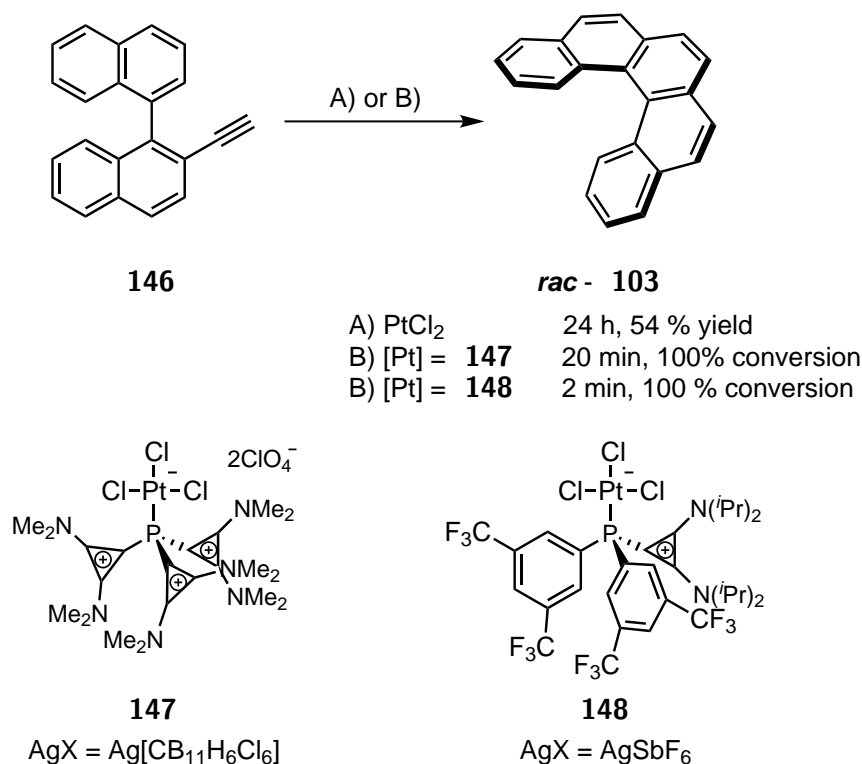
Scheme II.1.13. Synthesis of pentahelicene **103** by a Pt(II)-catalyzed hydroarylation. Conditions A) $PtCl_2$ (5 mol%), toluene, 80 °C. Conditions B) [Pt] (5 mol%), AgX (5 mol%), DCE, 80 °C.

The best results were obtained employing **148**, bearing a ligand with two electron-poor aromatic substituents and just one cyclopropenium moiety, probably due to an enhanced solubility and stability compared with the dicationic complex **147**.[27b] The reaction with the novel cationic phosphine ligands displayed a wide substrate scope, including the synthesis of different pentahelicenes, tetrahelicenes and heterohelicenes. The scope could be further extended to sterically hindered *ortho*-substituted biaryls employing gold(I) catalysts, bearing similar cationic phosphine ligand (see Subject overview, *Scheme 8*) and applied to the synthesis of natural products.[28]

Other research groups have employed π-acid catalysts, such as $PtCl_2$, $PtCl_4$ or $AuCl_3$, for the preparation of tetra-, penta- and hexahelicenes with different substitution patterns,[195] as well as heterohelicenes, including azahexahelicenes and silaheptahelicene.[196] This method has also been extended to the synthesis of tetrahydrooctahelicene by four consecutive hydroarylation reactions, albeit just with 20 %,[197] further evidencing the generality of the methodology.

Some asymmetric π-acid catalysed hydroarylation reactions leading to enantioen-

riched helicenes have also been reported. One strategy is based on the utilisation of enantiomerically pure biaryl subtrates with a stable chiral axis, such as (*S*)-**149** (94 %*ee*, **Scheme II.1.14**), which afforded the expected azahexahelicene **150** in 51 % yield and 92 %*ee*.[196b] Nevertheless, this only transfers the problem of the resolution of enantiomers to a previous step, since enantioselective synthesis of the required substrates is not obvious.[198] Furthermore, heating the reaction mixture is required and substrates less stable towards racemisation could result in diminished enantiomeric excess.

Scheme II.1.14. Asymmetric synthesis of azahexahelicene **150** by Pt(IV)-catalysed hydroarylation.

Tanaka and co-workers have recently reported an enantioselective Au(I)-catalysed hydroarylation reaction of **151**, leading to helicene **152** with excellent yield and moderate enantioselectivity, using (*R*)-BINAP as chiral ligand (**Scheme II.1.15**). The substrate scope included five more examples, obtained with lower %*ee*s, displaying that the *o*-MeO-(C$_6$H$_4$)- substituent on the alkyne and the protecting group of the amide have a major impact on the enantioselectivity.[199]

Scheme II.1.15. Enantioselective Au(I)-catalysed hydroarylation of **151** to afford **152**.

Additionally, they reported the synthesis of an S-shaped double azahelicene with more than 99 %*ee* and, more recently, the extension of the methodology to the synthesis of a [10]-helicene analogue with 96 %*ee* and 35 % yield, proving that, although the reaction scope is narrow and limited to azahelicenes, enantioselective gold(I)-catalysed hydroarylation reactions have potential for the enantioselective synthesis of helicenes.

In summary, although many different strategies have been developed to synthesise helicenes, there are few examples of enantioselective transformations. Moreover, the enantioselective reactions leading to helicenes display a lack of generality compared with the racemic methodologies, reaching good enantioselectivities only for a limited number of substrates.

The list of enantioselective reactions leading to carbohelicenes is even shorter and, except for the results obtained by the Tanaka and Starý research groups, they normally afford lower enantioselectivities than for heterohelicenes. Diasteroselective strategies have been more successful, but they require the introduction of a chiral group, which needs to be removed to obtain the fully conjugated carbohelicenes. Therefore, the development of new catalytic enantioselective methodologies towards the synthesis of carbohelicenes is required to facilitate access to enantiomerically pure compounds and foster the study of their properties and utilisation in different potential applications.

II.2. Objective of the project

Although helicenes display a variety of applications pertaining to their chirality, catalytic enantioselective methods leading to carbohelicenes are scarce in the literature. Consequently we planned to apply the expertise of our research group in π-acid catalysis to the development of an enantioselective Au(I)-catalysed hydroarylation of achiral alkynes, such as **27**, which through a double intramolecular hydroarylation would lead to hexahelicenes **26** with different substitution patterns (**Scheme II.2.1**).
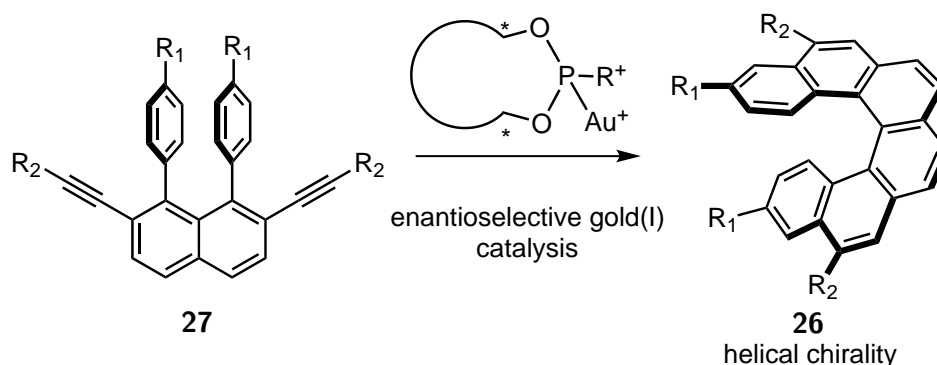
Scheme II.2.1. Proposal of transformation leading to hexahelicenes with different substitution patterns.

Since the rate determining step of the π-acid catalysed hydroarylation of aryl-tethered alkynes is the nucleophilic attack to the alkyne, poor σ-donor and strong π-acceptor ligands are the most appropriate for the transformation proposed in **Scheme II.2.1**. This compliments the work of our group with phosphorus-based positive charged ligands and, in order to achieve high enantioselectivities under milder conditions, a new class of chiral cationic ligands, TADDOL-based cationic phosphonites, was developed.

II.3.   Results and discussion

II.3.1   Synthesis of chiral cationic phosphonites based on TADDOL scaffolds

As previously discussed, we envisioned that a new class of chiral, cationic ligands would be ideal for the helicene forming reaction. In the first place, it was important to identify which chiral scaffold could be appropriate for the proposed gold(I)-catalysed transformation.

Chiral ligands such as chiral carbenes, phosphoramidites or axially chiral bisphosphines have been employed successfully in enantioselective Au(I)-catalysis. Chiral carbenes are the less adequate for the reaction proposed in *Scheme II.2.1* due to their electronic properties; since they are strong electron-releasing ligands, the rate of nucleophilic attack to the alkyne would decrease. Therefore, phosphorus-based ligands, such as phosphines, phosphoramidites or phosphites are a better choice for this particular transformation.

The most employed ligands in enantioselective gold(I)-catalysis are atropoisomeric bisphosphines, bearing a substituent with axial chirality, such as BINAP, SEGPHOS or BIPHEP derivatives.[200] On the other hand, phosphoramidites — based on BINOL, SPINOL or TADDOL scaffolds — have been also succesfully applied to enantioselective gold(I)-promoted transformations, such as cycloisomerisations of enynes and allene-(di)enes, allene hydroalkoxylations and hydroaminations, olefin cyclopropanation with sulfonium ylides and [4+2] and [3+2] intermolecular cycloadditions.[20c, 25,201]

The synthesis of phosphoramidites allows the easy modification of their backbone, and therefore simplifies the screening of catalysts. Normally they are obtained through the reaction of PCl_3 with the desired chiral diol in the presence of a base, to afford the corresponding chlorophosphite, which is subsequently treated with a lithium amide. We envisaged that the lithium amide could be replaced by another nucleophile, such as a carbene, to afford a chiral cationic phosphonite (*Scheme II.3.1*).
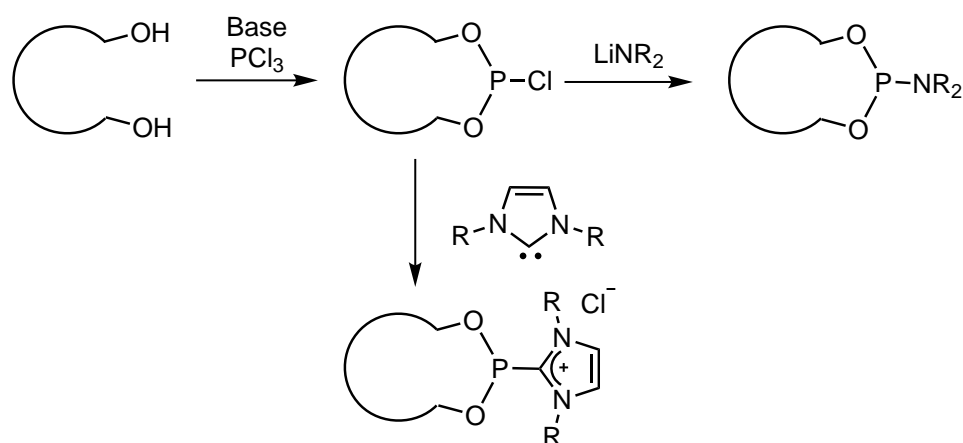
Scheme II.3.1. General procedure leading to phosphoramidites and proposed synthesis of chiral cationic phosphonites.

This proposed strategy has been already used by Chauvin and co-workers in a non-chiral fashion to synthesise achiral cationic phosphonites **154a–c**, obtained in good yields by treatment of carbenes IMes or IPr (**153**) with $(RO)_2PCl$ at low temperature (***Scheme II.3.2***).[202]

a : Ar = Mes, OR = OEt	70 %	
b : Ar = Mes, OR = OCH$_2$-	83 %	
c : Ar = Dipp, OR = OEt	89 %	
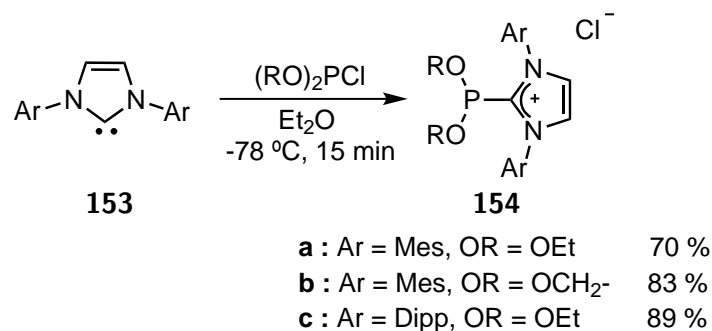
Scheme II.3.2. Synthesis of cationic phosphonites **154a–c** through the reaction of a free carbene with a chlorophosphite reported by Chauvin and co-workers.

Two are the components of the P-M bond in coordination complexes: σ-donation of the lone-pair at the phosphorus centre to a metal's empty orbital and π-backdonation from the metal to σ^*(P-R) orbitals. The cationic imidazolium substituent in **154** acts as an electron withdrawing group, lowering the energy of all the molecular orbitals, including the frontier orbitals responsible for the σ-donor and π-acceptor properties. Moreover, the imidazolium π-system may delocalise electron density from the phosphorus lone pair or, alternatively, it can overlap with the σ^*(P-O) orbital involved in π-backdonation. In both cases, the overall electron release from the ligand to the metal is reduced.[26d] As a consequence of these inductive and mesomeric effects, cationic phosphonites should behave as poor σ-donor and strong π-acceptor ligands.

The impact of the introduction of a cationic imidazolium substituent in **154** was evaluated by DFT calculations, obtaining the energy of the ligand's frontier orbitals and the theoretical CO stretching frequencies of the corresponding $[\text{RhClL(CO)}_2]$ compounds, often used to determine the donating ability of ligands. The computed stretching frequencies were higher for $\text{NHC}-\text{P(OEt)}_2$, attributing an overall weaker electron releasing ability to $\text{NHC}-\text{P(OEt)}_2$, than for phosphites P(OEt)_3 and P(OPh)_3, and rather displaying a similar value to the unstable and pyrophoric, but strong π-acceptor, PF_3. Additionally, calculation of the frontier orbitals supported the expected effect of electronegative -OR substituents, since compound $\text{NHC}-\text{P(OEt)}_2$ resulted a weaker donor and much better acceptor than its phosphine analogue $\text{NHC}-\text{PPh}_2$, displaying similar calculated HOMO and LUMO energies to the dicationic phosphine $(\text{NHC})_2-\text{PPh}$.[202]

Encouraged by this study, we considered that the synthesis of chiral analogues of **154** could be possible just by simply replacing the alcohol for a chiral diol in the reaction leading to the chlorophosphite.

Among the diols applied to the synthesis of phosphoramidites, TADDOLs constitute a highly convenient scaffold, since a myriad of analogues can be easily prepared in one step through the reaction of the desired Grignard or organolithium reagent with protected tartaric esters — inexpensive and readily available starting materials.[203]

Because of this, we chose initially to attempt the synthesis of the chiral cationic phosphonites with a TADDOL backbone. In order to test the effect of the structural and electronic features in the enantioselectivity, we planned to synthesise several TADDOLs with different aromatic groups.
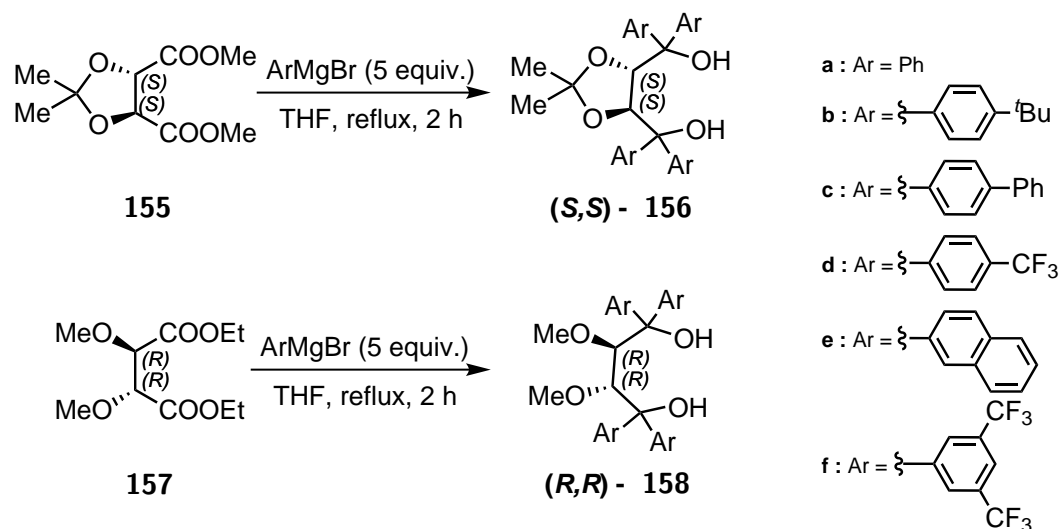
Scheme II.3.3. Synthesis of TADDOLs with different protecting groups and aromatic substituents.
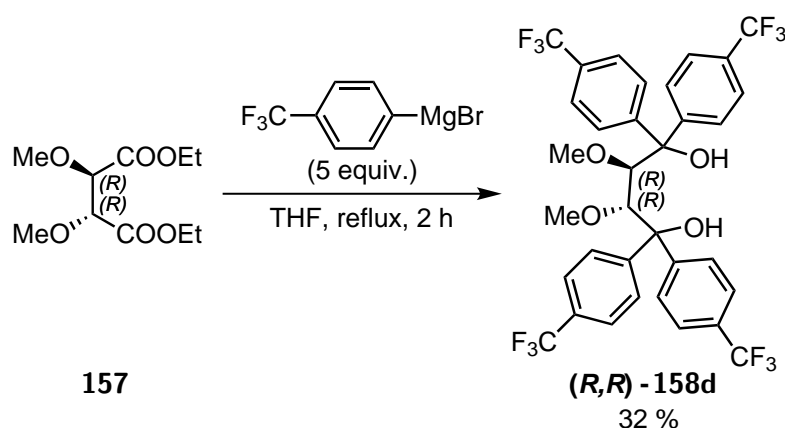
Scheme II.3.4. Synthesis of TADDOL **158d**.

Although acetonide protected TADDOL-based phosphoramidites have been employed in many enantioselective metal-catalysed reactions,[204] the Fürstner group reported that the more flexible MeO-protected phosphoramidites afforded higher enantioselectivities in the gold(I)-catalysed cyclisation of enynes.[25] Therefore, we decided to consider both protecting groups on the TADDOL backbone, and synthesised compounds **156** and **158** through the addition of excess of the Grignard reagents to **155** or **157** respectively (*Scheme II.3.3*).

The target TADDOLs (*S,S*)-**156a–f*** and (*R,R*)-**158a–c** are already known in the literature and were obtained in similar yields than those reported, whereas (*R,R*)-**158d** was not described. Following a similar procedure, compound **158d** was obtained in 32 % yield through the addition of an excess of the 4-trifluoromethyl-phenylmagnesium bromide to **157** (*Scheme II.3.4*).

With this variety of TADDOLs in hand, we decided to test our proposal for the synthesis of chiral cationic phosphonite **159b**, first preparing the corresponding chlorophosphite by treating **156b** with NEt$_3$ and PCl$_3$ (*Scheme II.3.5*, conditions A), following the procedure reported by the Fürstner group for the synthesis of phosphoramidites.[25] A solution of the chlorophosphite in diethylether was then treated with a solution in the same solvent of IMes at -78 °C, and the reaction was allowed to stir overnight, slowly warming to room temperature. After workup we were pleased to observe a ^{31}P-NMR signal at 144 ppm, similar to the phosphonites reported by Chauvin *et al.*[202]

Instead of using the cationic phosphonite with a chloride counteranion directly as ligand, a counteranion exchange was performed using an excess of NaSbF$_6$ in CH$_3$CN solution. Finally, we were able to isolate the desired cationic phosphonite (*S,S*)-**159b** by crystallisation in 29 % yield (*Table II.3.1*, entry 2). Employing MeO-substituted

---

*TADDOL **156f** was kindly provided by Fürstner group

TADDOL **158b** did not improved the yield under the same conditions (conditions A, entry 8), and the methoxy-protected analogue (R,R)-**160b** was obtained in 20 % yield.

156 PG = acetonide
158 PG = Me

159 PG = acetonide
160 PG = Me
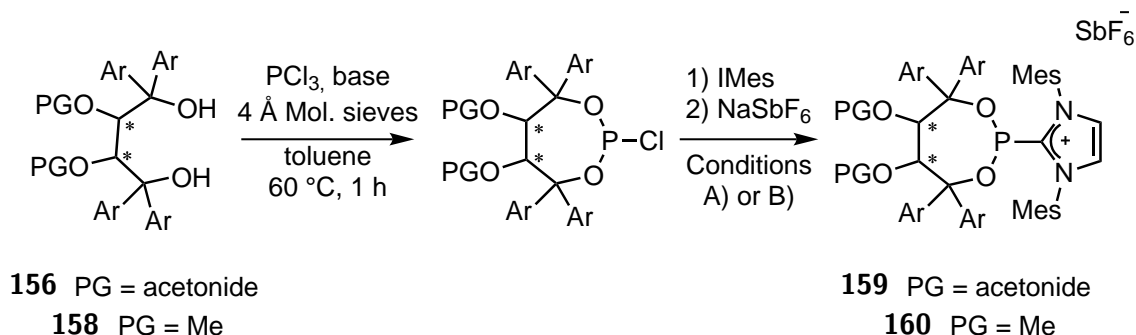
Scheme II.3.5. Synthesis of TADDOL-based cationic phosphonites.

Entry	TADDOL	PG	Ar	Cond.	Ligand	Yield (%)
1[a]	(S,S)-**156a**	acetonide	Ph	B	(S,S)-**159a**	69
2	(S,S)-**156b**	acetonide	4-^{t}Bu(C_6H_4)	A	(S,S)-**159b**	29
3	(S,S)-**156c**	acetonide	4-Ph(C_6H_4)	B	(S,S)-**159c**	48
4	(S,S)-**156d**	acetonide	4-CF_3(C_6H_4)	B	(S,S)-**159d**	72
5	(S,S)-**156e**	acetonide	2-naphthyl	B	(S,S)-**159e**	64
6	(R,R)-**156f**	acetonide	3,5-(CF_3)$_2$(C_6H_4)	B	(R,R)-**159f**	55
7[a]	(R,R)-**158a**	Me	Ph	B	(R,R)-**160a**	79
8	(R,R)-**158b**	Me	4-^{t}Bu(C_6H_4)	A	(R,R)-**160b**	20
9	(R,R)-**158c**	Me	4-Ph(C_6H_4)	B	(R,R)-**160c**	69
10	(R,R)-**158d**	Me	4-CF_3(C_6H_4)	B	(R,R)-**160d**	65

Table II.3.1: Synthesis of TADDOL-based cationic phosphonites; Conditions (Cond.) A) base = NEt$_3$; 1) IMes, Et$_2$O, -78 °C -rt, overnight; 2) NaSbF$_6$ (3 equiv.), CH$_3$CN, rt, 2 h. Conditions B) base = pyridine; 1) IMes, Et$_2$O, -78°C, 2 h; 2) NaSbF$_6$ (3 equiv.), -78 °C-rt, overnight. [a]Compounds synthesised by Leo Nicholls.

Fortunatedly, the reaction outcome could be improved by replacement of NEt$_3$ by pyridine as base during the formation of the chlorophosphite. Triethylammonium chloride, formed as byproduct, is partially soluble in toluene and diethylether and could not be completely separated from the chlorophosphite by filtration; this inevitably hydrolysed part of the carbene. The counteranion exchange could also be performed directly in ethereal solution, without the isolation of the chloride, facilitating the procedure.

Under these optimised conditions (conditions B) the rest of the cationic phospho-nites were obtained with moderate to good yields (48–79 %), independently of the protecting group and the aromatic substituent, as summarised in **Table II.3.1**. All the phosphonites exhibited a similar characteristic ^{31}P-NMR shift lying between 143.8–148.9 ppm.

The reaction was then extended to include other stable carbenes and related species, such as CAACs and carbodiphosphoranes (**Scheme II.3.6**).
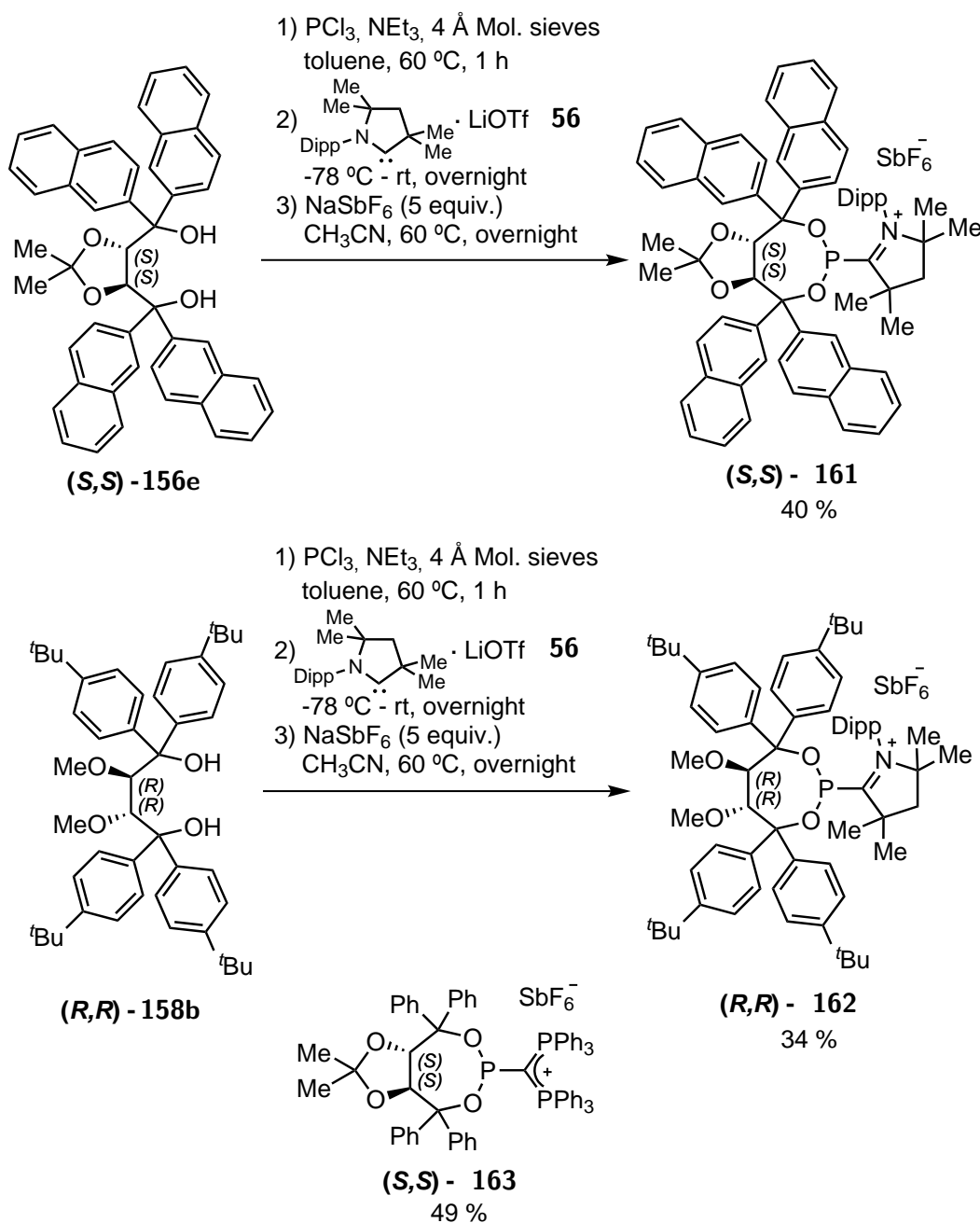
Scheme II.3.6. TADDOL-based cationic phosphonites bearing different cationic substituents.

The chlorophosphites obtained from **156e** and **158b** were treated with CAAC **56** at low temperature and, after counteranion exchange, cationic phosphonites **161** and **162** were obtained with 40 % and 34 % yields, respectively (***Scheme II.3.6***). Compounds **161** and **162** displayed a downfield ^{31}P-NMR shift compared with **159a–f** and **160a–d**, displaying a singlet at 160 and 158 ppm respectively. Additionally, compound **163** bearing a carbodiphosphorane unit, was synthesised through an analogous procedure.[†]

Hexafluoroantimonate was selected as a counteranion for the cationic phosphonites due to several advantages: first of all, it is a weakly coordinating counteranion, hence it should interact poorly with the gold centre during the catalysis and enhance the reactivity of the catalyst; secondly, it is not hygroscopic and, therefore, should enhance the stability of the compounds and facilitate their isolation.

In contrast to the phosphonites prepared by Chauvin and co-workers (**154**), which were unstable in solution, compounds **159a–f**, **160a–d**, **161**, **162** and **163** were stable to air and, with the exception of (*R,R*)-**159b**, they were purified by column chromatography in silica gel at low temperature. Their enhanced stability compared to the smaller **154** is likely due to steric reasons, since the bulkier TADDOL backbone might protect the phosphorus-cationic substituent bond towards hydrolysis. Furthermore, the cyclic TADDOL scaffold can confer additional stability through the chelation of the phosphorus centre.

[†]Synthesised by Leo Nicholls

II.3.2   Coordination of TADDOL-based cationic phosphonites to gold(I)

After the synthesis of the aforementioned cationic phosphonites, we decided to study their coordination to gold(I), through the reaction of the ligands with $(Me_2S)AuCl$ under the conditions depicted in **Scheme II.3.7**.
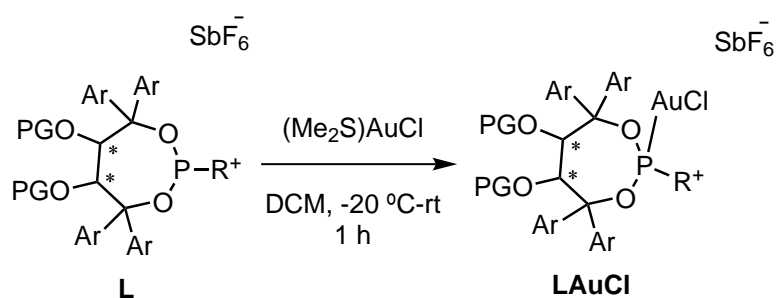
Scheme II.3.7. Coordination of cationic phosphonites to gold(I).

Entry	R^+	PG	Ar	L (LAuCl)	Yield (%)
1[a]	IMes$^+$	acetonide	Ph	(S,S)-**159a** (**164a**)	99
2	IMes$^+$	acetonide	4-^{t}Bu(C$_6$H$_4$)	(S,S)-**159b** (**164b**)	98
3	IMes$^+$	acetonide	4-Ph(C$_6$H$_4$)	(S,S)-**159c** (**164c**)	91
4	IMes$^+$	acetonide	4-CF$_3$(C$_6$H$_4$)	(S,S)-**159d**(**164d**)	91
5	IMes$^+$	acetonide	2-naphthyl	(S,S)-**159e** (**164e**)	77
6[b]	IMes$^+$	acetonide	3,5-(CF$_3$)$_2$(C$_6$H$_4$)	(R,R)-**159f** (**164f**)	56
7[a]	IMes$^+$	Me	Ph	(R,R)-**160a** (**165a**)	94
8	IMes$^+$	Me	4-^{t}Bu(C$_6$H$_4$)	(R,R)-**160b** (**165b**)	decomp.
9	IMes$^+$	Me	4-Ph(C$_6$H$_4$)	(R,R)-**160c** (**165c**)	decomp.
10	IMes$^+$	Me	4-CF$_3$(C$_6$H$_4$)	(R,R)-**160d** (**165d**)	99
11	CAAC$^+$	Ac	2-naphthyl	(S,S)-**161** (**166**)	decomp.
12	CAAC$^+$	Me	4-^{t}Bu(C$_6$H$_4$)	(R,R)-**162** (**167**)	decomp.
13[a]	[C(PPh$_3$)$_2$]$^+$	Me	Ph	(S,S)-**163** (**168**)	99

Table II.3.2: Results of the coordination of cationic phosphonites to gold(I). CAAC$^+$ = 1-[2,6-di(*iso*-propyl)-phenyl]-3,3,5,5-tetramethyl-2-pyrrolidinium.[a]Compounds synthesised by Leo Nicholls.[b]$(Me_2S)AuCl$ (1.2 equiv.), DCM, rt, overnight.

As summarised in ***Table II.3.2***, coordination of the phosphonites **159** proceeded to afford the desired gold(I)-complexes **164** (***Figure II.3.1***) in very good yields, except for (*R,R*)-**159f**, which required an extended reaction time and excess of (Me$_2$S)AuCl to reach complete conversion. Coordination to gold(I) was evidenced by ^{31}P-NMR; the signals shifted upfield compared with the free ligands, found between 108.6–113.4 ppm in a similar range to similar phosphoramidite-gold(I) chlorides.[25] The difficulty of (*R,R*)-**159f** to coordinate gold(I) could be attributed to the greater steric impediment generated by the large 3,5-bis(trifluoromethyl)-phenyl substituents.

a : Ar = Ph
b : Ar = 4-^{t}Bu(C$_6$H$_4$)
c : Ar = 4-Ph(C$_6$H$_4$)
d : Ar = 4-CF$_3$(C$_6$H$_4$)
e : Ar = 2-naphthyl
f : Ar = 3,5-(CF$_3$)$_2$(C$_6$H$_4$)

a : Ar = Ph
d : Ar = 4-CF$_3$(C$_6$H$_4$)

164   **165**
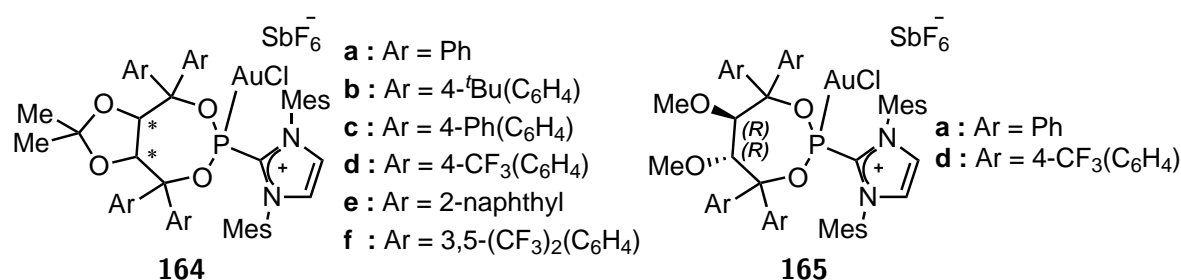
Figure II.3.1. Imidazolium-substituted phosphonite gold(I) complexes.

Unexpectedly, the formation of the methoxy-protected analogues **165** was not straightforward. Complex **165a**[‡] (***Figure II.3.1***) proved to be slightly sensitive in DCM solution at room temperature, with the coordination reaction working best when conducted entirely at -20 °C. Nevertheless, it could be isolated and characterised, presenting the expected ^{31}P-NMR chemical shift, 108.6 pm, attributed to the formation of the complex.

Contrarily, upon mixing **160b** with (Me$_2$S)AuCl following the general procedure, the crude exhibited instead a broad ^{31}P-NMR signal at 80.0 ppm. Similar behaviour was observed for the ligand **160c**. Although initially the formation of the complex could be detected by ^{31}P-NMR (signal at 108.8 ppm), after some minutes in CD$_3$CN solution, the intensity of the signal decreased, with a broad signal at 80.0 ppm increasing concomitantly.

These differences in the stability of methoxy-protected phosphonites **165** were better explained with the coordination study of ligand **162**. Upon treatment of **162** with (Me$_2$S)AuCl a ^{31}P-NMR broad signal at 92.4 ppm was observed. Two fractions could be isolated by addition of CH$_3$CN and identified as naphthalene **169** and complex **170** (***Scheme II.3.8***).

[‡]Synthesised by Leo Nicholls
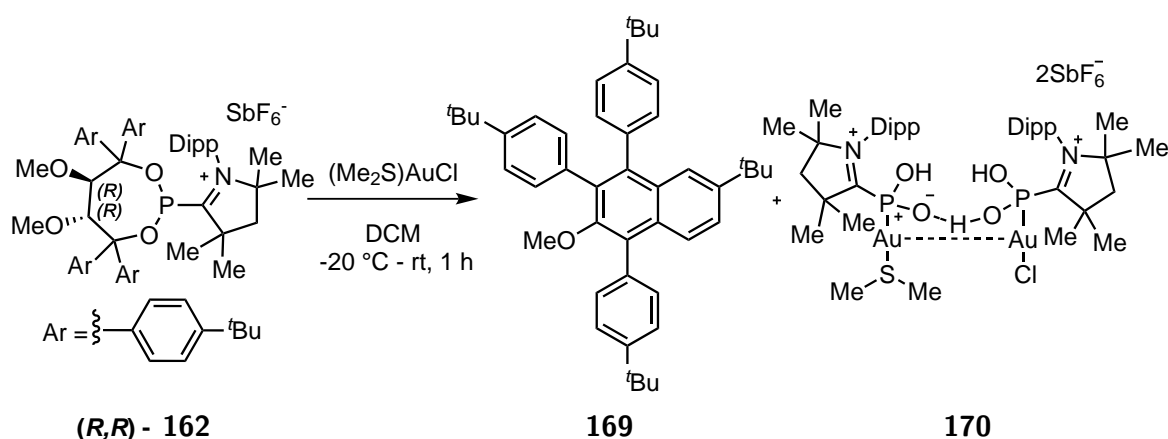
Scheme II.3.8. Reaction of **162** with (Me₂S)AuCl.

The structure of both products **169** and **170**, presented in ***Figure II.3.3*** and ***Figure II.3.2*** respectively, could be confirmed by X-ray analysis. The solid state structure of **170** displayed a dimeric species, consisting of two phosphonous acid-gold(I) fragments linked through an aurophilic interaction (Au1-Au2 = 3.090 Å) and a proton bridge, localised by the X-ray measurement. Each phosphorus centre retains one imidazolium substituent, whereas one gold is coordinated by dimethylsulfide and the other by a chloride. Despite of the coordination found in the solid state structure, just one set of signals could be identified in the ^{1}H-NMR, indicating that in solution the compound is probably a monomer.

On the other hand, the polysubstituted naphthalene **169** is constituted by the TADDOL-fragment of the cationic phosphonite, where one of the aromatic substituents has cyclised and one MeO-group has been eliminated.
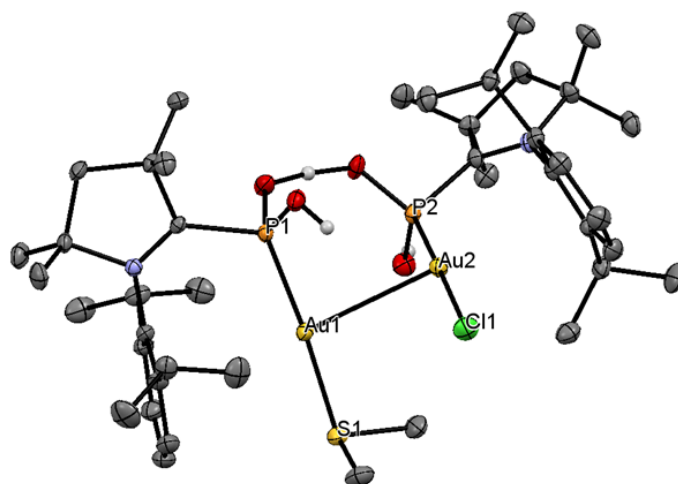
Figure II.3.2. X-ray structure of **170**. Counteranions, hydrogen atoms and solvent molecules have been omitted for clarity. Thermal ellipsoids set at 50 % probability. Selected bond lengths (Å) : Au1-Au2 = 3.090, Au1-P1 = 2.262 , Au2-P2 = 2.214 , P1-C1 = 1.869, P2-C21 = 1.882.
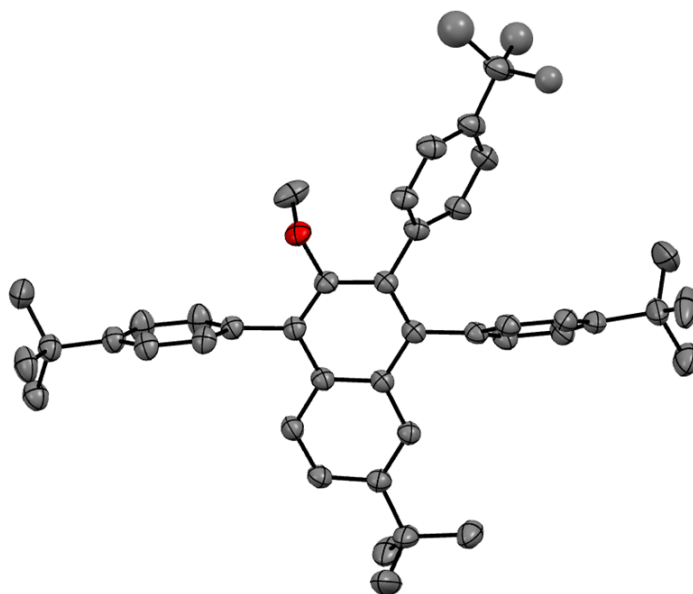
Figure II.3.3. X-ray structure of **169**. Hydrogen atoms have been omitted for clarity. Thermal ellipsoids set at 50 % probability.

The same phenomena was observed in the reaction of **160b** with (Me$_2$S)AuCl and two distinct fractions, with just one of them a ^{31}P-NMR signal, could be separated upon addition of CH$_3$CN and filtration. Based on the structure of **170** and the recorded NMR data, the isolated gold complex could be identified as **171** (***Scheme II.3.9***), whereas the organic fraction matched the analytical data of napththalene **169**. In the case of **160c**, a mixture containing **171**, **172** and the desired gold complex (**160c**)AuCl was obtained.

***(R,R)*-160b** R = ^{t}Bu
***(R,R)*-160c** R = Ph

169　R = ^{t}Bu
172　R = Ph
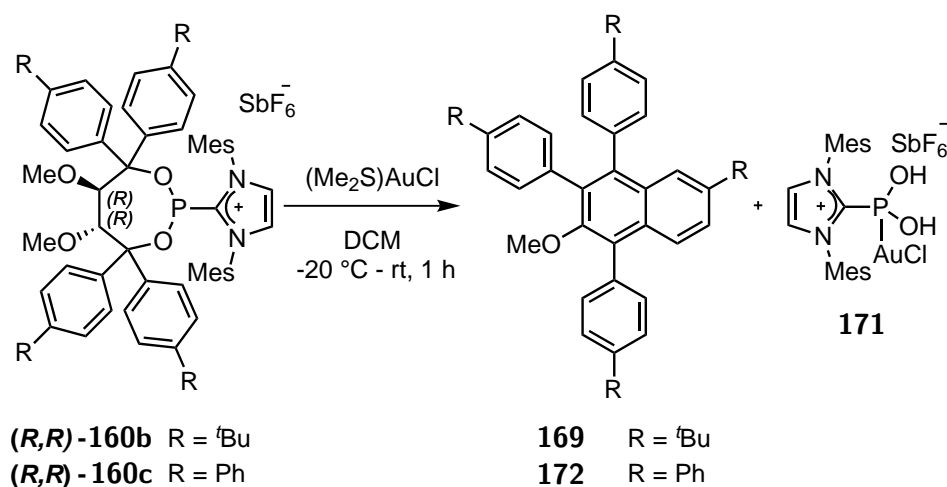
Scheme II.3.9. Decomposition of **160b** and **160c** upon treatment with (Me$_2$S)AuCl.

In view of these results, we hypothesised that initially the desired gold(I) complexes (**160b**)AuCl, (**160c**)AuCl and (**162**)AuCl were formed, but they decomposed into two different fragments: a gold complex with a cationic phosphonous acid ligand and a naphthalene derivative.

Seebach and coworkers reported the acid-promoted decomposition of TADDOL **173**, leading to naphthalene **174**, an analogue of **169**. They proposed a mechanism involving two consecutive acid-promoted eliminations to form a carbocation **175**, which generates after a Friedel-Crafts type intramolecular attack, the intermediate **176**. Acid-promoted opening of the acetonide and Wagner-Meerwein shift affords **177**, which after rearomatisation, acetone elimination and acetylation leads to the formation of **174**.[205]
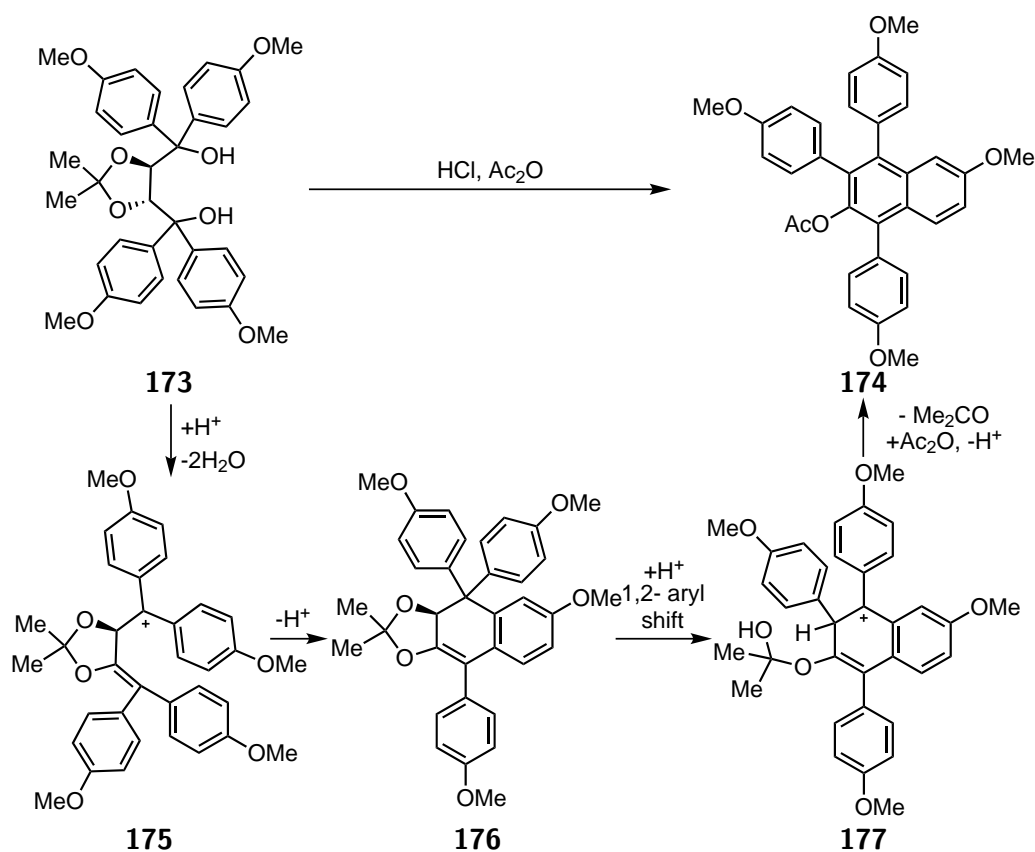
Scheme II.3.10. Acid-promoted decomposition of **173**.

An analogous mechanism could be proposed for the decomposition of (**162**)AuCl. In the same fashion, upon coordination to gold(I) and formation of the complex **167**, the removal of electron density from the phosphorus promotes two consecutive elimination processes. Release of complex **178**, which would lead to **170**, delivers the carbocation **180**. Intermediate **180** then undergoes intramolecular attack by one of the aromatic rings to form the bicycle **181**, which after elimination of MeOH, affords the carbocation

182. Finally, after 1,2-aryl shift and rearomatisation, the observed naphthalene **169** is formed.
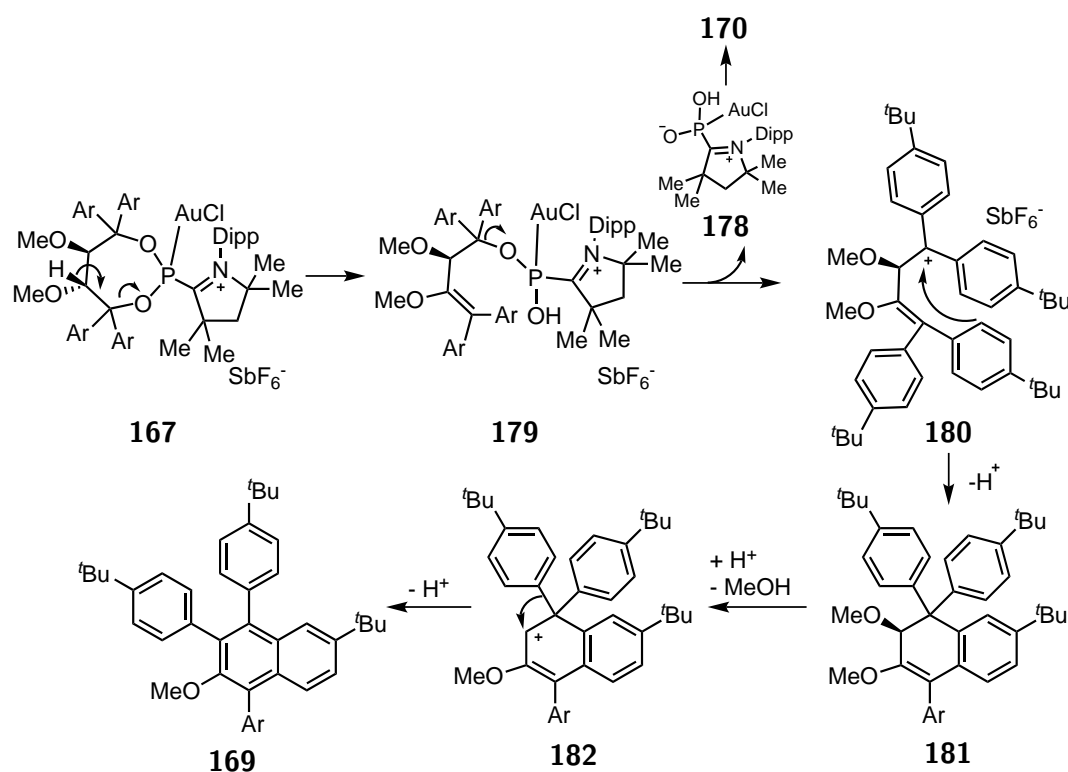
Scheme II.3.11. Proposed decomposition mechanism of **167**.

Through a similar pathway, **165b** and **165c** would then initially be formed, before decomposing to afford the corresponding naphthalenes and phosphonous acid gold complex **171**.

This decomposition pathway can be circumvented by using TADDOLs with electron-poor aromatic rings that would destabilise the intermediate carbocation **180**, disfavouring the initial elimination steps. Hence, upon treatment of the cationic phosphonite (*R,R*)-**160d**, bearing 4-CF$_3$(C$_6$H$_4$) substituents, with (Me$_2$S)AuCl under the general conditions, the formation of (*R,R*)-**165d** (***Figure II.3.1***) proceeded with excellent yield (***Table II.3.2***, entry 10), displaying a greater stability than **165a**.

In contrast, complexes **164** containing acetonide protecting group are stable, probably due to the higher rigidity of the seven-membered ring that prevents the adoption of the antiperiplanar geometry required for an E_2 elimination. Nevertheless, both acetonide-protected **161** and methoxy-protected **162** iminium-substituted phosphonites, decomposed upon coordination to gold(I), regardless of the backbone. Unfortunately, the presence of the more electron-withdrawing iminium substituent promotes the elimination of the **178** fragment.

The connectivity of the cationic phosphonite gold(I) complexes (*S,S*)-**164e**, (*R,R*)-**164f** and (*R,R*)-**165d** could be confirmed by X-ray analysis. Compounds with the acetonide backbone (*S,S*)-**164e** and (*R,R*)-**164f**, bearing 2-naphthyl and 3,5-$(CF_3)_2(C_6H_4)$ substituents respectively, are depicted in *Figure II.3.4* and the bis-methoxy derivative (*R,R*)-**165d** with 4-$CF_3(C_6H_4)$ groups, in *Figure II.3.5*. Complex (*R,R*)-**164f** shows two different conformations in the unit cell, with similar structural features, but for clarity the one that presents the least disorder is displayed. Both complexes with trifluoromethyl-substituted aromatic rings, **164f** and **165d**, present disorder in some CF_3 units that was removed from the figures for clarity reasons.

All the complexes present the expected linear geometry at the gold centre, with a shorter Au-P distance (2.185 Å) in the case of (*R,R*)-**165d**, indicating a stronger interaction. The structural features around the phosphorus centre present very similar values, although the P-$C_{imidazolium}$ bond length (P2-C61) is longer in the case of (*R,R*)-**164f**, probably a consequence of the higher steric hindrance between the mesityl and the bulky 3,5-bis(trifluoromethyl)-phenyl substituents.
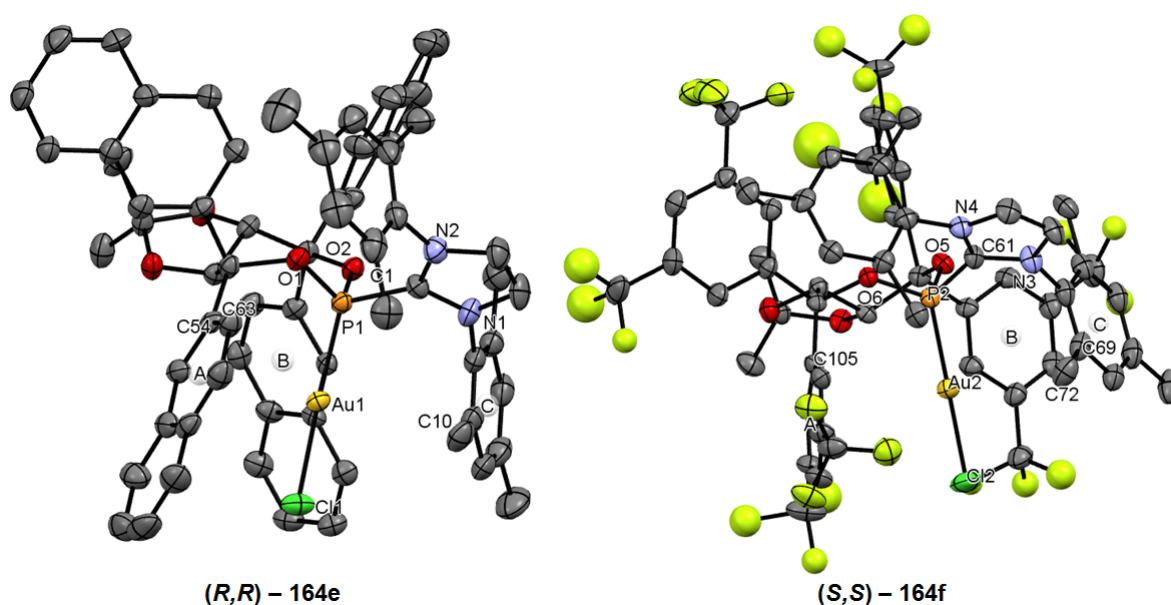
(R,R) – 164e   **(S,S) – 164f**

Figure II.3.4. Molecular structures of (*S,S*)-**164e** and (*R,R*)-**164f** in the solid state. Counteranions, hydrogen atoms and solvent molecules have been omitted for clarity. Thermal ellipsoids at 50 % probability. Selected bond lengths (Å) (*S,S*)-**164e** : Au1-P1 = 2.197, P1-C1 = 1.824, Au1-C54 = 3.277, Au1-C63 = 3.266, Au1-C10 = 3.350, Au1-centroid A = 3.556, Au1-centroid B = 4.318, Au1-centroid C = 4.029; (*R,R*)-**164f** : Au2-P2 = 2.191, P2-C61 = 1.841, Au2-C69 = 3.321, Au2-C72 = 3.355, Au2-C105 = 3.235, Au2-centroid A = 3.296, Au2-centroid B = 4.616, Au2-centroid C = 3.954.
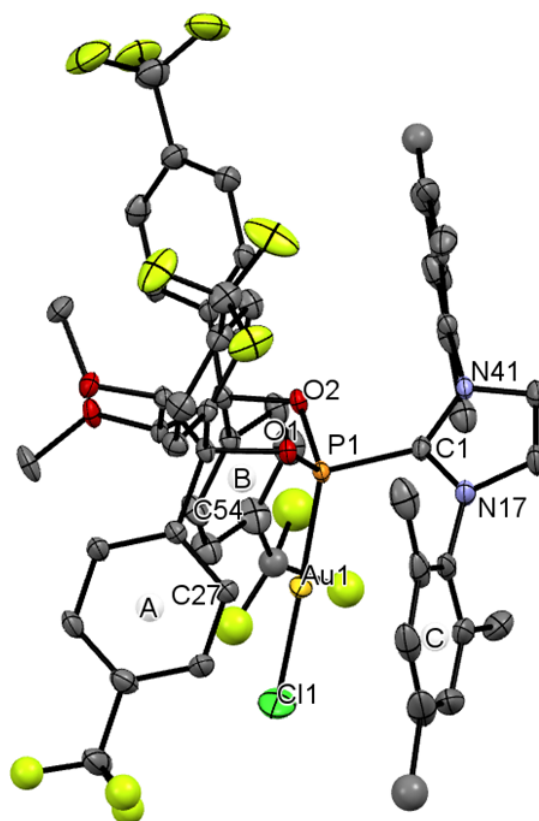
Figure II.3.5. Molecular structure of (*R,R*)-**165d** in the solid state. Counteranions, hydrogen atoms and solvent molecules have been omitted for clarity. Thermal ellipsoids at 50 % probability. Selected bond lengths (Å) (*R,R*)-**165d** : Au1-P1 = 2.185, P1-C1 = 1.829, Au1-C27 = 3.272, Au1-C54 = 3.285, Au1-centroid A = 3.940, Au1-centroid B = 3.978, Au1-centroid C = 3.957.

The α-substituents on the TADDOL backbone pointing towards the gold(I) centre are of major importance for the formation of the chiral pocket during the catalysis. Moreover, the proximity of the α-aromatic rings to the metal centre can foster gold-arene interactions, which provide additional stability to the active species during the catalysis and confer rigidity to the chiral pocket.

The distances from the gold(I) atom to the centroids of the A, B and C rings are very informative in this regard. Both complexes with the acetonide protectig group, **164e** and **164f**, show a strong arene-gold interaction between the ring A and the metal centre (Au1-centroid A = 3.556 Å for **164e** and Au2-centroid A = 3.296 Å for **164f**). In the naphthyl-substituted phosphonite **164e**, ring A interacts with the gold centre *via* C54-C63 bond through an η^2-arene-gold interaction (Au1-C54 = 3.277 Å, C63-Au = 3.266 Å; $\sum r_{vdW}$ (Au,C) = 3.36),[97] whereas in complex **164f** the gold centre interacts with the *ipso*-carbon (Au2-C105 = 3.235 Å). Conversely, the centroids of the rings B and C in both complexes are located further away from the gold (Au1-centroid B = 4.318, Au1-centroid C = 4.029 Å for **164e**; Au2-centroid B = 4.616, Au2-centroid C =

3.954 Å for **164f**), although short contacts are observed between the gold centre and one methyl groups of the mesityl ring C.

In contrast, the α-substituents in the methoxy-protected complex **165d** are more evenly distributed, with almost equal Au-centroid distances (Au1-centroid A = 3.940 Å, Au1-centroid B = 3.978 Å, Au1-centroid C = 3.957 Å), a situation that probably occurs due to its more flexible backbone or to the lesser bulkiness of the $4\text{-}CF_3(C_6H_4)$ aromatic rings. Short contacts are observed in this case between the gold centre and one *ortho*-carbon of the rings A and B (Au1-C27 = 3.272 Å, Au1-C54 = 3.285 Å).

II.3.3 Substrate synthesis

Based on the previous literature concerning helicene and phenanthrene synthesis through π-acid catalysis (see Introduction), we envisaged that hexahelicene derivatives could be obtained through a gold(I)-catalysed double hydroarylation reaction of alkyne-tethered aromatic substrates. Among the possible disconnections of hexahelicene **26**, the one depicted in **Figure II.3.6** constitutes the best option, since it leads to a C_{2v}-symmetric achiral substrate (**27**) whereas other alternatives might lead to aromatic compounds with a stable chiral axis.
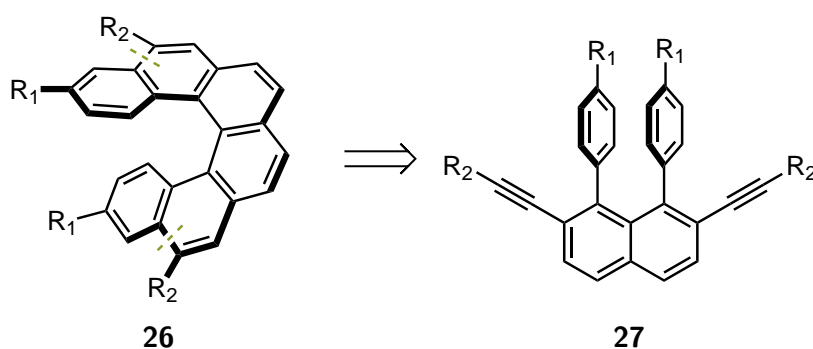
Figure II.3.6. Selected disconnection of hexahelicene **26**.

The bis-alkynyl naphthalene **27** was not described; therefore we devised a robust and scalable synthetic strategy for its synthesis, based on literature modified procedures.

The starting material for all of the substrates was 2,7-dimethyl-naphthalene **183**, which can be easily accessed through a well-established two-step procedure in multi-kilogram scale.[206] Selective bromination of positions 1 and 8 of **183** with *N*-bromo-succinimide led to **184** (**Scheme II.3.12**), this procedure was already reported by Laarkem *et al.*[207] Unfortunately, under the reported conditions, the reaction was sluggish, requiring an extended reaction time and the addition of extra portions of NBS to reach completion.

With **184** in hand, a Suzuki coupling was employed to introduce aromatic groups in the positions 1 and 8. Owing to the steric hindrance created after coupling of the first aromatic ring, the conditions reported by Buchwald and co-workers for bulky coupling partners were applied.[208] As can be seen in **Table II.3.3**, compounds **185a–e** were obtained in good yields.
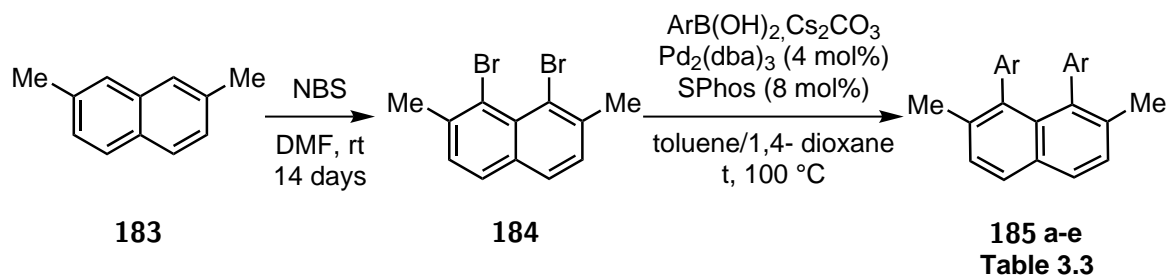
Scheme II.3.12. Synthesis of **185**.

Entry	Ar	185	t(h)	Yield (%)
1	Ph	**185a**	4	75
2	4-MeO-(C_6H_4)	**185b**	2	75
3	4-Ph-(C_6H_4)	**185c**	3	69
4	4-Cl-(C_6H_4)	**185d**	overnight	75
5	2-naphthyl	**185e**	4	68

Table II.3.3: Results of the Suzuki coupling between **184** and different aromatic boronic acids.

Depending on their substitution pattern, 1,8-diaryl-naphthalenes are known to display hindered rotation across the naphthalene-Ar bond, raising the energetic barrier with the increase of steric hindrance.[209] Because of this, compound **185e**, interesting since it could open a route to benzo-fused hexahelicenes, exhibited two sets of signals attributable to *anti-* and *syn-* isomers — indicating the relative orientations of the 2-naphthalene substituents — in the ^{1}H-NMR at room temperature (ratio *anti*:*syn*, 55:45). Increasing the temperature until 60 °C did not result in the broadening of the signals, implying that there is no rotation and therefore, no exchange between the conformers in the NMR time scale even at that temperature. Therefore, compound **185e** and its derivatives are less suitable substrates for the initially proposed reaction, and the synthesis of other substrates with *meta*-substituted aromatic rings was not pursued.

The synthesis of the substrates **27** continued as detailed in *Scheme II.3.13*. In order to install the alkyne moiety, methyl groups in **185** were functionalised selectively using a radical bromination with NBS in the presence of benzoyl peroxide. The resulting bromides **186** were subsequently hydrolysed with $CaCO_3$, affording diols **187**, which could be, after filtration, directly submitted to the oxidation reaction with PCC, leading to the dialdehydes **188** with good yields over the three steps. Compounds **188** were then submitted to Seyferth-Gilbert homologation, using the Ohira-Bestmann conditions, obtaining thus the terminal diynes **189** with good yields.

188 a-d
a : R$_1$ = H   80%
b : R$_1$ = OMe   59%
c : R$_1$ = Ph   52%
d : R$_1$ = Cl   42%
yield over three steps

27 aa
80%

189 a-d
a : R$_1$ = H   60%
b : R$_1$ = OMe   83%
c : R$_1$ = Ph   66%
d : R$_1$ = Cl   77%

27 ab-d
Table 3.4
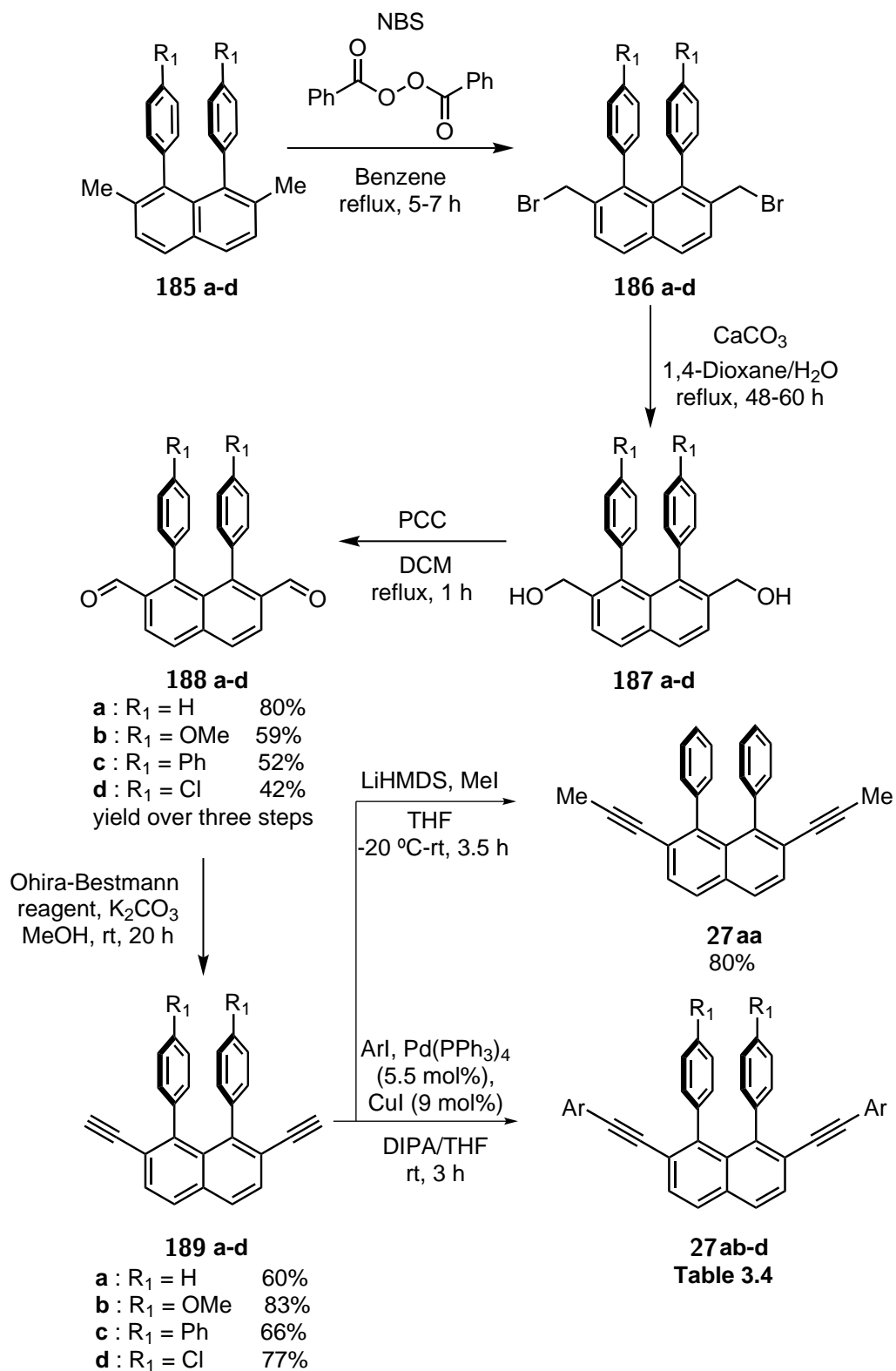
Scheme II.3.13. Synthesis of substrates **27aa–d**.

Using this strategy alkyne **189a** could be obtained in up to 1.18 g in a global yield of 36 %, with straightforward reaction procedures and just two chromatographic separations, highlighting the convenience of the synthetic pathway.

The alkynes **189** could be further funtionalised through deprotonation and methylation, as is the case for **27aa**, or with a Sonogashira coupling. The latter allowed the synthesis of a variety of substrates **27ab–d** with different aromatic residues with good yields, summarised in **Table II.3.4**.

Entry	R_1	Ar	27	Yield (%)
1	H	4-Me(C_6H_4)	**27ab**	80
2	H	Ph	**27ac**	55
3	H	3,5−Me$_2$(C_6H_4)	**27ad**	86
4	H	4-Cl(C_6H_4)	**27ae**	65
5	MeO	4-Me(C_6H_4)	**27ba**	97
6	MeO	Ph(S)\O—Me〜	**27bb**	75
7	Ph	4-Me(C_6H_4)	**27c**	73
8	Cl	4-Me(C_6H_4)	**27d**	66

Table II.3.4: Sonogashira coupling leading to substrates **27ab–d**.

The connectivity of the substrates could be confirmed by the crystallisation and X-ray analysis of compounds **27aa** (**Figure II.3.7**) and **27ac** (**Figure II.3.8**). Both molecules present similar structural features with the characteristic distortion on the 1,8 positions observed for other 1,8-diaryl-naphthalenes,[209c] generated by the steric clash between the phenyl rings.
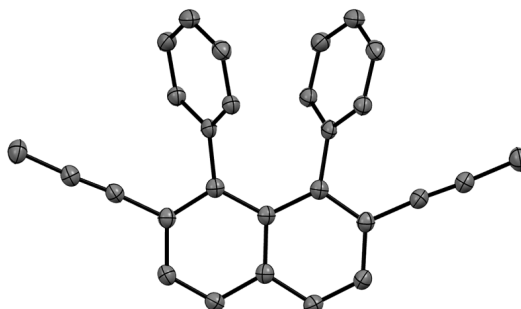
Figure II.3.7. Molecular structure of **27aa** in the solid state. Thermal ellipsoids at 50 % probability. Hydrogen atoms and solvent molecules have been omitted for clarity.
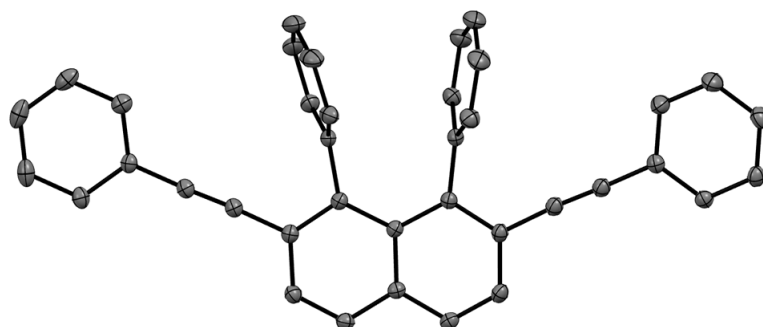
Figure II.3.8. Molecular structure of **27ac** in the solid state. Thermal ellipsoids at 50 % probability. Hydrogen atoms and solvent molecules have been omitted for clarity.

It is important to highlight the modularity of the developed synthetic strategy that allows an efficient formation of a wide variety of substrates with different substituents on the phenyl rings and the alkyne, which could later be evaluated in the enantioselective synthesis of the corresponding helicenes. Moreover, the reactions proved to be general, affording high yields regardless of the nature of the substituents, meaning that the same synthetic pathway could be later extended to other substrates with similar results.

II.3.4   Catalysis

II.3.4.1   Gold(I)-catalysed hydroarylation with achiral complexes

In the first place, it was necessary to investigate the viability of the proposed synthesis of hexahelicenes from alkynes **189** or **27** using gold(I)-catalysis, as well as the utility of our strategy in employing strong π-acceptor ligands.
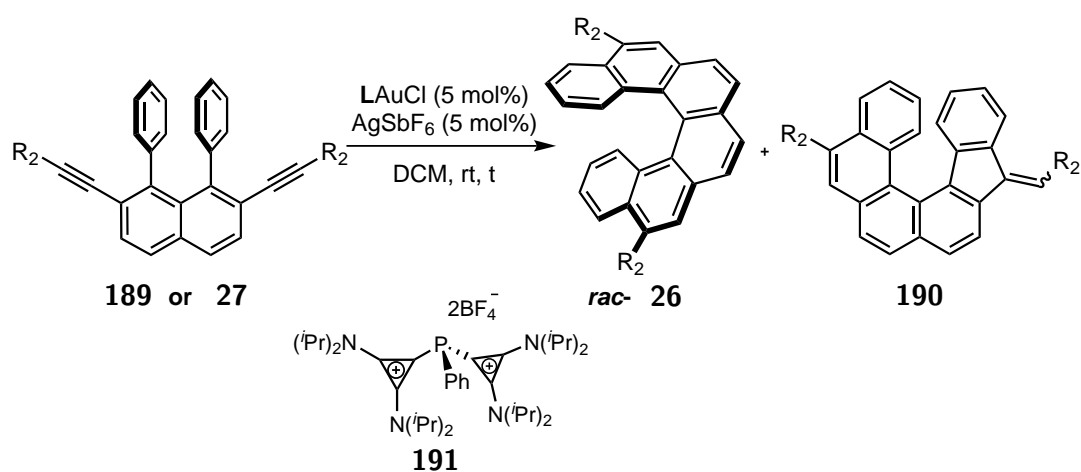
Scheme II.3.14. Gold(I) catalysed cycloisomerisation of akynes **189a** and **27aa–ac**. Results are summarised in **Table II.3.5**.

Entry	Substrate	R_2	L	t (min)	26:190	% mass recovered
1	**189a**	H	**191**	10	64:36	98
2	**27aa**	Me	**191**	2	95:5	> 99
3	**27aa**	Me	PPh$_3$	60	84:16	n.d.
4	**27aa**	Me	IMes	300	71:29	> 99
5	**27ab**	tolyl	**191**	45	81:19	> 99
6	**27ac**	Ph	**191**	30	77:23	> 99

Table II.3.5: Gold(I) catalysed cycloisomerisation of akynes **189a** and **27aa–ac** with achiral ligands at rt. Ratio **26**:**190** determined by ^{1}H-NMR, except for entries 5 and 6, that were obtained by HPLC.

Initially the terminal alkyne **189a** (**Table II.3.5**, entry 1) was submitted to gold(I)-catalysis conditions depicted in **Scheme II.3.14**, employing as precatalyst dicationic complex (**191**)AuCl, developed previously in our group.[28] Although the formation

of hexahelicene was confirmed by NMR analysis, matching the data reported in the literature,[210] the formation of another isomer was observed. The isolation of the latter was not possible due to partial decomposition during HPLC separation, but we hypothesise, by comparison with results elaborated below, that the isomer corresponds to **190**.

The reaction leading to **26** consists of two consecutive gold(I)-catalysed alkyne hydroarylations, the first one forming the intermediate **192** with a tetrahelicene backbone, after a 6-*endo*-dig cyclisation. Intermediate **192aa**, with R_1 = H and R_2 = Me, could be isolated and its structure confirmed by multinuclear NMR analyses. The second cycloisomerisation could then proceed *via* a 6-*endo*-dig or or 5-*exo*-dig cyclisation, leading to hexahelicene **26** or the isomer **190** respectively.
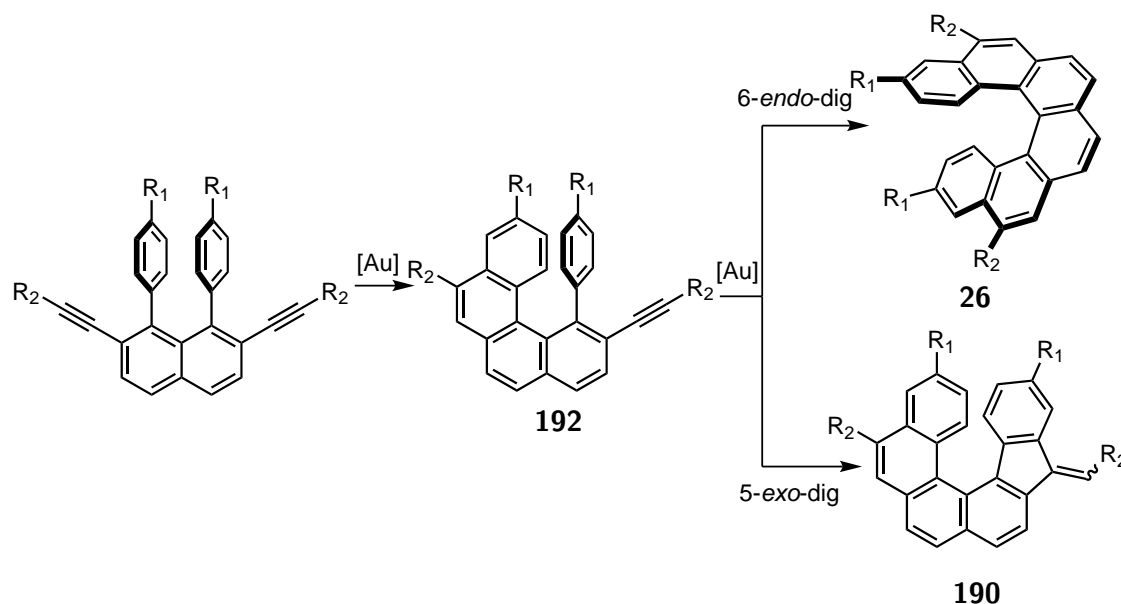
Scheme II.3.15. Steps for the formation of **26** and **190**.

Both reaction pathways are observed in the PtCl$_2$-catalysed synthesis of phenantrenes reported by Fürstner and co-workers and the regioselectivity of the reaction was dependant on the substituents attached to the aromatic nucleophile and to the terminal alkyne.[193] Calculations revealed that, even though the final aromatic 6-*endo*-dig product is more stable, the activation barriers for the initial nucleophilic attack are very similar, their energy difference being related to the electronic and steric nature of the substituents.[194]

The work of our research group in the synthesis of phenantrenes has showed that the regioselectivity of the Pt(II)- or Au(I)-catalysed cycloisomerisation is excellent when cationic phosphines are employed as ligands, such as **191**.[27,28] The diminished regios-

electivity obtained with substrate **189a** compared to the synthesis of phenanthrenes might account for the higher steric hindrance generated in the twisted helicene structure which could favour the formation of isomer 5-*exo*-dig **190** in the second cyclisation, since the five-membered ring would reduce the overlap of the terminal aromatic rings.

Since the regioselectivity with the terminal alkyne **189a** was just moderate for the formation of hexahelicene, the methyl-tethered substrate **27aa** was tested under the same conditions (*Table II.3.5*, entry 2). In this case, the regioselectivity increased significantly compared with the terminal alkyne to a ratio of helicene(**26aa**):5-*exo*-isomer(**190aa**) of 95:5.

We also evaluated the effect of the electronic properties of the ligand in the cycloisomerisation of the methylated substrate **189aa**; (Ph$_3$P)AuCl and (IMes)AuCl were tested, resulting in both cases in poorer regioselectivities compared with complex (**191**)AuCl (*Table II.3.5*, entries 3 and 4 respectively). Moreover, similarly to the synthesis of phenanthrenes, we could confirm following the reaction by GC/MS (entries 2 and 3), that the utilisation of dicationic ligand **191** is beneficial for the reaction rate, since complete formation of helicene was achieved in 2 minutes at room temperture, in contrast with 60 minutes required for (Ph$_3$P)AuCl.

Substrates bearing aromatic groups in the alkyne, tolyl-substituted **27ab** and phenyl substituted **27ac**, also cyclised using (**191**)AuCl, leading to a mixture of the corresponding hexahelicene and 5-*exo*-isomer, **26**:**190**, of 81:19 and 77:23 respectively (*Table II.3.5*, entries 5 and 6).

The 5-*exo*-isomer bearing tolyl-substituents in R_2, *E*-**190ab**, could be separated by semipreparative HPLC and its structure confirmed with the help of two-dimensional NMR experiments. The resulting chromatogram after the hydroarylation reaction of the tolyl-substituted substrate **27ab** (*Table II.3.5*, entry 5) showed 14 % of the identified isomer *E*-**190ab** and additionally a minor quantity of another isomer, just 5 %, that could not be isolated. The latter corresponds likely to the *Z*-isomer, since a sample of pure isomer *E*-**190ab** in DCM solution showed after several hours the formation of the other species, probably due to a proton-catalysed double bond isomerisation.

The formation of the desired helicenes could be confirmed by X-ray analysis of crystals from the 5,12-dimethylhexahelicene **26aa** and 5,12-diphenylhexahelicene **26ac**, grown from their racemic mixtures. Their solid state structures are depicted in *Figure II.3.9*, showing the characteristic helical distorted structure of hexahelicenes.

In the same fashion as other helicenes, their structures in the solid state are not C_2-symmetric, a fact that still is not well understood. Additionally, they display shorter outer bonds than benzene (1.39 Å), whereas, the inner bonds are longer, thus indicating the diminished aromaticity characteristic of helicenes (see Introduction). Their inner

pitches, determined as the C16-C22 distance for **26aa** and C19-C25 for **26ac**, are 3.137 and 3.062 Å respectively, similar to the 3.24 Å observed in hexahelicene **99**.[211,212] The inner torsional angles are also comparable with those of hexahelicene **99**, both structures exhibiting greater distortion of the aromatic rings in the centre of the helix than in the terminal rings (C16-C17-C18-C19 < C17-C18-C19-C20 for **26aa**). Although the terminal inner torsions are smaller for the methyl-substituted **26aa** than in the phenyl-tethered analogue **26ac** (C16-C17-C18-C19 in **26aa** < C19-C20-C21-C22 in **26ac**), the central torsion angle is larger.

rac – 26aa   **rac – 26ac**
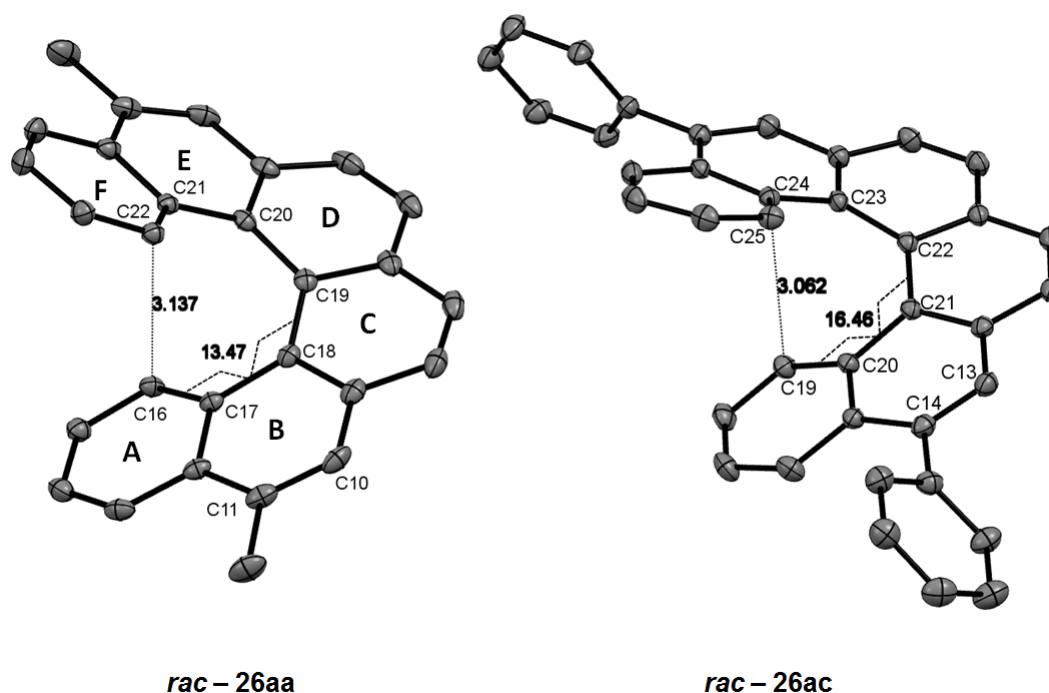
Figure II.3.9. X-ray structure of **26aa** and **26ac**. Thermal ellipsoids at 50 % probability. Selected structural features for **26aa**: distances (Å) C10-C11 = 1.354, C17-C18 = 1.456, C16-C22 (inner pitch) = 3.137; torsional angles (°) C16-C17-C18-C19 (terminal inner torsion) = 13.47 , C19-C20-C21-C22 (terminal inner torsion) = 12.85, C21-C20-C19-C18 (central torsion) = 30.16. Selected structural features for **26ac**: distances (Å) C13-C14 = 1.364, C20-C21 = 1.454, C19-C25 (inner pitch) = 3.062; torsion angles (°) C19-C20-C21-C22 (terminal inner torsion) = 16.46, C22-C23-C24-C25 (terminal inner torsion) = 16.04, C20-C21-C22-C23 (central torsion) = 25.52.

Both helicenes crystallised in a racemic space group, showing interactions between opposite enantiomers. In 5,12-dimethylhexahelicene **26aa**, depicted in ***Figure II.3.10***, π-stacking between D and E rings of opposite enantiomers could be observed, evidenced by a C21-C5 distance of 3.334 Å ($\sum r_{vdW}$(C,C) = 3.40 Å[97]). In the other direction, the A ring of one helicene molecule shows short contacts with the A ring of the opposite enantiomer (C13-C13 = 3.370 Å) and with one proton of a methyl group (C14-H28A =

2.749 Å, $\sum r_{vdW}(\text{C,C}) = 2.90$ Å^{97}).
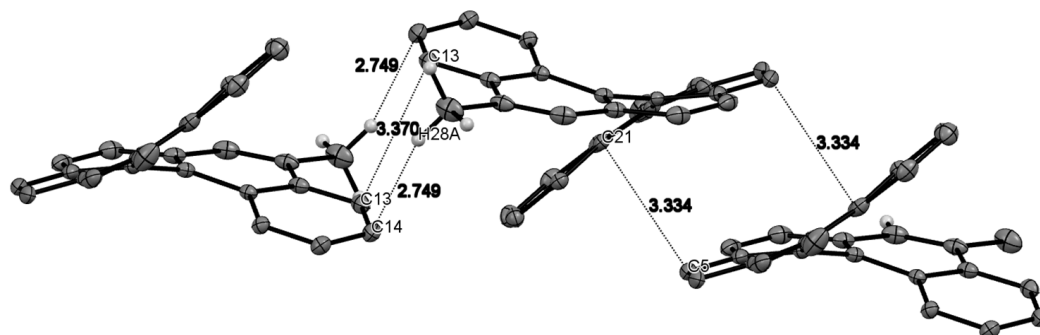
Figure II.3.10. Interactions in the solid state of the different enantiomers of **26aa**.
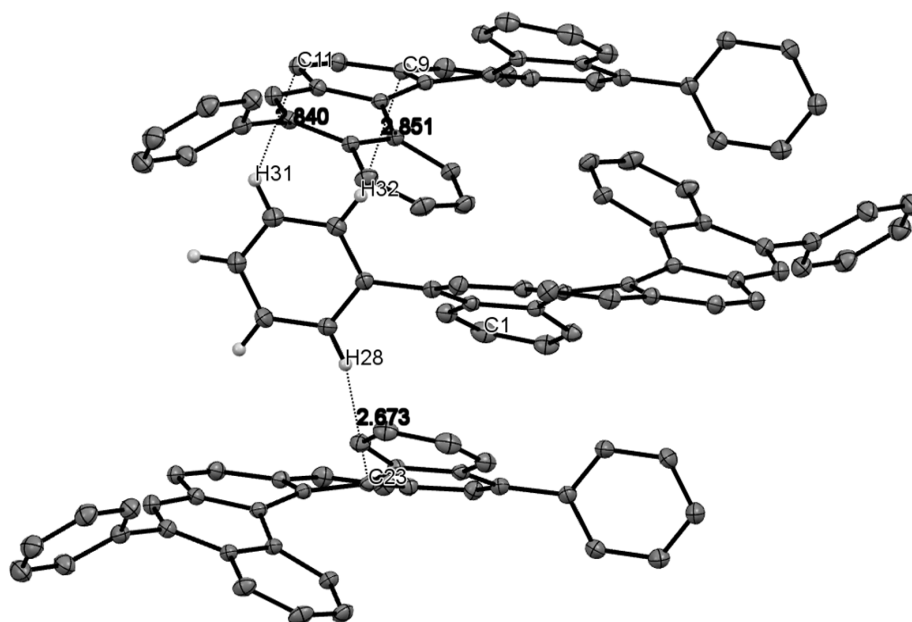
Figure II.3.11. Interactions in the solid state of the different enantiomers of **26ac**.

In the case of 5,12-diphenylhexahelicene **26ac**, the presence of the phenyl substituent forces a different arrangement in the crystal. As can be seen in ***Figure II.3.11***, opposite enantiomers alternate and, even though the helicene backbones are more separated and no C-C short contact is observed, H-π interactions can be found between the hydrogens of the phenyl substituent and two other molecules with opposite helicity. Thus, short contacts are observed between H31-C11 (2.840 Å), H32-C9 (2.851 Å) and H28-C23 (2.673 Å).

II.3.4.2 Enatioselective gold(I)-catalysed hydroarylation

Initial studies:

Since the hydroarylation reaction was successfully tested employing achiral cationic phosphines as ligands, we began a screening of chiral ligands (**Scheme II.3.16**). Initially, the methyl-substituted substrate **27aa** was selected as a test substrate due to the increased regioselectivity of the cyclisation.

In the first place, binuclear gold complexes with chiral bisphosphines BINAP **193** and BIPHEP **194** were tested. These ligands are commercially available and their analogues have proven to successfully promote several enantioselective gold(I)-catalysed transformations.[200] The employment of the binuclear complexes **193** and **194** led to poor regioselectivities and almost no enantioselectivity, as displayed in **Table II.3.6**. Using different amounts of silver salt, 5 mol% or 10 mol%, did not improved significantly the results (entries 1–4).

The worse regioselectivities of the bulky chiral bisphosphine ligands compared with PPh$_3$ highlights additionally that, although the selectivity could depend on the electronic properties of the ligands, sterics also play an important role. This can be explained because, after the nucleophilic attack, the 5-*exo*-dig cyclisation places the gold centre attached to the bulky ligand further away from the substrate backbone, thus relieving steric strain.

The better π-acceptor mononuclear phosphoramidite complexes **195** and **196** (entries 5 and 6), whose BINOL-based ligands are also commercially available, afforded better regioselectivities, but no induction of enantioselectivity was observed. A slight enantiomeric excess (entry 7) was obtained with 3,3'-substituted phosphoramidite gold(I) complex **197**,[§] which has been employed in the enantioselective gold(I)-catalysed cyclopropanation of styrenes.[25a]
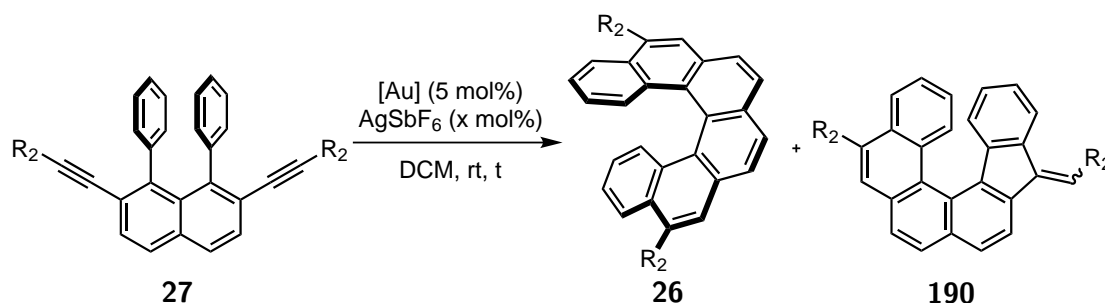
Scheme II.3.16. Gold(I)-catalysed cycloisomerisation of akynes **27** with chiral gold(I) complexes. Results are summarised in **Table II.3.6**.

[§]Compound kindly provided by Fürstner group.
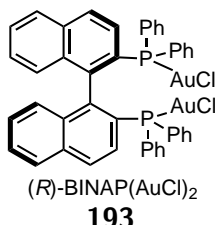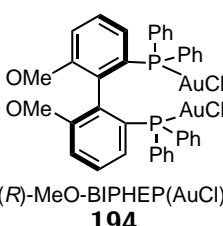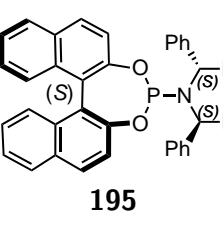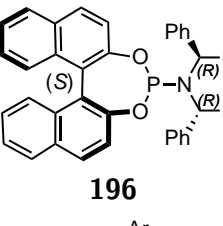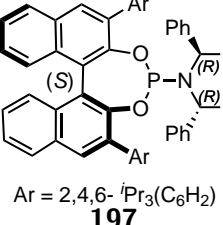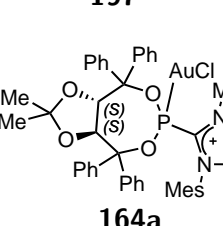
Entry	27	R$_2$	[Au]	x mol%	t(h)	26:190	%ee
1	**27aa**	Me	(R)-BINAP(AuCl)$_2$ **193**	5	15	42:58	0
2	**27aa**	Me	**193**	10	3	52:48	0
3	**27aa**	Me	(R)-MeO-BIPHEP(AuCl)$_2$ **194**	5	1.5	77:23	+8
4	**27aa**	Me	**194**	10	1.5	79:21	+9
5	**27aa**	Me	**195**	5	0.5	86:14	0
6	**27aa**	Me	**196**	5	0.5	98:2	0
7	**27aa**	Me	Ar = 2,4,6-^{i}Pr$_3$(C$_6$H$_2$) **197**	5	0.5	98:2	−8
8	**27aa**	Me	**164a**	5	0.5	90:10	−26
9	**27ab**	tolyl	**164a**	5	0.5	56:44	−80

Table II.3.6: Gold(I)-catalysed cycloisomerisation of alkynes **27aa** and **27ab** employing chiral ligands. Ratio **26**:**190** and %ee were determined by HPLC.

These results contrast with the performance of the newly developed cationic phosphonite gold complex **164a**, which afforded already 26 %*ee*, with also high regioselectivity (entry 8).

Since the substrate substitution pattern could have a major importance to archive good enantioselectivities, substrate **27ab**, with tolyl-substituted alkynes, was tested. The aromatic substituent on the alkyne had a dramatic effect on the enantioselectivity and, under the same conditions with complex **164a**, 5,12-bis(4-methylphenyl)hexahelicene **26ab** was obtained with 80 *ee*%, albeit with lower regioselectivity compared with the methyl-tethered helicene **26aa**.

Optimisation:

Encouraged by the high enantioselectivity obatined with **27ab**, the newly developed cationic phosphonite gold(I) complexes **164a–f**, **165a** and **165d** were tested under the conditions depicted in *Scheme II.3.17*. The obtained results are summarised in *Table II.3.7*.

Initially, lowering the temperature to 0 °C improved the regioselectivity obtained with ligand **159a** at room temperature (compare *Table II.3.6*, entry 9 with *Table II.3.7*, entry 1), at the expense of an increased reaction time. Since utilisation of colder temperatures (entry 2) did not affect the results significantly, 0 °C was selected as standard conditions to test all the developed ligands, to ensure the completion of the reaction in all the cases and to properly evaluate the effect of the different structural features.

Screening of the acetonide-substituted ligands **159b–e**, revealed decreased enantioselectivities when the phenyl groups of the TADDOL were replaced by other aromatic rings (entries 3–7). Biphenyl (L = **159c**, entry 4) and 2-naphthyl (L = **159e**, entry 6) substituents afforded the worse enantioselectivities. Surprisingly, the latter favoured the opposite enantiomer, which probably accounts for a different transition state during the catalysis. Additionally, the gold complex bearing ligand **159f**, with $3,5\text{-}(CF_3)_2(C_6H_4)$ moieties, failed to catalyse the reaction efficiently under the selected conditions likely due to its bulkiness, resulting in a mixture containing mainly the starting material (entry 7).

The regioselectivity decreased with the electron-rich $4\text{-}^tBu(C_6H_4)$ substituents (entry 2) and, conversely, improved with the electron-poor $4\text{-}CF_3(C_6H_4)$ (entry 5). The biphenyl and 2-naphthyl substituted analogues also resulted in increased selectivity towards the formation of hexahelicene compared with ligand **159a**.
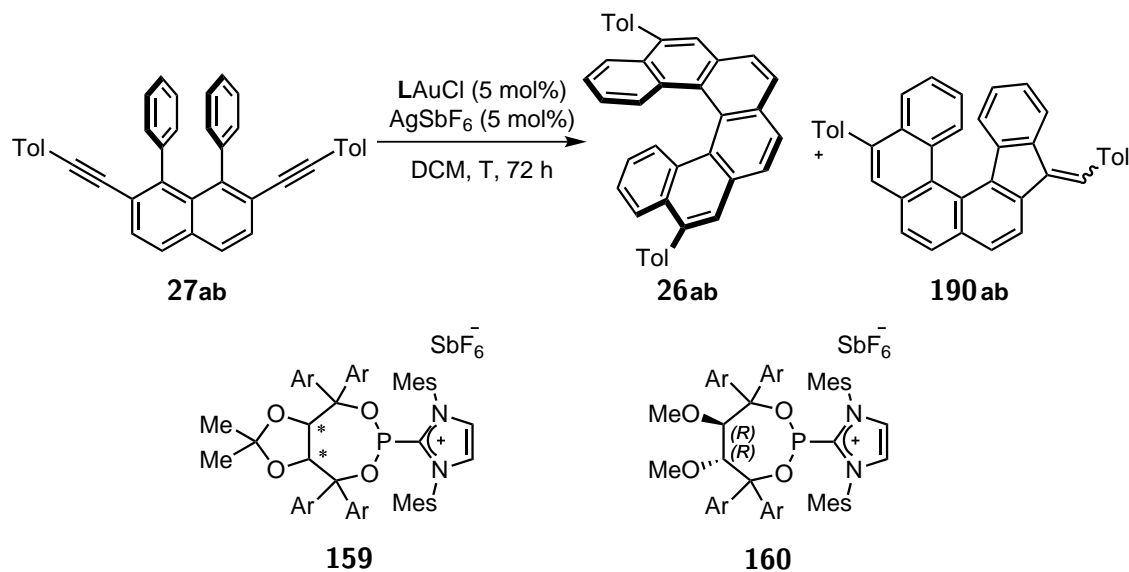
Scheme II.3.17. Gold(I)-catalysed cycloisomerisation of alkyne **27ab** with chiral gold(I) complexes. Results are summarised in **Table II.3.7**.

Entry	L	Ar	T (°C)	Conversion(%)	26:190	%ee
1	(*S*,*S*)-**159a**	Ph	0	99	71:29	−86
2	(*S*,*S*)-**159a**	Ph	-20	98	74:26	−88
3	(*S*,*S*)-**159b**	4-^{t}Bu(C$_6$H$_4$)	0	100	69:31	−63
4	(*S*,*S*)-**159c**	4-Ph(C$_6$H$_4$)	0	100	88:12	−36
5	(*S*,*S*)-**159d**	4-CF$_3$(C$_6$H$_4$)	0	100	89:11	−57
6	(*S*,*S*)-**159e**	2-naphthyl	0	100	98:2	+14
7	(*R*,*R*)-**159f**	3,5-(CF$_3$)$_2$(C$_6$H$_4$)	0	15	89:11	n.d.
8	(*R*,*R*)-**160a**	Ph	0	100	80:20	+77
9	(*R*,*R*)-**160a**	Ph	-20	100	90:10	+82
10	(*R*,*R*)-**160d**	4-CF$_3$(C$_6$H$_4$)	0	100	93:7	+63
11	(*R*,*R*)-**160d**	4-CF$_3$(C$_6$H$_4$)	-20	97	95:5	+82

Table II.3.7: Screening of TADDOL-based cationic phosphonite ligands for the gold(I) catalysed cycloisomerisation of **27ab**. Conversion, ratio **26ab:190ab** and %*ee* were determined by HPLC. All the crude mixtures presented less than 3 % of intermediate **192ab**, except entries 7 and 11 with 47 and 22 % respectively.

Under the same conditions, the utilisation of methoxy-substituted cationic phosphonite ligands such as **160a** and **160d** resulted in diminished enantioselectivities compared with **159a** (entries 8 and 10). Nevertheless, both ligands afforded better

regioselectivities, consisting ligand **160d**, bearing the electron-withdrawing $4\text{-}CF_3(C_6H_4)$ groups, one of the best in this aspect. The greater flexibility of the methoxy protected ligands could explain the improved results, since they can likely more readily adopt conformations with less steric strain between the ligand and the substrate.

Interestingly, the methoxy-substituted gold complexes **165a** and **165d** behaved differently with temperature compared with the acetonide-substituted counterpart **164a**, since a temperature decrease to -20 °C resulted in a greater increase of both enantioselectivities and regioselectivities, reaching 82 % *ee* in both cases (entries 9 and 11). This different temperature effect might be a benefit of the more flexible backbone in the MeO-TADDOL based cationic phosphonites. Unfortunately, the reaction at -20 °C with ligand **160d** did not converted completely to the helicene after 72 h and the resulting mixture still contained 22 % of intermediate **192ab**, the product of just one cyclisation.

In view of the results summarised in *Table II.3.7*, considering enantioselectivity and preference for the 6-*endo*-dig pathway, ligand **160d** afforded the best results. It was therefore selected to further test different reaction conditions to improve the enantioselectivity and reach full conversion without the loss of either enantio- nor regioselectivity.

At -20 °C, substrate **27ab** showed decreased solubility in DCM, slowing the reaction rate further and preventing its completion. Because of this, a variety of solvents were tested in the cycloisomerisation of **27ab** using the selected gold(I) precatalyst **165d** at different temperatures (*Scheme II.3.18*), resulting in the data displayed in *Table II.3.8*. As shown in *Table II.3.8*, other halogenated solvents, such as chloroform, fluorobenzene and chlorobenzene (entries 1–3 respectively), resulted even in decreased conversion compared with DCM at -20 °C, but in a significant increase in the enantioselectivities; the best being with $CHCl_3$ with a 96 % *ee* but just 30 % conversion. The reaction failed in toluene and CCl_4, even at -10 °C and with longer reaction times, recovering only the starting material (entries 4 and 5). Coordinating solvents such as THF, DME and acetone were not tested, since in a preliminary screening with substrate **27aa** they proved to inhibit the cycloisomerisation with cationic phosphonite gold complexes, probably due to the coordination of the solvent to the gold vacant position.

The reaction mixtures with the tested solvents were always not homogeneous, since partial precipitation of the substrate could be observed at low temperatures. Low solubility is a common problem in the chemistry of polyaromatic compounds, and it could account for the lower reactivity of the catalytic system, since the substrate is not in the same phase than the homogeneous gold(I) catalyst, thus preventing substrate activation.
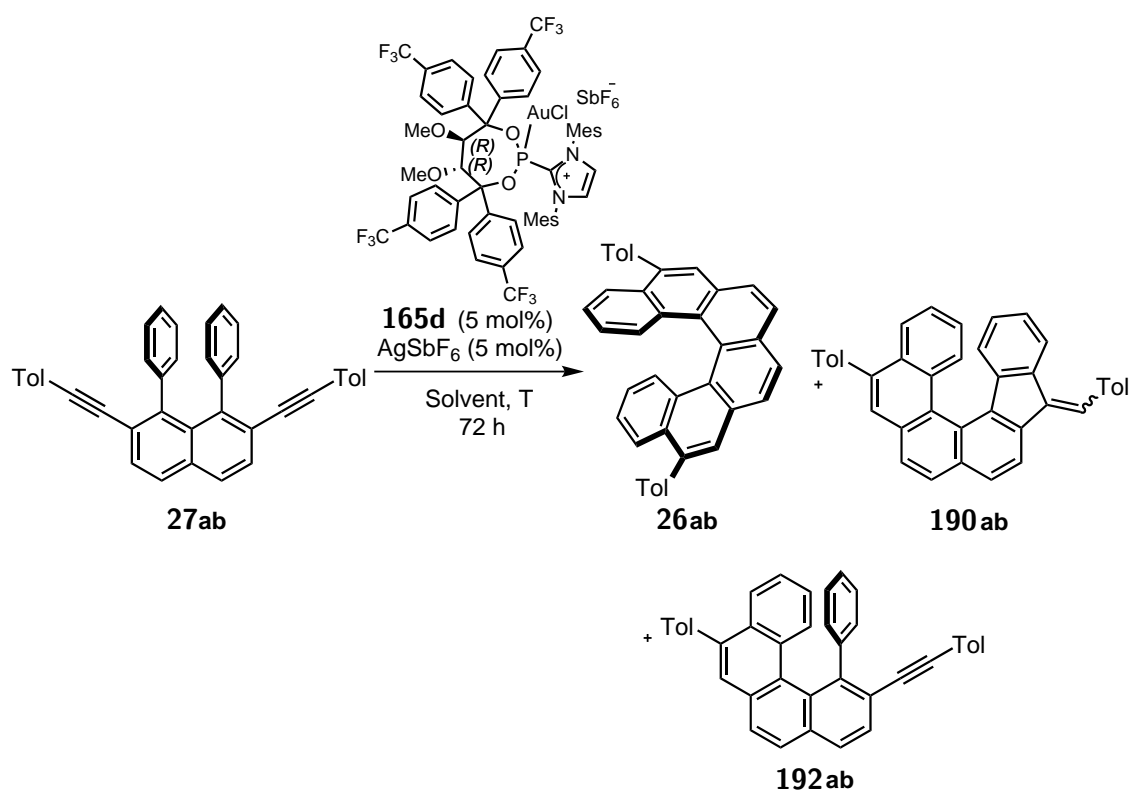
Scheme II.3.18. Gold(I)-catalysed cycloisomerisation of alkyne **27ab** with **165d**. Results are summarised in **Table II.3.8**.

Entry	Solvent	T (°C)	Conversion(%)	26:190:192	%*ee*
1	CHCl$_3$	-20	30	40:0:60	+96
2	C$_6$H$_5$F	-20	68	88:5:7	+90
3	C$_6$H$_5$Cl	-20	53	72:2:26	+92
4[a]	toluene	-10	0	-	-
5[a]	CCl$_4$	-10	0	-	-
6	CHCl$_3$	-10	99	95:5:0	+81
7	CHCl$_3$/1,2-Cl$_2$(C$_6$H$_5$) (1/1)	-20	46	57:2:41	+92
8	CHCl$_3$/1,2-Cl$_2$(C$_6$H$_5$) (1/1)	-10	81	49:3:48	+72
9[a]	CHCl$_3$/DCM (1/1)	-20	86	53:2:45	+86
10[a,b,c]	C$_6$H$_5$F	-20	98	96:3:1	+91

Table II.3.8: Screening of reaction conditions for the enantioselective gold(I)-catalysed cycloisomerisation of **27ab** with **165d**. Conversion, ratio **26ab:190ab:192ab** and %*ee* were determined by HPLC. [a]Reactions were stirred for for 96 h. [b] **165d** 10 mol% and AgSbF$_6$ 10 mol%.[c] 88 % mass recovered.

One approach to increase the solubility is raising the temperature, but, even though at -10 °C the reaction with CHCl$_3$ reached almost full conversion, the enantioselectivity dropped to 82 %*ee* (entry 6). An alternative was to employ solvent mixtures, with chloroform that afforded the highest enantiomeric excess, and another solvent, which would better dissolve the substrate and/or the reaction intermediate. Although CHCl$_3$/1,2-Cl$_2$(C$_6$H$_5$) (1/1) and CHCl$_3$/DCM (1/1) mixtures improved the conversion compared to only chloroform, the reaction was not finished and additionally worse *ee* values were obtained (entries 7 and 8).

Since the reactions in chloroform did not succeed on reaching full conversion with good enantioselectivity, we decided to employ fluorobenzene, the solvent displaying higher conversion at -20 °C, and increase the loading of **165d** and AgSbF$_6$ to 10 mol%. We were pleased to observe that the reaction under this conditions reached completion, with excellent regioselectivity for the formation of the hexahelicene **26ab** and with very good enantioselectivity, reaching 91 %*ee*. The measurement of the specific rotation of this sample, $[\alpha]_D^{20} = +1402$ ($c = 0.25$, DCM), showed that the configuration of the major enantiomer of **26ab** is likely the (*P*)-enantiomer, since as a general trend, (*P*)-helicenes are dextrorotatory ($\lambda = 589$ nm).

Additionally, the control experiments summarised in ***Table II.3.9*** were conducted. The cycloisomerisation under the optimised conditions did not proceed without the presence the gold precatalyst, recovering completely the starting material, discarding the activation of the alkyne by silver that would lead to a racemic product.

In order to evaluate the effect of the imidazolium substituent, phosphoramidite gold complexes **198** and **199**, with the same TADDOL backbone as **165d**, were synthesised employing an analogous procedure to the one developed by Fürstner and co-workers for other phosphoramidite gold complexes.[25] Under the optimised conditions, compound **198** showed no catalytic activity and the starting material could be recovered.

Because of this, to compare the performance of TADDOL-based phosphoramidite gold complexes **198** and **199** with the cationic phosphonite counterparts, the reaction temperature was increased to 0 °C, and conducted in DCM, thus reaching completion in both cases. The regioselectivity proved to be worse with both phosphoramidite-gold complexes than with **165d** and, although the enantioselectivity was higher with the matched diasteromer **198**, low enantiomeric excess values were obtained in both cases (entries 3 and 4). Bis-phosphine gold(I) complex BINAP(AuCl)$_2$ **193** was additionally tested under these conditions, showing no reactivity in the cycloisomerisation of **27ab** (entry 5).
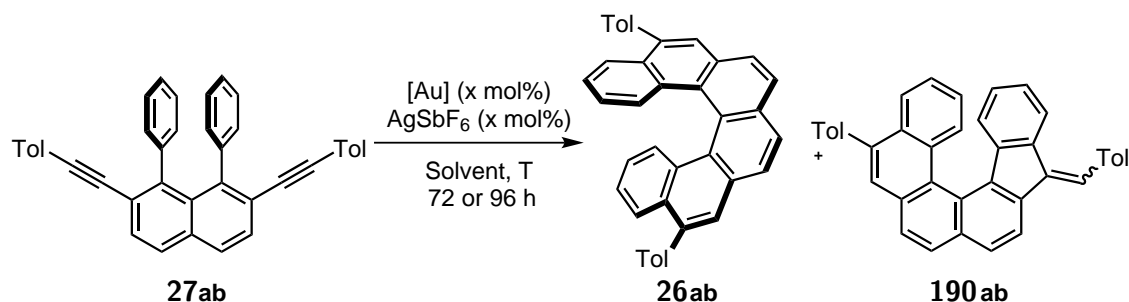
Scheme II.3.19. Control experiments on the Gold(I) catalysed cycloisomerisation of akyne **27ab**. Results are summarised in **Table II.3.8**
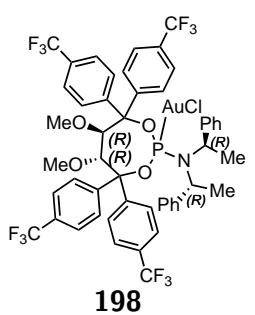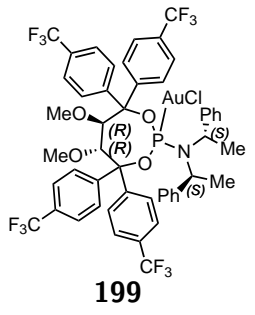
Entry	[Au]	x mol%	solvent	T(°C)	Conversion(%)	26:190	%ee
1[a]	none	10	C_6H_5F	−20	0	-	-
2[a]	**198**	10	C_6H_5F	−20	0	-	-
3[b]	**198**	5	DCM	0	100	81:19	+40
4[b]	**199**	5	DCM	0	100	73:27	+24
5[b]	BINAP(AuCl)$_2$ **193**	5	DCM	0	0	-	-

Table II.3.9: Control experiments on the gold(I)-catalysed cycloisomerisation of alkyne **27ab**. Conversion, ratio **26ab:190ab** and %ee were determined by HPLC. [a]Reactions were stirred for 96 h. [b]Reactions were stirred for 72 h.

These control experiments support that the introduction of the imidazolium substituent has the expected effect, rendering the cationic phosphonites less electron releasing and more π-accepting ligands than phosphoramidites and, therefore, their gold complexes are more Lewis acidic and reactive in the cycloisomerisation of **27ab** leading

to **26ab**. Furthermore, the imidazolium substituent was beneficial for the enantioselectivity of the reaction since, under the same conditions, complex **165d** afforded higher enantiomeric excess (***Table II.3.7***, entry 8) than phosphoramidite-gold(I) complexes **198** and **199**.

These results highlight the convenience of cationic phosphonites in the selected transformation, since compound **165d** could promote the formation of the desired helicene **26ab** with excellent regioselectivity and enantioselectivity under reaction conditions on which other chiral gold complexes remained unreactive. Furthermore, unlike the parent phosphoramidites in gold(I) catalysis, good enantioselectivities were obtained when the chiral information was carried solely on the diol part of the molecule, avoiding the utilisation of expensive secondary chiral amines.$^{\|}$

Furthermore, the regio- and enantioselectivities (94 % selectivity, 91 %*ee*) obtained for hexahelicene **26ab** open a novel pathway for the synthesis of carbohelicenes, which have been rarely synthesised enantioselectively in the existing literature.

$^{\|}$(-)-Bis[(*S*)-1-phenylethyl]amine 38.3 €/g; (+)-Bis[(*R*)-1-phenylethyl]amine 42.5 €/g (Sigma-Aldrich).

Preliminary scope:

With the optimised conditions in hand, we decided to test the cycloisomerisation in the series of substrates whose preparation was presented in Section II.3.3, and evaluate the substrate scope. The results are summarised in ***Table II.3.10***.
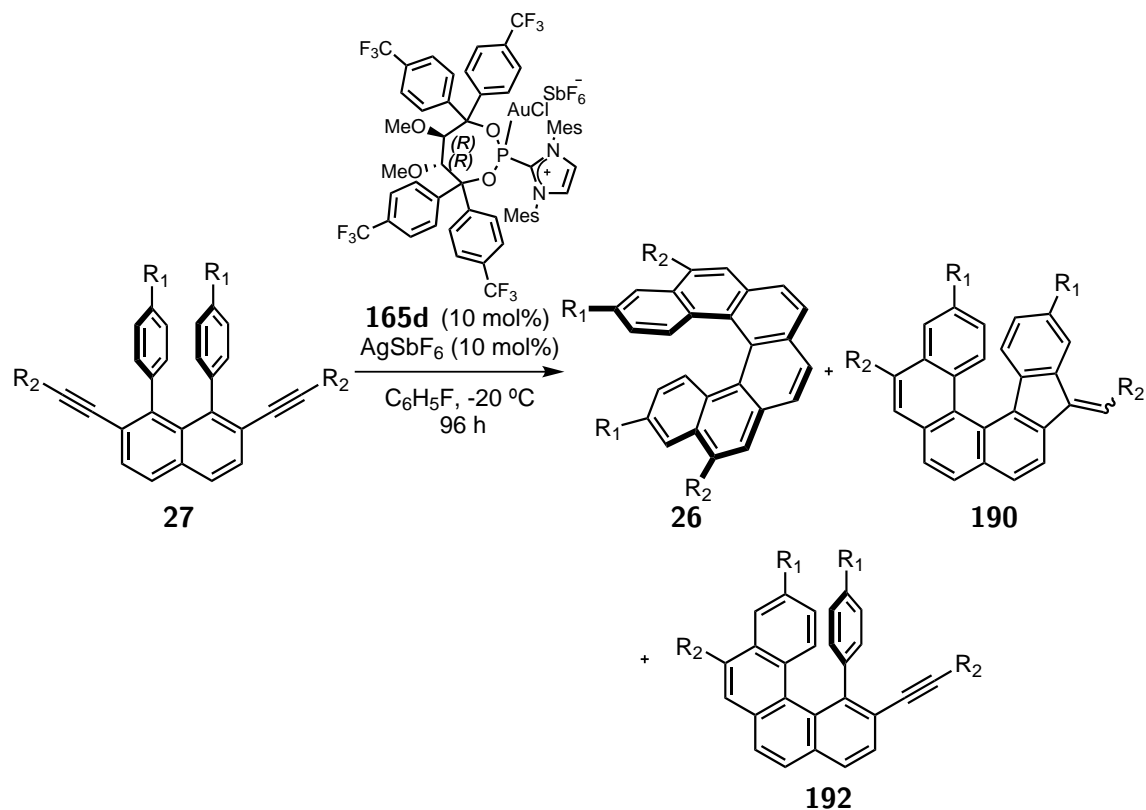
Scheme II.3.20. Gold(I) catalysed cycloisomerisation of substrates **27** with different substitution patterns under the optimised conditions. Results are summarised in ***Table II.3.10***.

Entry	27	R$_1$	R$_2$	Conv.(%)	26:190:192	% mass recov.	%*ee*
1	**27aa**	H	Me	100	99:1:0	82	63
2	**27ac**	H	Ph	95	82:4:14	77	92
3	**27ad**	H	xylyl	94	57:4:38	99	89
4[a]	**27ae**	H	4-Cl(C$_6$H$_4$)	31	81:3:16	-	97
5	**27ba**	OMe	tolyl	100	88:12:0	99	78
6	**27c**	Ph	tolyl	100	97:3:0	84	82
7	**27d**	Cl	tolyl	0	-	-	-

Table II.3.10: Preliminary scope of the cycloisomerisation reaction leading to hexahelicene derivatives. Conversion (Conv.), ratio **26:190:192** and %*ee* were determined by HPLC. Mass recov. = mass recovered. [a]Reaction conducted by Leo Nicholls.

As previously observed in the initial screening, replacing the aromatic substituent on the alkyne by a methyl group resulted in a significant drop of enantioselectivity (entry 1, 63 %*ee*). Nevertheless, the outcome under the optimised conditions improved compared with the initial results and 5,12-dimethylhexahelicene **26aa** was obtained with excellent regioselectivity.

The presence of an aromatic substituent on R_2 proved to be crucial for obtaining excellent enantioselectivities, which may result from additional π-interactions between the substrate and the chiral ligand. Replacing the tolyl substituent by other aromatic groups did not affect substantially the enantioselectivity of the reaction (entries 2–5), and compounds **27ac-ae** were obtained with very good enantioselectivities (89–97 %*ee*) and excellent regioselectivities. Unfortunately, some reactions were not complete, obtaining thus mixtures of the desired hexahelicene derivatives **26** with the intermediate **192** and the starting material **27**. These differences in reactivity are probably caused by the lower solubility in fluorobenzene at the optimised conditions of substrates **27ac-ae** and/or the corresponding intermediates compared with the tolyl-substituted analogue **27ab**.

The introduction of different substituents on R_1 led to different outcomes. The reaction of the substrate **27ba**, bearing the electron releasing MeO-groups, led to diminished regioselectivity and enantioselectivity (entry 5). Conversely, the formation of **26c**, with $R_1 =$ Ph, occurred under the optimised conditions with excellent regioselectivity and still high enantiomeric excess (entry 6, 82 %*ee*). Unfortunately, substrate **27d**, with the electron-withdrawing chloro-substituents, was completely unreactive under the optimised conditions. This could be explained by the decreased electron density on the Cl-tethered aromatic rings, that renders them less nucleophilic, inhibiting thus the attack to the alkyne.

The specific rotation measurement of hexahelicenes **26aa–c** solutions revealed that all the compounds are dextrorotatory ($\lambda = 589$ nm), in analogy with 5,12-bis(4-methylphenyl)hexahelicene **26ab**, meaning that the same enantiomer is obtained with all of the tested substrates. Since in most of the cases (P)-helicenes are dextrorotatory, it is highly likely that the major enantiomer of the obtained hexahelicenes has (P)-helicity.

In view of this results, we can conclude that the developed enantioselective gold(I)-catalysed hydroarylation of substrates **27** affords a series of hexahelicenes **26** with different substituents with good to excellent regioselectivities and moderate to very good enantioselectivities. The outcome of the reaction was sensitive to the nature of the substituents on both the alkyne and the aromatic rings involved in the nucleophilic attack and further evaluation of their effect is still necessary.

As discussed during the Introduction, efficient catalytic enantioselective reactions

leading to carbohelicenes are very scarce in the literature, and they normally suffer from narrow substrate scopes. The preliminary scope is very promising, since it showed that the proposed strategy seems to tolerate a variety of substituents and hexahelicene derivaties **26ab–c** were obtained with good to excellent enantioselectivities. Nevertheless, to prove the generality of the developed methodology, the substrate scope still needs to be extended.

Synthesis of 5-*exo*/5-*exo* isomer:

It is important to highlight that complex **168**, with a carbodiphosphorane substituent, was also tested at 0 °C in DCM (***Scheme II.3.21***), affording a compound that was not observed before and did not match the spectroscopic data of the hexahelicene **26ab**, the isomer **190ab** or the intermediate **192ab**, although mass spectrometry analysis revealed that it corresponded to another isomer of these compounds.
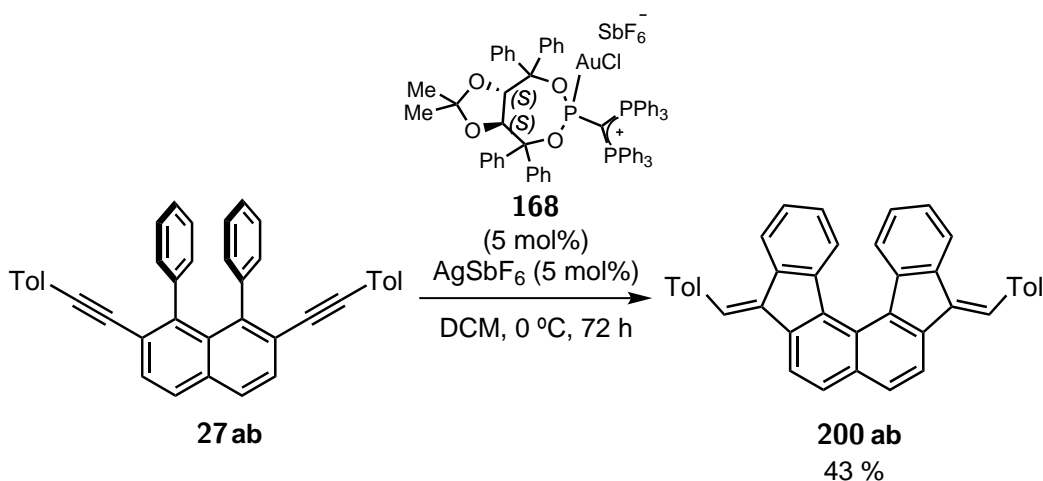
Scheme II.3.21. Gold(I) catalysed cycloisomerisation of akyne **27ab** with **168**.

Finally, its structure could be elucidated by X-ray (***Figure II.3.12***), confirming the formation of isomer **200ab**, the product of two consecutive 5-*exo* cyclisations. This difference in selectivity again validates the influence of the ligand bulkiness in the selectivity of this cycloisomerisation, since the huge size of compound **168** resulted almost exclusively in the formation of the isomer **200ab** (78 % selectivity according HPLC), that avoids steric clashes between the bulky ligand and the helicene backbone.

The solid state structure of the isomer **200ab** shows the characteristic distorted aromatic structure of helicenes, but, due to the presence of two five-membered rings, the in-plane turn is smaller and the terminal aromatic rings do not overlap to any extent. Because of this less hindered helical structure, enantiomers may racemise under milder

conditions than hexahelicenes **99** and **26**. Indeed, all the attempts to separate the enantiomers by HPLC failed, thus indicating that probably compound **200ab** isomerises at room temperature. Nevertheless, compounds such as **200ab** have not been previously described in the literature and their study might warrant attention in the future.
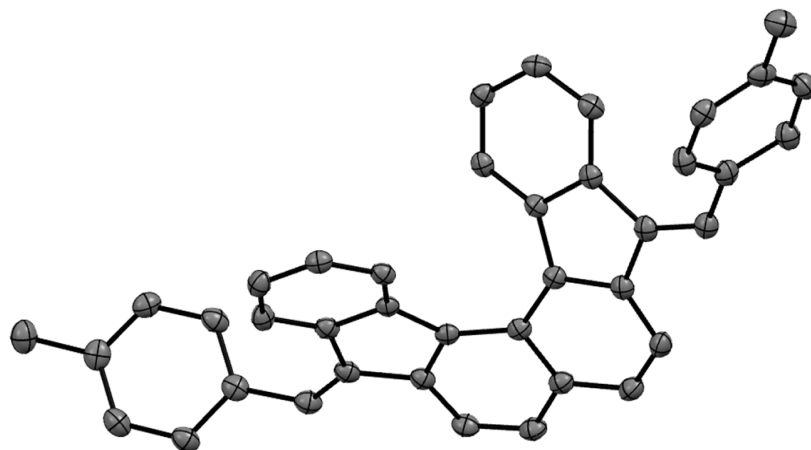
Figure II.3.12. Solid state structure of **200ab**. Thermal elipsoids at 50 % probability.

II.3.5   Dynamic NMR studies

In parallel with the optimisation of the double hydroarylation reaction, dynamic NMR studies were conducted in order to gain insight into the reaction mechanism and find the enantio-determining step.[#]

As mentioned in Section II.3.4., the reaction of **27** leading to hexahelicene **26** consists of two consecutive hydroarylation reactions (***Scheme II.3.22***). Therefore, if intermediate **192** has already a stable chiral axis, the enantioselectivity of the reaction would be determined in the first cyclisation. Conversely, if intermediate **192** rapidly racemises, the enantioselectivity of the hexahelicene derivative **26** would result from a dynamic kinetic resolution, stemming from the preferred reaction of the chiral catalyst with one of the intermediate enantiomers.
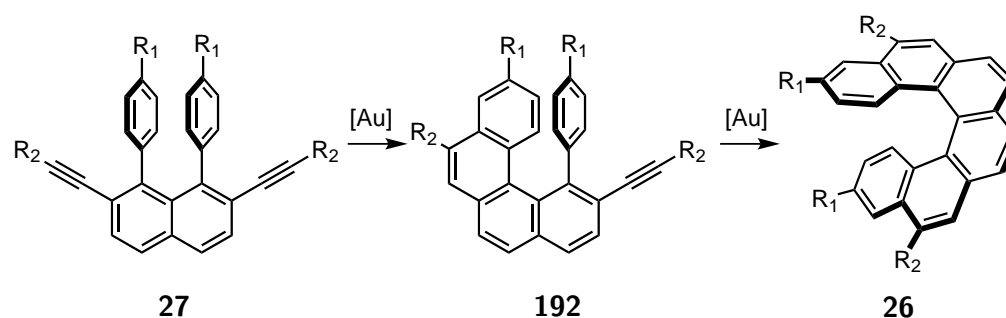
Scheme II.3.22. Steps in the gold(I)-catalysed cycloisomerisation of substrates **27**.
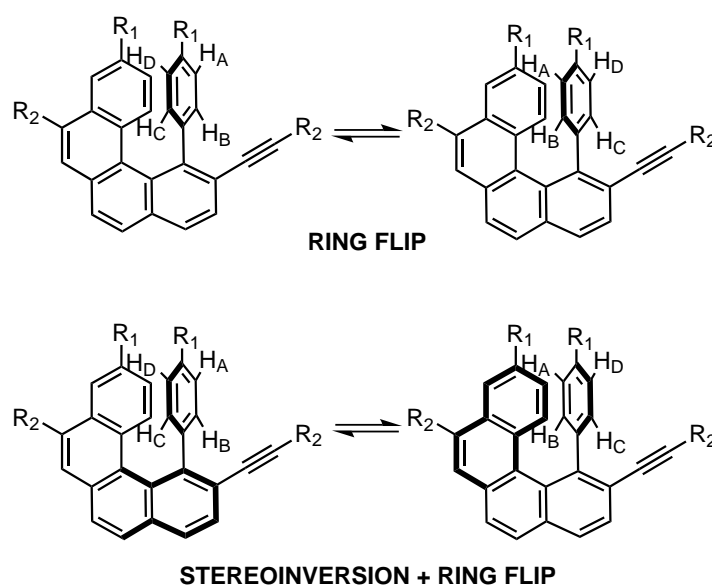
Figure II.3.13. Motions on **192** leading to conformational changes.

Two relevant motions in compound **192** can be considered (**Figure II.3.13**), the rotation of the aromatic ring (ring flip) and the racemisation of the tetrahelicene backbone, that probably involves a concomitant counter-clockwise rotation of the aromatic unit in a cog-wheel-like movement (stereoinversion+ringflip).[213] We can consider both motions as an equilibrium between two conformers, with the same energy and equivalent rate constants in both directions, following a first order kinetics. In order to ascertain which is the enantio-determining step, the kinetic constants and thermodynamic parameters of these two motions in the intermediates **192aa** and **192bb** were determined by DNMR studies.

Initially, intermediate **192aa**, with $R_1 = $ H and $R_2 = $ Me, could be isolated and fully assigned by multinuclear NMR analysis, displaying broad signals in its ^{1}H-NMR spectrum.
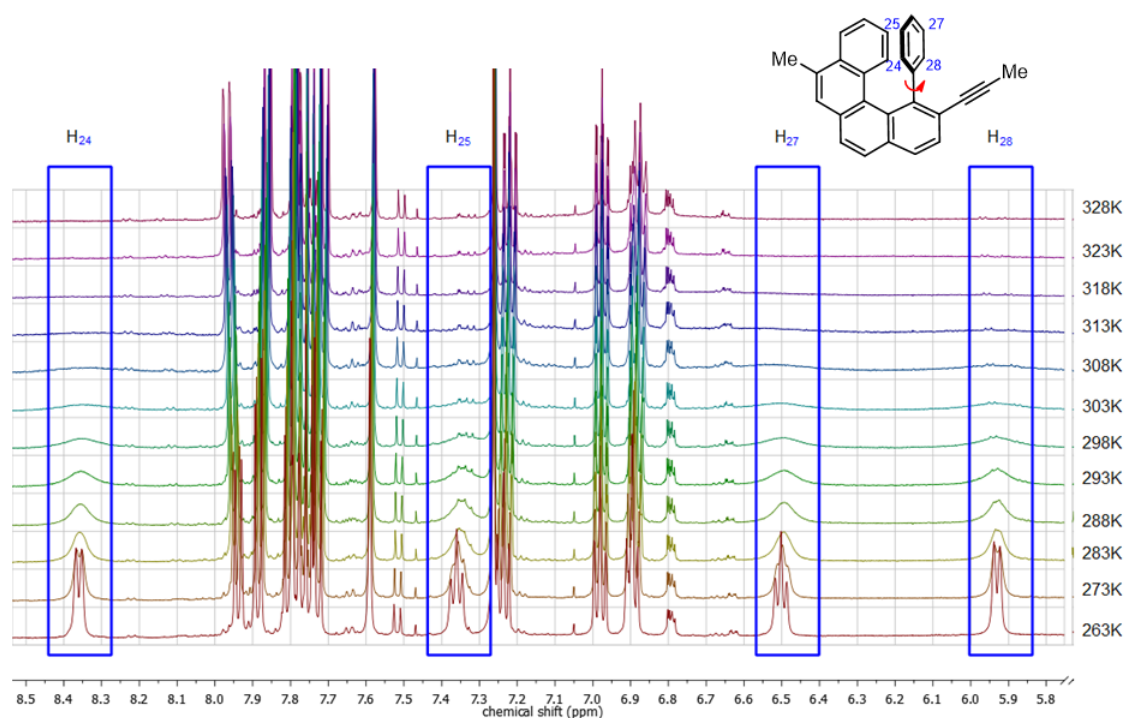
Figure II.3.14. Stacked ^{1}H-NMR spectra of **192aa** at different temperatures (263–328 K).

Variable temperature ^{1}H-NMR studies revealed the presence of a chemical exchange process due to the signal broadening in the aromatic region, which were assigned to *meta*- (H25 and H27 at 7.36 and 6.90 ppm respectively) and *ortho*- protons (H24 and H28 at 8.37 and 5.94 ppm respectively) on the phenyl ring (see Experimental section and Appendix A for the assignment). These signals merged to afford two peaks, one for H25-H27 and another for H24-H28, at an approximate coalescence temperature (T_c) of $\sim$ 318 K (**Figure II.3.14**).

The line shape of a NMR signal can be related with the exchange rate that produces the signal broadening through the Bloch equations. At the coalescence point, several approximations can be made and the exchange rate is determined by **Equation II.3.1**, where $\Delta\delta$ is the chemical shift difference in Hz of the exchanging nuclei.

$$k_{exchange} = \frac{\pi\Delta\delta}{\sqrt{2}} \qquad (II.3.1)$$

We can then estimate the energetic barrier of the exchange process ($\Delta G^{\ddagger}$) by replacing $k_{exchange}$ in the Eyring equation (**Equation II.3.2**) and solving for $\Delta G^{\ddagger}$, resulting in **Equation II.3.3**. Thus, the energetic barrier of the rotation can be estimated with **Equation II.3.3**, where T_c is the coalescence temperature and a is a conversion constant (4.575×10^{-3} kcal/molK).[214]

$$k = \frac{k_b T}{h} e^{\frac{-\Delta G^{\ddagger}}{RT}} \qquad (II.3.2)$$

$$\Delta G^{\ddagger} = aT_c\left[9,972 + \log\left(\frac{T_c}{\Delta\delta}\right)\right] \qquad (II.3.3)$$

Using this equation, estimate values of $\Delta G^{\ddagger} = 14.7$ kcal/mol (61.5 kJ/mol) were obtained for the ring flip of the phenyl group in the intermediate **192aa** at the coalescence temperature (318 K). This corresponds to an energy barrier to rotation higher than for mono-*ortho*-substituted biphenyls (5.9–10.2 kcal/mol, 24.7–42.7 kJ/mol)[215] but considerably lower than for 2,2'-di-*iso*-butylbiphenyl (26.4 kcal/mol, 110.4 kJ/mol), whose atropoisomers can be separated at room temperature.[216]

In order to obtain more details concerning the enthalpic $\Delta H^{\ddagger}$ and entropic $\Delta S^{\ddagger}$ contributions on this process, the obtained exchange rates at different temperatures were plotted in an Eyring plot using **Equation II.3.5**: the linear form of the Eyring equation (**Equation III.1.2**); which is obtained after substitution of $\Delta G^{\ddagger}$ according to the third law of thermodynamics (**Equation II.3.4**). The exchange rates at the temperature range 263–328 K could be determined by line-shape analysis using the DNMR module of Topspin 3.2, fitting the simulated spectra with the experimental signal lines.

$$\Delta G^{\ddagger} = \Delta H^{\ddagger} - T\Delta S^{\ddagger} \qquad (II.3.4)$$

$$\ln\left(\frac{k}{T}\right) = -\frac{\Delta H^{\ddagger}}{RT} + \frac{\Delta S^{\ddagger}}{R} + \ln\left(\frac{k_b}{h}\right) \qquad (II.3.5)$$

The resulting Eyring plot (**Figure II.3.15**) displayed the expected linear tendency, affording after linear regression the values of $\Delta H^{\ddagger} = 55.57$ kJ/mol and $\Delta S^{\ddagger} = -0.0163$

kJ/molK. With these values it is possible to calculate $\Delta G^{\ddagger}_{253K}$ at -20 °C, the optimal temperature for the catalysis, as 59.70 kJ/mol and also the rate of the ring flip as $k_{ringflip} = 2.49$ s^{-1}, indicating that the rotation of the phenyl ring is a fast motion.
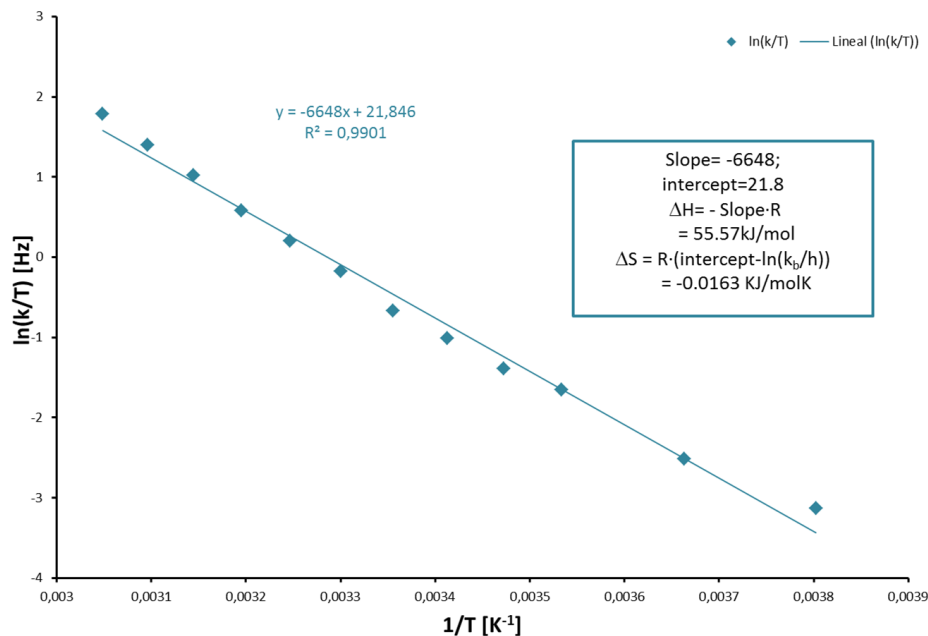
Figure II.3.15. Eyring plot for the ring flip of **192aa**.

The stereoinversion of the tetrahelicene backbone in this case could not be determined, since the racemisation leads to two enantiomers, that cannot be differentiated by NMR analysis.

Because of this, chiral intermediate **192bb** was synthesised (see structure in ***Figure III.1.4***). The presence of the additional chiral centres renders both isomers with different helicity diastereomers, and therefore, their analysis should be possible by ^{1}H-NMR spectroscopy. Indeed, compound **192bb** exhibits two sets of NMR data at low temperatures (233 K, see Appendix A), when the racemisation is slow on the NMR-time scale.

In the measured temperature series, two coalescence phenomena at different coalescence temperatures can be observed. In the same fashion as **192aa**, one involves the coalescence of the *ortho-* (H21 and H25) and *meta-* (H22 and H24) protons in the *p*-methoxyphenyl group due to the ring rotation ($T_c \sim 318K$). The other is the coalescence of diastereomeric pairs for all of the ^{1}H-NMR signals due to the stereoinversion of the tetrahelicene ($T_c \sim 338K$) and can be directly related with the stability of the chiral axis in the intermediate **192bb**. In order to calculate $\Delta G^{\ddagger}$ of these processes, we focused on the phenyl ^{1}H-NMR signals (*ortho-*^{1}H: 6.11 and 8.31 ppm, *meta-*^{1}H: 5.91 and 6.88 ppm at 233 K) for the ring flip motion (***Figure II.3.16***) and on the methoxy

[1]H signals (3.26 and 3.16 ppm at 333 K) for the stereoinversion (*Figure II.3.17*).
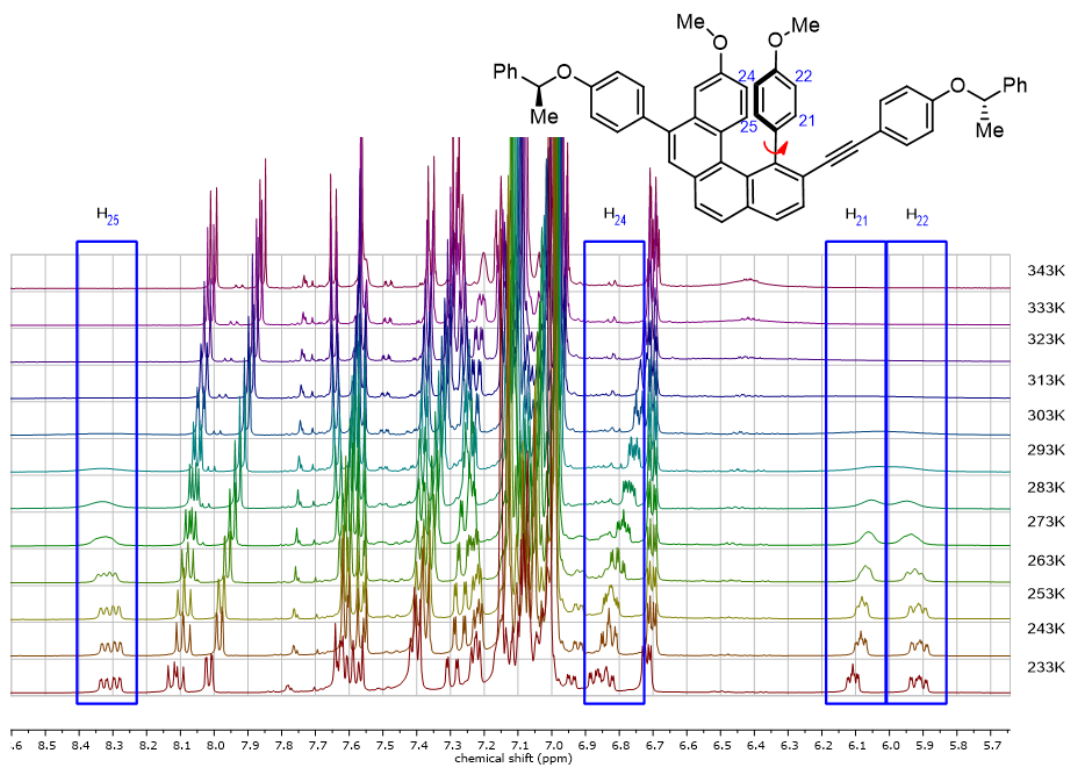
Figure II.3.16. Stacked ^{1}H-NMR spectra of **192bb** at different temperatures (233–343 K).
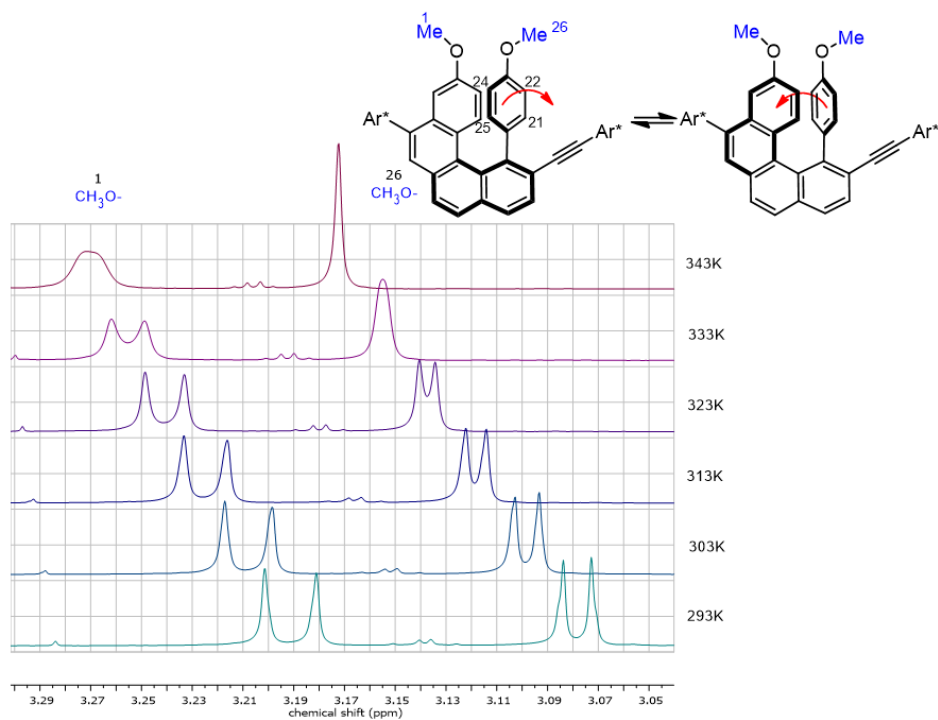
Figure II.3.17. Stacked ^{1}H-NMR spectra of **192bb** at different temperatures (293–343 K). Ar* = (*S*)-4-(1-phenylethoxy)phenyl

Estimation of the free energy of activation ($\Delta G^{\ddagger}$) using **_Equation II.3.3_**, afforded values of $\Delta G^{\ddagger}_{ringflip}$ = 14.2 kcal/mol (59.4 kJ/mol) and $\Delta G^{\ddagger}_{stereoinv.}$ = 17.8 kcal/mol (74.5 kJ/mol) for the ring flip and for the stereoinversion processes respectively at the corresponding coalescence temperatures. These results are in agreement with the results for **192aa** and with those obtained in a previous study by Laarhoven *et al.* They studied the energy barriers for the motions on 1-aryl-tetrahelicenes, including the ring flip of the aryl group and the stereoinversion of the tetrahelicene, reporting values of $\Delta G^{\ddagger}_{ringflip}$ between 13.2–16.4 kcal/mol, depending of the substitution pattern of the aryl group, and $\Delta G^{\ddagger}_{stereoinv.}$ of 16.1–17.0 kcal/mol.[213]

The estimated $\Delta G^{\ddagger}$ values obtained for the intermediate **192bb** indicate that the stereoinversion of the tetrahelicene backbone is more difficult than the simple rotation of the aromatic ring, but still both processes occur rapidly at room temperature. In comparison, the stereoinversion barrier for hexahelicene **99**, the first analogue in the helicene series with configurationally stable axis at room temperature, is 35.8 kcal/mol (149.8 kJ/mol),[119a] considerably higher than the stereoinversion of the tetrahelicene in compound **192bb**.

Again, in order to determine the contributions of the enthalpy $\Delta H^{\ddagger}$ and entropy $\Delta S^{\ddagger}$ of activation, the data was plotted $(1/T)$ *vs* $\ln(k/T)$ (**_Figure II.3.18_**). The chemical exchange rates were obtained in the same fashion as for the intermediate **192aa**, by line fitting of simulated spectra with the obtained NMR data. Lineal regression of the data $(1/T)$ *vs* $\ln(k/T)$ and **_Equation II.3.5_** allowed us to calculate the values of $\Delta H^{\ddagger}_{ringflip}$ = 51.71 kJ/mol and $\Delta S^{\ddagger}_{ringflip}$ = -0.025 kJ/molK for the ring flip and $\Delta H^{\ddagger}_{stereoinv.}$ = 33.47 kJ/mol and $\Delta S^{\ddagger}_{stereoinv.}$ = -0.128 kJ/molK for the stereoinversion.

Surprisingly, the $\Delta H^{\ddagger}$ for the stereoinversion is lower than for the flip of the aromatic moiety. In contrast, the contribution of $\Delta S^{\ddagger}$ is much larger for the stereoinversion motion, indicating that the entropy decreases in order to attain the transition state. This hints to an interplay between the two motions, since in order for the racemisation of **192bb** to be possible, the free aromatic ring must rotate and slip around the tetrahelicene backbone, reaching a highly ordered transition state where the aromatic ring and the tetrahelicene backbone are perpendicular. These results are consistent with the high entropy contributions found in the racemisation of other helicenes, where similar transition states have been proposed.[118,119]

The thermodynamic parameters $\Delta H^{\ddagger}$ and $\Delta S^{\ddagger}$ allowed us to calculate $\Delta G^{\ddagger}$ for both motions at -20 °C employing **_Equation II.3.4_** ($\Delta G^{\ddagger}_{ringflip,253K}$ = 58.04 kJ/mol and $\Delta G^{\ddagger}_{stereoinv.,253K}$ = 65.85 kJ/mol). Thus, the rate of the motions at -20 °C, the temperature of the optimised conditions, could be obtained from **_Equation II.3.2_** affording $k_{ringflip,253K}$ = 5.48 s^{-1} and $k_{stereoinv.,253K}$ = 0.134 s^{-1} for the ring flip and

stereoinversion respectively.
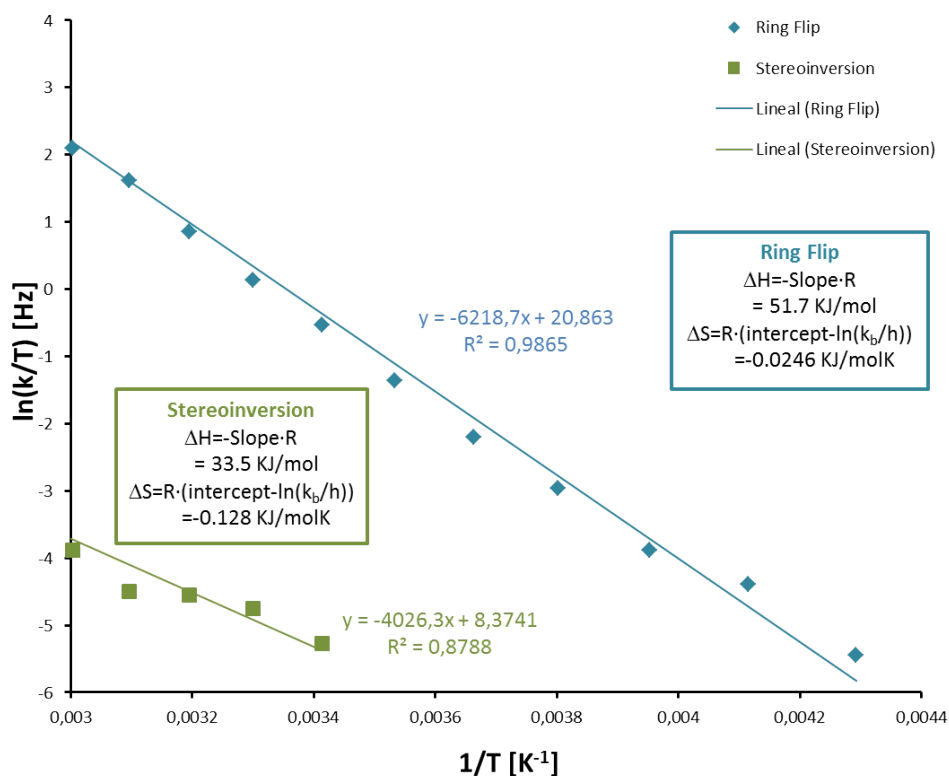
Figure II.3.18. Eyring plots for the ring flip and stereoinversion motions in intermediate **192bb**.

The half life of one diastereomer can be additionally calculated from the rate of stereoinversion of the tetrahelicene scaffold employing ***Equation II.3.6***, considering that the racemisation follows a first-order kinetics, in analogy to the racemisation of other helicenes.

$$t_{1/2}(diasteromer) = \frac{\ln 2}{k_{stereoinv.}} \qquad (II.3.6)$$

Thus the half life of each diastereomer of **192bb** at -20 °C is 5.17 s, a very small time lapse, compared with the reaction time (96 h). Since the substitution patterns for the rest of the substrates are similar, we can extrapolate these results and conclude that the racemisation of intermediate **192** at -20 °C is facile and therefore, the enantioselectivity determining step is the second cyclisation, resulting in a dynamic kinetic resolution of **192**.

II.4. Conclusion and Summary

In summary, we were able to obtain hexahelicenes **26** with a novel substitution pattern, through a gold(I)-catalysed double hydroarylation of aryl-tethered bis-alkynes **27** in excellent regio- and enantioselectivities. The developed reaction constitutes a novel enantioselective approach to helicenes. Even though the chirality of helicenes is normally a crucial property for their applications, enantioselective syntheses are still scarce.

Chiral, cationic phosphonite gold(I) complexes, described for the first time in this thesis, proved to be superior in the selected transformation in terms of regio- and enantioselectivity if compared with other classical chiral gold(I) complexes. Moreover, they were able to maintain their catalytic activity even at low temperatures, under conditions at which the reactivity of other catalysts bearing phosphoramidite and/or phosphine chiral ligands was completely inhibited. These results proved that, in the same fashion as the synthesis of phenanthrenes, the reaction rate of the gold(I)-catalysed hydroarylation of **27** is enhanced when using excellent π-acceptor and poor σ-donor ligands. Lowering the temperature and using fluorobenzene as solvent, was decisive to achieve excellent enantioselectivities for the synthesis of **26ab**, that could be obtained in up to 91 %*ee* with 94 % of selectivity towards the formation of 5,12-bis(4-methyl-phenyl)hexahelicene.

The optimised conditions could be further applied to different substrates **26aa–c**, which were synthesised through a highly modular and reliable approach. Moderate to excellent enantioselectivities were obtained with a variety of substituents. Note however that aromatic groups on the alkyne moiety proved to be necessary to obtain good enantioselectivities.

Finally, using dynamic NMR spectroscopy studies, we could examine the enantio-determining step of the reaction, concluding that the enantioselectivity is produced by a dynamic kinectic resolution of the enantiomers of intermediate **192**.

Now further research in the broadening and improvement of the substrate scope of this reaction is being conducted in our research group to prove the generality of the developed methodology. The introduction of other functional groups on the substrates, such as silanes and benzylic alcohols, could allow the derivatisation of the obtained helicenes by cross-coupling or substitution reactions. Scaling-up of the procedure would

also be interesting in order to obtain larger quantities of the hexahelicenes **26aa-c** and study their properties in more detail.

Since helicenes **26aa–c** have an unprecedented substitution pattern, the study of their electronic and chiroptical properties and their variation depending on the substituents is important in order to evaluate their potential applications in material science, molecular electronics and photonics and self-assembling properties. The presence of additional functional groups, like in the case of MeO-substituted **26ba**, could also allow their application in molecular recognition and asymmetric catalysis, since they could serve as a functional group handle to be employed in synthesising novel chiral ligands or organocatalysts.

Part III

Experimental section

III.1. Experimental procedures and characterisations

III.1.1 General considerations

III.1.1.1 General experimental procedures

All manipulations were carried out under argon atmosphere either in flame-dried glassware on a Schlenk line or in an MBraun Labmaster 130 Glovebox, unless stated otherwise. The solvents employed for the reactions were purified by distillation over the drying agents indicated and were stored and handled under argon atmosphere: THF, Et$_2$O (Mg/anthracene), CH$_2$Cl$_2$, CHCl$_3$, fluorobenzene, chlorobenzene, 1,2-dichloro-benzene, pyridine, NEt$_3$ (CaH$_2$, stored over 4 Å molecular sieves), n-pentane, toluene (Na/K), MeOH (Mg, stored over 3 Å molecular sieves).[217] DMF, 1,4-dioxane and CH$_3$CN were dried by an adsorption solvent purification system based on molecular sieves. Benzene was dried by treatment of a freshly opened bottle with activated 4 Å molecular sieves and then stored under inert atmosphere.

Flash chromatography separations were performed using Merck 60 silica gel (40-63 µm), whereas preparative thin-layer chromatography (TLC) was performed on Merck 25-DC-Plastic sheets (20 x 20 cm) coated with 60 silica gel. Determined compounds needed to be separated by semipreparative HPLC, using a Shimadzu preparative LC-8A system with a diode array detector at the indicated conditions. System control and chromatogram analysis were carried out with LabSolutions® software. The semi-preparative HPLC of compounds **26ab**, **26ac**, **26ba** and **190ab** were conducted by Sandra Kestermann and Alfred Deege (department for chromatography at the Max-Planck-Institut für Kohlenforschung).

Reactions were controlled by TLC analysis, performed using Merck silica gel 60 F254 TLC plates and visualised by UV irradiation and/or ceric ammonium molybdate or potassium permanganate dip. When it was possible, the reactions were additionally followed by GC/MS measurements performed on Agilent Technology GC 6890 Series and MSD 5973 (carrier gas: helium) with HP6890 Series Injector, employing a MN

Optima 5 column (30 mm × 0.25 mm × 0.25 mm).

All commercially available compounds (Acros, ABCR, Alfa Aesar, Aldrich) were used as received, unless stated otherwise.

III.1.1.2 General analytical methods

NMR spectra were recorded on a Bruker AV600, AV500, AV400 or DPX300 as stated for each case, using dry deuterated solvents. ^{1}H and ^{13}C chemical shifts (δ) are given in ppm relative to TMS, using the solvent signals as references and converting the chemical shifts to the TMS scale. ^{31}P and ^{19}F chemical shifts are given in ppm relative to H_3PO_4 and $CFCl_3$ respectively (external standard). The NMR signals of compounds **185e**, **192aa**, **192bb** and *E*-**190ab** were assigned by the NMR department at the Max-Planck-Institut für Kohlenforschung, using multinuclear and two-dimensional NMR spectra. Dynamic NMR studies of compounds **192aa** and **192bb** were conducted by Dr. Christophe Farès.

Mass spectrometry analysis was performed by the department for mass spectrometry at the Max-Planck-Institut für Kohlenforschung, using the following equipment: Finnigan MAT 8200 (70 eV, EI), Finnigan MAT 95 (ESI) and Bruker APEX III FT-MS (7 T magnet, HRMS). Infrared spectra were recorded on Nicolet FT-7199 or Bruker ALPHA FT-IR Platinum ATR spectrometers at room temperature. The specific rotation for chiral compounds was obtained using Perkin Elmer 343 polarimeter with Na spectral line at 589 nm, *c* is given in g/100mL.

X-Ray diffraction analysis was performed by the department of chemical at the Max-Planck-Institut für Kohlenforschung and Hendrik Tinnermann. X-Ray diffraction analysis of compounds **80**, **84**, **87**, **88**, **90**, **93**, **94** and **97** was performed by Jörg Rust. The X-ray intensity data were measured on a Bruker AXS Proteum X8, Bruker AXS KappaCCD and Bruker AXS Apex II diffractometers. The crystal structures were solved by direct methods using SHELXS-97 and refined with SHELXL-2014. The crystalls suitable for X-ray analysis were grown by slow diffusion of *n*-pentane into DCM solutions of the metal complexes or by slow solvent evaporation of saturated solutions of the organic compounds.

The ratio of regioisomers in the hexahelicene synthesis, was determined by HPLC using Shimadzu Prominence LC-20A system, employing 50 × 4.6 mm Agilent Eclipse Plus C18 column and CH_3CN/H_2O mixtures as mobile phase. Detection was performed using a diode array detector at the given wavelengths. System control and chromatogram analysis were carried out with LabSolutions® software. Enantiomeric excess was determined by the department for chromatography at the Max-Planck-Institut für Kohlenforschung (Sandra Kestermann, Marie Sophie Sterling and Alfred Deege) by

2D HPLC using an Agilent 2D 1290 Infinity system: in the first dimension an achiral separation of substrate, helicene and isomers was performed with a 50 × 3 mm Agilent Eclipse Plus C18 column using CH_3CN/H_2O mixtures. The helicene peak was then transferred with a heart cut to a second dimension equipped with a chiral 150 × 4.6 mm Chiralpak IC-3 column and eluted with CH_3CN/CH_3OH mixtures. Detection of both separations was performed *via* a diode array detector at the given wavelengths. System control and chromatogram analysis were carried out with the Agilent OpenLAB ChemStation software.

III.1.2   Synthesis and reactivity of acyclic (amino)-(ylide)carbene metal complexes

III.1.2.1   Starting materials

Isonitrile-gold(I) complexes **12a**, **12b** and **12c** were prepared using the method described by Hashmi *et al.* in quantitative yields.[75c] Phenylisocyanide and 2-pyridylisocyanide were prepared by the method of Weber *et al.* from aniline and 2-aminopyridine respectively.[218] The ylides **79d**,[219] **79e**,[220] **79f**,[221] **83**,[222] **85** and **86**[102] were prepared according to literature procedures.

III.1.2.2   Synthesis of AAYC-gold(I) complexes

General procedure A: Synthesis of AAYC-gold(I) complexes bearing phosphorus ylides

12	**79**	**81**	**80**
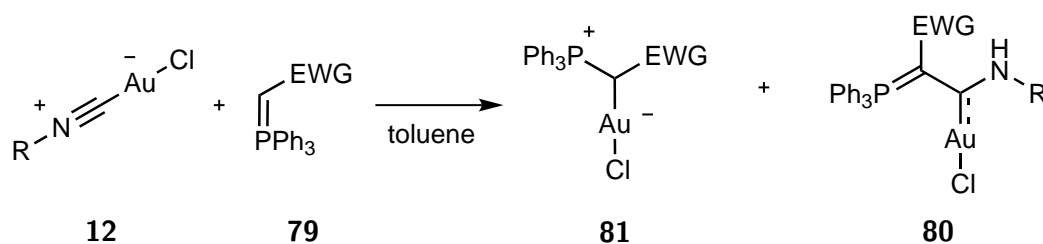
In a typical procedure, the isonitrile-gold(I) chloride **12** was suspended in toluene (0.024 M) followed by the addition of ylide **79** at the indicated temperature. After stirring the reaction for the referred time, the mixture was allowed to reach room temperature and the solvents filtered out. The remaining white solid thus obtained was then washed with small portions of *n*-pentane and dried under vacuum.

Compound 80a :
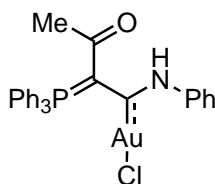
Following the general procedure described above, a mixture of phenylisocyanide gold(I) chloride **12a** (40 mg, 0.12 mmol) and ylide **79a** (38 mg, 0.12 mmol) afforded pure **80a** (66 mg, 85 %) after a reaction time of 3 days at room temperature.

^{31}P-NMR (162 MHz, CD_2Cl_2) δ : 19.6 ppm.

^{1}H-NMR (400 MHz, CD_2Cl_2) δ : 14.54 (s, 1H), 7.97-7.92 (m, 6H), 7.72-7.69 (m, 3H), 7.65-7.59 (m, 8H), 7.34-7.31 (m, 2H), 7.24-7.21 (m, 1H), 1.47 (s, 3H) ppm.

^{13}C-NMR (101 MHz, CD_2Cl_2) δ : 200.9 (d, J_{C-P}= 36.0 Hz), 195.3 (d, J_{C-P}= 24.0 Hz), 144.1, 134.5 (d, J_{C-P}= 8.6 Hz), 133.5 (d, J_{C-P}= 3.0 Hz), 129.8 (d, J_{C-P}= 12.3 Hz), 129.1, 126.6, 125.8 (d, J_{C-P}= 91.6 Hz), 123.7, 93.0 (d, J_{C-P}= 124.9 Hz), 31.7 (d, J_{C-P}= 2.3 Hz) ppm.

HRMS calculated m/z for $C_{28}H_{24}NOAuClPNa^+$: 676.084174; found (ESI) 676.084426.

IR (neat) $\tilde{\nu}$: 3052, 1587, 1567, 1506, 1482, 1438, 1415, 1365, 1253, 1227, 1182, 1133, 1095, 1052, 1024, 998, 983, 901, 875, 756, 749, 736, 721, 706, 690, 680 cm^{-1}.

Compound 80b :
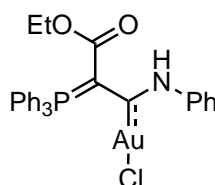
Following the general procedure described above, a mixture of phenylisocyanide gold(I) chloride **12a** (41 mg, 0.12 mmol) and ylide **79b** (45 mg, 0.12 mmol) afforded pure **80a** (62 mg, in 74 %) after a reaction time of 1 day at 35 °C .

^{31}P-NMR (162 MHz, CD_2Cl_2) δ : 22.0 ppm.

^{1}H-NMR (400 MHz, CD_2Cl_2) δ : 12.67 (s, 1H), 7.89-7.84 (m, 6H), 7.67-7.63 (m, 5H), 7.58-7.53 (m, 6H), 7.34-7.30 (m, 2H), 7.23-7.19 (m, 1H), 3.73 (q, J= 7.2 Hz, 2H), 0.59 (t, J= 7.2 Hz, 3H) ppm.

^{13}C-NMR (101 MHz, CD_2Cl_2) δ : 200.6 (d, J_{C-P}= 35.9 Hz), 168.8 (d, J_{C-P}= 17.2 Hz), 144.4, 134.1 (d, J_{C-P}= 9.0 Hz), 133.0 (d, J_{C-P}= 2.6 Hz), 129.4 (d, J_{C-P}= 12.7 Hz), 129.1, 126.3, 126.2(d, J_{C-P}= 94.0 Hz), 123.4, 79.4 (d, J_{C-P}= 134.4 Hz), 60.0, 13.6 ppm.

HRMS calculated m/z for $C_{29}H_{26}NO_2AuClPNa^+$: 706.094742; found (ESI) 706.095558.

IR (neat) $\tilde{\nu}$: 3054, 2976, 2907, 1629, 1588, 1517, 1479, 1436, 1392, 1368, 1336, 1292, 1233, 1197, 1185, 1164, 1156, 1103, 1081, 1071, 1024, 997, 937, 905, 849, 819, 799, 748, 760, 710, 698, 688, 681 cm^{-1}.

Compound 80c :
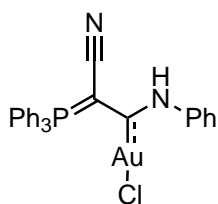
Following the general procedure described above, a mixture of phenylisocyanide gold(I) chloride **12a** (23 mg, 0.07 mmol) and ylide **79c** (21 mg, 0.07 mmol) afforded pure **80c** (38 mg, 88 %) after a reaction time of 3 days at 35 °C .

^{31}P-NMR (162 MHz, CD$_2$Cl$_2$) δ : 21.8 ppm.

^{1}H-NMR (400 MHz, CD$_2$Cl$_2$) δ : 8.89 (s, 1H), 7.83-7.75 (m, 9H), 7.71-7.69 (m, 2H), 7.69-7.61 (m, 6H), 7.38-7.34 (m, 2H), 7.28-7.24 (m, 1H) ppm.

^{13}C-NMR (101 MHz, CD$_2$Cl$_2$) δ : 201.9 (d, J_{C-P}= 35.9 Hz), 143.0, 134.8 (d, J_{C-P}= 9.8 Hz), 134.4 (d, J_{C-P}= 2.9 Hz), 129.8 (d, J_{C-P}= 13.0 Hz), 129.3, 126.8, 123.1, 122.9 (d, J_{C-P}= 94.1 Hz), 117.8 (d, J_{C-P}= 22.1 Hz), 60.1 (d, J_{C-P}= 154.6 Hz) ppm.

HRMS calculated m/z for C$_{27}$H$_{21}$N$_2$AuClPNa$^+$: 659.068858; found (ESI) 659.069049.

IR (neat) $\tilde{\nu}$: 3242, 2175, 1594, 1529, 1491, 1436, 1343, 1319, 1300, 1284, 1225, 1190, 1120, 1102, 1073, 1026, 996, 923, 900, 850, 788, 758, 748, 727, 715, 687 cm^{-1}.

Compound 80d :
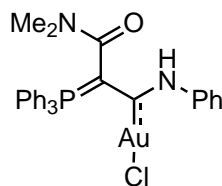
Following the general procedure described above, a mixture of phenylisocyanide gold(I) chloride **12a** (23 mg, 0.07 mmol) and ylide **79d** (24 mg, 0.07 mmol) afforded pure **80d** (38 mg, 81 %) after a reaction time of 6 h at 35 °C .

^{31}P-NMR (162 MHz, CD$_2$Cl$_2$) δ : 18.1 ppm.

^{1}H-NMR (400 MHz, CD$_2$Cl$_2$) δ : 7.98 (s, 1H), 7.85-7.80 (m, 6H), 7.69-7.65 (m, 3H), 7.61-7.53 (m, 8H), 7.29-7.25 (m, 2H), 7.14-7.06 (m, 1H), 2.88 (s, 6H) ppm.

^{13}C-NMR (101 MHz, CD$_2$Cl$_2$) δ : 188.9 (d, J_{C-P}= 32.0 Hz), 167.8 (d, J_{C-P}= 19.1 Hz), 144.4, 134.6 (d, J_{C-P}= 9.3 Hz), 133.4 (d, J_{C-P}= 2.9 Hz), 129.3 (d, J_{C-P}= 12.4 Hz), 129.0, 125.1 (d, J_{C-P}= 92.0 Hz), 125.0, 122.4, 86.1 (d, J_{C-P}= 132.3 Hz), 37.0 ppm.

HRMS calculated m/z for C$_{29}$H$_{27}$N$_2$OAuClPNa$^+$: 705.110727; found (ESI) 705.110773.

IR (neat) $\tilde{\nu}$: 3275, 3042, 1597, 1542, 1496, 1481, 1446, 1435, 1384, 1304, 1271, 1215, 1188, 1158, 1098, 1070, 1048, 1027, 998, 937, 900, 841, 756, 729, 691 cm^{-1}.

Compound 81e :
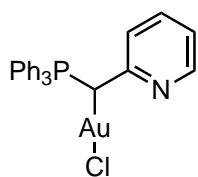
Phenylisocyanide gold(I) chloride **12a** (230 mg, 0.63 mmol) is added to a cooled solution of the phosphorus ylide **79e** (224 mg, 0.63 mmol) in toluene (26 ml) at -78 °C . After 2 h controlling the temperature, it is allowed to warm up to room temperature overnight. Filtration of the obtained suspension afforded a white solid (306 mg, 83 %), which corresponds to **81e**.

^{31}P-NMR (162 MHz, CD$_2$Cl$_2$) δ : 28.3 ppm.

^{1}H-NMR (400 MHz, CD$_2$Cl$_2$) δ : 7.64 (ddd, J= 5.0, 1.8, 0.9 Hz, 1H), 7.90-7.85 (m, 6H), 7.66-7.61 (m. 3H), 7.52-7.45 (m, 7H), 7.23-7.21 (m, 1H), 6.82-6.79 (m, 1H), 4.5 (d, J_{H-P}= 7.9 Hz, 1H) ppm.

^{13}C-NMR (101 MHz, CD$_2$Cl$_2$) δ : 161.0 (d, J_{C-P}= 5.5 Hz), 147.9, 136.5, 134.5 (d, J_{C-P}= 9.2 Hz), 133.3 (d, J_{C-P}= 12.1 Hz), 125.9 (d, J_{C-P}= 87.9 Hz), 122.7 (d, J_{C-P}= 13.1 Hz), 119.3, 29.6 (d, J_{C-P}= 49.1 Hz) ppm.

^{31}P-NMR (162 MHz, CD$_2$Cl$_2$) δ : 28.3 ppm.

HRMS calculated m/z for C$_{31}$H$_{31}$N$_2$OAuClPNa$^+$: 733.142026; found (ESI) 733.142583.

IR (neat) $\tilde{\nu}$: 3269, 3059, 3007, 2951, 2915, 2848, 1606, 1586, 1488, 1436, 1384, 1357, 1293, 1263, 1212, 1192, 1160, 1102, 1051, 1028, 997, 946, 918, 854, 767, 755, 743, 712, 694 cm^{-1}.

Compound 80e :
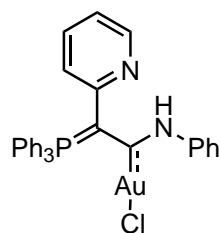
Following the general procedure described above, a mixture of phenylisocyanide gold(I) chloride **12a** (89 mg, 0.26 mmol) and ylide **79e** (94 mg, 0.26 mmol) afforded pure **80e** (180 mg, 98 %) after a reaction time of 6 h at 35 °C .

^{1}H-NMR (400 MHz, CD$_2$Cl$_2$) δ : 9.77 (s, 1H), 8.45 (d, J= 4.6 Hz, 1H), 7.82 (dd, J= 12.1, 8.1 Hz, 6H), 7.62-7.58 (m, 5H), 7.52-7.47 (m, 6H), 7.30-7.22 (m, 3H), 7.06 (t, J= 7.1 Hz, 1H), 6.93-6.90 (m, 1H), 6.81 (d, J= 7.9 Hz, 1H) ppm.

^{13}C-NMR (101 MHz, CD$_2$Cl$_2$) δ : 189.6 (d, J_{C-P}= 35.7 Hz), 156.4 (d, J_{C-P}= 20.1 Hz), 149.6, 144.5, 136.3, 134.7 (d, J_{C-P}= 9.1 Hz), 133.0 (d, J_{C-P}= 2.6 Hz), 129.2 (d, J_{C-P}= 12.1 Hz), 128.8, 126.8 (d, J_{C-P}= 3.0 Hz), 126.2 (d, J_{C-P}= 91.8 Hz), 124.4, 121.7, 120.8, 87.9 (d, J_{C-P}= 134.4 Hz) ppm.

^{31}P-NMR (162 MHz, CD$_2$Cl$_2$) δ : 20.0 ppm.

HRMS calculated m/z for C$_{31}$H$_{25}$N$_2$AuClPNa$^+$: 711.100164; found (ESI) 711.100454.

IR (neat) $\tilde{\nu}$: 3056, 1582, 1557, 1514, 1494, 1460, 1435, 1425, 1379, 1312, 1263, 1183, 1154, 1098, 1051, 1017, 997, 900, 862, 793, 742, 711, 688 cm^{-1}.

Compound 80f :
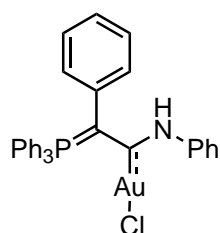
Phenylisocyanide gold(I) chloride **12a** (44 mg, 0.12 mmol) was added to a cooled solution of the phosphorus ylide **79f** (43 mg, 0.12 mmol) at -78 °C . After 2 h, it was allowed to warm up to room temperature overnight. Filtration of the obtained suspension afforded a white solid which contains both **80f** and the side product **81f**. Three consecutive crystallisations in DCM/n-pentane allowed

the isolation of pure **80f** (4 mg) in 5 % yield.

^{31}P-NMR (162 MHz, CD$_2$Cl$_2$) δ : 21.0 ppm.

^{1}H-NMR (400 MHz, CD$_2$Cl$_2$) δ : 7.71-7.66 (m, 5H), 7.64-7.59 (m, 3H), 7.52-7.45 (m, 9H), 7.30 (s, 1H), 7.22-7.13 (m, 5H), 7.06-6.70 (m, 3H) ppm..

^{13}C-NMR (101 MHz, CD$_2$Cl$_2$) δ : 187.1 (d, J_{C-P}= 37.7 Hz), 144.5, 134.8 (d, J_{C-P}= 9.0 Hz), 134.0 (d, J_{C-P}= 3.8 Hz), 133.1 (d, J_{C-P}= 2.8 Hz), 133.1 (d, J_{C-P}= 2.8 Hz), 132.3 (d, J_{C-P}= 9.9 Hz), 129.6 (d, J_{C-P}= 1.7 Hz), 129.1 (d, J_{C-P}= 12.3 Hz), 129.0 (d, J_{C-P}= 12.1 Hz), 128.9, 127.9 (d, J_{C-P}= 2.3 Hz), 125.8 (d, J_{C-P}= 91.1 Hz), 124.0, 121.2, 88.9 (d, J_{C-P}= 132.1 Hz) ppm.

HRMS calculated m/z for C$_{31}$H$_{31}$N$_2$OAuClPNa$^+$: 710.104912; found (ESI) 710.105881.

IR (neat) $\tilde{\nu}$: 3551, 3494, 3331, 3051, 2961, 2922, 2851, 1590, 1508, 1493, 1480, 1444, 1433, 1372, 1326, 1305, 1261, 1220, 1159, 1098, 1071, 1027, 1009, 996, 913, 887, 853, 800, 784, 716, 744, 704, 689 cm^{-1}.

Compound 80g :
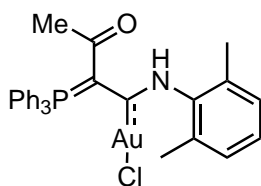
Following the general procedure described above, a mixture of 2,6-dimethyl-phenylisocyanide gold(I) chloride **12b** (100 mg, 0.28 mmol) and phosphorus ylide **79a** (88 mg, 0.28 mmol) pure **80g** (54 mg, 30 %) after a reaction time of 3 days at 50 °C .

^{31}P-NMR (162 MHz, CD$_2$Cl$_2$) δ : 20.5 ppm.

^{1}H-NMR (400 MHz, CD$_2$Cl$_2$) δ : 13.70 (s, 1H), 7.97-7.92 (m, 6H), 7.73-7.68 (m, 3H), 7.64-7.58 (m, 6H), 7.13-7.06 (m, 3H), 2.26 (s, 6H), 1.48 (s, 3H) ppm.

^{13}C-NMR (101 MHz, CD$_2$Cl$_2$) δ : 206.6 (d, J_{C-P}= 34.8 Hz), 195.0 (d, J_{C-P}= 28.0 Hz), 142.6, 135.0, 134.6, (d, J_{C-P}= 8.6 Hz), 133.6 (d, J_{C-P}= 2.9 Hz), 129.7 (d, J_{C-P}= 12.4 Hz), 128.4, 127.6, 125.9 (d, J_{C-P}= 92.0 Hz), 91.1 (d, J_{C-P}= 124.3 Hz), 31.6 (d, J_{C-P}= 2.0 Hz), 19.1 ppm.

HRMS calculated m/z for C$_{30}$H$_{28}$NOAuClPNa$^+$: 704.115849; found (ESI) 704.115049.

IR (neat) $\tilde{\nu}$: 2975, 1572, 1500, 1435, 1418, 1360, 1342, 1268, 1250, 1213, 1142, 1098, 1046, 1018, 998, 982, 920, 873, 842, 781, 768, 755, 734, 720, 693, 682 cm^{-1}.

Compound 80h :
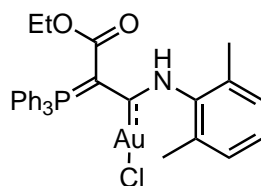
Following the general procedure described above, a mixture of 2,6-dimethyl-phenylisocyanide gold(I) chloride **12b** (46 mg, 0.13 mmol) and phosphorus ylide **79b** (47 mg, 0.13 mmol) afforded afforded after 4 days at 50 °C a white solid that was further purified by crystallisation from DCM/n-pentane. Thus, **80h** was obtained in 37 % yield (33 mg).

^{31}P-NMR (162 MHz, CD$_2$Cl$_2$) δ : 22.4 ppm.

^{1}H-NMR (400 MHz, CD$_2$Cl$_2$) δ : 11.89 (s, 1H), 7.88-7.83 (m, 6H), 7.67-7.63 (m, 3H), 7.58-7.53 (m, 6H), 7.15-7.07 (m, 3H), 3.75 (q, J= 7.1 Hz, 2H), 2.20 (s, 6H), 0.59 (t, J= 7.1 Hz, 3H) ppm.

^{13}C-NMR (101 MHz, CD$_2$Cl$_2$) δ : 206.1 (d, J_{C-P}= 34.8 Hz), 168.8 (d, J_{C-P}= 16.9 Hz), 142.9, 135.6, 134.2 (d, J_{C-P}= 9.2 Hz), 133.0 (d, J_{C-P}= 3.0 Hz), 129.3 (d, J_{C-P}= 12.3 Hz), 128.4, 127.6, 126.2 (d, J_{C-P}= 93.6 Hz), 76.9 (d, J_{C-P}= 135.0 Hz), 59.7, 19.1, 13.7 ppm.

HRMS calculated m/z for C$_{31}$H$_{30}$NO$_2$AuClPNa$^+$: 734.126042; found (ESI) 734.125744.

IR (neat) $\tilde{\nu}$: 3063, 2982, 1635, 1521, 1480, 1436, 1390, 1368, 1339, 1300, 1258, 1216, 1182, 1162, 1103, 1078, 1025, 997, 938, 802, 776, 748, 722, 709, 698, 683 cm^{-1}.

Compound 80i :
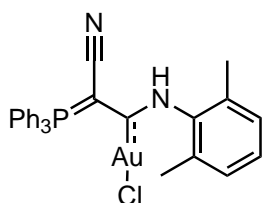
Following the general procedure described above, a mixture of 2,6-dimethyl-phenylisocyanide gold(I) chloride **12b** (86 mg, 0.24 mmol) and phosphorus ylide **79d** (71 mg, 0.24 mmol) afforded after 4 d at 50 °C a white solid that was further purified by three consecutive crystallisations from DCM/n-pentane. Thus, **80i** was obtained in 25 % yield (40 mg).

^{31}P-NMR (162 MHz, CD$_2$Cl$_2$) δ : 22.1 ppm.

^{1}H-NMR (400 MHz, CD$_2$Cl$_2$) δ : 8.30 (s, 1H), 7.83-7.75 (m, 9H), 7.66-7.61 (m, 6H), 7.21-7.17 (m, 1H), 7.13-7.11 (m, 2H), 2.33 (s, 6H) ppm.

^{13}C-NMR (101 MHz, CD$_2$Cl$_2$) δ : 207.0 (d, J_{C-P}= 29.5 Hz), 141.2, 136.1, 134.7 (d, J_{C-P}= 9.9 Hz), 134.4 (d, J_{C-P}= 2.7 Hz), 129.8 (d, J_{C-P}= 13.1 Hz), 128.7, 128.4, 123.1 (d, J_{C-P}= 95.0 Hz), 117.9 (d, J_{C-P}= 22.2 Hz), 57.3 (d, J_{C-P}= 154.6 Hz), 19.1 ppm.

HRMS calculated m/z for C$_{29}$H$_{25}$N$_2$AuClPNa$^+$: 687.100159; found (ESI) 687.100556.

IR (neat) $\tilde{\nu}$: 3282, 2962, 2180, 1505, 1482, 1436, 1375, 1328, 1312, 1260, 1217, 1186, 1165, 1123, 1105, 1025, 997, 952, 927, 907, 804, 780, 749, 716, 697, 687 cm^{-1}.

Compound 80j :
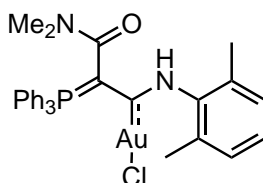
Following the general procedure described above, a mixture of 2,6-dimethyl-phenylisocyanide gold(I) chloride **12b** (94 mg, 0.26 mmol) was added to a cooled solution of the phosphorus ylide **79d** (90 mg, 0.26 mmol) at -78 °C . After 2 h, the reaction mixture was allowed to warm up to room temperature overnight. Filtration of the obtained suspension afforded a white solid which was purified by three consecutive crystallisations in DCM/n-pentane. Thus, **80j** was obtained as colourless

crystals (21 mg, 12 %).

^{31}P-NMR (162 MHz, CD$_2$Cl$_2$) δ : 18.8 ppm.

^{1}H-NMR (400 MHz, CD$_2$Cl$_2$) δ : 7.87-7.81 (m, 6H), 7.70-7.65 (m, 3H), 7.59-7.54 (m, 6H), 7.24 (s, 1H), 7.13-7.07 (m, 3H), 2.96 (s, 6H), 2.33 (s, 6H) ppm.

^{13}C-NMR (101 MHz, CD$_2$Cl$_2$) δ : 194.4 (d, J_{C-P}= 31.0 Hz), 168.0 (d, J_{C-P}= 19.2 Hz), 142.4, 136.6, 134.5 (d, J_{C-P}= 9.1 Hz), 133.3 (d, J_{C-P}= 2.6 Hz), 129.2 (d, J_{C-P}= 12.3 Hz), 128.5, 127.6, 125.5 (d, J_{C-P}= 92.7 Hz), 82.2 (d, J_{C-P}= 134.1 Hz), 37.1, 19.4 ppm.

HRMS calculated m/z for C$_{31}$H$_{31}$N$_2$OAuClPNa$^+$: 733.142026; found (ESI) 733.142583.

IR (neat) $\tilde{\nu}$: 3269, 3059, 3007, 2951, 2915, 2848, 1606, 1586, 1488, 1436, 1384, 1357, 1293, 1263, 1212, 1192, 1160, 1102, 1051, 1028, 997, 918, 854, 767, 755, 743, 712, 694 cm^{-1}.

Compound 80k :
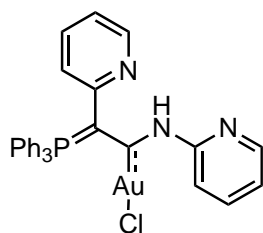
Following the general procedure described above, a mixture of 2-pyrydilisocyanide gold(I) chloride **12c** (41 mg, 0.12 mmol) and ylide **79e** (43 mg, 0.12 mmol) afforded pure **80k** (75 mg, 89 %) after a reaction time of 8 h at 35 °C.

^{31}P-NMR (162 MHz, CD$_2$Cl$_2$) δ : 20.5 ppm.

^{1}H-NMR (400 MHz, CD$_2$Cl$_2$) δ : 9.14 (s, 1H), 8.49 (d, J= 8.4 Hz, 1H), 8.46 (dt, J= 5.0, 1.2 Hz, 1H), 8.13 (ddd, J= 4.9, 1.8, 0.8 Hz, 1H), 7.87-7.76 (m, 6H), 7.68-7.59 (m, 3H), 7.57 (ddd, J= 8.8, 7.3, 2.0 Hz, 1H), 7.50 (m, 6H), 7.39 (td, J = 7.7, 1.9 Hz, 1H), 7.04-6.93 (m, 2H), 6.91 (ddd, J= 7.3, 4.9, 1.0 Hz, 1H) ppm.

^{13}C-NMR (101 MHz, CD$_2$Cl$_2$) δ : 185.8 (d, J_{C-P}= 36.3 Hz), 156.1, 155.5 (d, J_{C-P}= 18.2 Hz), 150.3, 148.0, 137.7, 136.7, 134.8 (d, J_{C-P}= 9.1 Hz), 133.1 (d, J_{C-P}= 3.0 Hz), 129.2 (d, J_{C-P}= 12.5 Hz), 127.6 (d, J_{C-P}= 3.6 Hz), 126.1, 125.2, 121.7, 118.9, 112.4, 93.05 (d, J_{C-P}= 131.8 Hz) ppm.

HRMS calculated m/z for C$_{30}$H$_{24}$AuClN$_3$PNa$^+$: 712.095413; found (ESI) 712.095817.

IR (neat) $\tilde{\nu}$: 3211, 1577, 1556, 1525, 1490, 1461, 1440, 1420, 1376, 1308, 1261, 1183, 1154, 1098, 1051, 1013, 997, 905, 789, 741, 711, 690 cm^{-1}.

Compound 84:
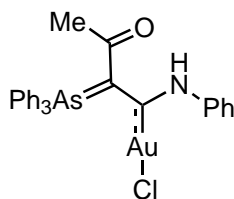
A suspension of phenylisocyanide gold(I) chloride **12a** (38 mg, 0.11 mmol) in toluene (4.7 ml) was cooled at -10 °C and then the arsenic ylide **83** (41 mg, 0.11 mmol) was added. After stirring the obtained suspension for 1 day, the reaction mixture was allowed to reach room temperature. The solvents were then filtered out and the remaining a white solid washed with small portions of toluene and dried under

vacuum. Thus, **84** was obtained as a white solid (32 mg, 40 %).

^{1}H-NMR (400 MHz, CD$_2$Cl$_2$) δ : 14.45 (s, 1 H), 7.85 (d, J= 7.2 Hz, 6H), 7.70-7.60 (m, 11H), 7.31 (t, J= 7.7 Hz, 2H), 7.21 (t, J= 7.3 Hz, 1H), 1.61 (br, 3H) ppm.

^{13}C-NMR (75 MHz, CD$_2$Cl$_2$) δ : 198.0, 144.1, 133.3, 133.1, 130.5, 129.1, 129.0, 126.4, 123.4, 31.3 ppm

HRMS calculated m/z for C$_{28}$H$_{24}$AsAuClNONa$^+$: 720.032365; found (ESI) 720.033071.

IR (neat) $\tilde{\nu}$: 2955, 2922, 2853, 1589, 1565, 1509, 1459, 1441, 1371, 1259, 1078, 1014, 865, 793, 756, 741, 691 cm^{-1}.

Compound 87:
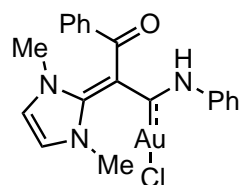
A mixture of phenylisocyanide gold (I) chloride **12a** (25 mg, 0.08 mmol) and diaminoalkene **85** (16 mg, 0.08 mmol) was suspended in toluene (3 ml) and warmed to 35 ºC . After 8 h the mixture was allowed to reach room temperature. Elimination of the solvents by filtration afforded pure **87** as a yellow solid (40 mg, 95 % yield).

^{1}H-NMR (400 MHz, CD$_2$Cl$_2$) δ : 14.73 (s, 1H), 7.86 (d, J= 7.8 Hz, 2H), 7.43-7.40 (m, 2H), 7.35-7.32 (m, 1H), 7.29-7.25 (m, 3H), 7.06 (s, 2H), 7.05-7.03 (m, 2H) 3.63 (s, 6H) ppm.

^{13}C-NMR (101 MHz, CD$_2$Cl$_2$) δ : 194.6, 187.4, 151.5, 143.7, 142.3, 130.2, 129.3, 128.9, 126.2, 125.9, 122.7, 121.3, 98.4, 36.0 ppm.

HRMS calculated m/z for C$_{20}$H$_{19}$N$_3$OAuClNa: 572.077435; found (ESI) 572.078099.

IR (neat) $\tilde{\nu}$: 3125, 1595, 1519, 1488, 1446, 1384, 1278, 1235, 1173, 1155, 1071, 1025, 906, 792, 760, 728, 704, 691 cm^{-1}.

Compound 88:
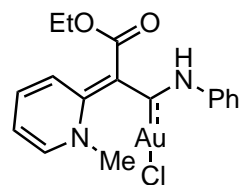
A mixture of phenylisocyanide gold(I) chloride **12a** (26 mg, 0.08 mmol) and enamine **86** (14 mg, 0.08 mmol) was suspended in toluene (3.3 ml) and warmed to 35 ºC . After 18 h the mixture was allowed to reach room temperature. Elimination of the solvents by filtration afforded pure **88** as a yellow solid (35 mg, 87 % yield).

^{1}H-NMR (400 MHz, CD$_2$Cl$_2$) δ : 12.09 (s, 1H), 8.33 (d, J= 6.2 Hz, 1H), 8.23 (t, J= 7.9 Hz, 1H), 8.16 (d, J= 7.9 Hz, 1H), 7.78-7.76 (m, 2H), 7.67-7.63 (m, 1H), 7.36-7.31 (m, 2H), 7.18-7.14 (m, 1H), 4.17 (s, 3H), 4.14-4.04 (m, 2H), 1.13 (t, J= 7.0 Hz, 3H) ppm.

^{13}C-NMR (101 MHz, CD$_2$Cl$_2$) δ : 189.6, 165.9, 162.2, 144.2, 143.1, 142.8, 135.3, 129.2, 125.0, 124.4, 122.0, 98.4, 59.5, 46.2, 14.8 ppm.

HRMS calculated m/z for C$_{17}$H$_{18}$N$_2$O$_2$AuClNa$^+$: 537.061450; found (ESI) 537.061877.

IR (neat) $\tilde{\nu}$: 3055, 2975, 1640, 1622, 1588, 1527, 1493, 1447, 1373, 1336, 1299, 1218,

1256, 1175, 1091, 1074, 1028, 954, 931, 893, 788, 759, 749, 694, 680 cm^{-1}.

III.1.2.3   Reactivity of AAYC-gold(I) complexes

Compound 90:
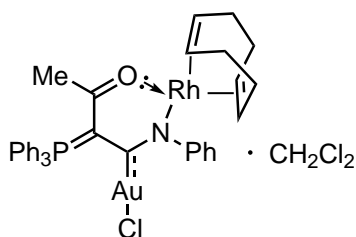
KOMe (5.5 mg, 0.078 mmol) and [{Rh(cod)Cl}$_2$] (19.3 mg, 0.039 mmol) were suspended in THF (2 ml) and stirred for 10 min, at 5 °C . Then, **80a** was added and the mixture stirred for 36 h. Along this time a light yellow precipitate was slowly formed. The reaction was then allowed to reach room temperature and the solvent evaporated *in vacuo*. The yellow solid thus obtained was washed with small portions of DCM to afford **90** (54 mg, 72 %).

^{31}P-NMR (162 MHz, CDCl$_3$) δ : 19.9 ppm.

^{1}H-NMR (400 MHz, CDCl$_3$) δ : 8.06-8.01 (m, 6H), 7.67-7.57 (m, 9H), 7.12 (t, J= 7.6 Hz, 2H), 6.97 (t, J= 7.4 Hz, 1H), 6.82 (d, J= 7.2 Hz, 2H), 4.18 (br, 2H), 3.34 (br, 2H), 2.44-2.35 (m, 4H), 1.83-1.72 (m, 4H) 1.49 (s, 3H) ppm.

^{13}C-NMR (126 MHz, CDCl$_3$) δ : 197.6 (d, J_{C-P}= 35.0 Hz), 180.7 (d, J_{C-P}= 24.1 Hz), 155.9, 134.1 (d, J_{C-P}= 8.7 Hz), 133.1 (d, J_{C-P}= 2.8 Hz), 129.4 (d, J_{C-P}= 12.4 Hz), 128.2, 125.5 (d, J_{C-P}= 91.6 Hz), 124.8, 124.6, 95.3 (d, J_{C-P}= 126.6 Hz), 82.7 (d, J_{C-Rh}= 11.8 Hz), 75.1 (d, J_{C-Rh}= 11.8 Hz), 53.6, 31.6, 29.6, 28.7 ppm.

HRMS calculated m/z for C$_{36}$H$_{35}$AuClNOPRhNa$^+$:   886.075756; found (ESI) 886.076414.

IR (neat) $\tilde{\nu}$: 3052, 2994, 2942, 2858, 2838, 2228, 1591, 1494, 1483, 1440, 1404, 1362, 1350, 1262, 1218, 1187, 1142, 1096, 1070, 1023, 998, 964, 911, 869, 800, 776, 759, 741, 725, 708, 687 cm^{-1}.

Compound 91:
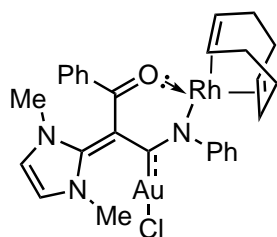
KOMe (11.5 mg, 0.16 mmol) and [{Rh(cod)Cl}$_2$] (40.4 mg, 8.2×10^{-2} mmol) were suspended in THF (4 ml) and stirred for 10 min. Then, **87** (90.2 mg, 0.16 mmol) was added and the mixture stirred for 2.5 days. Along this time a light yellow precipitate was slowly formed. The solvent was removed *in vacuo* and the remaining yellow solid was washed with DCM to afford the desired bimetallic compound **91** as a pale yellow solid (94 mg, 75 % yield).

^{1}H-NMR (400 MHz, CD$_2$Cl$_2$) δ : 7.32-7.19 (m, 5H), 7.11 (ddt, J= 7.8, 7.0, 1.3 Hz, 1H), 7.01-6.96 (m, 4H), 6.96 (s, 2H), 4.32 (br, 2H), 3.55 (s, 6H), 3.35 (br, 2H), 2.48-2.23 (m,

4H), 1.88-1.66 (m, 4H) ppm.

^{13}C-NMR (101 MHz, CD$_2$Cl$_2$) δ : 195.0, 177.5, 171.3, 157.5, 141.5, 129.4, 128.6, 128.1, 126.4, 126.1, 124.5, 120.8, 114.8, 83.1 (d, J_{C-Rh}= 11.7 Hz), 75.5 (d, J_{C-Rh}= 14.6 Hz), 35.8, 31.9, 29.3 ppm.

HRMS decomposition of the sample.

IR (neat) $\tilde{\nu}$: 3040, 2992, 2941, 2858, 2833, 2222, 1615, 1553, 1494, 1488, 1439, 1380, 1281, 1242, 1174, 1163, 1070, 1024, 906, 965, 865, 803, 763, 725, 701, 698 cm^{-1}.

Compound 92:
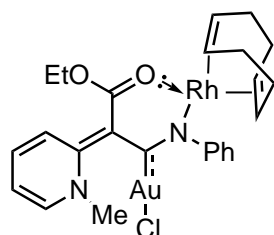
KOMe (9.0 mg, 0.13 mmol) and [{Rh(cod)Cl}$_2$] (31.6 mg, 6.4×10^{-2} mmol) were suspended in THF (3.2 ml) and stirred for 10 min. Then, **88** (65.8 mg, 0.13 mmol) was added and the mixture stirred for 36 h. Along this time a light yellow precipitate was slowly formed. The solvent was removed *in vacuo* and the remaining yellow solid was washed with DCM to afford the desired bimetallic compound **92** as a pale yellow solid (53 mg, 57 % yield).

^{1}H-NMR (400 MHz, CD$_2$Cl$_2$) δ : 8.26 (dd, J= 6.2, 1.5 Hz, 1H), 8.14 (td, J= 7.8, 1.5 Hz, 1H), 8.00 (dd, J= 8.0, 1.6 Hz, 1H), 7.60 (ddd, J= 7.7, 6.3, 1.6 Hz, 1H), 7.23 (td, J= 7.3, 1.3 Hz, 2H), 7.05 (tt, J= 7.3, 1.3 Hz, 1H), 6.94 (br, 2H), 4.23 (br, 2H), 4.15 (s, 3H), 3.95 (dq, J= 8.5, 7.0 Hz, 2H), 3.30 (br, 2H), 2.39-2.35 (m, 4H), 1.80-1.70 (m, 4H), 1.07 (t, J= 7.0 Hz, 3H) ppm.

^{13}C-NMR (101 MHz, CD$_2$Cl$_2$) δ : 198.0, 162.5, 161.8, 157.9, 142.7, 142.3, 135.8, 128.1, 126.9, 124.2, 124.1, 114.6, 82.1 (d, J_{C-Rh}= 11.3 Hz), 75.2 (d, J_{C-Rh}= 12.8 Hz), 60.8, 46.2, 32.0, 31.9, 29.3, 15.2 ppm.

HRMS calculated m/z for C$_{25}$H$_{29}$AuClN$_2$O$_2$RhNa$^+$: 747.052324; found (ESI) 747.053507.

IR (neat) $\tilde{\nu}$: 3045, 2975, 2937, 2863, 2832, 2220, 1608, 1585, 1530, 1494, 1442, 1368, 1357, 1295, 1217, 1241, 1182, 1093, 1072, 1024, 969, 890, 801, 763, 749, 703, 681 cm^{-1}.

Compound 93:
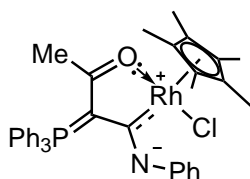
[{RhCp*Cl$_2$}$_2$] (5.0 mg, 0.009 mmol) and **80**a(10.2 mg, 0.016 mmol) were disolved in DCE (0.2 ml) and NEt$_3$ (0.04 ml, 0.272 mmol) was added drop-wise. This solution was heated at 50 °C and stirred at this temperature for 4 days. Then, the reaction mixture was allowed to cool down to room temperature and filtered in order to remove the formed precipitate. The bright red solution thus obtained was evaporated *in vacuo* affording a red solid that was redissolved in a small

amount of toluene and filtrated again. Evaporation of the toluene produced an orange solid that could be further purified by consecutive crystallizations (two times from DCM/n-pentane). Thus **93** was obtained as an orange solid (9.0 mg, 83 %).

^{31}P-NMR (162 MHz, CDCl$_3$) δ : 11.4 (d, J_{P-Rh}= 2.9 Hz) ppm.

^{1}H-NMR (400 MHz, CDCl$_3$) δ : 7.75-7.66 (m, 6H), 7.53-7.50 (m, 3H), 7.47-7.43 (m, 6H), 6.96-6.92 (m, 2H), 6.69 (t, J= 7.2 Hz, 1H), 6.54 (br, 2H), 1.36 (s, 3H), 1.34 (s, 15H) ppm.

^{13}C-NMR (101 MHz, CDCl$_3$) δ : 201.7 (dd, J_{C-P}= 35.8 Hz, J_{C-Rh}= 2.9 Hz), 194.0 (d, J_{C-P}= 27.7 Hz), 150.4, 133.8 (d, J_{C-P}= 9.9 Hz), 131.7 (d, J_{C-P}= 3.1 Hz), 128.7 (d, J_{C-P}= 12.4 Hz), 127.7, 127.3 (d, J_{C-P}= 93.3 Hz), 122.3, 120.8, 94.7 (d, J_{C-Rh}= 6.7 Hz), 94.0 (d, J_{C-P}= 95.7 Hz), 23.3, 9.6 ppm.

HRMS calculated m/z for C$_{38}$H$_{39}$ClNOPRh: 694.150034; found (ESI) 694.150324.

IR (neat) $\tilde{\nu}$: 3044, 2911, 1588, 1554, 1473, 1435, 1392, 1353, 1309, 1278, 1225, 1187, 1154, 1119, 1105, 1062, 1021, 994, 984, 905, 843, 768, 756, 742, 722, 708, 695 cm^{-1}.

Compound 94:
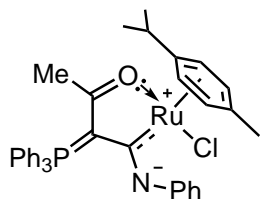
[{Ru(cym)Cl$_2$}$_2$] (10.6 mg, 0.017 mmol) and **80a** (22.6 mg, 0.035 mmol) were dissolved in DCE (0.7 ml) and then NEt$_3$ (0.08 ml, 0.595 mmol) was added drop-wise. The reaction mixture was heated at 50 ºC and stirred for 1 day. Then, the mixture was allowed to cool down to room temperature and filtered. The bright red solution was evaporated *in vacuo* and the remaining orange solid was purified by consecutive crystallisations (two times from DCM/n-pentane) to afford **94** (14.1 mg, 59 %) as an orange solid.

^{31}P-NMR (162 MHz, CD$_2$Cl$_2$) δ : 11.6 ppm.

^{1}H-NMR (400 MHz, CD$_2$Cl$_2$) δ : 7.72 (dd, J= 12.3, 7.9 Hz, 6H), 7.56-7.55 (m, 3H), 7.49-7.47 (m, 6H), 7.00 (t, J= 7.4 Hz, 2H), 6.78 (t, J= 7.4 Hz, 1H), 6.40 (br, 2H), 5.42 (d, J= 5.9 Hz, 1H), 4.96 (d, J= 5.9 Hz, 1H), 4.70 (d, J= 5.4 Hz, 1H), 3.77 (d, J= 5.4 Hz, 1H), 2.42 (quint J= 6.8 Hz, 1H), 1.94 (s, 3H), 1.28 (s, 3H), 1.08 (d, J= 6.8 Hz, 3H), 1.03 (d, J= 6.8 Hz, 3H) ppm.

^{13}C-NMR (101 MHz, CD$_2$Cl$_2$) δ : 208.8 (d, J_{C-P}= 2.8 Hz), 194.9 (d, J_{C-P}= 28.1 Hz), 155.5, 134.2 (d, J_{C-P}= 9.9 Hz), 132.1 (d, J_{C-P}= 2.9 Hz), 128.9 (d, J_{C-P}= 12.4 Hz), 128.1, 127.3 (d, J_{C-P}= 93.0 Hz), 122.0, 120.8, 102.5, 98.0, 93.2 (d, J_{C-P}= 97.3 Hz), 91.0, 84.2, 82.1, 76.6, 31.4, 23.2, 22.5, 22.2, 19.0 ppm.

HRMS calculated m/z C$_{38}$H$_{38}$ClNOPRu: 692.141123; found (ESI) 692.141970.

IR (neat) $\tilde{\nu}$: 3057, 2958, 2849, 1917, 1738, 1589, 1556, 1472, 1436, 1384, 1260, 1191, 1160, 1103, 1025, 983, 864, 844, 801, 743, 726, 710, 692 cm^{-1}.

Compound 97:
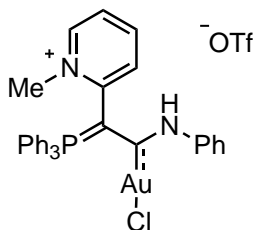
Complex **80e** (39 mg, 5.7×10^{-2} mmol) was dissolved in DCM (0.6 ml) and cooled to -50 °C . Then, MeOTf (6.4 µl, 5.7×10^{-2} mmol) was added drop-wise and the mixture was stirred for 1 day at the same temperature, observing the formation of a yellow precipitate. The reaction mixture was warmed to room temperature and the solution filtered via cannula to a second flask, affording pure **97** as a pale yellow solid. A second crop of **97** could be obtained from the remaining solution after solvent evaporation and washing the remaining solid with small portions of DCM (43 mg in total, 88 %).

^{31}P-NMR (162 MHz, CD$_3$CN) δ : 21.1 ppm.

^{1}H-NMR (400 MHz, CD$_3$CN) δ : 8.56 (dd, J= 6.2, 1.5 Hz, 1H), 8.13 (s, 1H), 8.04 (td, J= 7.9, 1.5 Hz, 1H), 7.78 (br, 4H), 7.75-7.62 (m, 6H), 7.62-7.47 (m, 7H), 7.35-7.28 (m, 2H), 7.24-7.13 (m, 1H), 4.28 (s, 3H) ppm.

^{13}C-NMR (101 MHz, CD$_3$CN) δ : 195.5 (d, J_{C-P}= 31.8 Hz), 153.0 (d, J_{C-P}= 20.0 Hz), 148.7, 146.4, 145.2, 136.3 (d, J_{C-P}= 2.6 Hz), 135.2 (d, J_{C-P}= 9.4 Hz), 134.7 (d, J_{C-P}= 2.9 Hz), 130.4 (d, J_{C-P}= 12.6 Hz), 129.5, 127.9, 126.8, 125.1, 124.5 (d, J_{C-P}= 92.4 Hz), 78.3 (d, J_{C-P}= 141.2 Hz), 47.2 ppm.

HRMS calculated m/z C$_{32}$H$_{28}$AuClN$_2$P$^+$: 703.133866; found 703.133492.

IR (neat) $\tilde{\nu}$: 3052, 3023, 1624, 1584, 1490, 1482, 1434, 1375, 1312, 1269, 1183, 1140, 1098, 1056, 1017, 994, 861, 786, 742, 709 cm^{-1}.

Compound 98:
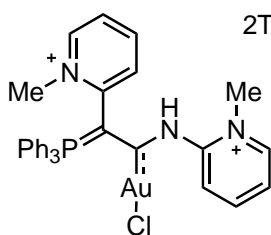
Complex **80k** (24.0 mg, 3.5×10^{-2} mmol) was dissolved in DCM (0.5 ml) and cooled to -50 °C . Then, MeOTf (8 µl, 7.0×10^{-2} mmol) was added drop-wise and the mixture was stirred for 1 day at the same temperature, observing the formation of a precipitate. The reaction was warmed to room temperature and the solution filtered via cannula, washing the resulting solid with portions of DCM. After drying the remaining yellow solid *in vacuo*, pure **98** was obtained (23 mg, 65 %).

^{31}P-NMR (122 MHz, CD$_3$CN) δ : 21.7 ppm

^{1}H-NMR (300 MHz, CD$_3$CN) δ : 8.67-8.50 (m, 2H), 8.47-8.36 (m, 3H), 8.31-8.16 (m, 1H), 7.98-7.70 (m, 12H), 7.65-7.59 (m, 6H), 4.20 (s, 3H), 4.09 (s, 3H) ppm.

HRMS calculated m/z for C$_{34}$H$_{29}$Au$_1$Cl$_1$F$_6$N$_3$O$_6$P$_1$S$_2$$^+$: 1016.048826; found 1016.050100.

III.1.3   Enantioselective synthesis of hexahelicenes through gold(I)-catalysis

III.1.3.1   Starting materials

PCl_3 was distilled prior use. 4 Å molecular sieves were activated by heat at 200 °C under high vacuum for 3 days. $NaSbF_6$ was ground and dried under high vacuum at 120 °C for 3 days. $AgSbF_6$ was always stored and handled inside the glovebox.

TADDOLs **156a**, **156b**,[223] **156c**, **156d**[224] and **156e**[225] were prepared according literature procedures from (+)-Dimethyl-2,3-*O*-isopropylidene-D-tartrate (Aldrich, 98 %*ee*) and the corresponding arylmagnesium bromide. (*2R,3R*)-Diethyl-2,3-dimethoxy-succinate and methoxy-protected TADDOLs **158a**, **158b** and **158c** were prepared from (+)-Diethyl-L-tartrate (Aldrich, *ee* ≥ 99 %) following the procedure described by Fürstner and co-workers.[25,226] IMes was obtained from the corresponding imidazolium salt, synthesised according Ritter *et al.*,[227] using the procedure established by Nolan and co-workers.[228] 1-[2,6-di(*iso*-propyl)phenyl]-3,3,5,5-tetramethyl-2-pyrrolidinylidene lithium triflate adduct **201** was provided by Dr. Estela Haldon Hermoso, synthesised according to the literature.[81] Compounds **156f** and **197** were provided by the group of Prof. Fürstner. Cationic chiral phosphonites **159a**, **160a** and **163** and their corresponding gold(I) chlorides **164a**, **165a** and **168** were synthesised by Leo Nicholls. The starting material for all the substrates was 2,7-dimethylnaphthalene **183**, prepared according to the described procedure by Siegel and co-workers.[206] The Ohira-Bestmann reagent,[229] (*S*)-1-iodo-4-(1-phenylethoxy)benzene[230] and chiral gold(I) complexes **193**,[23] **194**,[200] **195** and **196**[20c] were prepared according literature procedures.

III.1.3.2   Synthesis of ligands and gold(I) complexes

Compound 158d :
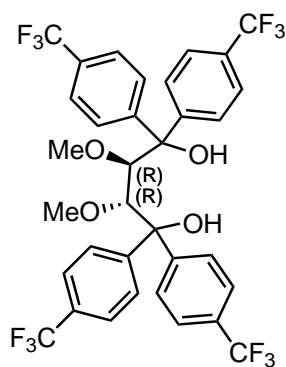
Prepared by a modified procedure reported by Fürstner and co-workers.[25,226] Activated Mg turnings (531 mg, 21.85 mmol) were placed in a Schlenk and suspended in THF (5 ml). A solution of 1-bromo-4-(trifluoromethyl)benzene (3 ml, 21.43 mmol) in THF (17 ml) was then added drop-wise, maintaining a gentle reflux. Once all the bromide was added, the resulting mixture was heated to reflux for 1 h, before cooling to 0 °C . At this temperature, a solution of (*2R,3R*)-Diethyl-2,3-dimethoxysuc-cinate (1.00 g, 4.28 mmol) in THF (5 ml) was slowly added and

the mixture was heated to reflux for 2 h more. The reaction was quenched by slow addition of saturated NH_4Cl solution (20 ml) and 1 M HCl (2 ml). The two phases were separated and the aqueous fraction washed with portions of MTBE. The organic layers were combined, dried over Na_2SO_4 and the solvent evaporated *in vacuo* to afford a red oil. The crude was purified by flash chromatography (hexanes/EtOAc, 8/2), to obtain a light yellow foam, which was washed with portions of *n*-pentane, thus obtaining the desired compound **158d** as a white solid (1.00 g, 32 %).

^{1}H-NMR (400 MHz, $CDCl_3$) δ : 7.71-7.66 (m, 12H), 7.55 (d, J= 8.4 Hz, 4H), 4.67 (s, 2H), 4.39 (s, 2H), 2.60 (s, 6H) ppm.

^{13}C-NMR (101 MHz, $CDCl_3$) δ : 148.4, 147.8, 130.2 (q, J_{C-F}= 32.9 Hz), 129.8 (q, J_{C-F}= 32.8 Hz), 126.7, 126.3, 126.0 (q, J_{C-F}= 3.5 Hz), 125.3 (q, J_{C-F}= 3.7 Hz), 124.0 (q, J_{C-F}= 273.2 Hz), 123.9 (q, J_{C-F}= 273.4 Hz), 84.7, 80.0, 61.4 ppm.

^{19}F-NMR (282 MHz, $CDCl_3$) δ : -62.6, -62.7 ppm.

HRMS calculated m/z for $C_{34}H_{26}F_{12}O_4Na^+$: 749.153171; found (ESI) 749.153490.

IR (neat) $\tilde{\nu}$: 3471, 2982, 2936, 2845, 1617, 1413, 1324, 1163, 1117, 1069, 1016, 840, 771, 734, 706, 674, 629, 600, 500, 436 cm^{-1}.

$[\alpha]_D^{20}$= -87.6 (c = 1.11, DCM).

Synthesis of chiral cationic phosphonites
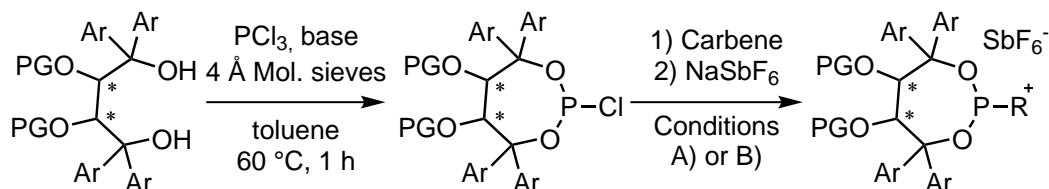
Conditions A) base = pyridine; 1) IMes, Et_2O, -78°C, 2 h ; 2) $NaSbF_6$ (3 equiv.), -78 °C-rt, overnight (general procedure B). Conditions B) base = NEt_3; 1) IMes or CAAC, Et_2O, -78 °C -rt, overnight; 2) $NaSbF_6$ (3 equiv.), CH_3CN, rt, 2 h (general procedure C).

General Procedure B:

The synthesis of the chlorophosphites was based on the procedure reported by Fürstner and co-workers.[25,226] The desired TADDOL (1 equiv.) and powdered 4 Å molecular sieves (100 mg) were placed in a Schlenk, suspended in toluene (0.02 M) and cooled to 0 °C . Then, dry pyridine (3 equiv.) and PCl_3 (1.05 equiv.) were successively added, stirring the reaction mixture at this temperature for 10 min, after which was heated to 60 °C for 1 h. After cooling to room temperature, the reaction was filtered under argon atmosphere using a cannula fitted with a glass-fibre filter. The filtrate was evaporated and the resulting chlorophosphite dried under vacuum.

The obtained residue was suspended in Et_2O (0.087 M), cooled to -78 °C and a solution of IMes (0.7–0.9 equiv.) in Et_2O (0.14 M) was added drop-wise. The reaction mixture was stirred at this temperature for 2 h, after which $NaSbF_6$ (3 equiv.) was added, allowing the reaction mixture to reach room temperature slowly overnight.

The solvent was removed *in vacuo* and the resulting solid washed with two portions of Et_2O and one of *n*-pentane. Then, DCM was added and the resulting suspension filtered under an argon atmosphere, using a cannula fitted with a glass-fibre filter, washing the remaining solid with more portions of DCM. The filtrate was evaporated affording a white solid that was further purified by flash chromatography at -10 °C as specified for each case.

General Procedure C:

The chlorophosphite was first prepared analogously to general procedure B, but using NEt_3 as a base instead of pyridine. After evaporation of the solvent, the obtained residue was redissolved in Et_2O (0.087 M), cooled to -78 °C and a solution of the carbene (0.9 equiv.) in Et_2O (0.14 M) was added drop-wise. The reaction mixture was stirred at this temperature for 2 h, after which was allowed to reach room temperature slowly overnight.

The solvent was removed *in vacuo*, adding to the resulting solid $NaSbF_6$ (3 equiv.) and dry CH_3CN (0.1 M). The mixture was stirred for 2 h, after which, the solvent was removed *in vacuo* and the remaining solid extracted with dry DCM. The filtrate was then evaporated and the desired compound was further purified as specified for each case.

Compound 159b :
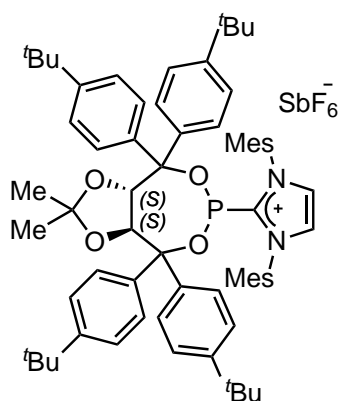
Prepared using general procedure C, obtaining first the chlorophosphite from diol **156b** (144 mg, 0.21 mmol), NEt_3 (89 µl, 0.64 mmol) and PCl_3 (19 µl, 0.22 mmol). This intermediate was then treated with IMes (58 mg, 0.19 mmol). After solvent evaporation, the resulting solid was treated with $NaSbF_6$ (163 mg, 0.63 mmol) in dry CH_3CN. After workup, the crude was further purified dissolving the remaining solid in Et_2O (3 ml) and filtering the mixture via cannula. The filtrate was evaporated and the resulting white solid dried *in vacuo* to afford **159b** (70 mg, 29 %).

^{31}P-NMR (162 MHz, CD_3CN) δ : 144.0 ppm.

^{1}H-NMR (400 MHz, CD_3CN) δ : 7.78 (d, J_{H-P}= 1.1 Hz, 2H), 7.43 (d, J= 8.7 Hz, 2H), 7.39 (dt, J= 8.6, 2.2 Hz, 2H), 7.36 (s, 4H), 7.29-7.23 (m, 6H), 7.11 (br, 2H), 6.78 (dt,

J= 8.6, 2.2 Hz, 2H), 6.51 (dt, J= 8.6, 2.2 Hz, 2H), 5.11 (dd, J= 8.6 Hz, J_{H-P}= 4.8 Hz, 1H), 4.58 (d, J= 8.6 Hz, 1H), 2.49 (s, 6H), 2.09 (s, 6H), 1.74 (s, 6H), 1.34 (s, 9H), 1.34 (s, 21H), 1.30 (s, 9H), -0.05 (s, 3H) ppm.

^{13}C-NMR (101 MHz, CD$_3$CN) δ : 153.0, 152.8, 152.7, 152.5, 145.5 (d, J_{C-P}= 64.3 Hz), 142.7, 142.0, 141.2 (d, J_{C-P}= 4.7 Hz), 136.8 (d, J_{C-P}= 2.9 Hz), 136.5 , 136.1, 136.0 (d, J_{C-P}= 1.2 Hz), 132.2, 131.1, 130.7, 129.8, 129.2, 129.0 (d, J_{C-P}= 3.7 Hz), 128.3, 128.1, 126.5, 126.2, 125.8, 125.1, 113.5, 87.2 (d, J_{C-P}= 11.4 Hz), 86.1 (d, J_{C-P}= 8.1 Hz), 83.5 (d, J_{C-P}= 3.1 Hz), 81.6 (d, J_{C-P}= 28.3 Hz), 35.3, 35.2, 35.1, 31.5, 31.4, 27.6, 24.5, 21.5, 18.2, 18.0, 18.0 ppm.

HRMS calculated m/z for C$_{68}$H$_{84}$N$_2$O$_4$P$^+$: 1023.616322; found (ESI) 1023.616810.

IR (neat) $\tilde{\nu}$: 2961, 2906, 2870, 1636, 1603, 1578, 1508, 1460, 1407, 1383, 1367, 1292, 1268, 1231, 1167, 1148, 1109, 1092, 1021, 980, 950, 930, 878, 851, 838, 766, 710, 656, 610, 586, 565, 509 cm^{-1}.

$[\alpha]_D^{20}$= +65.5 (c = 0.99, DCM).

Compound 159c :
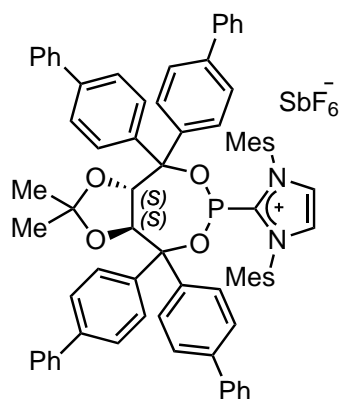
Prepared using general procedure B, obtaining first the chlorophosphite from diol **156c** (158 mg, 0.20 mmol), pyridine (50 µl, 0.61 mmol) and PCl$_3$ (19 µl, 0.21 mmol). This intermediate was then treated with IMes (44 mg, 0.14 mmol) and NaSbF$_6$ (156 mg, 0.60 mmol). After workup, the crude was further purified by flash chromatography at -10 ºC (gradient from DCM to DCM/EtOAc, 9/1) to afford **159c** as a white solid (93 mg, 48 %).

^{31}P-NMR (162 MHz, CD$_3$CN) δ : 146.7 ppm.

^{1}H-NMR (400 MHz, CD$_3$CN) δ : 7.83 (d, J_{H-P}= 1.0 Hz, 2H), 7.71-7.63 (m, 14H), 7.61-7.58 (m, 2H) , 7.56-7.46 (m, 12H), 7.45-7.38 (m, 4H), 7.31 (s, 2H), 7.12 (s, 2H), 7.04 (d, J= 8.4 Hz, 2H), 6.78 (d, J= 8.5 Hz, 2H), 5.33 (dd, J= 8.6 Hz, J_{H-P}= 4.8 Hz, 1H), 4.72 (d, J= 8.6 Hz, 1H), 2.43 (s, 6H), 2.16 (s, 6H), 1.79 (s, 6H), 1.42 (s, 3H), 0.10 (s, 3H) ppm.

^{13}C-NMR (101 MHz, CD$_3$CN) δ : 145.1 (d, J_{C-P}= 62.6 Hz), 143.5, 142.8, 142.8, 142.5, 142.2, 142.0, 141.7, 140.8, 140.7, 140.7, 140.3, 138.7 (d, J_{C-P}= 2.5 Hz), 138.3, 136.0, 136.0, 132.1, 131.0, 130.8, 130.7, 130.1, 130.0, 130.0, 129.9, 129.9, 129.3 (d, J_{C-P}= 4.2 Hz), 129.0, 129.0, 128.9, 128.9, 128.8, 128.1, 128.0, 127.8, 127.8, 127.7, 127.5, 126.7, 113.8, 87.2 (d, J_{C-P}= 11.7 Hz), 86.2 (d, J_{C-P}= 8.4 Hz), 83.6 (d, J_{C-P}= 3.1 Hz), 81.3 (d, J_{C-P}= 28.9 Hz), 27.6, 24.8, 21.4, 18.2, 18.0, 18.0 ppm.

HRMS calculated m/z for C$_{76}$H$_{68}$N$_2$O$_4$P$^+$: 1103.491122; found (ESI) 1103.491010.

IR (neat) $\tilde{\nu}$: 2962, 2919, 2853, 1599, 1577, 1542, 1485, 1448, 1404, 1373, 1342, 1327, 1260, 1229, 1208, 1163, 1089, 1020, 1009, 981, 961, 875, 847, 799, 762, 743, 697, 655, 603, 570, 554, 538, 505, 488 cm^{-1}.

$[\alpha]_D^{20}$= +91.0 (c = 1.01, DCM).

Compound 159d :
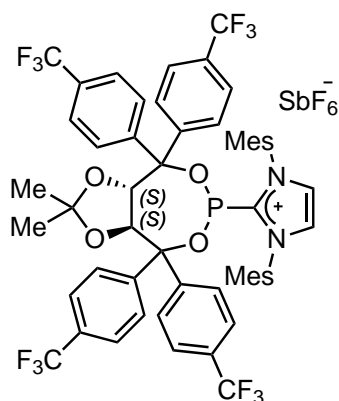
Prepared using general procedure B, obtaining first the chlorophosphite from diol **156d** (499 mg, 0.68 mmol), pyridine (164 µl, 2.03 mmol) and PCl$_3$ (62 µl, 0.71 mmol). This intermediate was then treated with IMes (179 mg, 0.59 mmol) NaSbF$_6$ (528 mg, 2.04 mmol). After workup, the crude was further purified by flash chromatography at -10 °C (DCM/EtOAc, 9.5/0.5) to afford **159d** as a white solid (556 mg, 72 %).

^{31}P-NMR (162 MHz, CD$_3$CN) δ : 147.0 ppm.

^{1}H-NMR (400 MHz, CD$_3$CN) δ : 7.85 (d, J_{H-P}= 1.1 Hz, 2H), 7.74 (d, J= 7.9 Hz, 2H), 7.70 (d, J= 7.9 Hz, 2H), 7.63 (d, J= 8.1 Hz, 2H), 7.56 (d, J= 8.1 Hz, 2H), 7.52 (d, J= 7.9 Hz, 2H), 7.50 (d, J= 8.1 Hz, 2H), 7.24 (s, 2H), 7.14 (d, J= 8.1 Hz, 2H), 7.10 (s, 2H), 6.78 (d, J= 7.9 Hz, 2H), 5.21 (dd, J= 8.6 Hz, J_{H-P}= 4.9 Hz, 1H), 4.60 (d, J= 8.6 Hz, 1H), 2.45 (s, 6H), 2.08 (s, 6H), 1.73 (s, 6H), 1.33 (s, 3H), 0.08 (s, 3H) ppm.

^{13}C-NMR (101 MHz, CD$_3$CN) δ : 147.6, 147.0, 143.9 (d, J_{C-P}= 60.8 Hz), 143.2, 142.9, 135.9, 135.8, 135.8, 131.9 (d, J_{C-P}= 1.3 Hz), 131.7 (q, J_{C-F}= 32.5 Hz), 131.3 (q, J_{C-F}= 32.5 Hz), 131.3 (q, J_{C-F}= 32.5 Hz), 131.0, 130.9, 130.8, 130.5, 130.1 (d, J_{C-P}= 5.4 Hz), 129.7, 129.5, 129.4, 126.9 (q, J_{C-F}= 3.8 Hz), 126.4 (q, J_{C-F}= 3.8 Hz), 126.2 (q, J_{C-F}= 3.8 Hz), 125.4 (q, J_{C-F}= 3.8 Hz), 125.0 (q, J_{C-F}= 272.5 Hz), 125.1 (q, J_{C-F}= 272.5 Hz), 125.0 (q, J_{C-F}= 272.5 Hz, 2C), 114.6, 86.6 (d, J_{C-P}= 12.1 Hz), 85.8 (d, J_{C-P}= 7.6 Hz), 82.5 (d, J_{C-P}= 3.5 Hz), 80.6 (d, J_{C-P}= 29.6 Hz), 27.4, 24.9, 21.3, 18.2, 17.9, 17.8 ppm.

^{19}F-NMR (282 MHz, CD$_3$CN) δ : -63.2, -63.3, -63.4, -63.4, -124.0 (sext, $J_{F-^{121}Sb}$ = 1952.9 Hz), -124.0 (oct, $J_{F-^{123}Sb}$ = 1055.0 Hz) ppm.

HRMS calculated m/z for C$_{56}$H$_{48}$F$_{12}$N$_2$O$_4$P$^+$: 1071.315464; found (ESI) 1071.317040.

IR (neat) $\tilde{\nu}$: 3172, 3146, 2991, 1608, 1455, 1411, 1376, 1324, 1229, 1166, 1121, 1069, 1043, 1018, 992, 964, 951, 925, 879, 852, 827, 756, 731, 656, 612, 575, 533, 508 cm^{-1}.

$[\alpha]_D^{20}$= +88.1 (c = 1.05, DCM).

Compound 159e :
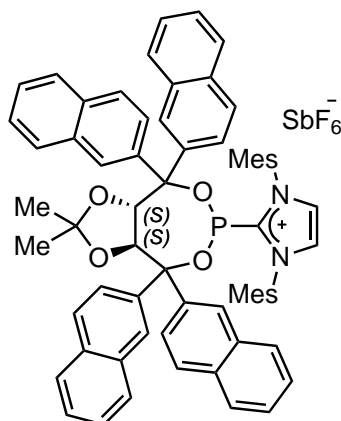
Prepared using general procedure B, obtaining first the chlorophosphite from diol **156e** (147 mg, 0.22 mmol), pyridine (54 µl, 0.66 mmol) and PCl_3 (20 µl, 0.23 mmol). This intermediate was then treated with IMes (60 mg, 0.20 mmol) and $NaSbF_6$ (171 mg, 0.66 mmol). After workup, the crude was further purified by flash chromatography at -10 °C (gradient from DCM to DCM/EtOAc, 9/1) to afford **159e** as a white solid (157 mg, 64 %).

^{31}P-NMR (162 MHz, CD_3CN) δ : 145.1 ppm.

^1H-NMR (400 MHz, CD_3CN) δ : 8.42 (s, 1H), 8.03 (d, $J=$ 1.5 Hz, 1H), 7.98-7.91 (m, 5H), 7.89-7.75 (m, 8H), 7.70 (d, $J=$ 8.0 Hz, 1H), 7.66-7.48 (m, 8H), 7.40 (br, 1H), 7.34 (dd, $J=$ 8.7, 2.0 Hz, 1H), 7.30 (d, $J=$ = 1.9 Hz, 1H), 7.26 (dd, $J=$ 8.7, 1.9 Hz, 1H), 7.19 (br, 2H), 7.11 (dd, $J=$ 8.7, 2.0 Hz, 1H), 6.94 (dd, $J=$ 8.6, 1.9 Hz, 1H), 6.74 (s, 2H), 5.71 (dd, $J=$ 8.6 Hz, $J_{H-P}=$ 5.3 Hz, 1H), 5.02 (d, $J=$ 8.6 Hz, 1H), 2.33 (s, 6H), 2.14 (s, 6H), 1.62 (s, 6H), 1.39 (s, 3H), -0.19 (s, 3H) ppm.

^{13}C-NMR (101 MHz, CD_3CN) δ : 145.1 (d, $J_{C-P}=$ 63.8 Hz), 142.7, 141.4, 141.1 (d, $J_{C-P}=$ 4.9 Hz), 137.4 (d, $J_{C-P}=$ 2.7 Hz), 136.8, 135.9, 135.8, 134.1, 134.0, 133.8, 133.3, 133.3, 133.1, 133.1, 132.1, 130.9, 130.7, 130.2, 129.9, 129.8, 129.3, 129.3, 129.3, 129.2, 129.0, 128.7, 128.5, 128.5, 128.6, 128.4, 128.4, 128.3, 128.2, 128.1, 127.9, 127.8, 127.8, 127.7, 127.6, 127.5, 127.5, 127.4, 127.1, 126.9, 126.0, 113.8, 87.9 (d, $J_{C-P}=$ 11.5 Hz), 87.1 (d, $J_{C-P}=$ 7.7 Hz), 83.2 (d, $J_{C-P}=$ 3.3 Hz), 80.9 (d, $J=$ 30.6 Hz), 27.7, 25.1, 21.3, 18.2, 17.9, 17.8 ppm.

HRMS calculated m/z for $C_{68}H_{60}N_2O_4P^+$: 999.428522; found (ESI) 999.429250.

IR (neat) $\tilde{\nu}$: 3146, 3056, 2986, 2921, 1601, 1505, 1481, 1453, 1372, 1274, 1229, 1215, 1162, 1127, 1091, 1047, 1018, 992, 958, 942, 896, 878, 854, 816, 773, 757, 747, 640, 607, 589, 568, 510 cm^{-1}.

$[\alpha]_D^{20}=$ +110.2 (c = 1.17, DCM).

Compound 159f :
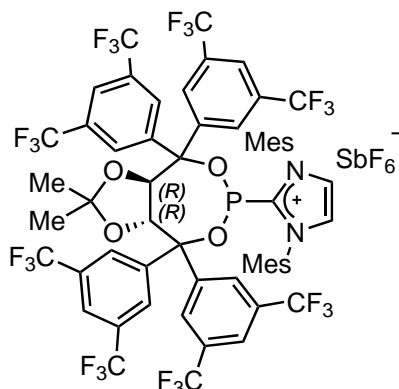
Prepared using general procedure B, obtaining first the chlorophosphite from diol **156f** (498 mg, 0.49 mmol), pyridine (120 µl, 1.48 mmol) and PCl_3 (45 µl, 0.52 mmol). Due to its insolubility in toluene, after cooling the reaction mixture to room temperature, the solvent was evaporated and the resulting solid was taken in Et_2O (25 ml). The mixture was filtered under argon atmosphere using a cannula fitted with a glass-fibre filter. The filtrate was evaporated and the resulting chlorophosphite dried under . Afterwards, it was treated with IMes (105 mg, 0.35 mmol) and $NaSbF_6$ (380 mg, 1.47 mmol) following general procedure B. After workup, the crude was further purified by flash chromatography at -10 ºC (DCM/EtOAc, 9.5/0.5) to afford **159f** as a white solid (248 g, 55 %).

^{31}P-NMR (162 MHz, CD_3CN) δ : 148.9 ppm.

^{1}H-NMR (400 MHz, CD_3CN) δ : 8.24 (s, 1H), 8.21 (s, 1H), 8.17 (s, 1H), 8.16 (s, 1H), 7.81 (s, 2H), 7.81 (s, 2H), 7.79 (br, 2H), 7.54 (s, 2H), 7.47 (s, 2H), 7.16 (s, 2H), 6.49 (s, 2H), 5.28 (dd, J= 8.1 Hz, J_{H-P}= 5.9 Hz, 1H), 4.75 (d, J= 8.1 Hz, 1H), 2.26 (s, 6H), 2.16 (s, 6H), 1.59 (s, 6H), 0.89 (s, 3H), 0.20 (s, 3H) ppm.

^{13}C-NMR (101 MHz, CD_3CN) δ : 144.61 (d, J_{C-P}= 2.7 Hz), 143.6, 143.0, 141.69 (d, J_{C-P}= 61.5 Hz), 141.08 (d, J_{C-P}= 3.0 Hz), 140.3, 135.0, 134.9, 134.7, 134.7, 132.9 (q, J_{C-F}= 33.7 Hz), 132.4 (q, J_{C-F}= 33.7 Hz), 131.8 (q, J_{C-F}= 33.7 Hz), 131.6 (q, J_{C-F}= 33.7 Hz), 131.2, 131.2, 131.0 (br), 130.7, 130.5 (br), 130.4 (br), 130.2, 129.8, 129.5 (q, J_{C-F}= 3.8 Hz), 125.6-125.5 (m), 125.0 (sept, J_{C-F}= 3.5 Hz), 124.9-124.5 (m), 124.1 (q, J_{C-F}= 273.3 Hz), 124.0 (q, J_{C-F}= 273.5 Hz), 123.9 (q, J_{C-F}= 273.5 Hz), 116.6, 86.4, 86.1 (d, J_{C-P}= 13.6 Hz), 79.0 (d, J_{C-P}= 3.7 Hz), 77.9 (d, J_{C-P}= 32.5 Hz), 27.0, 26.2, 21.0, 17.8, 17.8, 17.6 ppm.

^{19}F-NMR (282 MHz, CD_3CN) δ : -63.0, -63.1, -63.2, -63.3, -124.1 (sext, $J_{F-^{121}Sb}$ = 1912.0 Hz), -124.1 (oct, $J_{F-^{123}Sb}$ = 1030.7 Hz) ppm.

HRMS calculated m/z for $C_{60}H_{44}F_{24}N_2O_4P^+$: 1343.265006; found (ESI) 1343.266970.

IR (neat) $\tilde{\nu}$: 2993, 2924, 1625, 1609, 1483, 1467, 1456, 1373, 1278, 1231, 1177, 1135, 1008, 986, 901, 876, 847, 835, 805, 707, 683, 657, 570, 523, 514, 500 cm^{-1}.

$[\alpha]_D^{20}$= -24.3 (c = 1.23, DCM).

Compound 160b :
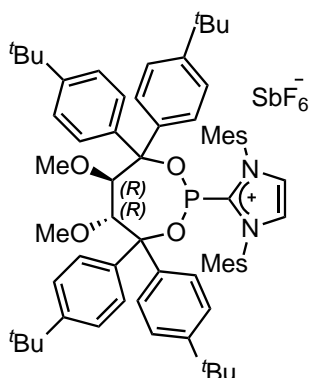
Prepared using general procedure C, obtaining first the chlorophosphite from diol **158b** (303 mg, 0.44 mmol), NEt$_3$ (186 µl, 1.25 mmol) and PCl$_3$ (41 µl, 0.48 mmol). This intermediate was then treated with IMes (122 mg, 0.40 mmol) and NaSbF$_6$ (342 mg, 1.32 mmol). After workup, the crude was further purified by flash chromatography (DCM/EtOAc, 9/1) to afford **160b** as a white solid (100 mg, 20 %).

^{31}P-NMR (162 MHz, CD$_3$CN) δ : 144.6 ppm.

^{1}H-NMR (400 MHz, CD$_3$CN) δ : 7.71 (d, J_{H-P}= 0.9 Hz, 2H), 7.40-7.35 (m, 4H), 7.31 (d, J= 9.0 Hz, 2H), 7.27-7.25 (m, 4H), 7.18 (d, J= 8.1 Hz, 2H), 7.14 (s, 2H), 6.97 (d, J= 8.6 Hz, 2H), 6.71 (dt, J= 8.6, 2.2 Hz, 2H), 6.61 (dt, J= 8.5, 2.2 Hz, 2H), 4.42 (t, J= 7.1 Hz, 1H), 3.98 (d, J= 7.1 Hz, 1H), 3.29 (s, 3H), 2.51 (s, 6H), 2.22 (s, 3H), 1.98 (s, 6H), 1.57 (s, 6H), 1.35 (s, 9H), 1.33 (s, 9H), 1.33 (s, 9H), 1.32 (s, 9H) ppm.

^{13}C-NMR (101 MHz, CD$_3$CN) δ : 152.8, 152.6, 152.4, 152.1, 145.8 (d, J_{C-P}= 67.7 Hz), 142.7, 141.5 (d, J_{C-P}= 4.2 Hz), 141.4, 136.6 (d, J_{C-P}= 2.9 Hz), 136.6, 136.1, 135.9, 132.3, 131.0, 130.8, 129.8, 128.8, 128.8 (d, J_{C-P}= 5.1 Hz), 128.5, 128.3, 126.3, 125.8, 125.7, 124.3, 89.0 (d, J_{C-P}= 3.9 Hz), 86.9 (d, J_{C-P}= 14.7 Hz), 84.1, 81.5 (d, J_{C-P}= 28.5 Hz), 61.0, 59.7, 35.3, 35.2, 35.2, 35.1, 31.5, 31.5, 31.5, 31.5, 21.5, 17.9, 17.5, 17.4 ppm.

HRMS calculated m/z for C$_{67}$H$_{84}$N$_2$O$_4$P$^+$: 1011.616322; found (ESI) 1011.616600.

IR (neat) $\tilde{\nu}$: 3177, 3153, 2960, 2904, 2869, 1556, 1510, 1475, 1459, 1405, 1375, 1321, 1306, 1258, 1214, 1162, 1092, 971, 930, 884, 847, 836, 821, 771, 738, 708, 655, 583, 515, 502 cm^{-1}.

$[\alpha]_D^{20}$= -66.5 (c = 1.00, DCM).

Compound 160c :
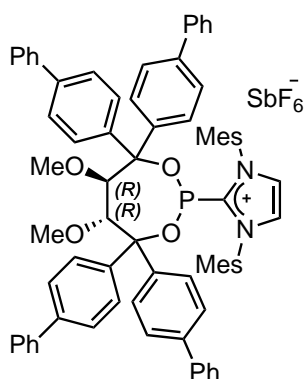
Prepared using general procedure B, obtaining first the chlorophosphite from diol **158c** (460 mg, 0.60 mmol), pyridine (147 µl, 1.82 mmol) and PCl$_3$ (55 µl, 0.64 mmol). This intermediate was then treated with IMes (129 mg, 0.42 mmol) and NaSbF$_6$ (466 mg, 1.80 mmol). After workup, the crude was further purified by flash chromatography at -10 °C (gradient from DCM to DCM/EtOAc, 9.5/0.5) to afford **160c** as a white solid (387 mg, 69 %).

^{31}P-NMR (162 MHz, CD$_3$CN) δ : 143.8 ppm.

^{1}H-NMR (400 MHz, CD$_3$CN) δ : 7.76 (s, 2H), 7.74-7.60 (m, 14H), 7.58-7.55 (m, 4H), 7.54-7.37 (m, 12H), 7.32 (s, 2H), 7.17 (d, J= 8.5 Hz, 2H), 7.14 (s, 2H), 6.92 (dd, J= 8.6, 2.4 Hz, 4H), 4.71 (t, J= 7.1 Hz, 1H), 4.05 (d, J= 7.1 Hz, 1H), 3.50 (s, 3H), 2.48 (s, 6H), 2.34 (s, 3H), 2.06 (s, 6H), 1.65 (s, 6H) ppm.

^{13}C-NMR (101 MHz, CD$_3$CN) δ : 145.2 (d, J_{C-P}= 64.9 Hz), 143.2 (d, J_{C-P}= 4.5 Hz), 142.9, 142.3, 142.0, 141.7, 141.4, 140.8, 140.7, 140.7, 140.5, 138.6 (d, J_{C-P}= 2.9 Hz), 138.3, 136.0, 135.9, 132.1, 130.9, 130.8, 130.1, 130.0, 130.0, 129.9, 129.8, 129.8, 129.2, 129.02, 128.9 (d, J_{C-P}= 8.1 Hz), 128.8, 128.7, 128.0, 127.9, 127.9, 127.8, 127.6, 127.2, 126.0, 88.9 (d, J_{C-P}= 5.3 Hz), 87.0 (d, J_{C-P}= 14.9 Hz), 85.3, 81.2 (d, J_{C-P}= 28.6 Hz), 61.4, 60.4, 21.4, 18.0, 17.6, 17.5 ppm.

HRMS calculated m/z for C$_{75}$H$_{68}$N$_2$O$_4$P$^+$: 1091.4911; found (ESI) 1091.4910.

IR (neat) $\tilde{\nu}$: 3155, 3130, 3077, 3054, 3030, 2922, 2835, 1600, 1561, 1517, 1485, 1401, 1378, 1297, 1229, 1184, 1123, 1076, 1021, 993, 957, 921, 854, 762, 746, 696, 655, 608, 572, 528, 503 cm^{-1}.

$[\alpha]_D^{20}$= -64.0 (c = 1.08, DCM).

Compound 160d :
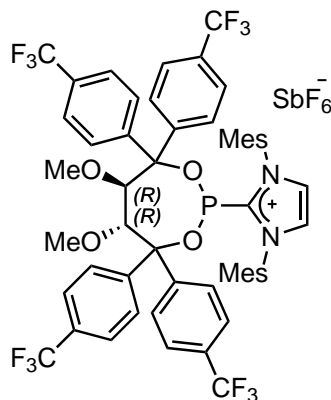
Prepared using general procedure B, obtaining first the chlorophosphite from diol **158d** (302 mg, 0.42 mmol), pyridine (101 µl, 1.25 mmol) and PCl$_3$ (38 µl, 0.44 mmol). This intermediate was then treated with IMes (89 mg, 0.29 mmol) and NaSbF$_6$ (326 mg, 1.26 mmol). After workup, the crude was further purified by flash chromatography at -10 °C (gradient from DCM to DCM/EtOAc, 9/1) to afford **160d** as a white solid (246 mg, 65 %).

^{31}P-NMR (162 MHz, CD$_3$CN) δ : 146.2 ppm.

^{1}H-NMR (400 MHz, CD$_3$CN) δ : 7.78 (d, J= 0.9 Hz, 2H), 7.69-7.64 (m, 6H), 7.60 (d, J= 8.3 Hz, 2H), 7.46 (d, J= 8.1 Hz, 2H), 7.22 (s, 2H), 7.19 (d, J= 8.3 Hz, 2H), 7.14 (s, 2H), 6.96 (d, J= 7.8 Hz, 2H), 6.94 (d, J= 7.7 Hz, 2H), 4.62 (dd, J= 7.5 Hz, J_{H-P}= 6.5 Hz, 1H), 3.87 (d, J= 7.5 Hz, 1H), 3.40 (s, 3H), 2.46 (s, 6H), 2.28 (s, 3H), 1.93 (s, 6H), 1.65 (s, 6H) ppm.

^{13}C-NMR (101 MHz, CD$_3$CN) δ : 147.2 (d, J_{C-P}= 4.5 Hz), 146.7, 143.9 (d, J_{C-P}= 62.6 Hz), 143.1, 142.8, 135.9, 135.7, 131.9, 131.4 (q, J_{C-F}= 32.7 Hz), 131.3 (q, J_{C-F}= 32.5 Hz), 131.0, 130.9, 130.9 (q, J_{C-F}= 32.5 Hz), 130.8, 130.8 (q, J_{C-F}= 32.6 Hz), 129.8 (d, J_{C-P}= 4.5 Hz), 129.6, 129.4, 129.3, 126.7-126.4 (m), 126.0 (q, J_{C-F}= 3.5 Hz), 125.2 (q, J_{C-F}= 272.4 Hz), 125.0 (q, J_{C-F}= 272.7 Hz), 124.9 (q, J_{C-F}= 272.6 Hz), 124.8 (q, J_{C-F}= 3.8 Hz), 88.2 (d, J_{C-P}= 5.4 Hz), 86.4 (d, J_{C-P}= 15.1 Hz), 84.9, 80.5

(d, J_{C-P}= 28.7 Hz), 61.4, 60.5, 21.3, 17.9, 17.5, 17.4 ppm.

^{19}F-NMR (282 MHz, CD$_3$CN) δ : -63.2, -63.2, -63.3, - 63.3, -124.1 (sext, $J_{F-^{121}Sb}$ = 1937.9 Hz), -124.1 (oct, $J_{F-^{123}Sb}$ = 1069.6 Hz) ppm.

HRMS calculated m/z for C$_{55}$H$_{48}$F$_{12}$N$_2$O$_4$P$^+$: 1059.315464; found (ESI) 1059.315390.

IR (neat) $\tilde{\nu}$: 3154, 3129, 1455, 1410, 1327, 1229, 1165, 1124, 1071, 1017, 996, 962, 933, 854, 828, 815, 776, 717, 654, 619, 573, 479 cm^{-1}

$[\alpha]_D^{20}$= -46.7 (c = 1.23, DCM).

Compound 161:
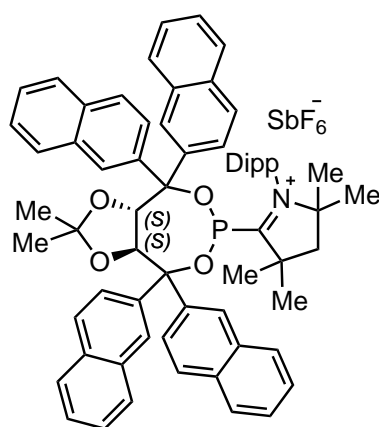
Prepared using general procedure C, obtaining first the chlorophosphite from diol **156e** (211 mg, 0.32 mmol), NEt$_3$ (132 µl, 0.95 mmol) and PCl$_3$ (29 µl, 0.33 mmol). This intermediate was then treated with CAAC·LiOTf adduct **56** (126 mg, 0.28 mmol). Since the removal of the triflate proved to be more difficult, the counteranion exchange in this case was performed stirring the reaction crude with NaSbF$_6$ (409 mg, 1.58 mmol) in CH$_3$CN (10 ml) at 60 ºC overnight. After workup, the crude was further purified by flash chromatography at -10 ºC (DCM/EtOAc, 9.5/0.5) to afford **161** as a bright yellow solid (140 mg, 40 %).

^{31}P-NMR (162 MHz, CD$_3$CN) δ : 160.1 ppm.

^{1}H-NMR (400 MHz, CD$_3$CN) δ : 8.30 (s, 1H), 8.27 (br, 1H), 8.05 (d, J= 7.8 Hz, 1H), 7.94-7.86 (m, 7H), 7.82-7.68 (m, 6H), 7.63-7.45 (m, 11H), 7.36 (dd, J= 8.7, 1.9 Hz, 1H), 7.33-7.28 (m, 2H), 6.60 (d, J= 8.7 Hz, 1H), 5.63 (d, J= 8.0 Hz, 1H), 5.32 (dd, J= 8.0 Hz, J_{H-P}= 3.5 Hz, 1H), 2.66 (d,J= 13.5 Hz, 1H), 2.58 (d,J= 13.5 Hz, 1H), 2.48 (sept, J= 6.5 Hz, 1H), 2.43 (s, 3H), 2.27 (s, 3H), 2.01 (sept, J= 6.5 Hz, 1H), 1.65 (s, 3H), 1.44 (s, 3H), 1.40 (s, 3H), 1.13 (d, J= 6.5 Hz, 3H), 0.98 (d, J= 6.5 Hz, 3H), 0.60 (d, J= 6.5 Hz, 3H), 0.10 (s, 3H), -0.37 (d, J= 6.5 Hz, 3H) ppm.

^{13}C-NMR (101 MHz, CD$_3$CN) δ : 207.0 (d, J_{C-P}= 63.2 Hz), 146.9, 144.1, 142.3, 139.8 (d, J_{C-P}= 3.5 Hz), 137.8 (d, J= 2.9 Hz), 134.4, 134.2, 134.0, 133.9, 133.8, 133.7, 133.7, 133.3, 133.3, 133.1, 130.4, 130.0 (d, J_{C-P}= 4.0 Hz), 129.7, 129.6, 129.4, 129.1, 129.1 (br), 129.0, 128.9, 128.8, 128.5 (br), 128.5, 128.4, 128.4, 128.3, 128.3, 128.2, 128.1, 128.1, 128.0, 127.9, 127.8, 127.6, 127.5, 126.9, 126.3, 126.3, 125.8, 114.9, 88.9 (d, J_{C-P}= 2.5 Hz), 88.2 (d, J_{C-P}= 11.2 Hz), 88.0 (d, J_{C-P}= 2.9 Hz), 84.3 (d, J_{C-P}= 4.0 Hz), 83.8 (d, J_{C-P}= 20.7 Hz), 55.3 (d, J_{C-P}= 3.1 Hz), 52.3, 30.5, 30.3, 30.1, 30.0, 29.8, 29.3, 27.7, 27.6, 25.4, 25.1, 25.1, 25.0, 23.0, 22.9 ppm.

^{19}F-NMR (282 MHz, CD$_3$CN) δ : -124.1 (sext, $J_{F-^{121}Sb}$ = 1955.0 Hz), -124.1 (oct,

$J_{F-^{123}Sb}$ = 1037.6 Hz) ppm.

HRMS calculated m/z for $C_{67}H_{67}NO_4P^+$: 980.480223; found (ESI) 980.480930.

IR (neat) $\tilde{\nu}$: 3059, 2972, 2938, 2873, 1598, 1505, 1459, 1374, 1273, 1244, 1214, 1161, 1127, 1097, 1052, 993, 958, 942, 878, 857, 810, 775, 758, 746, 709, 656, 568, 509, 477 cm^{-1}.

$[\alpha]_D^{20}$= +81.2 (c = 1.06, DCM).

Compound 162:
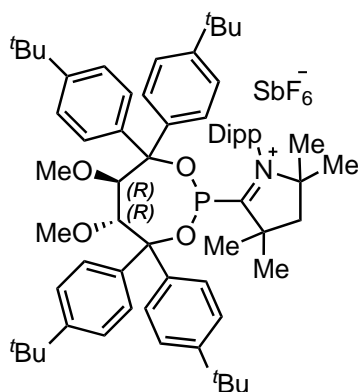
Prepared using general procedure C, obtaining first the chlorophosphite from diol **158b** (161 mg, 0.24 mmol), NEt$_3$ (99 µl, 0.71 mmol) and PCl$_3$ (22 µl, 0.25 mmol). This intermediate was then treated with CAAC·LiOTf adduct (94 mg, 0.21 mmol). The counteranion exchange in this case was performed stirring the reaction crude with NaSbF$_6$ (306 mg, 1.18 mmol) in CH$_3$CN (14 ml) at 60 ºC overnight. After workup, the crude was further purified by flash chromatography (DCM/EtOAc, 9.5/0.5) to afford **162** as a bright yellow solid (90 mg, 34 %).

^{31}P-NMR (162 MHz, CD$_3$CN) δ : 158.3 ppm.

^{1}H-NMR (400 MHz, CD$_3$CN) δ : 7.75 (t, J= 7.9 Hz, 1H), 7.45-7.42 (m, 3H), 7.38-7.30 (m, 7H), 7.15 (d, J= 9.0 Hz, 2H), 7.08-7.03 (m, 4H), 6.78 (d, J= 8.1 Hz, 2H), 4.42 (d, J= 7.2 Hz, 1H), 4.21 (dd, J= 7.2 Hz, J_{H-P}= 5.0 Hz, 1H), 3.27 (s, 3H), 2.54 (d,J= 13.5 Hz, 1H), 2.49 (d,J= 13.5 Hz, 1H), 2.44 (s, 3H), 2.37 (sept, J= 6.5 Hz, 1H), 2.10 (s, 3H), 2.07-2.01 (m, 4H), 1.58 (s, 3H), 1.43 (s, 3H), 1.32 (s, 9H), 1.30 (s, 9H), 1.30 (s, 9H), 1.28 (s, 9H), 1.16 (d, J= 6.6 Hz, 3H), 1.10 (d, J= 6.5 Hz, 3H), 0.54 (d, J= 6.6 Hz, 3H), 0.21 (d, J= 6.5 Hz, 3H) ppm.

^{13}C-NMR (101 MHz, CD$_3$CN) δ : 207.9 (d, J_{C-P}= 66.1 Hz), 152.4, 152.3, 152.2, 146.8, 144.6, 142.2, 140.7 (d, J_{C-P}= 3.6 Hz), 137.6 (d, J_{C-P}= 3.0 Hz), 135.0, 133.4, 130.1 (d, J_{C-P}= 3.9 Hz), 129.6, 128.8, 128.7, 128.5, 127.9, 127.9, 127.7, 126.6, 125.8, 125.5, 125.0, 90.6, 87.3 (d, J_{C-P}= 3.1 Hz), 87.0 (d, J_{C-P}= 13.7 Hz), 85.7 (d, J_{C-P}= 2.4 Hz), 83.8 (d, J_{C-P}= 21.7 Hz), 60.9, 60.3, 54.9 (d, J_{C-P}= 3.2 Hz), 52.1, 35.2, 35.1, 35.1, 31.5, 31.4, 30.4, 30.2, 30.2, 30.1, 29.6, 29.0, 27.8, 25.7, 25.4, 24.4, 23.8, 23.7 ppm.

^{19}F-NMR (282 MHz, CD$_3$CN) δ : -124.1 (sext, $J_{F-^{121}Sb}$ = 1934.2 Hz), -124.1 (oct, $J_{F-^{123}Sb}$ = 1079.8 Hz) ppm.

HRMS calculated m/z for $C_{66}H_{91}NO_4P^+$: 992.668023; found (ESI) 992.668340.

IR (neat) $\tilde{\nu}$: 2960, 2868, 1510, 1462, 1438, 1395, 1365, 1270, 1188, 1129, 1100, 1019, 995, 900, 841, 788, 745, 711, 690, 655, 567, 523, 499 cm^{-1}.

$[\alpha]_D^{20}$= -18.0 (c = 0.67, DCM).

Compound 202:
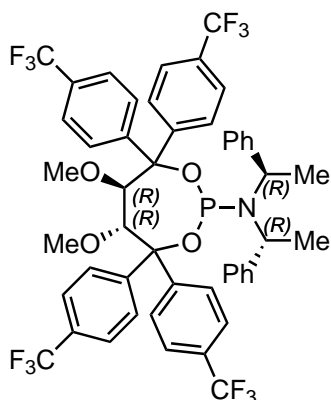
The phosphoramidite **202** was prepared using a modification of the procedure described by Fürstner and co-workers.[25,226] The chlorophosphite (92 mg, 0.12 mmol) was prepared analogously to **160d** from TADDOL **158d**, following the general procedure B. In parallel, (+)-Bis[(R)-1-phenylethyl]amine (29.0 µl, 0.13 mmol) was dissolved in THF (0.5 ml), cooled to -10 °C and treated with n-BuLi solution (1.6 M in hexanes, 80 µl, 0.13 mmol).

The mixture was stirred at room temperature for 30 min, before transferring *via* cannula to a solution of the previously prepared chlorophosphite in THF (2 ml), cooled to 0 °C. The reaction was stirred overnight and the solvent was removed *in vacuo* to afford the desired phosphoramidite as a white solid (90 mg of crude), which was used in the next step without further purification.

^{31}P-NMR (162 MHz, CD$_3$CN) δ : 139.3 ppm.

Compound 203:
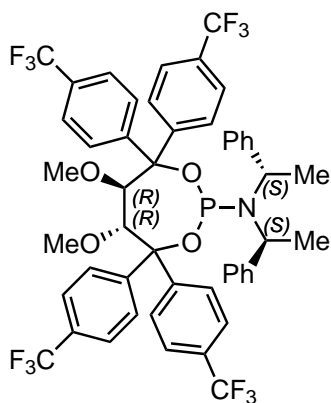
The phosphoramidite **203** was prepared using a modification of the procedure described by Fürstner and co-workers.[25,226] The chlorophosphite (46 mg, 5.8×10^{-2} mmol) was prepared analogously to **160d** from TADDOL **158d**, following the general procedure B. In parallel, (-)-Bis[(S)-1-phenylethyl]amine (14.6 µl, 6.4×10^{-2} mmol) was dissolved in THF (0.5 ml), cooled to -10 °C and treated with n-BuLi solution (1.6 M in hexane, 40 µl, 6.4×10^{-2} mmol).

The mixture was stirred at room temperature for 30 min, before transferring *via* cannula to a solution of the previously prepared chlorophosphite in THF (2 ml), cooled to 0 °C. The reaction was stirred overnight and the solvent was removed *in vacuo* to afford the desired phosphoramidite as a white solid (57 mg of crude), which was used in the next step without further purification.

^{31}P-NMR (162 MHz, CD$_3$CN) δ : 138.7 ppm.

General Procedure D : Synthesis of gold(I) complexes
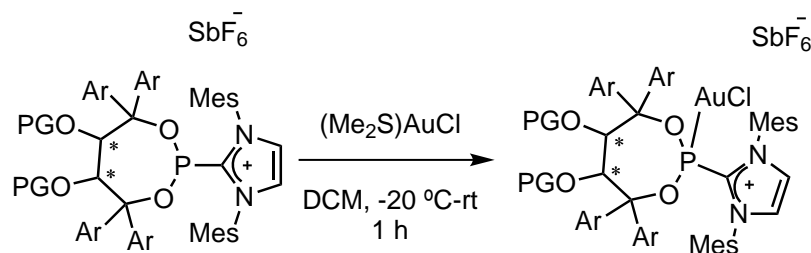
   The cationic phosphonite was placed in a Schlenk, solved in DCM (0.03 M) and cooled to -20 °C . At this temperature (Me$_2$S)AuCl (1 equiv.) was added, the reaction was warmed to room temperature and stirred for 1 h. The solvent was then removed *in vacuo* to afford the desired gold(I) complex.

Compound 164b :
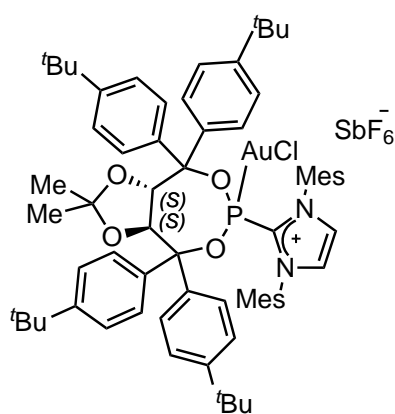
   Prepared using general procedure D from **159b** (30 mg, 2.4×10^{-2} mmol) and (Me$_2$S)AuCl (7.0 mg, 2.4×10^{-2} mmol). The solvent was removed *in vacuo* and the resulting residue re-precipitated from DCM/n-pentane. The solid was filtered and dried *in vacuo* to afford **164b** as a white solid (34.8 mg, 98 %).

^{31}P-NMR (162 MHz, CD$_3$CN) δ : 108.7 ppm.

^{1}H-NMR (600 MHz, CD$_3$CN) δ : 7.91 (d, J_{H-P}= 2.3 Hz, 2H), 7.46 (dt, J= 8.6, 2.3 Hz, 2H), 7.41-7.39 (m, 4H), 7.34 (d, J= 8.3 Hz, 2H), 7.27 (d, J= 8.0 Hz, 2H),7.17 (s, 2H), 7.13 (s, 3H), 7.11 (d, J= 8.4 Hz, 2H), 6.88 (dt, J= 8.6, 2.3 Hz, 2H),6.64 (d, J= 8.3 Hz, 2H), 6.21 (dd, J= 8.5 Hz, J_{H-P}= 1.9 Hz, 1H), 4.87 (d, J= 8.5 Hz, 1H), 2.40 (s, 6H), 2.01 (s, 6H), 1.98 (s, 6H), 1.41 (s, 3H), 1.36 (s, 9H), 1.34 (s, 9H), 1.32 (s, 9H), 1.31 (s, 9H), -0.03 (s, 3H) ppm.

^{13}C-NMR (151 MHz, CD$_3$CN) δ : 154.4, 154.0, 153.9, 153.3, 143.6, 139.3, 139.2, 139.2,138.6 (d, J_{C-P}= 100.8 Hz), 135.8, 135.7, 135.3 (d, J_{C-P}= 6.6 Hz), 133.4 (d, J_{C-P}= 1.8 Hz), 132.2, 131.7, 131.4, 131.4, 129.4 (br), 128.9, 128.6, 126.9, 126.7, 126.2, 125.5, 114.2, 93.4, 92.0 (d, J_{C-P}= 1.9 Hz), 83.0, 81.0 (d, J_{C-P}= 13.5 Hz), 35.4, 35.4, 35.3, 35.3, 31.5, 31.5, 31.4, 31.4, 27.6, 24.0, 21.5, 18.8, 18.3 ppm.

HRMS calculated m/z for C$_{68}$H$_{84}$AuClN$_2$O$_4$P$^+$: 1255.551727; found (ESI) 1255.552900.

IR (neat) $\tilde{\nu}$: 3167, 3118, 3078, 3061, 3038, 2962, 2906, 2870, 1609, 1552, 1510, 1477, 1462, 1404, 1365, 1320, 1270, 1216, 1164, 1111, 1092, 1046, 1019, 973, 932, 883, 840, 822, 797, 773, 740, 710, 659, 619, 585, 566, 506 cm^{-1}.

$[\alpha]_D^{20}$= +33.1 (c = 0.74, DCM).

Compound 164c :
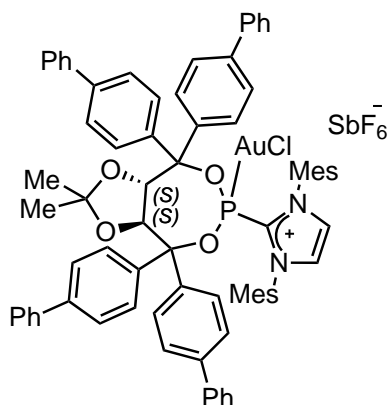
Prepared using general procedure D from **159c** (62.1 mg, 4.6×10^{-2} mmol) and $(Me_2S)AuCl$ (13.6 mg, 4.6×10^{-2} mmol). The solvent was removed *in vacuo* and the resulting residue re-precipitated from DCM/n-pentane. The solid was filtered and dried *in vacuo* to afford **164c** as a white solid (66.0 mg, 91 %).

^{31}P-NMR (162 MHz, CD_3CN) δ : 109.0 ppm.

^{1}H-NMR (400 MHz, CD_3CN) δ : 7.97 (d, J_{H-P}= 2.3 Hz, 2H), 7.76-7.65 (m, 14H), 7.62 (d, J= 9.0 Hz, 2H), 7.54-7.47 (m, 10H), 7.46-7.39 (m, 4H), 7.33 (d, J= 8.1 Hz, 2H), 7.23 (s, 2H), 7.21 (s, 2H), 7.14 (d, J= 8.6 Hz, 2H) , 6.88 (br, 2H), 6.37 (dd, J= 8.5 Hz, J_{H-P}= 1.9 Hz, 1H), 5.03 (d, J= 8.5 Hz, 1H), 2.38 (s, 6H), 2.10 (s, 6H), 2.06 (s, 6H), 1.50 (s, 3H), 0.12 (s, 3H) ppm.

^{13}C-NMR (101 MHz, CD_3CN) δ : 143.8, 143.7, 143.3, 143.1, 142.3, 140.8, 140.8, 140.6, 140.5, 140.5, 140.4, 138.0 (d, J_{C-P}= 103.4 Hz), 137.0 (d, J= 6.7 Hz), 135.8, 135.7, 135.0 (d, J_{C-P}= 2.0 Hz), 132.1, 131.6, 131.6 (J_{C-P}= 4.0 Hz), 131.3, 130.3 (br), 130.0, 130.0, 129.9, 129.8, 129.7, 129.1, 129.0, 129.0, 128.7, 128.2, 128.1, 128.0, 127.9, 127.7, 127.0, 114.6, 93.3, 92.0 (d, J_{C-P}= 1.9 Hz), 83.1, 80.8 (d, J_{C-P}= 13.2 Hz), 27.6, 24.2, 21.4, 18.8, 18.4 ppm.

HRMS calculated m/z for $C_{76}H_{68}AuClN_2O_4P^+$: 1335.426528; found (ESI) 1335.426850.

IR (neat) $\tilde{\nu}$: 3010, 2926, 2880, 1486, 1374, 1213, 1099, 934, 828, 762, 743, 697, 680, 618, 554, 519 cm^{-1}.

$[\alpha]_D^{20}$= +34.4 (c = 1.00, DCM).

Compound 164d :
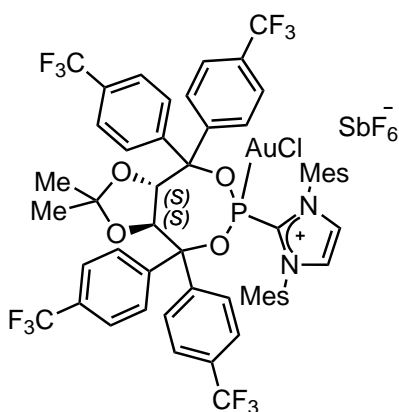
Prepared using general procedure D from **159d** (100.4 mg, 7.7×10^{-2} mmol) and $(Me_2S)AuCl$ (22.6 mg, 7.7×10^{-2} mmol), to afford **164d** as a white solid (107.4 mg, 91 %).

^{31}P-NMR (162 MHz, CD_3CN) δ : 111.3 ppm.

^{1}H-NMR (400 MHz, CD_3CN) δ : 8.01 (d, J_{H-P}= 2.5 Hz, 2H), 7.77-7.74 (m, 4H), 7.69 (d, J= 8.4 Hz, 2H), 7.63 (d, J= 8.1 Hz, 2H), 7.57 (d, J= 8.1 Hz, 2H), 7.43 (d, J= 8.1 Hz, 2H), 7.22 (s, 2H), 7.19-7.17 (m, 4H), 6.86 (d, J= 8.0 Hz, 2H), 6.25 (dd, J= 8.7 Hz, J_{H-P}= 1.9 Hz, 1H), 4.81 (d, J= 8.7 Hz, 1H), 2.38 (s, 6H), 2.07 (s, 6H), 2.01 (s, 6H), 1.47 (s,

3H), 0.03 (s, 3H) ppm.

^{13}C-NMR (101 MHz, CD$_3$CN) δ : 145.2, 144.7, 144.3, 141.2 (d, J_{C-P}= 6.6 Hz), 140.2, 136.8 (d, J_{C-P}= 107.1 Hz), 135.7, 135.7, 132.7 (q, J_{C-F}= 32.8 Hz), 132.5 (q, J_{C-F}= 32.8 Hz), 132.2 (d, J= 4.1 Hz), 132.0, 131.9, 131.4, 130.6, 130.0, 129.9, 127.4 (q, J_{C-F}= 3.7 Hz), 127.1 (q, J_{C-F}= 3.7 Hz), 126.4 (q, J_{C-F}= 3.7 Hz), 125.8 (q, J_{C-F}= 3.7 Hz), 125.0 (q, J_{C-F}= 272.6 Hz), 124.9 (q, J_{C-F}= 272.6 Hz), 124.8 (q, J_{C-F}= 272.6 Hz), 115.2, 92.3, 90.6, 82.7, 80.4 (d, J_{C-P}= 12.8 Hz), 27.3, 24.0, 21.3, 18.8, 18.4 ppm.

^{19}F-NMR (282 MHz, CD$_3$CN) δ : -63.3, -63.3, -63.4 (s, 6F), -124.0 (sext, $J_{F-^{121}Sb}$ = 1935.6 Hz), -124.0 (oct, $J_{F-^{123}Sb}$ = 1048.4 Hz) ppm.

HRMS calculated m/z for C$_{56}$H$_{48}$AuClF$_{12}$N$_2$O$_4$P$^+$: 1303.250870; found (ESI) 1303.252520.

$\tilde{\nu}$3167, 3148, 1619, 1607, 1480, 1454, 1411, 1390, 1365, 1322, 1258, 1229, 1215, 1170, 1124, 1070, 1018, 972, 930, 882, 828, 795, 787, 767, 731, 654, 621, 607, 525, 512 cm^{-1}.

$[\alpha]_D^{20}$= + 39.3 (c = 1.00, DCM).

Compound 164e :
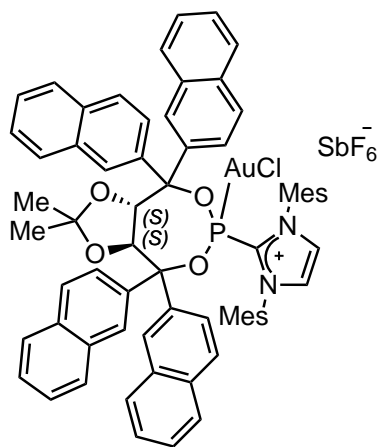
Prepared using general procedure D from **159e** (35.9 mg, 2.9 × 10^{-2} mmol) and (Me$_2$S)AuCl (8.6 mg, 2.9 × 10^{-2} mmol). The solvent was removed *in vacuo* and the resulting residue re-precipitated from DCM/n-pentane. The solid was filtered and dried *in vacuo* to afford **164e** as a white solid (32.7 mg, 77 %).

^{31}P-NMR (162 MHz, CD$_3$CN) δ : 109.7 ppm.

^{1}H-NMR (400 MHz, CD$_3$CN) δ : 8.56 (s, 1H), 8.10 (s, 1H), 8.06 (d, J= 8.8 Hz, 1H), 8.02–7.95 (m, 4H), 7.94 (d, J_{H-P}= 2.3 Hz, 2H), 7.92-7.83 (m, 6H), 7.71 (d, J= 8.0 Hz, 1H), 7.68–7.50 (m, 8H), 7.36 (dd, J= 8.8 Hz, J_{H-P}= 2.1 Hz, 2H), 7.28 (d, J= 2.0 Hz, 1H), 7.13 (d, J= 9.7 Hz, 1H), 7.09 (s, 4H), 6.97 (br, 1H), 6.91 (d, J= 8.8 Hz, 1H), 6.69 (dd, J= 8.5, 2.0 Hz, 1H), 5.36 (d, J= 8.5 Hz, 1H), 2.27 (s, 6H), 2.04 (s, 6H), 2.03 (s, 6H), 1.53 (s, 3H), -0.20 (s, 3H) ppm.

^{13}C-NMR (101 MHz, CD$_3$CN) δ : 143.7, 138.8 (d, J_{C-P}= 8.5 Hz), 138.6, 138.1 (d, J_{C-P}= 102.8 Hz), 135.8, 135.6, 135.5 (d, J_{C-P}= 6.5 Hz), 134.6, 134.4, 134.3, 133.9, 133.3, 133.2, 133.2, 133.0, 132.8, 132.2, 131.6 (d, J_{C-P}= 3.9 Hz), 131.5, 131.3, 130.1, 130.1, 130.0, 130.0, 129.8, 129.7, 129.5, 129.4, 129.0, 128.7, 128.6, 128.5, 128.3, 128.3, 127.9, 127.9, 127.7, 127.2, 126.6, 125.4, 114.7, 94.2, 92.9 (d, J_{C-P}= 2.6 Hz), 82.8, 80.7 (d, J_{C-P}= 13.4 Hz), 27.7, 24.4, 21.3, 18.7, 18.4 ppm.

HRMS calculated m/z for C$_{68}$H$_{60}$AuClN$_2$O$_4$P$^+$: 1231.363927; found (ESI) 1231.364860.

IR (neat) $\tilde{\nu}$: 3070, 2925, 2879, 1496, 1473, 1443, 1360, 1192, 1135, 1110, 1071, 1030, 985, 940, 796, 775, 754, 738, 698, 629, 615, 571, 504 cm^{-1}.

$[\alpha]_D^{20}$= +44.5 (c = 0.83, DCM).

Compound 164f :
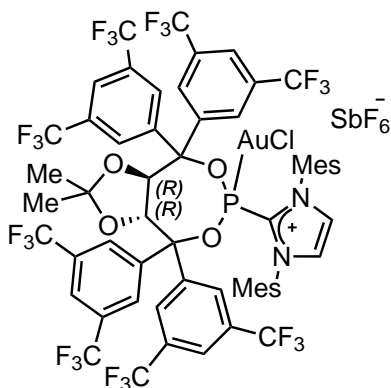
Prepared using general procedure D from **159f** (13.3 mg, 8.4×10^{-3} mmol) and (Me$_2$S)AuCl (3.0 mg, 10.1×10^{-3} mmol), stirring the reaction in this case overnight. After evaporation of the solvent the compound was purified by two consecutive re-precipitations using DCM/n-pentane to afford **164f** as a white solid (8.5 mg, 56 %).

^{31}P-NMR (162 MHz, CD$_3$CN) δ : 113.4 ppm.

^{1}H-NMR (400 MHz, CD$_3$CN) δ : 8.25 (br, 3H), 8.22 (s, 1H), 8.14 (s, 2H), 7.99 (d, J_{H-P}= 2.7 Hz, 2H), 7.90 (br, 2H), 7.43 (s, 2H), 7.30 (s, 2H), 7.12 (s, 2H), 6.87 (s, 2H), 6.31 (dd, J= 8.4 Hz, J_{H-P}= 2.5 Hz, 1H), 4.87 (d, J= 8.4 Hz, 1H), 2.27 (s, 6H), 2.10 (s, 6H), 1.84 (s, 6H), 1.36 (s, 3H), 0.12 (s, 3H) ppm.

^{13}C-NMR (101 MHz, CD$_3$CN) δ : 144.5, 142.4 (d, J_{C-P}= 8.1 Hz), 142.0, 139.1 (d, J_{C-P}= 6.7 Hz), 137.7, 135.2 (d, J_{C-P}= 84.5 Hz), 135.0, 135.0, 133.7 (q, J_{C-F}= 34.1 Hz), 133.3 (d, J_{C-P}= 4.2 Hz), 133.3 (q, J_{C-F}= 34.1 Hz), 132.9 (q, J_{C-F}= 34.1 Hz), 132.5 (q, J_{C-F}= 34.1 Hz), 131.8, 131.7, 131.4, 130.7 (br), 130.3 – 130.2 (m), 129.4 (q, J_{C-F}= 3.2 Hz), 127.1-126.9 (m), 126.7-126.6 (m), 126.2-125.9 (m), 124.0 (q, J_{C-F}= 273.7 Hz), 123.9 (q, J_{C-F}= 273.7 Hz), 123.9 (q, J_{C-F}= 273.7 Hz), 123.8 (q, J_{C-F}= 273.7 Hz), 117.0, 91.6, 90.6, 81.4, 79.3 (d, J_{C-P}= 15.1 Hz), 27.1, 25.4, 21.3, 19.2, 18.3 ppm.

^{19}F-NMR (282 MHz, CD$_3$CN) δ : -62.9, -63.0 (br), -63.1, -63.2 ppm.

HRMS calculated m/z for C$_{60}$H$_{44}$AuClF$_{24}$N$_2$O$_4$P$^+$: 1575.200412; found (ESI) 1575.201250.

IR (neat) $\tilde{\nu}$: 3180, 2989, 2944, 2919, 2885, 2858, 1624, 1478, 1468, 1458, 1375, 1342, 1321, 1277, 1219, 1181, 1142, 1097, 1034, 989, 974, 960, 905, 865, 846, 827, 812, 784, 744, 707, 683, 658, 640, 575, 551, 532, 503 cm^{-1}.

$[\alpha]_D^{20}$= -20.0 (c = 0.21, DCM).

Compound 165d :
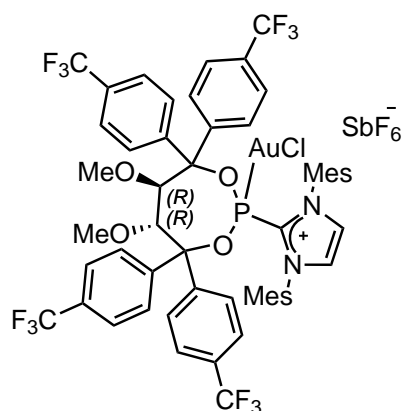
Prepared using general procedure D from **160d** (54.4 mg, 4.2×10^{-2} mmol) and (Me$_2$S)AuCl (12.4 mg, 4.2×10^{-2} mmol), to afford **165d** as a white solid (64.0 mg, 99 %).

^{31}P-NMR (162 MHz, CD$_3$CN) δ : 110.3 ppm.

^{1}H-NMR (400 MHz, CD$_3$CN) δ : 7.96 (d, J_{H-P}= 2.3 Hz, 2H), 7.76-7.65 (m, 8H), 7.45 (br, 2H), 7.24 (s, 2H), 7.18 (d, J= 8.2 Hz, 2H), 7.09 (s, 2H), 7.07 (d, J= 8.5 Hz, 2H), 6.97 (d, J= 8.2 Hz, 2H), 5.47 (dd, J= 8.0, 2.0 Hz, 1H), 4.19 (d, J= 8.0 Hz, 1H), 3.68 (s, 3H), 2.39 (s, 3H), 2.35 (s, 6H), 2.09 (s, 6H), 1.82 (s, 6H) ppm.

^{13}C-NMR (101 MHz, CD$_3$CN) δ : 145.2 (d, J_{C-P}= 9.6 Hz), 144.4, 144.1, 141.4 (d, J_{C-P}= 6.8 Hz), 139.6, 137.2 (d, J_{C-P}= 106.1 Hz), 135.8, 135.7, 132.5 (q, J_{C-F}= 32.8 Hz), 132.2 (q, J_{C-F}= 32.8 Hz), 131.8 (q, J_{C-F}= 32.8 Hz), 131.8, 131.8 (d, J_{C-P}= 4.1 Hz), 131.7, 131.3 (q, J_{C-F}= 32.8 Hz), 131.3, 130.8, 130.6 (br), 130.4, 129.6, 127.2 (q, J_{C-F}= 3.5 Hz), 126.9 (q, J_{C-F}= 3.8 Hz), 126.4 (q, J_{C-F}= 3.5 Hz), 125.0 (q, J_{C-F}= 272.6 Hz), 125.0 (q, J_{C-F}= 3.8 Hz), 124.9 (q, J_{C-F}= 272.6 Hz), 124.9 (q, J_{C-F}= 272.6 Hz), 124.8 (q, J_{C-F}= 272.6 Hz), 93.5 (d, J_{C-P}= 2.8 Hz), 91.8, 85.2, 80.7 (d, J_{C-P}= 11.2 Hz), 62.2, 61.4, 21.2, 18.9, 18.2 ppm.

^{19}F-NMR (282 MHz, CD$_3$CN) δ : -63.2, -63.3, -63.4, - 63.4 , -124.0 (sext, $J_{F-^{121}Sb}$ = 1935.6 Hz), -124.0 (oct, $J_{F-^{123}Sb}$ = 1048.4 Hz) ppm.

HRMS calculated m/z for C$_{55}$H$_{48}$AuClF$_{12}$N$_2$O$_4$P: 1291.250870; found (ESI) 1291.252230.

IR (neat) $\tilde{\nu}$: 3184, 3162, 3139, 1619, 1606, 1550, 1478, 1449, 1411, 1367, 1325, 1229, 1169, 1120, 1071, 1018, 990, 937, 881, 854, 824, 788, 773, 735, 715, 658, 622, 607, 586, 575, 542, 524, 505 cm^{-1}.

$[\alpha]_D^{20}$= -53.4 (c = 1.11, DCM).

Compound 170:
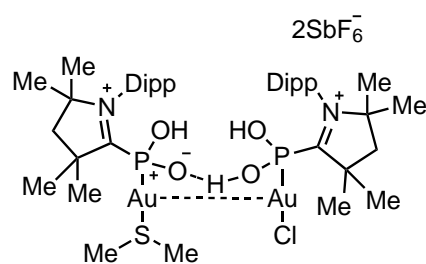
Prepared using general procedure D from **162** (42.4 mg, 3.5×10^{-2} mmol) and (Me$_2$S)AuCl (10.3 mg, 3.5×10^{-2} mmol). After evaporation of the solvent, CH$_3$CN is added and the solid is filtered off, corresponding the remaining solid to the naphthalene **169**. The resulting solution is evaporated and recrystallised from DCM/n-pentane to afford **170**.

^{31}P-NMR (202 MHz, CD$_3$CN) δ : 92.5 (br) ppm.

^{1}H-NMR (500 MHz, CD$_3$CN) δ : 7.59 (t, J= 7.8 Hz, 1H), 7.40 (d, J= 7.8 Hz, 2H), 2.64 (sept., J= 6.5 Hz, 2H), 2.36 (s, 2H), 1.77 (s, 6H), 1.48 (s, 6H), 1.38 (d, J= 6.5 Hz, 6H), 1.31 (d, J= 6.5 Hz, 6H) ppm.

^{13}C-NMR (126 MHz, CD$_3$CN) δ : 145.7, 132.7, 127.2, 126.0, 92.7, 50.7, 30.0, 29.9, 28.8, 27.7, 24.5 ppm.

MS found m/z (ESI): 1127.3 [M - Me$_2$S - 2SbF$_6^-$], 993.7, 818.7, 582.2 [monomer, C$_{20}$H$_{33}$AuClNO$_2$P$^+$].

IR (neat) $\tilde{\nu}$: 2963, 2907, 2875, 1592, 1462, 1412, 1392, 1375, 1259, 1198, 1086, 1015, 898, 874, 795, 700, 654, 611, 575, 546, 526 cm^{-1}.

Compound 169:
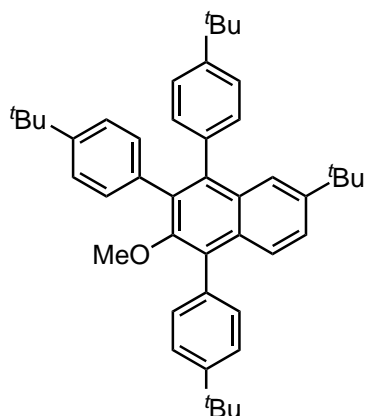
Prepared as stated above and separated from **170** through the addition of CH$_3$CN to the crude and filtering the resulting mixture, corresponding the reamining solid to the naphthalene **169**.

^{1}H-NMR (400 MHz, CDCl$_3$) δ : 7.67 (dd, J= 2.1, 0.6 Hz, 1H), 7.63 (dd, J= 8.9, 0.6 Hz, 1H), 7.52 (dt, J= 8.5, 2.0 Hz, 2H), 7.47-7.44 (m, 3H), 7.22 (dt, J= 8.4, 2.0 Hz, 2H), 7.12 (dt, J= 8.5, 2.0 Hz, 2H), 7.07-7.02 (m, 4H), 3.11 (s, 3H), 1.42 (s, 9H), 1.29 (s, 9H), 1.25 (s, 9H), 1.23 (s, 9H) ppm.

^{13}C-NMR (101 MHz, CDCl$_3$) δ : 152.8, 149.9, 149.1, 148.7, 147.3, 140.5, 136.1, 135.2, 134.9, 133.8, 131.4, 131.0, 130.7, 130.6, 130.2, 129.9, 125.8, 125.1, 124.7, 124.2, 123.9, 122.3, 60.9, 34.9, 34.8, 34.6, 34.4, 31.6, 31.5, 31.4, 31.4, 31.2 ppm.

HRMS calculated m/z for C$_{45}$H$_{54}$ONa$^+$: 633.406180; found (ESI) 633.406684.

IR (neat) $\tilde{\nu}$: 3064, 2959, 2902, 2866, 1497, 1460, 1362, 1268, 1151, 1109, 1052, 1019, 997, 832, 812, 641, 594, 552 cm^{-1}.

Compound 171:
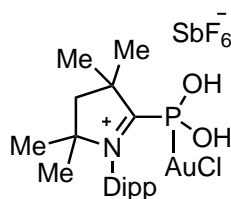
Prepared using general procedure D from **160b** (20 mg, 1.6×10^{-2} mmol) and (Me$_2$S)AuCl (4.7 mg, 1.6×10^{-2} mmol). After evaporation of the solvent, CH$_3$CN is added and the solid is filtered off. The resulting solution is evaporated and recrystallised from DCM/n-pentane to afford **171** (5.1 mg, 53 %).

^{31}P-NMR (122 MHz, CD$_3$CN) δ : 80.0 (br) ppm.

^{1}H-NMR (300 MHz, CD$_3$CN) δ : 7.63 (s, 2H), 7.08 (s, 4H), 2.79 (s, 1H), 2.36 (s, 6H),

2.05 (s, 9H) ppm.

^{13}C-NMR (101 MHz, CD$_3$CN) δ : 142.4, 135.7, 130.5, 130.5, 127.9 (br), 21.3, 18.0 ppm.

HRMS calculated m/z for C$_{21}$H$_{26}$Au$_1$Cl$_1$N$_2$O$_2$P$_1{}^+$: 601.109080; found (ESI) 601.108048.

Compound 204:
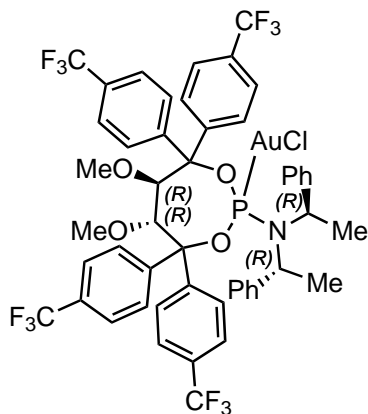
Prepared using general procedure D from **202** (90 mg of crude, 9.2×10^{-2} mmol) and (Me$_2$S)AuCl (27.0 mg, 9.2×10^{-2} mmol). After evaporation of the solvent the compound was purified by flash chromatography at -10 °C (gradient from Hexanes/DCM, 80/20 to 50/50), to afford **205** as a white solid (15.0 mg, 21 % over two steps).

^{31}P-NMR (202 MHz, CD$_3$CN) δ : 110.2 ppm.

^{1}H-NMR (500 MHz, CD$_3$CN) δ : 7.94-7.65 (m, 10H), 7.58 (t, J= 7.7 Hz, 6H), 7.27-7.10 (m, 10H), 5.30 (dd, J= 8.0 Hz, J_{H-P}= 1.8 Hz, 1H), 5.12 (d, J= 18.8 Hz, 2H), 4.39 (d, J= 8.0 Hz, 1H), 3.73 (s, 3H), 2.48 (s, 3H), 1.87 (d, J= 7.0 Hz, 6H) ppm.

^{13}C-NMR (126 MHz, CD$_3$CN) δ : 148.7, 148.6 (d, J_{C-P}= 9.1 Hz), 144.7 (d, J_{C-P}= 6.6 Hz), 143.0, 142.1 (d, J_{C-P}= 3.6 Hz), 131.4 (q, J_{C-F}= 32.3 Hz), 131.0 (q, J_{C-F}= 32.3 Hz), 130.7 (q, J_{C-F}= 32.2 Hz), 130.5, 129.7, 129.6, 129.1, 129.0, 126.4 (q, J_{C-F}= 3.7 Hz), 126.1 (q, J_{C-F}= 3.8 Hz), 125.2 (q, J_{C-F}= 271.3 Hz), 125.2 (q, J_{C-F}= 3.9 Hz), 125.1 (q, J_{C-F}= 271.7 Hz), 125.1 (q, J_{C-F}= 271.4 Hz), 125.1 (q, J_{C-F}= 271.7 Hz), 88.4 (d, J_{C-P}= 4.0 Hz), 85.6, 82.5 (d, J_{C-P}= 9.5 Hz), 61.8, 61.2, 54.2 (d, J_{C-P}= 7.8 Hz), 21.7 ppm.

^{19}F-NMR (470 MHz, CD$_3$CN) δ : -63.1 (s, 6F), -63.1, -63.1 ppm.

HRMS calculated m/z for C$_{50}$H$_{42}$AuClF$_{12}$NO$_4$PNa$^+$: 1234.190615; found (ESI) 1234.191850.

IR (neat) $\tilde{\nu}$: 2962, 1619, 1410, 1325, 1260, 1168, 1070, 1016, 888, 848, 798, 738, 660, 636, 620 cm^{-1}.

$[\alpha]_D^{20}$= - 8.0 (c = 0.977, DCM).

Compound 205:
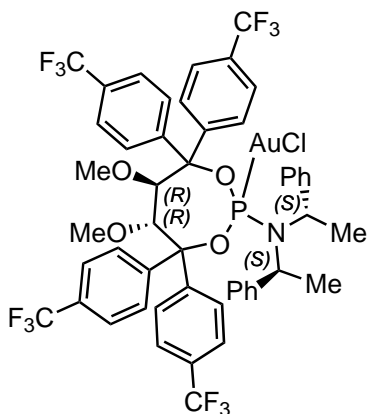
Prepared using general procedure D from **203** (57 mg of crude, 5.8×10^{-2} mmol) and (Me$_2$S)AuCl (17.1 mg, 5.8×10^{-2} mmol). After evaporation of the solvent the compound was purified by flash chromatography at -10 °C (gradient from Hexanes/DCM, 80/20 to 50/50), to afford **205** as a white solid (22.0 mg, 16 % over two steps).

^{31}P-NMR (202 MHz, CD$_3$CN) δ : 109.8 ppm.

^{1}H-NMR (500 MHz, CD$_3$CN) δ : 8.12 (d, J= 8.1 Hz, 2H), 7.81 (d, J= 8.1 Hz, 2H), 7.79 (d, J= 7.8 Hz, 2H), 7.72 (d, J= 7.8 Hz, 2H), 7.70 (d, J= 7.6 Hz, 2H), 7.55 (d, J= 7.5 Hz, 2H), 7.54 (d, J= 8.0 Hz, 2H), 7.44 (d, J= 8.0 Hz, 2H), 7.19 (t, J= 4.5 Hz, 4H), 7.15-7.13 (m, 6H), 5.49 (dd, J= 8.0 Hz, J_{H-P}= 1.6 Hz, 1H), 5.17 (dq, J_{H-P}= 20.4 Hz, J= 7.0 Hz, 2H), 4.30 (d, J= 8.0 Hz, 1H), 3.76 (s, 3H), 2.45 (s, 3H), 1.89 (d, J= 7.0 Hz, 6H) ppm.

^{13}C-NMR (126 MHz, CD$_3$CN) δ : 149.3 (d, J_{C-P}= 7.2 Hz), 148.1, 145.1 (d, J_{C-P}= 6.2 Hz), 144.0, 142.4, 132.1-130.7 (m), 131.2, 131.1, 129.8, 129.6, 129.4, 129.1, 128.6, 126.7 (br), 126.1 (br), 125.5 (q, J_{C-F}= 273.0 Hz), 125.5 (q, J_{C-F}= 273.0 Hz), 125.4 (q, J_{C-F}= 273.0 Hz), 125.4 (br), 88.7 (d, J_{C-P}= 5.5), 86.7, 86.4, 82.3 (d, J_{C-P}= 9.9 Hz), 62.0, 61.4, 54.8 (d, J_{C-P}= 8.2 Hz), 21.6 ppm.

^{19}F-NMR (470 MHz, CD$_3$CN) δ : -63.2, -63.2, -63.2 , -63.3 ppm.

^{15}N-NMR (50.7 MHz, CD$_3$CN) δ : -286 ppm.

HRMS calculated m/z for C$_{50}$H$_{42}$AuClF$_{12}$NO$_4$PNa$^+$: 1234.190615; found (ESI) 1234.190910.

IR (neat) $\tilde{\nu}$: 2962, 2932, 2919, 2897, 1483, 1449, 1409, 1380, 1323, 1260, 1167, 1116, 1069, 1015, 964, 934, 915, 868, 848, 818, 799, 770, 751, 715, 698, 671, 659, 629, 620, 604, 521, 505, 492 cm^{-1}.

$[\alpha]_D^{20}$= - 26.1 (c = 0.4, DCM).

III.1.3.3   Substrate Synthesis

Compound 184:
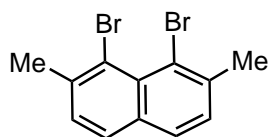
The procedure is a modification of the one described by Laarkem *et al.*[207] A Schlenk was charged with 5.89 g of 1,8-dimethylnaphthalene **183** (37.8 mmol) and 160 ml of dry DMF. Under vigorous stirring, one equivalent of NBS (6.71 g, 37.8 mmol) was added portion-wise. The mixture was stirred overnight at room temperature until completion of the first bromination step, confirmed by GC/MS, and then additional 1.2 equivalents of NBS were added (8.06 g, 45.3 mmol). The reaction was stirred for 14 days further at the same temperature, checking the reaction mixture periodically by GC/MS. After 7 days, the reaction slowed down and an additional 1.34 g of NBS (0.2 equiv., 7.6 mmol) were added, according to the amount of monobrominated compound shown in the GC/MS measurement. When the reaction reached complete conversion, it was quenched by slow addition of water. The mixture was then extracted with Et_2O, washing the aqueous phase with 2 additional portions of ether. The organic layers were combined, dried over Na_2SO_4, and the solvent evaporated *in vacuo* to afford an orange oil.

The compound was further purified by flash chromatography (hexanes/Et_2O/Et_3N, 9/1/ 0.2) as eluent, obtaining 5.52 g of **184** as a white crystalline solid. An additional crop of 400 mg compound could be obtained, combining impure fractions and purifying them again by a second flash chromatography under the same conditions, affording in total 5.92 g of **184** in 50 % yield. The analytical data matches that described in the literature.[207]

General Procedure E : Suzuki coupling
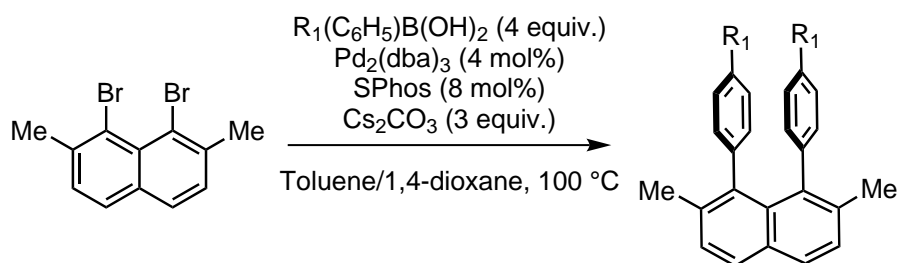
Based on the procedure described by Buchwald and co-workers.[208] A Schlenk was charged with **184**, $Pd_2(dba)_3$ (4 mol%), SPhos (8 mol%), Cs_2CO_3 (3 equiv.) and the corresponding aromatic boronic acid (4 equiv.). Degassed and dry toluene and 1,4-dioxane (0.065 M; toluene/1,4-dioxane, 6/1) were then added under vigorous stirring, heating the

resulting mixture to 100 ºC until the conversion to the desired coupling product, checked by GC/MS, was complete. The reaction was then allowed to cool to room temperature and filtered through a pad of silica, eluting with portions of EtOAc. The solvent was evaporated to afford the crude product, which was purified as specified for each case.

Compound 185a :
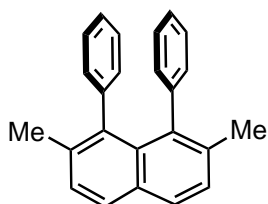
Prepared using general procedure E . A Schlenk was charged with **184** (4.37 g, 13.91 mmol), phenylboronic acid (6.78 g, 55.64 mmol), Cs_2CO_3 (13.6 g, 41.73 mmol), $Pd_2(dba)_3$ (510 mg, 0.56 mmol) and SPhos (457 mg, 1.11 mmol). Toluene (185 ml) and 1,4-dioxane (30 ml) were then added and the reaction was heated for 4 h. After workup, the compound was purified by crystallisation in EtOH, obtaining pure **185a** as a pale yellow crystalline solid. Additionally, the mother liquor was evaporated and purified by flash chromatography (gradient from hexanes to hexanes/EtOAc, 10/0.5) affording more **185a** (in total 3.22 g, 75 %).

^{1}H-NMR (400 MHz, CDCl$_3$) δ : 7.78 (d, J= 8.2 Hz, 2H), 7.33 (d, J= 8.2 Hz, 2H), 6.92-6.87 (m, 6H), 6.66-6.63 (m, 4H), 1.92 (s, 6H) ppm.

^{13}C-NMR (75 Hz, CDCl$_3$) δ : 142.4, 138.8, 135.9, 132.0, 131.7, 130.7, 127.9, 127.8, 127.4, 125.4, 21.8 ppm.

HRMS calculated m/z for $C_{24}H_{20}{}^+$: 308.156500; found (EI) 308.156359.

IR (neat) $\tilde{\nu}$: 3077, 3055, 3047, 3020, 2919, 2849, 1606, 1574, 1509, 1492, 1442, 1376, 1354, 1340, 1308, 1261, 1179, 1155, 1111, 1072, 1025, 1001, 954, 911, 838, 794, 756, 741, 696, 658, 632, 618, 605, 573, 531 cm^{-1}.

Compound 185b :
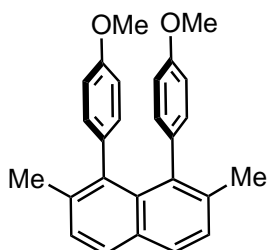
Prepared using general procedure E . A Schlenk was charged with **184** (854 mg, 2.72 mmol), 4-methoxyphenylboronic acid (1.65 g, 10.88 mmol), Cs_2CO_3 (2.66 g, 8.16 mmol), $Pd_2(dba)_3$ (100 mg, 0.11 mmol) and SPhos (90 mg, 0.22 mmol). Toluene (26 ml) and 1,4-dioxane (6 ml) were then added and the reaction was heated for 2 h. After workup, the compound was purified by flash chromatography (gradient from hexanes to hexanes/EtOAc, 9/1) to afford **185b** as a white solid (755 mg, 75 %).

^{1}H-NMR (400 MHz, CDCl$_3$) δ : 7.76 (d, J= 8.3 Hz, 2H), 7.32 (d, J= 8.3 Hz, 2H), 6.54 (dt, J= 8.7, 2.5 Hz, 4H), 6.48 (dt, J= 8.7, 2.5 Hz, 4H),3.76 (s, 6H), 1.96 (s, 6H) ppm.

^{13}C-NMR (101 MHz, CDCl$_3$) δ : 157.1, 138.4, 136.3, 135.1, 132.5, 132.0, 131.5, 127.9, 127.7, 113.0, 55.3, 22.0 ppm.

HRMS calculated m/z for $C_{26}H_{24}O_2Na^+$: 391.166849; found (ESI) 391.167140.

IR (neat) $\tilde{\nu}$: 3053, 3020, 2951, 2915, 2861, 2853, 1678, 1603, 1490, 1467, 1441, 1350, 1232, 1178, 1144, 1067, 1040, 1012, 987, 908, 883, 843, 816, 788, 762, 729, 695, 633, 607, 590, 542, 520 cm^{-1}.

Compound 185c :
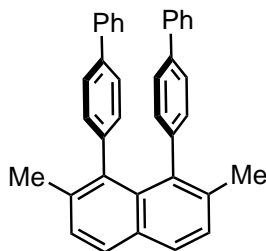
Prepared using general procedure E . A Schlenk was charged with **184** (533 mg, 1.70 mmol), 4-biphenylboronic acid (1.41 g, 6.79 mmol), Cs_2CO_3 (1.66 g, 5.09 mmol), $Pd_2(dba)_3$ (62 mg, 0.07 mmol) and SPhos (56 mg, 0.14 mmol). Toluene (23 ml) and 1,4-dioxane (4 ml) were then added and the reaction was heated for 3 h. After workup, the compound was purified by flash chromatography (gradient from hexanes to hexanes/EtOAc, 9.5/0.5) to afford two partially pure fractions. This fractions were combined and crystallised in EtOAc to afford **185c** as a white solid (541 mg, 69 %).

^{1}H-NMR (400 MHz, CDCl$_3$) δ : 7.82 (d, J= 8.3 Hz, 2H), 7.39-7.36 (m, 6H), 7.32-7.28 (m, 6H), 7.14 (dt, J= 8.2, 2.0 Hz, 4H), 6.73 (dt, J= 8.2, 2.0 Hz, 4H), 2.02 (s, 6H) ppm.

^{13}C-NMR (101 MHz, CDCl$_3$) δ : 141.6, 141.3, 138.3, 138.1, 135.9, 132.2, 131.9, 131.0, 128.7, 128.0, 127.8, 127.2, 126.9, 126.0, 21.9 ppm.

HRMS calculated for m/z $C_{36}H_{28}^+$: 460.219100; found (EI) 460.219205.

IR (neat) $\tilde{\nu}$: 3060, 3050, 3028, 2948, 2918, 2855, 1600, 1509, 1483, 1442, 1396, 1377, 1355, 1334, 1319, 1282, 1256, 1182, 1154, 1110, 1072, 1036, 1008, 959, 915, 885, 841, 827, 798, 699, 648, 638, 620, 611, 591, 571, 531, 497 cm^{-1}.

Compound 185d :
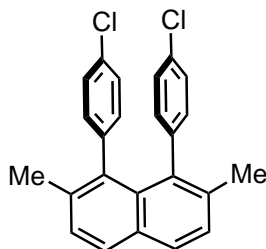
Prepared using general procedure E . A Schlenk was charged with **184** (466 mg, 1.48 mmol) and 4-chlorophenylboronic acid (928 mg, 5.93 mmol), Cs_2CO_3 (1.45 g, 4.45 mmol), $Pd_2(dba)_3$ (54 mg, 0.06 mmol) and SPhos (49 mg, 0.12 mmol). Toluene (20 ml) and 1,4-dioxane (3.2 ml) were then added and the reaction was heated overnight. After workup, the compound was purified by flash chromatography (hexanes) to afford **185d** as a white solid (420 mg, 75 %).

^{1}H-NMR (400 MHz, CDCl$_3$) δ : 7.79 (d, J= 8.3 Hz, 2H), 7.34 (d, J= 8.3 Hz, 2H), 6.96 (dt, J= 8.3, 2.2 Hz, 4H), 6.57 (dt, J= 8.3, 2.2 Hz, 4H), 1.95 (s, 6H) ppm.

^{13}C-NMR (101 MHz, CDCl$_3$) δ : 140.8, 137.0, 136.0, 132.0, 131.9, 131.8, 131.8, 128.4, 127.9, 127.7, 21.8 ppm.

HRMS calculated m/z for $C_{24}H_{18}Cl_2{}^+$: 376.078556; found (EI) 376.078900.

IR (neat) $\tilde{\nu}$: 3048, 3033, 2944, 2921, 1604, 1593, 1509, 1490, 1440, 1393, 1355, 1320, 1180, 1147, 1110, 1088, 1015, 959, 884, 844, 829, 798, 780, 737, 713, 609, 539, 497 cm^{-1}.

Compound 185e :
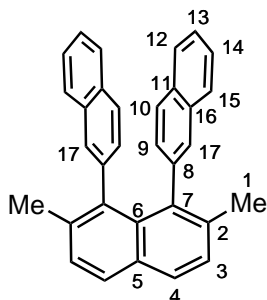
Prepared using general procedure E . A Schlenk was charged with **184** (392 mg, 1.25 mmol), 2-naphthylboronic acid (859 mg, 4.99 mmol), Cs$_2$CO$_3$ (1.22 g, 3.75 mmol), Pd$_2$(dba)$_3$ (46 mg, 0.05 mmol) and SPhos (41 mg, 0.10 mmol). Toluene (17 ml) and 1,4-dioxane (2.7 ml) were then added and the reaction was heated for 4 h. After workup, the compound was purified by flash chromatography (gradient from hexanes to hexanes/DCM, 9.5/0.5) to afford the desired compound **185e** as a white solid. An additional fraction of the compound could be obtained by crystallisation of impure fractions of the column in hot EtOAc (overall 349 mg, 68 %). NMR displayed a mixture of *anti-* and *syn-* conformers in 55:45 ratio respectively. Both conformers could be differentiated by NOEs between H17 and H9/H10 that can only take place in the *anti-* form. The analysis of the NMR spectra and the assigments can be found in ***Table A.1*** and ***Table A.2***.

^{1}H-NMR (500 MHz, CDCl$_3$) δ : 7.86 (d, J= 8.0 Hz, 2H, *anti-* 4), 7.85 (d, J= 8.4 Hz, 2H, *syn-* 4), 7.50 (d, J= 8.1 Hz, 2H, *anti-* 15), 7.39 (d, J= 8.3 Hz, 4H, 3), 7.36-7.31 (m, 4H), 7.29 (d, J= 8.1 Hz, 2H, *anti-* 12), 7.22 (t, J= 7.4 Hz, 2H, *anti-* 13), 7.18 (t, J= 7.4, 2H, *syn-* 13), 7.13-7.04 (m, 8H), 7.03 (s, 2H, *syn-* 17), 6.77 (d, J= 8.7 Hz, 2H, *anti-*10), 6.74 (d, J= 8.0 Hz, 2H, *syn-* 9), 6.71 (d, J= 8.1 Hz, 2H, *anti-* 9), 1.96 (s, 12H, 1) ppm.

^{13}C-NMR (126 MHz, CDCl$_3$) δ : 139.8 (*anti-* 8), 139.7 (*syn-* 8), 138.6 (*syn-* 7), 138.4 (*anti-* 7), 136.0 (*anti-* 2), 135.9 (*syn-* 2), 132.9 (*anti-* 16), 132.7 (*syn-* 16), 132.4 (*anti-* 6), 132.2 (*syn-* 6), 132.0 (5), 131.5 (*syn-* 11), 131.4 (*anti-* 11), 129.5 (*syn-* 17), 129.3 (*anti-* 9), 129.0 (*anti-* 17), 128.3 (*syn-* 9), 128.1 (*anti-* 4), 128.0 (*syn-* 4), 127.8 (*anti-* 3), 127.8 (*syn-* 3), 127.2 (*anti-* 15), 127.2 (*anti-* 12), 127.0 (*syn-* 15), 127.0 (*syn-* 12), 126.4 (*syn-* 10), 126.1 (*anti-* 10), 125.3 (14), 125.1 (*anti-* 13), 124.9 (*syn-* 13), 21.9 (*anti-* 1), 21.8 (*syn-* 1) ppm.

HRMS calculated m/z for $C_{32}H_{24}{}^+$: 408.187800; found (EI) 408.187501.

IR (neat) $\tilde{\nu}$: 3078, 3046, 3017, 2965, 2921, 2856, 1598, 1512, 1500, 1442, 1430, 1380, 1354, 1325, 1268, 1238, 1184, 1154, 1131, 1104, 1082, 1066, 1017, 960, 954, 893, 850, 837, 818, 795, 784, 766, 747, 734, 715, 659, 627, 614, 582, 558, 538, 509, 474 cm^{-1}.

General Procedure F: Radical bromination
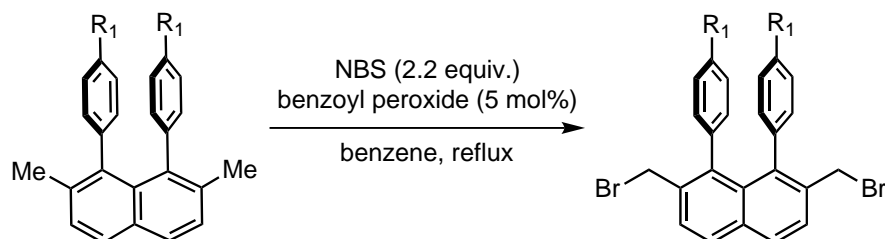
Based on the bromination of 2,7-dimethylnaphthalene described by Andrus *et al.*[231] The 1,8-diaryl-2,7-dimethylnaphthalenes were placed in a Schlenk and dissolved in dry benzene (0.05 M), followed by the addition of NBS (2.2 equiv.) and dibenzoyl peroxide (5 mol%). The resulting mixture was then heated under reflux for the specified time, before cooling to 0 °C and filtering with a cannula fitted with a glass fibre filter. The mother liqueur was concentrated *in vacuo* and the residue was purified as stated in each case.

Compound 186a :
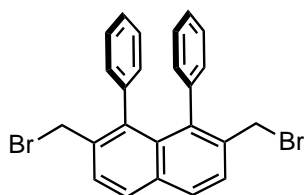
According to general procedure F, compound **185a** (2.46 g, 7.98 mmol) was placed in a Schlenk and dissolved in dry benzene (158 ml), followed by the addition of NBS (3.12 g, 17.56 mmol) and dibenzoyl peroxide (129 mg, 0.40 mmol). The reaction was heated for 5 h and the compound was purified by crystallisation, dissolving it first in warm $CHCl_3$ and then adding hexanes slowly, until precipitation in the interphase occurred. The mixture was stored in the freezer overnight, after which the obtained white crystals were collected and dried under vacuum. The solid thus obtained contained **186a** as the major product and was used directly in the next step without further purification.

^{1}H-NMR (400 MHz, $CDCl_3$) δ : 7.89 (d, J= 8.5 Hz, 2H), 7.60 (d, J= 8.5 Hz, 2H), 7.00-6.92 (m, 6H), 6.77-6.75 (m, 4H), 4.10 (s, 4H) ppm.

HRMS calculated for $C_{24}H_{18}Br_2^+$: 463.977000; found (APPIpos) 463.977860.

Compound 186b :
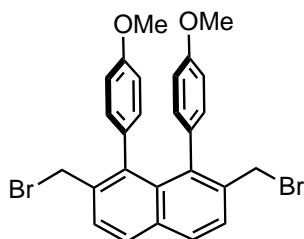
According to general procedure F, compound **185b** (652 mg, 1.77 mmol) was placed in a Schlenk and dissolved in dry benzene (35 ml), followed by the addition of NBS (693 mg, 3.89 mmol) and dibenzoyl peroxide (29 mg, 0.09 mmol). The reaction was heated for 5 h and the compound was purified by crystallisation, dissolving it first in warm $CHCl_3$ and then adding hexanes slowly, until precipitation in the interphase occurred. The mixture was

stored in the freezer overnight, after which the obtained white crystals were collected. In order to eliminate traces of remaining succinimide, the crystals were dissolved in DCM and filtered through a short pad of silica. The solvent was evaporated *in vacuo* to afford **186b** as a white solid (660 mg, 71 %).

^{1}H-NMR (400 MHz, CDCl$_3$) δ : 7.87 (d, J= 8.5 Hz, 2H), 7.59 (d, J= 8.5 Hz, 2H), 6.66 (dt, J= 8.6, 2.5 Hz, 4H), 6.51 (dt, J= 8.6, 2.5 Hz, 4H), 4.16 (s, 4H), 3.78 (s, 6H).

^{13}C-NMR (101 MHz, CDCl$_3$) δ : 157.8, 140.4, 136.4, 134.3, 132.6, 131.9, 131.4, 129.1, 128.2, 113.0, 55.3, 33.6 ppm.

HRMS calculated m/z for C$_{26}$H$_{22}$Br$_2$O$_2^+$: 523.998680; found (EI) 523.998328.

IR (neat) $\tilde{\nu}$: 3035, 2995, 2950, 2906, 2831, 1609, 1574, 1509, 1453, 1435, 1410, 1342, 1280, 1243, 1200, 1176, 1106, 1029, 956, 880, 834, 816, 787, 727, 637, 600, 569, 550, 509 cm^{-1}.

Compound 186c :
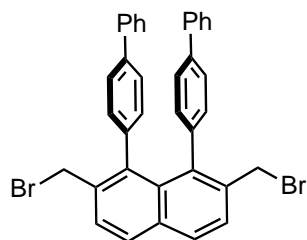
According to general procedure F, compound **185c** (477 mg, 1.04 mmol) was placed in a Schlenk and dissolved in dry benzene (21 ml), followed by the addition of NBS (406 mg, 2.28 mmol) and dibenzoyl peroxide (17 mg, 0.05 mmol). The reaction was heated for 7 h and the compound was purified by crystallisation, dissolving it first in warm CHCl$_3$ and then adding hexanes slowly, until precipitation in the interphase occurred. The mixture was stored in the freezer overnight, after which the obtained white crystals were collected and dried under vacuum. The solid thus obtained contained **186c** as the major product and was used directly in the next step without further purification.

^{1}H-NMR (300 MHz, CDCl$_3$) δ : 7.92 (d, J= 8.5 Hz, 2H), 7.64 (d, J= 8.5 Hz, 2H), 7.44-7.28 (m, 10H), 7.20-7.13 (m, 4H), 6.89-6.82 (m, 4H), 4.20 (s, 2H) ppm.

HRMS calculated m/z for C$_{36}$H$_{26}$Br$_2^+$: 616.040151; found (EI) 616.039996.

Compound 186d :
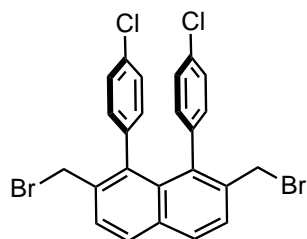
According to general procedure F, compound **185d** (426 mg, 1.13 mmol) was placed in a Schlenk and dissolved in dry benzene (22 ml), followed by the addition of NBS (442 mg, 2.48 mmol) and dibenzoyl peroxide (18 mg, 0.06 mmol). The reaction was heated for 7 h and the compound was purified by flash chromatography (hexanes/EtOAc, 9.8/0.2) to afford **186d** as a white solid (327 mg, 54 %).

^{1}H-NMR (400 MHz, CDCl$_3$) δ : 7.91 (d, J= 8.5 Hz, 2H), 7.60 (d, J= 8.5 Hz, 2H), 7.01

(d, $J=$ 8.4 Hz, 4H), 6.70 (d, $J=$ 8.4 Hz, 4H), 4.10 (s, 4H) ppm.

^{13}C-NMR (101 MHz, CDCl$_3$) δ : 138.8, 137.8, 136.3, 134.2, 133.0, 131.9, 131.8, 129.6, 128.3, 127.7, 32.8 ppm.

HRMS calculated m/z for C$_{24}$H$_{16}$Br$_2$Cl$_2^+$: 531.899606; found (EI) 531.899790.

IR (neat) $\tilde{\nu}$: 3048, 3017, 1592, 1489, 1435, 1410, 1392, 1342, 1241, 1204, 1188, 1110, 1084, 1013, 965, 884, 869, 845, 832, 790, 763, 735, 713, 644, 608, 540, 518, 499 cm^{-1}.

General Procedure G: Hydrolysis
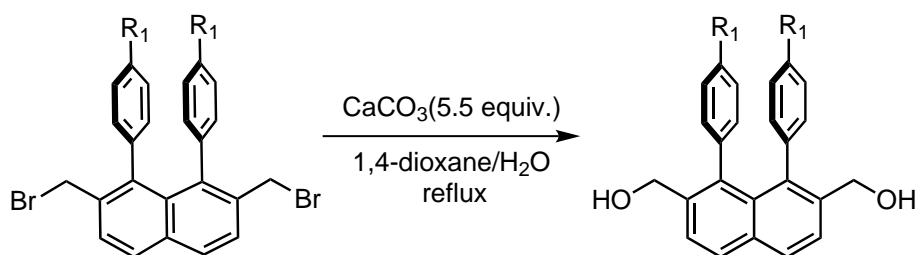
Based on the analogous hydrolysis reaction of 2,7-bis(bromomethyl)naphthalene described by Granzhan *et al.*[232] A round bottomed flask was charged with one of the 1,8-diaryl-2,7-bis(bromomethyl) naphthalenes, CaCO$_3$ (5.5 equiv.), 1,4-dioxane and water (0.077 M, 1,4-dioxane/water, 5/1) and the resulting mixture was heated under reflux for the specified time with vigorous stirring. The reaction mixture was then filtered hot, washing the filter cake with portions of hot 1,4-dioxane. The filtrate was concentrated *in vacuo*, and the resulting solid washed with small portions of 2 M aqueous HCl solution and water to afford the desired diol, that was dried *in vacuo* and used directly in the next step without further purification.

Compound 187a :

According to general procedure G, a round bottomed flask was charged with **186a** (3.71 g, 7.97 mmol) and CaCO$_3$ (4.38 g, 43.81 mmol). 1,4-Dioxane (86 ml) and water (17 ml) were added and the resulting mixture was heated for 48 h. After workup, a yellow solid was obtained, containing **187a** as the major product, and was used in the next step without purification.
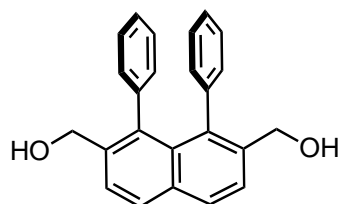
^{1}H-NMR (400 MHz, CDCl$_3$) δ : 7.95 (d, $J=$ 8.4 Hz, 2H), 7.68 (d, $J=$ 8.4 Hz, 2H), 6.96-6.89 (m, 6H), 6.70-6.68 (m, 4H), 4.22 (s, 4H), 1.39 (brs, 2H) ppm.

HRMS calculated m/z for C$_{24}$H$_{20}$O$_2$Na$^+$: 363.135549; found (ESI) 363.135560.

Compound 187b :
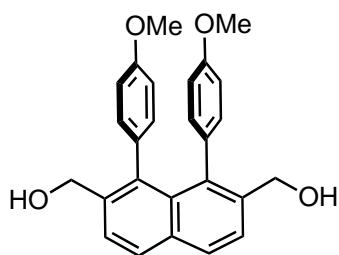
According to general procedure G, a round bottomed flask was charged with **186b** (652 mg, 1.24 mmol) and CaCO$_3$ (682 mg, 6.81 mmol). 1,4-Dioxane (13 ml) and water (2.7 ml) were added and the resulting mixture was heated for 60 h. After workup, a yellow solid was obtained, containing **187b** as the major product, and was used in the next step without purification.

^{1}H-NMR (400 MHz, CDCl$_3$) δ : 7.93 (d, $J=$ 8.4 Hz, 2H), 7.66 (d, $J=$ 8.4 Hz, 2H), 6.59-6.57 (m, 4H), 6.49-6.47 (m, 4H), 4.27 (brs, 4H), 3.76 (s, 6H), 1.45 (brs, 2H) ppm.
HRMS calculated m/z for C$_{26}$H$_{24}$O$_4$Na$^+$: 423.156679; found (ESI) 423.156900.

Compound 187c :
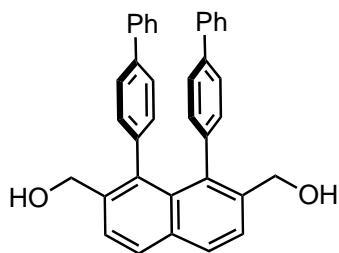
According to general procedure G, a round bottomed flask was charged with **186c** (346 mg, 0.56 mmol) and CaCO$_3$ (308 mg, 3.08 mmol). 1,4-Dioxane (6 ml) and water (1.2 ml) were added and the resulting mixture was heated for 48 h. After workup, a yellow solid was obtained, containing **187c** as the major product, and was used in the next step without purification.

^{1}H-NMR (400 MHz, CDCl$_3$) δ : 7.98 (d, $J=$ 8.4 Hz, 2H), 7.73 (d, $J=$ 8.4 Hz, 2H), 7.36-7.28 (m, 10H), 7.16-7.13 (m, 4H), 6.79-6.76 (m, 4H), 4.33 (s, 4H), 1.50 (brs, 2H) ppm.
HRMS calculated m/z for C$_{36}$H$_{28}$O$_2$Na$^+$: 515.198149; found (ESI) 515.198570.

Compound 187d :
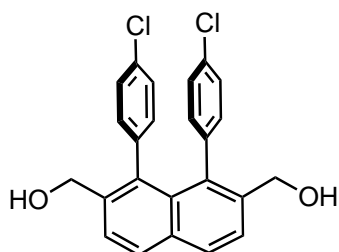
According to general procedure G, a round bottomed flask was charged with **186d** (257 mg, 0.48 mmol) and CaCO$_3$ (264 mg, 2.64 mmol). 1,4-Dioxane (5 ml) and water (1 ml) were added and the resulting mixture was heated for 60 h. After workup, a yellow solid was obtained, containing **187d** as the major product, and was used in the next step without purification.

^{1}H-NMR (400 MHz, CDCl$_3$) δ : 7.97 (d, $J=$ 8.5 Hz, 2H), 7.71 (d, $J=$ 8.5 Hz, 2H), 7.00-6.96 (m, 4H), 6.64-6.61 (m, 4H), 4.25 (s, 4H), 1.46 (brs, 2H) ppm.
HRMS calculated m/z for C$_{24}$H$_{18}$Cl$_2$O$_2$Na$^+$: 431.057605; found (ESI) 431.057870.

General Procedure H: Oxidation
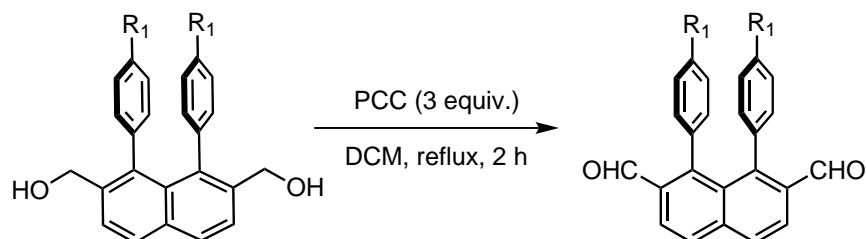
Based on the procedure for the oxidation of 2,7-bis(hydroxymethyl)naphthalene described by Granzhan *et al.*[232] A suspension of the corresponding diol in DCM (0.08 M) was heated to 40 ºC and, once it reached this temperature, PCC (3 equiv.) was added in one portion. The reaction mixture was vigorously stirred for 2 h at reflux, cooled to room temperature and poured into an Erlenmeyer with Et_2O. The mixture was triturated until the black tar solidified and then filtered through a pad of silica, eluting with an additional portion of Et_2O, to afford the crude material that was purified as specified for each case.

Compound 188a :
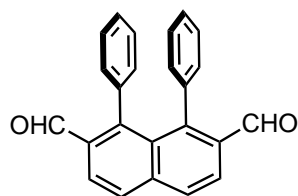
Using general procedure H, compound **188a** was prepared from **187a** (2.39 g, 7.02 mmol) and PCC (4.54 g, 21.06 mmol). The dialdehyde **188a** was obtained directly after filtration as a yellow solid (2.15 g, 80 % over three steps).

^{1}H-NMR (400 MHz, CDCl$_3$) δ : 9.41 (d, J= 0.9 Hz, 2H), 8.16 (d, J= 8.7 Hz, 2H), 8.04 (dd, J= 8.7, 0.9 Hz, 2H), 7.06 (tt, J= 7.4, 1.3 Hz, 2H), 7.00-6.95 (m, 4H), 6.87-6.84 (m, 4H) ppm.

^{13}C-NMR (101 MHz, CDCl$_3$) δ : 193.0, 192.7, 148.1, 139.6, 136.4, 134.5, 131.3, 130.8, 129.4, 127.4, 127.4, 127.3, 125.3 ppm.

HRMS calculated m/z for $C_{24}H_{16}O_2^+$: 335.1078; found (ESI) 335.1103.

IR (neat) $\tilde{\nu}$: 3021, 2959, 2924, 2883, 2858, 1677, 1600, 1490, 1442, 1260, 1180, 1144, 1092, 1003, 908, 881, 850, 798, 770, 762, 694, 666, 651, 629, 619, 609, 581 cm^{-1}.

Compound 188b :
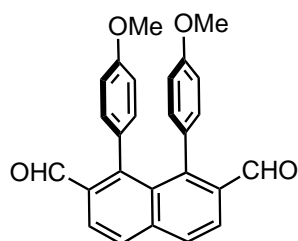
Using general procedure H, compound **188b** was prepared from **187b** (421 mg, 1.05 mmol) and PCC (680 mg, 3.15 mmol). The dialdehyde **188b** was obtained directly after filtration as an orange solid (390 mg, 83 % over two steps).

^{1}H-NMR (400 MHz, CDCl$_3$) δ : 9.52 (brs, 2H), 8.13 (d, J= 8.7 Hz, 2H), 8.00 (d, J= 8.7, 2H), 6.74 (dt, J= 8.6, 2.5 Hz, 4H), 6.54 (dt, J= 8.6, 2.5 Hz, 4H), 3.78 (s, 6H) ppm.

^{13}C-NMR (101 MHz, CDCl$_3$) δ : 193.1, 158.5, 148.0, 139.6, 134.9, 132.3, 131.6, 129.4, 128.9, 125.3, 113.0, 55.4 ppm.

HRMS calculated m/z for C$_{26}$H$_{20}$O$_4$Na$^+$: 419.125379; found (ESI) 419.125500.

IR (neat) $\tilde{\nu}$: 2962, 2983, 2901, 2879, 2836, 1677, 1606, 1593, 1509, 1461, 1439, 1289, 1236, 1181, 1172, 1141, 1106, 982, 857, 831, 804, 789, 767, 733, 721, 651, 612, 584 cm^{-1}.

Compound 188c :
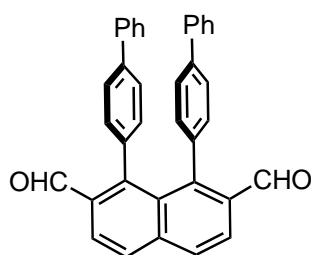
Using general procedure H, compound **188c** was prepared from **187c** (240 mg, 0.49 mmol) and PCC (317 mg, 1.47 mmol). The dialdehyde was purified by flash chromatography (gradient from hexanes to hexanes/EtOAc, 8/2), obtaining **188c** as a pale yellow foam (117 mg, 52% over three steps).

^{1}H-NMR (400 MHz, CDCl$_3$) δ : 9.60 (d, J= 0.9 Hz, 2H), 8.21 (d, J= 8.6 Hz, 2H), 8.07 (dd, J= 8.6, 0.9 Hz, 2H), 7.37-7.30 (m, 10H), 7.22-7.19 (m, 4H), 6.96-6.93 (m, 4H) ppm.

^{13}C-NMR (101 MHz, CDCl$_3$) δ : 192.8, 147.8, 140.3, 140.1, 139.7, 135.6, 134.5, 131.7, 131.4, 129.6, 128.9, 127.6, 127.2, 126.0, 125.3 ppm.

HRMS calculated m/z for C$_{36}$H$_{24}$O$_2$Na$^+$: 511.166849; found (ESI) 511.167280.

IR (neat) $\tilde{\nu}$: 3045, 3033, 3011, 2962, 2858, 1719, 1677, 1595, 1500, 1488, 1397, 1358, 1234, 1195, 1142, 1093, 1016, 964, 907, 851, 819, 792, 768, 739, 712, 655, 642, 628, 569, 528 cm^{-1}.

Compound 188d :
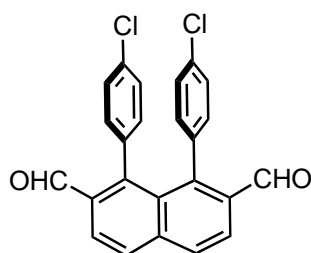
Using general procedure H, compound **188d** was prepared from **187d** (161 mg, 0.39 mmol) and PCC (252 mg, 1.17 mmol). The dialdehyde was purified by flash chromatography (hexanes/EtOAc, 9/1), obtaining **188d** as white solid (125 mg, 78% over two steps).

^{1}H-NMR (400 MHz, CDCl$_3$) δ : 9.51 (d, J= 0.9 Hz, 2H), 8.17 (d, J= 8.7 Hz, 2H), 8.06 (dd, J= 8.7, 0.9 Hz, 2H), 7.06 (dt, J= 8.3, 2.3 Hz, 4H), 6.81-6.78 (dt, J= 8.3, 2.3 Hz, 4H) ppm.

^{13}C-NMR (101 MHz, CDCl$_3$) δ : 192.0, 146.2, 139.7, 134.9, 134.5, 134.1, 132.4, 130.9, 130.0, 127.8, 125.5 ppm.

HRMS calculated m/z for C$_{24}$H$_{14}$Cl$_2$O$_2$Na$^+$: 427.026305; found (ESI) 427.026500.

IR (neat) $\tilde{\nu}$: 3053, 2962, 2905, 2876, 2861, 1676, 1597, 1506, 1488, 1436, 1397, 1358, 1337, 1259, 1232, 1185, 1140, 1087, 1015, 907, 884, 855, 794, 763, 725, 712, 655, 642, 614, 559, 528 cm^{-1}.

General Procedure I: Seyferth-Gilbert homologation
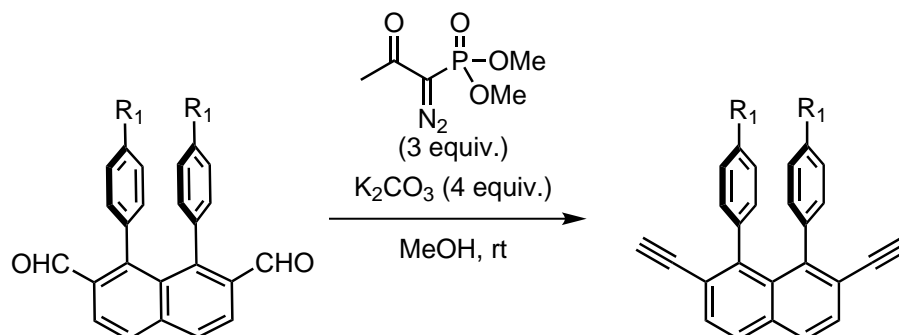
Based on the procedure for biphenyl systems described by our group.[27] The Ohira-Bestmann reagent (3 equiv.) was placed in a Schlenk and dissolved in dry MeOH (0.5 M), pouring the resulting solution into another Schlenk where the dialdehyde (1 equiv.) was placed previously. Afterwards, K_2CO_3 (4 equiv.) was added and the mixture was stirred at room temperature overnight. Then, the solvent was evaporated and the resulting oil was partitioned between DCM and Brine. The organic layers were combined, dried with Na_2SO_4, and the solvent evaporated *in vacuo* to afford the crude material that was purified by flash chromatography.

Compound 189a :
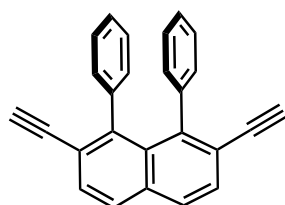
According to general procedure I, the dialdehyde **188a** (2.00 g, 5.96 mmol) was placed in a Schlenk and the Ohira-Bestmann reagent (3.43 g, 17.88 mmol), dissolved in MeOH (31 ml), and K_2CO_3 (3.30 g, 23.84 mmol) were consecutively added, stirring the resulting mixture overnight. After workup and purification by flash chromatography (hexanes/EtOAc, 9.5/0.5) the alkyne **189a** was obtained as a light yellow solid. Additionally, impurer fractions of the column were combined and washed with portions of EtOAc to afford more **189a** (1.18 g in total, 60 %).

^{1}H-NMR (400 MHz, CDCl$_3$) δ : 7.83 (d, *J*= 8.5 Hz, 2H), 7.64 (d, *J*= 8.5 Hz, 2H), 6.98-6.91 (m, 6H), 6.83-6.80 (m, 4H), 2.88 (s, 2H) ppm.

^{13}C-NMR (101 MHz, CDCl$_3$) δ : 144.7, 140.7, 134.3, 130.8, 130.8, 130.0, 128.2, 127.1, 126.4, 122.9, 83.4, 81.8 ppm.

HRMS calculated *m/z* for $C_{26}H_{16}^+$: 328.125200; found (EI) 328.124971.

IR (neat) $\tilde{\nu}$: 3282, 3074, 3057, 3019, 1596, 1573, 1488, 1439, 1348, 1305, 1259, 1169, 1070, 1027, 837, 804, 780, 756, 729, 695, 648, 635, 607, 593, 556, 525, 510 cm^{-1}.

Compound 189b :
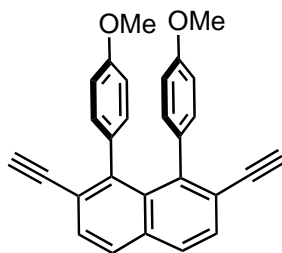
According to general procedure I, the dialdehyde **188b** (346 mg, 0.87 mmol) was placed in a Schlenk and the Ohira-Bestmann reagent (501 mg, 2.61 mmol), dissolved in MeOH (5 ml), and K_2CO_3 (481 mg, 3.48 mmol) were consecutively added, stirring the resulting mixture overnight. After workup and purification by flash chromatography (hexanes/EtOAc, 8/2) the alkyne **189b** was obtained as a light green solid (283 mg, 83 %).

^{1}H-NMR (400 MHz, CDCl$_3$) δ : 7.81 (d, J= 8.5 Hz, 2H), 7.63 (d, J= 8.5 Hz, 2H), 6.71 (dt, J= 8.8, 1.8 Hz, 4H), 6.49 (dt, J= 8.8, 1.8 Hz, 4H), 3.75 (s, 6H), 2.92 (s, 2H) ppm.

^{13}C-NMR (101 MHz, CDCl$_3$) δ : 157.8, 144.4, 134.4, 133.4, 131.8, 131.5, 129.9, 128.1, 123.1, 112.7, 83.7, 81.8, 55.3 ppm.

HRMS calculated m/z for $C_{28}H_{20}O_2$: 388.146330; found (EI) 388.146189.

IR (neat) $\tilde{\nu}$: 3273, 2953, 2933, 2903, 2834, 1608, 1574, 1533, 1506, 1463, 1436, 1350, 1304, 1282, 1241, 1175, 1104, 1031, 953, 885, 844, 828, 809, 786, 759, 722, 666, 640, 621, 608, 592, 579 cm^{-1}.

Compound 189c :
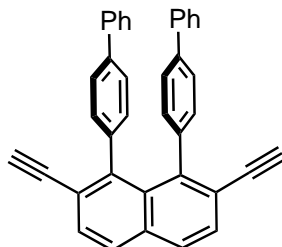
According to general procedure I, the dialdehyde **188c** (85 mg, 0.17 mmol) was placed in a Schlenk and the Ohira-Bestmann reagent (100 mg, 0.52 mmol), dissolved in MeOH (0.9 ml), and K_2CO_3 (94 mg, 0.68 mmol) were consecutively added, stirring the resulting mixture overnight. After workup and purification by flash chromatography (hexanes/DCM, 8/2) the alkyne **189c** was obtained as a yellow foam (55 mg, 66 %).

^{1}H-NMR (400 MHz, CDCl$_3$) δ : 7.86 (d, J= 8.5 Hz, 2H), 7.67 (d, J= 8.5 Hz, 2H), 7.38-7.34 (m, 4H), 7.32-7-27 (m, 6H), 7.15 (d, J= 8.2 Hz, 4H), 6.88 (d, J= 8.2 Hz, 4H), 2.92 (s, 2H) ppm.

^{13}C-NMR (101 MHz, CDCl$_3$) δ : 144.3, 141.1, 139.9, 139.0, 134.3, 131.4, 131.1, 130.0, 128.6, 128.3, 127.2, 127.0, 125.7, 122.8, 83.4, 82.2 ppm.

HRMS calculated m/z for $C_{38}H_{24}^+$: 480.187800; found (EI) 480.187667.

IR (neat) $\tilde{\nu}$: 3271, 3028, 2960, 2922, 2853, 1513, 1497, 1446, 1434, 1399, 1279, 1261, 1175, 1155, 1108, 1077, 1026, 1008, 966, 949, 923, 915, 883, 851, 842, 810, 771, 748, 699, 678, 659,, 648, 641 cm^{-1}.

Compound 189d :
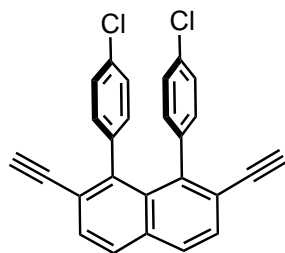
According to general procedure I, the dialdehyde **188d** (100 mg, 0.25 mmol) was placed in a Schlenk and the Ohira-Bestmann reagent (144 mg, 0.75 mmol), dissolved in MeOH (1.3 ml), and K_2CO_3 (138 mg, 1.00 mmol) were consecutively added, stirring the resulting mixture overnight. After workup and purification by flash chromatography (hexanes/EtOAc, 8/2) the alkyne **189d** was obtained as a white solid (76 mg, 77 %).

^{1}H-NMR (400 MHz, CDCl$_3$) δ : 7.85 (d, J= 8.5 Hz, 2H), 7.64 (d, J= 8.5 Hz, 2H), 6.97 (dt, J= 8.4, 2.2 Hz, 4H), 6.72 (dt, J= 8.4, 2.2 Hz, 4H), 2.93 (s, 2H) ppm.

^{13}C-NMR (101 MHz, CDCl$_3$) δ : 142.9, 139.1, 134.2, 132.8, 132.1, 130.8, 130.0, 128.7, 127.4, 123.1, 83.0, 82.7 ppm.

HRMS calculated for m/z $C_{26}H_{14}Cl_2$: 396.047256; found (EI) 396.047147.

IR (neat) $\tilde{\nu}$: 3285, 3220, 1592, 1488, 1396, 1346, 1330, 1301, 1245, 1176, 1108, 1085, 1015, 984, 962, 939, 889, 845, 833, 823, 806, 770, 754, 733, 651, 628, 603, 597, 563, 512, 491 cm^{-1}.

Compound 27aa :
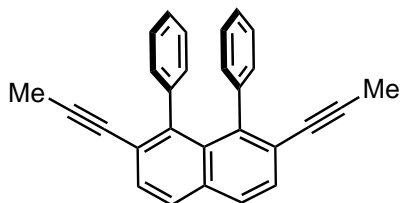
LiHMDS (1.98 g, 11.82 mmol) was placed in a Schlenk, dissolved in THF (23 ml) and cooled to -20 °C . To this solution, the diyne **189a** (1.11 g, 3.38 mmol) was added portion-wise and the reaction mixture was stirred for 1 h at the same temperature. MeI (1.0 ml, 16.88 mmol) was then added slowly, before allowing the mixture to warm to room temperature and stirring for 2.5 h more. The reaction was quenched with a saturated solution of ammonium chloride and extracted with DCM. The organic layers were combined, dried over Na_2SO_4 and the solvent removed *in vacuo* to afford a brown oily solid which was further purified by flash chromatography (hexanes/EtOAc, 9/1) to afford the desired compound **27aa** as a pale yellow solid (963 mg, 80%).

^{1}H-NMR (400 MHz, CDCl$_3$) δ : 7.76 (d, J= 8.4 Hz, 2H), 7.53 (d, J= 8.4 Hz, 2H), 6.92-6.90 (m, 6H), 6.82-6.80 (m, 4H), 1.72 (s, 6H) ppm.

^{13}C-NMR (101 MHz, CDCl$_3$) δ : 143.2, 141.4, 133.3, 131.1, 131.0, 129.2, 127.9, 126.8, 125.9, 124.4, 90.7, 80.0, 4.4 ppm.

HRMS calculated m/z for $C_{28}H_{20}^+$: 357.163775; found (APPI) 357.163270.

IR (neat) $\tilde{\nu}$: 3057, 3028, 3016, 2958, 2913, 2847, 2229, 1597, 1573, 1503, 1488, 1439,

1398, 1374, 1351, 1331, 1305, 1275, 1259, 1186, 1171, 1149, 1070, 1026, 966, 952, 909, 834, 803, 760, 733, 696, 619, 607, 594, 560 cm^{-1}.

General Procedure J: Sonogashira coupling
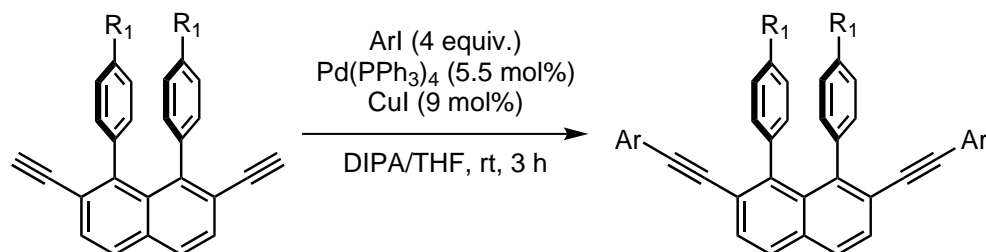
Based on the procedure reported by Starý for aryl-tethered triynes.[185] A Schlenk was charged with the diyne (1 equiv.), the corresponding aromatic iodide (4 equiv.), Pd(PPh$_3$)$_4$ (5.5 mol%), CuI (9 mol%) and a mixture of DIPA/THF (2/1, 0.047 M for the diyne) was added. The reaction mixture was degassed for 15 minutes and then stirred at room temperature for 3 h. The solvents were removed *in vacuo* and to the resulting residue was added EtOAc, observing the precipitation of a white solid. The solvent was then filtered out, the white solid was washed with two additional portions of EtOAc and dried under vacuum. Toluene was added to the crude, and the resulting suspension was directly purified by a short flash chromatography.

Compound 27ab :
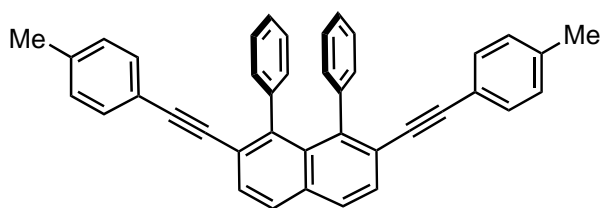
According to general procedure J, a Schlenk was charged with the diyne **189a** (81 mg, 0.25 mmol), 4-iodotoluene (218 mg, 1.0 mmol), Pd(PPh$_3$)$_4$ (15.9 mg, 1.4×10^{-2} mmol) and CuI (4.3 mg, 2.3×10^{-2} mmol). DIPA (3.5 ml) and THF (1.7 ml) were added and the reaction was stirred for 3 h and 15 min. After workup and purification by flash chromatography (toluene), compound **27ab** was obtained as a white solid (100 mg, 80 %).

^{1}H-NMR (400 MHz, CDCl$_3$) δ : 7.85 (d, J= 8.5 Hz, 2H), 7.66 (d, J= 8.5 Hz, 2H), 7.00-6.95 (m, 10H), 6.93-6.88 (m, 8H), 2.28 (s, 6H) ppm.

^{13}C-NMR (101 MHz, CDCl$_3$) δ : 143.8, 141.4, 138.2, 133.7, 131.4, 131.3, 130.9, 129.0, 128.8, 128.2, 127.0, 126.1, 124.2, 120.3, 94.6, 89.6, 21.6 ppm.

HRMS calculated m/z for C$_{40}$H$_{28}$$^+$: 508.219100; found (EI) 508.219002.

IR (neat) $\tilde{\nu}$: 3051, 3021, 2990, 1596, 1512, 1491, 1442, 1404, 1354,1340, 1307, 1277, 1264, 1238, 1179, 1160, 1105, 1073, 1038, 1020, 1000, 977, 961, 942, 929, 915, 894, 877,

849, 834, 812, 785, 757, 695, 608, 596, 551, 525 cm^{-1}.

Compound 27ac :

According to general procedure J, a Schlenk was charged with the diyne **189a** (185 mg, 0.56 mmol), iodobenzene (457 mg, 2.24 mmol), Pd(PPh$_3$)$_4$ (35.8 mg, 3.1×10^{-2} mmol) and CuI (9.7 mg, 5.1×10^{-2} mmol). DIPA (8 ml) and THF (4 ml) were added and the reaction was stirred for 3 h and 15 min. In this case, the crude was dissolved in DCM and the solution was purified by flash chromatography (hexanes/EtOAc, 9/1). The purer fractions from the column were collected and precipitated, dissolving the solid in toluene and adding EtOH until a white solid appeared. The thus obtained **27ac** was collected and dried *in vacuo* (150 mg, 55 %).

^{1}H-NMR (300 MHz, CDCl$_3$) δ : 7.87 (d, $J=$ 8.5 Hz, 2H), 7.68 (d, $J=$ 8.5 Hz, 2H), 7.21-7.14 (m, 6H), 7.02-6.90 (m, 14H) ppm.

^{13}C-NMR (101 MHz, CDCl$_3$) δ : 144.0, 141.3, 133.9, 131.5, 131.3, 130.8, 128.9, 128.3, 128.2, 128.1, 127.0, 126.2, 124.1, 123.4, 94.4, 90.2 ppm.

HRMS calculated m/z for C$_{38}$H$_{24}{}^+$: 480.187800; found (EI) 480.187643.

IR (neat) $\tilde{\nu}$: 3051, 3021, 2990, 1596, 1512, 1491, 1442, 1404, 1354,1340, 1307, 1277, 1264, 1238, 1179, 1160, 1105, 1073, 1038, 1020, 1000, 977, 961, 942, 929, 915, 894, 877, 849, 834, 812, 785, 757, 695, 608, 596, 551, 525 cm^{-1}.

Compound 27ad :

According to general procedure J, a Schlenk was charged with the diyne **189a** (29 mg, 8.9×10^{-2} mmol), 5-iodo-*m*-xylene (52 µl, 0.36 mmol), Pd(PPh$_3$)$_4$ (5.7 mg, 4.9×10^{-3} mmol) and CuI (1.5 mg, 8.0×10^{-3} mmol). DIPA (1.2 ml) and THF (0.6 ml) were added and the reaction was stirred for 3 h and 15 min. After workup and purification by flash chromatography (toluene), compound **27ad** was obtained as a white solid (41 mg, 86 %).

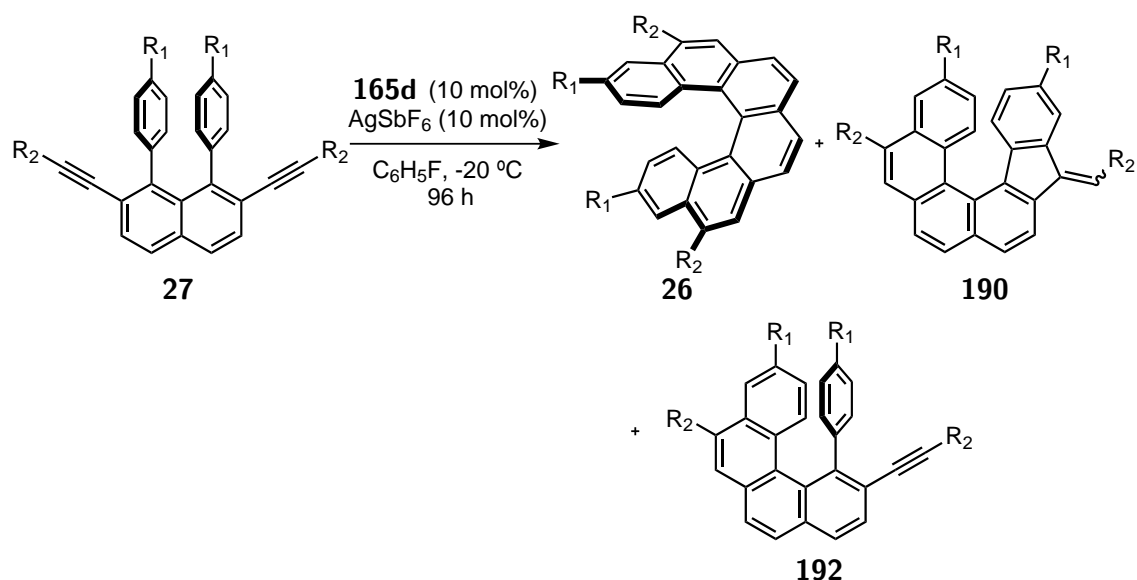^{1}H-NMR (400 MHz, CDCl$_3$) δ : 7.85 (d, $J=$ 8.4 Hz, 2H), 7.66 (d, $J=$ 8.4 Hz, 2H), 7.02-6.96 (m, 6H), 6.94-6.90 (m, 4H), 6.83 (s, 2H), 6.63 (s, 4H), 2.19 (s, 12H) ppm.

^{13}C-NMR (101 MHz, CDCl$_3$) δ : 143.9, 141.4, 137.7, 133.8, 131.3, 130.9, 130.0, 129.2, 128.9, 128.2, 127.0, 126.1, 124.2, 123.0, 94.9, 89.6, 21.2 ppm.

HRMS calculated m/z for C$_{42}$H$_{32}{}^+$: 536.250400; found (EI) 536.250302.

IR (neat) $\tilde{\nu}$: 3055, 3026, 2997, 2966, 2914, 1594, 1504, 1442, 1375, 1237, 1152, 1133, 1097, 1072, 1002, 947, 881, 842, 807, 773, 756, 730, 687, 633, 624, 609, 595, 573, 536, 512 cm^{-1}.

Compound 27ae :

According to general procedure J, a Schlenk was charged with the diyne **189a** (73 mg, 0.22 mmol), 4-chloroiodobenzene (213 mg, 0.89 mmol), Pd(PPh$_3$)$_4$ (14.2 mg, 1.2×10^{-2} mmol) and CuI (3.8 mg, 2.0×10^{-2} mmol). DIPA (3.2 ml) and THF (1.6 ml) were added and the reaction was stirred for 3 h and 15 min. After workup and purification by flash chromatography (toluene), compound **27ae** was obtained as a white solid (80 mg, 65 %).

^{1}H-NMR (400 MHz, CDCl$_3$) δ : 7.87 (d, J= 8.4 Hz, 2H), 7.66 (d, J= 8.4 Hz, 2H), 7.17-7.13 (m, 4H), 7.02-6.95 (m, 6H), 6.92-6.88 (m, 8H) ppm.

^{13}C-NMR (101 MHz, CDCl$_3$) δ : 144.2, 141.2, 134.1, 134.0, 132.7, 131.2, 130.7, 128.8, 128.6, 128.4, 127.0, 126.3, 123.8, 121.8, 93.4, 91.1 ppm.

HRMS calculated m/z for C$_{38}$H$_{22}$Cl$_2$: 548.109856; found (EI) 548.110089.

IR (neat) $\tilde{\nu}$: 3055, 3026, 1505, 1484, 1441, 1396, 1336, 1083, 1027, 1011, 842, 823, 805, 763, 716, 692, 623, 608, 598, 542, 520, 492 cm^{-1}.

Compound 27ba :

According to general procedure J, a Schlenk was charged with the diyne **189b** (60 mg, 0.15 mmol), 4-iodotoluene (131 mg, 0.60 mmol), Pd(PPh$_3$)$_4$ (9.5 mg, 8.3×10^{-3} mmol) and CuI (2.6 mg, 1.4×10^{-2} mmol). DIPA (2.2 ml) and THF (1.1 ml) were added and the reaction was stirred for 3 h and 15 min. After workup and purification by flash chromatography (toluene), compound **27ba** was obtained as a light yellow solid (85 mg, 97 %).

^{1}H-NMR (400 MHz, CDCl$_3$) δ : 7.83 (d, J= 8.4 Hz, 2H), 7.65 (d, J= 8.4 Hz, 2H), 7.01 (d, J= 8.1 Hz, 4H), 6.97 (d, J= 8.1 Hz, 4H), 6.81 (dt, J= 8.6, 2.4 Hz, 4H), 6.54 (dt, J= 8.6, 2.4 Hz, 4H), 3.77 (s, 6H), 2.29 (s, 6H) ppm.

^{13}C-NMR (101 MHz, CDCl$_3$) δ : 157.8, 143.4, 138.2, 134.1, 133.9, 132.3, 131.6, 131.4, 129.0, 128.9, 128.1, 124.4, 120.5, 112.7, 94.5, 89.8, 55.5, 21.6 ppm.

HRMS calculated m/z for C$_{42}$H$_{32}$O$_2$Na$^+$: 591.229449; found (ESI) 591.229740.

IR (neat) $\tilde{\nu}$: 3061, 3024, 3012, 2995, 2945, 2926, 2854, 2831, 1610, 1577, 1530, 1508, 1462, 1440, 1406, 1358, 1339, 1287, 1245, 1177, 1107, 1035, 968, 946, 885, 848, 819, 787, 722, 709, 695, 652, 633, 611, 589, 579, 551, 530, 494 cm^{-1}.

Compound 27bb :

According to general procedure J, a Schlenk was charged with the diyne **189b** (34 mg, 8.8×10^{-2} mmol), (*S*)-1-iodo-4-(1-phenylethoxy)benzene (113 mg, 0.35 mmol), Pd(PPh$_3$)$_4$ (5.6 mg, 4.8×10^{-3} mmol) and CuI (1.5 mg, 7.9×10^{-3} mmol). DIPA (1.2 ml) and THF (0.6 ml) were added and the reaction was stirred for 3 h and 15 min. After workup and purification by flash chromatography (toluene), compound **27bb** was obtained as a light brown oil, that precipitated upon addition of hexanes to give a pale yellow powder (51 mg, 75 %).

^{1}H-NMR (400 MHz, C$_6$D$_6$) δ : 7.74 (d, *J*= 8.4 Hz, 2H), 7.51 (d, *J*= 8.4 Hz, 2H), 7.14-7.04 (m, 12H), 7.01-6.97 (m, 2H), 6.85 (dd, *J*= 8.3, 2.3 Hz, 2H), 6.81 (dd, *J*= 8.3, 2.3 Hz, 2H), 6.62 (d, *J*= 8.8 Hz, 4H), 6.43 (dd, *J*= 8.3, 2.6 Hz, 2H), 6.47 (dd, *J*= 8.3, 2.6 Hz, 2H), 4.84 (q, *J*= 6.4 Hz, 2H), 3.33 (s, 6H), 1.34 (d, *J*= 6.4 Hz, 6H) ppm.

^{13}C-NMR (101 MHz, C$_6$D$_6$) δ : 158.3, 158.2, 143.8, 143.2, 134.5, 134.2, 133.3, 132.7, 132.7, 132.4, 129.0, 128.8, 128.6, 127.6, 125.7, 125.3, 116.3, 116.1, 113.0, 112.9, 95.2, 90.0, 75.9, 54.8, 24.4 ppm.

HRMS calculated m/z for C$_{56}$H$_{44}$O$_4$Na$^+$: 803.313179; found (ESI) 803.313210.

IR (neat) $\tilde{\nu}$: 3082, 3057, 3028, 2971, 2962, 2926, 2866, 2833, 1605, 1543, 1506, 1451, 1371, 1353, 1329, 1303, 1275, 1237, 1173, 1109, 1096, 1067, 1029, 1010, 997, 959, 930, 891, 828, 810, 797, 758, 698, 638, 611, 595, 559, 534, 499 cm^{-1}.

Compound 27c :

According to general procedure J, a Schlenk was charged with the diyne **189c** (34 mg, 7.1×10^{-2} mmol), 4-iodotoluene (62 mg, 28.4×10^{-2} mmol), Pd(PPh$_3$)$_4$ (4.5 mg, 3.9×10^{-3} mmol) and CuI (1.2 mg, 6.4×10^{-3} mmol). DIPA (1.0 ml) and THF (0.5 ml) were added and the

reaction was stirred for 3 h and 15 min. After workup and purification by flash chromatography (toluene), compound **27c** was obtained as a white solid (34 mg, 73 %).

^{1}H-NMR (400 MHz, CDCl$_3$) δ : 7.89 (d, J= 8.4 Hz, 2H), 7.70 (d, J= 8.4 Hz, 2H), 7.41-7.38 (m, 4H), 7.36-7.31 (m, 6H), 7.20 (d, J= 8.0 Hz, 4H), 7.00 (d, J= 8.0 Hz, 4H), 6.93 (d, J= 7.9 Hz, 4H), 6.87 (d, J= 7.9 Hz, 4H), 2.25 (s, 6H) ppm.

^{13}C-NMR (101 MHz, CDCl$_3$) δ : 143.4, 141.6, 140.7, 139.0, 138.3, 133.7, 131.7, 131.4, 131.2, 129.0, 128.7, 128.7, 128.4, 127.4, 127.0, 125.8, 124.2, 120.2, 95.1, 89.7, 21.6 ppm.

HRMS calculated m/z for C$_{52}$H$_{36}$$^+$: 660.281700; found (EI) 660.281973.
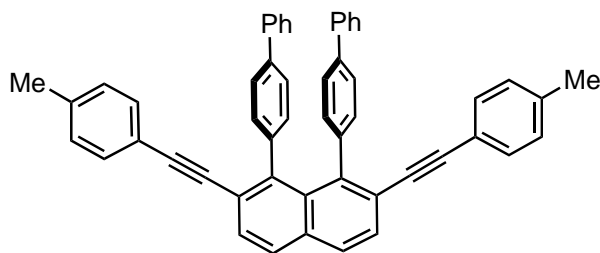
IR (neat) $\tilde{\nu}$: 3021, 2964, 2944, 2915, 2874, 2859, 1598, 1579, 1511, 1486, 1446, 1429, 1403, 1378, 1360, 1305, 1278, 1261, 1209, 1181, 1153, 1107, 1073, 1021, 963, 890, 823, 758, 735, 721, 693, 641, 612, 578, 566, 509 cm^{-1}.

Compound 27d :
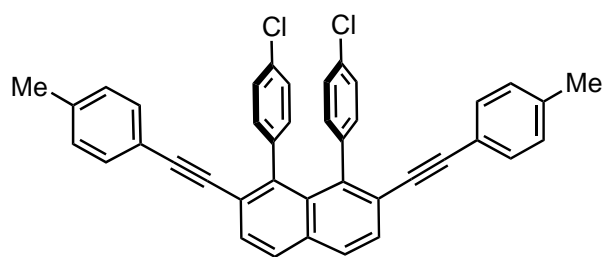
According to general procedure J, a Schlenk was charged with the diyne **189d** (50 mg, 0.13 mmol), 4-iodotoluene (113 mg, 0.52 mmol), Pd(PPh$_3$)$_4$ (8.3 mg, 7.1 × 10^{-3} mmol) and CuI (2.2 mg, 1.2 × 10^{-2} mmol). DIPA (1.8 ml) and THF (0.9 ml) were added and the reaction was stirred for 3 h and 15 min. After workup and purification by flash chromatography (hexanes/toluene, 4/6), compound **27d** was obtained as a white solid (48 mg, 66 %).

^{1}H-NMR (400 MHz, CDCl$_3$) δ : 7.87 (d, J= 8.5 Hz, 2H), 7.66 (d, J= 8.5 Hz, 2H), 7.05-7.01 (m, 8H), 6.94-6.91 (m, 4H), 6.85-6.81 (m, 4H), 2.30 (s, 6H) ppm.

^{13}C-NMR (101 MHz, CDCl$_3$) δ : 141.8, 139.8, 138.6, 133.6, 132.6, 132.5, 131.4, 130.9, 129.2, 128.9, 128.7, 127.2, 124.4, 120.0, 95.4, 89.1, 21.6 ppm.

HRMS calculated m/z for C$_{40}$H$_{26}$Cl$_2$$^+$: 576.141156; found (EI) 576.140833.

IR (neat) $\tilde{\nu}$: 3076, 3046, 3020, 2914, 2850, 2203, 1590, 1510, 1488, 1436, 1396, 1358, 1336, 1294, 1263, 1180, 1160, 1139, 1099, 1037, 1015, 961, 943, 883, 862, 844, 813, 782, 733, 716, 710, 677, 645, 590 cm^{-1}.

III.1.3.4   Catalysis

General Procedure K: Enantioselective gold(I)-catalysed hydroarylation of 27

The substrate **27** (10-25 mg) and the gold precatalyst **165d** (10 mol%) were placed in a Schlenk and dry fluorobenzene (0.05 M) was added. The mixture was pre-stirred at room temperature for 2 min, then cooled to -20 °C and stirred 15 min further. Then, $AgSbF_6$ solution (0.05 M in DCM) was added (10 mol%) and the reaction was stirred for 4 days at the same temperature. The reaction was quenched, filtering the mixture through a short pad of silica and eluting with portions of DCM. After evaporation of the solvent a mixture of isomers was obtained, the helicene being the major compound.

Compound 26aa :

According to general procedure K, substrate **27aa** (7.3 mg, 2.0×10^{-2} mmol) was treated with **165d** (3.1 mg, 2.0×10^{-3} mmol) and $AgSbF_6$ (41 µl, solution 0.05 M in DCM). After workup, a mixture of isomers was obtained (6.0 mg, 82 % mass recovered), the helicene **27aa** being the major compound (conversion 100 %, ratio **26aa**:**190aa**:**192aa**, 99:1:0). Conversion and the ratio of compounds was determined by HPLC, in this case with the Agilent system: 50×3 mm Agilent Eclipse Plus C18 column, CH_3CN/H_2O = 95/5 (v/v), 0.5 ml min^{-1}, 19.1 MPa, 308 K, 254 nm; helicene **26aa** t_R= 2.85 min, isomer **190aa** t_R= 3.15 min.

Enantiomeric excess: 63 %. The *ee* was determined by 2D HPLC: 50×3 mm Agilent Eclipse Plus C18 column, CH_3CN/H_2O = 95/5 (v/v), 0.5 ml min^{-1}, 19.1 MPa,

308 K, 254 nm, helicene **26aa** t_R= 2.85; then 150 × 4.6 mm Chiralpak IC-3 column, CH_3CN = 100 (v/v), 1.0 ml min^{-1}, 7.6 MPa, 298 K, 254 nm; major enantiomer t_R= 2.80 min, minor enantiomer t_R= 2.94 min.

^{1}H-NMR (400 MHz, CDCl$_3$) δ : 8.00-7.96 (m, 4H), 7.88 (d, J= 8.2 Hz, 2H), 7.76 (s, 2H), 7.67 (dd, J= 8.5, 1.2 Hz, 2H), 7.26 (ddd, J= 8.2, 6.9, 1.2 Hz, 2H), 6.68 (ddd, J= 8.5, 6.9, 1.4 Hz, 2H), 2.86 (s, 6H) ppm.

^{13}C-NMR (101 MHz, CDCl$_3$) δ : 133.6, 132.6 , 131.5, 131.3, 130.2, 128.4, 127.3, 127.1, 126.5, 126.4, 125.5, 124.3, 124.2, 123.6, 20.0 ppm.

HRMS calculated m/z for $C_{28}H_{20}^+$: 356.156500; found (EI) 356.156258.

IR (neat) $\tilde{\nu}$: 2962, 2933, 2907, 1470, 1437, 1399, 1362, 1324, 1259, 1195, 1087, 1015, 875, 796, 760, 746, 703, 664, 630, 622, 607, 559, 546, 516 cm^{-1}.

$[\alpha]_D^{20}$= +1526 (c = 0.22, DCM)

Compound 26ab :

According to general procedure K, substrate **27ab** (11.0 mg, 2.2×10^{-2} mmol) was treated with **165d** (3.3 mg, 2.2×10^{-3} mmol) and AgSbF$_6$ (43 µl, solution 0.05 M in DCM). After workup, the mixture of isomers was obtained (9.7 mg, 88 % mass recovered), the helicene **26ab** being the major compound (conversion 98 %, ratio **26ab**:**190ab**:**192ab**, 96:3:1). Conversion and the ratio of compounds was determined by HPLC: 50 × 3 mm Agilent Eclipse Plus C18 column, CH$_3$CN/ H$_2$O = 90/10 (v/v), 1.0 ml min^{-1}, 6.7 MPa, 308 K, 254 nm; intermediate **192ab** t_R= 9.44 min, starting material **27ab** t_R= 9.83 min, helicene **26ab** t_R= 11.99 min, isomers **190ab** E t_R= 12.69 min and Z t_R= 13.27 min.

Enantiomeric excess: 91 %. The ee was determined by 2D HPLC: 50 × 3 mm Agilent Eclipse Plus C18 column, CH$_3$CN/ H$_2$O = 95/5 (v/v), 0.5 ml min^{-1}, 11.3 MPa, 308 K, 254 nm, helicene **26ab** t_R= 5.45 min; then 150 × 4.6 mm Chiralpak IC-3 column, CH$_3$CN/ CH$_3$OH = 95/5 (v/v), 1.0 ml min^{-1}, 5.9 MPa, 298 K, 254 nm; major enantiomer t_R= 2.81 min, minor enantiomer t_R= 3.10 min.

In order to obtain a purer sample for characterisation, the mixture was separated by semi-preparative HPLC. Separation conditions: 250 × 20 mm YMC PVA-SIL 5 µm column, i-hexane/MTBE = 99/1 (v/v), 15 ml min^{-1}, 1.8 MPa, 308 K, 239 nm.

^{1}H-NMR (400 MHz, CDCl$_3$) δ : 8.04 (d, J= 8.2 Hz, 2H), 7.99 (d, J= 8.2 Hz, 2H), 7.92-7.90 (m, 4H), 7.82 (d, J= 8.4 Hz, 2H), 7.63 (d, J= 7.7 Hz, 4H), 7.41 (d, J= 7.7 Hz, 4H), 7.17 (ddd, J= 8.2, 6.7, 1.3 Hz, 2H), 6.75 (ddd, J= 8.4, 6.7, 1.4 Hz, 2H), 2.51 (s, 6H) ppm.

¹³C-NMR (101 MHz, CDCl$_3$) δ : 139.7, 137.8, 137.3, 133.3, 131.0, 130.7, 130.5, 130.2, 129.3, 128.2, 127.6, 127.4, 127.3, 126.6, 126.0, 125.6, 124.6, 124.0, 21.5 ppm.

HRMS calculated m/z for C$_{40}$H$_{28}$$^+$: 508.219100; found (EI) 508.218991.

IR (neat) $\tilde{\nu}$: 3042, 3019, 2962, 2916, 2858, 1602, 1512, 1436, 1398, 1368, 1304, 1259, 1182, 1108, 1020, 956, 885, 819, 792, 765, 746, 714, 655, 624, 611, 573, 551, 510 cm^{-1}.

$[\alpha]_D^{20}$= +1402 (c = 0.25, DCM).

Compound *E*-190ab :
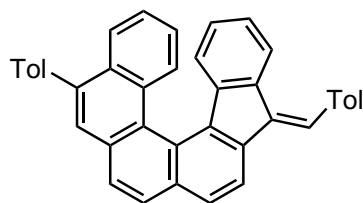
The substrate **27ab** (80 mg, 0.16 mmol) and the gold precatalyst **164a** (2.7 mg, 7.9×10^{-3} mmol) were placed in a Schlenk and dry DCM (0.05 M) was added. The mixture was pre-stirred at room temperature for 2 min, then cooled to 0 °C and stirred for 15 min further. Then, AgSbF$_6$ solution (158 µl solution 0.05 M in DCM, 7.9×10^{-3} mmol) was added and the reaction was stirred for 3 days at the same temperature. The reaction was quenched filtering the mixture through a short pad of silica and eluting with portions of DCM. After solvent evaporation, 60 mg of mixture of isomers was obtained, containing 32 % of compound *E*-**190ab** (calculated by HPLC).

E-**190ab** was separated by semi-preparative HPLC, obtaining 16.9 mg of pure material. Separation conditions: 250×20 mm YMC PVA-SIL 5 µm column, *i*-hexane/MTBE = 99/1 (v/v), 15 ml min^{-1}, 1.8 MPa, 308 K, 239 nm. Analysis of the NMR data and assignment of the signals are summarised in *__Table A.3__*.

¹H-NMR (500 MHz, C$_6$H$_6$) δ : 8.58 (dd, J= 8.4, 1.2 Hz, 1H), 8.23 (dd, J= 8.4, 1.3 Hz, 1H), 7.97 (d, J= 7.7 Hz, 1H), 7.94 (d, J= 8.1 Hz, 1H), 7.85 (s, 1H), 7.81 (d, J= 8.8, 1H), 7.80 (s, 1H), 7.80 (d, J= 6.7 Hz, 1H), 7.66 (d, J= 8.3 Hz, 1H), 7.54 (d, J= 7.8 Hz, 2H), 7.52 (d, J= 8.0, 2H), 7.24 (ddd, J= 8.2, 6.7, 1.2 Hz, 1H), 7.05 (ddd, J= 8.4, 6.7, 1.4 Hz, 1H), 7.04 (d, J= 8.0 Hz, 2H), 6.82 (d, J= 7.9 Hz, 1H), 6.78 (td, J= 7.5, 1.1 Hz, 1H), 6.65 (td, J= 7.6, 1.2 Hz, 1H), 2.26 (s, 3H), 2.15 (s, 3H) ppm.

¹³C-NMR (151 MHz, C$_6$D$_6$) δ : 142.8, 140.3, 140.1, 137.9, 137.8, 136.9, 136.8, 136.8, 136.6, 134.7, 134.2, 132.0, 131.2, 130.9, 130.8, 130.2, 129.7, 129.2, 129.1, 128.1, 127.9, 127.2, 126.9, 126.7, 126.5, 126.3, 126.1, 125.9, 125.7, 125.7, 125.1, 124.3, 123.5, 118.8, 21.0, 20.9 ppm.

HRMS calculated m/z for C$_{40}$H$_{28}$$^+$: 508.219100; found (EI) 508.219024.

IR (neat) $\tilde{\nu}$: 3042, 3019, 2981, 2959, 2918, 2884, 2850, 1510, 1454, 1407, 1378, 1341, 1312, 1260, 1204, 1181, 1161, 1149, 1107, 1085, 1040, 1020, 952, 906, 887, 831, 816, 791, 769, 746, 710, 637, 624, 603, 574, 563, 538, 510, 484 cm^{-1}.

Compound 200ab :

The substrate **27ab** (13.8 mg, 2.7×10^{-2} mmol) and the gold precatalyst **168** (2.0 mg, 1.4×10^{-3} mmol) were placed in a Schlenk and dry DCM (0.05 M) was added. The mixture was pre-stirred at room temperature for 2 min, then cooled to 0 °C and stirred for 15 min further. AgSbF$_6$ solution (27 µl solution 0.05 M in DCM, 1.4×10^{-3} mmol) was then added and the reaction was stirred for 3 days at the same temperature. The reaction was quenched, filtering the mixture through a short pad of silica and eluting with portions of DCM. After solvent evaporation, a yellow oil was obtained, that was further purified by preparative TLC (hexanes/EtOAc, 95/5) to afford **200ab** as a bright yellow solid (6.0 mg, 43 %).

^{1}H-NMR (400 MHz, CDCl$_3$) δ : 7.97 (d, J= 8.3 Hz, 2H), 7.87 (d, J= 8.3 Hz, 2H), 7.85 (s, 2H), 7.80 (d, J= 7.6 Hz, 2H), 7.67 (d, J= 7.7 Hz, 4H), 7.40 (d, J= 7.7 Hz, 2H), 7.32 (d, J= 7.7 Hz, 4H), 7.14 (t, J= 7.7 Hz, 2H), 7.03 (t, J= 7.6 Hz, 2H), 2.47 (s, 6H) ppm.

^{13}C-NMR (101 MHz, CDCl$_3$) δ : 142.7, 138.5, 136.8, 136.7, 134.6, 133.9, 130.3, 130.2, 129.9, 129.4, 129.0, 128.2, 127.6, 127.3, 125.5, 125.5, 123.4, 123.4, 118.2, 21.7 ppm.

HRMS calculated m/z for C$_{40}$H$_{28}$$^+$: 508.219100; found (EI) 508.218702.
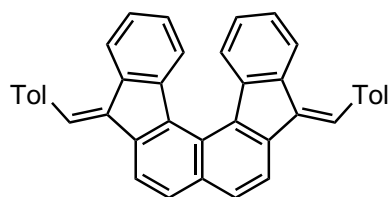
IR (neat) $\tilde{\nu}$: 3038, 3021, 2958, 2918, 2851, 1626, 1590, 1508, 1451, 1322, 1260, 1180, 1140, 1099, 1035, 1020, 942, 871, 834, 814, 798, 765, 760, 648, 627, 601, 552, 504 cm^{-1}.

Compound 26ac :
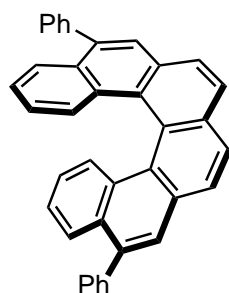
According to general procedure K, substrate **27ac** (10.5 mg, 2.2×10^{-2} mmol) was treated with **165d** (3.3 mg, 2.2×10^{-3} mmol) and AgSbF$_6$ (44 µl, solution 0.05 M in DCM). After workup, a mixture of isomers was obtained (8.1 mg, 77 % mass recovered), the helicene **26ac** being the major compound (conversion 95 %, ratio **26ac**:**190ac**:**192ac**, 82:4:14). Conversion and the ratio of compounds was determined by HPLC: 50 × 3 mm Agilent Eclipse Plus C18 column, CH$_3$CN/ H$_2$O = 90/10 (v/v), 1.0 ml min^{-1}, 6.4 MPa, 308 K, 254 nm; intermediate **192ac** t_R= 5.56 min, starting material **27ac** t_R= 5.96 min, helicene **26ac** t_R= 6.79 min, isomer E-**190ac** t_R= 7.10 min.

Enantiomeric excess: 92 %. The *ee* was determined by 2D HPLC: 50 × 3 mm Agilent Eclipse Plus C18 column, CH$_3$CN/ H$_2$O = 90/10 (v/v), 0.5 ml min^{-1}, 12.1 MPa, 308 K, 275 nm, helicene **26ac** t_R= 6.34 min; then 150 × 4.6 mm Chiralpak IC-3 column, CH$_3$CN/ CH$_3$OH = 95/5 (v/v), 1.0 ml min^{-1}, 6.8 MPa, 298 K, 275 nm; major enantiomer t_R= 2.73 min, minor enantiomer t_R= 3.03 min.

In order to obtain a purer sample for characterisation, the mixture was purified by HPLC, obtaining a 1.6 mg fraction with 89 % of **26ac**. Separation conditions: 250 × 20 mm YMC PVA-SIL 5 µm column, *i*-hexane/MTBE = 92/8 (*v/v*), 20 ml min^{-1}, 3.3 MPa, 308 K, 254 nm.

^{1}H-NMR (500 MHz, CDCl$_3$) δ : 8.05 (d, *J*= 8.1 Hz, 2H), 8.00 (d, *J*= 8.1 Hz, 2H), 7.92 (s, 2H), 7.87 (dd, *J*= 8.2, 1.4 Hz, 2H), 7.81 (dd, *J*= 8.5, 1.1 Hz, 2H), 7.73 (d, *J*= 6.8 Hz, 4H), 7.59 (t, *J*= 7.6 Hz, 4H), 7.51 (tt, *J*= 7.6, 1.2 Hz, 2H), 7.17 (ddd, *J*= 8.2, 6.8, 1.1 Hz, 2H), 6.74 (ddd, *J*= 8.5, 6.8, 1.4 Hz, 2H) ppm.

^{13}C-NMR (126 MHz, CDCl$_3$) δ : 140.7, 139.7, 133.4, 130.9, 130.6, 130.5, 130.3, 128.5, 128.2, 127.7, 127.6, 127.4, 127.3, 126.7, 125.9, 125.7, 124.6, 124.0 ppm.

HRMS calculated *m/z* for C$_{38}$H$_{24}^+$: 480.187800; found (EI) 480.187351.

IR (neat) $\tilde{\nu}$: 3049, 3025, 2984, 2960, 2927, 2918, 2849, 1596, 1502, 1489, 1467, 1441, 1398, 1366, 1306, 1259, 1240, 1214, 1177, 1153, 1138, 1092, 1072, 1046, 1028, 1001, 956, 914, 886, 827, 810, 772, 748, 728, 698, 651, 609, 593, 581, 522, 499 cm^{-1}.

Compound 26ba :
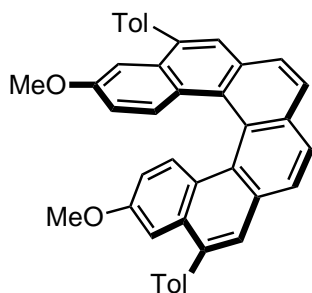
According to general procedure K, substrate **27ba** (14.2 mg, 2.5×10^{-2} mmol) was treated with **165d** (3.8 mg, 2.5×10^{-3} mmol) and AgSbF$_6$ (50 µl, solution 0.05 M in DCM). After workup, a mixture of isomers was obtained (14.1 mg, 99 % mass recovered), the helicene **26ba** being the major compound (conversion 100 %, ratio **26ba**:**190ba**:**192ba**, 88:12:0). Conversion and the ratio of compounds was determined by HPLC: 50 × 3 mm Agilent Eclipse Plus C18 column, CH$_3$OH/ H$_2$O = 93/7 (*v/v*), 1.0 ml min^{-1}, 11.3 MPa, 308 K, 254 nm; helicene **26ba** t_R= 8.55 min, isomers **190ba** t_R= 9.24 min and t_R= 9.47 min.

Enantiomeric excess: 78 %. The *ee* was determined by 2D HPLC: 50 × 3 mm Agilent Eclipse Plus C18 column, CH$_3$OH/ H$_2$O = 90/10 (*v/v*), 0.5 ml min^{-1}, 12.1 MPa, 308 K, 275 nm, helicene **26ba** t_R= 9.05 min; then 150 × 4.6 mm Chiralpak IC-3 column, CH$_3$CN/ CH$_3$OH = 95/5 (*v/v*), 1.0 ml min^{-1}, 6.8 MPa, 298 K, 275 nm; major enantiomer t_R= 2.87 min, minor enantiomer t_R= 3.22 min.

In order to obtain a purer sample for characterisation, the mixture was purified by semi-preparative HPLC, obtaining 6.4 mg of **26ba**. Separation conditions: 250 × 20 mm YMC PVA-SIL 5 µm column, *i*-hexane/MTBE = 98/2 (*v/v*), 20 ml min^{-1}, 3.3 MPa, 308 K, 254 nm.

^{1}H-NMR (400 MHz, CDCl$_3$) δ : 7.94 (AA'BB', 4H), 7.87 (s, 2H), 7.75 (d, *J*= 9.3 Hz, 2H), 7.62 (d, *J*= 8.0 Hz, 4H), 7.39 (d, *J*= 7.8 Hz, 4H), 7.28 (d, *J*= 2.7 Hz, 2H), 6.44

(dd, $J= 9.3$, 2.7 Hz, 2H), 3.69 (s, 6H), 2.52 (s, 6H) ppm.

^{13}C-NMR (101 MHz, CDCl$_3$) δ : 157.3, 139.0, 138.0, 137.2, 133.5, 132.2, 130.0, 129.9, 129.9, 129.3, 127.9, 127.2, 127.2, 126.4, 125.4, 123.5, 115.1, 106.23, 55.2, 21.5 ppm.

HRMS calculated m/z for C$_{42}$H$_{32}$O$_2$Na$^+$: 591.229449; found (ESI) 591.229610.

IR (neat) $\tilde{\nu}$: 3035, 3021, 2996, 2967, 2943, 2923, 2873, 2859, 2838, 1558, 1498, 1469, 1449, 1428, 1404, 1374, 1327, 1288, 1262, 1230, 1199, 1180, 1150, 1090, 1078, 1032, 959, 898, 887, 870, 850, 824, 796, 756, 736, 721, 694, 671, 612, 584, 550, 521, 503 cm^{-1}.

$[\alpha]_D^{20}= +1108$ ($c = 0.72$, DCM).

Compound 26c :
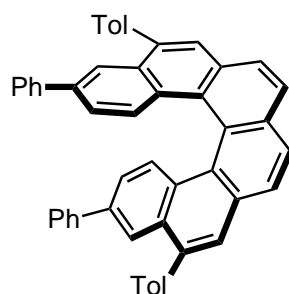
According to general procedure K, substrate **27c** (10.2 mg, 1.5×10^{-2} mmol) was treated with **165d** (2.4 mg, 1.5×10^{-3} mmol) and AgSbF$_6$ (31 µl, solution 0.05 M in DCM). After workup, a mixture of isomers was obtained (8.6 mg, 84% mass recovered), the helicene **26c** being the major compound (conversion 100 %, ratio **26c**:**190c**:**192c**, 97:3:0). Conversion and the ratio of compounds was determined by HPLC: 50 × 3 mm Agilent Eclipse Plus C18 column, CH$_3$CN = 100 (v/v), 1.0 ml min^{-1}, 5.6 MPa, 308 K, 275 nm; helicene **26c** $t_R= 5.98$ min, isomer **190c** $t_R= 6.73$ min. Enantiomeric excess: 82 %. The *ee* was determined by 2D HPLC: 50 × 3 mm Agilent Eclipse Plus C18 column, CH$_3$CN = 100 (v/v), 0.5 ml min^{-1}, 10.5 MPa, 308 K, 275 nm, helicene **26c** $t_R= 5.67$ min; then 150 × 4.6 mm Chiralpak IC-3 column, CH$_3$CN/ CH$_3$OH = 95/5 (v/v), 1.0 ml min^{-1}, 6.8 MPa, 298 K, 275 nm; major enantiomer $t_R= 3.95$ min, minor enantiomer $t_R= 5.41$ min.

^{1}H-NMR (400 MHz, CDCl$_3$) δ : 8.15 (d, $J= 2.0$ Hz, 2H), 8.06 (d, $J= 8.2$ Hz, 2H), 8.01 (d, $J= 8.2$ Hz, 2H), 7.94 (s, 2H), 7.90 (d, $J= 8.8$ Hz, 2H), 7.67 (d, $J= 8.0$ Hz, 4H), 7.42-7.39 (m, 8H), 7.33-7.28 (m, 4H), 7.27-7.23 (m, 2H), 6.99 (dd, $J= 8.8$, 2.0 Hz, 2H), 2.53 (s, 6H) ppm.

^{13}C-NMR (101 MHz, CDCl$_3$) δ : 141.1, 139.9, 138.1, 137.7, 137.4, 133.4, 131.1, 131.0, 130.2, 129.8, 129.4, 128.8, 128.7, 127.5, 127.5, 127.4, 127.3, 127.2, 124.1, 124.0, 123.8, 21.5 ppm.

HRMS calculated for C$_{52}$H$_{36}$: 660.281700; found (EI) 660.281253.

IR (neat) $\tilde{\nu}$: 3021, 2964, 2944, 2915, 2874, 2859, 1598, 1579, 1511, 1486, 1446, 1429, 1403, 1378, 1360, 1305, 1278, 1261, 1209, 1181, 1153, 1107, 1073, 1021, 963, 890, 823, 758, 735, 721, 693, 641, 612, 578, 566, 509 cm^{-1}.

$[\alpha]_D^{20}= +1421$ ($c = 0.32$, DCM).

III.1.4 Dynamic NMR studies

Compound 192aa :
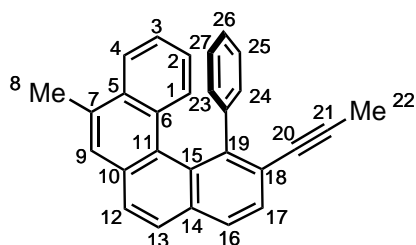
The substrate **27aa** (90.0 mg, 0.25 mmol), gold complex **164f** (22.9 mg, 1.3×10^{-2} mmol) and AgSbF$_6$ (4.3 mg, 1.3×10^{-2} mmol) were placed in a Schlenk and suspended in DCM (5 ml) at 23 °C . The reaction mixture was stirred at this temperature for 30 min, before filtering through a pad of silica and eluting with portions of DCM. After evaporation of the solvent, 45 mg of crude material was obtained, containing a mixture of helicene **26aa** and intermediate **192aa** (**26aa**/**192aa**, 22/78 calculated by ¹H-NMR). Intermediate **192aa** was separated by semi-preparative HPLC, obtaining 17 mg of pure material. Separation conditions: 250×20 mm MultiChrom SI 3 μm, i-hexane/MTBE = 99/1 (v/v), $10\,\mathrm{ml\,min^{-1}}$, 4.9 MPa, 308 K, 254 nm. Analysis of the NMR data and assignment of the signals are summarised in *Table A.4*.

¹H-NMR (600 MHz, CDCl$_3$) δ : 8.37 (br, 1H, 24), 7.96 (d, $J=$ 8.3 Hz, 1H, 1), 7.88 (d, $J=$ 8.2 Hz, 1H, 16), 7.81 (d, $J=$ 8.3 Hz, 1H, 13), 7.79 (d, $J=$ 8.3 Hz, 1H, 4), 7.76 (d, $J=$ 8.2 Hz, 1H, 17), 7.73 (d, $J=$ 8.3 Hz, 1H, 12), 7.59 (s, 1H, 9), 7.36 (br, 1H, 25), 7.24 (t, $J=$ 7.5 Hz, 1H, 3), 6.99 (t, $J=$ 7.2 Hz, 1H, 2), 6.90 (t, $J=$ 7.3 Hz, 1H, 26), 6.51 (br, 1H, 27), 5.94 (br, 1H, 28), 2.74 (s, 3H, 8), 1.99 (s, 3H, 22) ppm.

¹³C-NMR (151 MHz, CDCl$_3$) δ : 142.1 (19), 141.5 (23), 133.9 (7), 133.8 (14), 132.6 (br, 24), 132.1 (10), 131.0 (5), 130.73 (1), 130.4 (17), 130.3 (br, 28), 129.5 (6), 128.7 (15), 127.3 (16), 126.9 (25, 27), 126.8 (13), 126.8, 126.7 (12), 126.4 (11), 126.3 (26), 125.9 (9), 124.9 (3), 124.2 (2), 122.8 (18), 122.3 (4), 90.4 (21), 80.7 (20), 19.7 (8), 4.9 (22) ppm.

HRMS calculated m/z for C$_{28}$H$_{20}$$^+$: 356.156500; found (EI) 356.156744.

IR (neat) $\tilde{\nu}$: 2964, 2932, 1560, 1544, 1453, 1377, 1322, 1267, 1195, 1170, 1105, 1081, 1040, 982, 944, 915, 876, 838, 801, 771, 753, 722, 701, 687, 676, 657, 648, 610, 580, 568, 552, 538, 518 cm^{-1}.

Compound 192bb:

Substrate **27bb** (15.3 mg, 2.0×10^{-2} mmol was placed in a flask, disolved in CHCl$_3$

and one drop of concentrated aqueous HCl was added. The mixture is stirred for 10 min, after which water was added and the compound extracted into $CHCl_3$. After drying with Na_2SO_4 and solvent evaporation the desired compound **192bb** was obtained as a yellow foam (6.7 mg, 44 %). Analysis of the NMR data and assignment of the signals are summarised in *Table A.5*.

^{1}H-NMR (500 MHz, toluene$-$d$_8$,333 K) δ : 8.01 (d, J= 9.0 Hz, 1H, 6), 7.87 (d, J= 8.2 Hz, 1H, 17), 7.65 (d, J= 8.2 Hz, 1H, 16), 7.57 (s, 2H, 12, 13), 7.55 (s, 1H, 9), 7.36 (d, J= 8.6 Hz, 2H, 28), 7.29 (d, J= 8.8 Hz, 2H, 44), 7.27 (d, J= 7.7 Hz, 2H, 36), 7.21 (dd, J= 7.4, 2.8 Hz, 1H, 3), 7.15 (d, J= 7.4 Hz, 2H, 51), 7.14-7.10 (m, 3H, 52, 37), 7.04-7.02 (m, 2H, 38, 53), 6.96-6.95 (m, 2H, 29), 6.71 (d, J= 9.1 Hz, 1H, 7), 6.70 (d, J= 8.9 Hz, 2H, 45), 5.14 (q, J= 6.4 Hz, 1H, 33), 4.97 (qd, J= 6.5, 2.1 Hz, 1H, 49), 3.26 (d, J= 6.3 Hz, 3H, 1), 3.16 (s, 3H, 26), 1.52 (d, J= 6.4 Hz, 3H, 34), 1.42 (d, J= 6.4 Hz, 3H, 50) ppm. The peaks for H-21, H-22, H- 24 and H-25 could not be detected at this temperature because of the broadening of the signals, however they could be assigned at 233 K (see assignments in *Table A.5*).

^{13}C-NMR (126 MHz, toluene$-$d$_8$, 333 K) δ : 159.1 (23), 158.6 (46), 158.2 (30), 157.7 (2), 143.9 (56), 143.5 (35), 142.9 (19), 139.3 (8), 135.1 (14), 134.7 (20), 133.8 (27), 133.1 (44), 132.9 (6), 132.6 (4), 131.4 (28), 131.2 (10), 130.6 (17), 129.3 (15), 128.9 (37, 52), 128.0 (11), 127.7 (38), 127.7 (53), 127.5 (12), 127.4 (16), 126.3 (13) , 126.0 (36), 125.8 (51), 125.7 (5), 123.3 (18), 117.0 (43), 116.5 (29, 45), 115.5 (7), 105.6 (3), 94.2 (42), 90.7 (41), 76.6 (33), 76.5 (49), 54.7 (1), 54.7 (26), 24.5 (34), 24.3 (50) ppm.

HRMS calculated m/z for $C_{56}H_{45}O_4^+$: 781.331235; found (ESI) 781.331510.

IR (neat) $\tilde{\nu}$: 3082, 3057, 3028, 2971, 2962, 2926, 2866, 2850, 2833, 1605, 1543, 1506, 1451, 1371, 1353, 1329, 1303, 1275, 1237, 1173, 1109, 1096, 1067, 1029, 1010, 997, 959, 930, 891, 828, 810, 797, 758, 698, 638, 611, 595, 559, 534, 499 cm^{-1}.

A thermodynamic analysis was conducted from a series of ^{1}H-NMR spectra measured in the following conditions:

- Compound **192aa**: from 263 K to 328 K on a 15 mg sample of **192aa** dissolved in approximately 550 µl of CDCl$_3$

- Compound **192bb**: from 233K to 343K on a 15 mg sample of **192bb** dissolved in approximately 550 µl of toluene$-$d$_8$.

NMR spectra were recorded on an Advance III 500 spectrometer (499.89 MHz) from Bruker Biospin GmbH equipped with a 2-channel 1H/X (incl. 19F) probehead (BBFO smartprobe) with z-gradient and with a BCU-X for sample cooling. All NMR data were processed and analysed with Topspin 3.2 (Bruker) while the line fitting to extract the chemical exchange rates were conducted on the DNMR module of Topspin 3.2.

Two types of motion could be considered: 1) Rotation of the aromatic ring ; 2)

Stereoinversion of the tetrahelicene backbone with a concomitant counter-clockwise rotation of the aromatic unit (***Figure III.1.1***).

RING FLIP

STEREOINVERSION + RING FLIP

Figure III.1.1. Motions on intermediates **192aa** and **192bb**.

In **192aa**, coalescence of the *ortho-* H-24 and H-28 and *meta-* H-25 and H-27 ^{1}H-NMR signals could be observed, that could be attributed to the rotation motion of the phenyl ring (***Figure III.1.2***). The approximate coalescence temperature (T_c) could be estimated as 318 K for this motion.

Figure III.1.2. Stacked ^{1}H-NMR spectra of **192aa** at different temperatures.

Estimation of the Gibbs energy of activation ($\Delta G^{\ddagger}$) can be obtained with the approximate coalescence temperature (T_c) using **Equation III.1.1**, where a is a conversion constant (4.575×10^{-3} kcal/molK) and $\Delta\delta$ is the chemical shift difference in Hz of the exchanging nuclei.

$$\Delta G^{\ddagger} = aT_c\Big[9,972 + \log\Big(\frac{T_c}{\Delta\delta}\Big)\Big] \tag{III.1.1}$$

Using this equation, estimate values of $\Delta G^{\ddagger}$= 14.7 kcal/mol (61.5 kJ/mol) were obtained for the ring flip of the phenyl group in compound **192aa**.

In order to obtain more details concerning the enthalpic $\Delta H^{\ddagger}$ and entropic $\Delta S^{\ddagger}$ contributions on these processes, the exchange rates (k) were obtained by line-fitting of the obtained NMR data over the temperature range 263–328 K. The resulting data are summarised in **Table III.1.1**, and were plotted in an Eyring plot using **Equation III.1.4**, the linear form of the Eyring equation (**Equation III.1.2**).

$$k = \frac{k_b T}{h}e^{\frac{-\Delta G^{\ddagger}}{RT}} \tag{III.1.2}$$

since,

$$\Delta G^{\ddagger} = \Delta H^{\ddagger} - T\Delta S^{\ddagger} \tag{III.1.3}$$

$$\ln\Big(\frac{k}{T}\Big) = -\frac{\Delta H^{\ddagger}}{RT} + \frac{\Delta S^{\ddagger}}{R} + \ln\Big(\frac{k_b}{h}\Big) \tag{III.1.4}$$
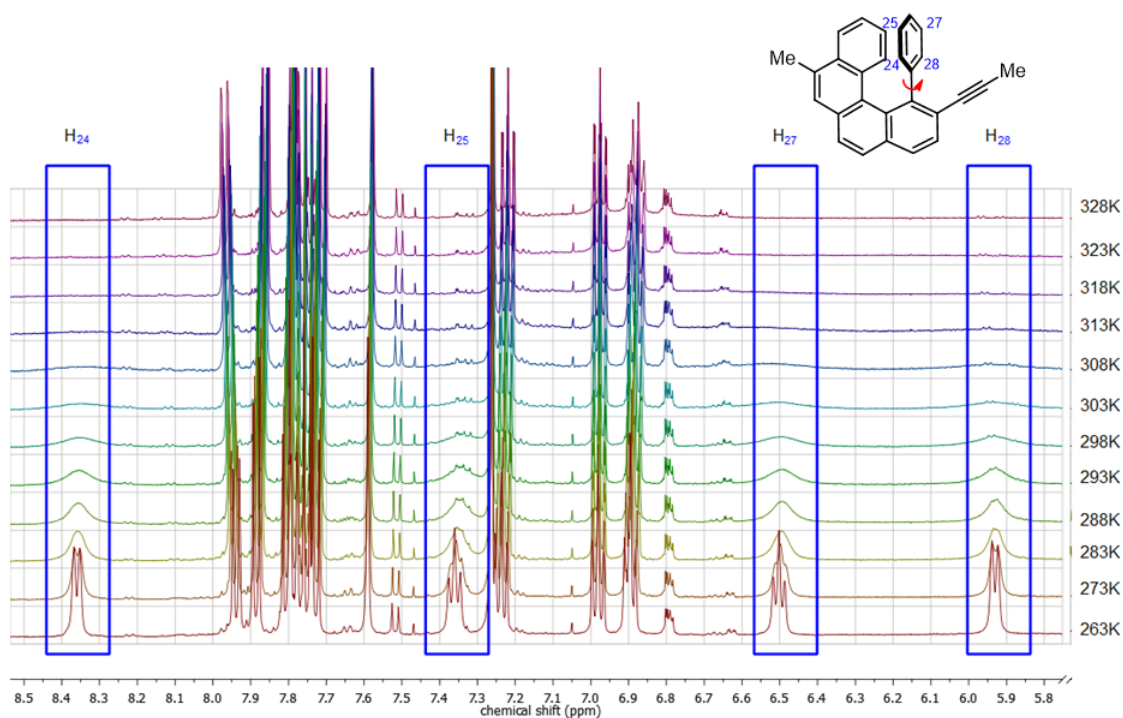
The Eyring plot (**Figure III.1.3**) displayed an expected linear tendency, affording after linear regression the values of $\Delta H^{\ddagger} = 55.57$ KJ/mol and $\Delta S^{\ddagger} = $ -0.0163 kJ/molK. With these values it is possible to calculate $\Delta G^{\ddagger}$ at -20 ºC — the optimal temperature for the catalysis — as 59.70 kJ/mol and also the rate of the ring flip as $k_{ringflip,253K}$ = 2.49 s^{-1}. The stereoinversion of the tetrahelicene backbone in this case could not be determined, since the racemisation leads to two enantiomers, which cannot be differentiated by NMR analysis.

In the case of compound **192bb**, in the measured temperature series (233–343K), two coalescence phenomena at different coalescence temperatures (T_c) can be observed.

One involves the coalescence of *ortho*- H-25 and H-21 and *meta*- H-24 and H-22 ^{1}H-NMR signals due to a aromatic ring rotation ($T_c \sim 318K$) whereas the other is the coalescence of diastereomeric pairs for all of the ^{1}H-NMR signals due to the stereoinversion of the phenylbenzo[c]phenanthrene ($T_c \sim 338K$).

T (K)	1/T	k (Hz)	ln(k)	k/T	ln(k/T)	$\Delta G^{\ddagger}$ (kJ/mol)
263	0,0038	11,5	2,44	0,04	-3,13	58,81
273	0,0037	22,1	3,09	0,08	-2,52	59,64
283	0,0035	54,0	3,99	0,19	-1,66	59,81
288	0,0035	72,1	4,28	0,25	-1,39	60,21
293	0,0034	106,4	4,67	0,36	-1,01	60,35
298	0,0034	153,2	5,03	0,51	-0,67	60,52
303	0,0033	253,4	5,53	0,84	-0,18	60,31
308	0,0032	375,8	5,93	1,22	0,20	60,34
313	0,0032	560,6	6,33	1,79	0,58	60,32
318	0,0031	879,3	6,78	2,76	1,02	60,13
323	0,0031	1311,7	7,18	4,06	1,40	60,05
328	0,0030	1956,0	7,58	5,96	1,79	59,93
					average $\Delta G^{\ddagger}$	**60,04 kJ/mol**
					std	**0,482372**

Table III.1.1: Thermodynamic parameters for the ring flip in **192aa**
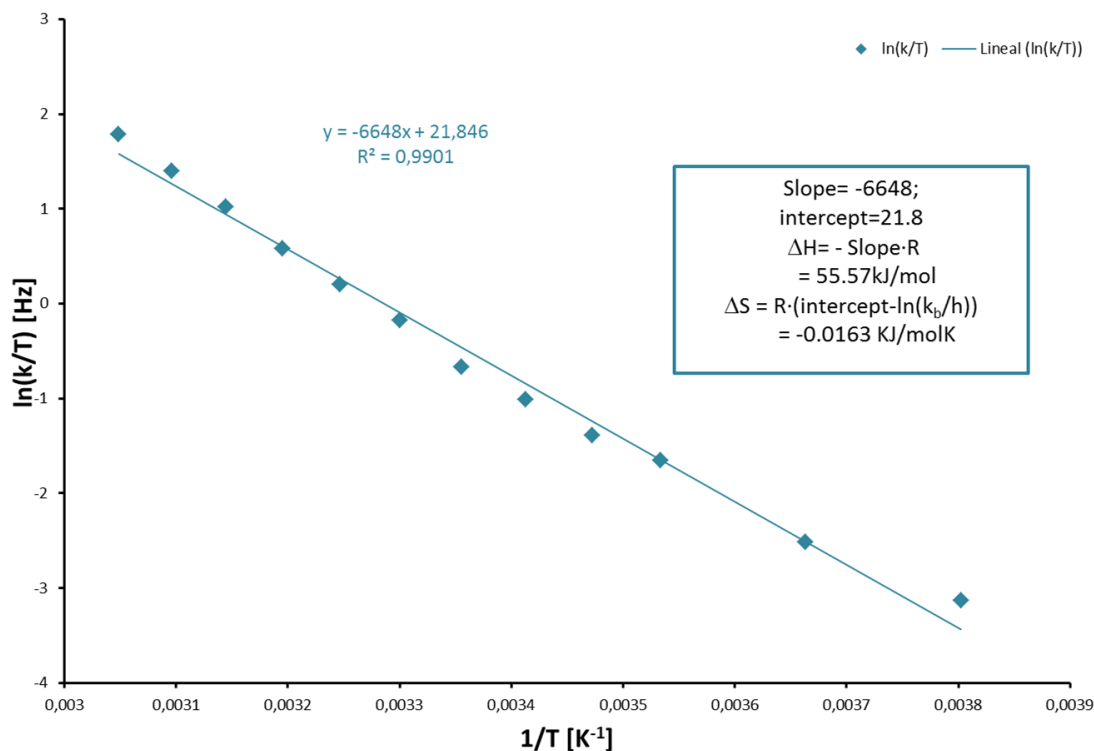
Figure III.1.3. Eyring plot for the ring flip of **192aa**.
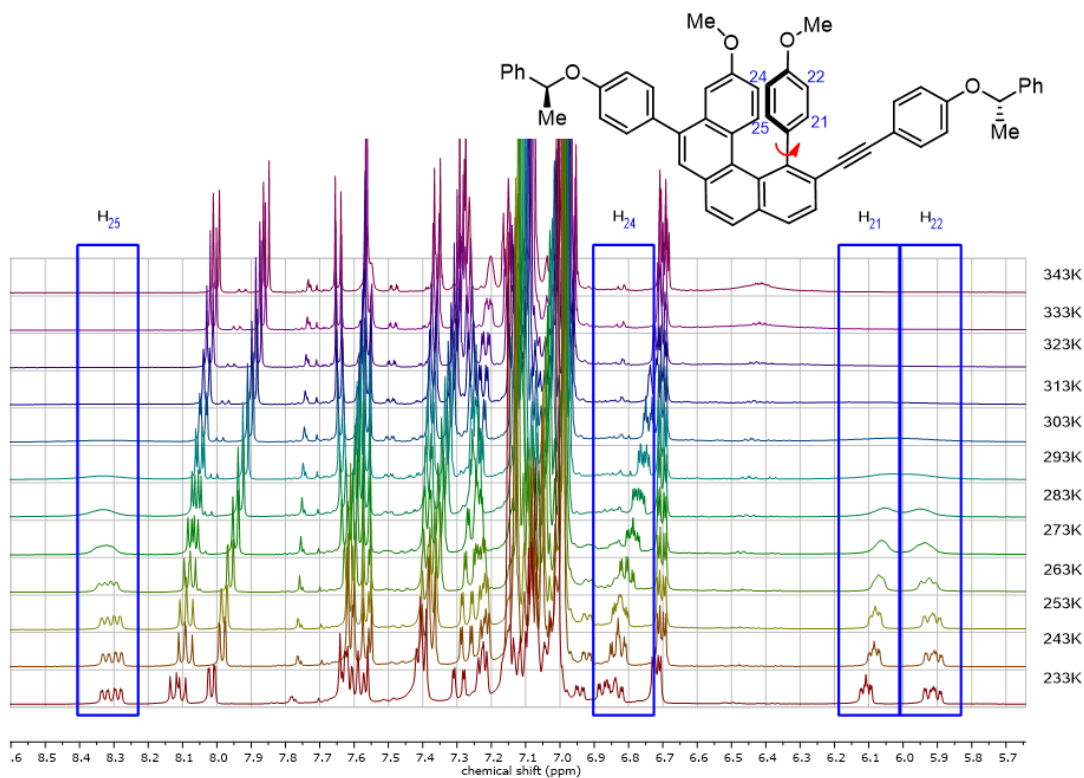
Figure III.1.4. Stacked ^{1}H-NMR spectra of **192bb** at different temperatures.
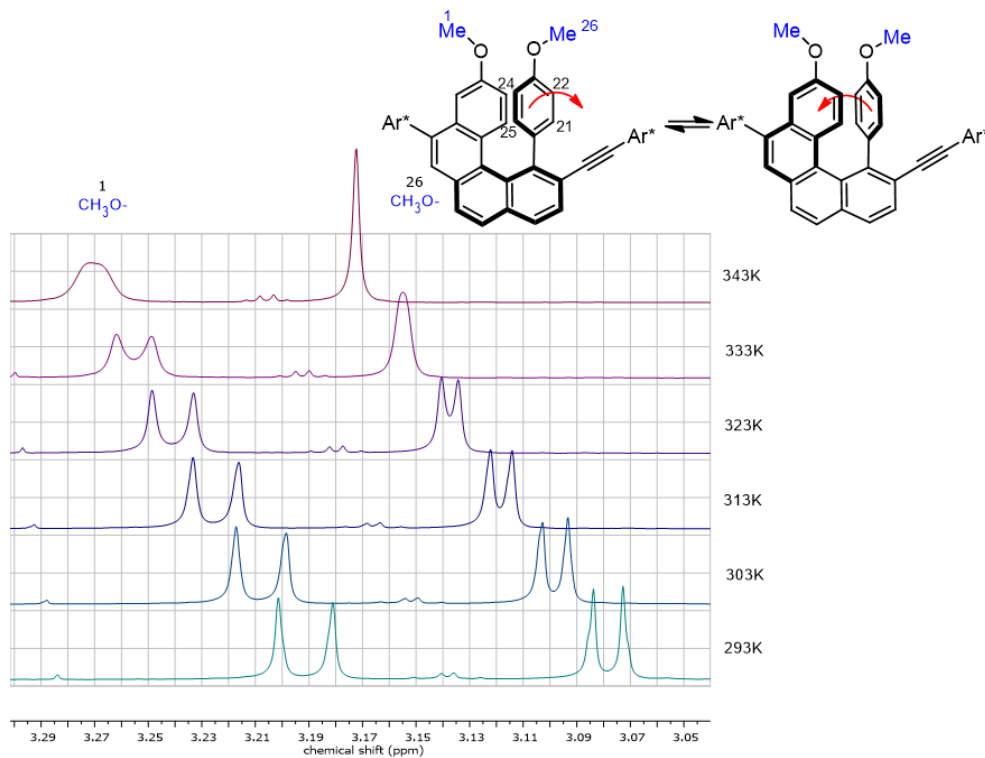
Figure III.1.5. Stacked ^{1}H-NMR spectra **192bb** at different temperatures.

184

Estimation of $\Delta G^{\ddagger}$ using **Equation III.1.1**, afforded values of 14.2 kcal/mol (59.4 kJ/mol) and 17.8 kcal/mol (74.5 kJ/mol) for the ring flip and for the stereoinversion processes, respectively. These values are in agreement with those obtained on similar molecules in a previous study by Laarhoven *et al.*[213] and with the results for **192aa**.

The chemical exchange rates were calculated by line fitting of the obtained NMR (values for the ring flip are displayed in **Table III.1.2** and for the stereoinversion in **Table III.1.3**) and plotted using the linear Eyring equation, **Equation III.1.4**.

The Eyring plots (**Figure III.1.6**) displayed an expected linear tendency, affording after linear regression the values of $\Delta H^{\ddagger} = 51.71\,kJ/mol$ and $\Delta S^{\ddagger} = -0.025\,kJ/molK$ for the ring flip and $\Delta H^{\ddagger} = 33.47\,\text{KJ/mol}$ and $\Delta S^{\ddagger} = -0.128$ kJ/molK for the stereoinversion.

With these values it is possible to calculate $\Delta G^{\ddagger}$ at -20 °C using **Equation III.1.3**, as $\Delta G^{\ddagger}_{ringflip,253K} = 58.04$ kJ/mol and $\Delta G^{\ddagger}_{stereoinv.,253K} = 65.85$ kJ/mol. Thus, the rate of the motions at -20 °C, temperature of the optimised conditions, could be obtained from **Equation III.1.2** affording $k_{ringflip,253K} = 5.48$ s^{-1} and $k_{stereoinv.,253K} = 0.134$ s^{-1} for the ring flip and stereoinversion respectively. The values thus obtained indicate that the stereoinversion of the tetrahelicene backbone is more difficult than the rotation of the *p*-methoxyphenyl unit, even though both processes are fast even at low temperatures. These results indicate that the racemisation of the tetrahelicene backbone is fast and, consequently, the enantioselectivity is determined by the second cyclisation step.

T (K)	1/T	k (Hz)	ln(k)	k/T	ln(k/T)	$\Delta G^{\ddagger}$ (kJ/mol)
233	0.0043	1,0	0,00	0,00	-5,45	56,59
243	0,0041	3,0	1,10	0,01	-4,39	56,88
253	0,0040	5,2	1,65	0,02	-3,88	58,15
263	0,0038	13,5	2,60	0,05	-2,97	58,45
273	0,0037	30,0	3,40	0,11	-2,21	58,94
283	0,0035	73,0	4,29	0,26	-1,35	59,09
293	0,0034	172,0	5,15	0,59	-0,53	59,18
303	0,0033	347,0	5,85	1,15	0,14	59,52
313	0,0032	735,0	6,60	2,35	0,85	59,61
323	0,0031	1636,0	7,40	5,07	1,62	59,45
333	0,0030	2700,0	7,90	8,11	2,09	59,99
343	0,0029	11500,0	9,35	33,53	3,51	57,74
					average $\Delta G^{\ddagger}$	**58,715 kJ/mol**
					std	**1,1085**

Table III.1.2: Thermodynamic parameters for the ring flip in **192bb**.

T (K)	1/T	k (Hz)	ln(k)	k/T	ln(k/T)	$\Delta G^{\ddagger}$ (kJ/mol)
293	0,0034	1,5	0,41	0,01	-5,27	70,73
303	0,0033	2,6	0,96	0,01	-4,76	71,84
313	0,0032	3,3	1,19	0,01	-4,55	73,68
323	0,0031	3,6	1,28	0,01	-4,50	75,88
333	0,0030	6,8	1,92	0,02	-3,89	76,56
343	0,0029	17,6	2,87	0,05	-2,97	76,23
					average $\Delta G^{\ddagger}$	**73,74 kJ/mol**
					std	**2,5092**

Table III.1.3: Thermodynamic parameters for the stereoinversion of the tetrahelicene backbone in **192bb**.
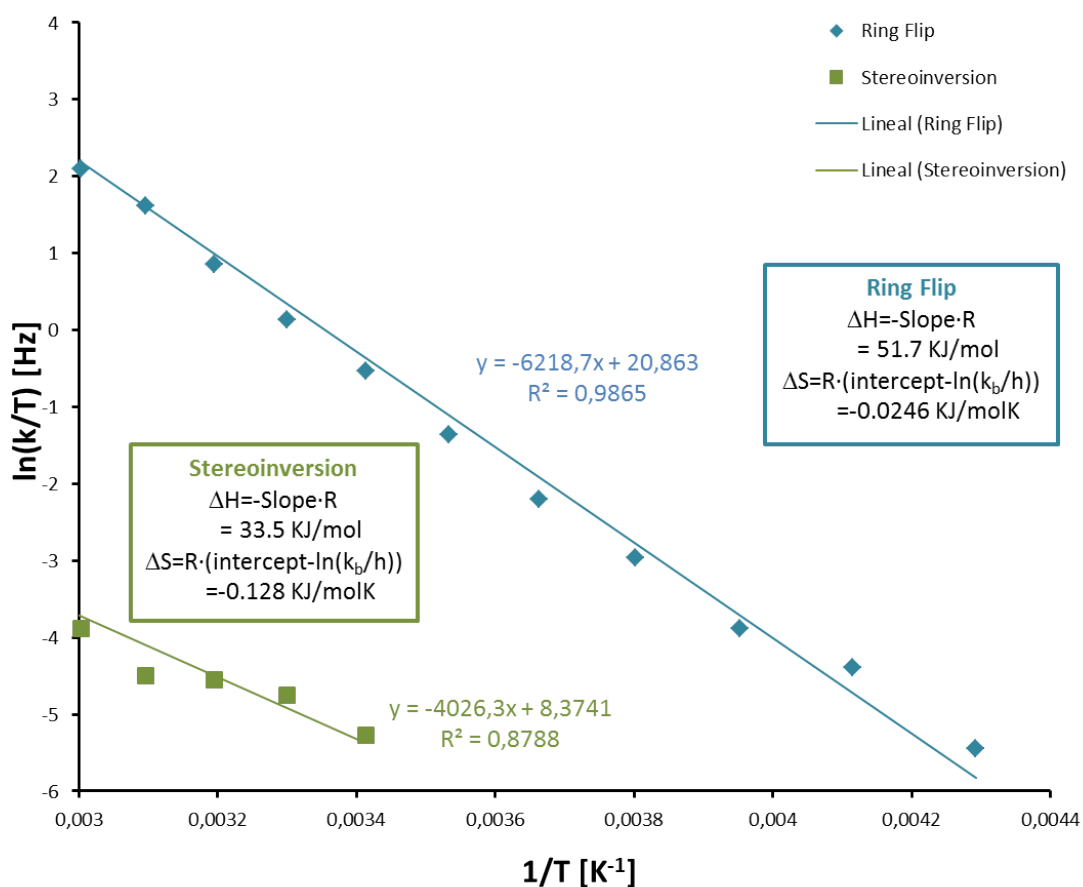
Figure III.1.6. Eyring plots for the ring flip (blue) and stereoinversion (red) motions of **192bb**.

Appendices

A. NMR of selected compounds

^{31}P-NMR(162 MHz, CD$_2$Cl$_2$) **81e**

^{1}H-NMR(400 MHz, CD$_2$Cl$_2$) **81e**

^{13}C-NMR(101 MHz, CD$_2$Cl$_2$) **81e**

^{31}P-NMR(162 MHz, CD$_2$Cl$_2$) **80a**

^{1}H-NMR(400 MHz, CD$_2$Cl$_2$) **80a**
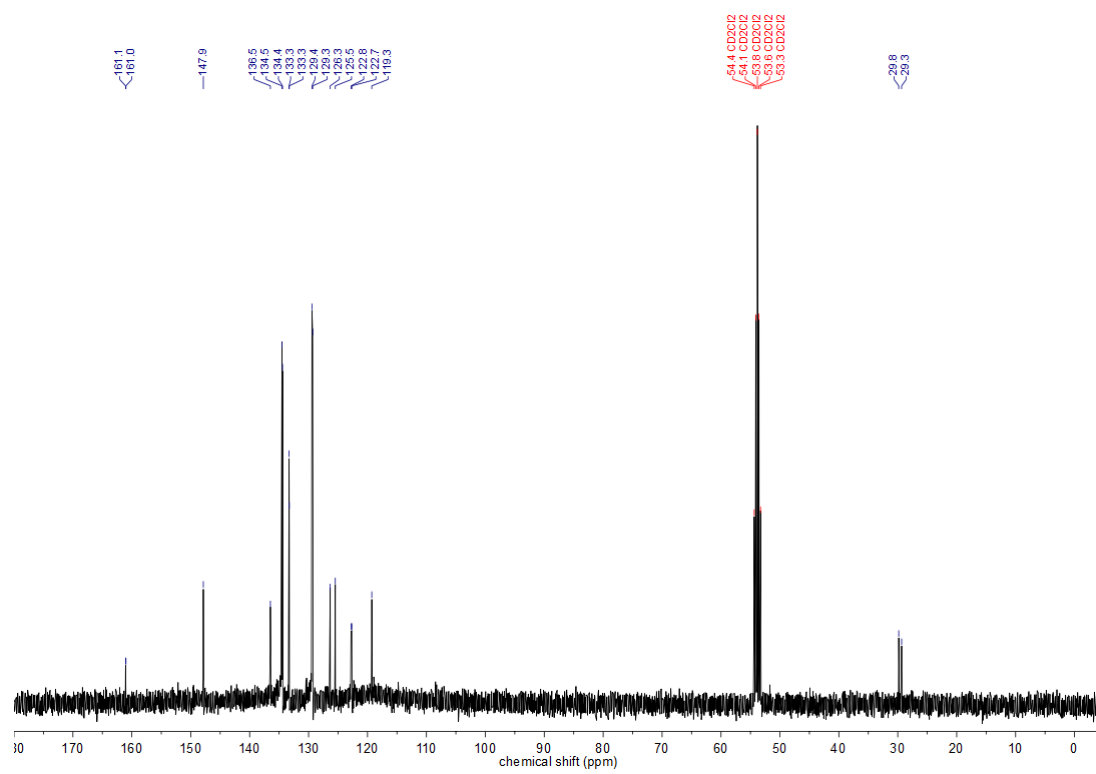
^{13}C-NMR(101 MHz, CD$_2$Cl$_2$) **80a**
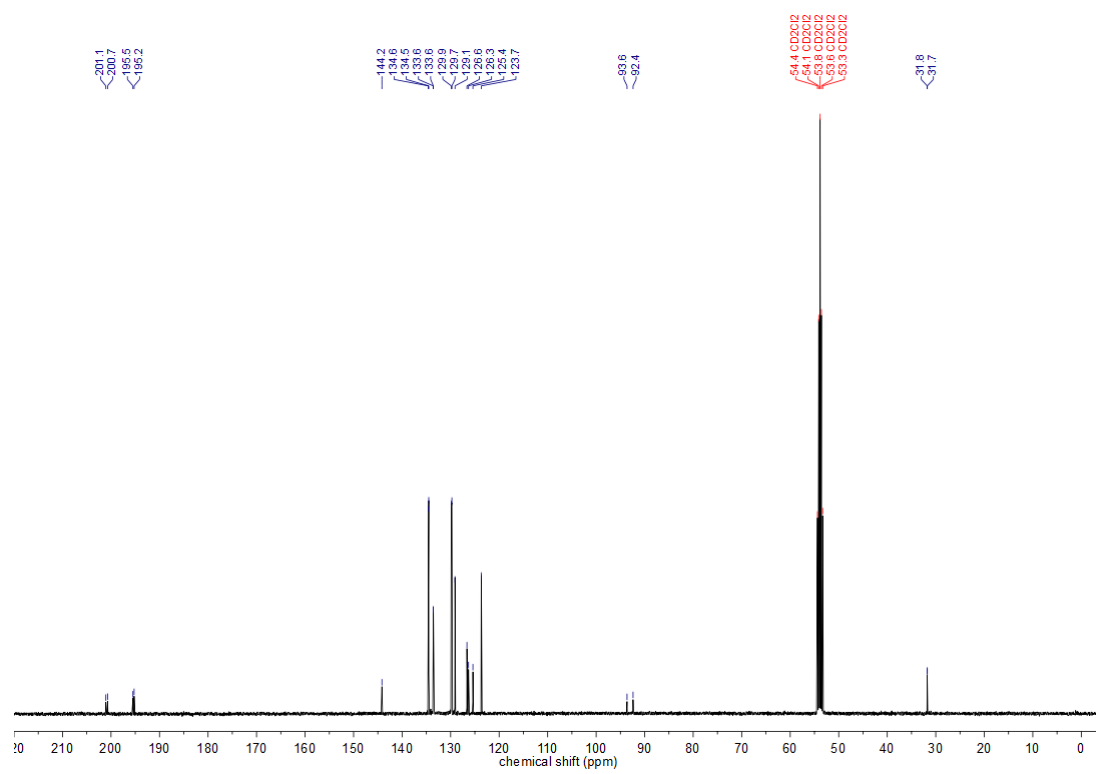
^{31}P-NMR(162 MHz, CD$_2$Cl$_2$) **80b**
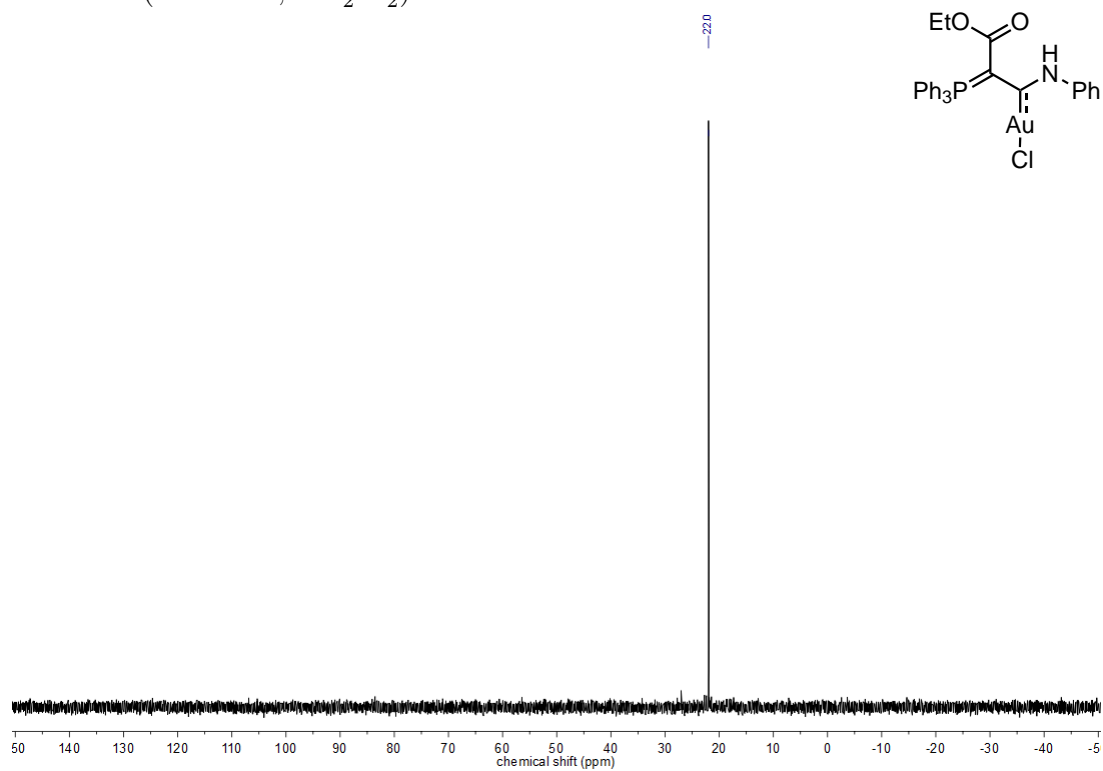
^{1}H-NMR(400 MHz, CD$_2$Cl$_2$) **80b**
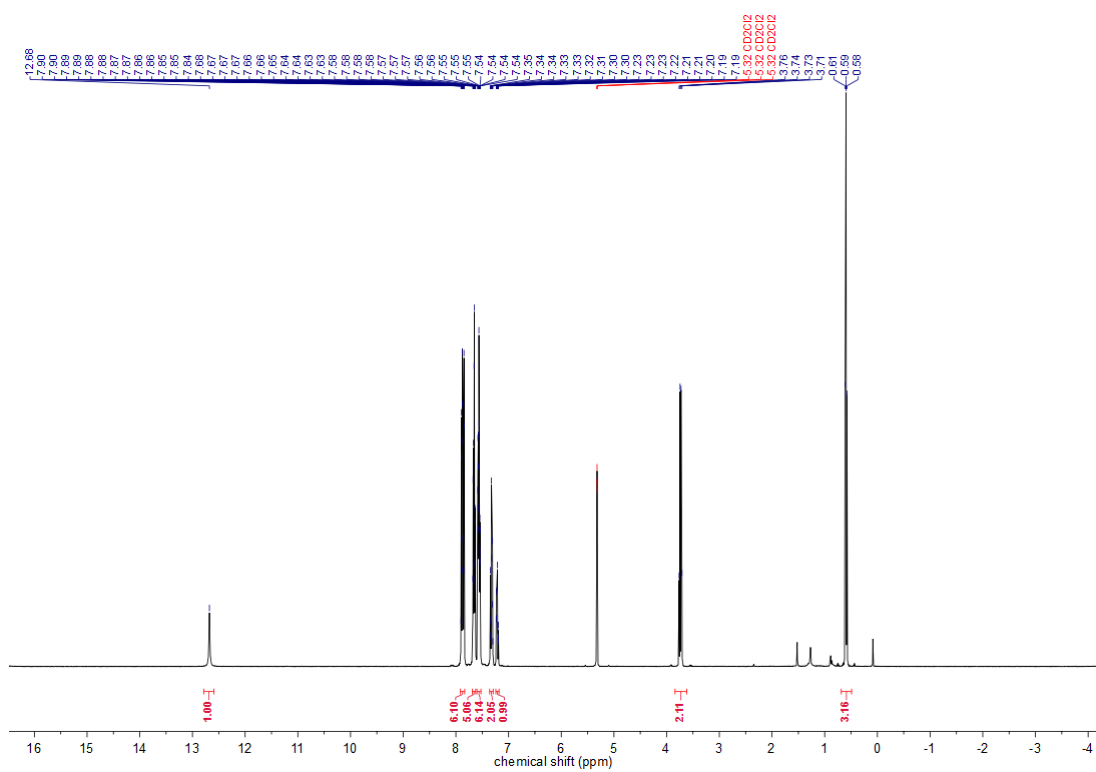
^{13}C-NMR(101 MHz, CD$_2$Cl$_2$) **80b**

^{31}P-NMR(162 MHz, CD$_2$Cl$_2$) **80c**
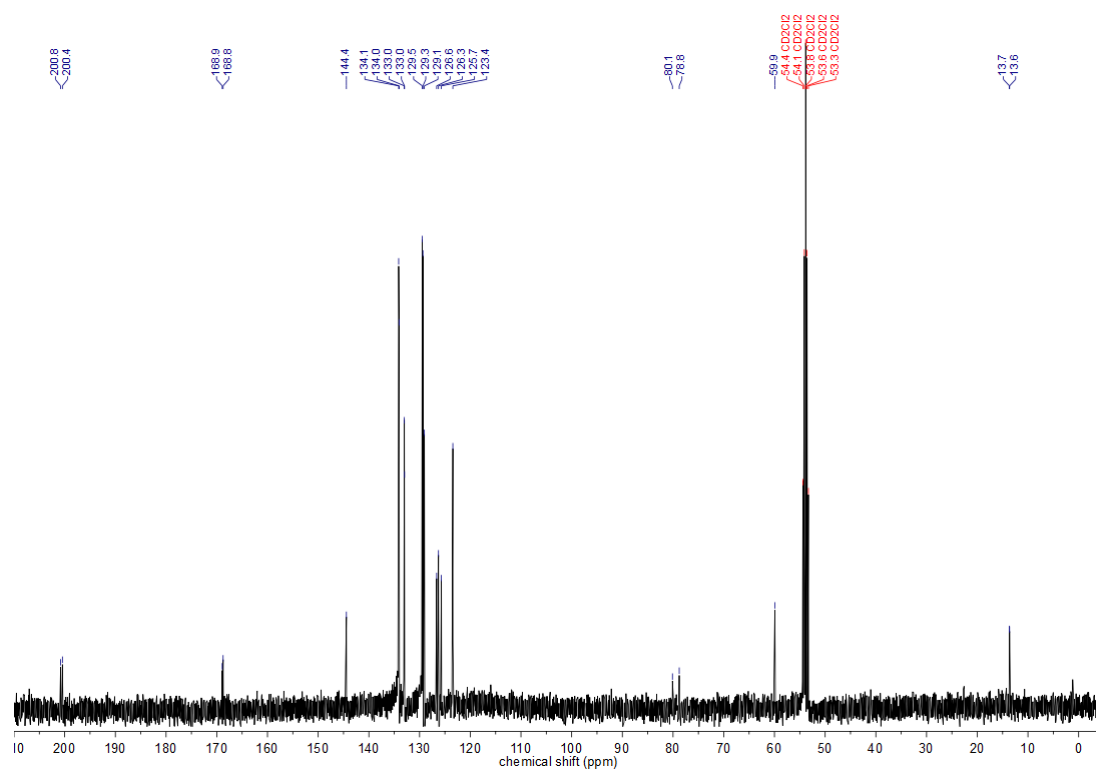
^{1}H-NMR(400 MHz, CD$_2$Cl$_2$) **80c**

^{13}C-NMR(101 MHz, CD$_2$Cl$_2$) **80c**

^{31}P-NMR(162 MHz, CD$_2$Cl$_2$) **80d**

^{1}H-NMR(400 MHz, CD$_2$Cl$_2$) **80d**
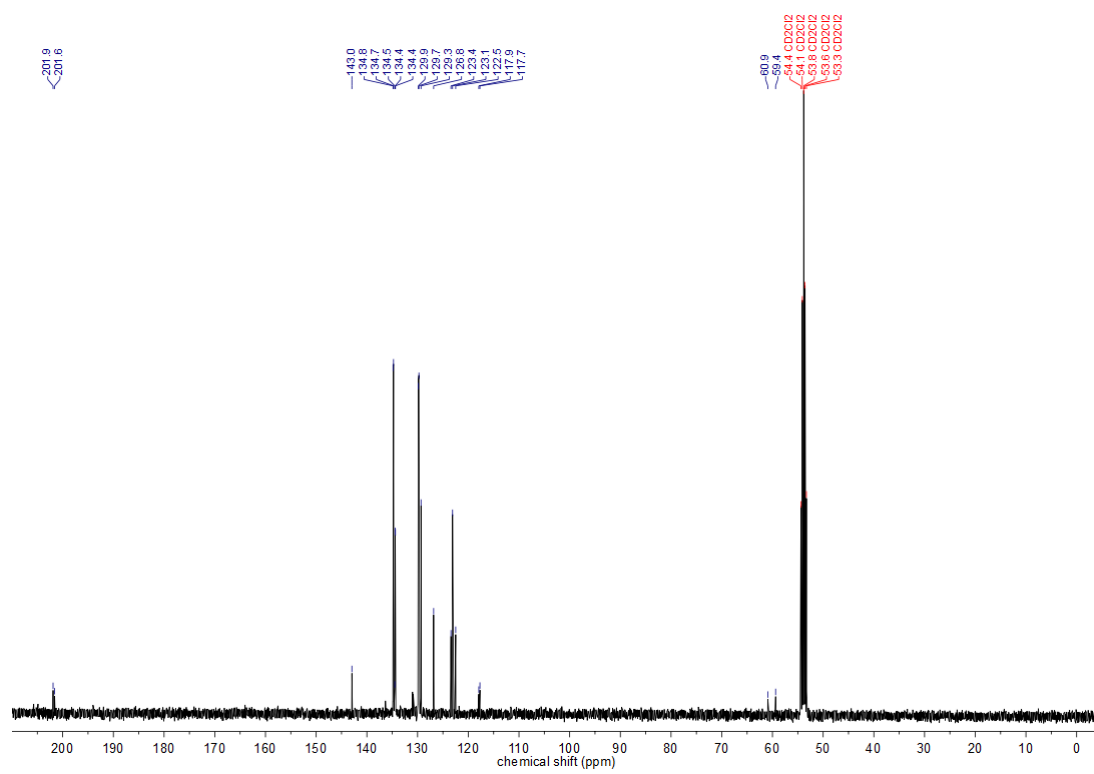
^{13}C-NMR(101 MHz, CD$_2$Cl$_2$) **80d**
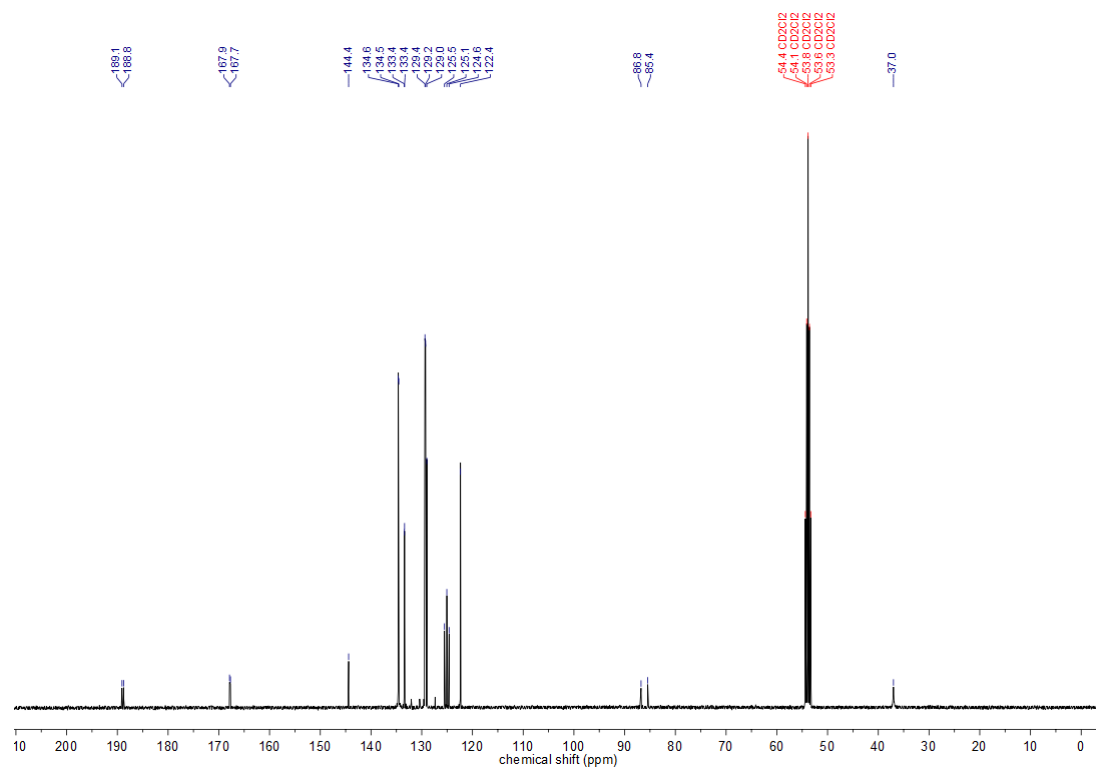
^{31}P-NMR(162 MHz, CD$_2$Cl$_2$) **80e**

^{1}H-NMR(400 MHz, CD$_2$Cl$_2$) **80e**
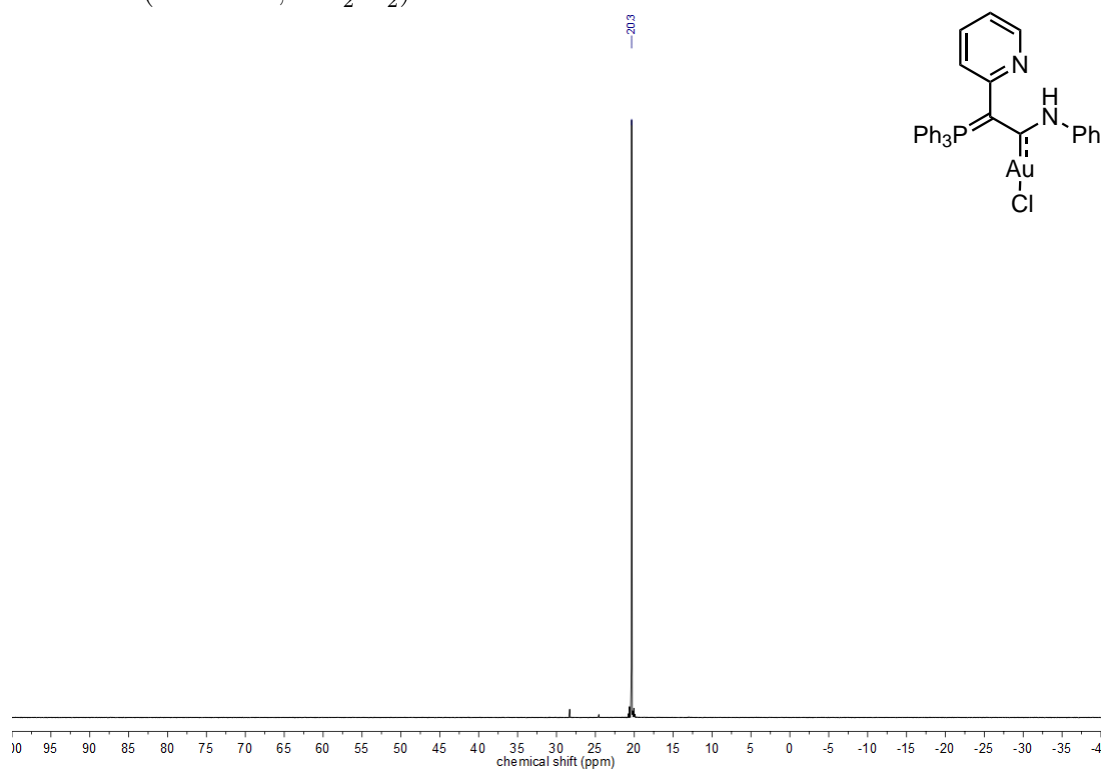
^{13}C-NMR(101 MHz, CD$_2$Cl$_2$) **80e**
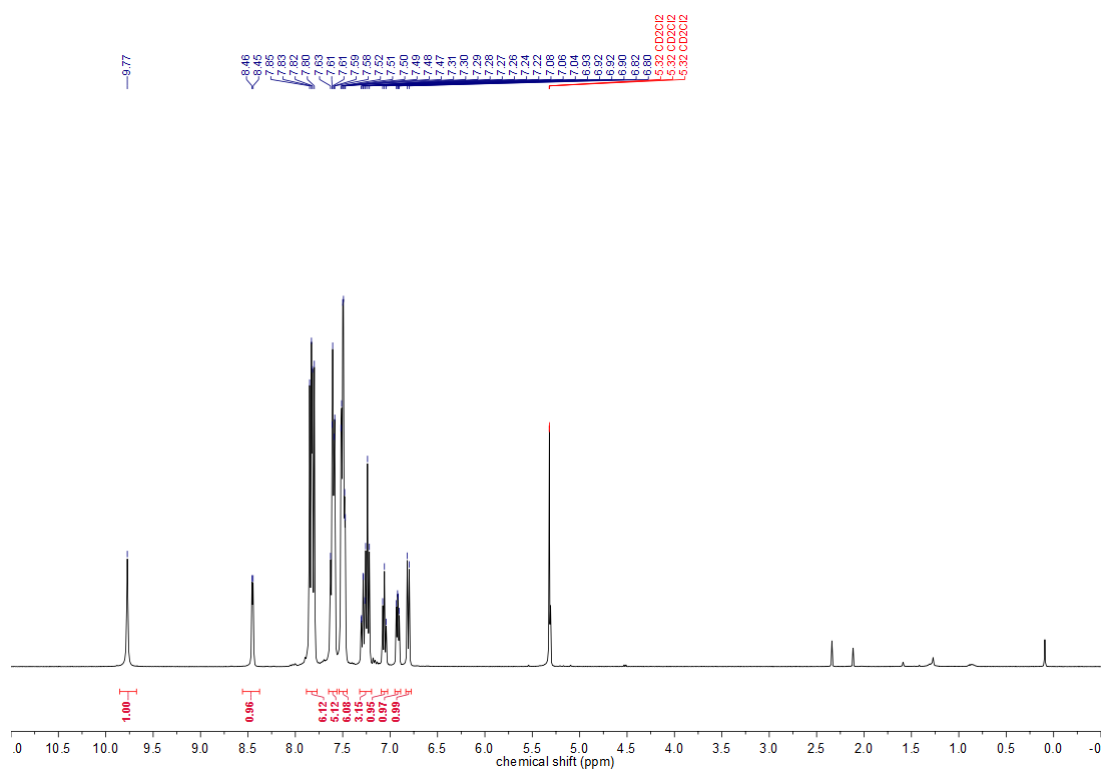
^{31}P-NMR(162 MHz, CD$_2$Cl$_2$) **80f**

^{1}H-NMR(400 MHz, CD$_2$Cl$_2$) **80f**
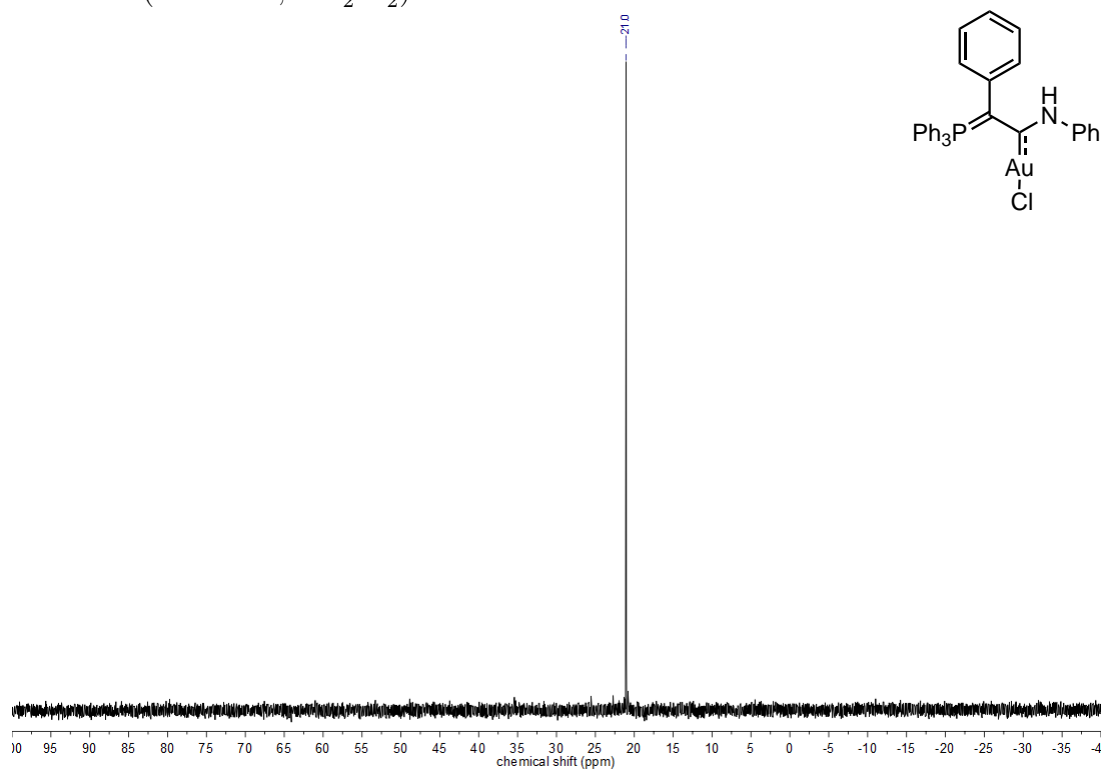
^{13}C-NMR(101 MHz, CD$_2$Cl$_2$) **80f**
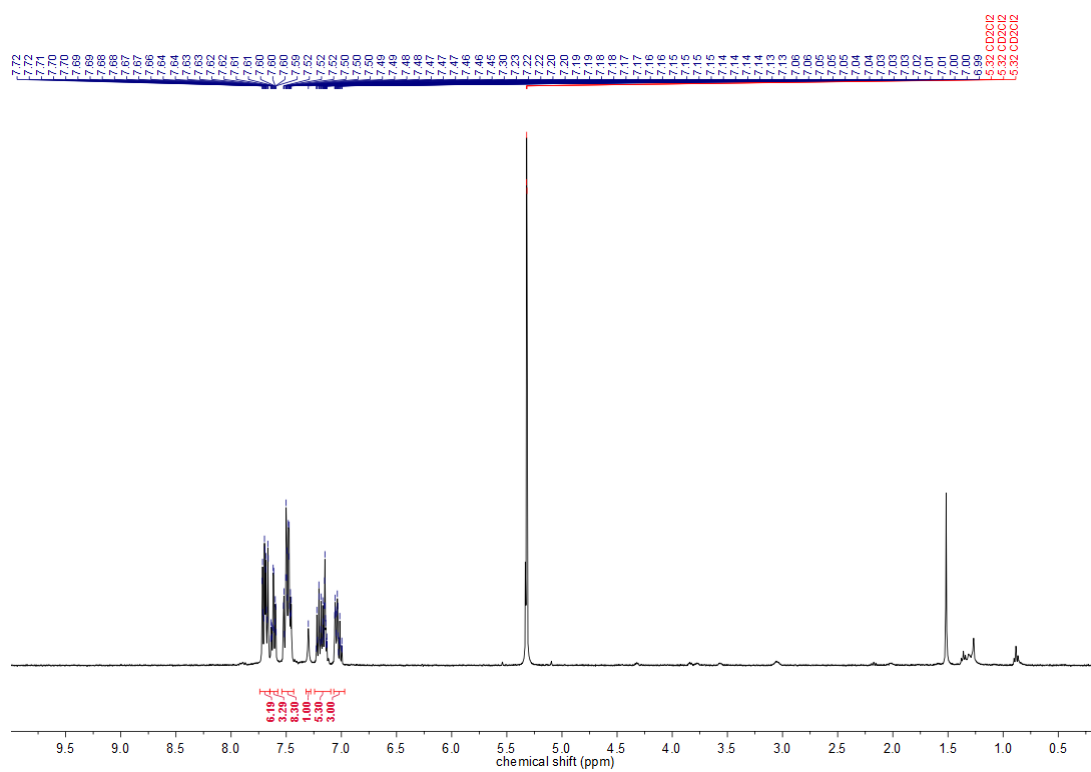
^{31}P-NMR(162 MHz, CD$_2$Cl$_2$) **80g**
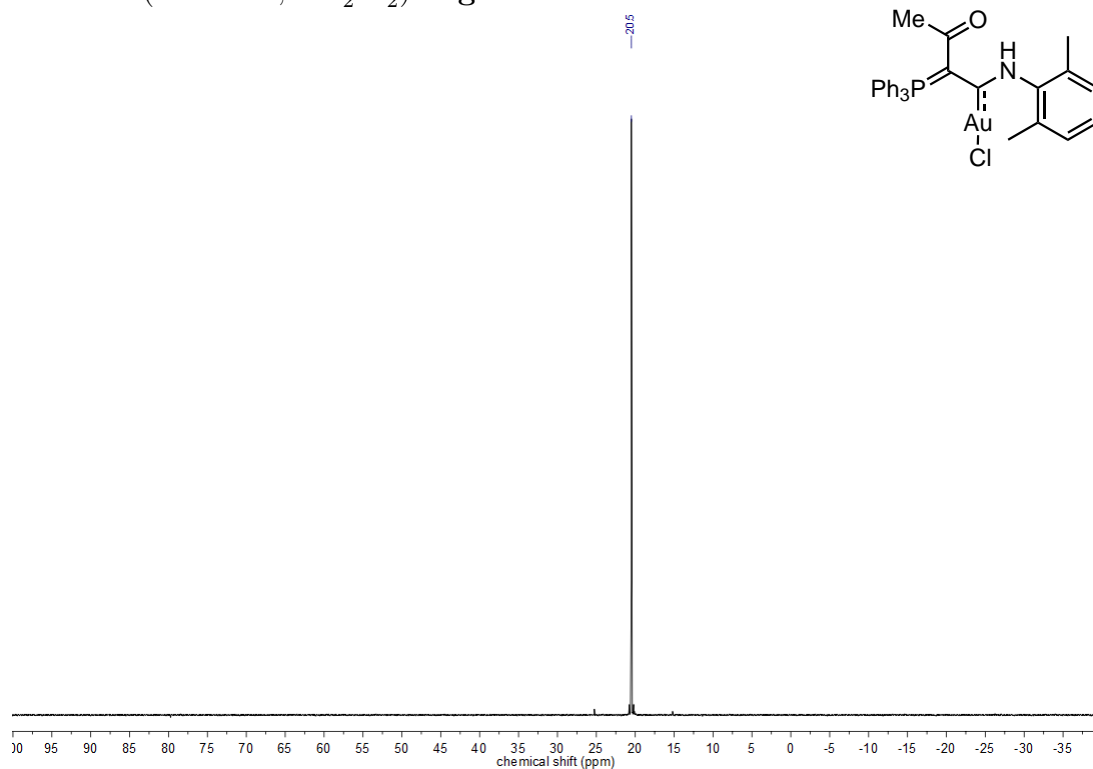
^{1}H-NMR(400 MHz, CD$_2$Cl$_2$) **80g**

^{13}C-NMR(101 MHz, CD$_2$Cl$_2$) **80g**

^{31}P-NMR(162 MHz, CD$_2$Cl$_2$) **80h**

^{1}H-NMR(400 MHz, CD$_2$Cl$_2$) **80h**
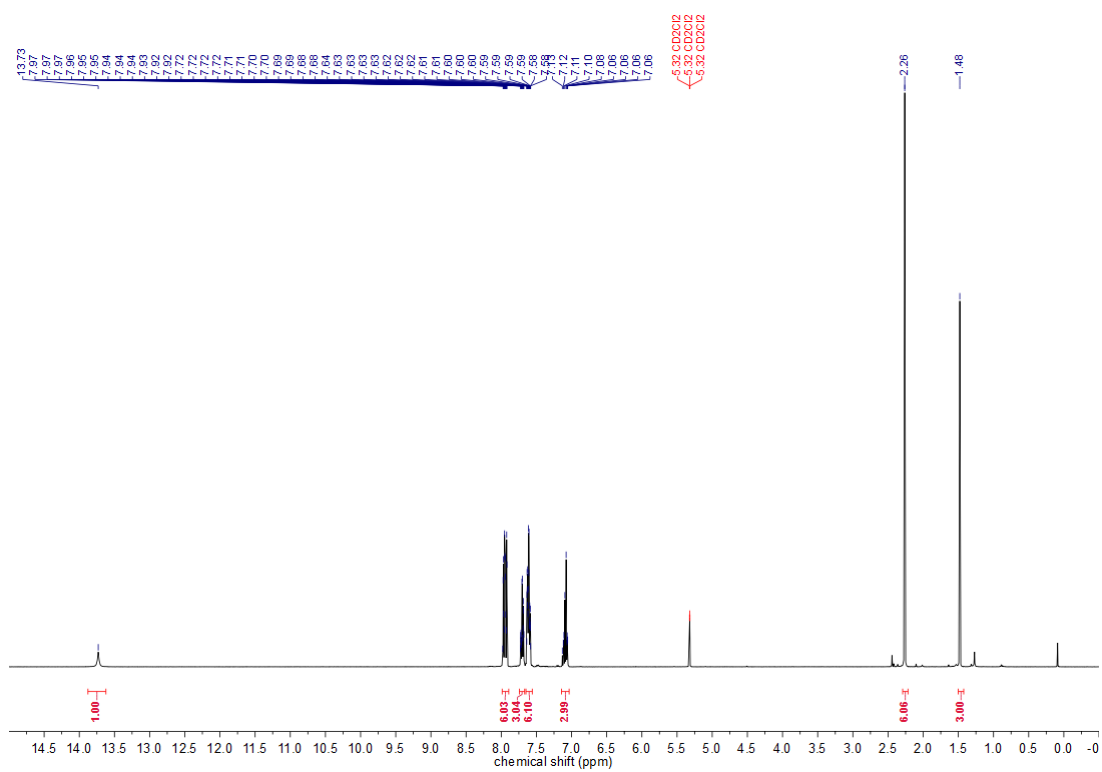
^{13}C-NMR(101 MHz, CD$_2$Cl$_2$) **80h**
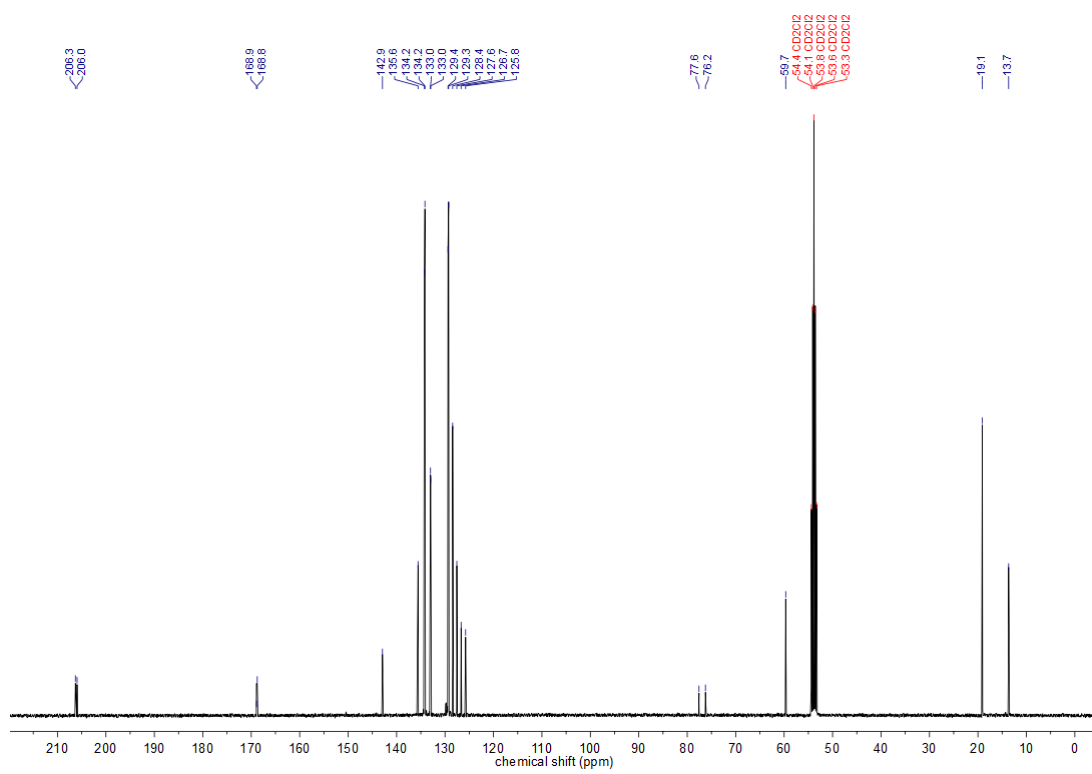
^{31}P-NMR(162 MHz, CD$_2$Cl$_2$) **80i**
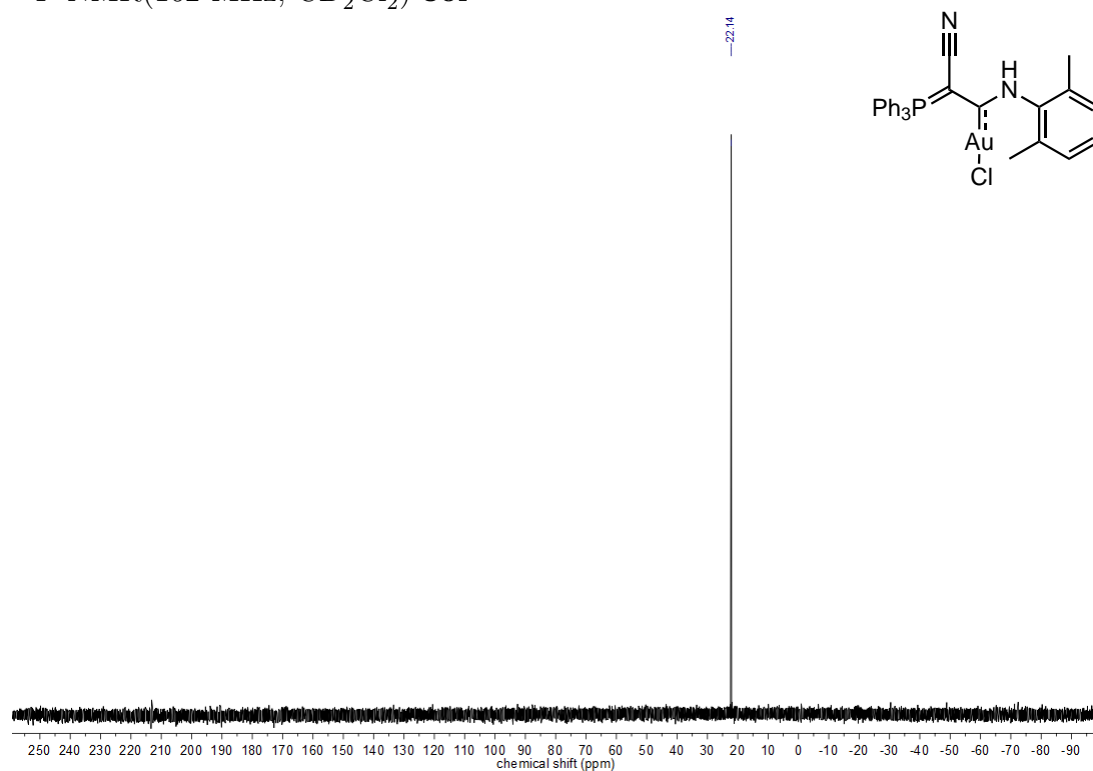
^{1}H-NMR(400 MHz, CD$_2$Cl$_2$) **80i**
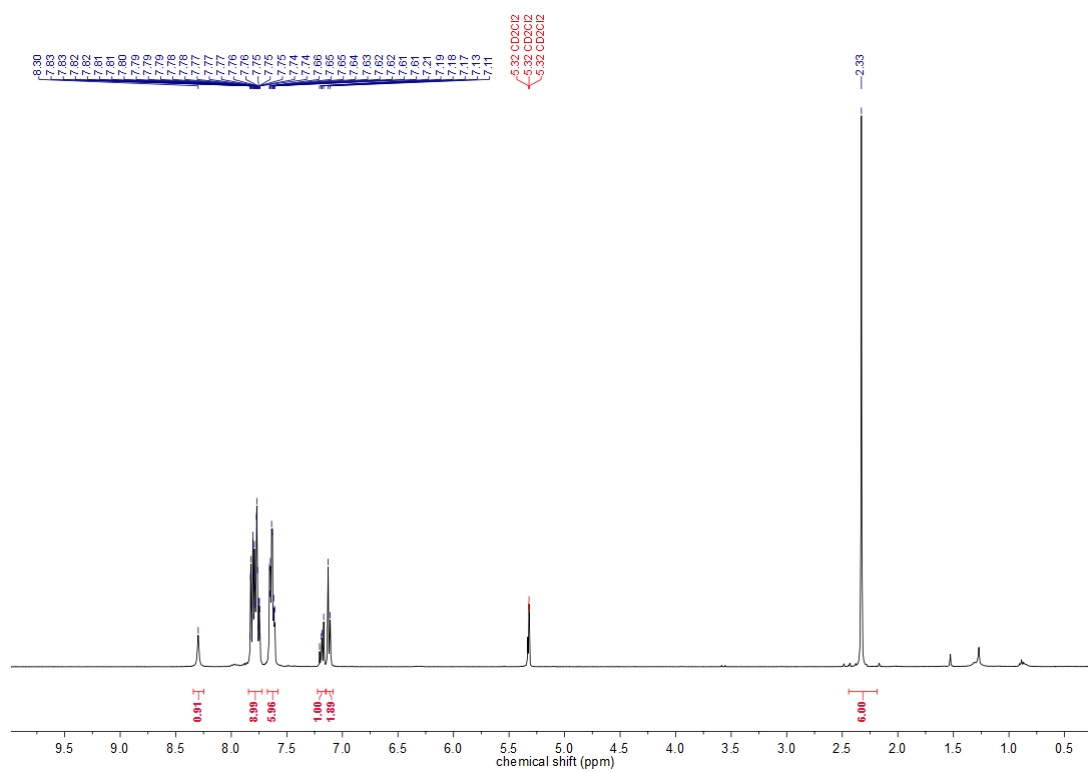
^{13}C-NMR(101 MHz, CD$_2$Cl$_2$) **80i**
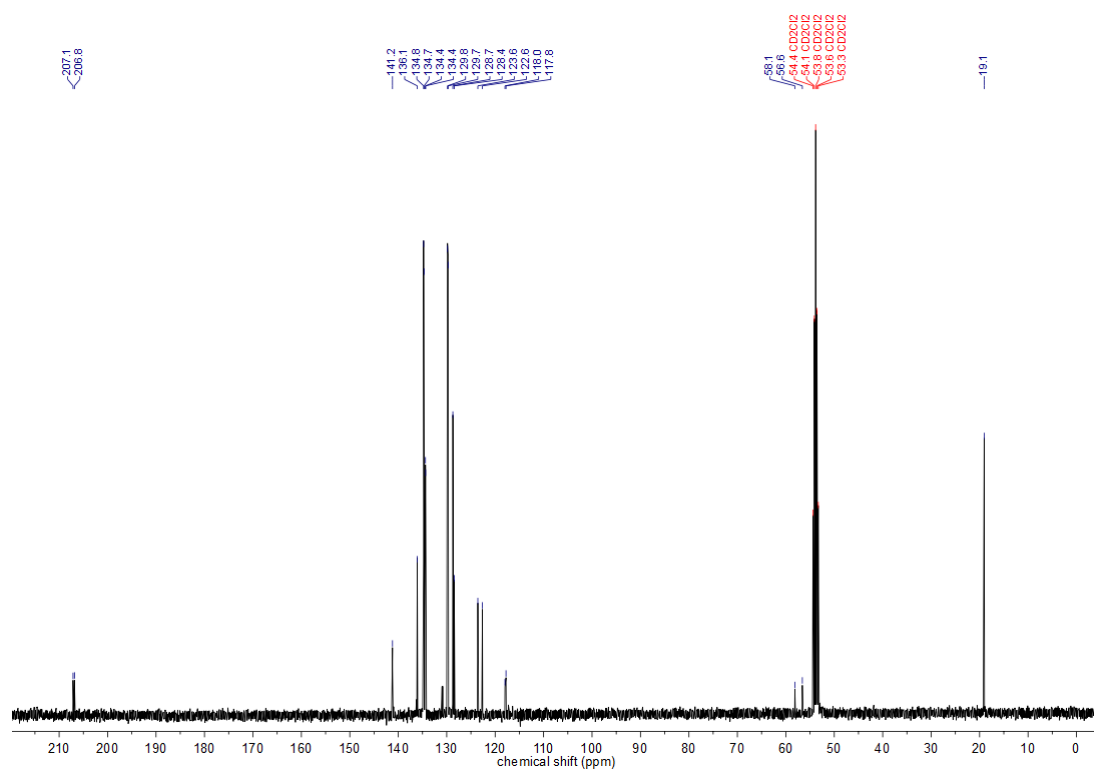
^{31}P-NMR(162 MHz, CD$_2$Cl$_2$) **80j**
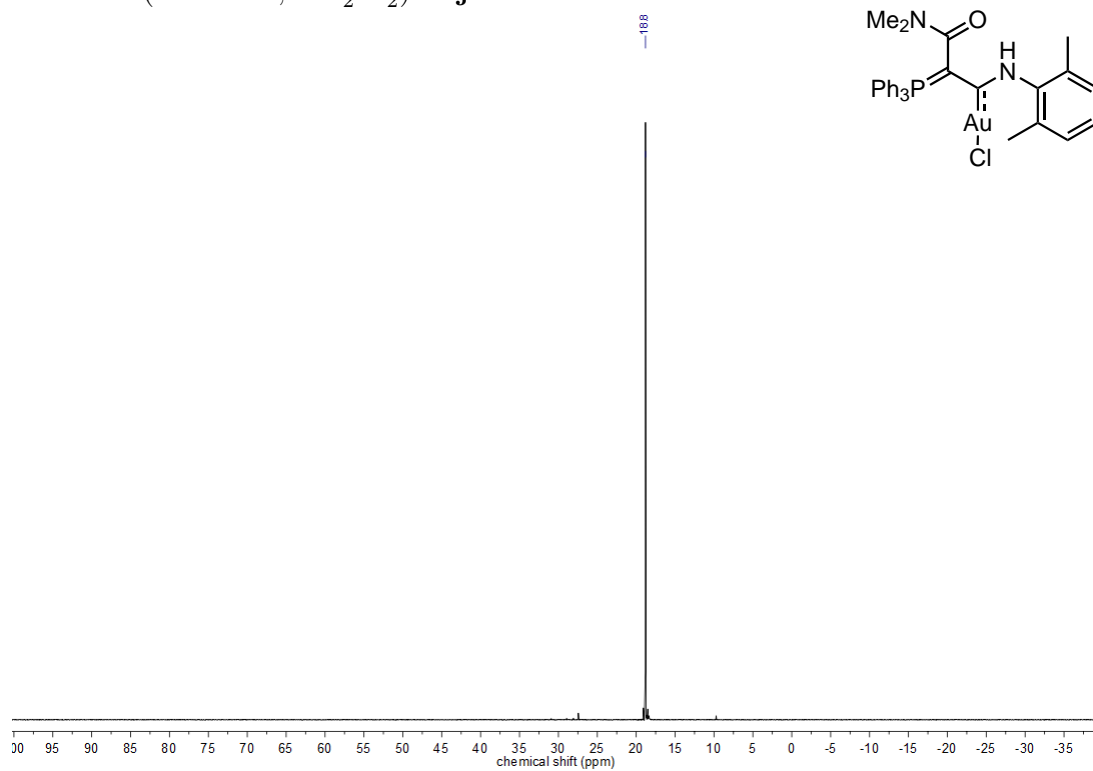
^{1}H-NMR(400 MHz, CD$_2$Cl$_2$) **80j**
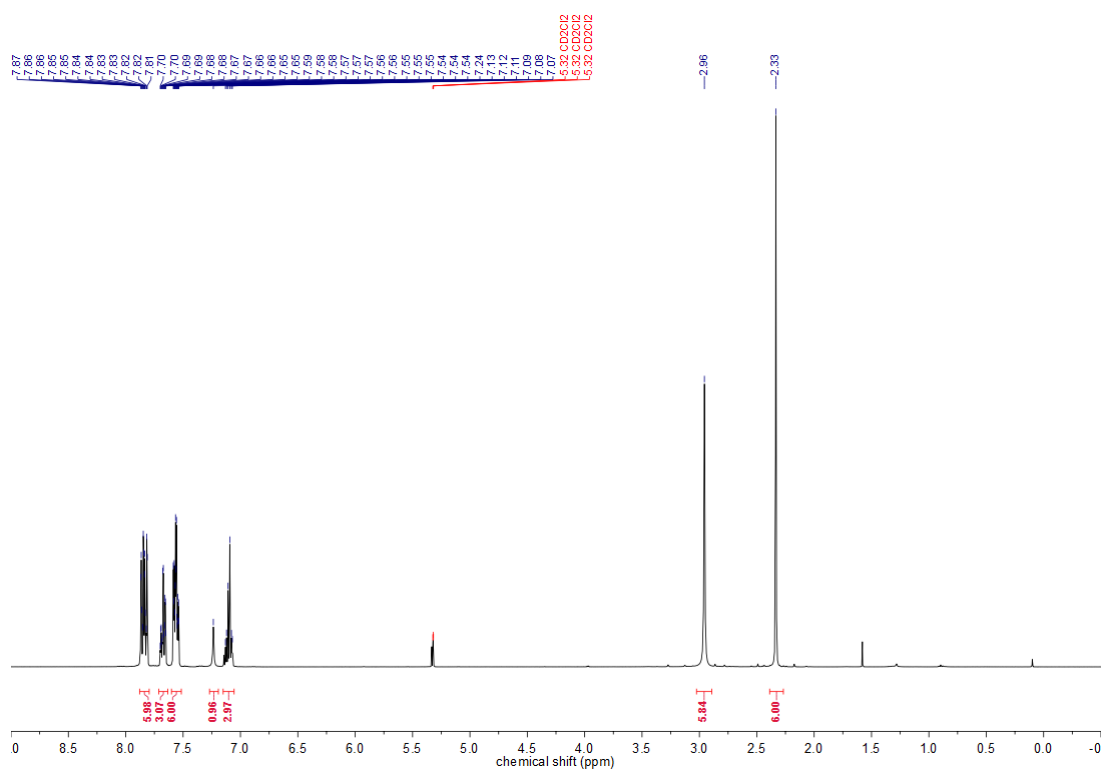
^{13}C-NMR(101 MHz, CD$_2$Cl$_2$) **80j**
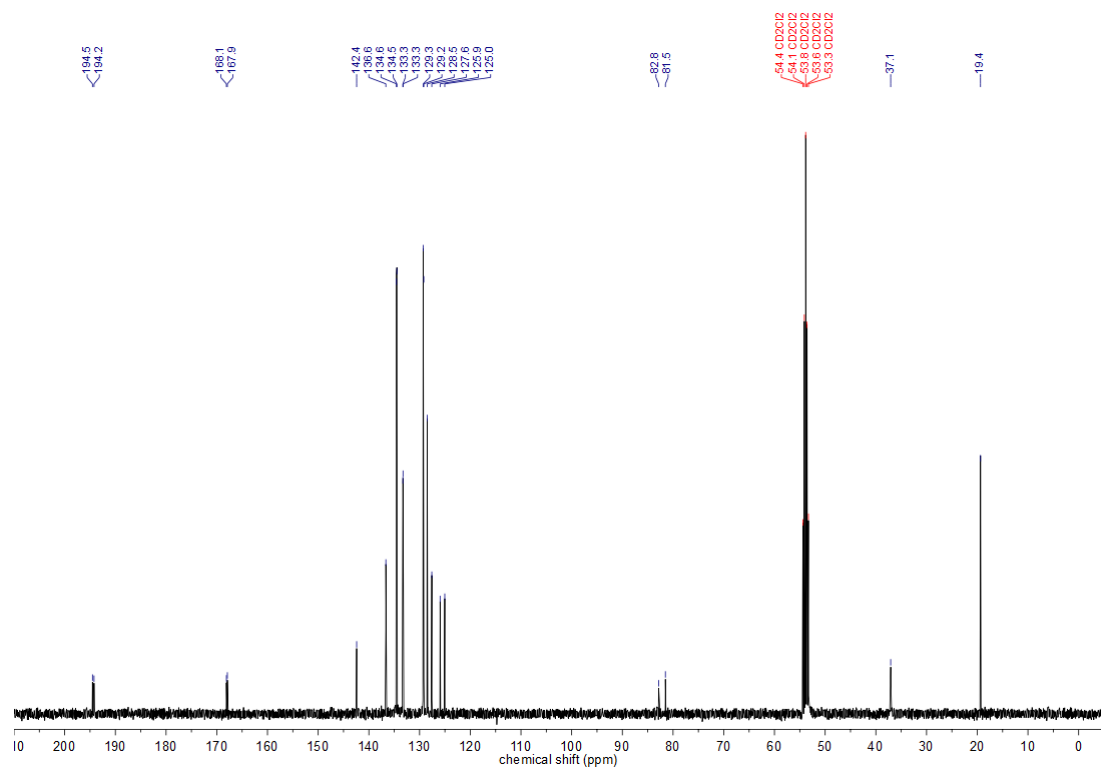
^{31}P-NMR(162 MHz, CD$_2$Cl$_2$) **80k**
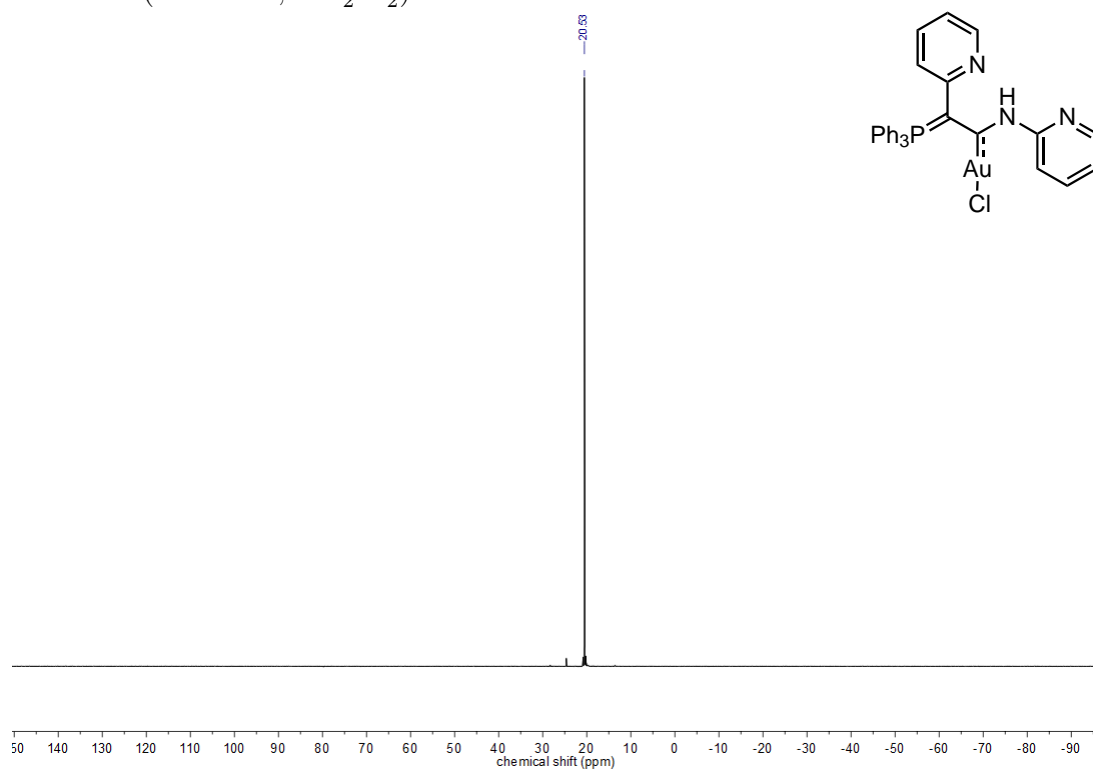
^{1}H-NMR(400 MHz, CD$_2$Cl$_2$) **80k**
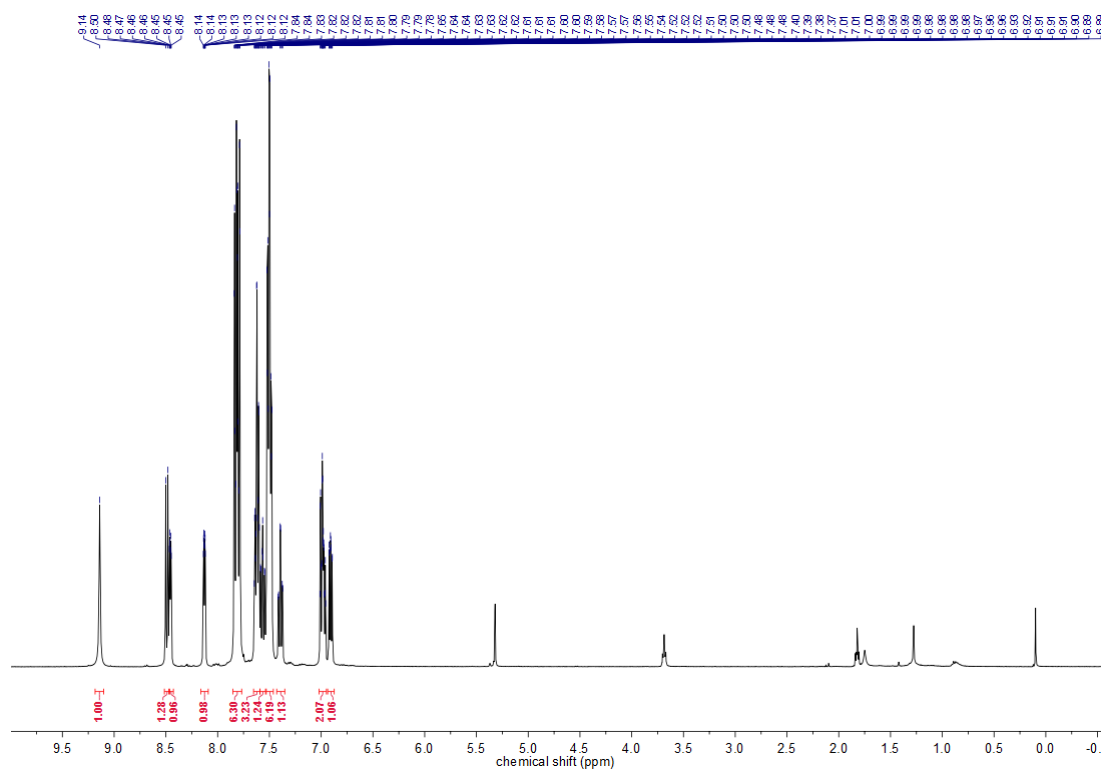
^{13}C-NMR(101 MHz, CD$_2$Cl$_2$) **80k**
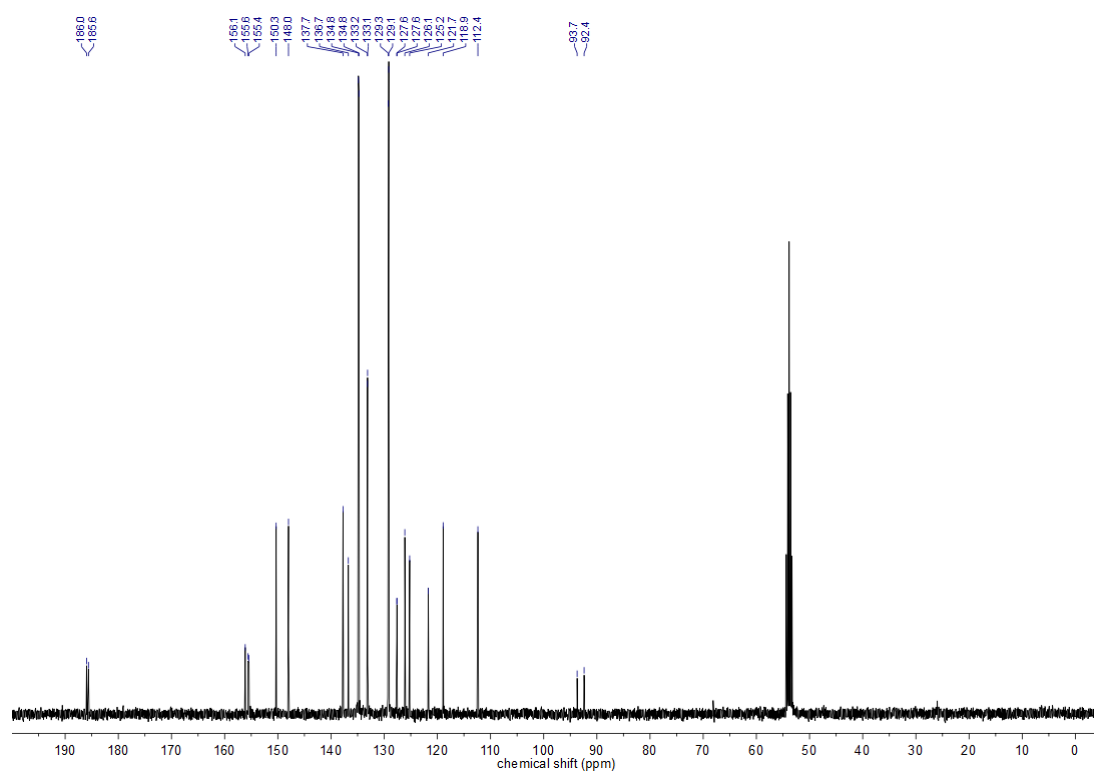
^{1}H-NMR(400 MHz, CD$_2$Cl$_2$) **84**
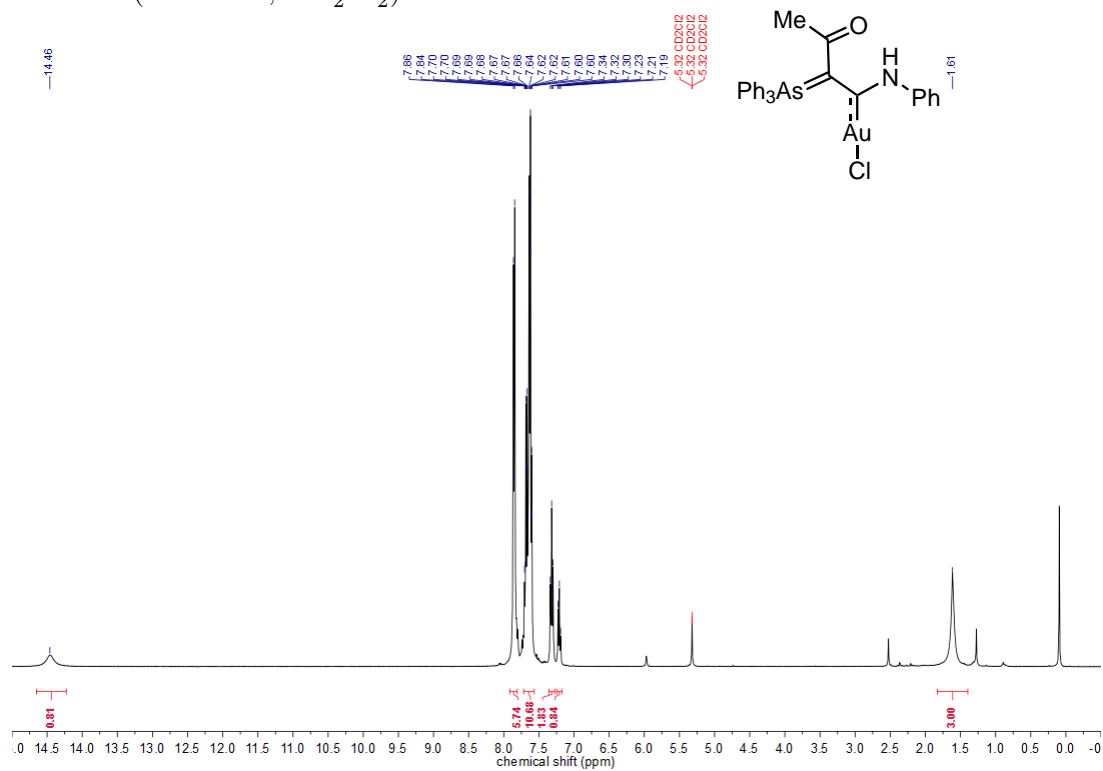
^{13}C-NMR(75 MHz, CD$_2$Cl$_2$) **84**
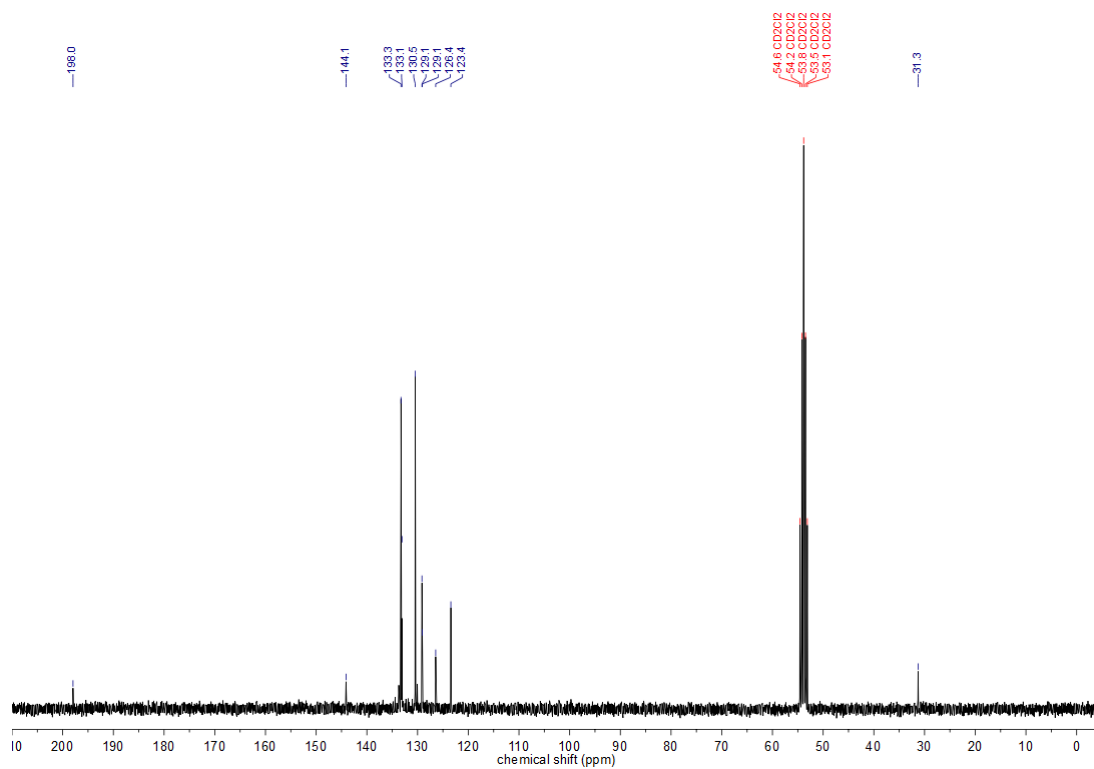
^{1}H-NMR(400 MHz, CD$_2$Cl$_2$) **87**
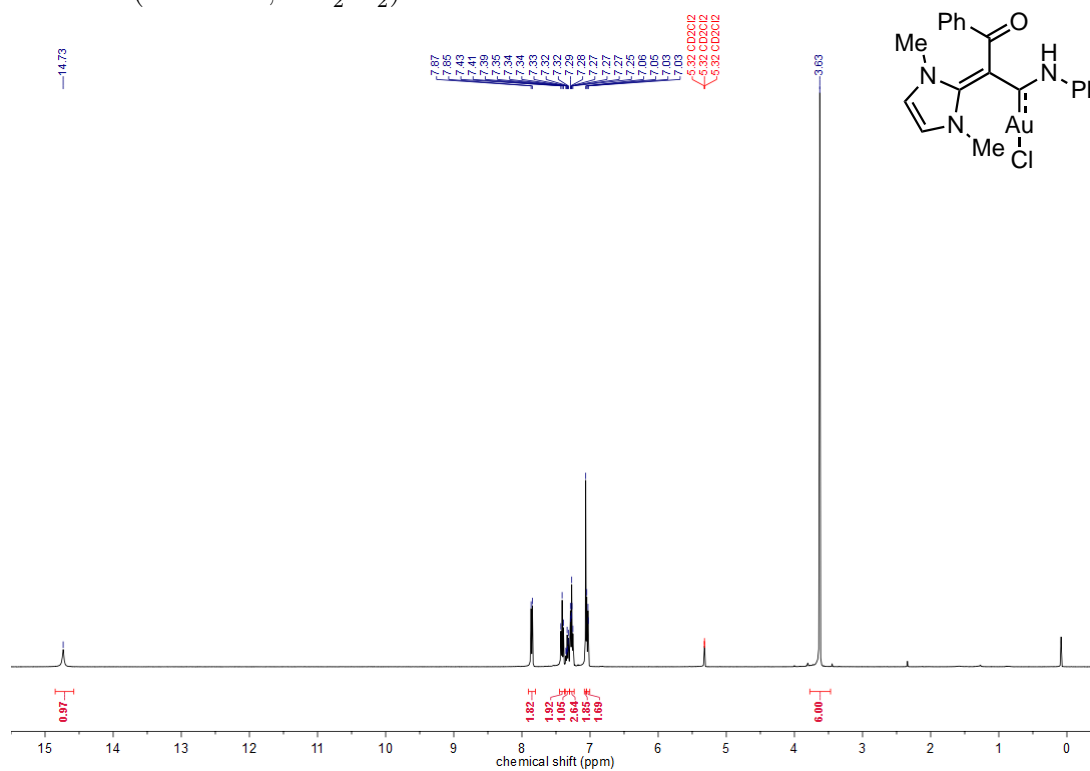
^{13}C-NMR(101 MHz, CD$_2$Cl$_2$) **87**
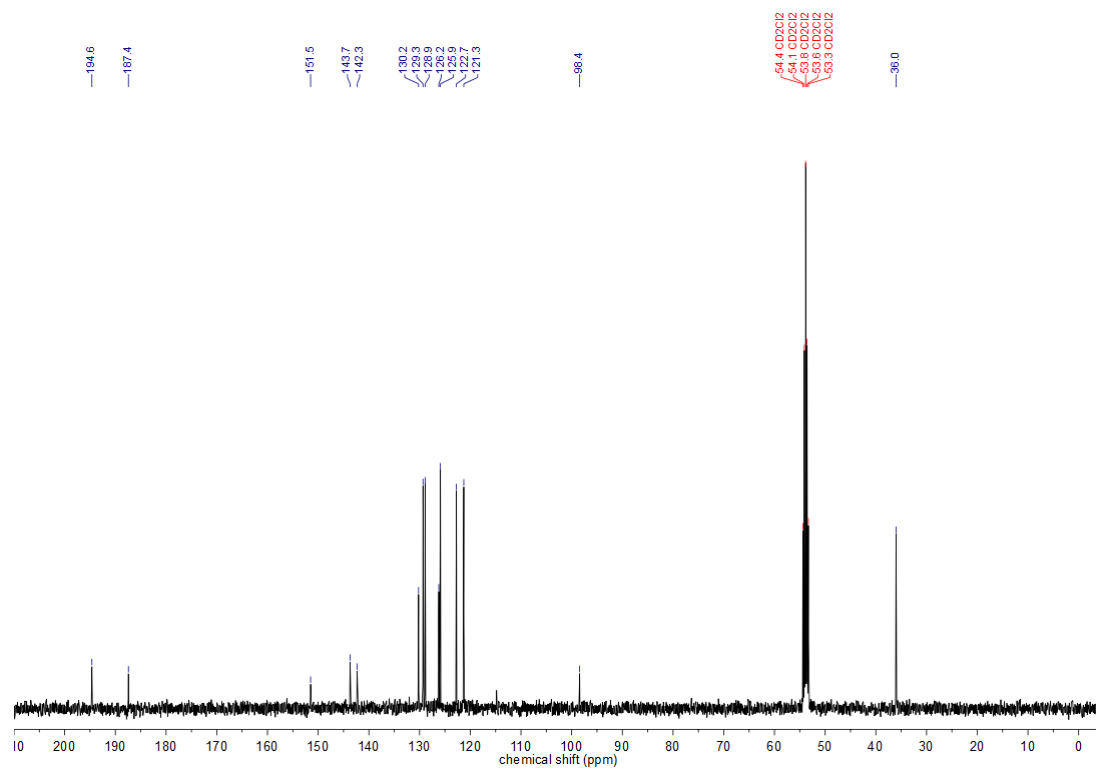
^{1}H-NMR(400 MHz, CD$_2$Cl$_2$) **88**

^{13}C-NMR(101 MHz, CD$_2$Cl$_2$) **88**

^{31}P-NMR(162 MHz, CDCl$_3$) **90**
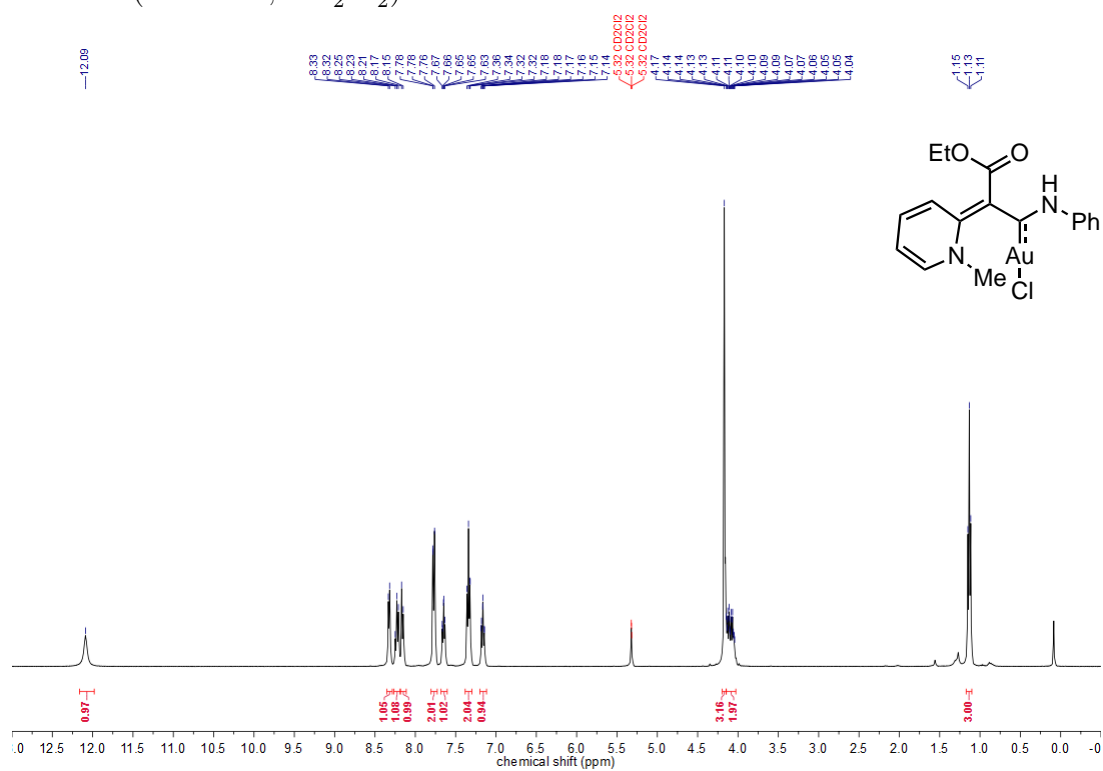
^{1}H-NMR(400 MHz, CDCl$_3$) **90**
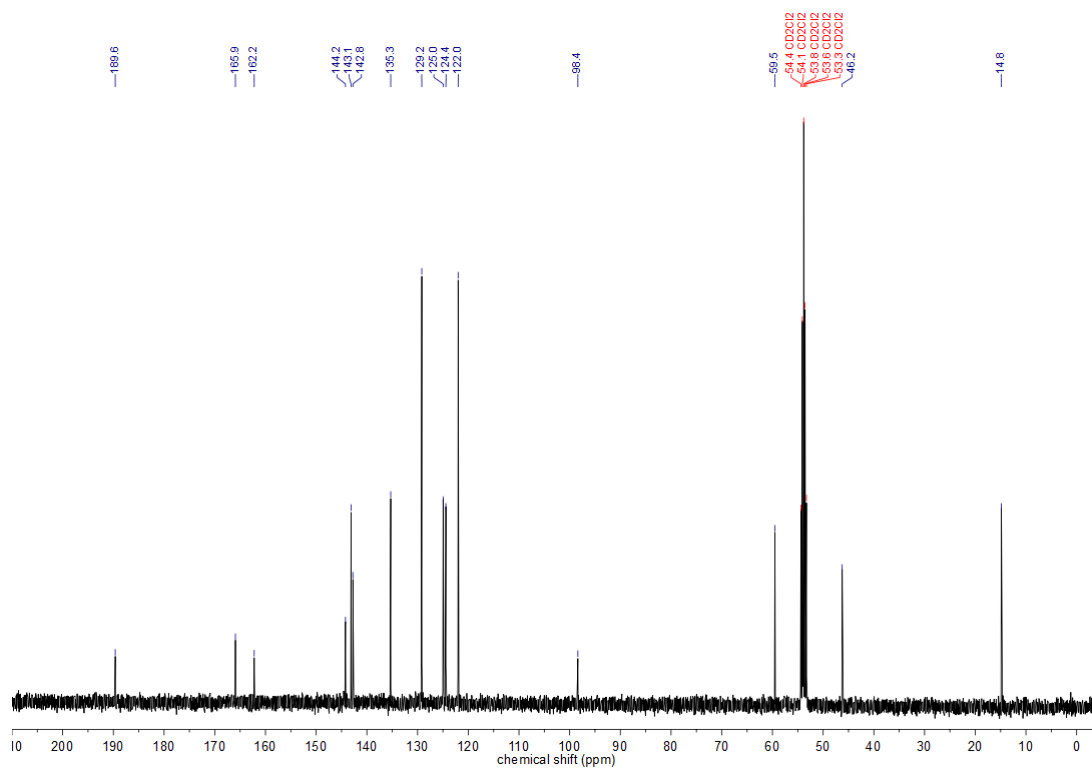
^{13}C-NMR(126 MHz, CDCl$_3$) **90**
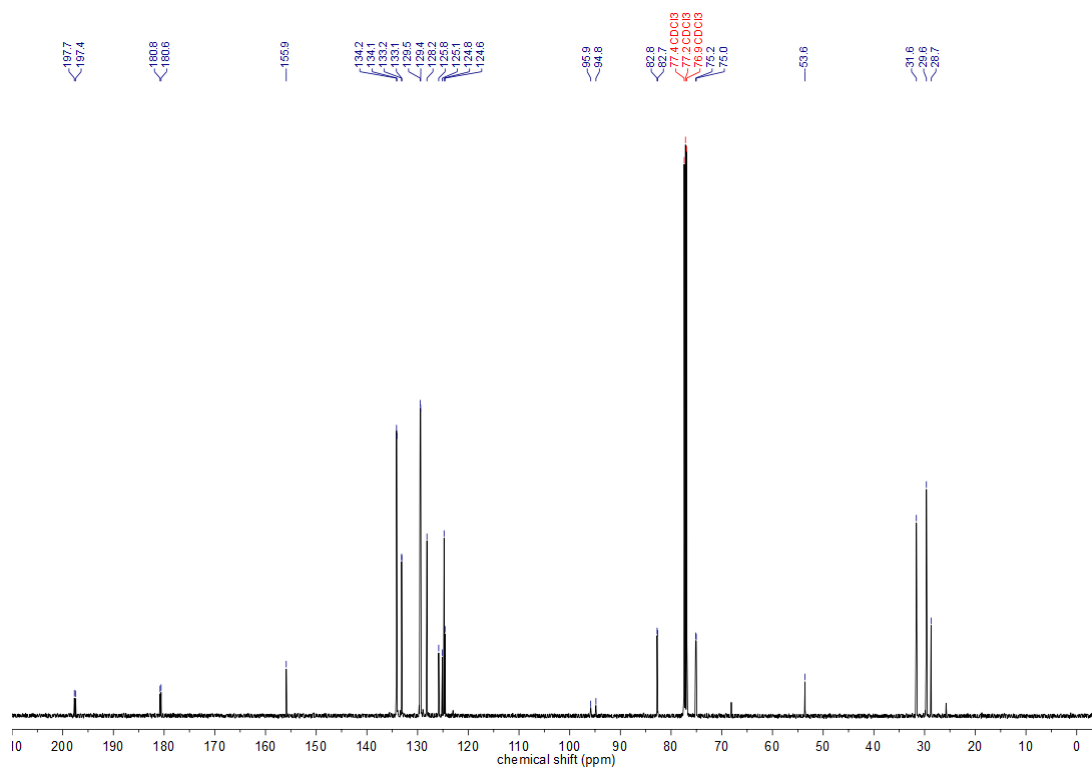
^{1}H-NMR(400 MHz, CD$_2$Cl$_2$) **91**
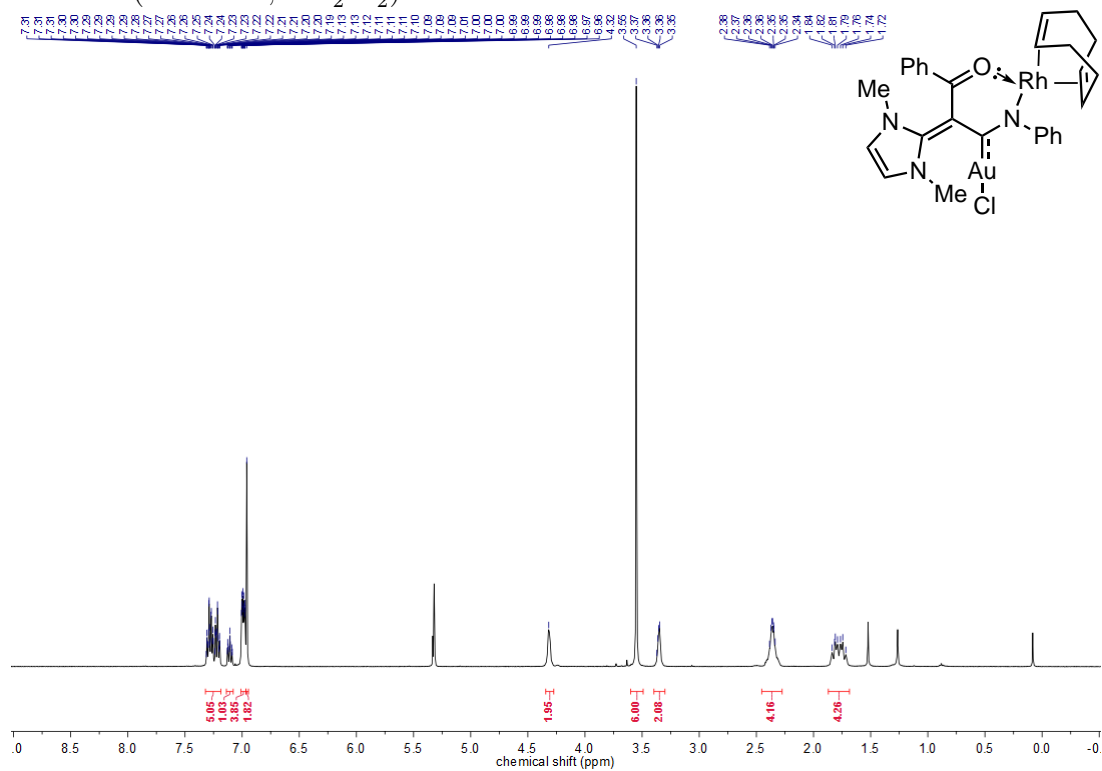
^{13}C-NMR(101 MHz, CD$_2$Cl$_2$) **91**
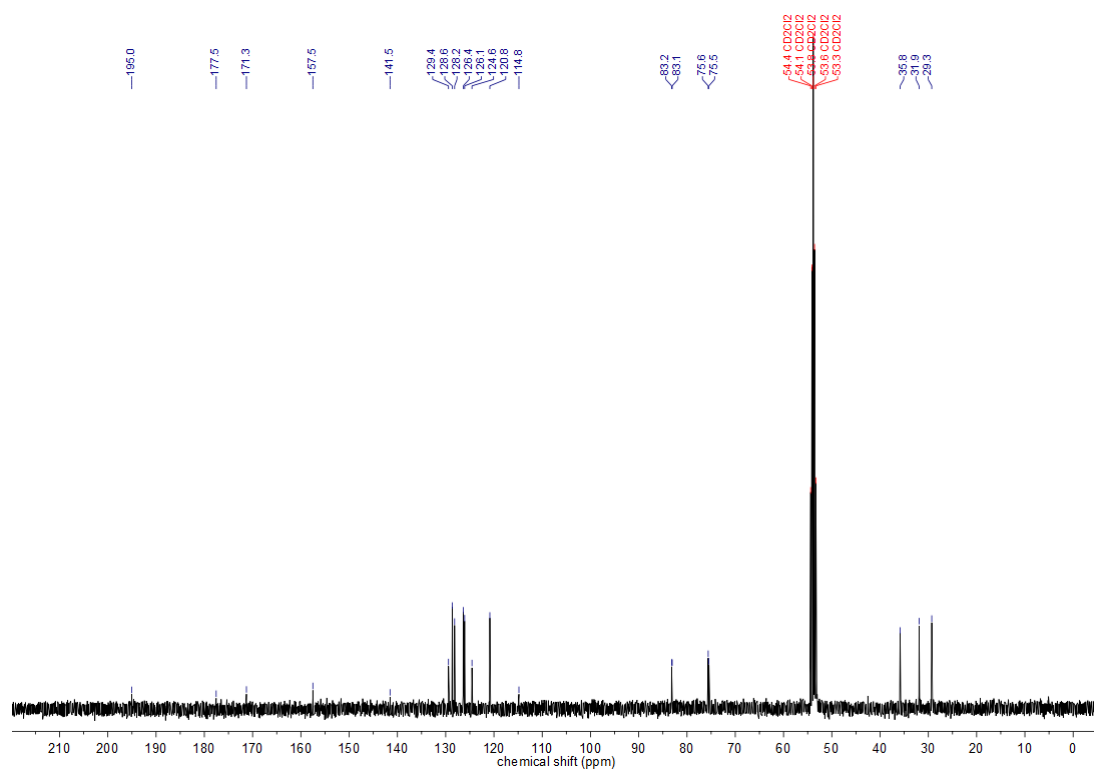
^{1}H-NMR(400 MHz, CD$_2$Cl$_2$) **92**
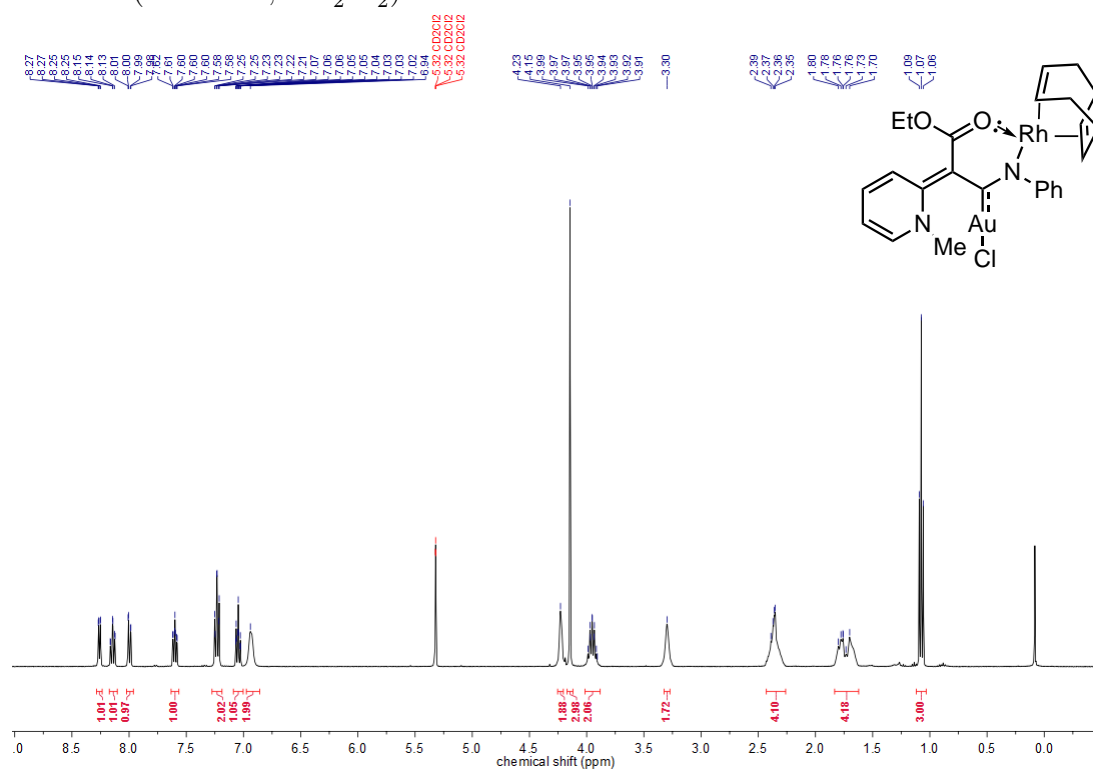
^{13}C-NMR(101 MHz, CD$_2$Cl$_2$) **92**
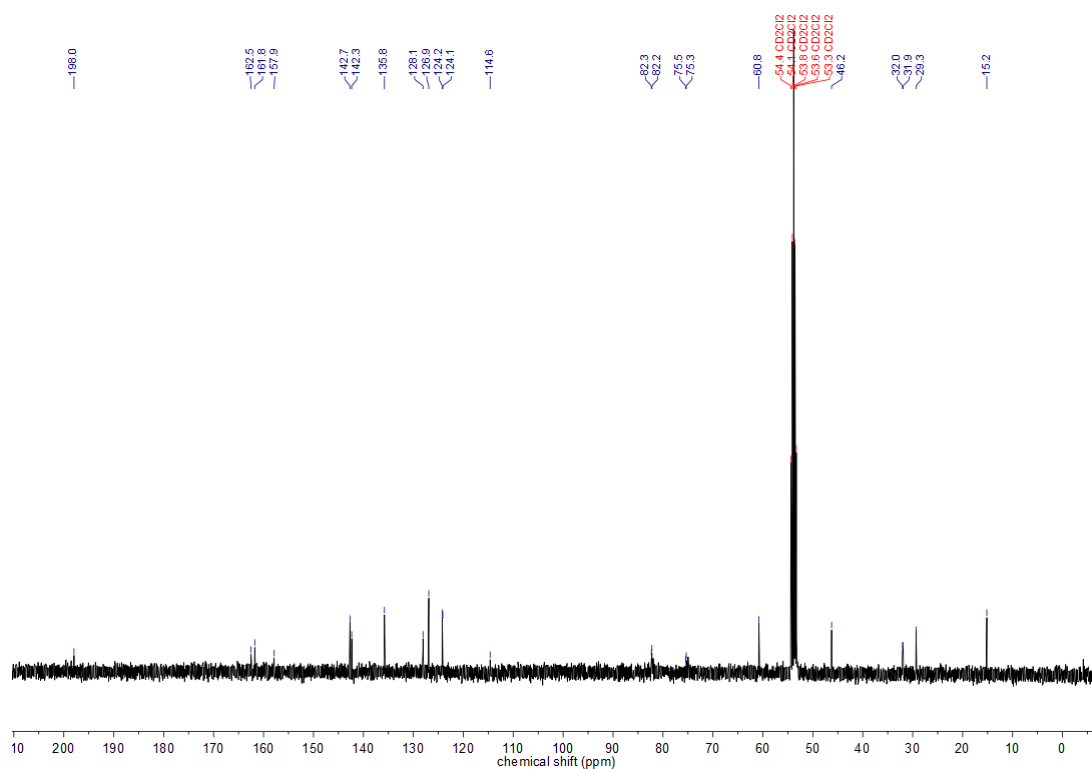
^{31}P-NMR(162 MHz, CDCl$_3$) **93**
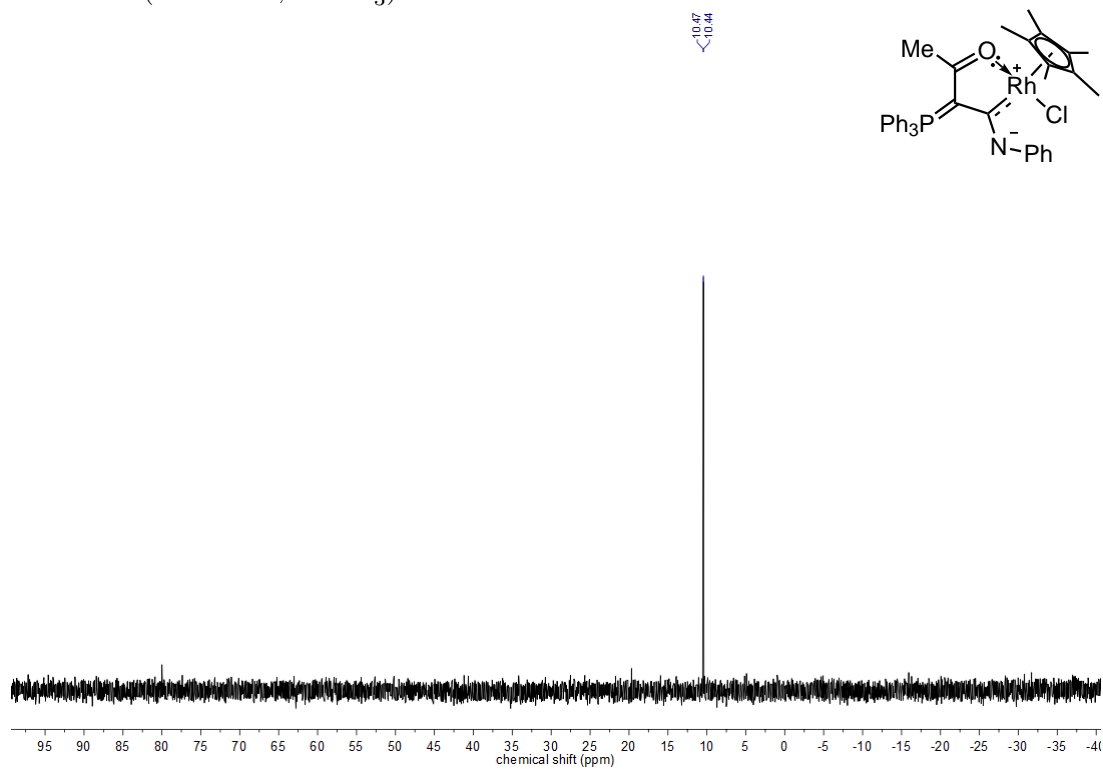
^{1}H-NMR(400 MHz, CDCl$_3$) **93**
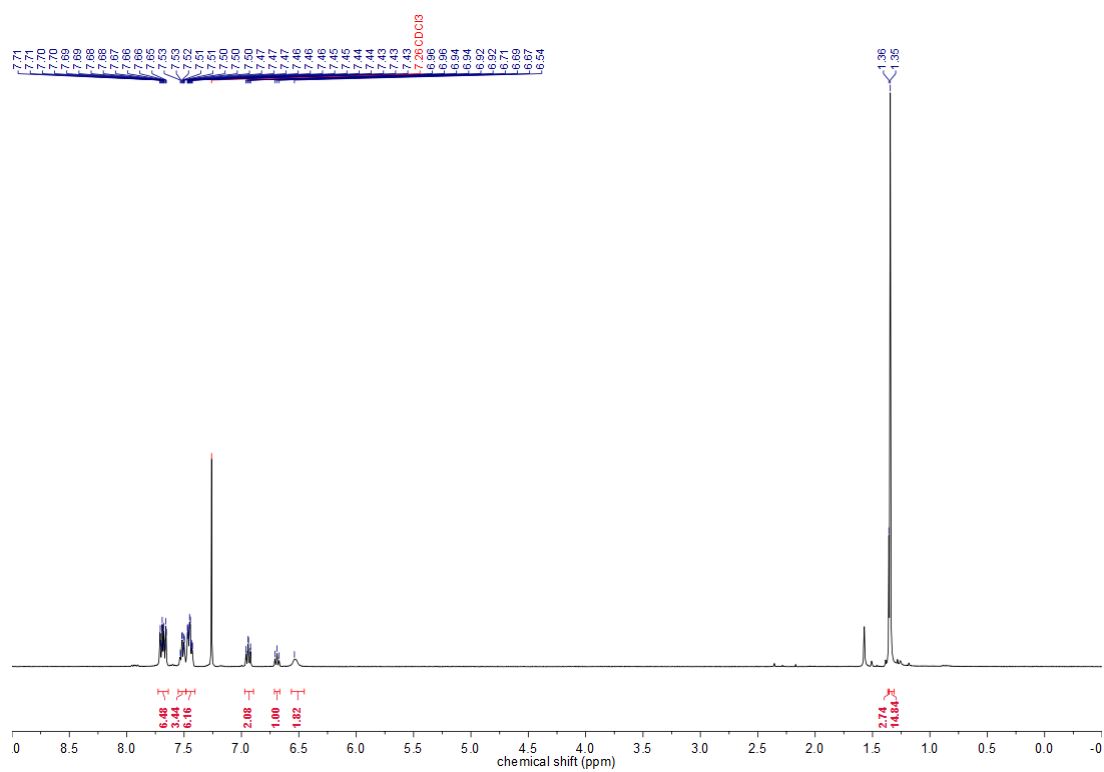
^{13}C-NMR(101 MHz, CDCl$_3$) **93**
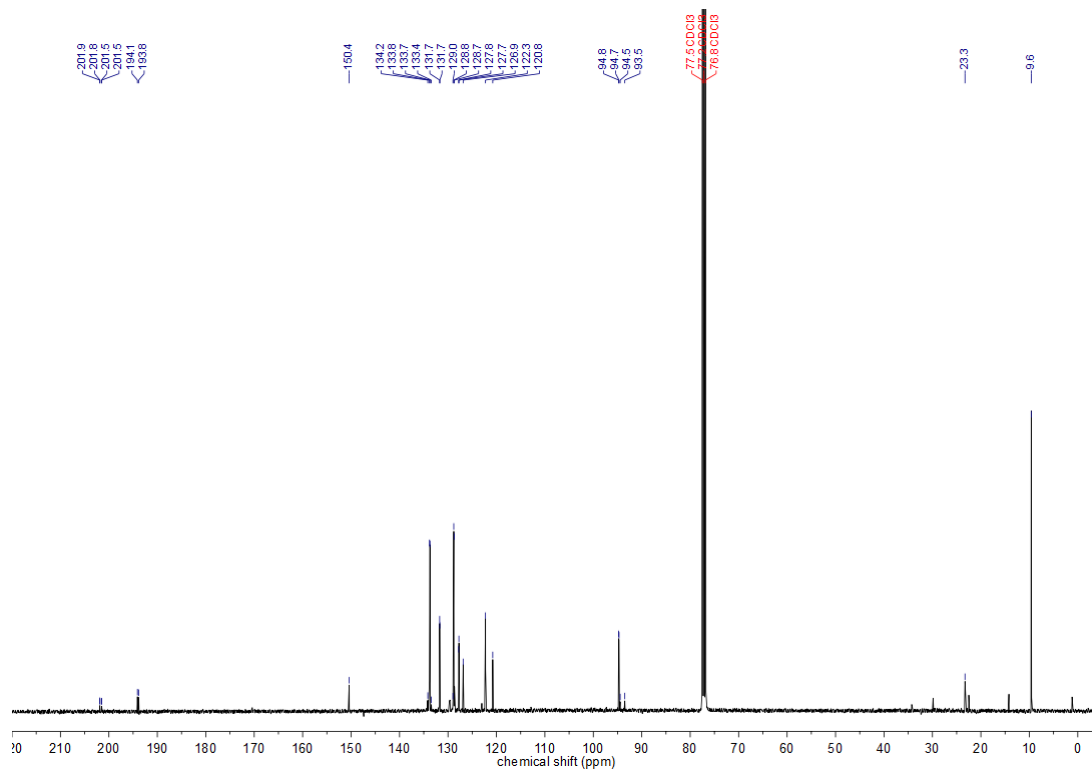
^{31}P-NMR(162 MHz, CD$_2$Cl$_2$) **94**
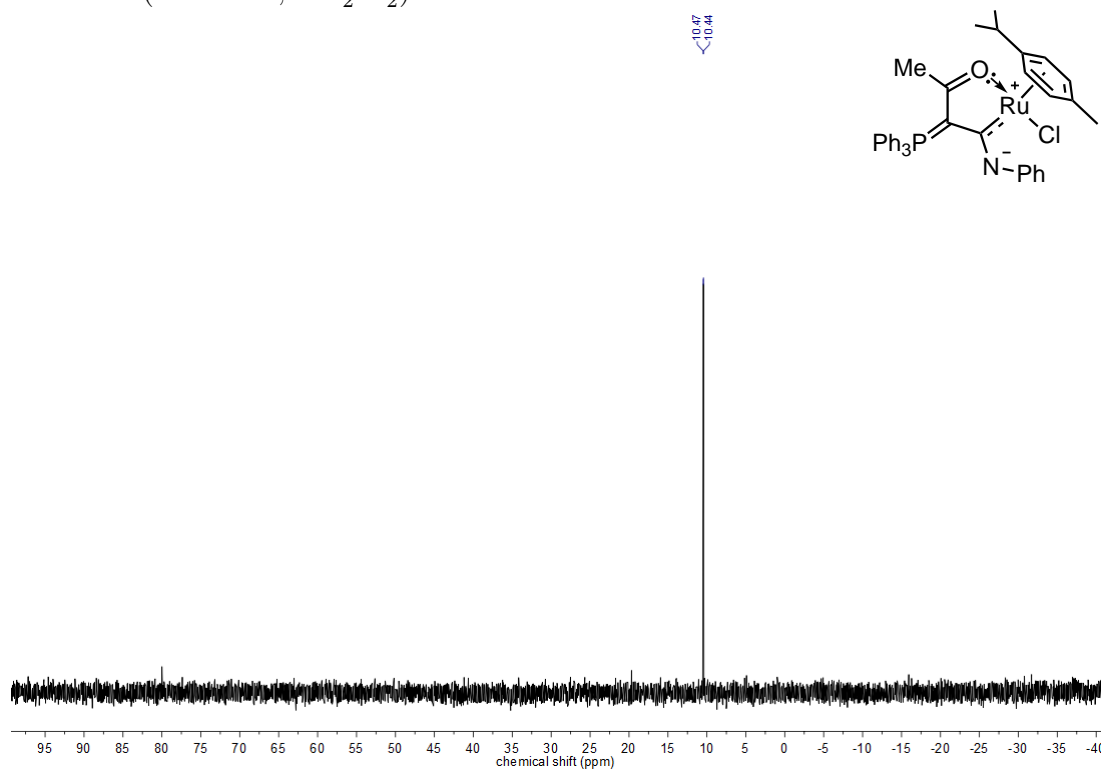
^{1}H-NMR(400 MHz, CD$_2$Cl$_2$) **94**
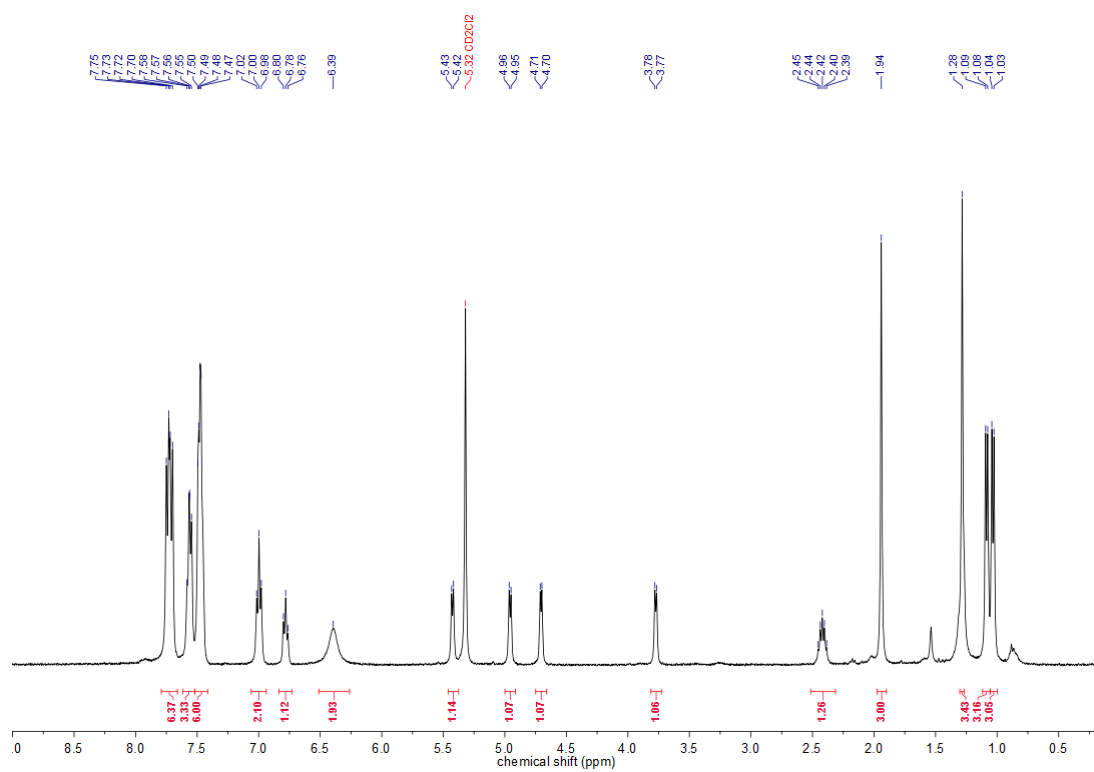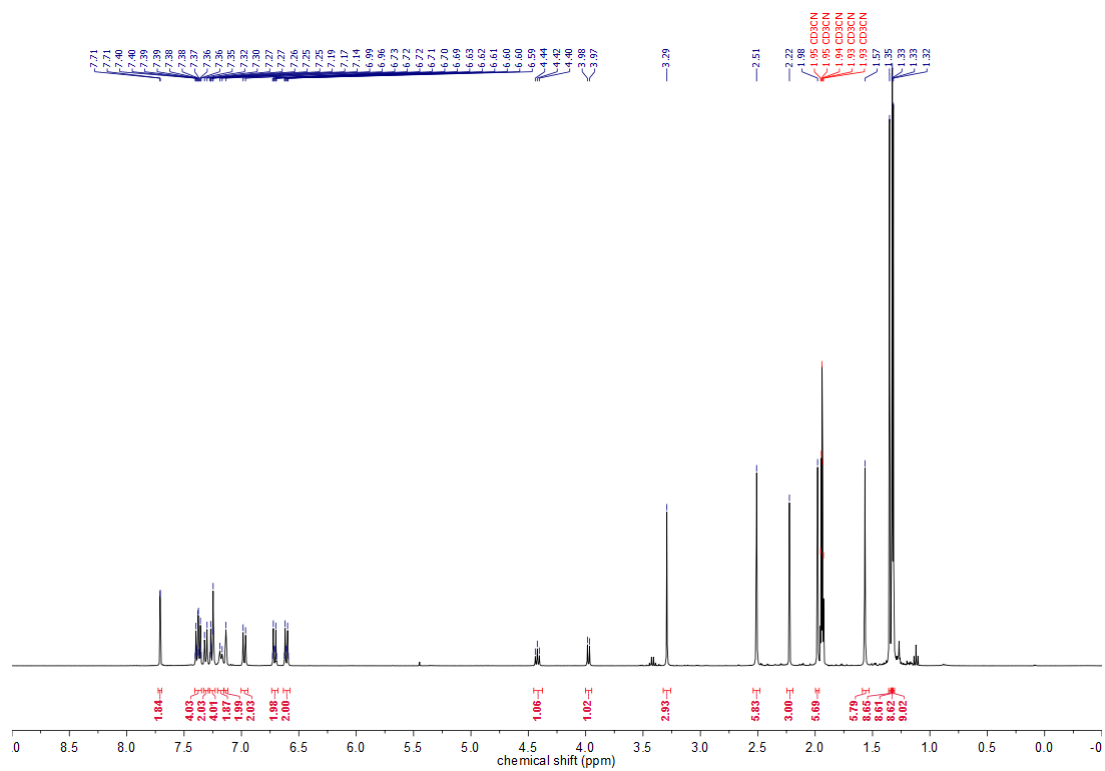
^{13}C-NMR(101 MHz, CD$_2$Cl$_2$) **94**

^{31}P-NMR(162 MHz, CD$_3$CN) **97**

^{1}H-NMR(400 MHz, CD$_3$CN) **97**
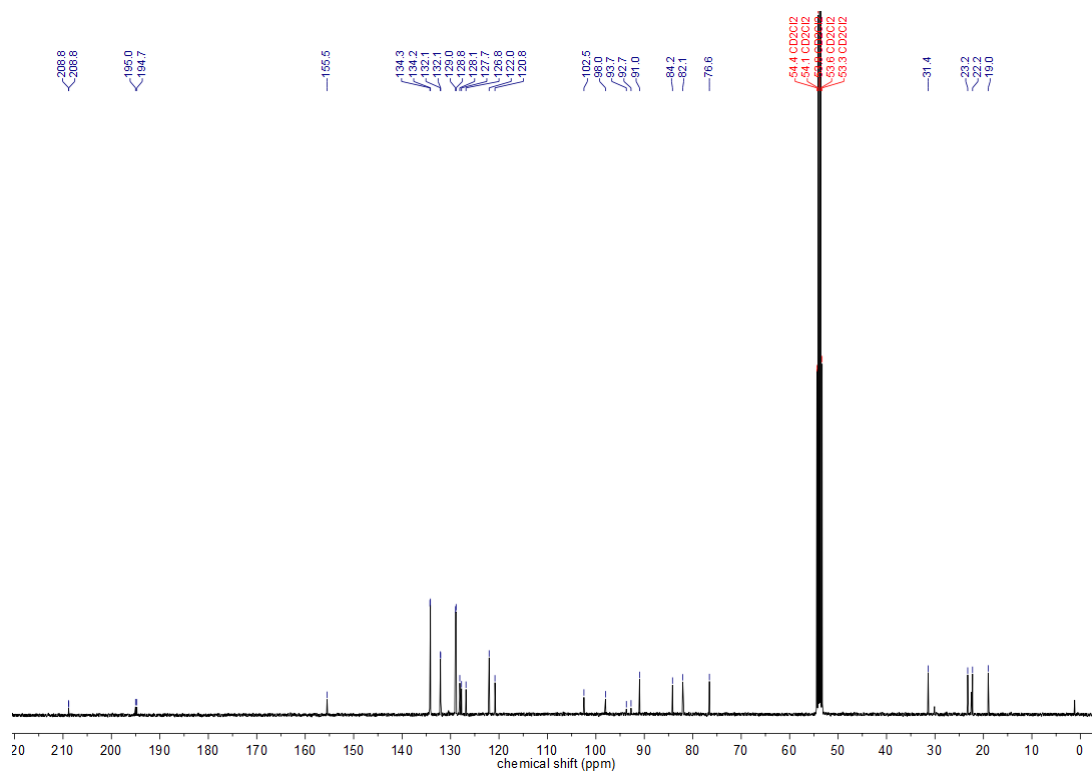
^{13}C-NMR(101 MHz, CD$_3$CN) **97**
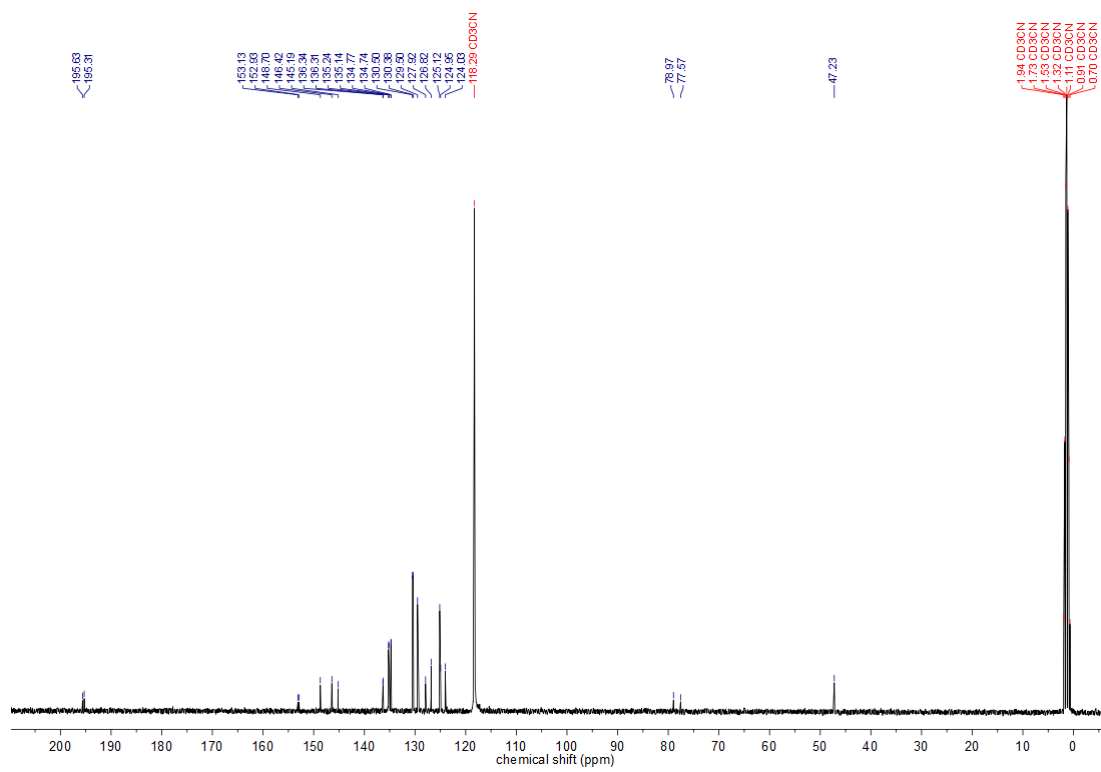
^{31}P-NMR(122 MHz, CD$_3$CN) **98**
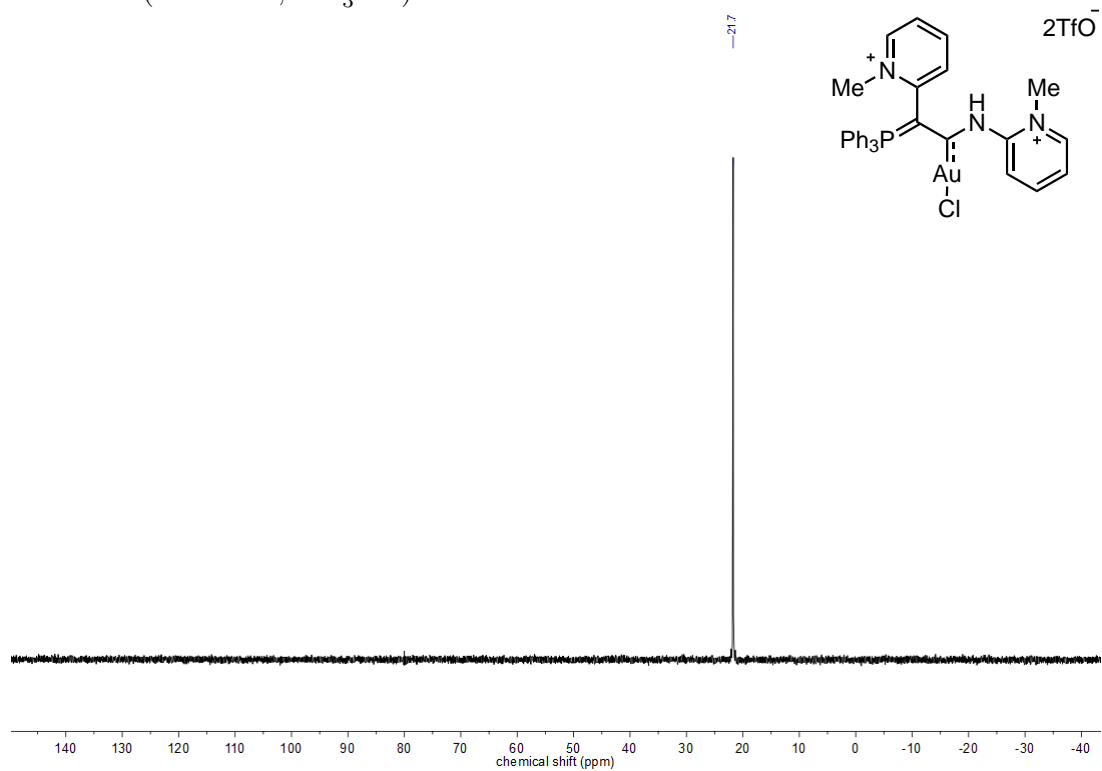
^{1}H-NMR(300 MHz, CD$_3$CN) **98**
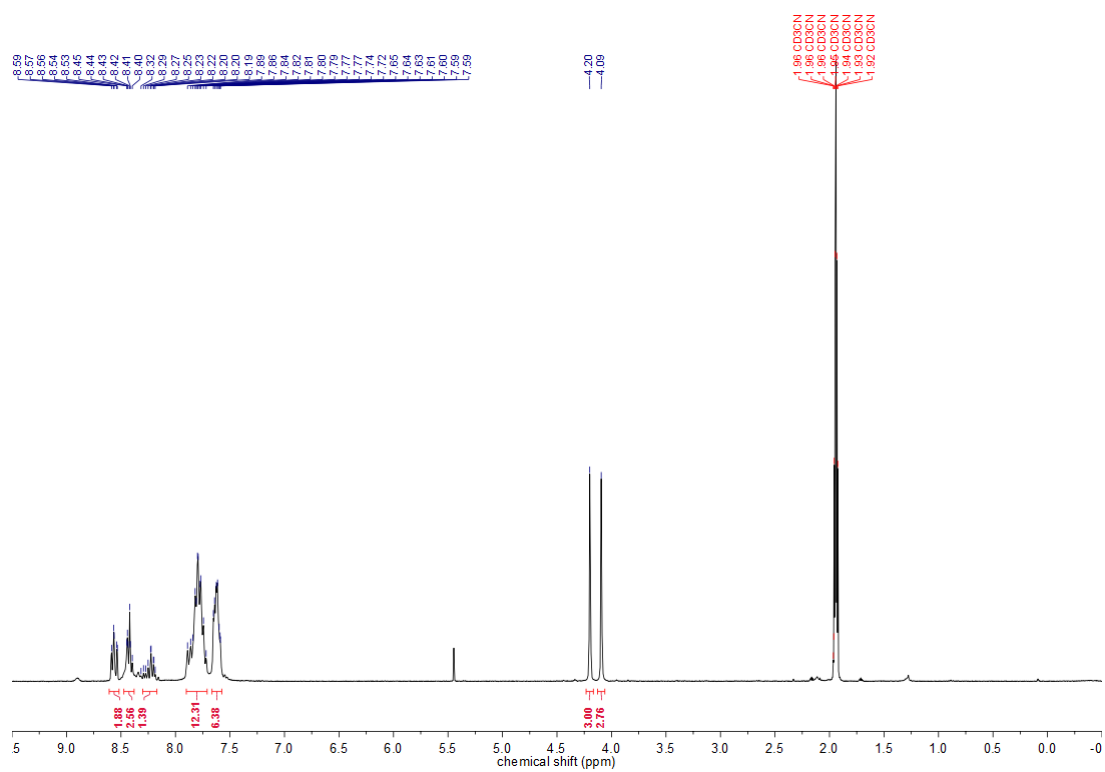
^{1}H-NMR(400 MHz, CDCl$_3$) **158d**
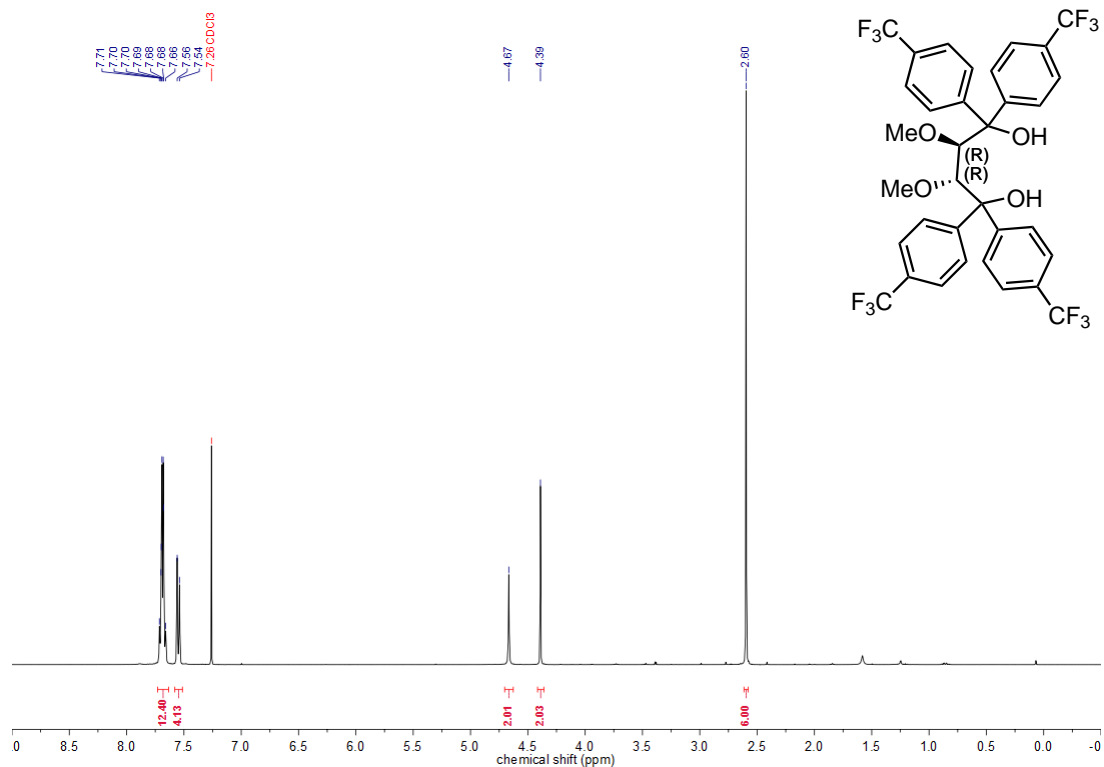
^{13}C-NMR(101 MHz, CDCl$_3$) **158d**
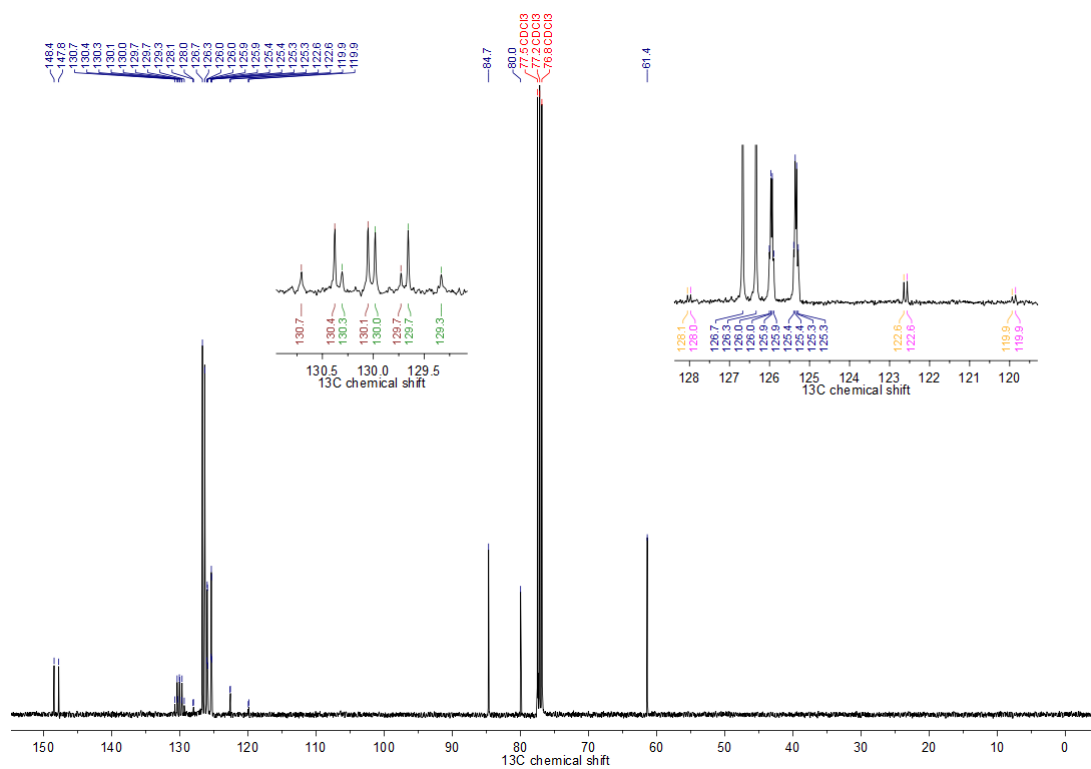
^{19}F-NMR(282 MHz, CDCl$_3$) **158d**
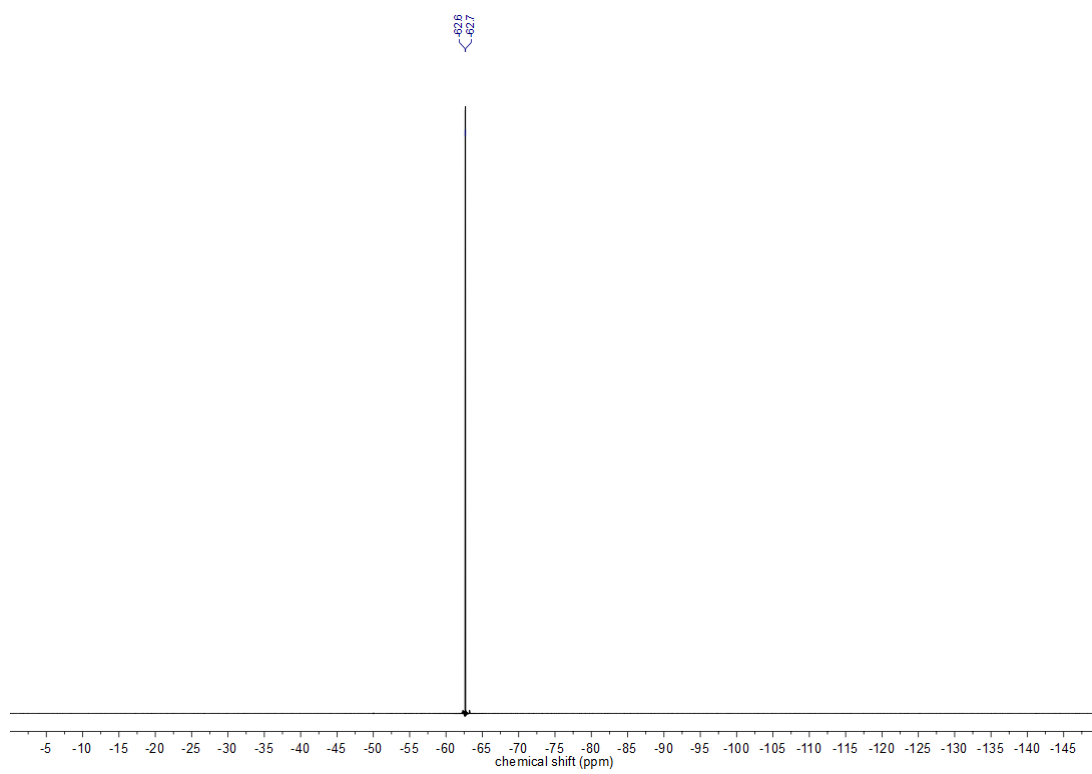
^{31}P-NMR(162 MHz, CD$_3$CN) **159b**
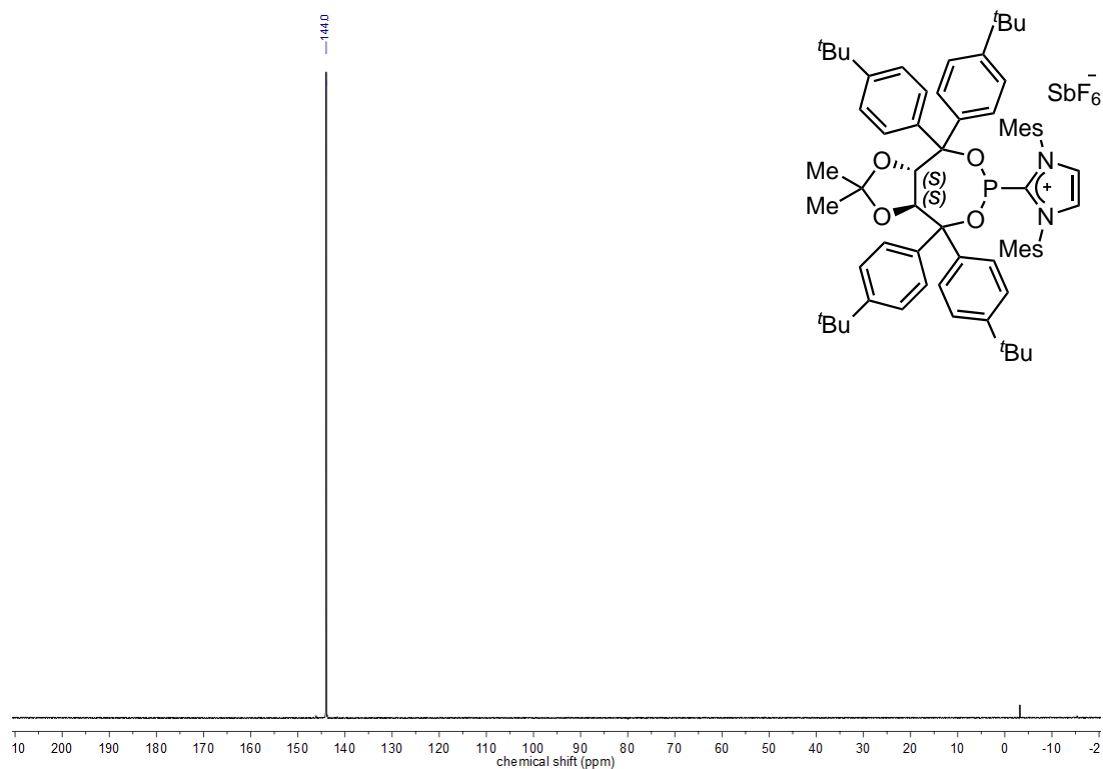
^{1}H-NMR(400 MHz, CD$_3$CN) **159b**
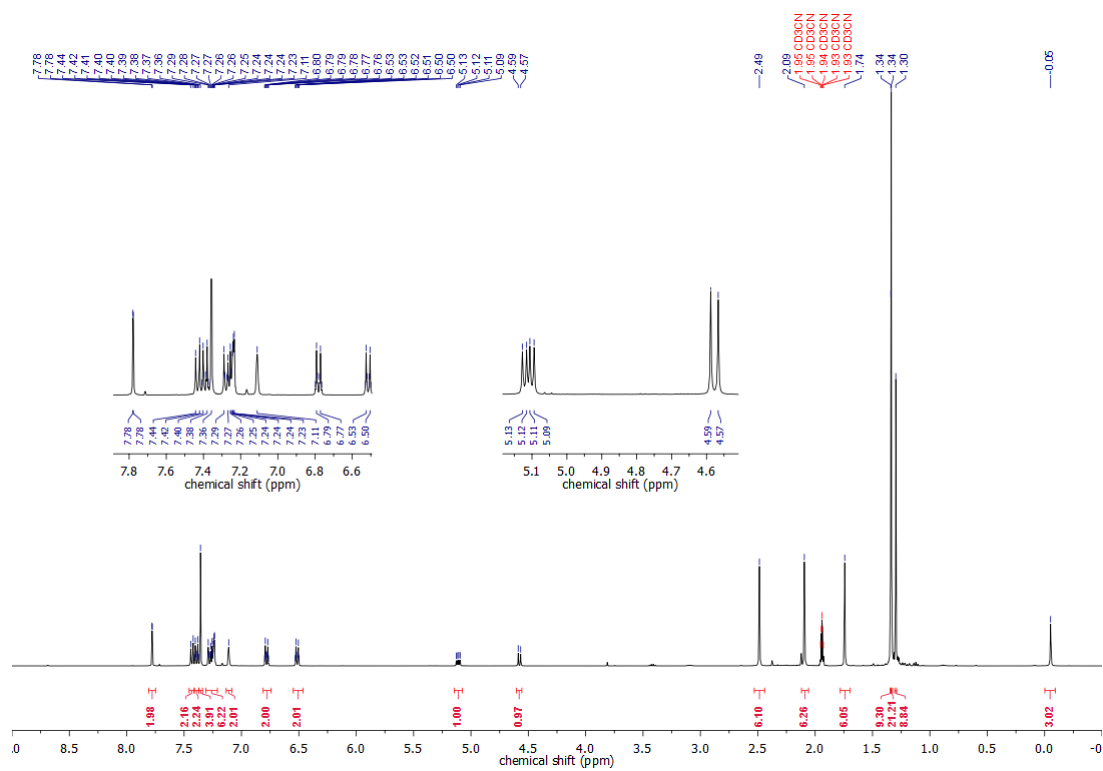
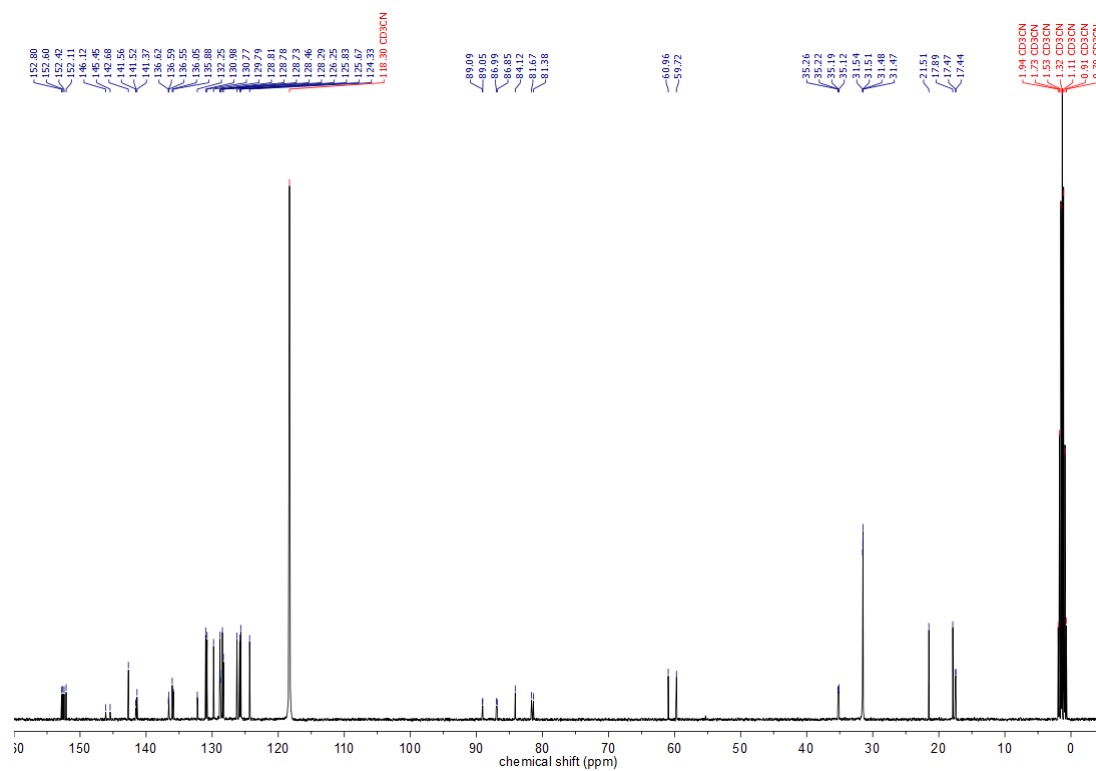^{13}C-NMR(101 MHz, CD$_3$CN) **159b**
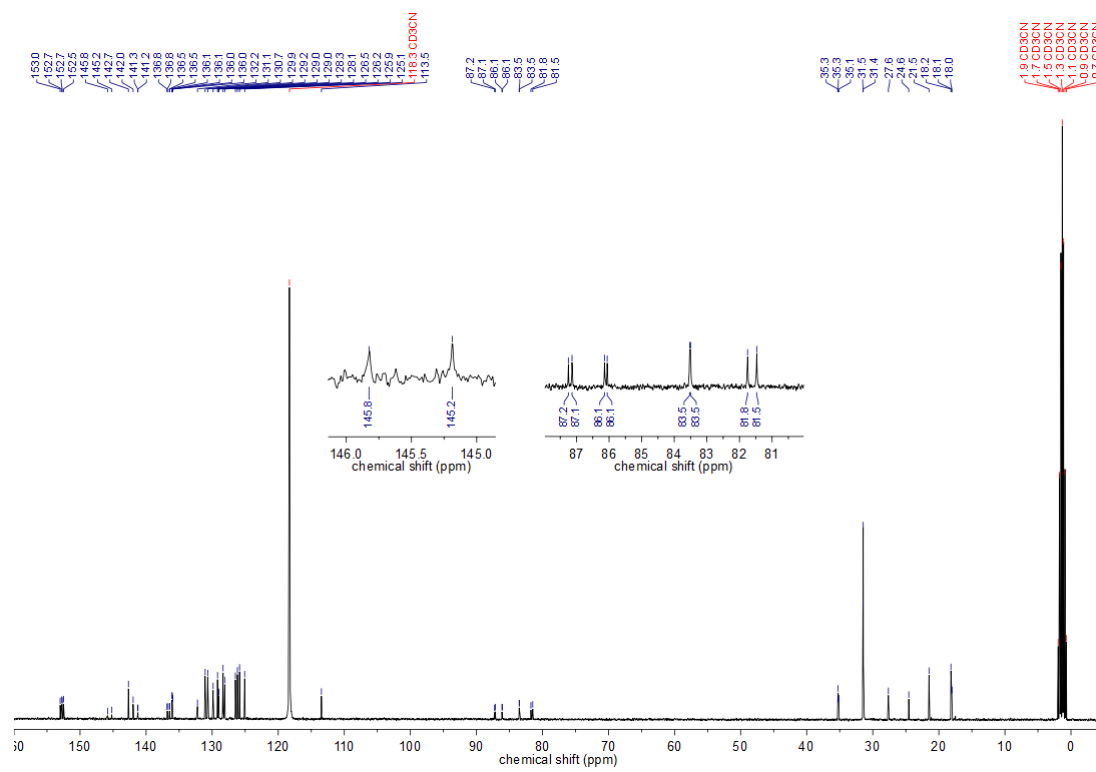
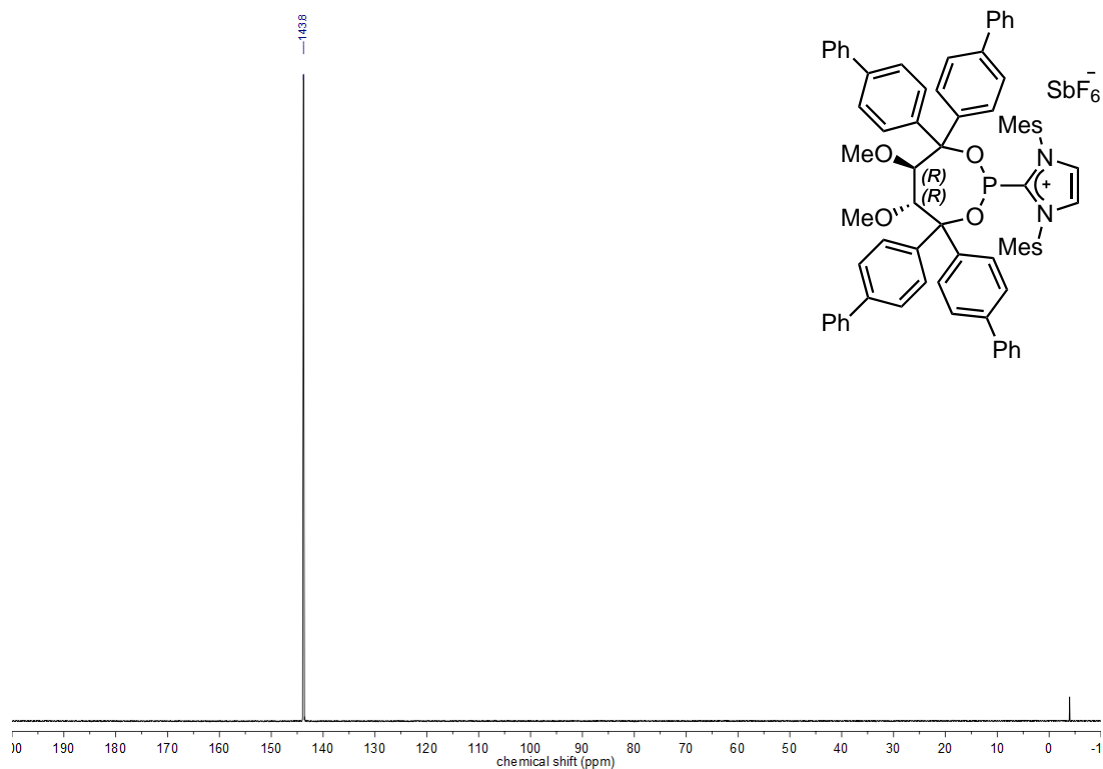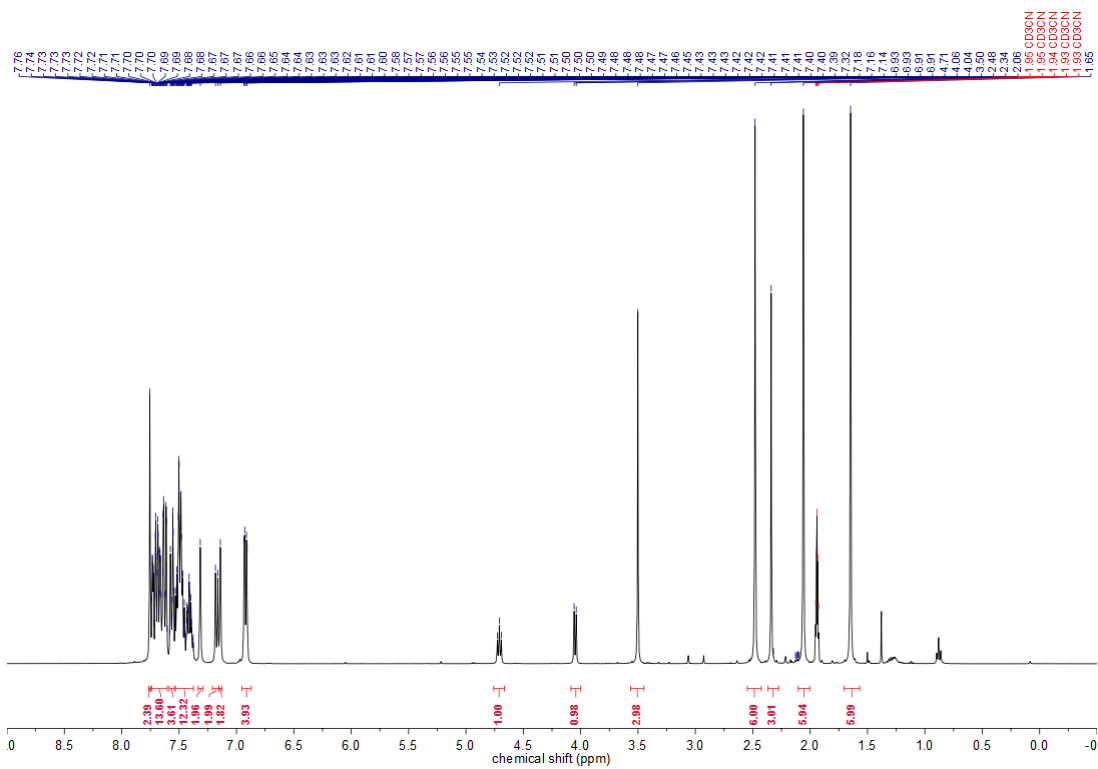^{31}P-NMR(162 MHz, CD$_3$CN) **159c**

^{1}H-NMR(400 MHz, CD$_3$CN) **159c**
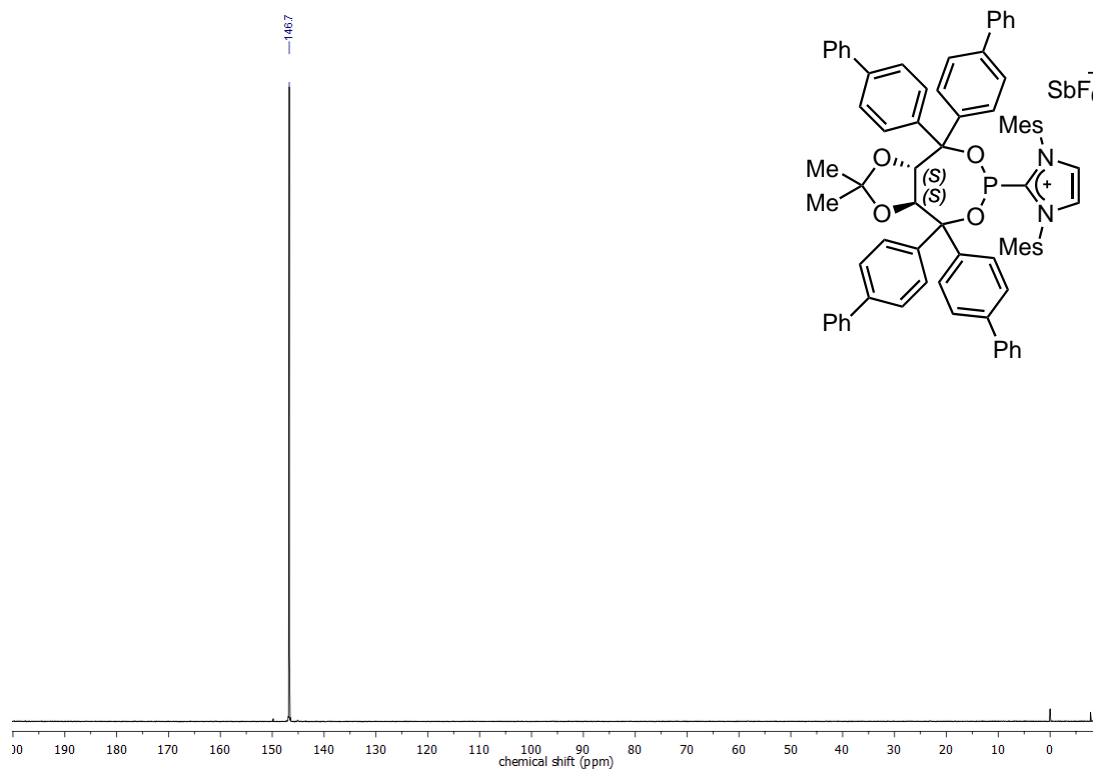
^{13}C-NMR(101 MHz, CD$_3$CN) **159c**
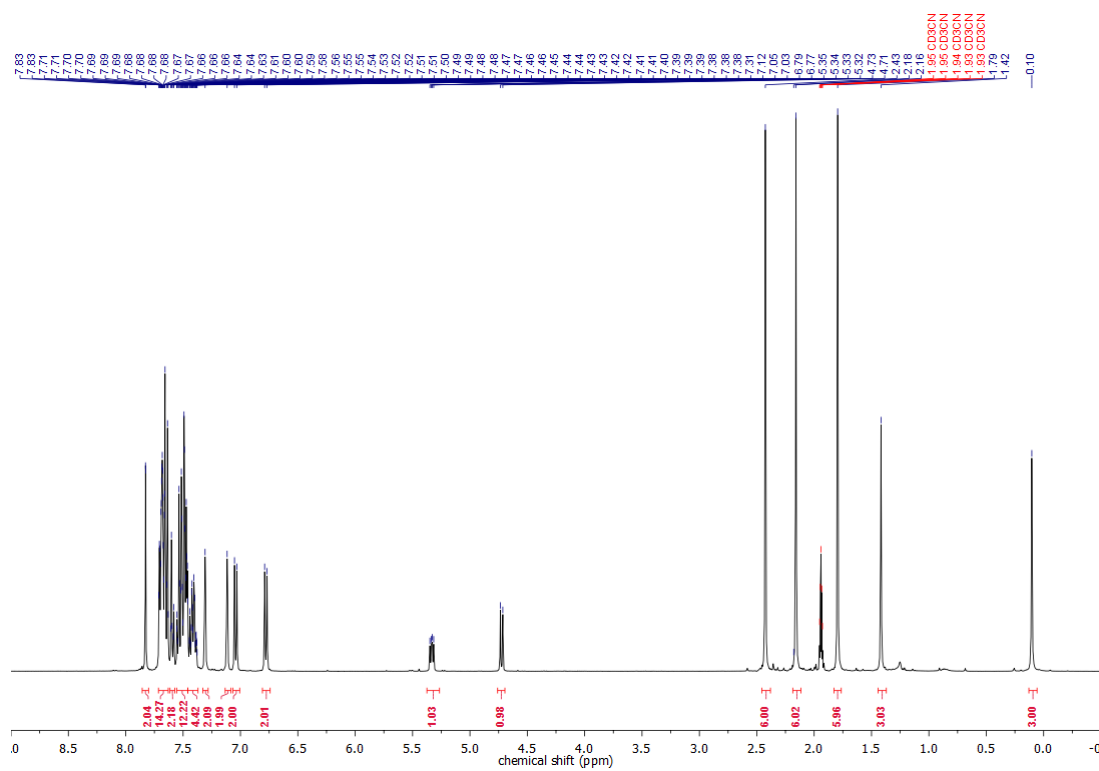
^{31}P-NMR(162 MHz, CD$_3$CN) **159d**

^{1}H-NMR(400 MHz, CD$_3$CN) **159d**

^{13}C-NMR(101 MHz, CD$_3$CN) **159d**
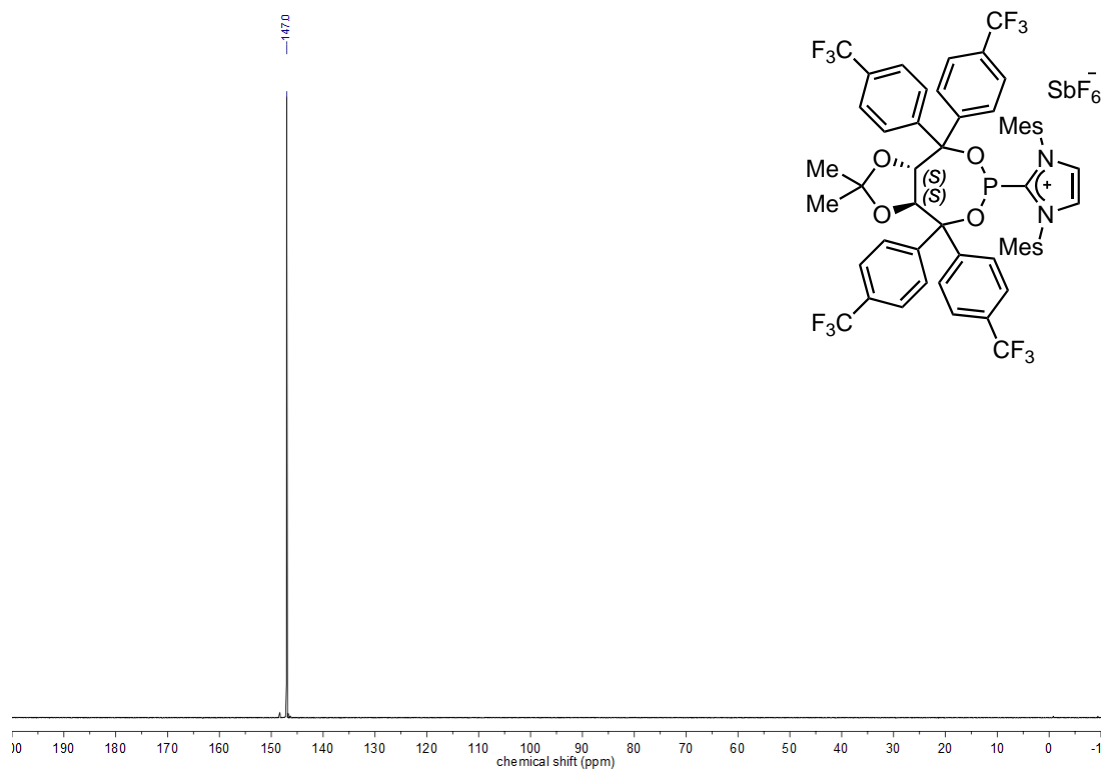
^{19}F-NMR(282 MHz, CD$_3$CN) **159d**

^{31}P-NMR(162 MHz, CD$_3$CN) **159e**

^{1}H-NMR(400 MHz, CD$_3$CN) **159e**

^{13}C-NMR(101 MHz, CD$_3$CN) **159e**
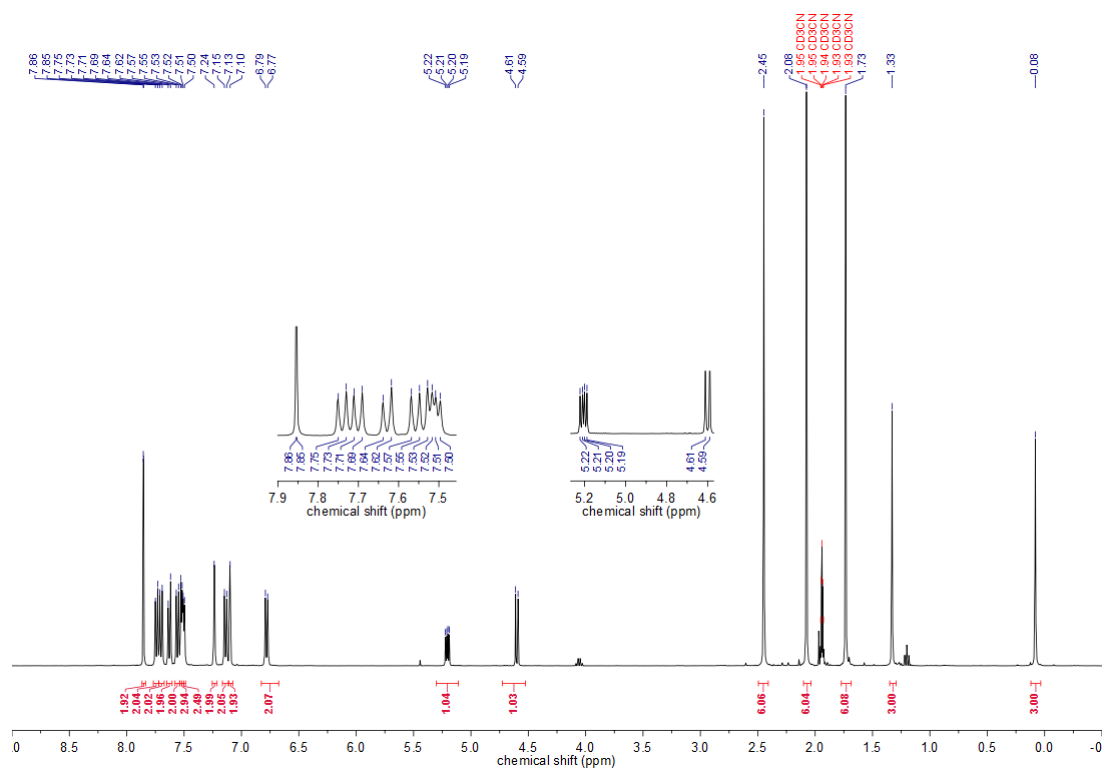
^{31}P-NMR(162 MHz, CD$_3$CN) **159f**

^{1}H-NMR(400 MHz, CD$_3$CN) **159f**
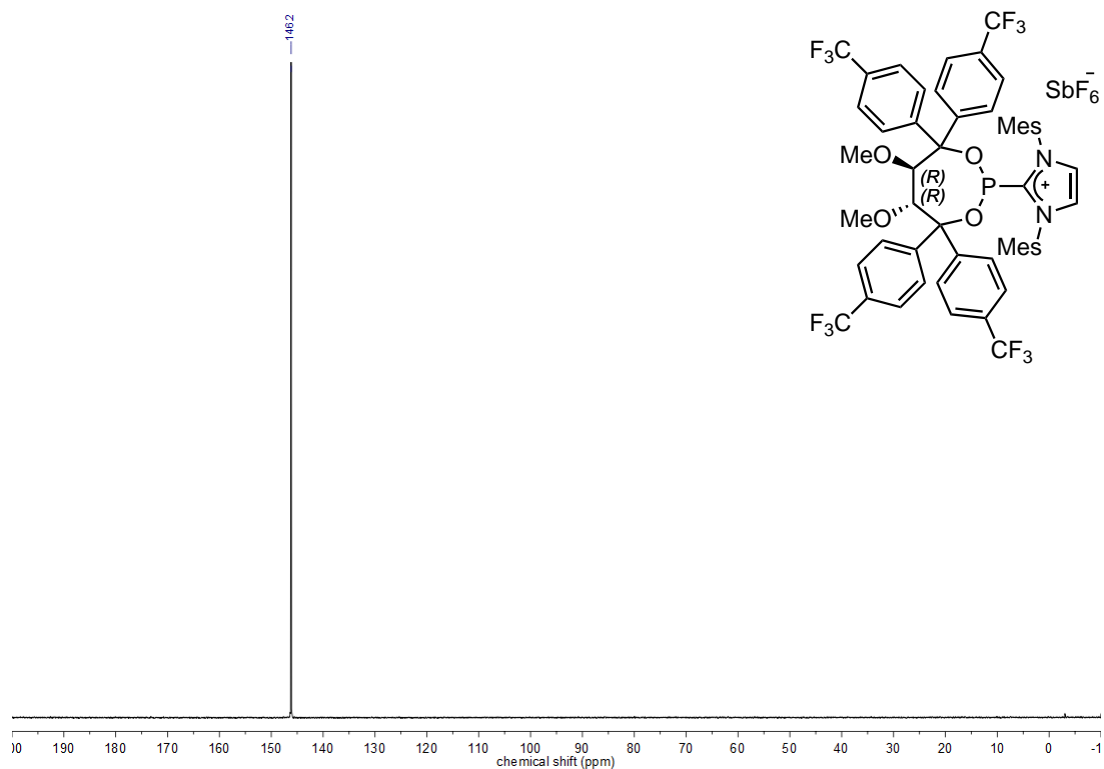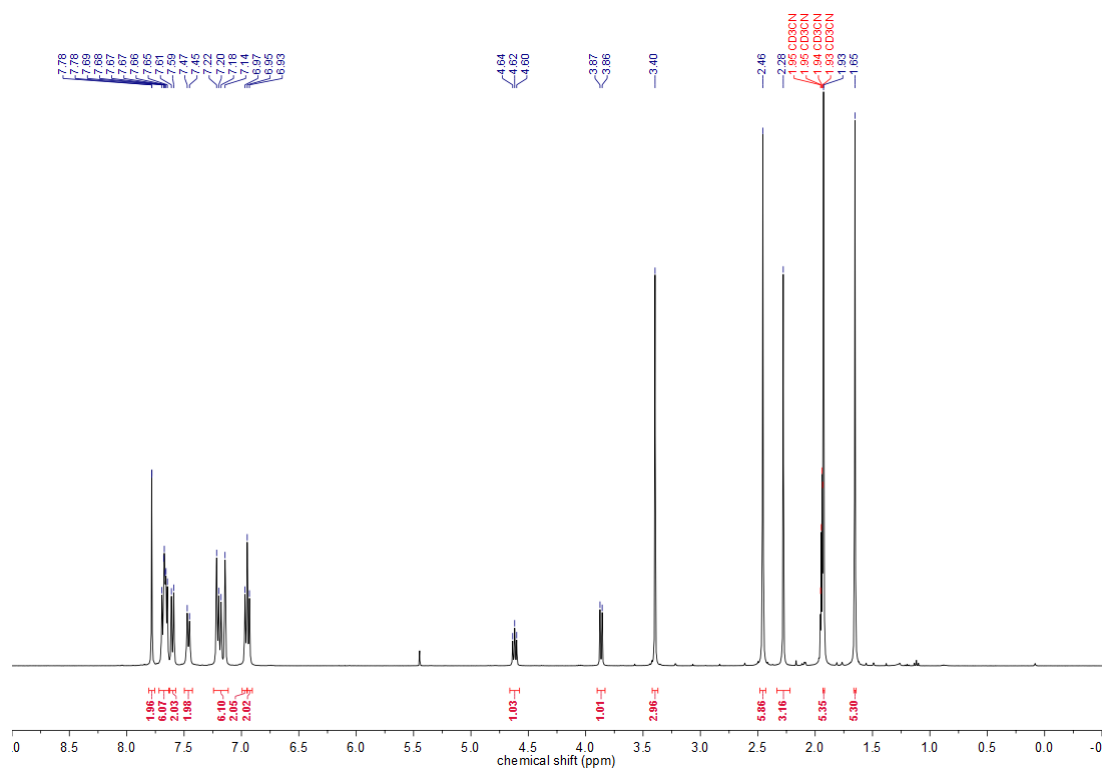
^{13}C-NMR(101 MHz, CD$_3$CN) **159f**
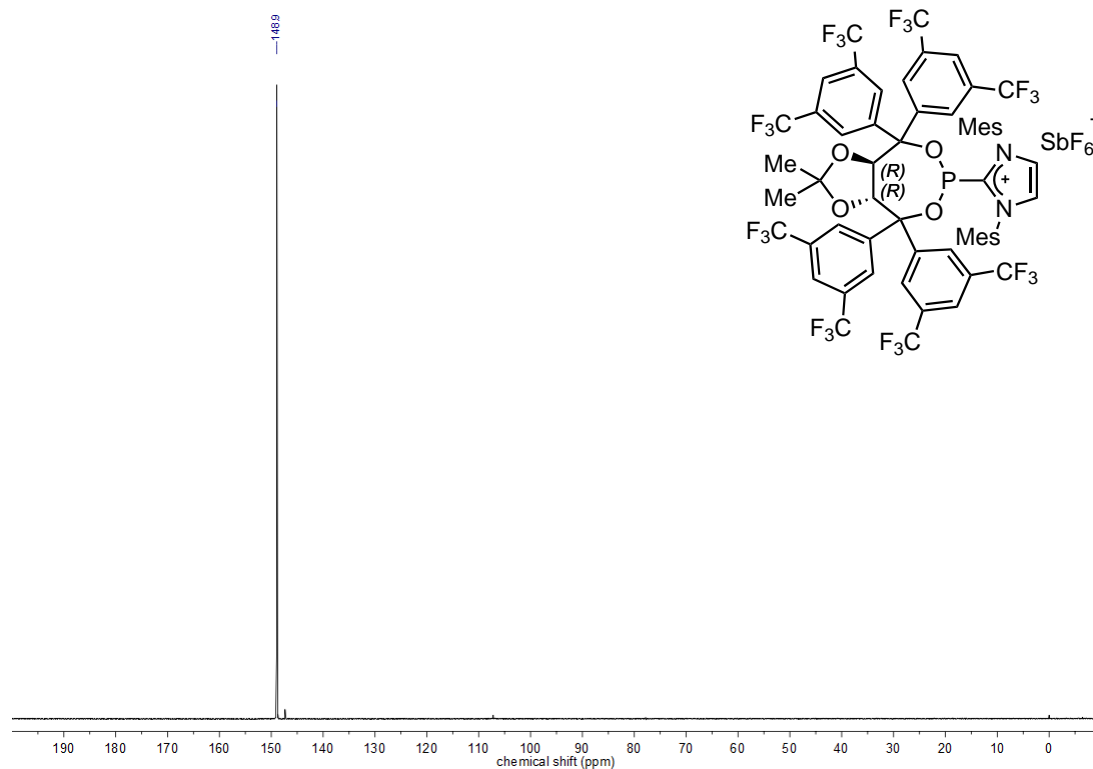
^{19}F-NMR(282 MHz, CD$_3$CN) **159f**
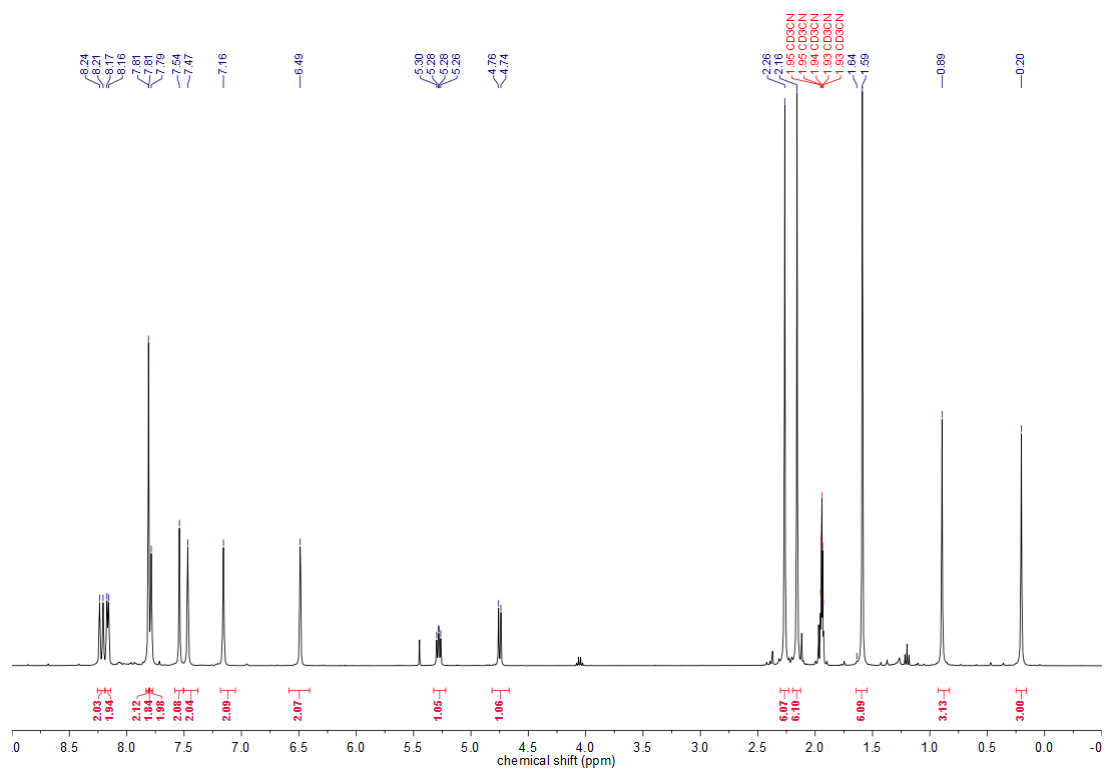
^{31}P-NMR(162 MHz, CD$_3$CN) **160b**
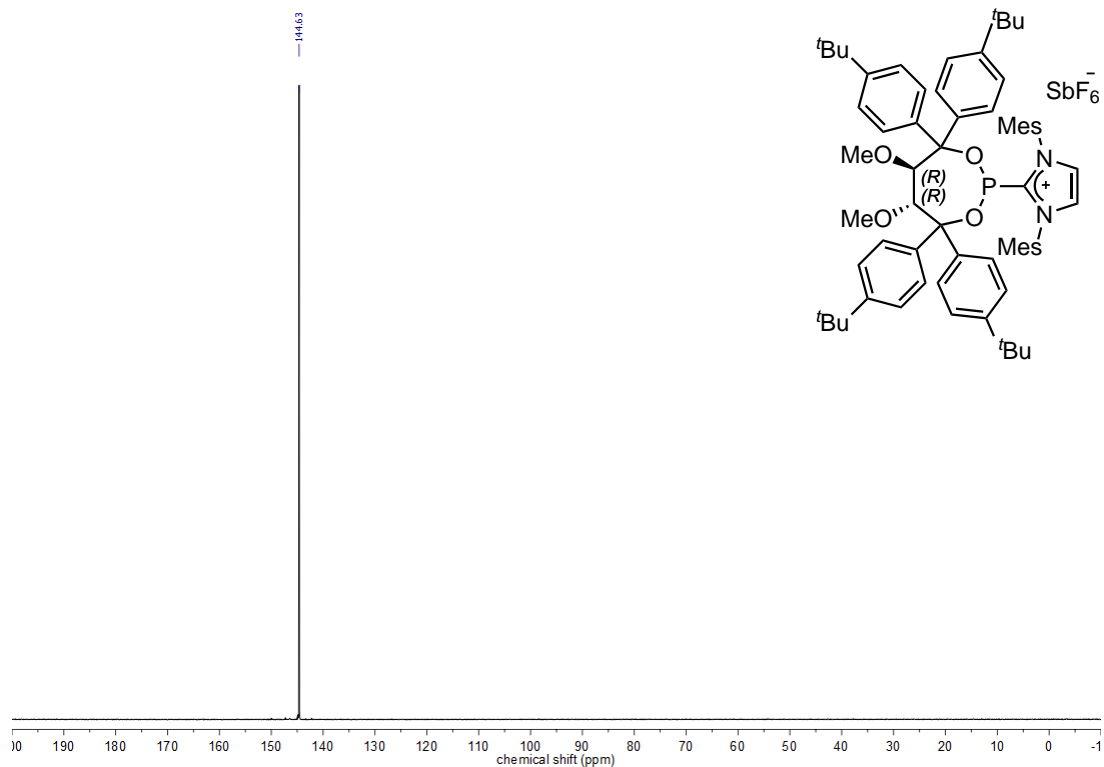
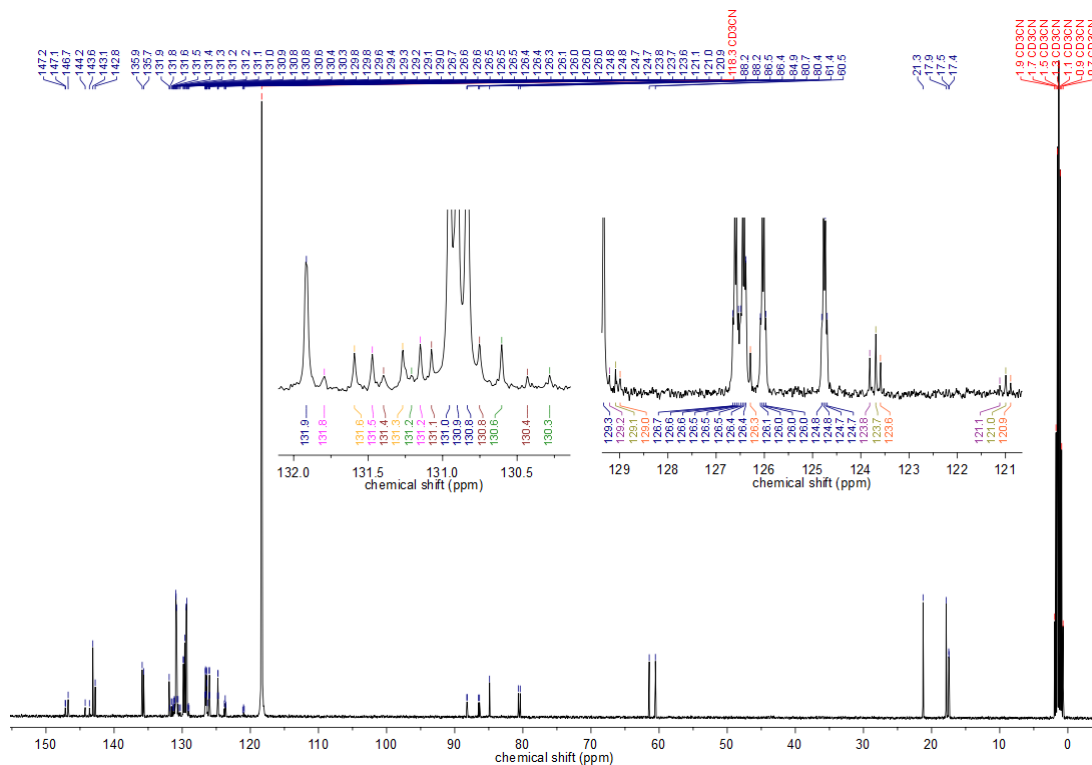^{1}H-NMR(400 MHz, CD$_3$CN) **160b**

^{13}C-NMR(101 MHz, CD$_3$CN) **160b**

^{31}P-NMR(162 MHz, CD$_3$CN) **160c**

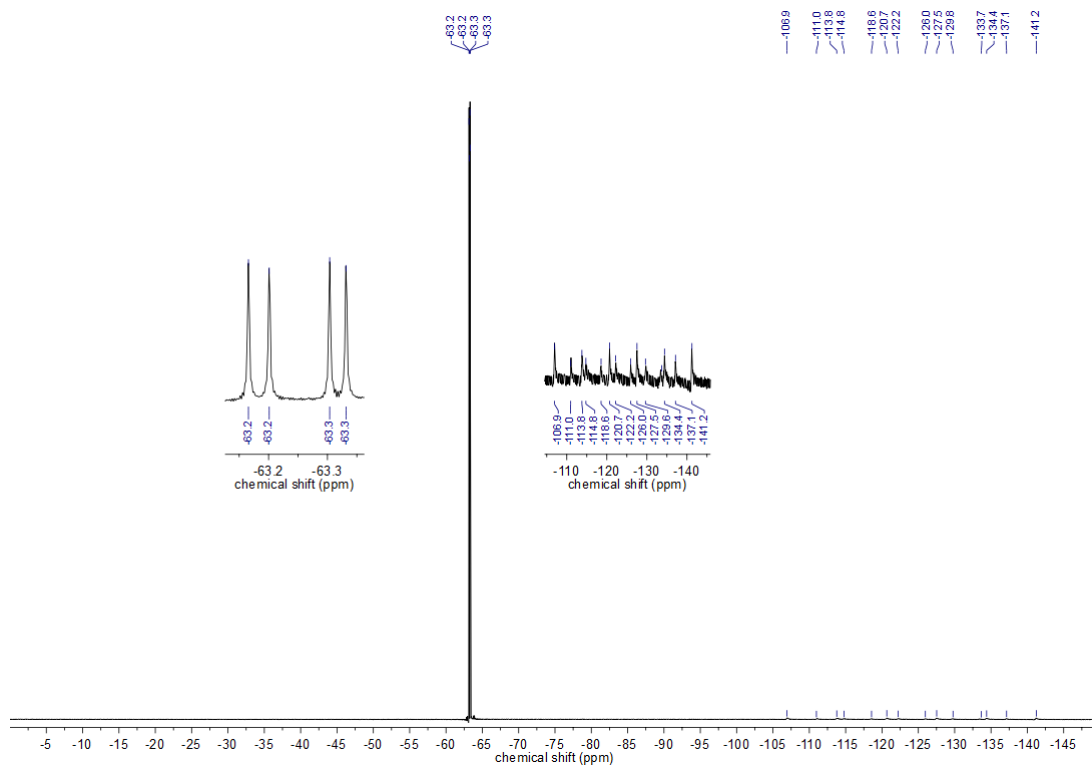^{1}H-NMR(400 MHz, CD$_3$CN) **160c**

^{13}C-NMR(101 MHz, CD$_3$CN) **160c**
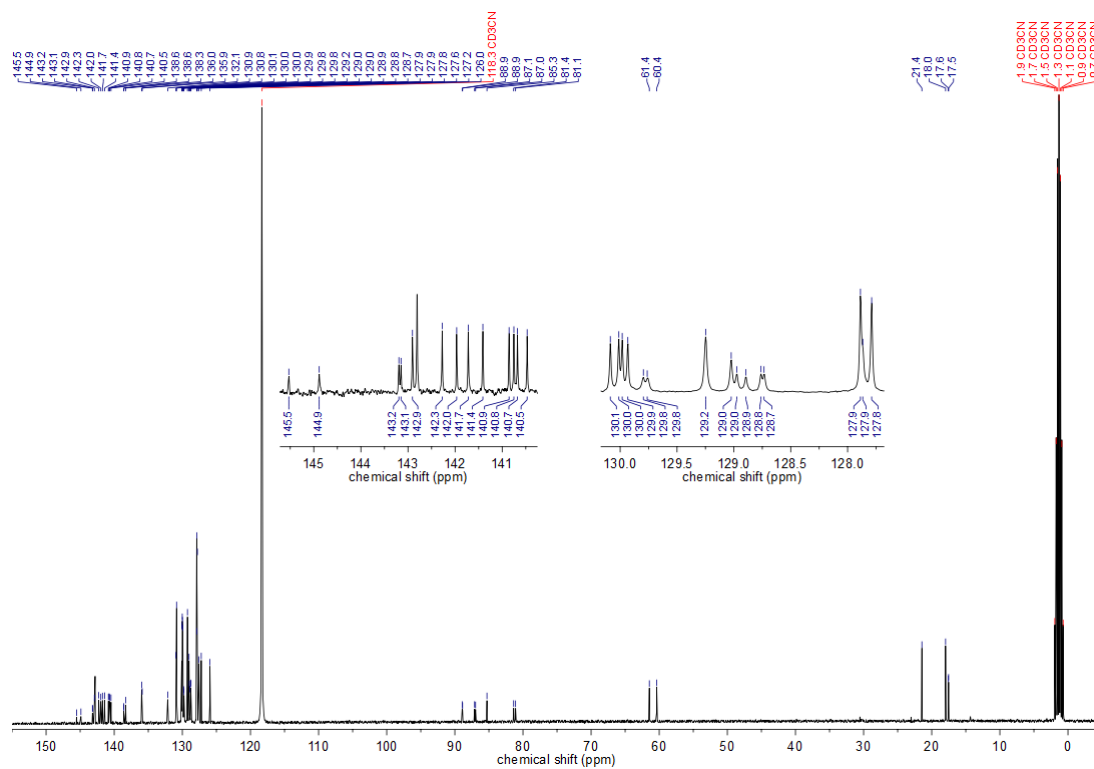
^{31}P-NMR(162 MHz, CD$_3$CN) **160d**

^{1}H-NMR(400 MHz, CD$_3$CN) **160d**

^{13}C-NMR(101 MHz, CD$_3$CN) **160d**

^{19}F-NMR(282 MHz, CD$_3$CN) **160d**

^{31}P-NMR(162 MHz, CD$_3$CN) **161**

^{1}H-NMR(400 MHz, CD$_3$CN) **161**

^{13}C-NMR(101 MHz, CD$_3$CN) **161**
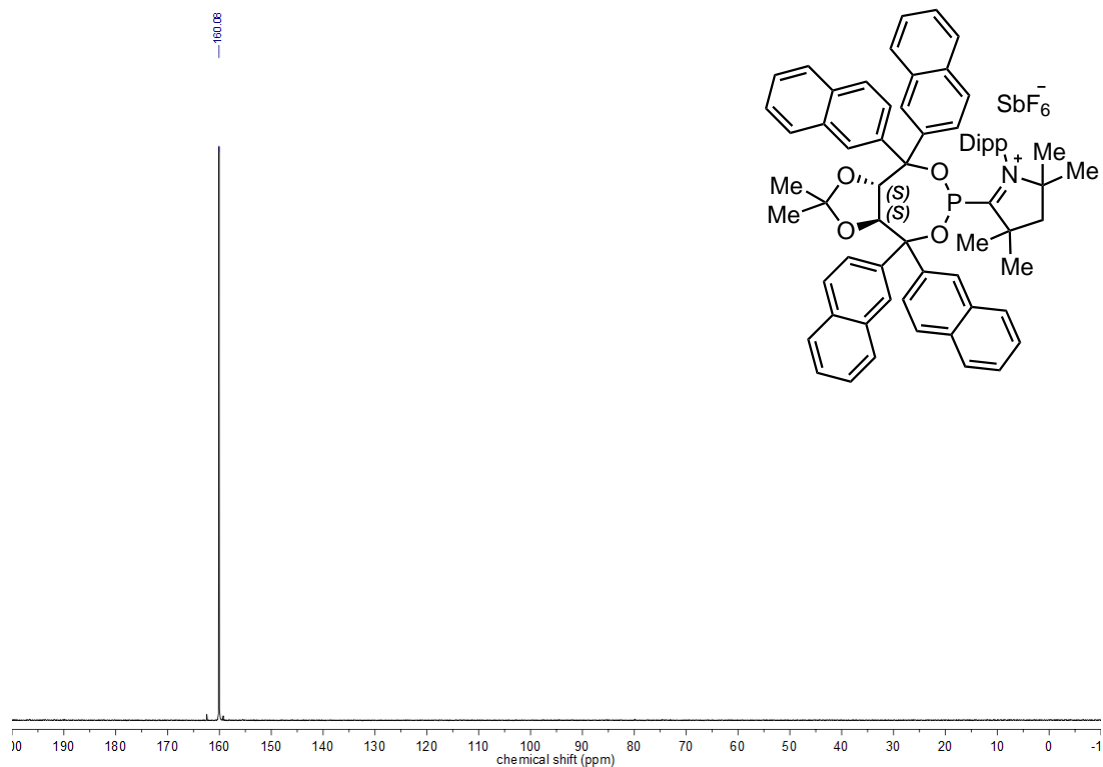
^{19}F-NMR(282 MHz, CD$_3$CN) **161**

^{31}P-NMR(162 MHz, CD$_3$CN) **162**

^{1}H-NMR(400 MHz, CD$_3$CN) **162**

^{13}C-NMR(101 MHz, CD$_3$CN) **162**
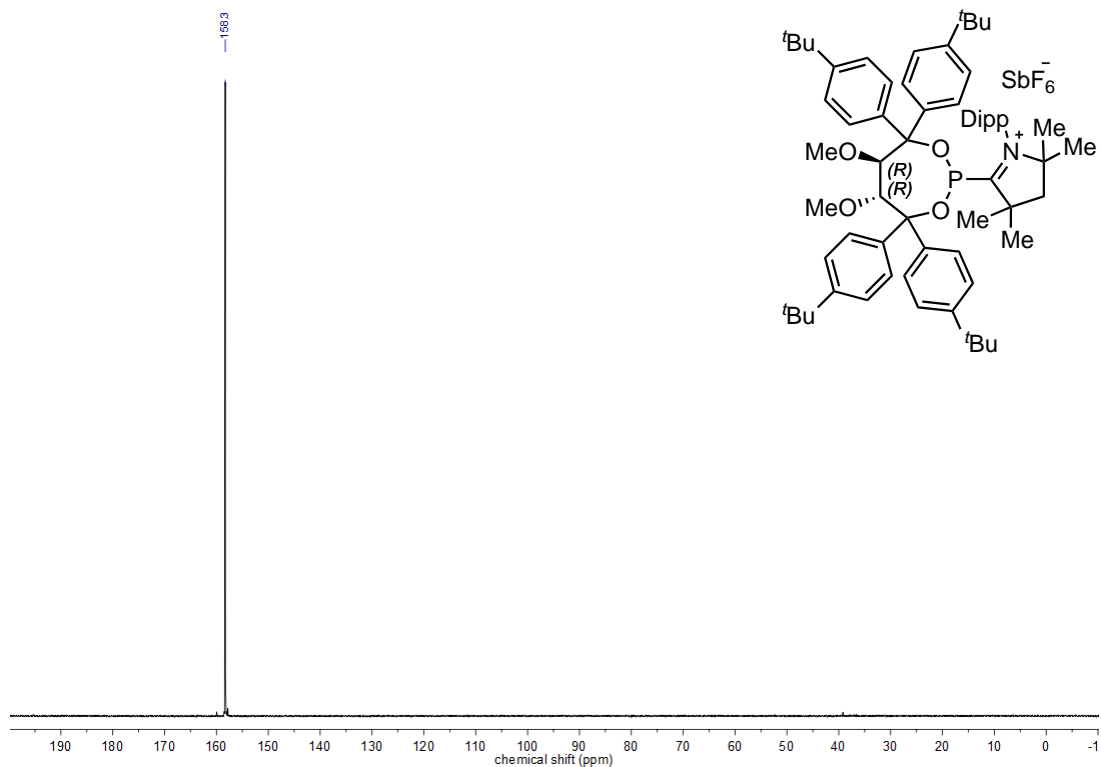
^{19}F-NMR(282 MHz, CD$_3$CN) **162**
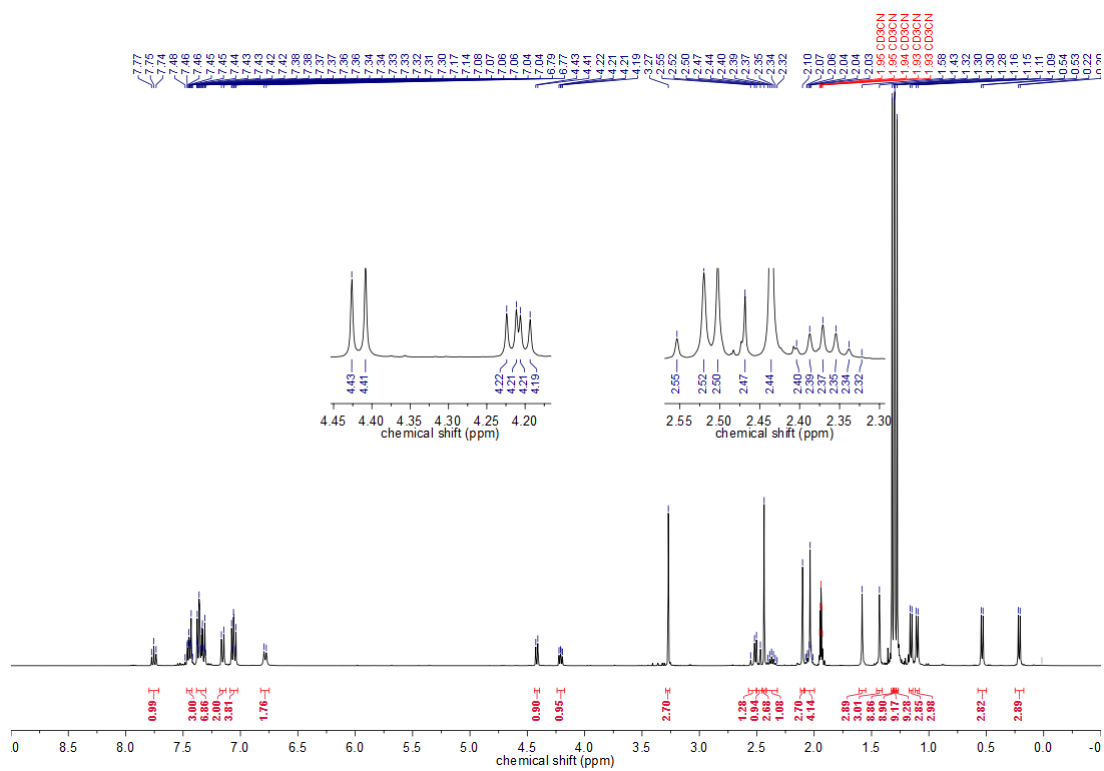
^{31}P-NMR(162 MHz, CD$_3$CN) **164b**

^{1}H-NMR(600 MHz, CD$_3$CN) **164b**
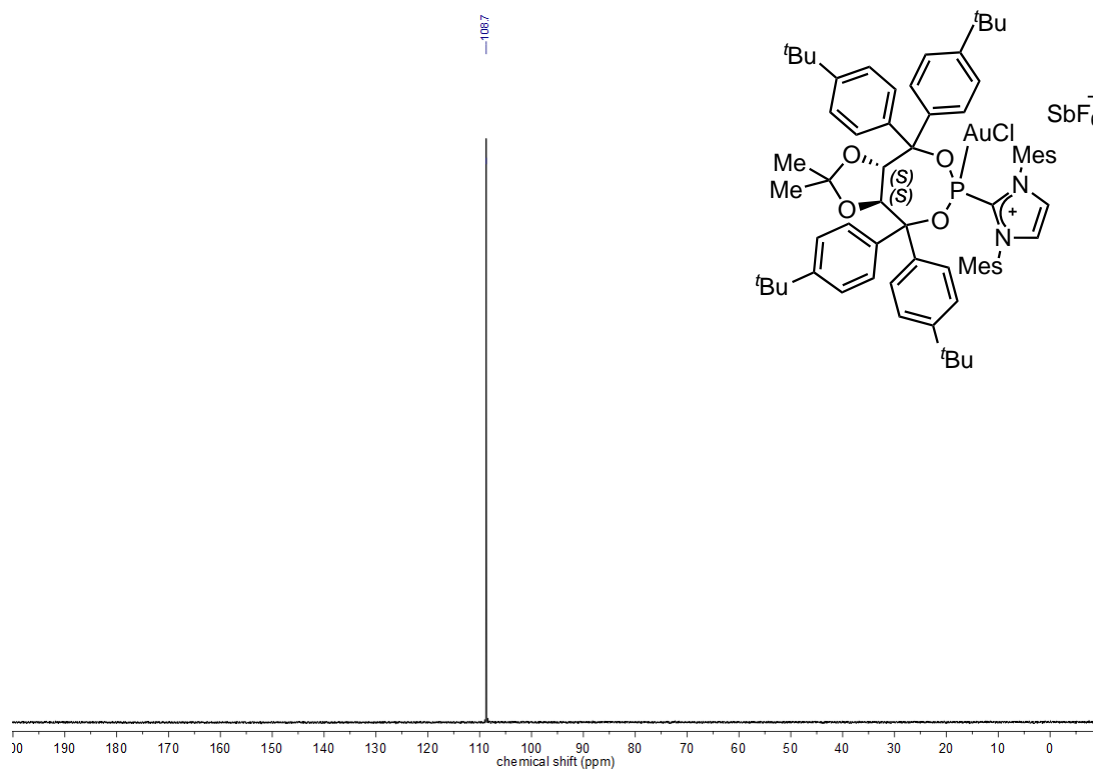
^{13}C-NMR(151 MHz, CD$_3$CN) **164b**
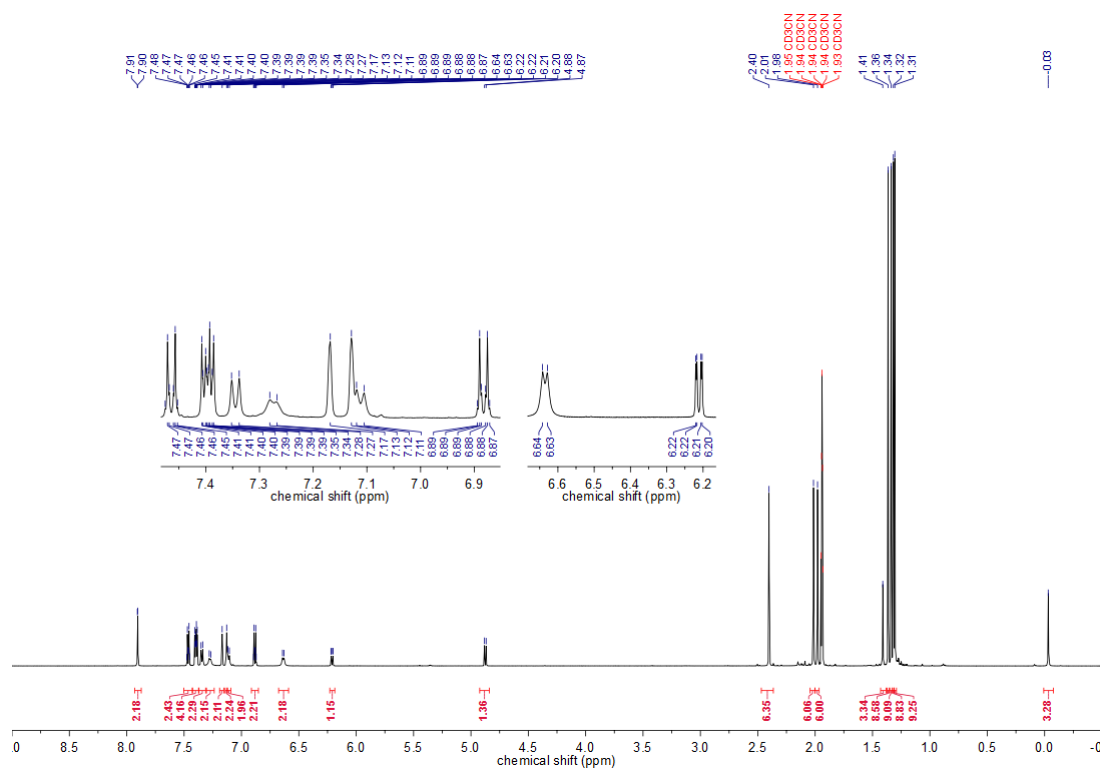
^{31}P-NMR(162 MHz, CD$_3$CN) **164c**

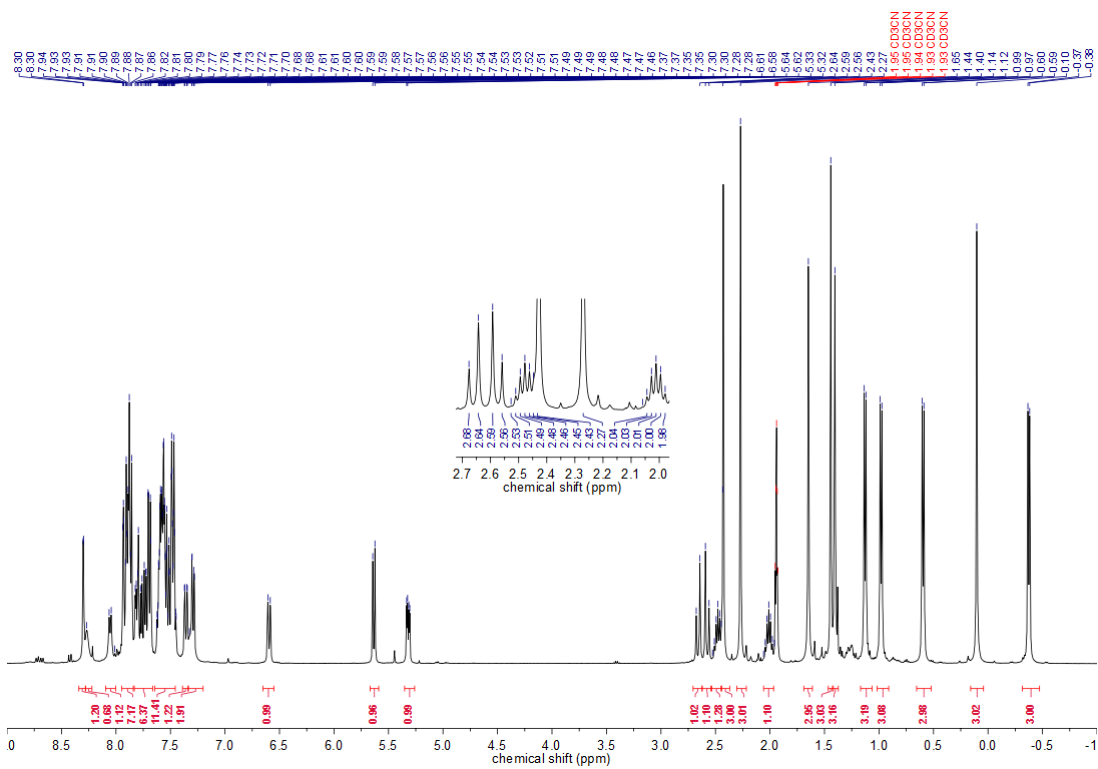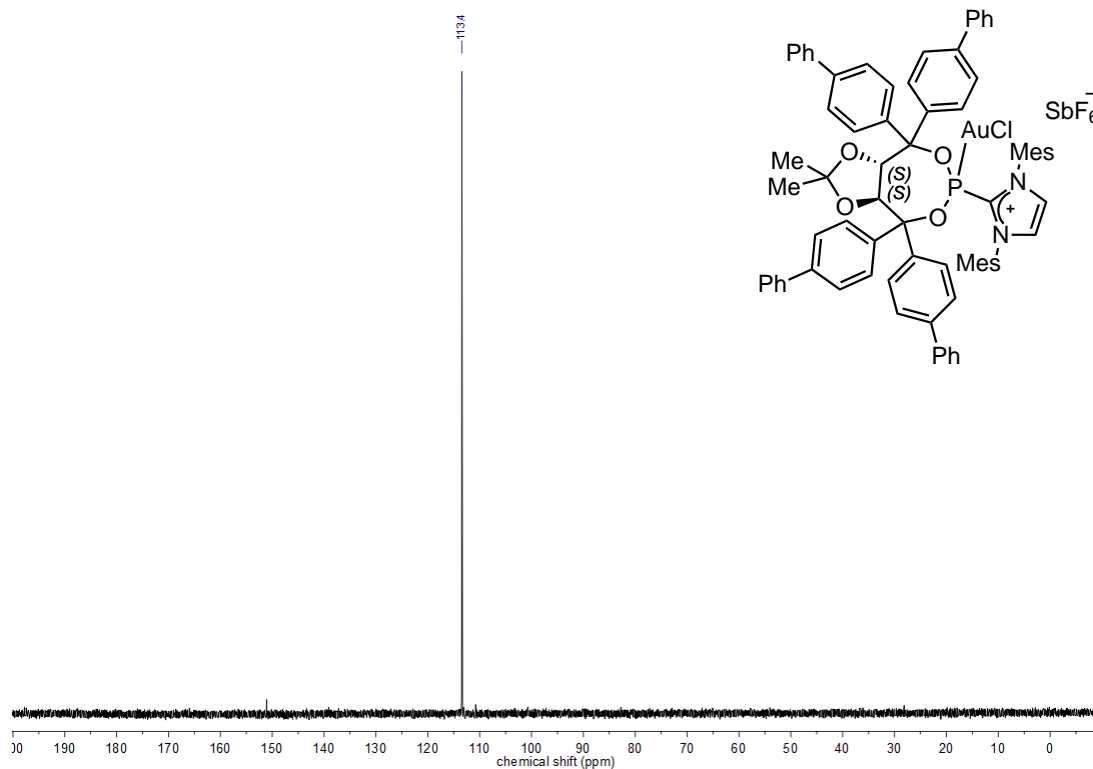^{1}H-NMR(400 MHz, CD$_3$CN) **164c**
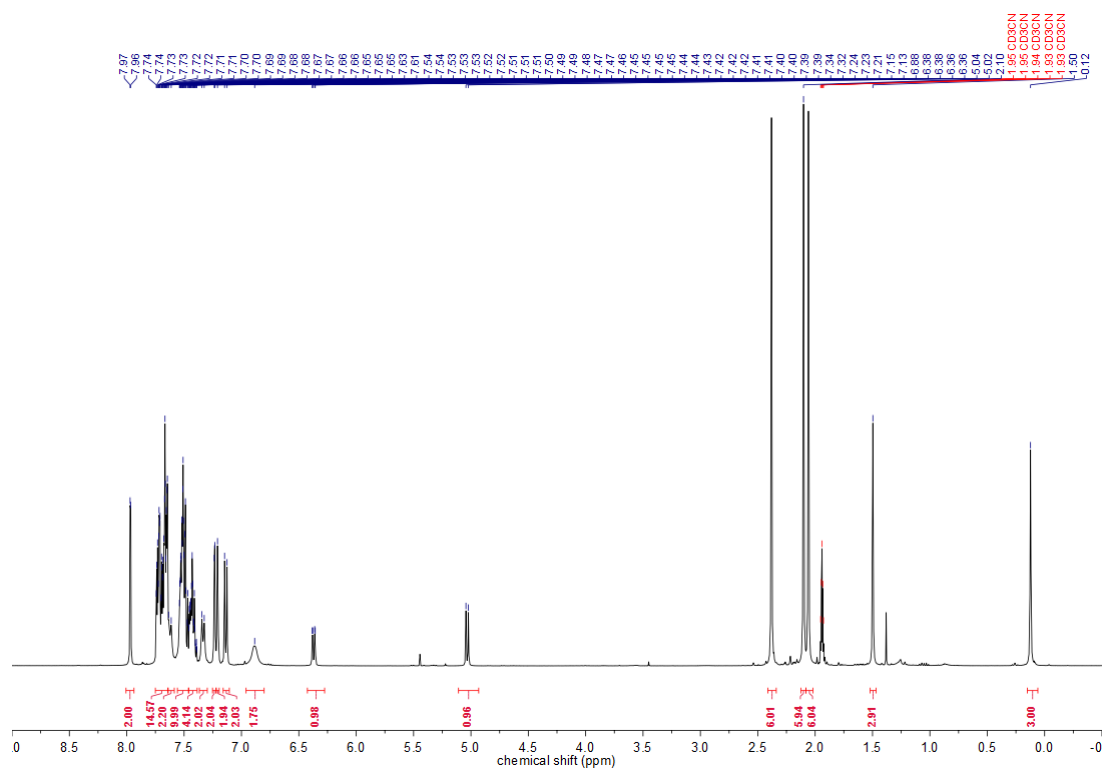
^{13}C-NMR(101 MHz, CD$_3$CN) **164c**

^{31}P-NMR(162 MHz, CD$_3$CN) **164d**

^{1}H-NMR(400 MHz, CD$_3$CN) **164d**

^{13}C-NMR(101 MHz, CD$_3$CN) **164d**

^{19}F-NMR(282 MHz, CD$_3$CN) **164d**
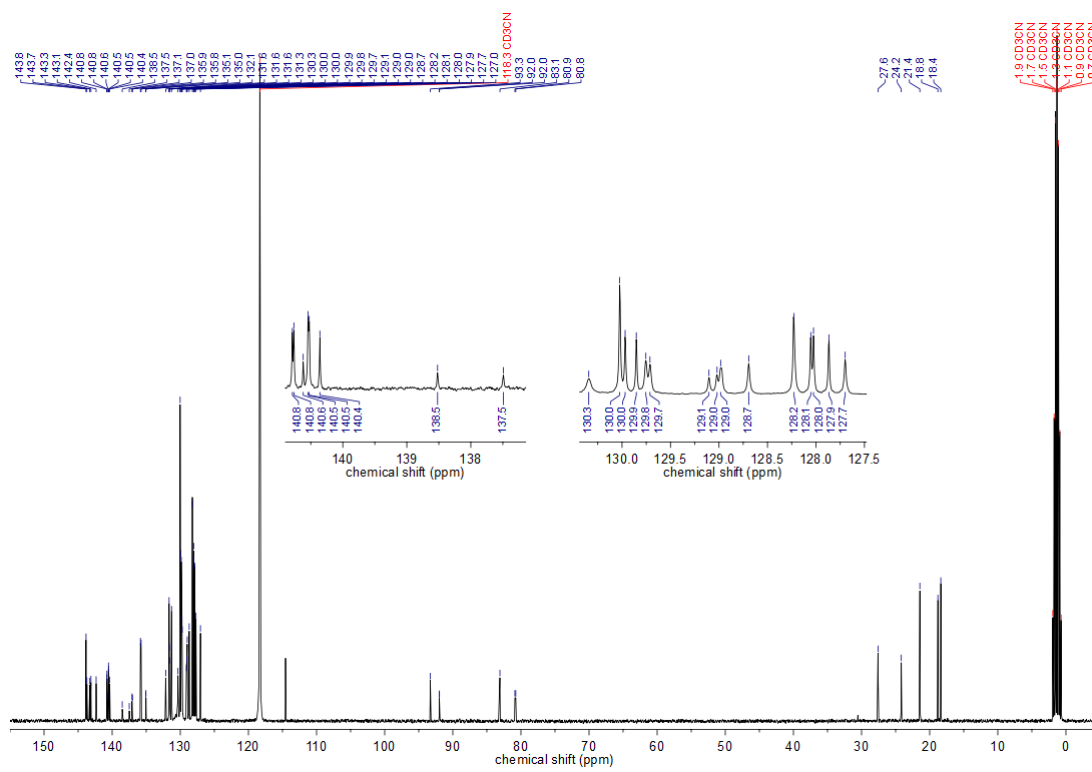
^{31}P-NMR(162 MHz, CD$_3$CN) **164e**
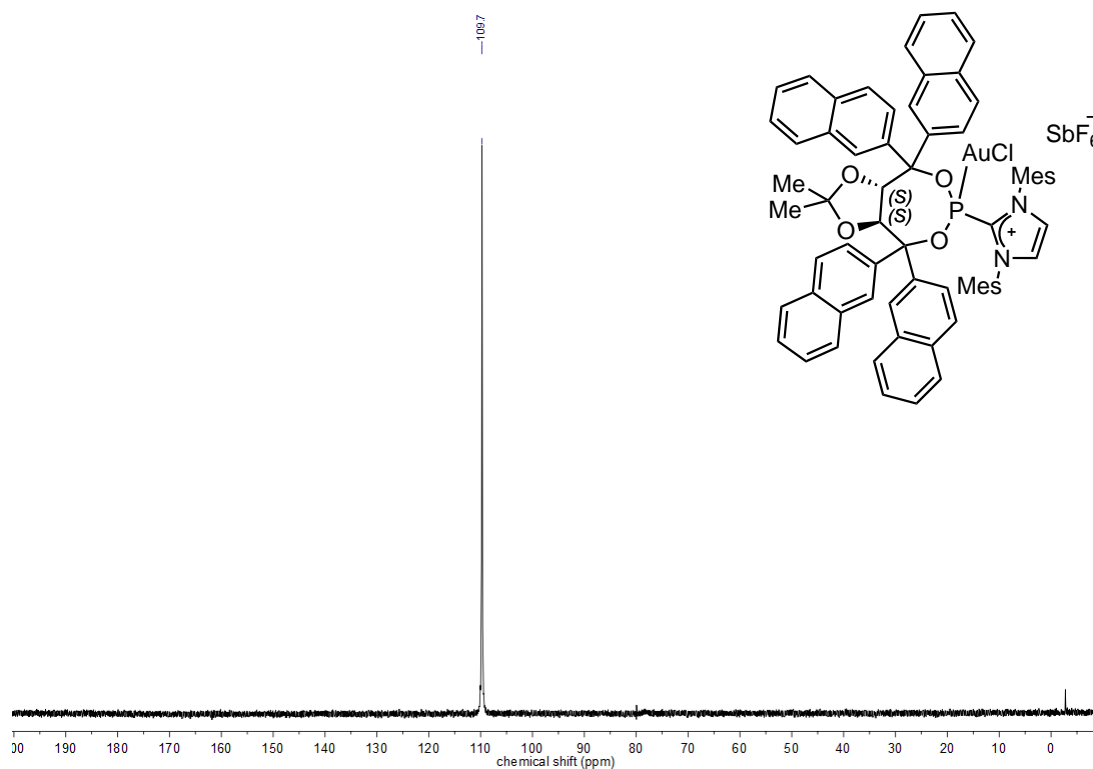
^{1}H-NMR(400 MHz, CD$_3$CN) **164e**
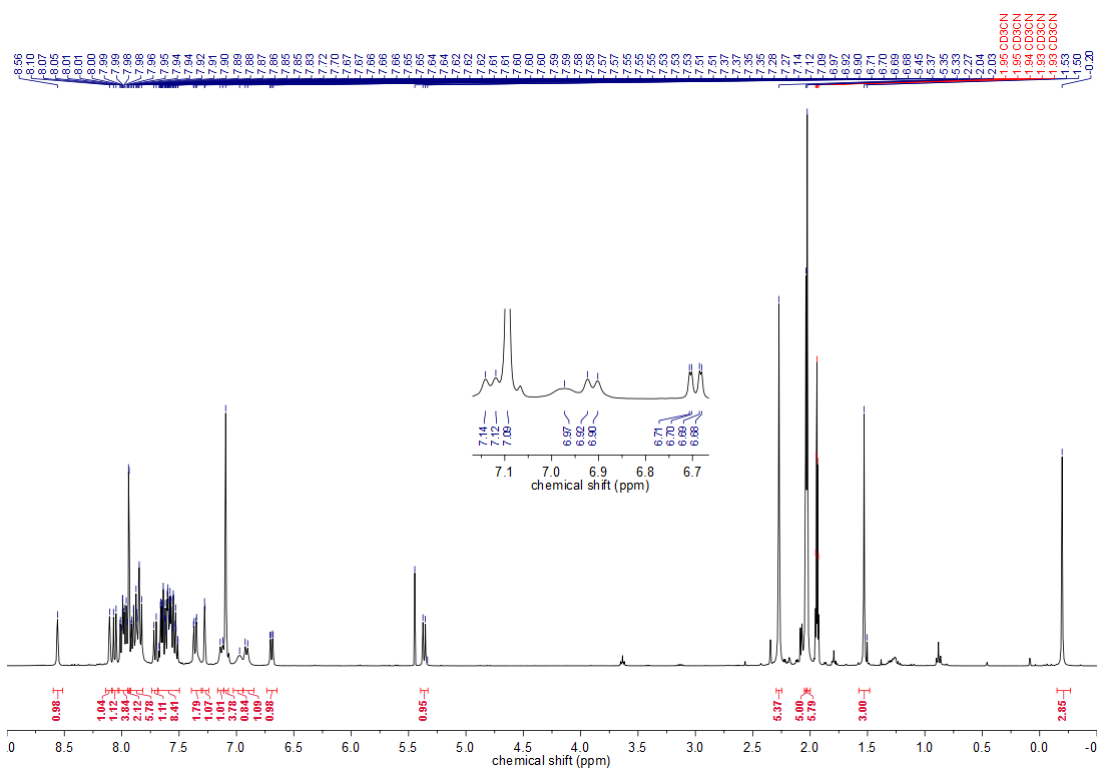
¹³C-NMR(101 MHz, CD₃CN) **164e**
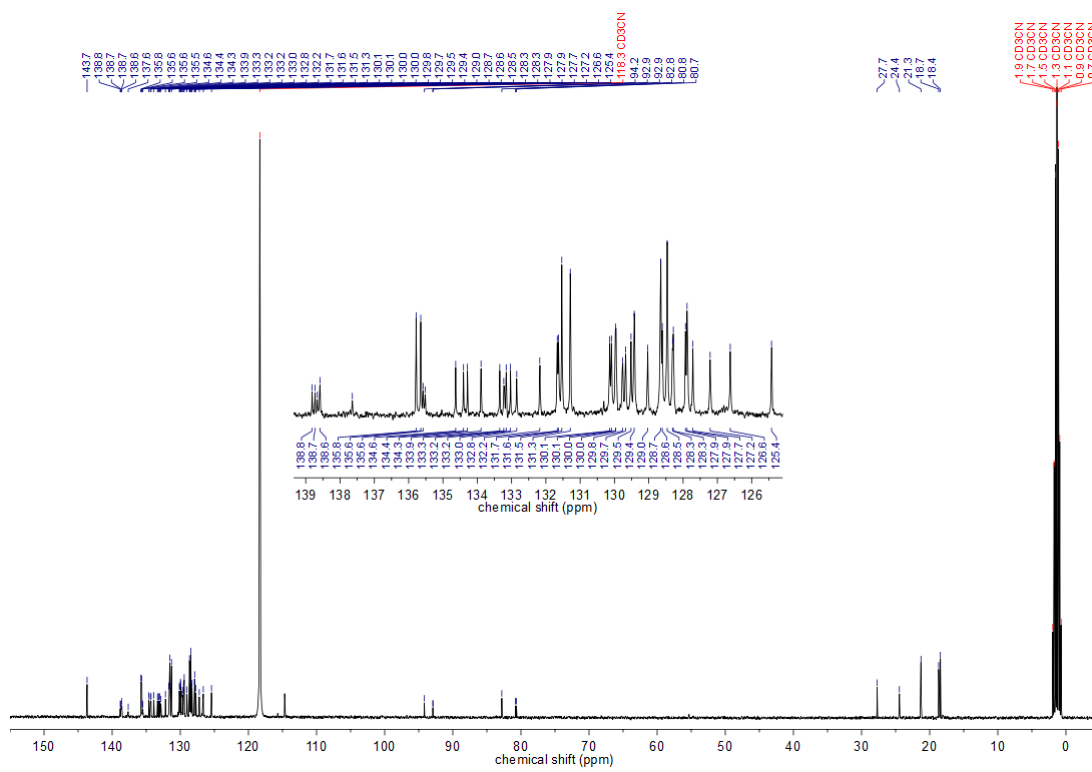
^{31}P-NMR(162 MHz, CD$_3$CN) **164f**

^{1}H-NMR(400 MHz, CD$_3$CN) **164f**

^{13}C-NMR(101 MHz, CD$_3$CN) **164f**
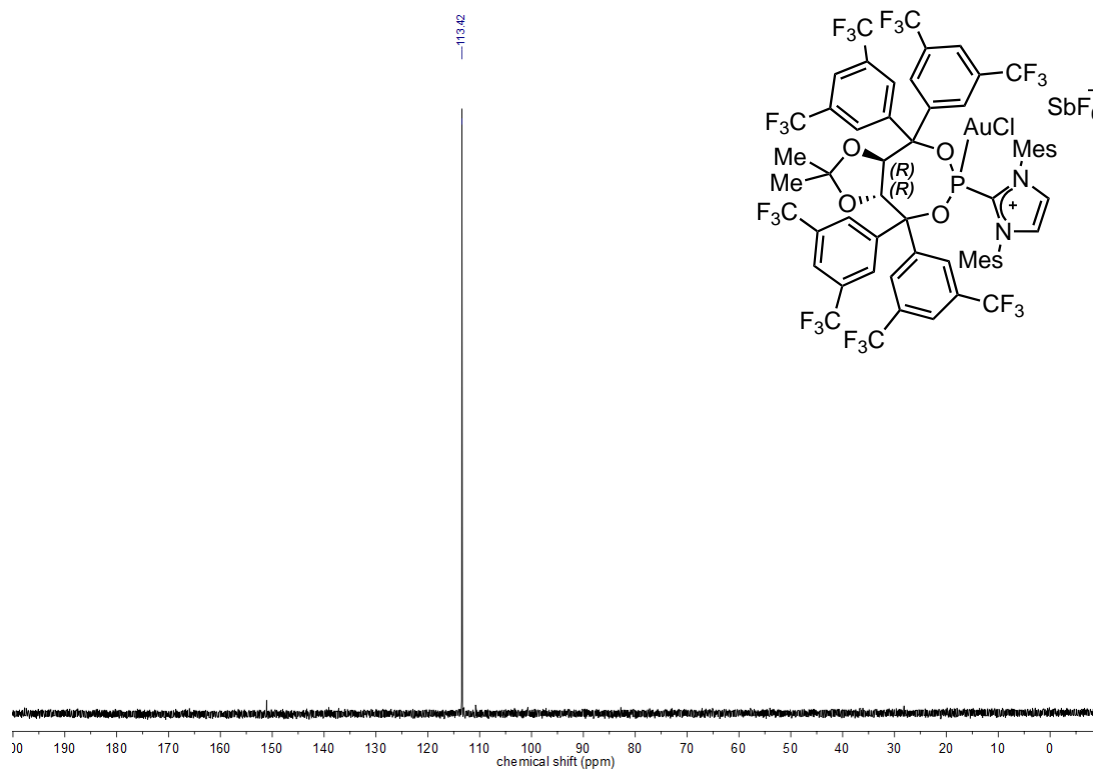
^{19}F-NMR(282 MHz, CD$_3$CN) **164f**
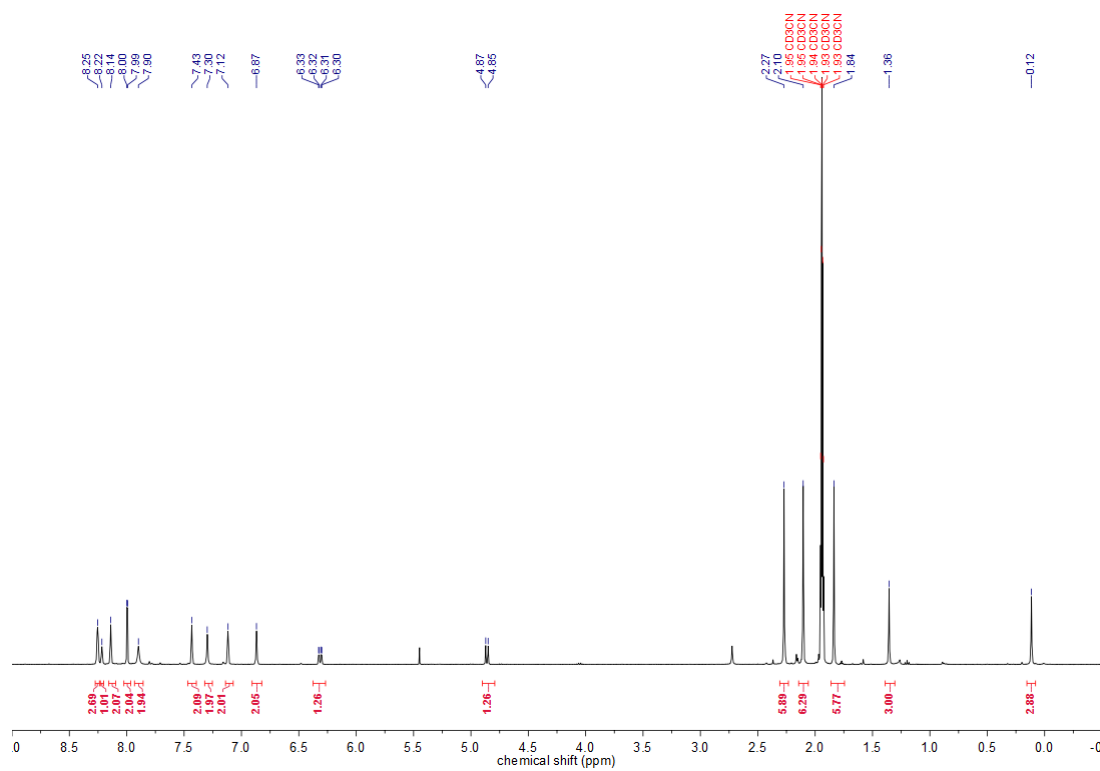
^{31}P-NMR(162 MHz, CD$_3$CN) **165d**

^{1}H-NMR(400 MHz, CD$_3$CN) **165d**

^{13}C-NMR(101 MHz, CD$_3$CN) **165d**
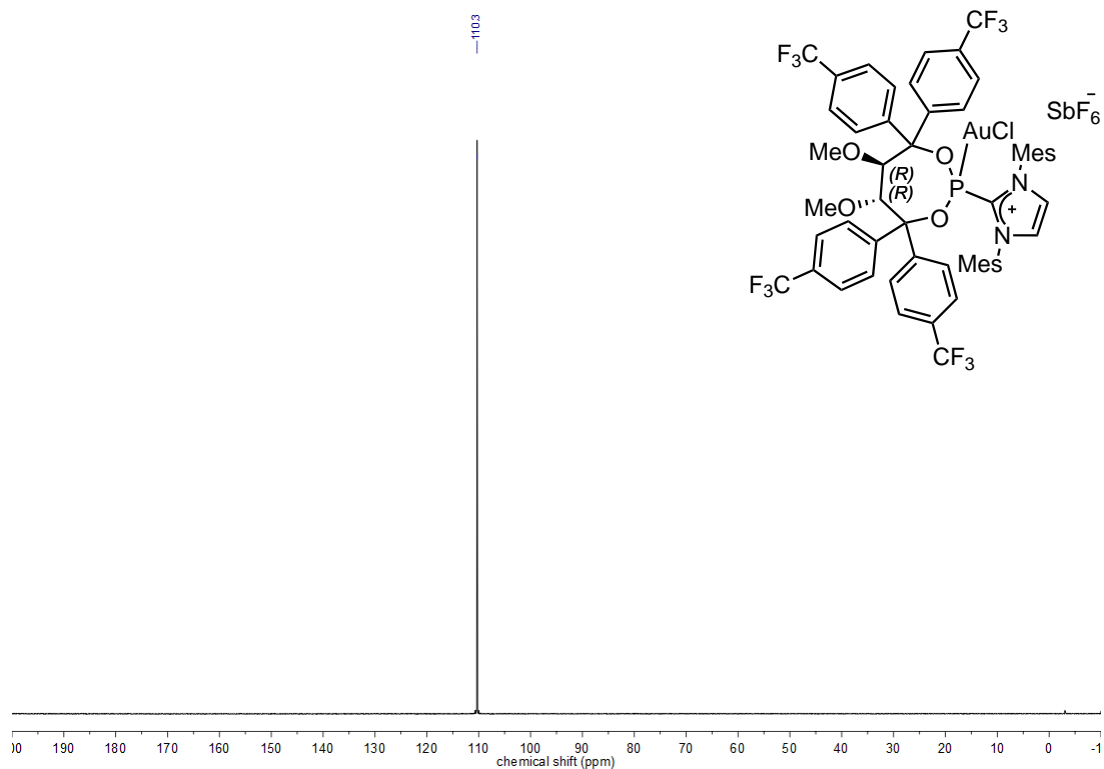
^{19}F-NMR(282 MHz, CD$_3$CN) **165d**
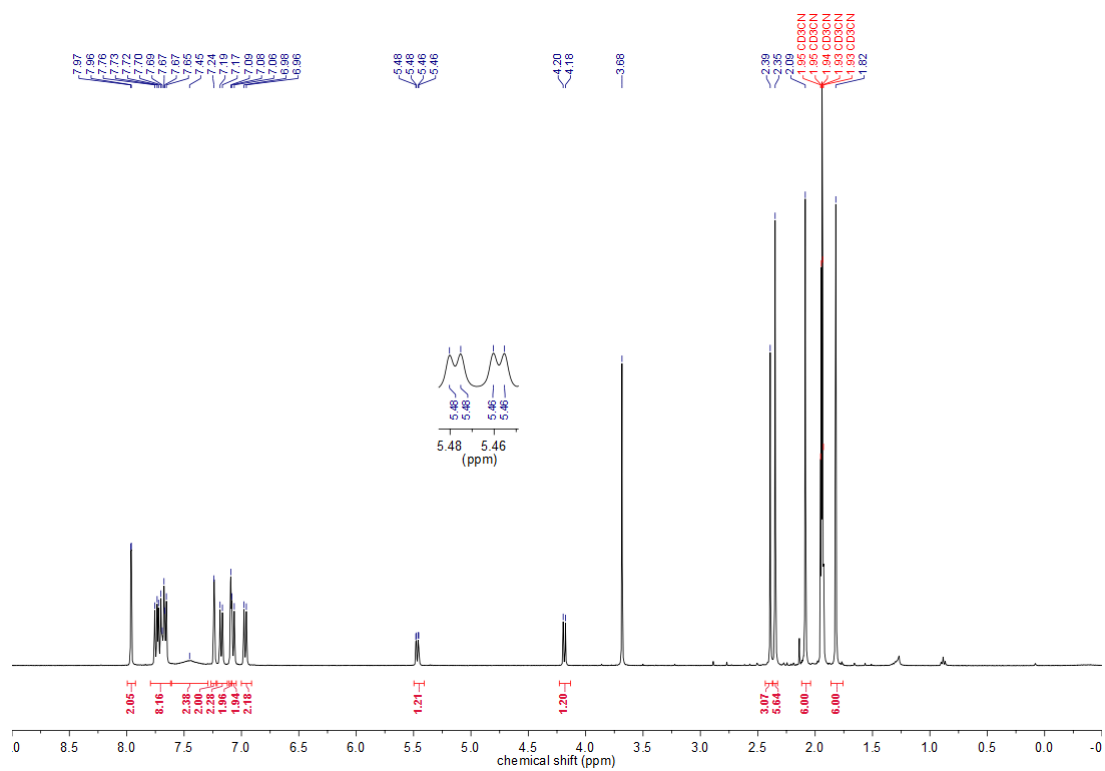
^{31}P-NMR(202 MHz, CD$_3$CN) **170**
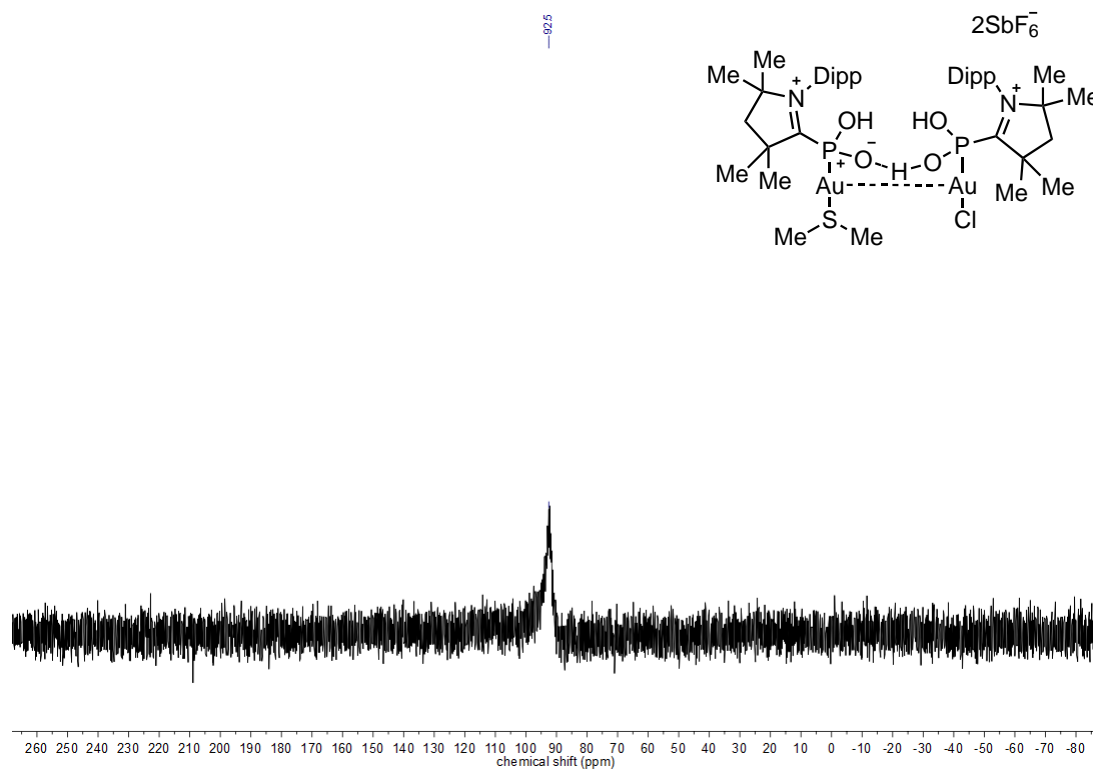
^{1}H-NMR(500 MHz, CD$_3$CN) **170**
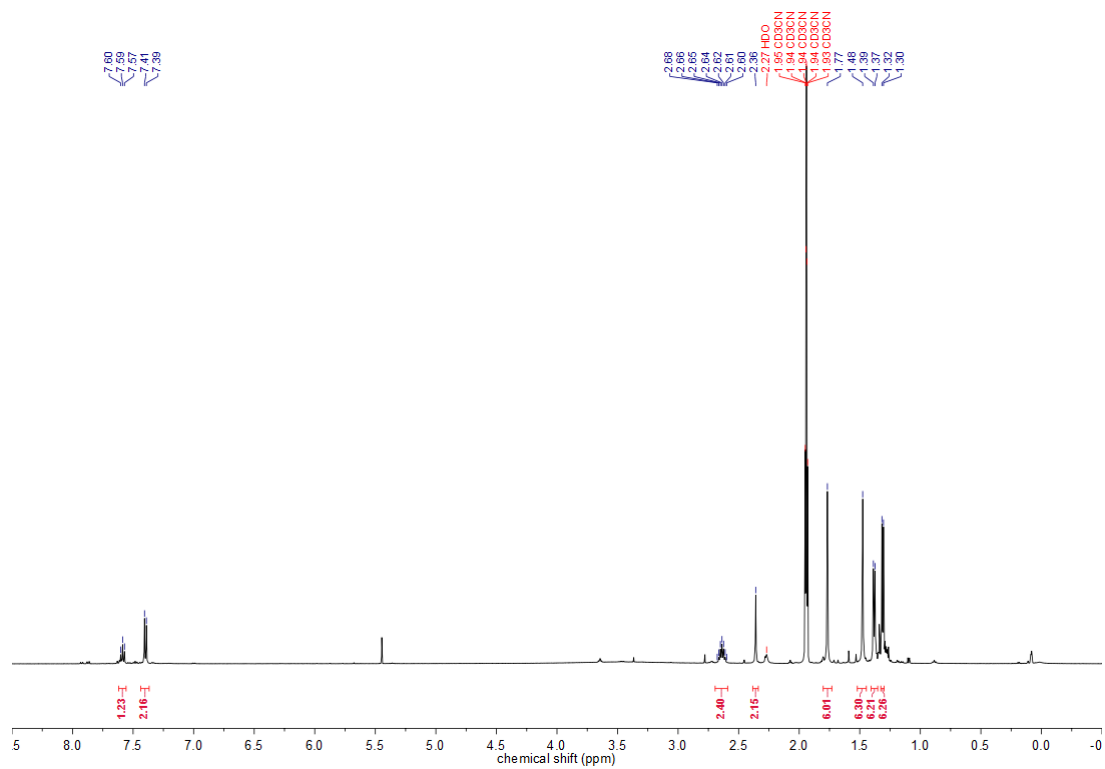
^{13}C-NMR(126 MHz, CD$_3$CN) **170**
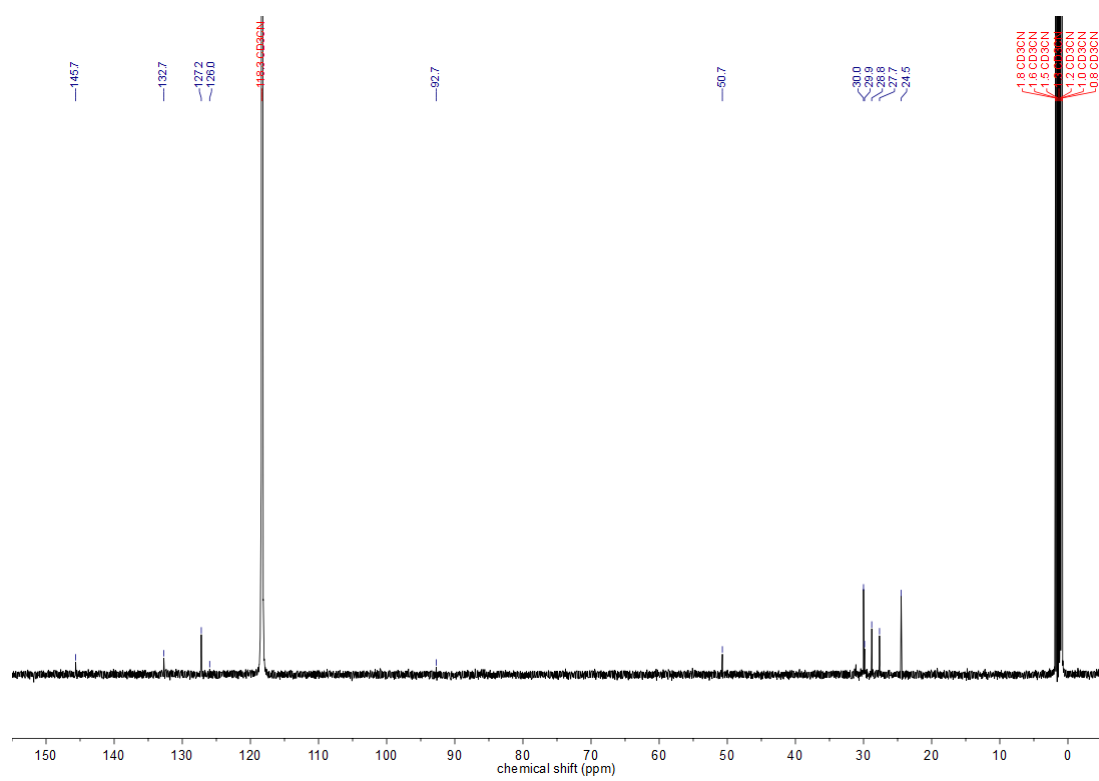
^{1}H-NMR(400 MHz, CDCl$_3$) **169**
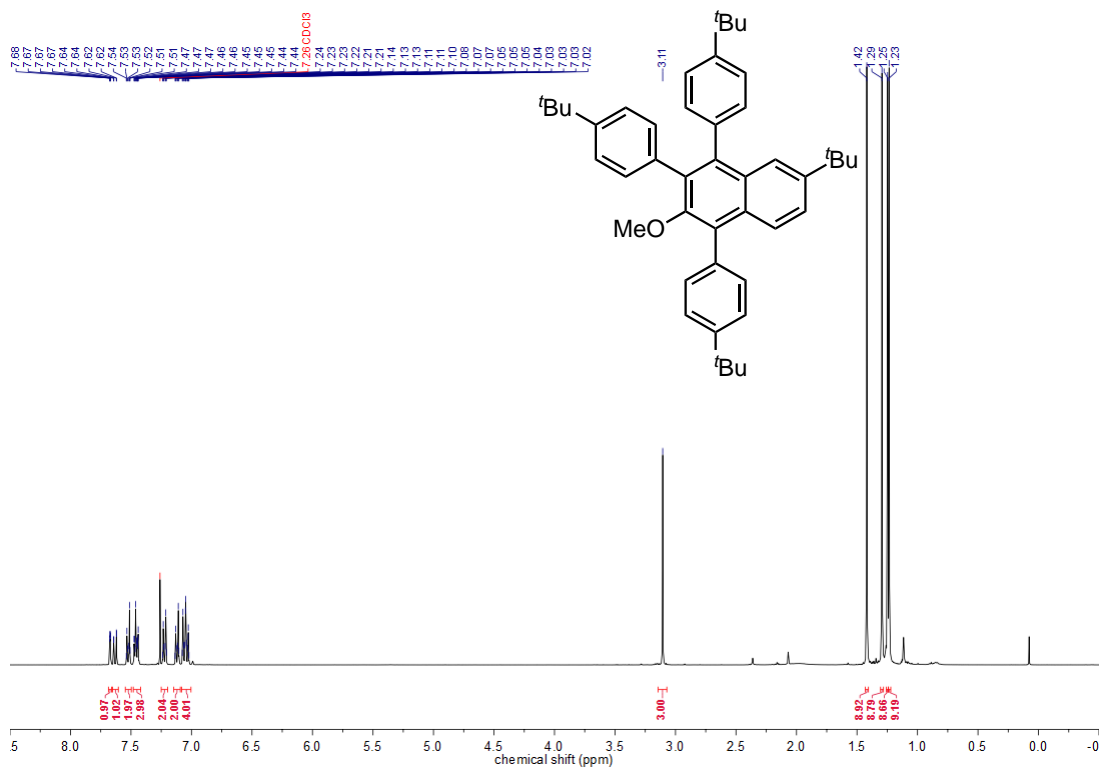
^{13}C-NMR(101 MHz, CDCl$_3$) **169**
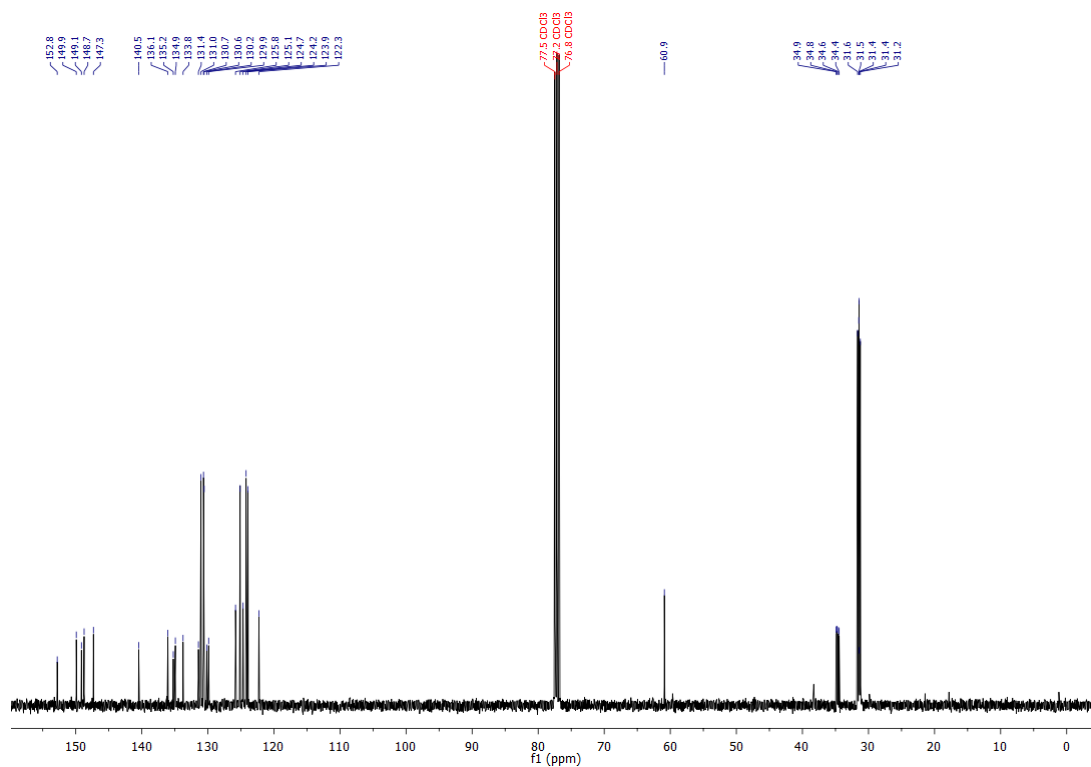
^{31}P-NMR(122 MHz, CD$_3$CN) **171**
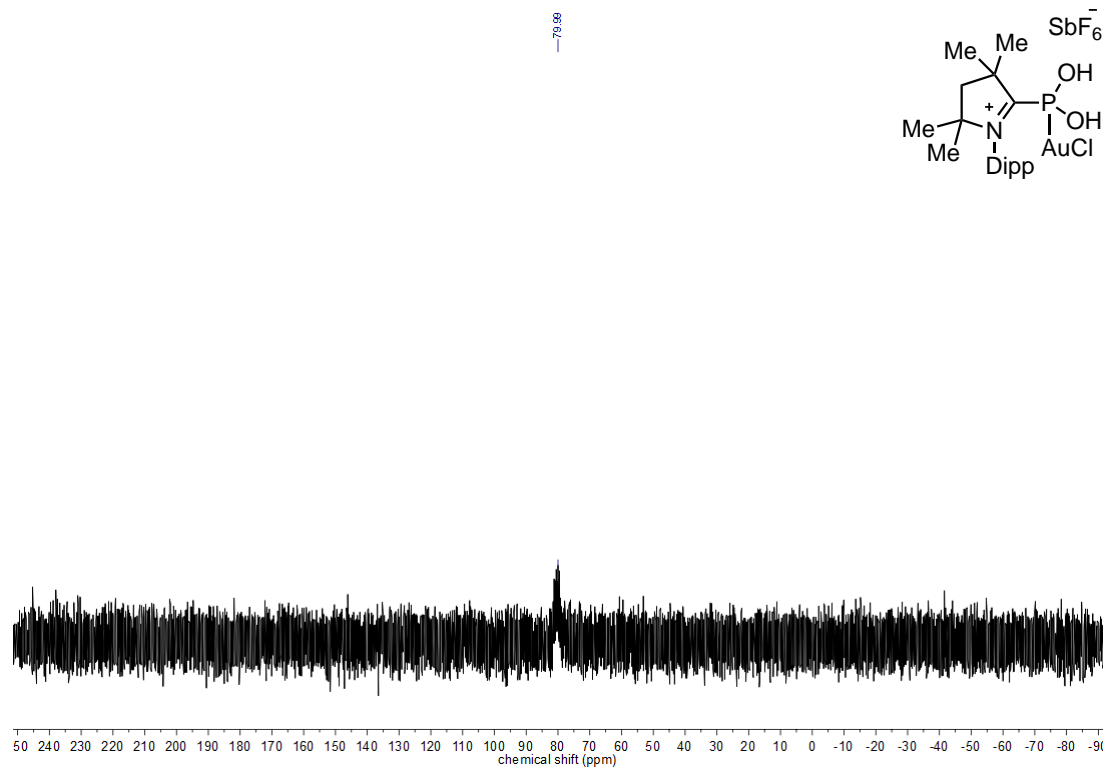
^{1}H-NMR(300 MHz, CD$_3$CN) **171**
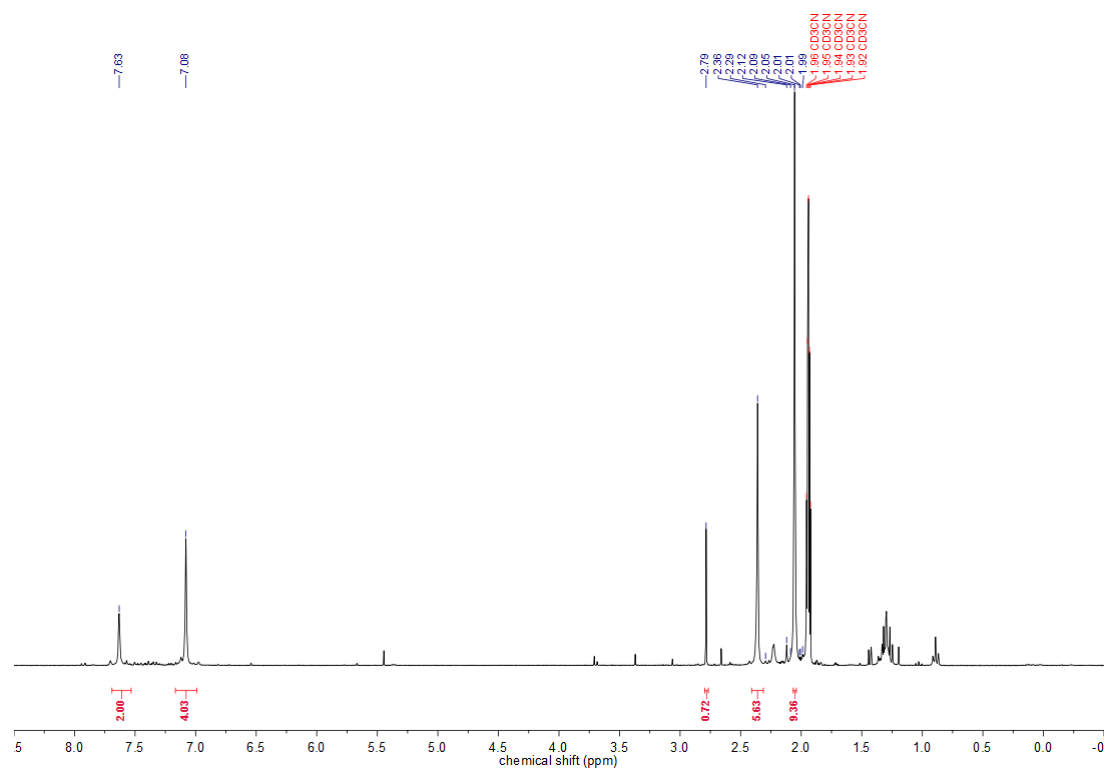
^{13}C-NMR(101 MHz, CD$_3$CN) **171**
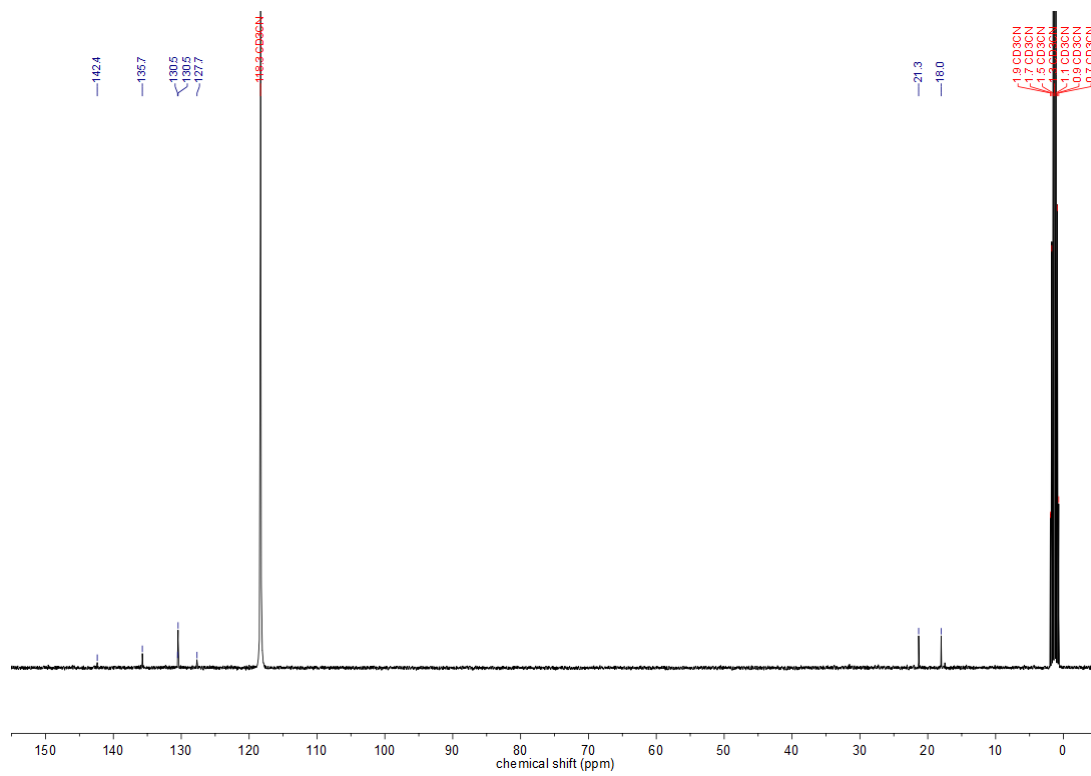
^{31}P-NMR(202 MHz, CD$_3$CN) **204**

^{1}H-NMR(500 MHz, CD$_3$CN) **204**

^{13}C-NMR(126 MHz, CD$_3$CN) **204**
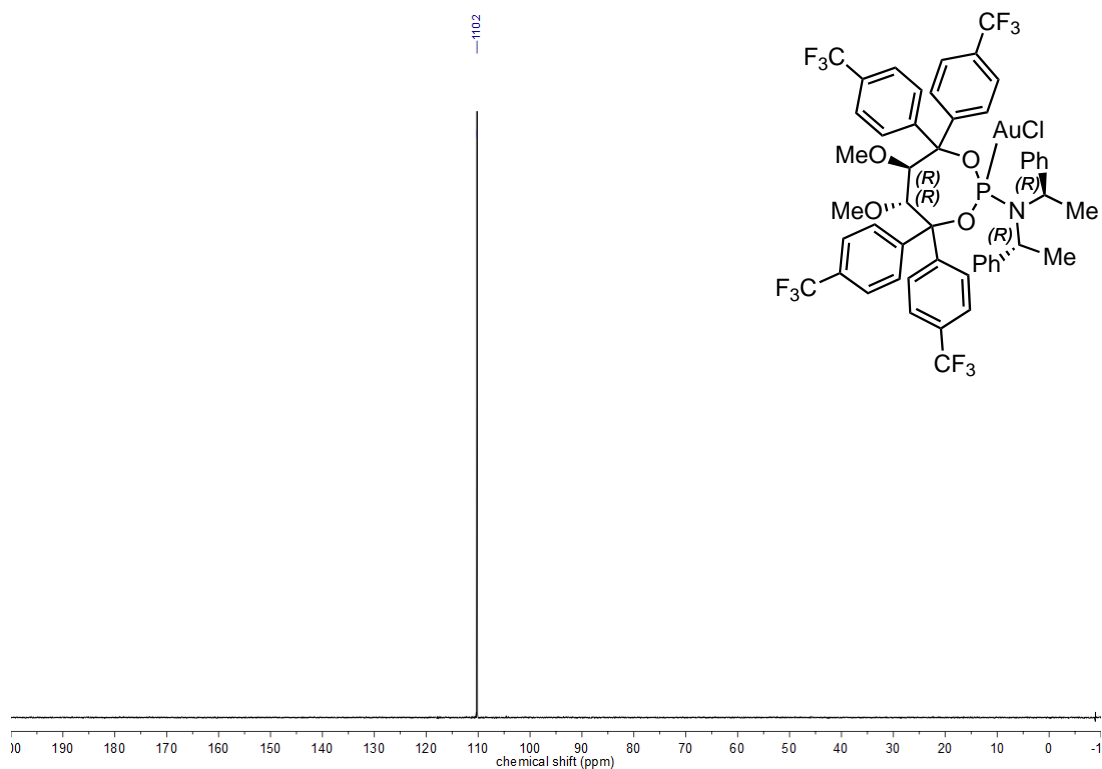
^{19}F-NMR(470 MHz, CD$_3$CN) **204**
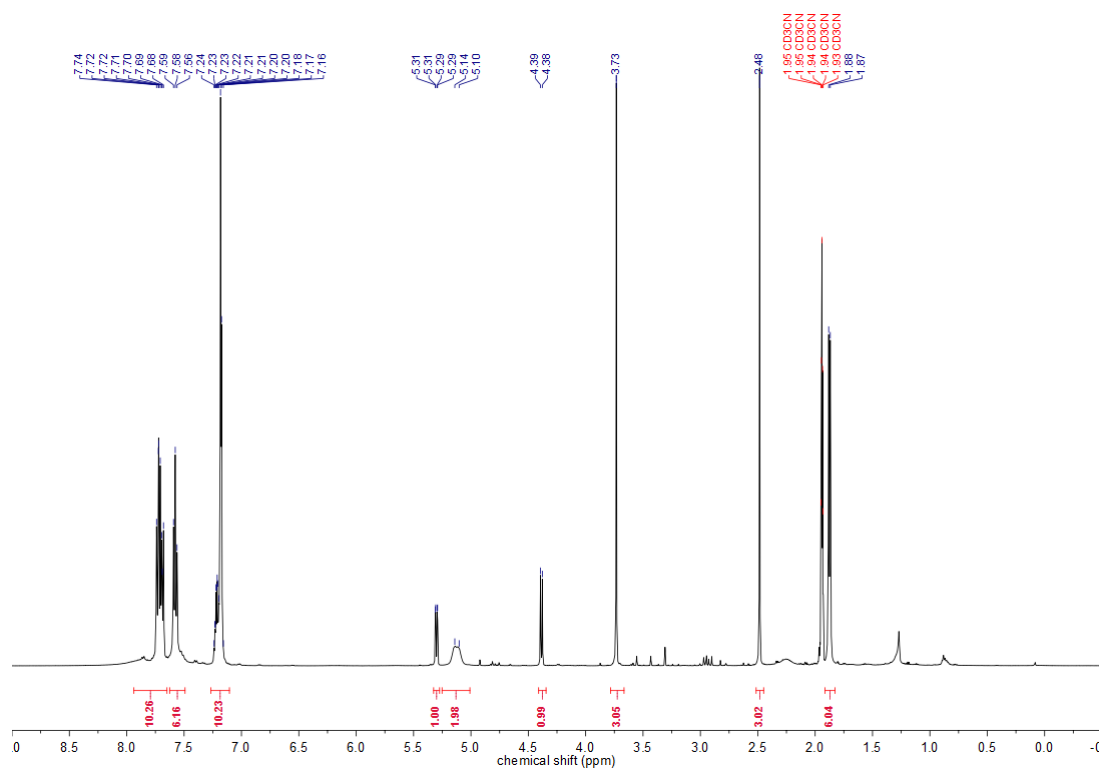
^{31}P-NMR(202 MHz, CD$_3$CN) **205**

^{1}H-NMR(500 MHz, CD$_3$CN) **205**

^{13}C-NMR(126 MHz, CD$_3$CN) **205**
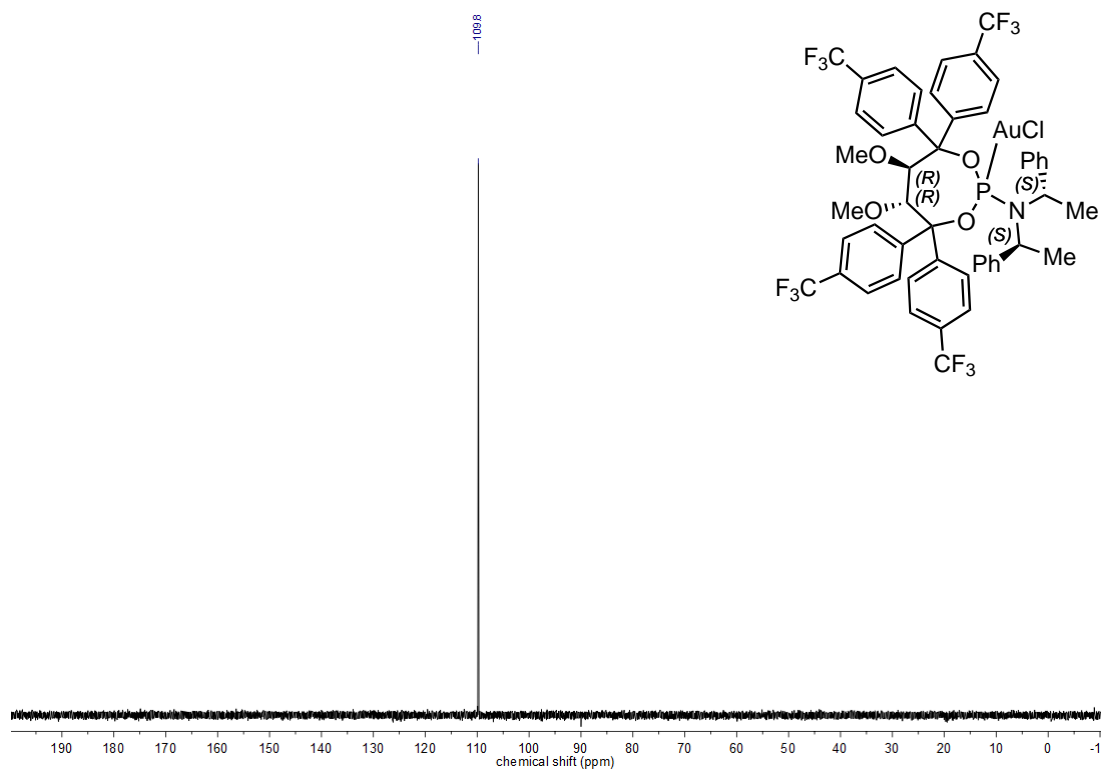
^{19}F-NMR(470 MHz, CD$_3$CN) **205**
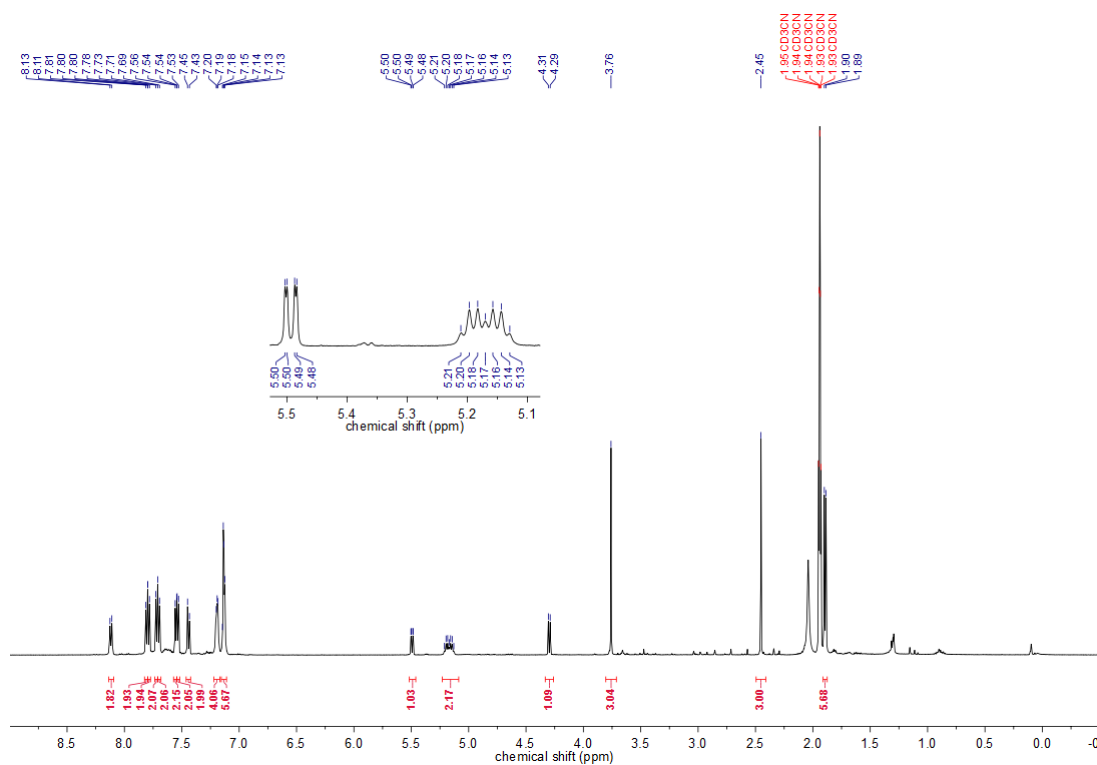
^{1}H-NMR(400 MHz, CDCl$_3$) **185a**
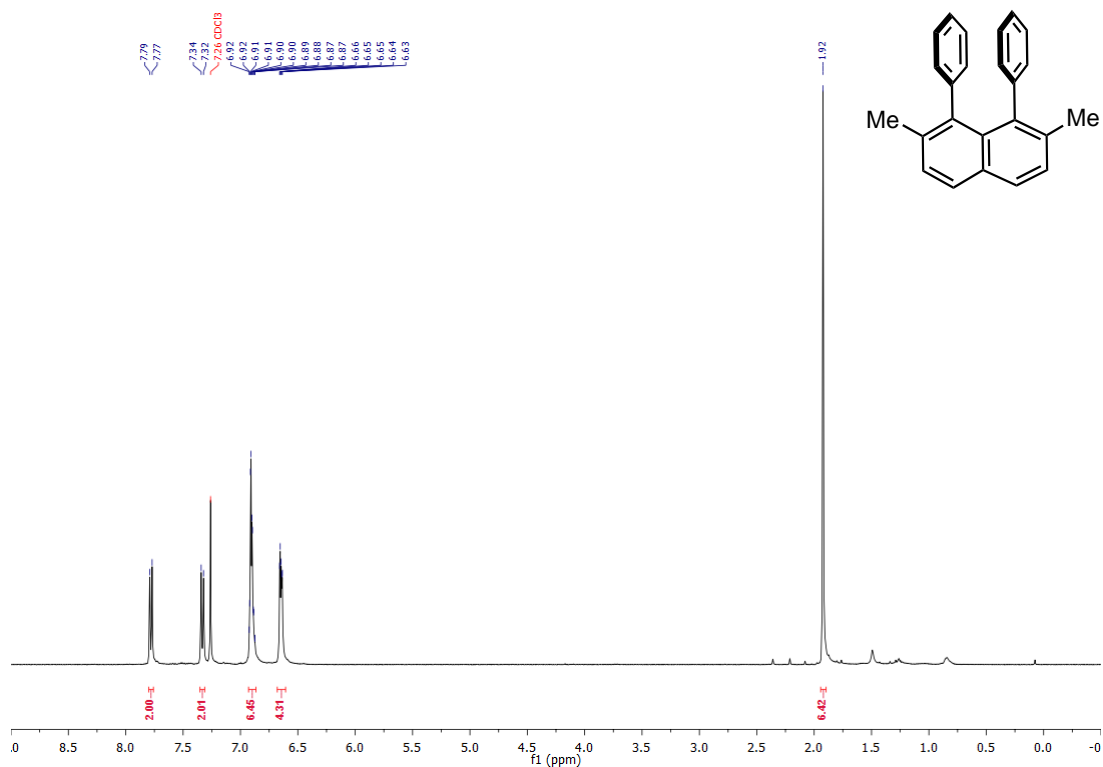
^{13}C-NMR(75 MHz, CDCl$_3$) **185a**
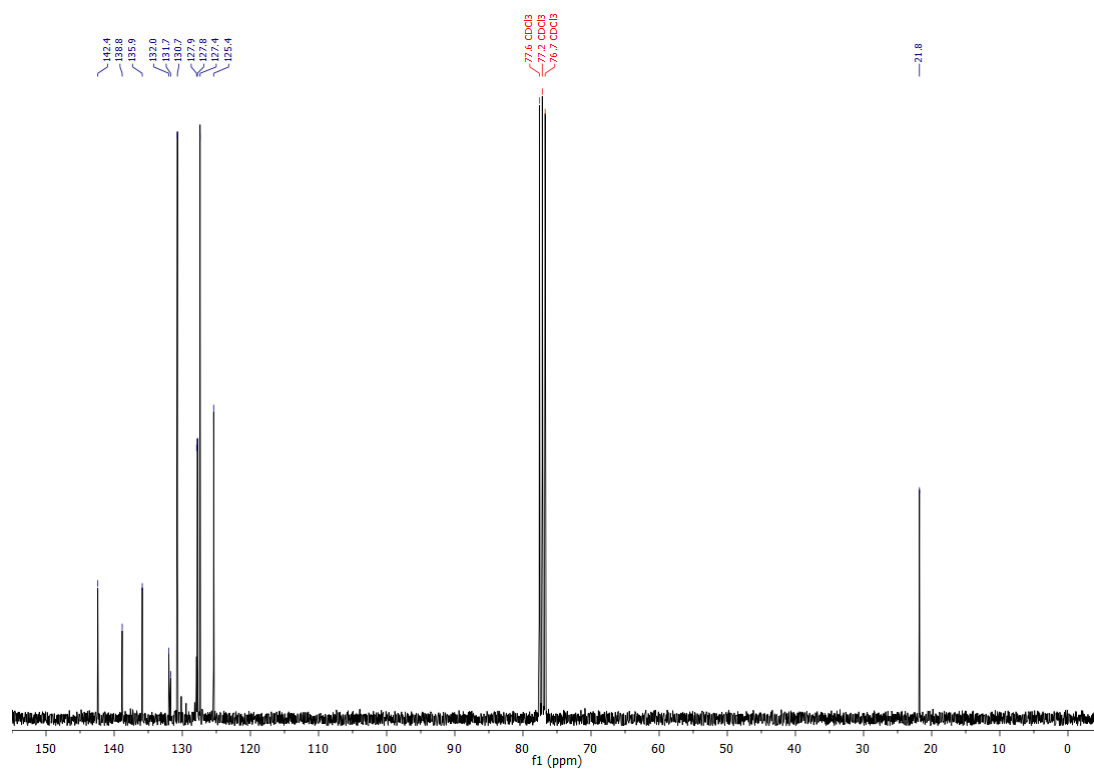
^{1}H-NMR(400 MHz, CDCl$_3$) **185b**
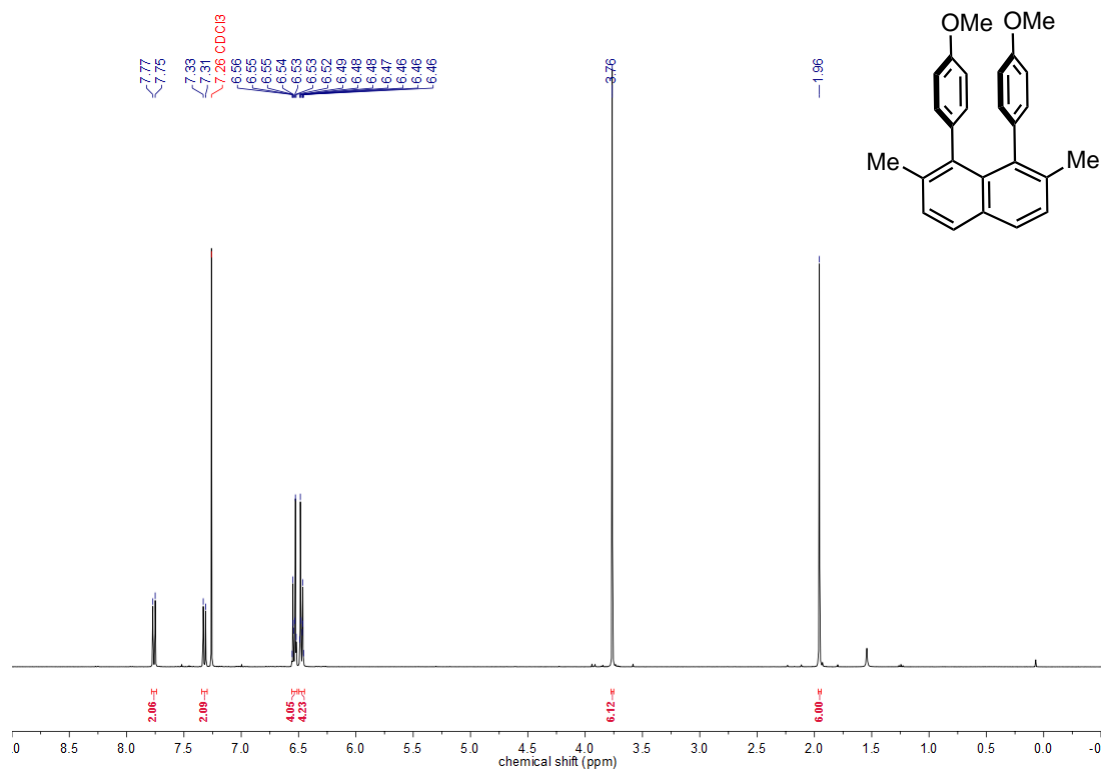
^{13}C-NMR(101 MHz, CDCl$_3$) **185b**
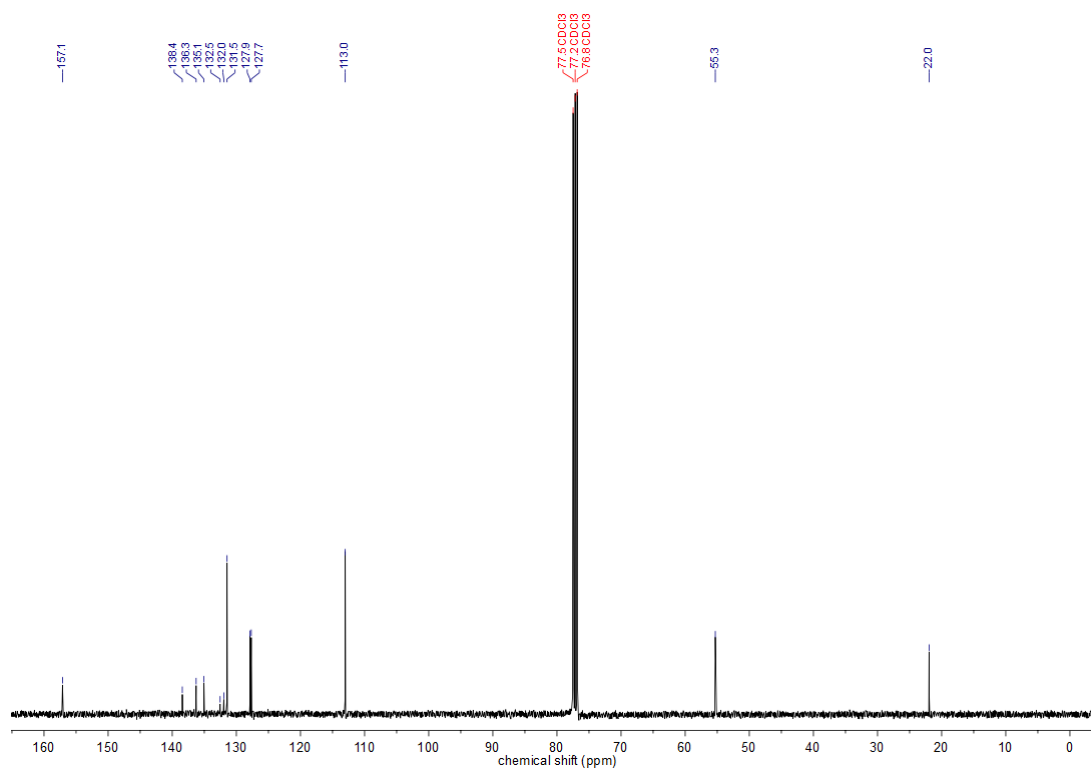
^{1}H-NMR(400 MHz, CDCl$_3$) **185c**
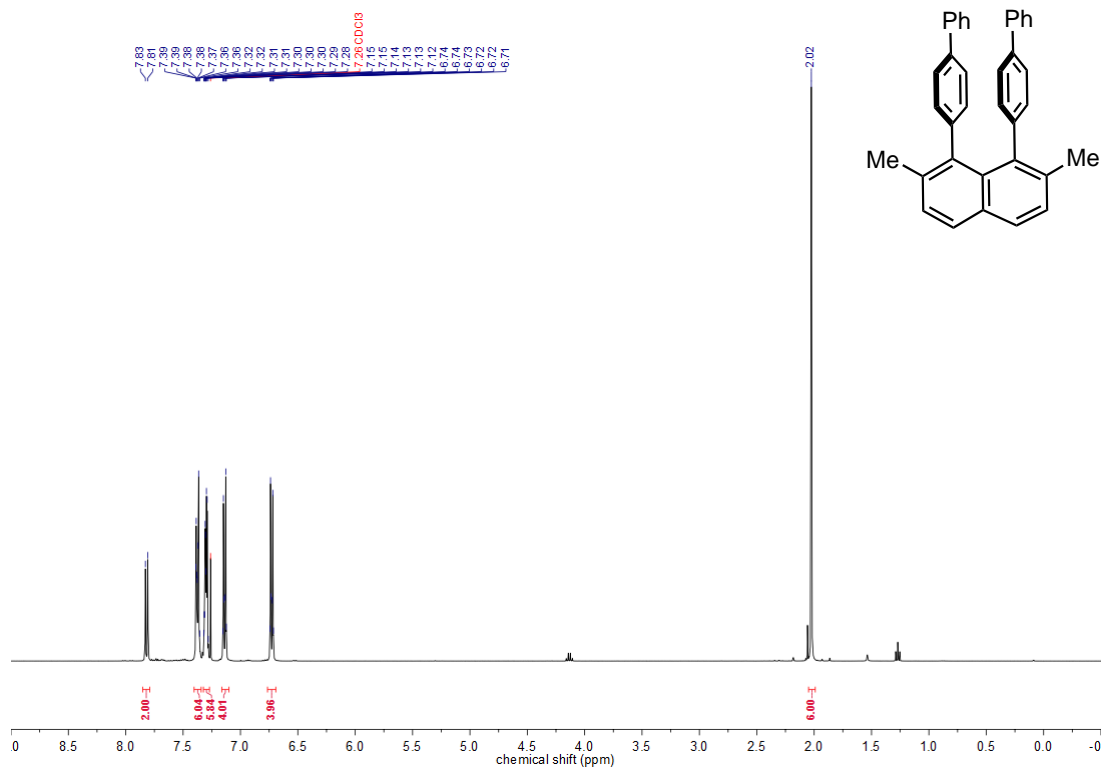
^{13}C-NMR(101 MHz, CDCl$_3$) **185c**
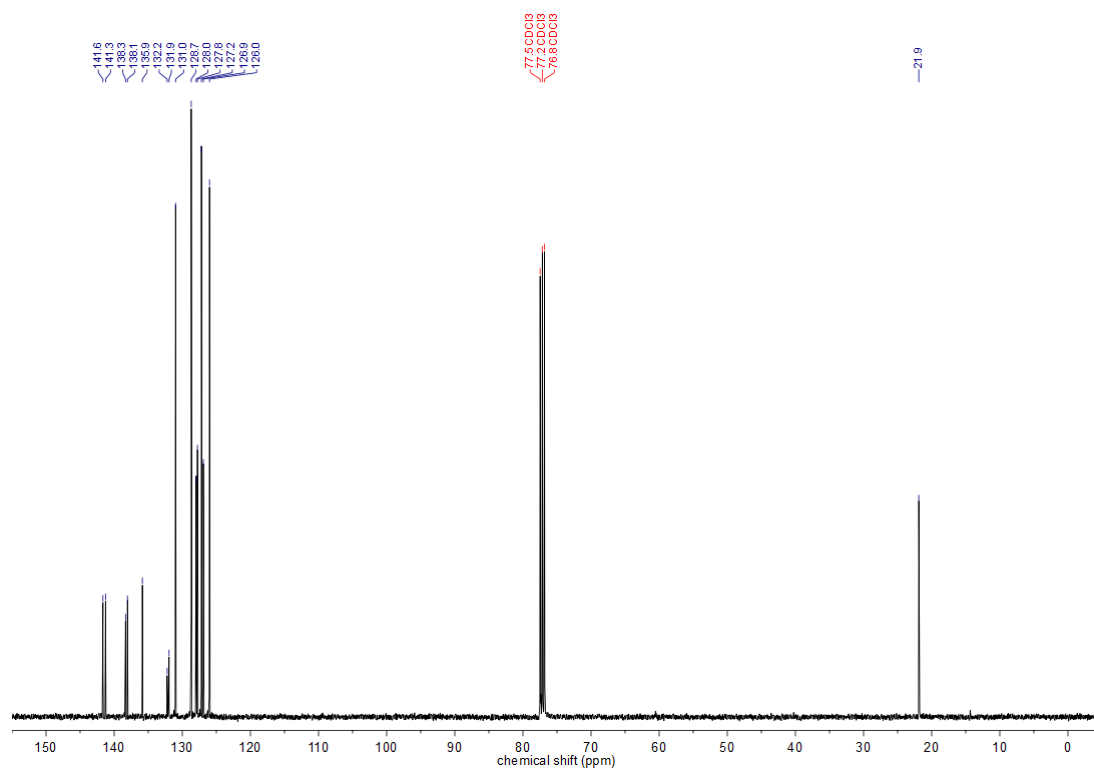
^{1}H-NMR(400 MHz, CDCl$_3$) **185d**

^{13}C-NMR(101 MHz, CDCl$_3$) **185d**

Assigments for compound **185e**

	185e	185e
	anti- conformer	*syn-* conformer
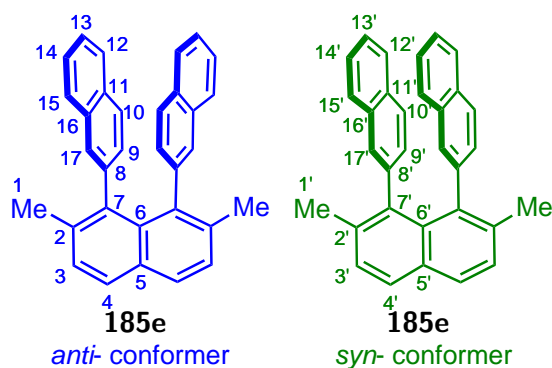
Atom	δ (ppm)		Correlations		
	experimental	predicted	COSY	HMBC	NOESY
1 C	21,868	22,46		3	
1 H(3)	1,962	2,4		2, 3, 7, 6	3, 9, 17
2 C	135,97	137,53		4, 1	
3 C	127,783	129,06		1	
3 H	7,387	7,41	4	5, 7, 1	1, 4
4 C	128,077	128,68			
4 H	7,855	7,87	3	6, 2, 4	3
5 C	131,974	133,6		3	
6 C	132,362	136,95		4, 1	
7 C	138,402	135,88		3, 9, 17, 1	
8 C	139,84	135,83		10	
9 C	129,252	126,56		17	
9 H	6,71	7,59	10	7, 11, 17	1, 10
10 C	126,127	128,35		12	
10 H	6,767	7,9	9	8, 12, 16	9, 12
11 C	131,419	134,78		15, 9, 13, 17	
12 C	127,194	127,74		10, 14	
12 H	7,291	8,03	13	10, 14, 16	10, 13
13 C	125,074	128,84		15	
13 H	7,224	7,51	12, 14	11, 15	12, 14
14 C	125,345	127,11		12	
14 H	7,333	7,57	13, 15	12, 16	13, 15
15 C	127,221	129,6		13, 17	
15 H	7,498	7,85	14	17, 11, 13	14, 17
16 C	132,941	132,79		10, 12, 14	
17 C	128,952	129,63		15, 9	
17 H	7,099	7,77	7, 9, 11, 15	1, 15, 9, 10	

Table A.1: Assignment of NMR signals for *anti*-**185e** . Spectrometer: Bruker AV500; Solvent: CDCl$_3$.*Interaction with the other half of the molecule.

| Atom | δ (ppm) | | Correlations | | |
	experimental	predicted	COSY	HMBC	NOESY
1' C	21,808	22,46		3'	
1' H(3)	1,962	2,4		2', 3', 7', 6'	3', 9', 17'
2' C	135,919	137,53		4', 1'	
3' C	127,774	129,06		1'	
3' H	7,387	7,41	4'	5', 7', 1'	1', 4'
4' C	128,019	128,68		4'	
4' H	7,848	7,87	3'	6', 2', 4'*	3'
5' C	131,974	133,6		3'	
6' C	132,23	136,95		4', 1'	
7' C	138,555	135,88		3', 9', 17', 1'	
8' C	139,664	135,83		10'	
9' C	128.266	126,56		17'	
9' H	6,745	7,59	10'	7', 11', 17'	1', 10'
10' C	126,427	128,35		12'	
10' H	7,086	7,9	9'	8', 12', 16'	9', 12'
11' C	131,47	134,78		15', 9', 13', 17'	
12' C	127	127,74		10', 14'	
12' H	7,325	8,03	13'	10', 14', 16'	10', 13'
13' C	124,902	128,84		15'	
13' H	7,181	7,51	12', 14'	11', 15'	12', 14'
14' C	125,345	127,11		12'	
14' H	7,08	7,57	13', 15'	12', 16'	13', 15'
15' C	127,033	129,6		13', 17'	
15' H	7,064	7,85	14'	17', 11', 13'	14', 17'
16' C	132,68	132,79		10', 12', 14'	
17' C	129,491	129,63		15', 9'	
17' H	7,027	7,77	7', 9', 11', 15'	1', 15'	

Table A.2: Assignment of NMR signals for *syn*-**185e** . Spectrometer: Bruker AV500; Solvent: CDCl$_3$.*Interaction with the other half of the molecule.
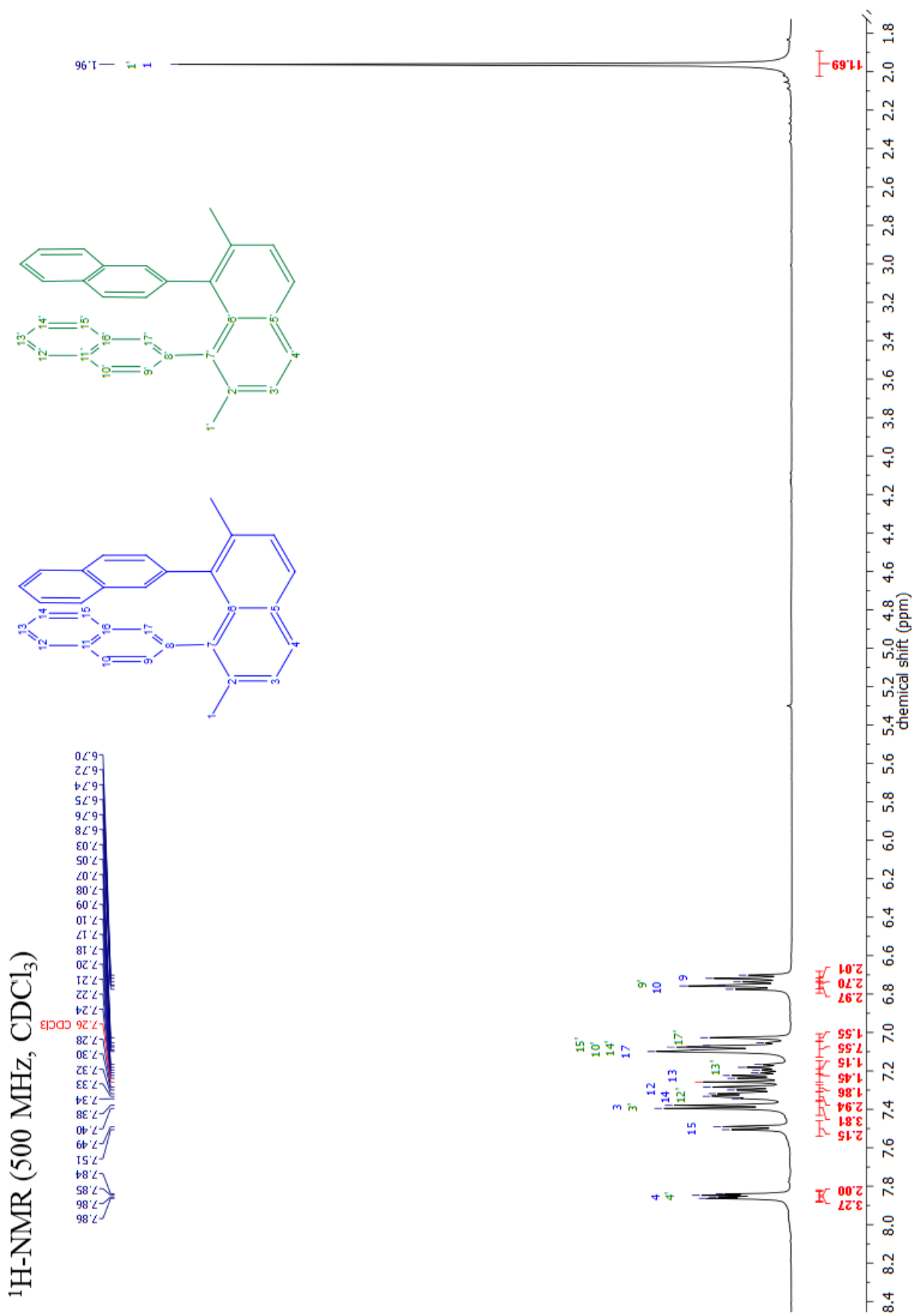
^{1}H-NMR (500 MHz, CDCl$_3$)

¹³C-NMR (126 MHz, CDCl$_3$)

HSQC
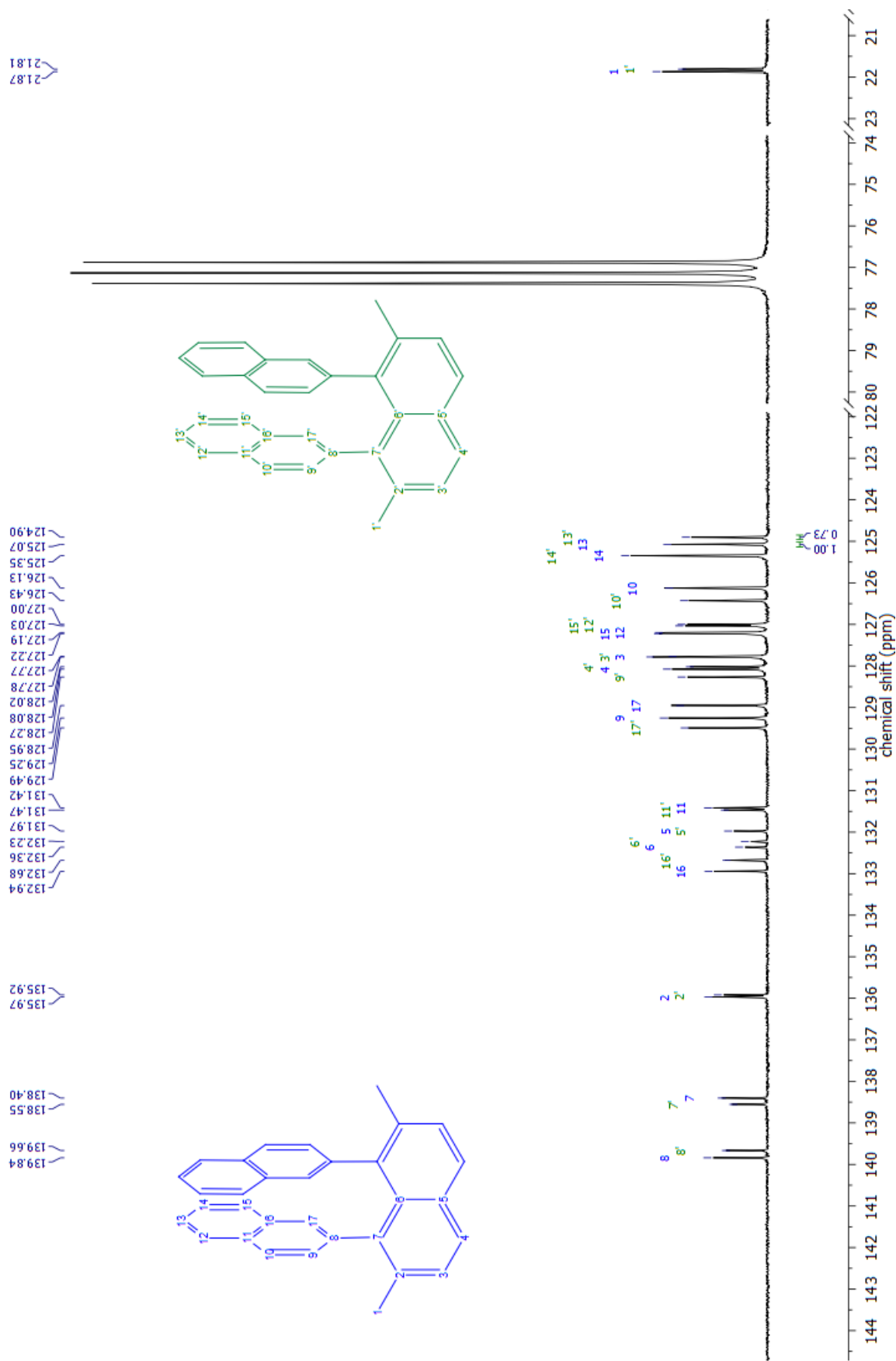
HMBC
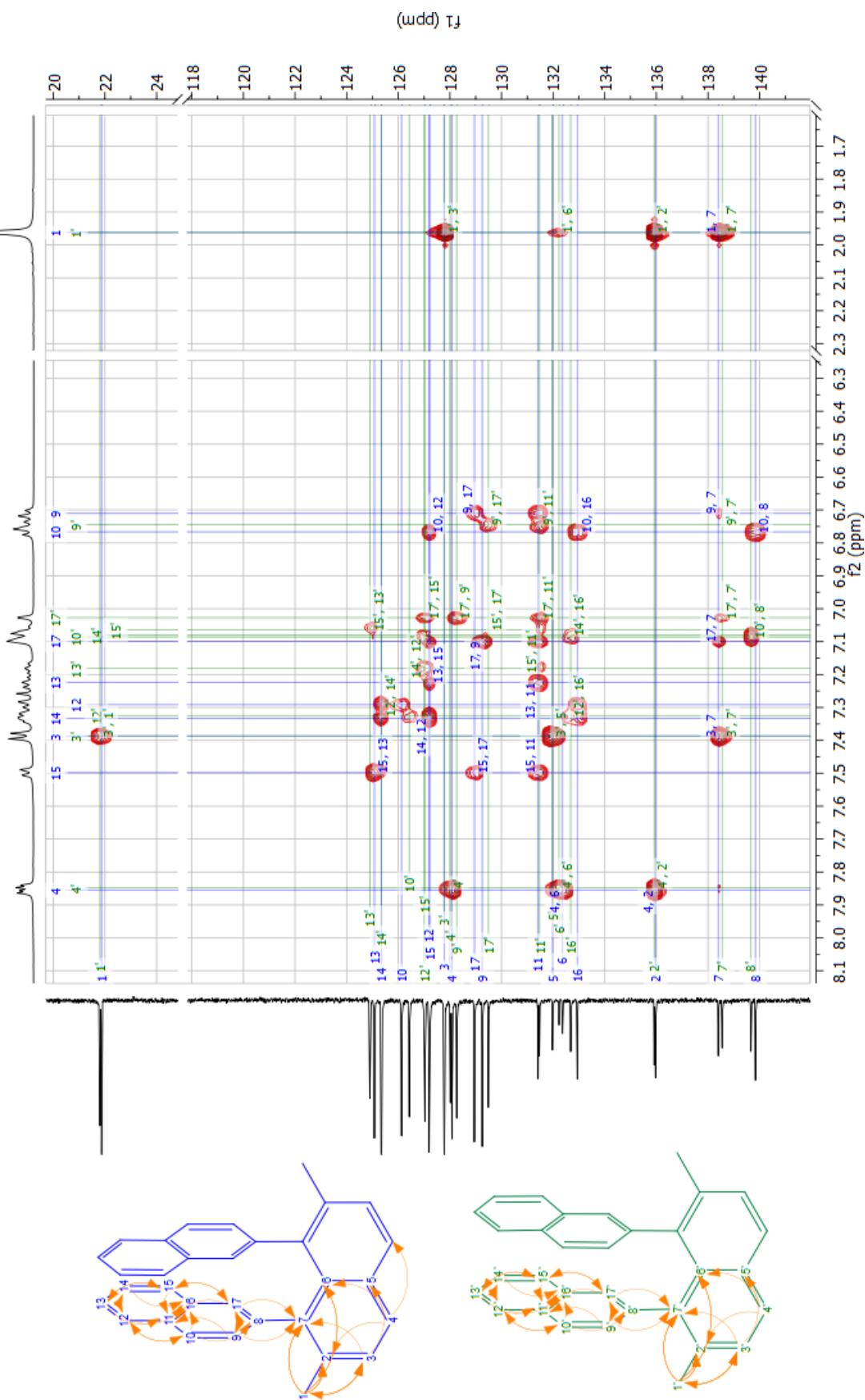
COSY
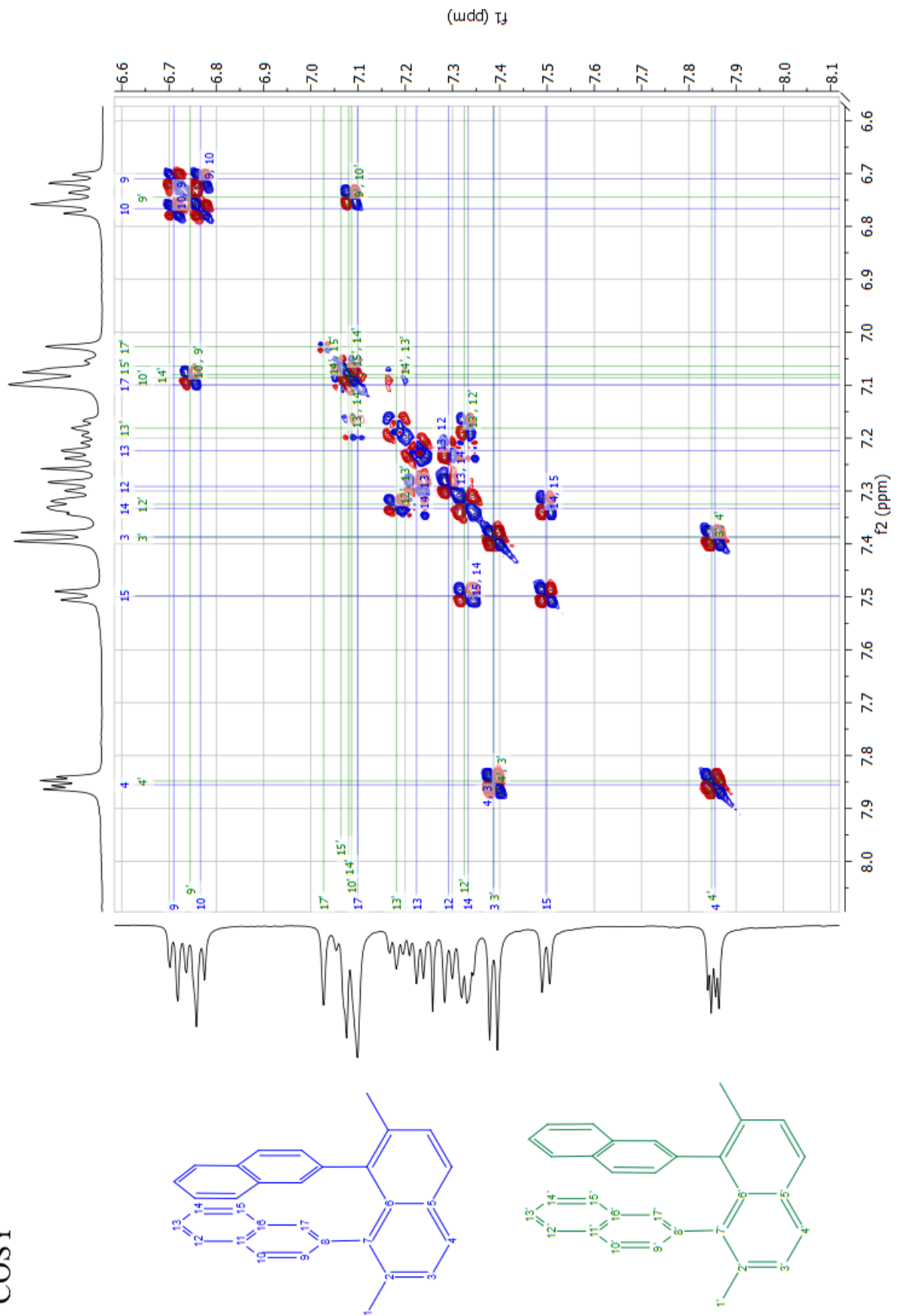
NOESY
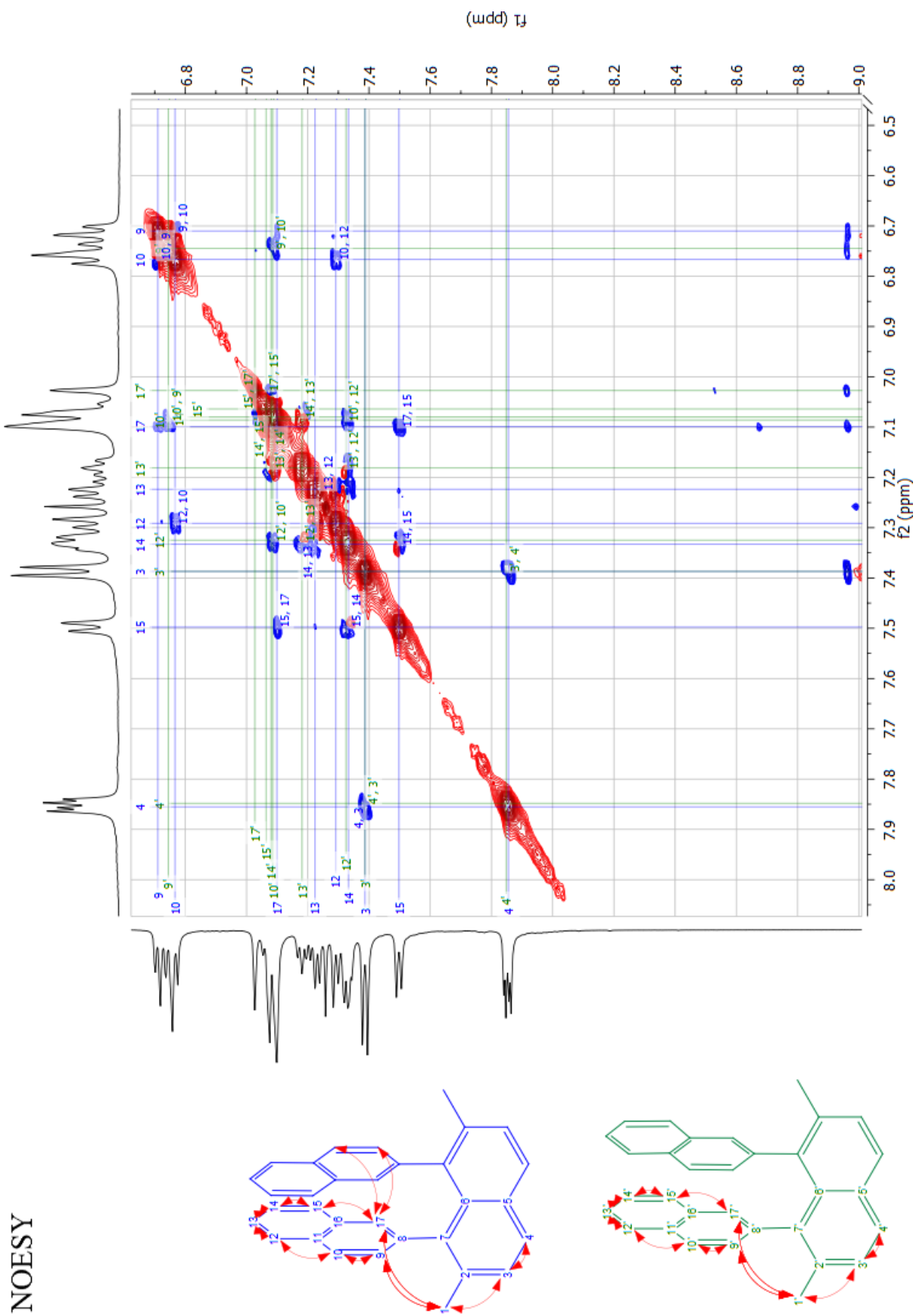
^{1}H-NMR(400 MHz, CDCl$_3$) **186b**
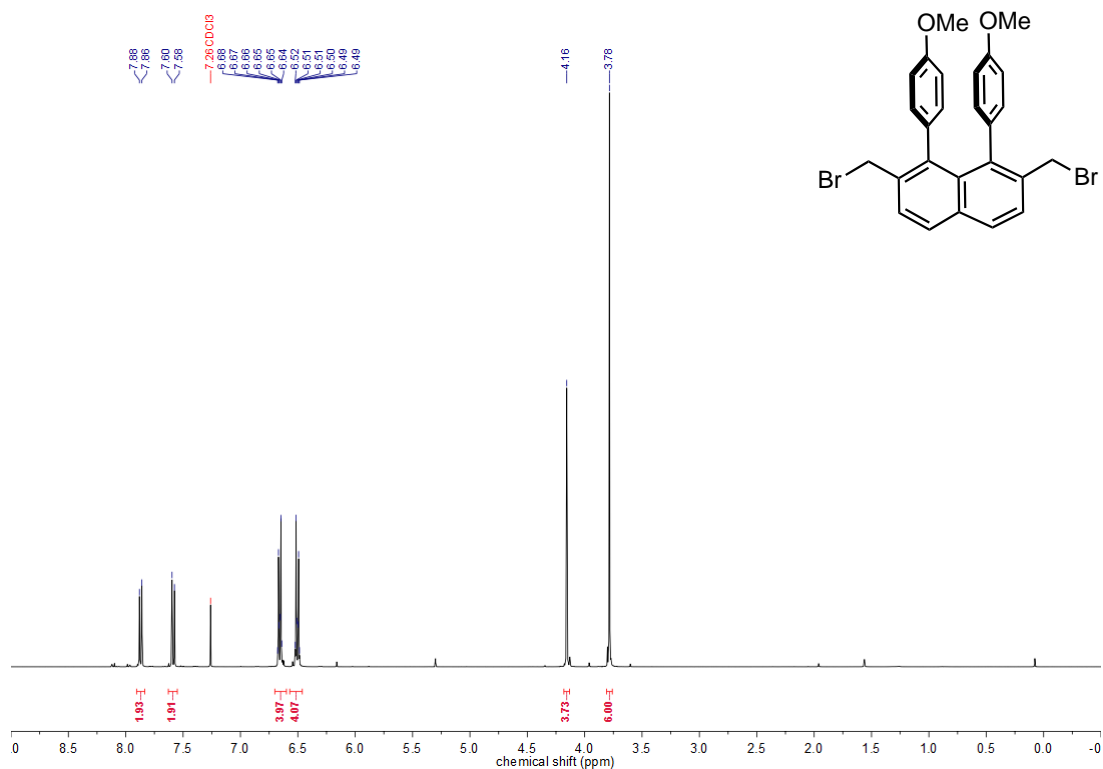
^{13}C-NMR(101 MHz, CDCl$_3$) **186b**
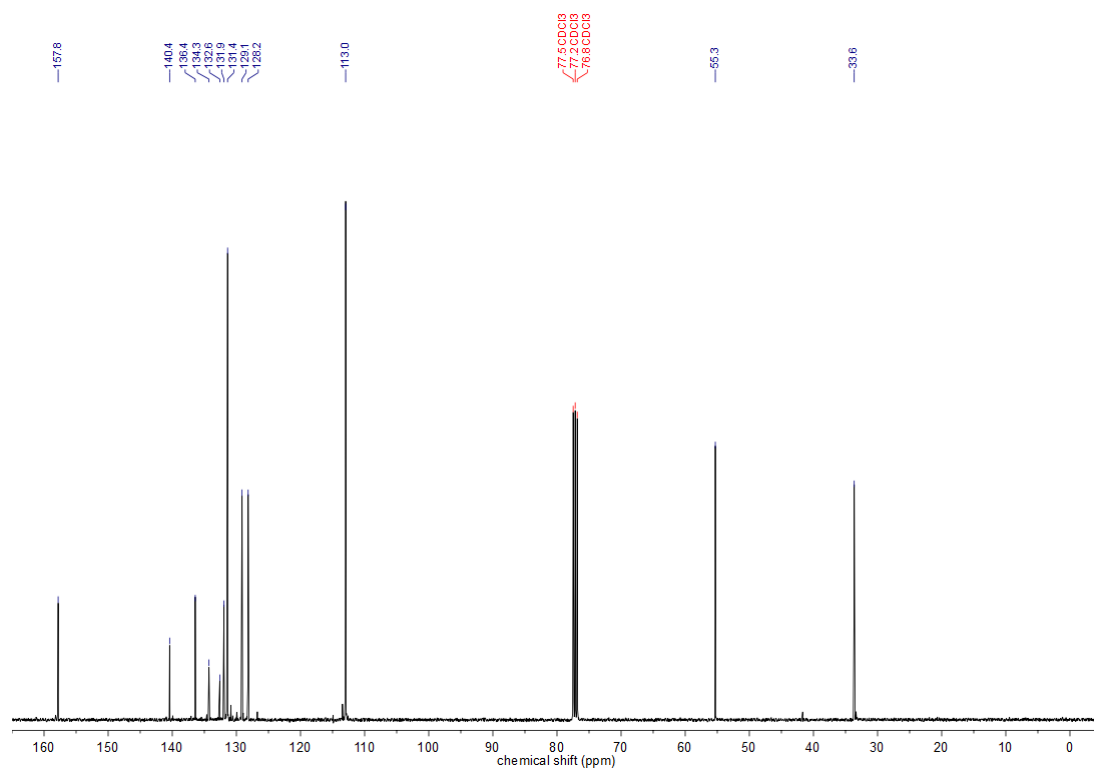
^{1}H-NMR(400 MHz, CDCl$_3$) **186d**
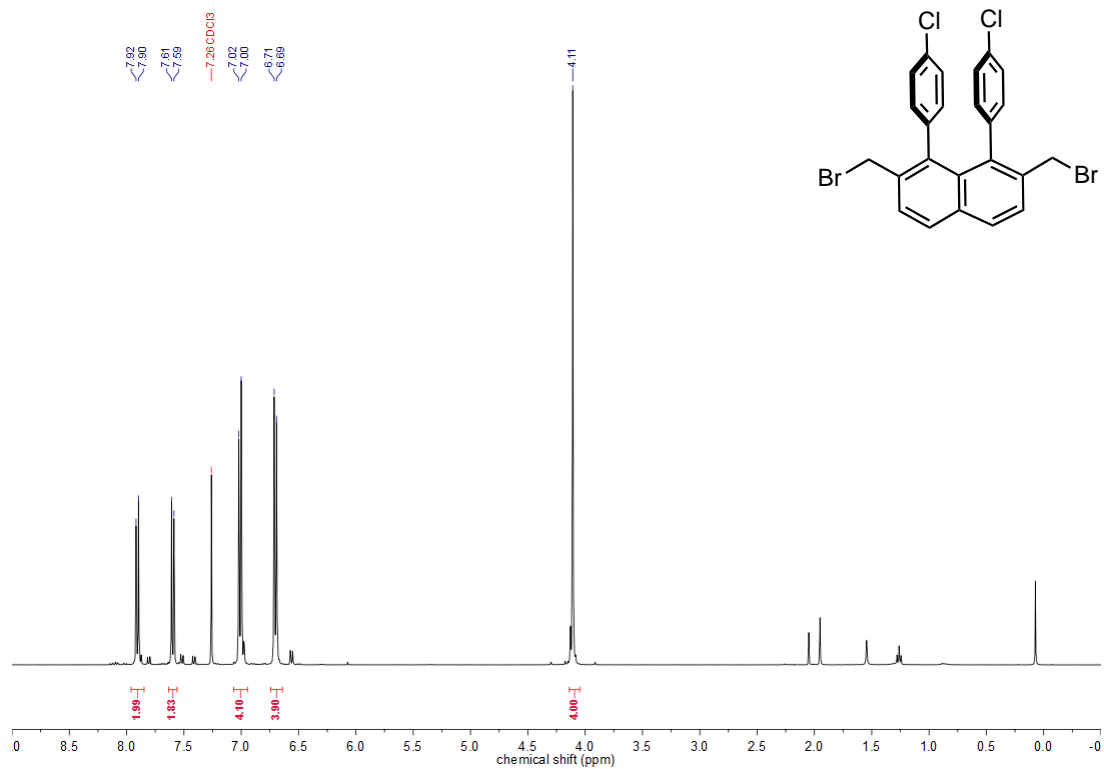
^{13}C-NMR(101 MHz, CDCl$_3$) **186d**
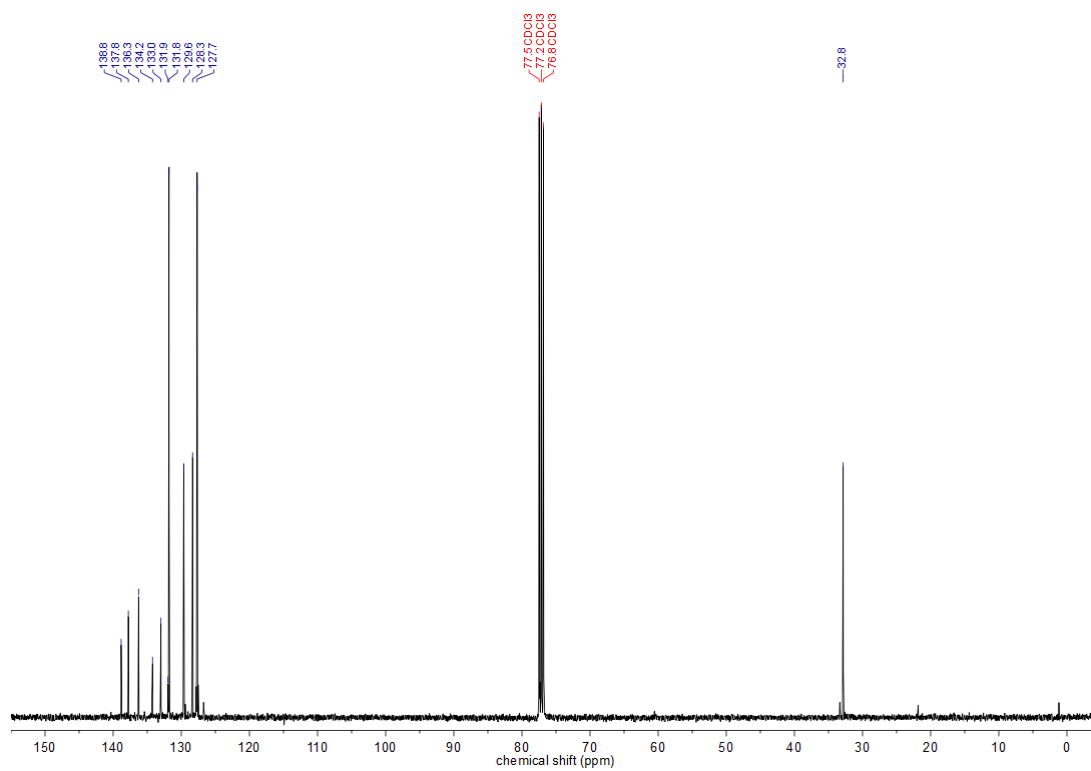
^{1}H-NMR(400 MHz, CDCl$_3$) **188a**
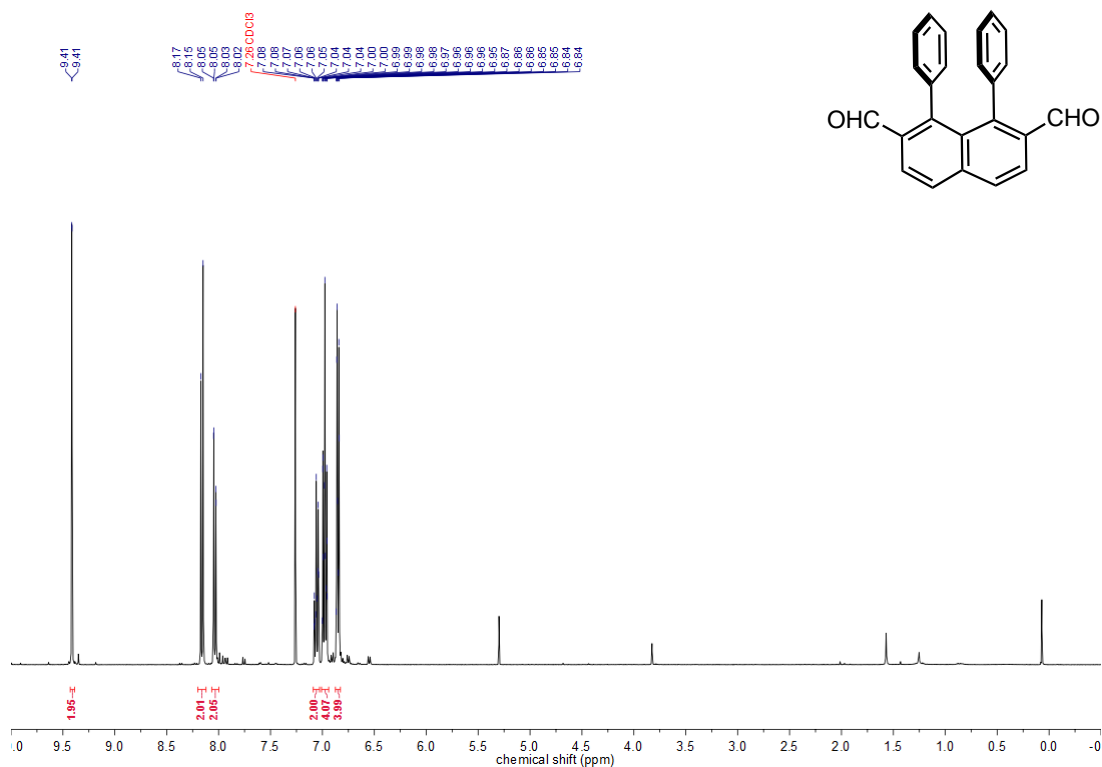
^{13}C-NMR(101 MHz, CDCl$_3$) **188a**
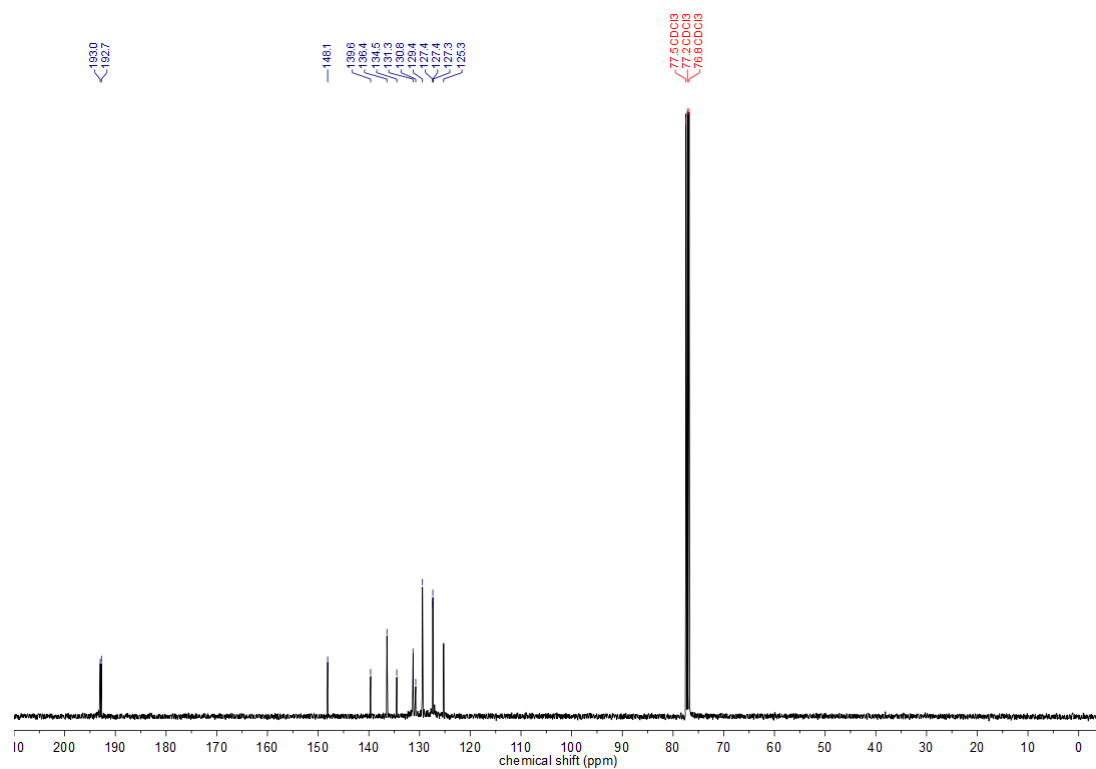
^{1}H-NMR(400 MHz, CDCl$_3$) **188b**
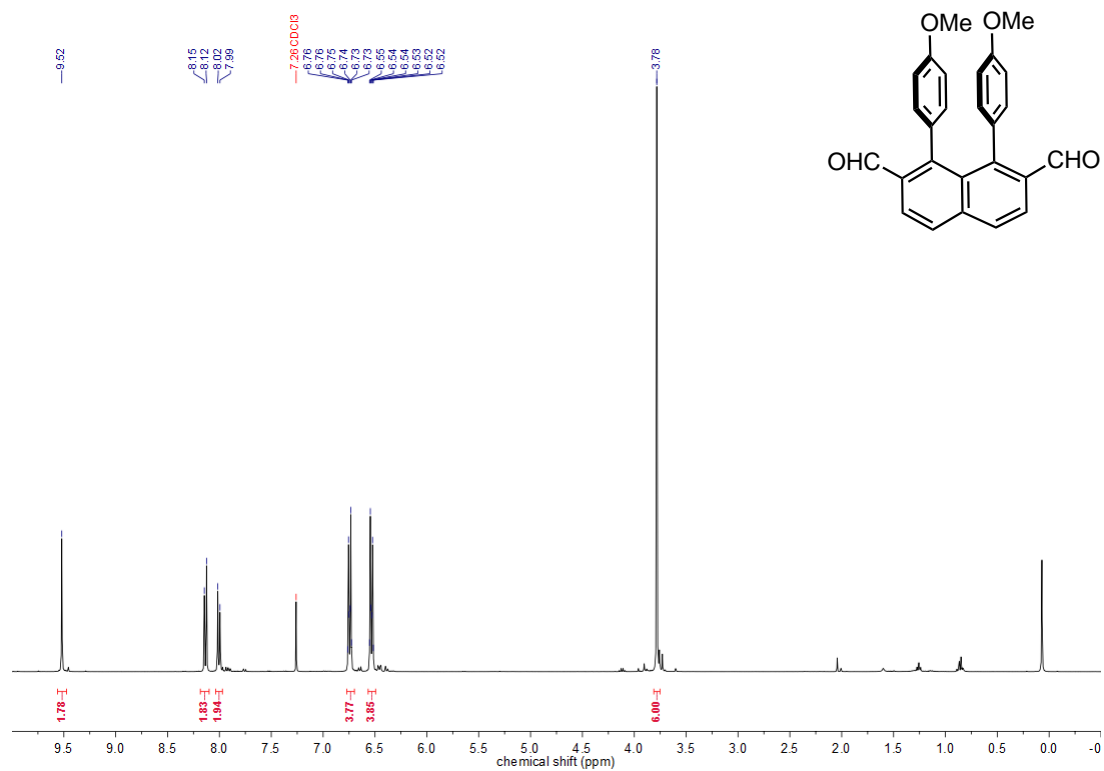
^{13}C-NMR(101 MHz, CDCl$_3$) **188b**
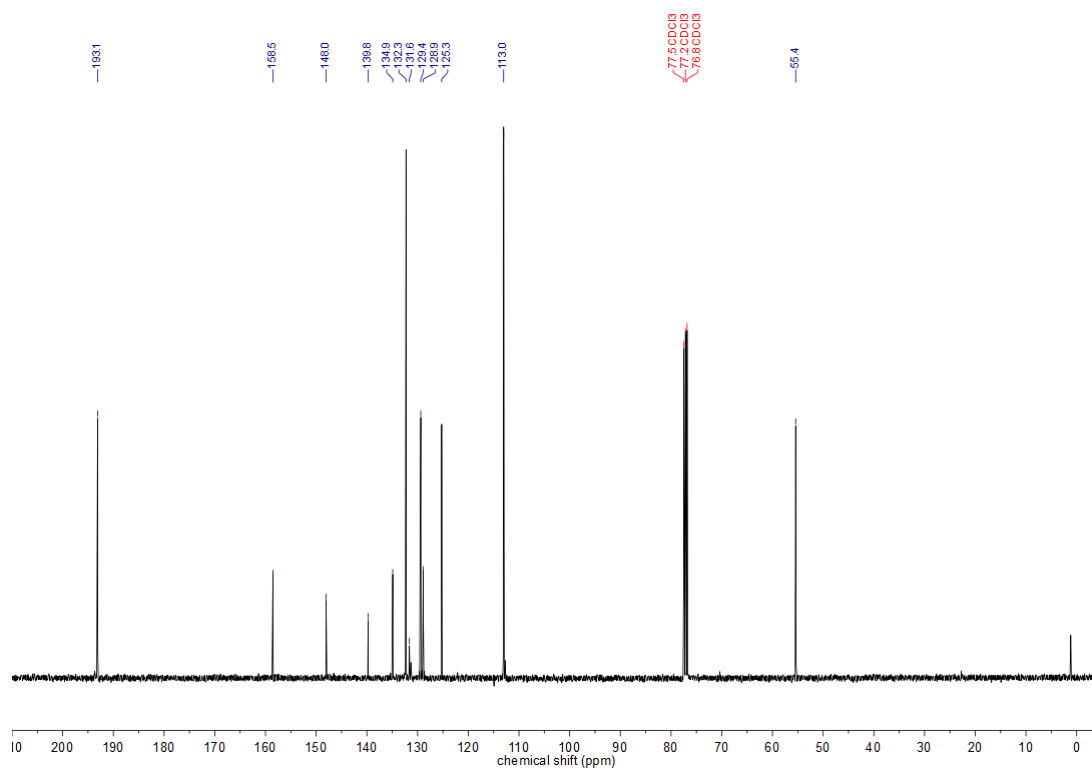
^{1}H-NMR(400 MHz, CDCl$_3$) **188c**
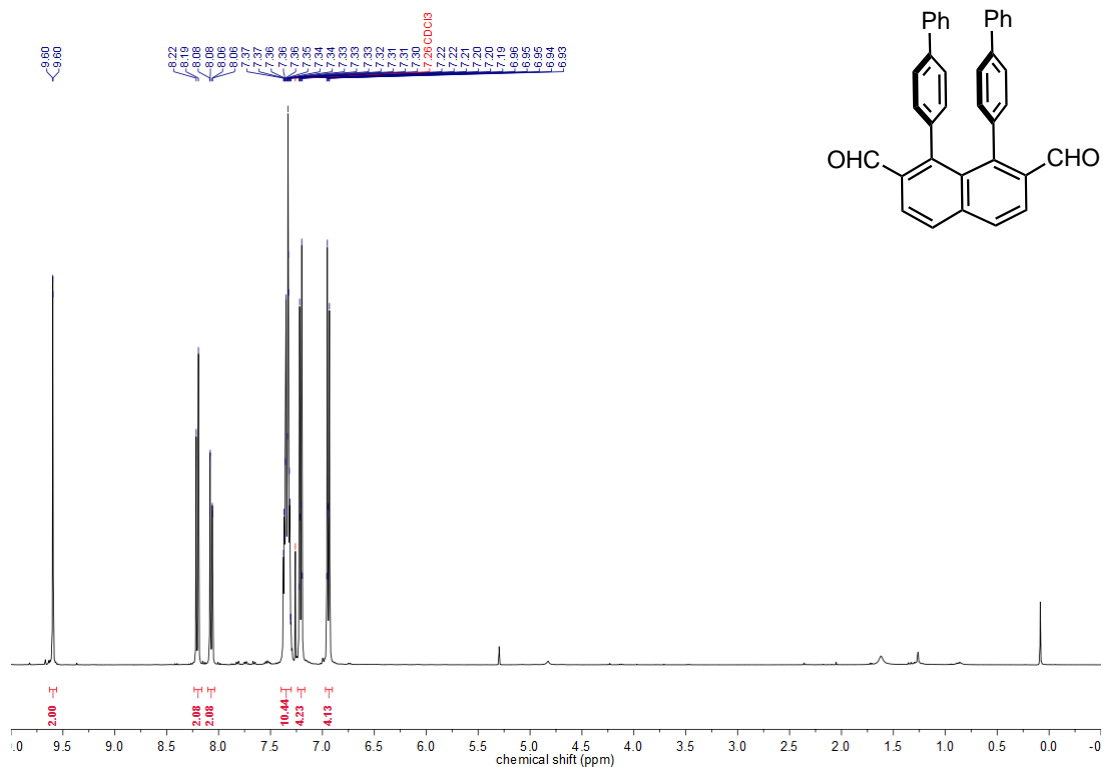
^{13}C-NMR(101 MHz, CDCl$_3$) **188c**
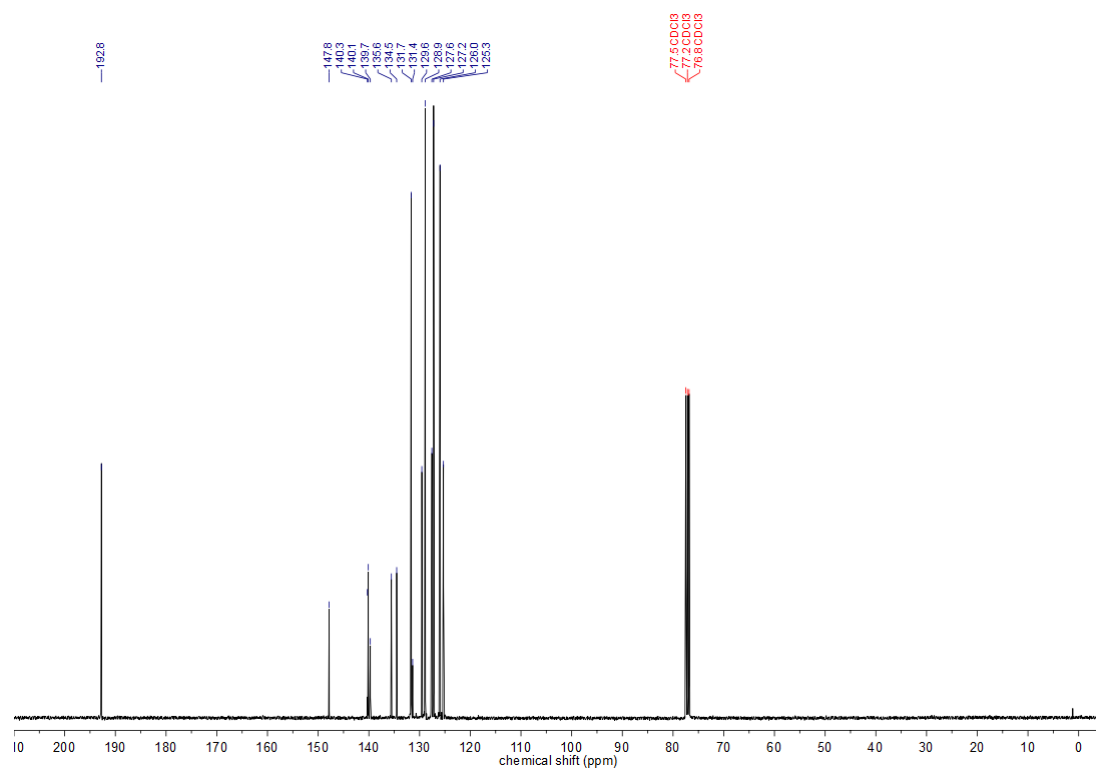
^{1}H-NMR(400 MHz, CDCl$_3$) **188d**
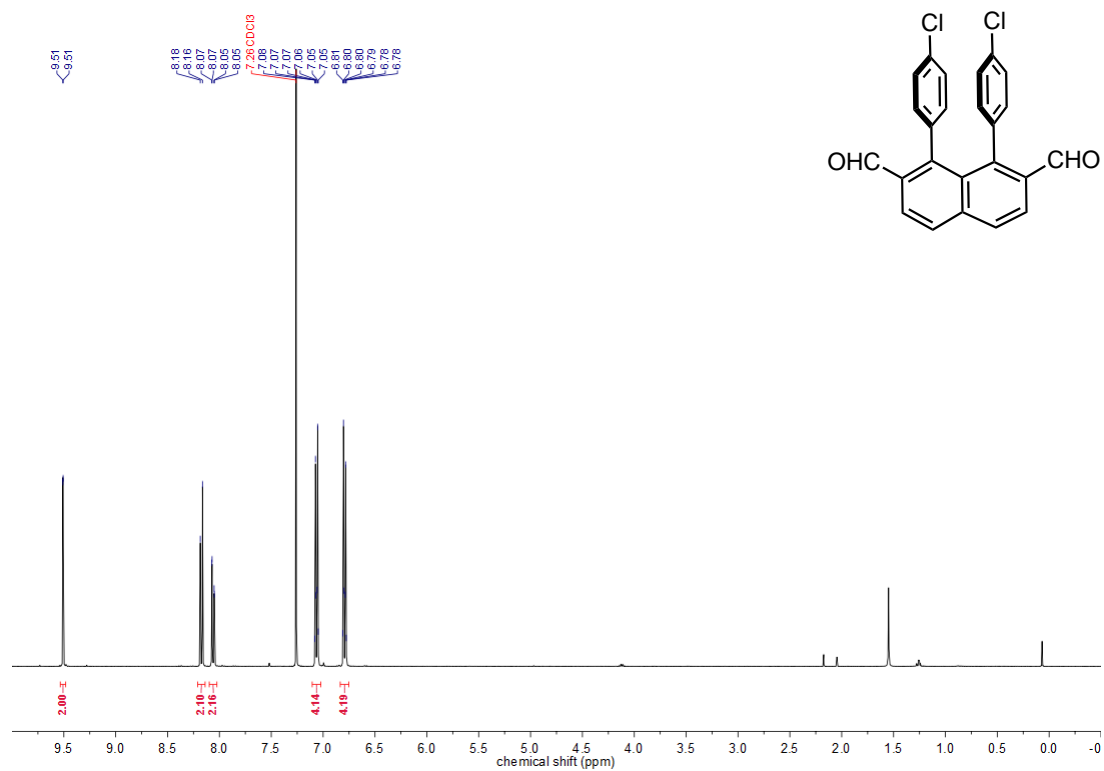
^{13}C-NMR(101 MHz, CDCl$_3$) **188d**
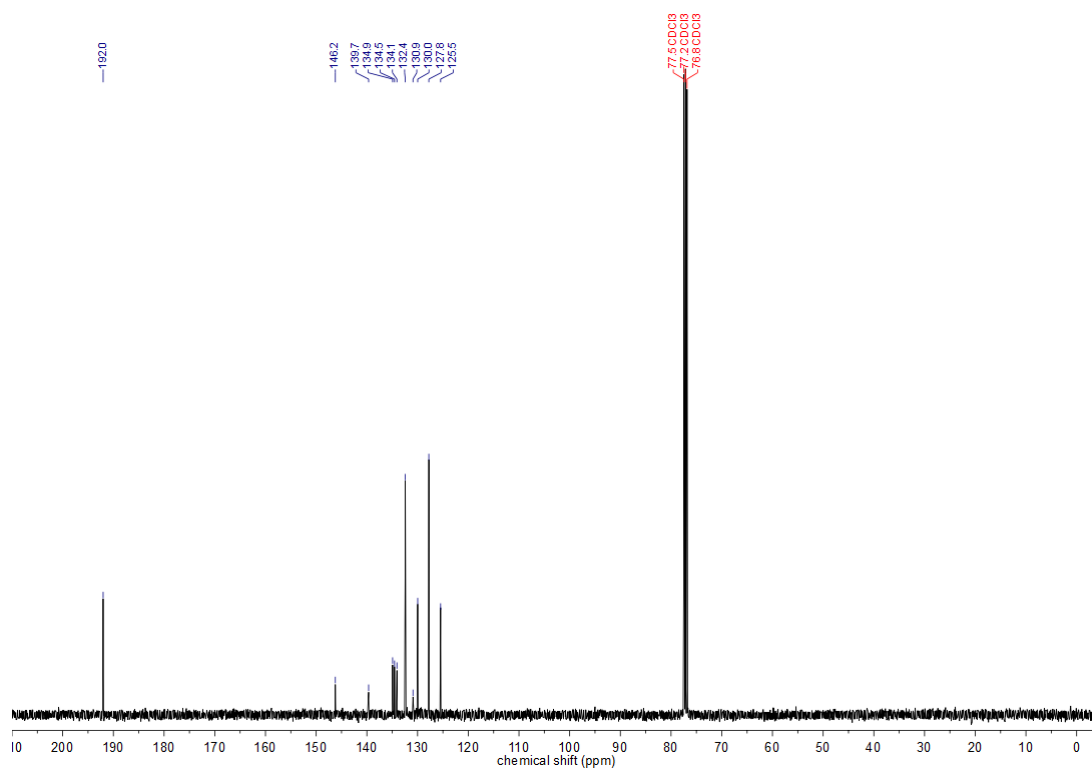
^{1}H-NMR(400 MHz, CDCl$_3$) **189a**
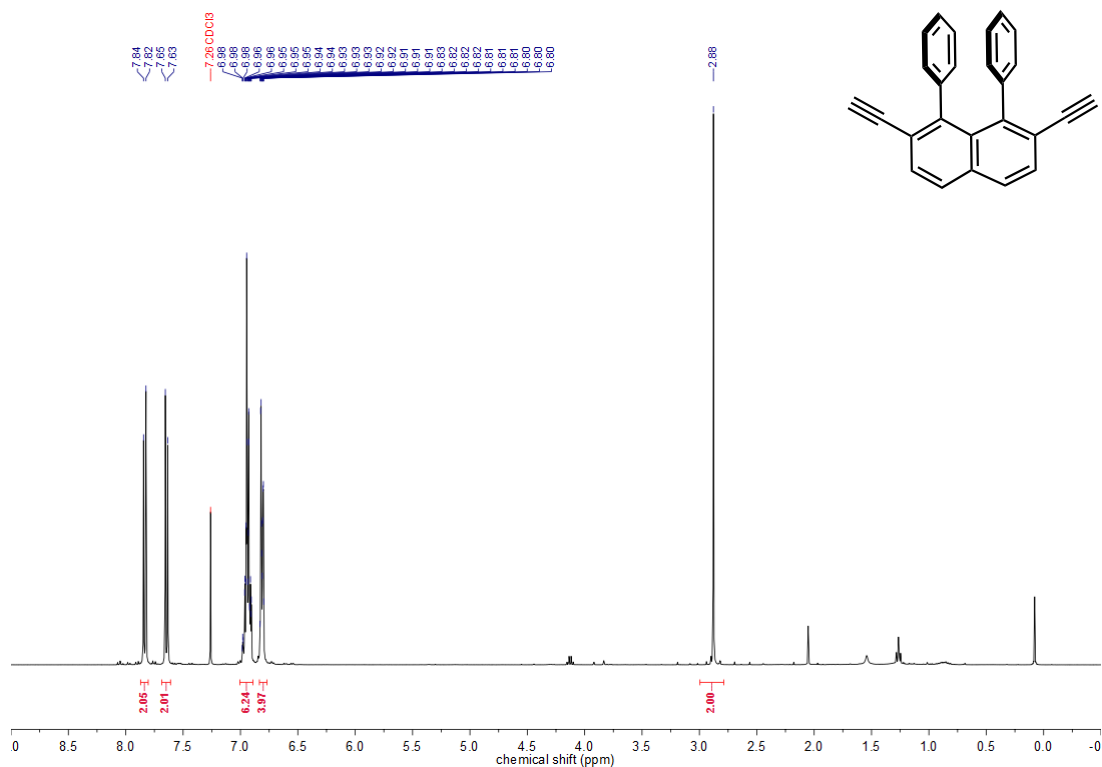
^{13}C-NMR(101 MHz, CDCl$_3$) **189a**
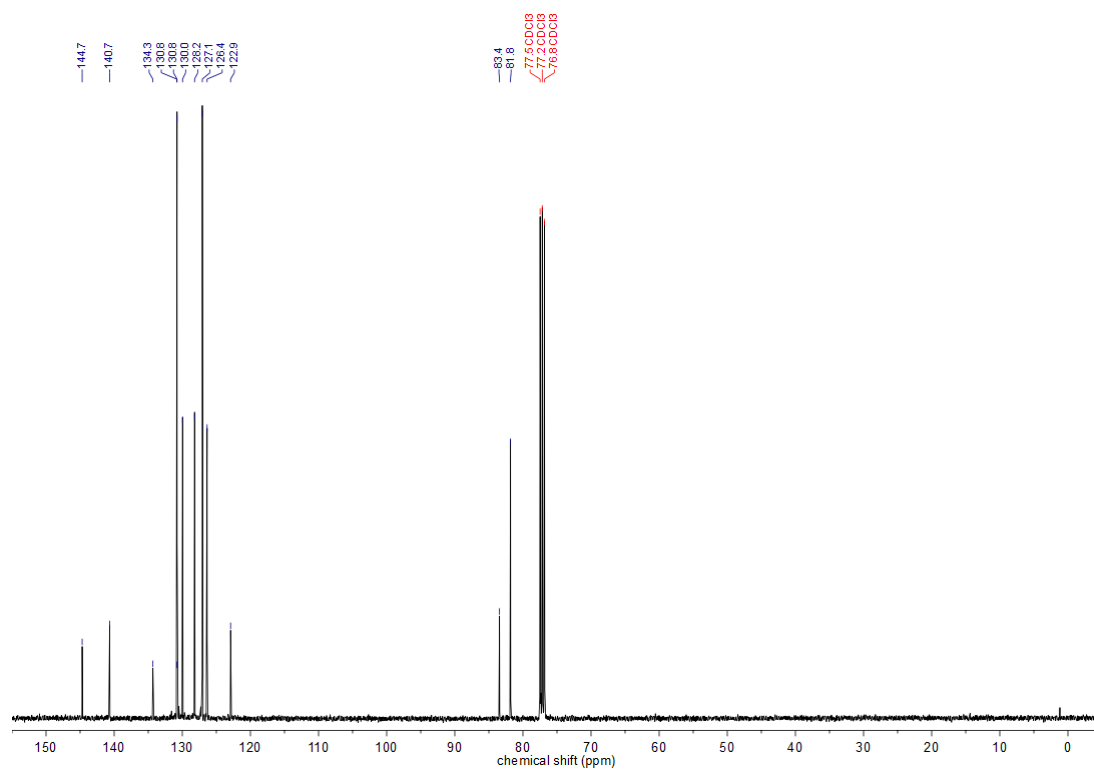
^{1}H-NMR(400 MHz, CDCl$_3$) **189b**
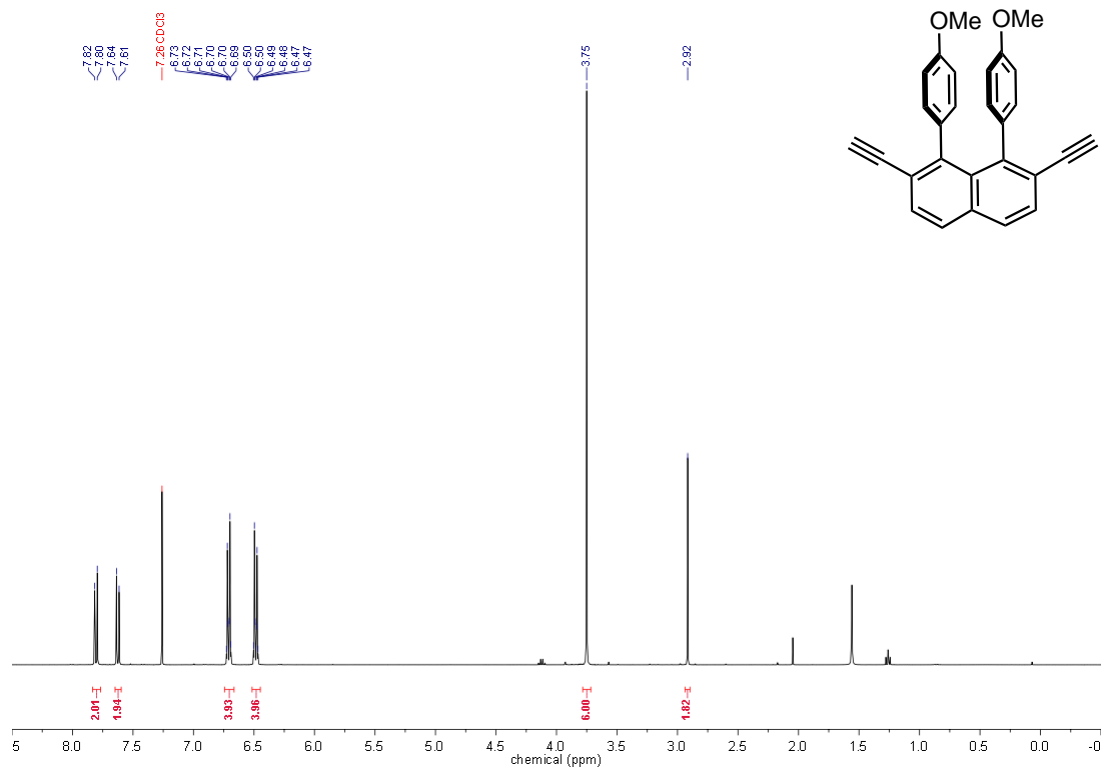
^{13}C-NMR(101 MHz, CDCl$_3$) **189b**
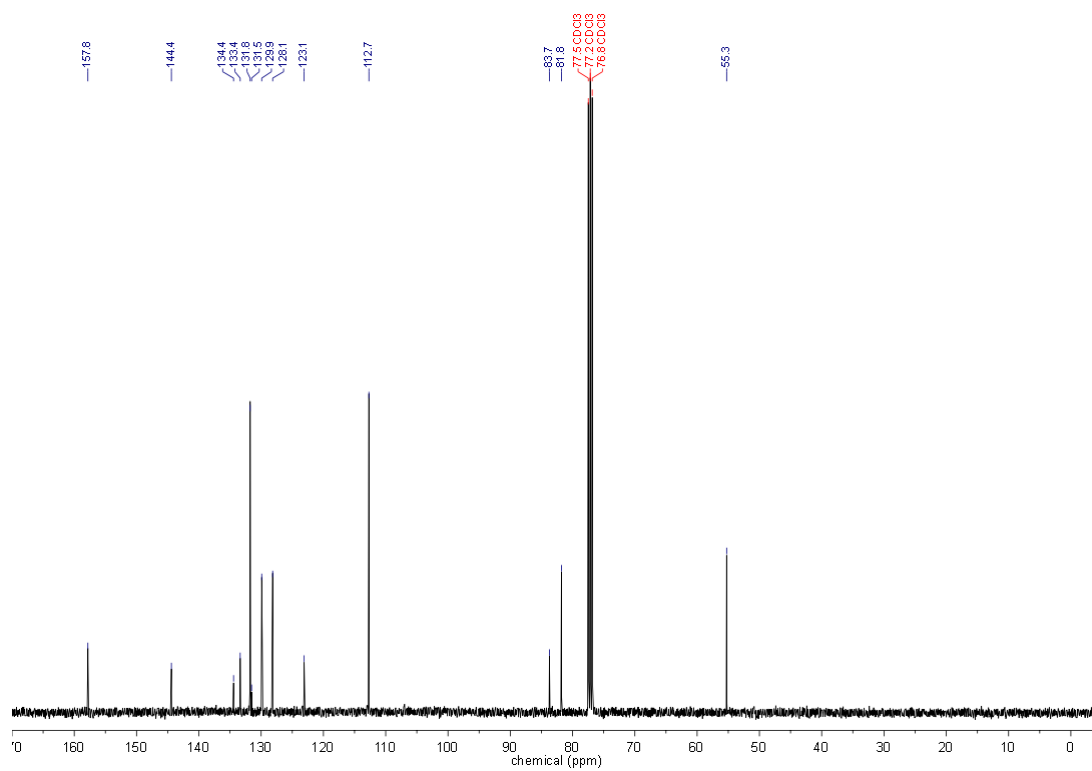
^{1}H-NMR(400 MHz, CDCl$_3$) **189c**
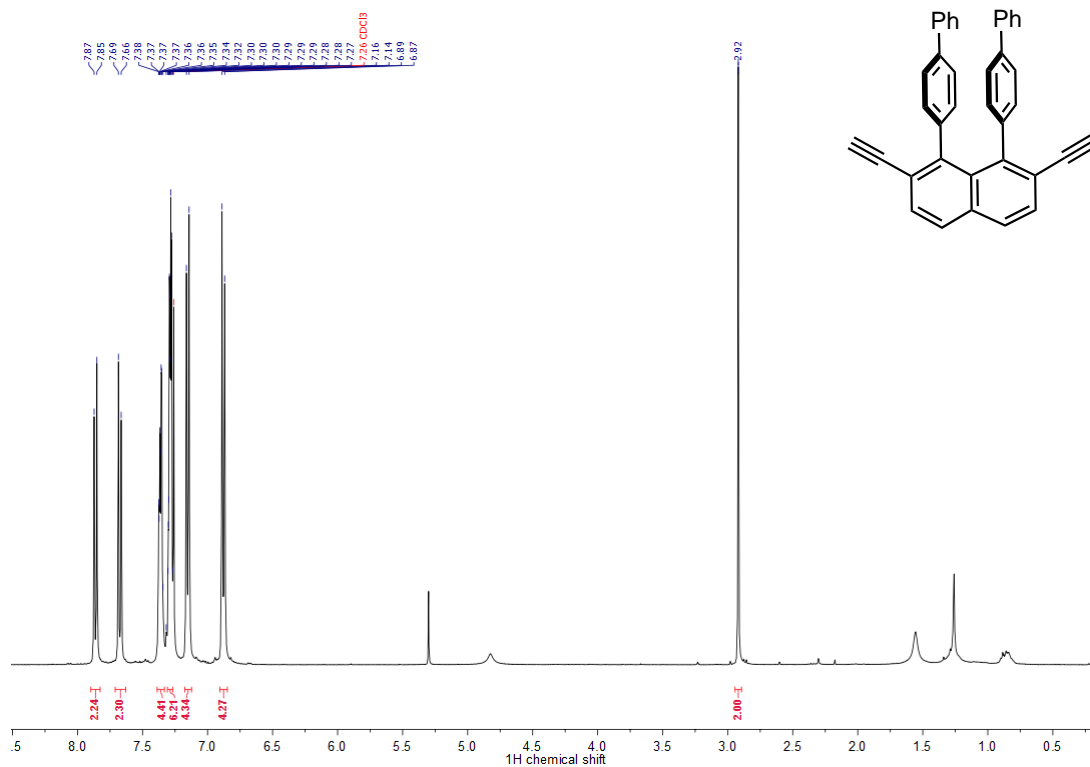
^{13}C-NMR(101 MHz, CDCl$_3$) **189c**
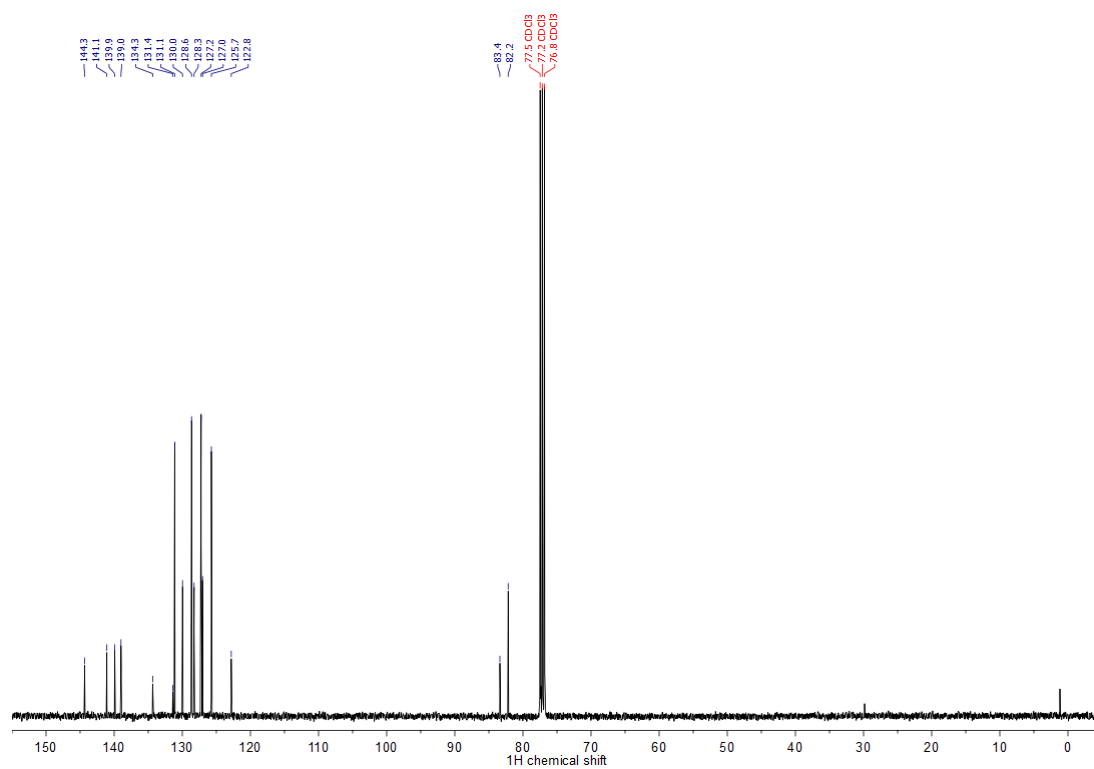
^{1}H-NMR(400 MHz, CDCl$_3$) **189d**
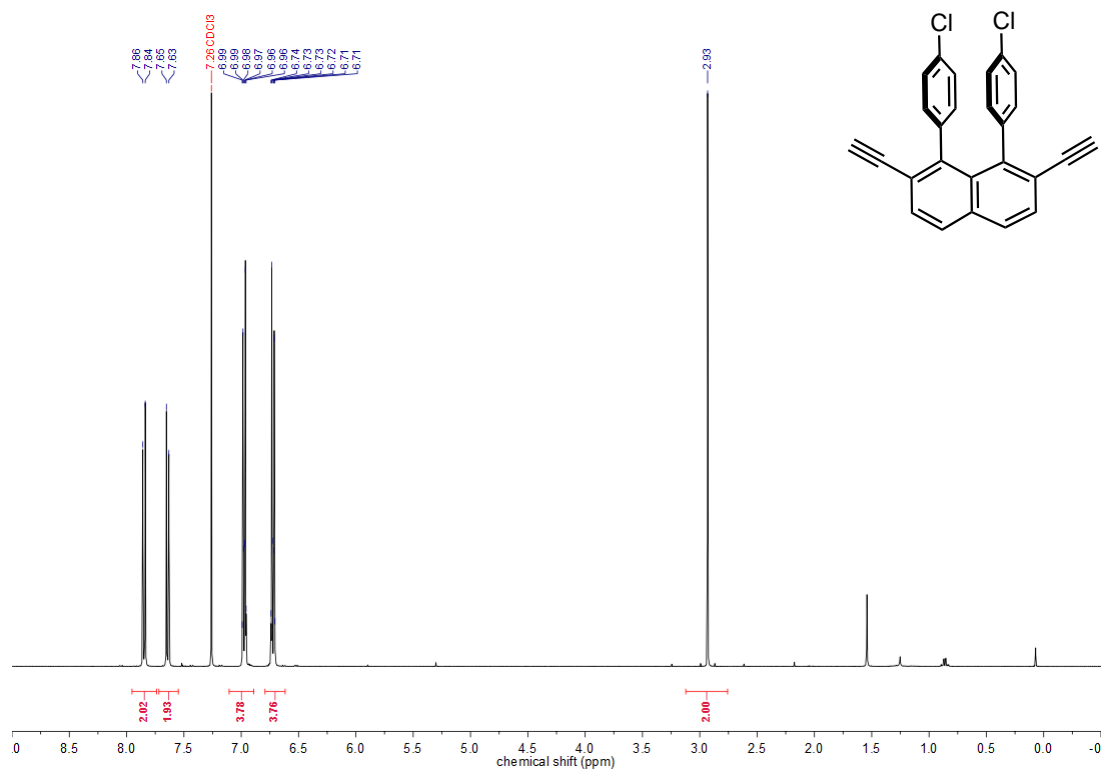
^{13}C-NMR(101 MHz, CDCl$_3$) **189d**
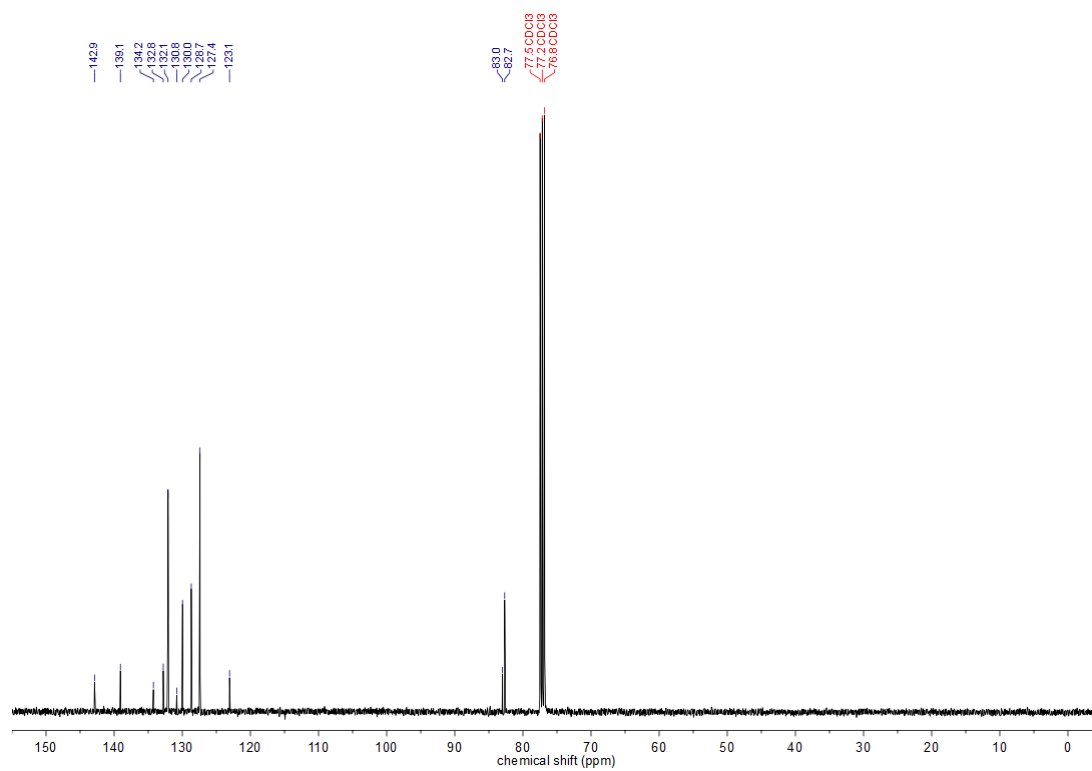
^{1}H-NMR(400 MHz, CDCl$_3$) **27aa**
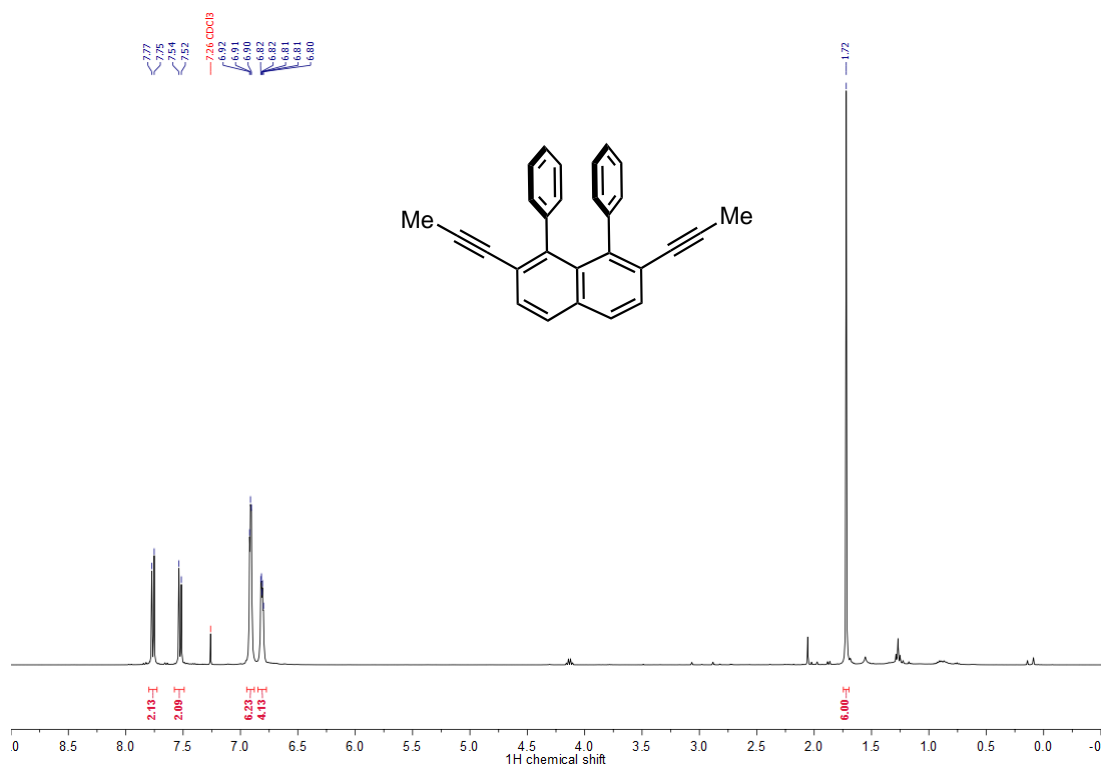
^{13}C-NMR(101 MHz, CDCl$_3$) **27aa**
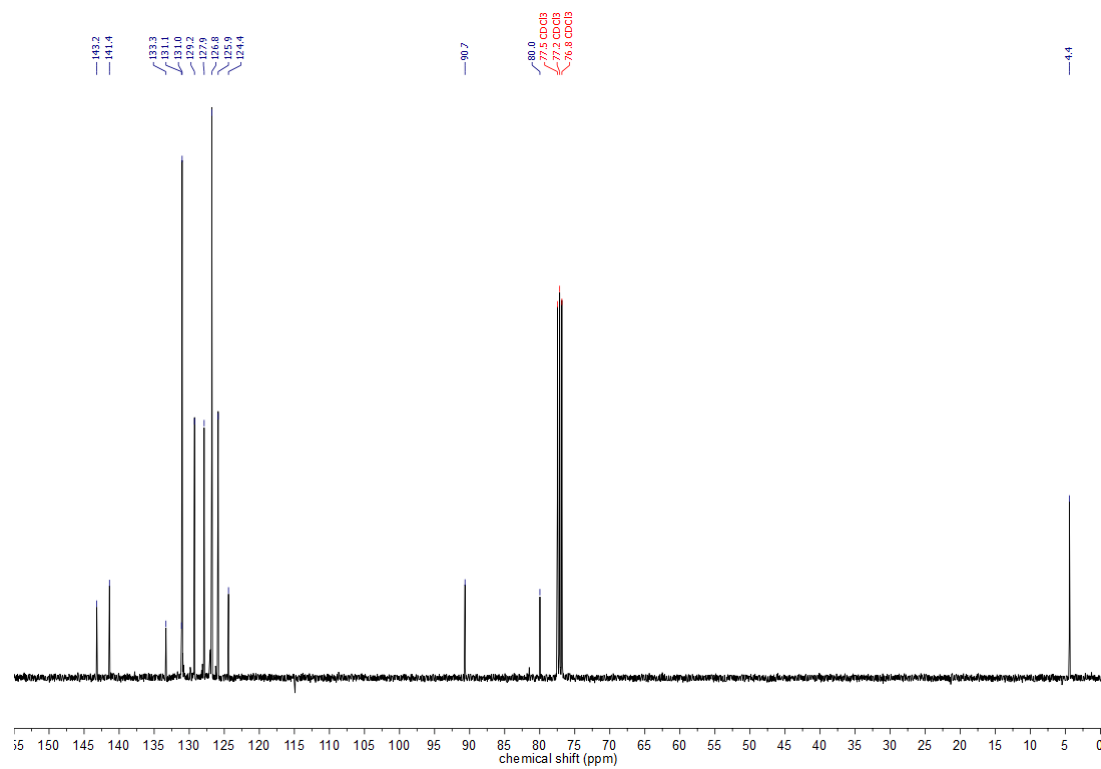
^{1}H-NMR(400 MHz, CDCl$_3$) **27ab**
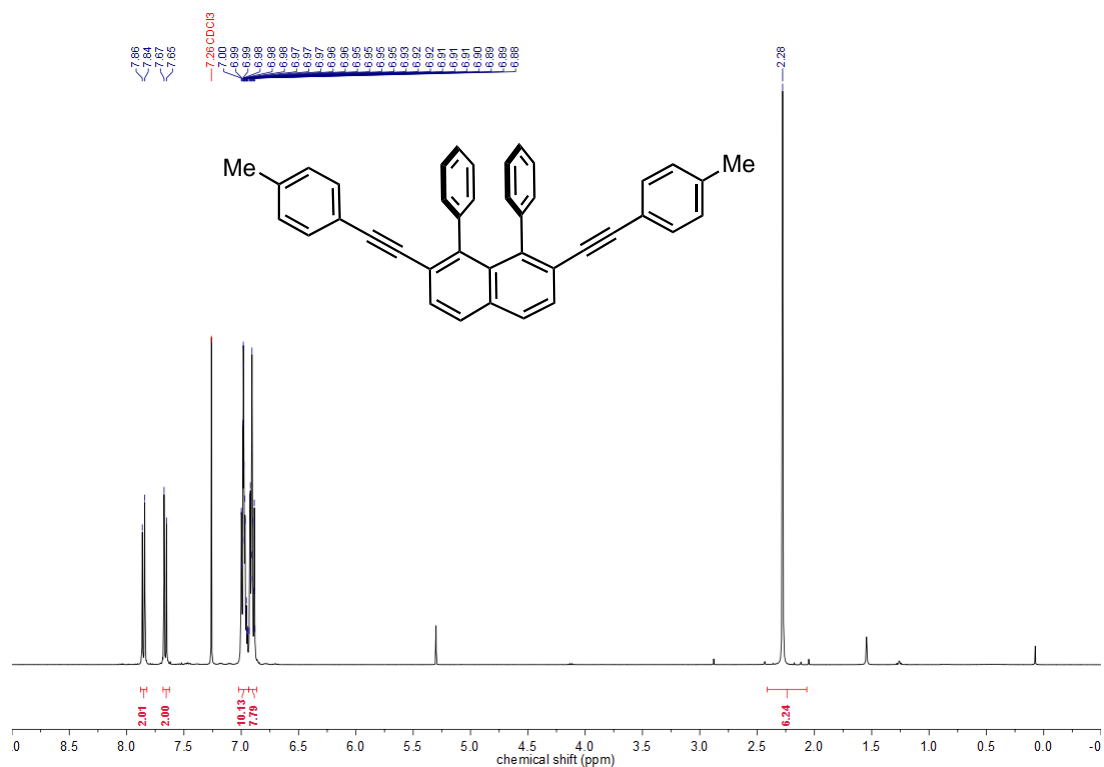
^{13}C-NMR(101 MHz, CDCl$_3$) **27ab**
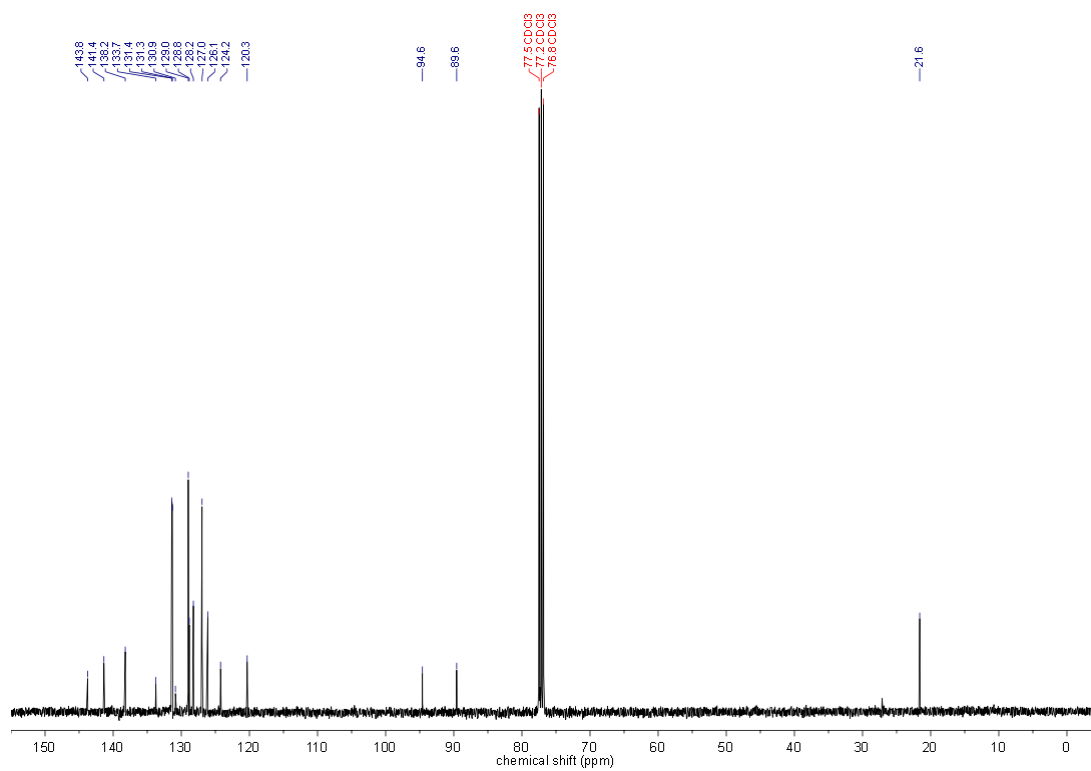
^{1}H-NMR(300 MHz, CDCl$_3$) **27ac**
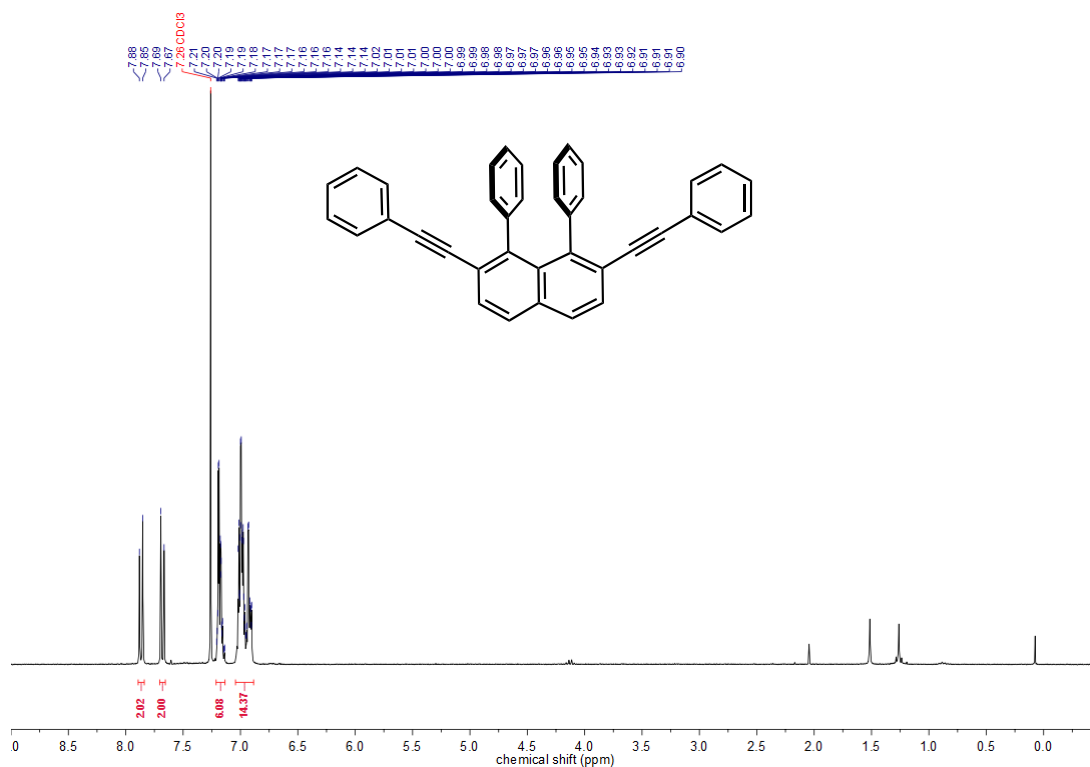
^{13}C-NMR(101 MHz, CDCl$_3$) **27ac**
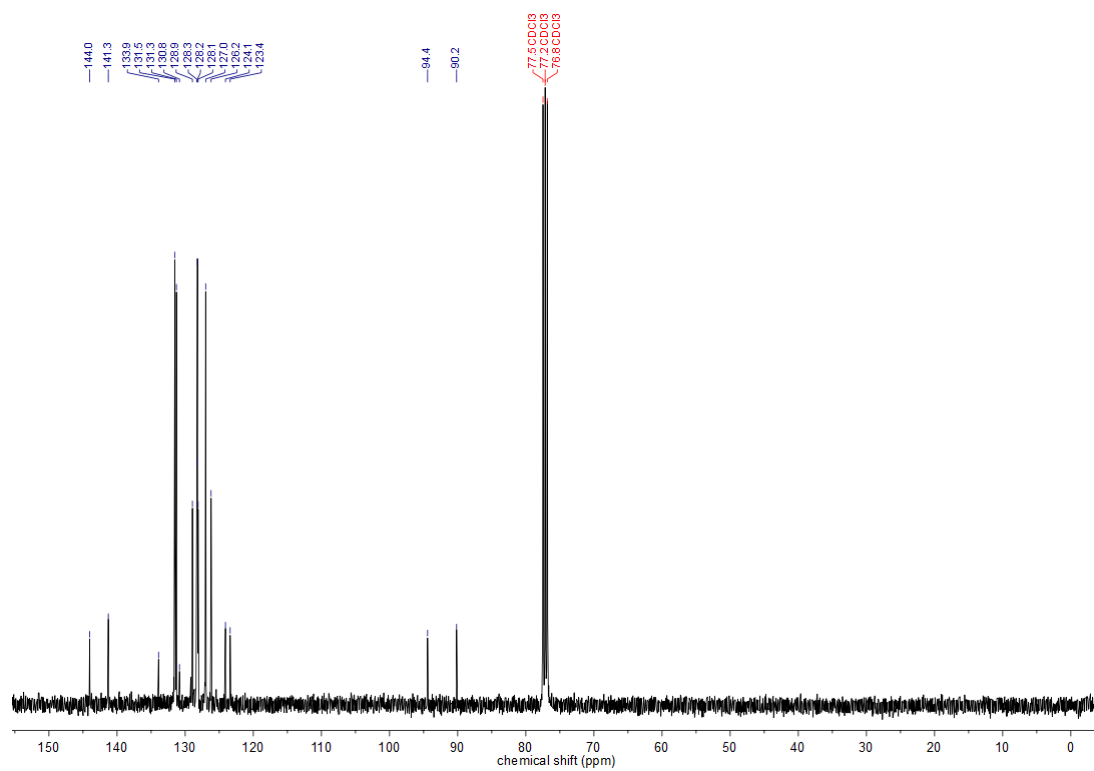
^{1}H-NMR(400 MHz, CDCl$_3$) **27ad**
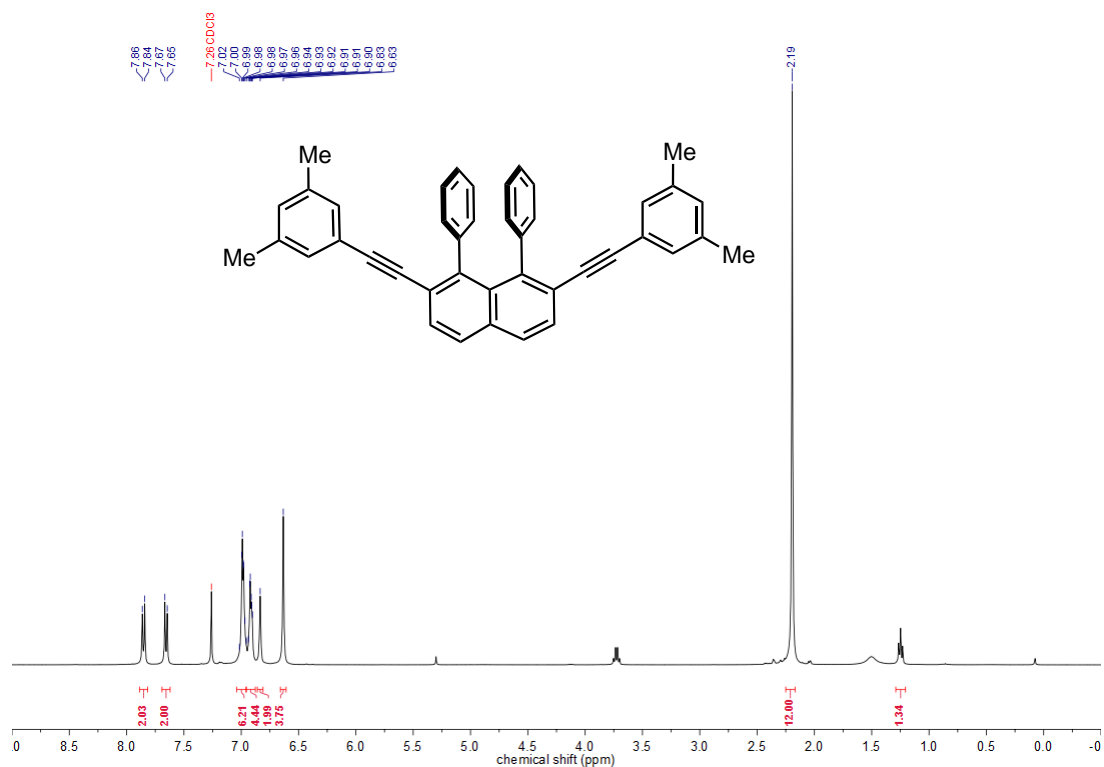
^{13}C-NMR(101 MHz, CDCl$_3$) **27ad**

^{1}H-NMR(400 MHz, CDCl$_3$) **27ae**

^{13}C-NMR(101 MHz, CDCl$_3$) **27ae**
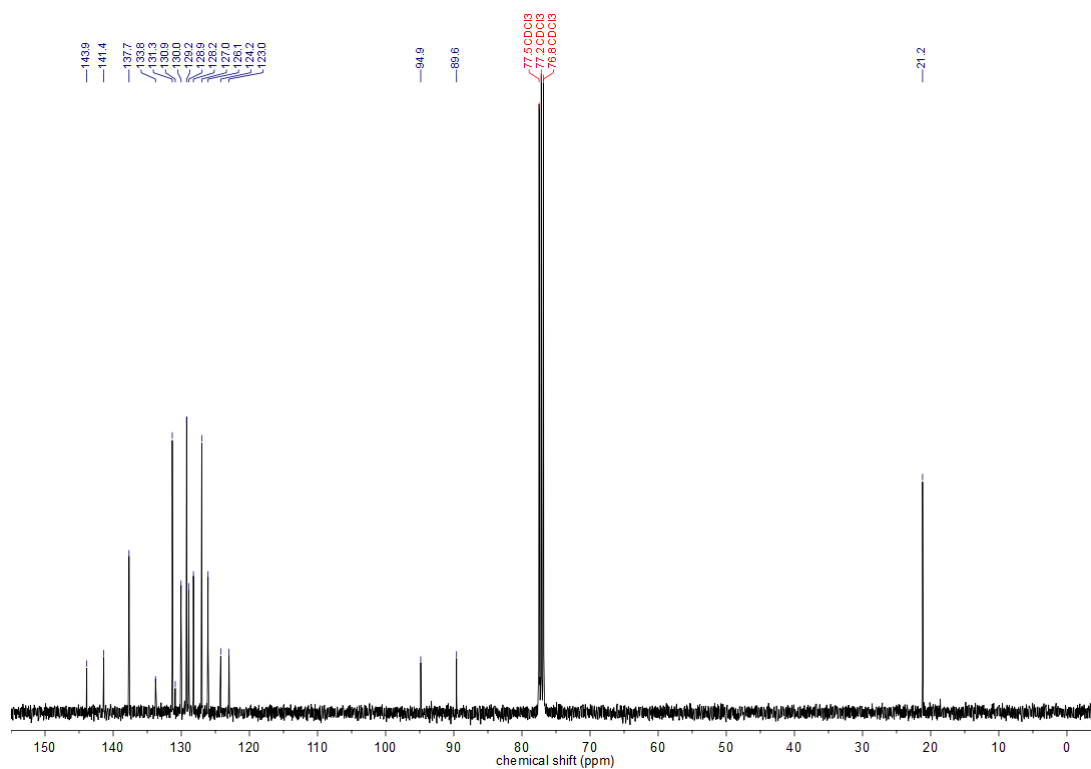
^{1}H-NMR(400 MHz, CDCl$_3$) **27ba**
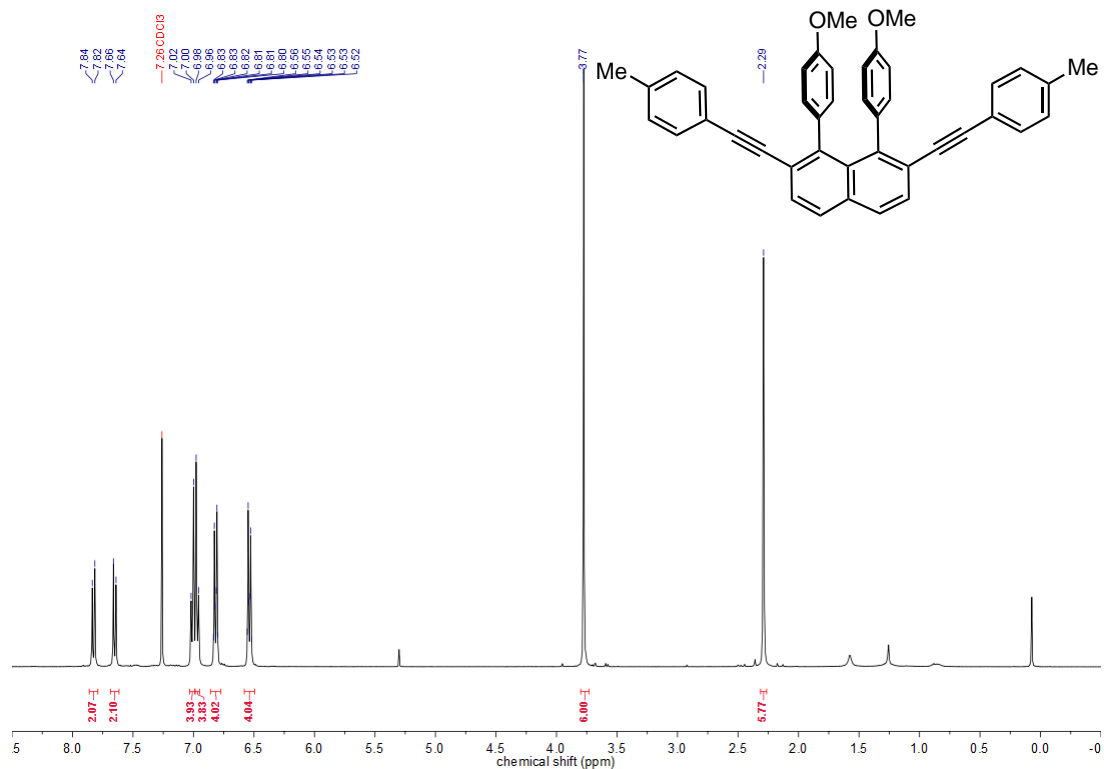
^{13}C-NMR(101 MHz, CDCl$_3$) **27ba**
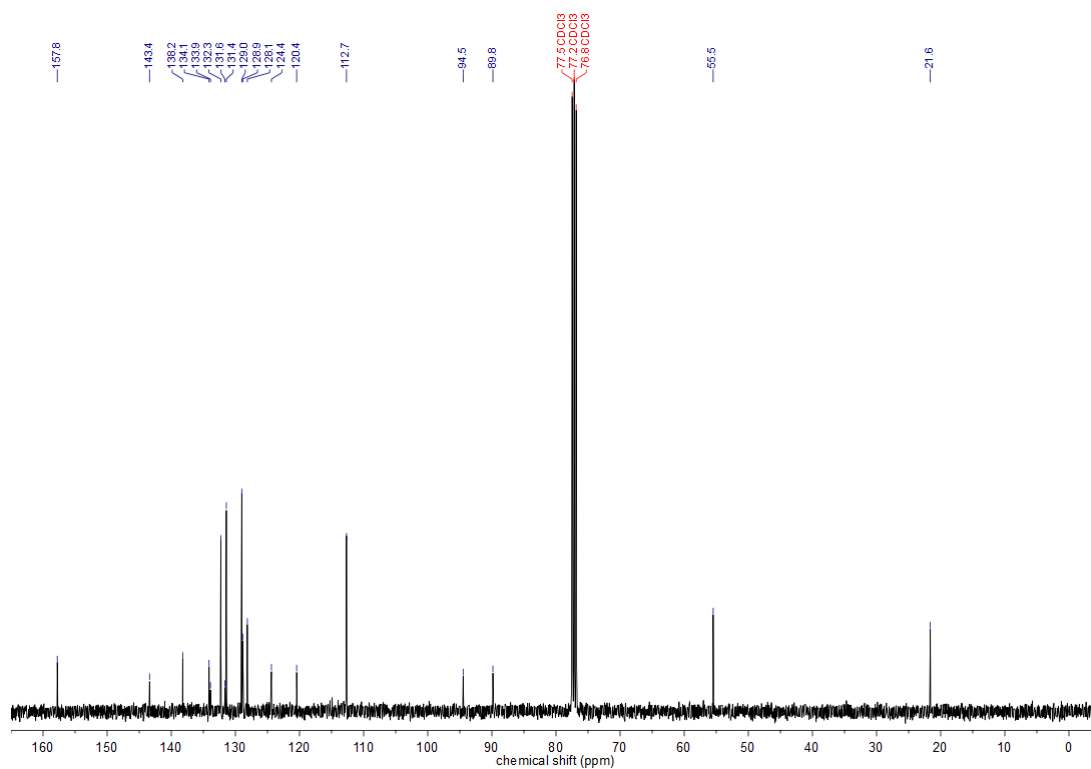
^{1}H-NMR(400 MHz, C$_6$D$_6$) **27bb**

^{13}C-NMR(101 MHz, C$_6$D$_6$) **27bb**
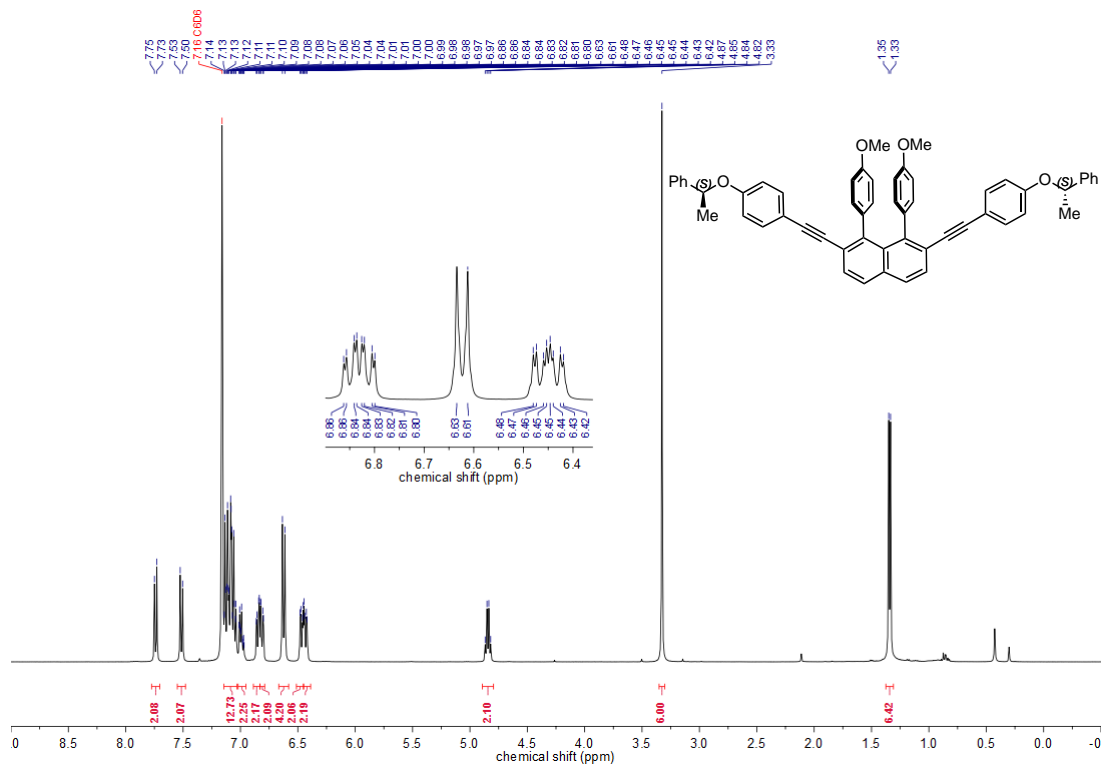
^{1}H-NMR(400 MHz, CDCl$_3$) **189g**
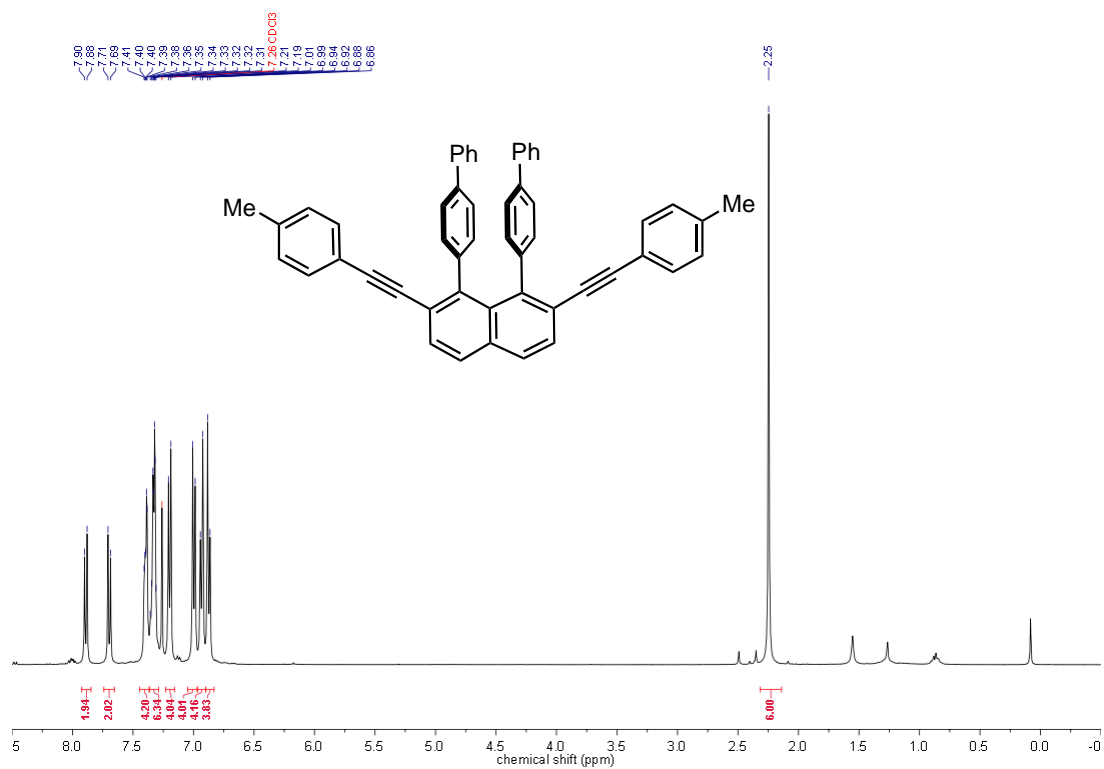
^{13}C-NMR(101 MHz, CDCl$_3$) **189g**
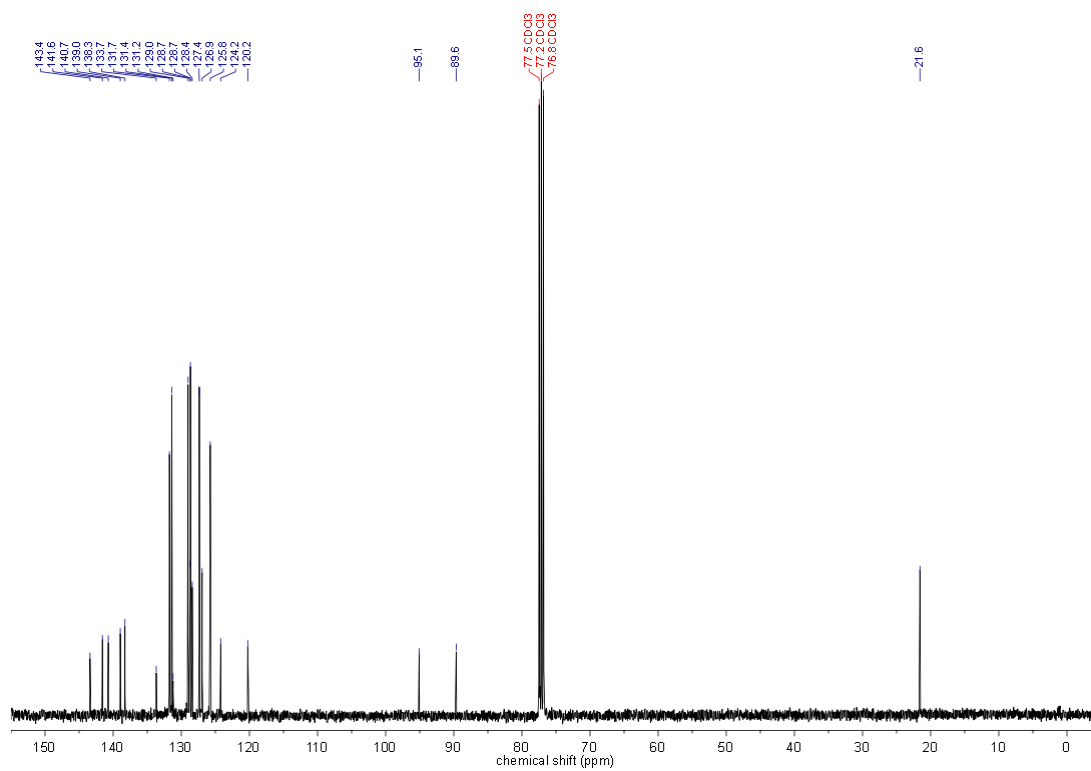
^{1}H-NMR(400 MHz, CDCl$_3$) **189h**
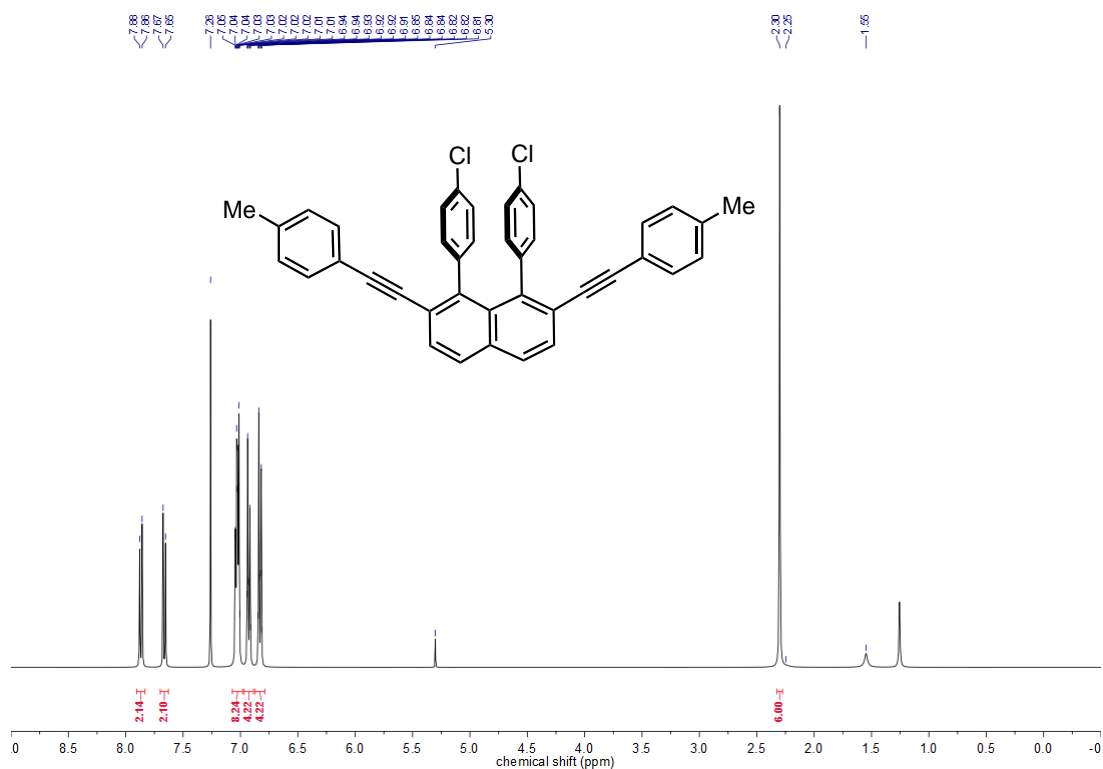
^{13}C-NMR(101 MHz, CDCl$_3$) **189h**
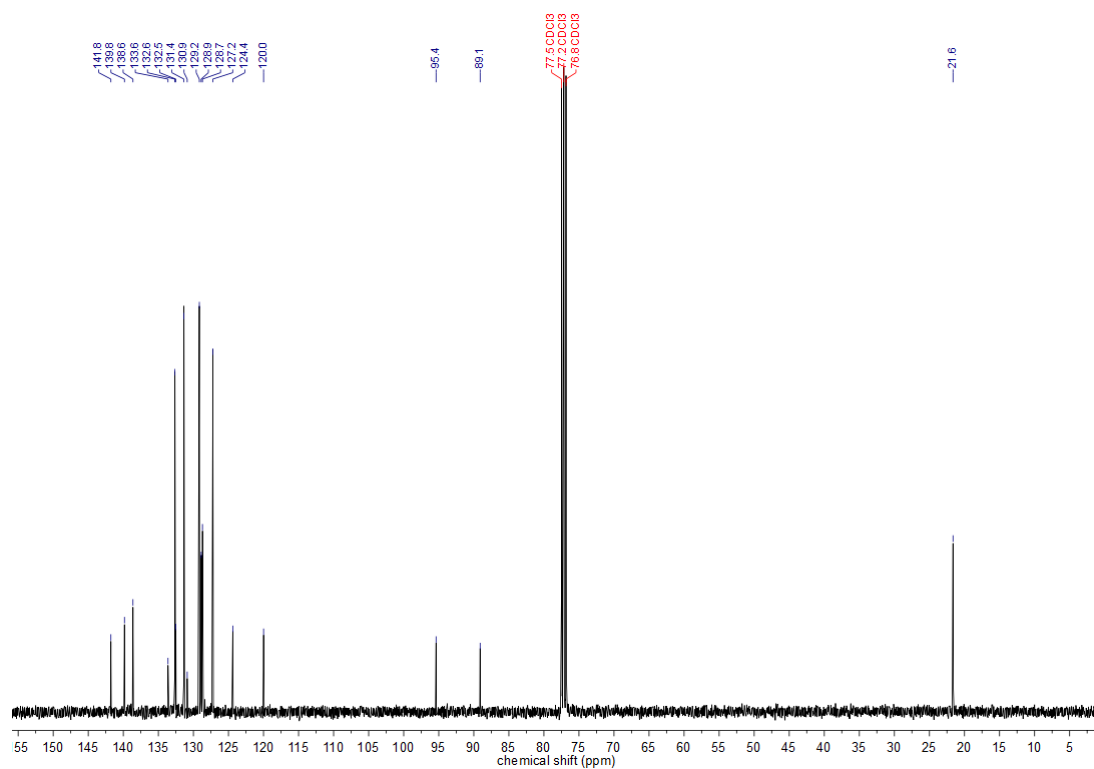
^{1}H-NMR(400 MHz, CDCl$_3$) **26aa**
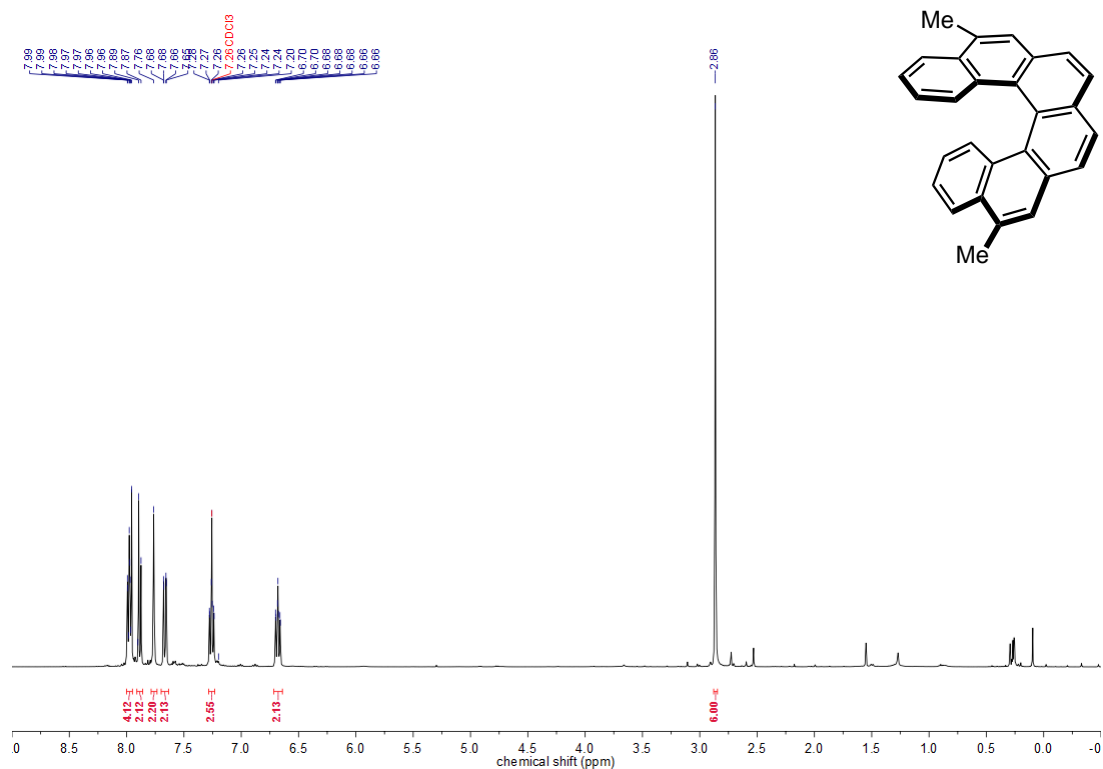
^{13}C-NMR(101 MHz, CDCl$_3$) **26aa**
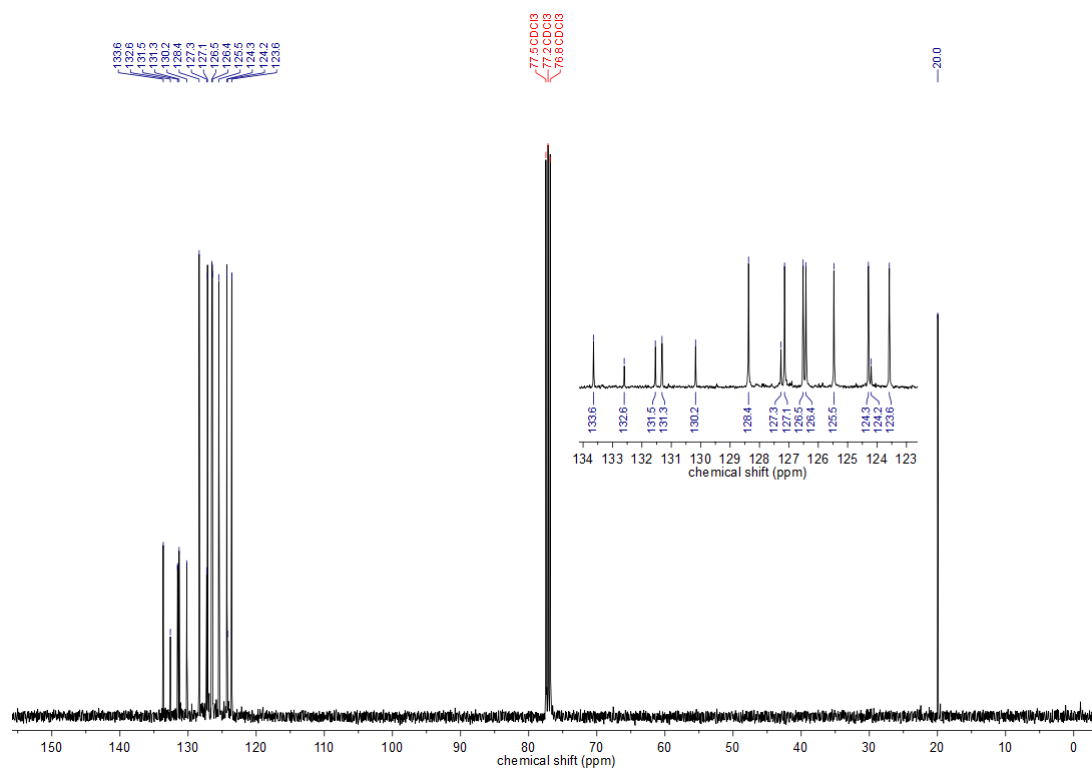
^{1}H-NMR(400 MHz, CDCl$_3$) **26ab**
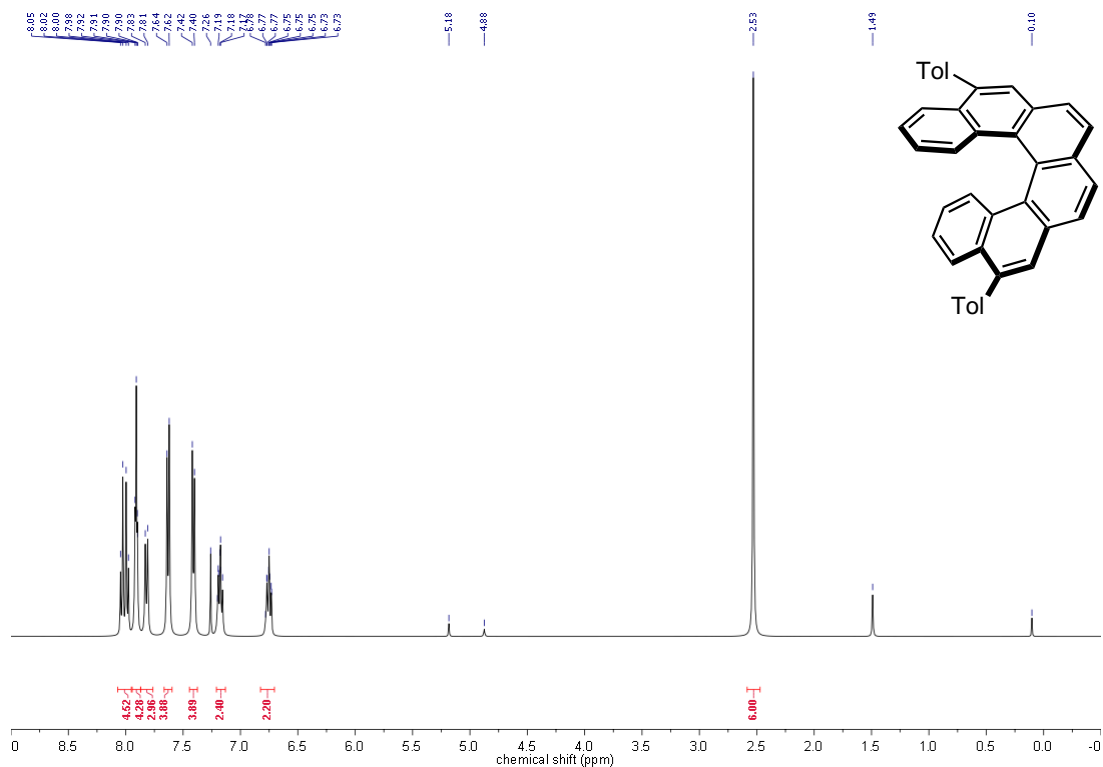
^{13}C-NMR(101 MHz, CDCl$_3$) **26ab**
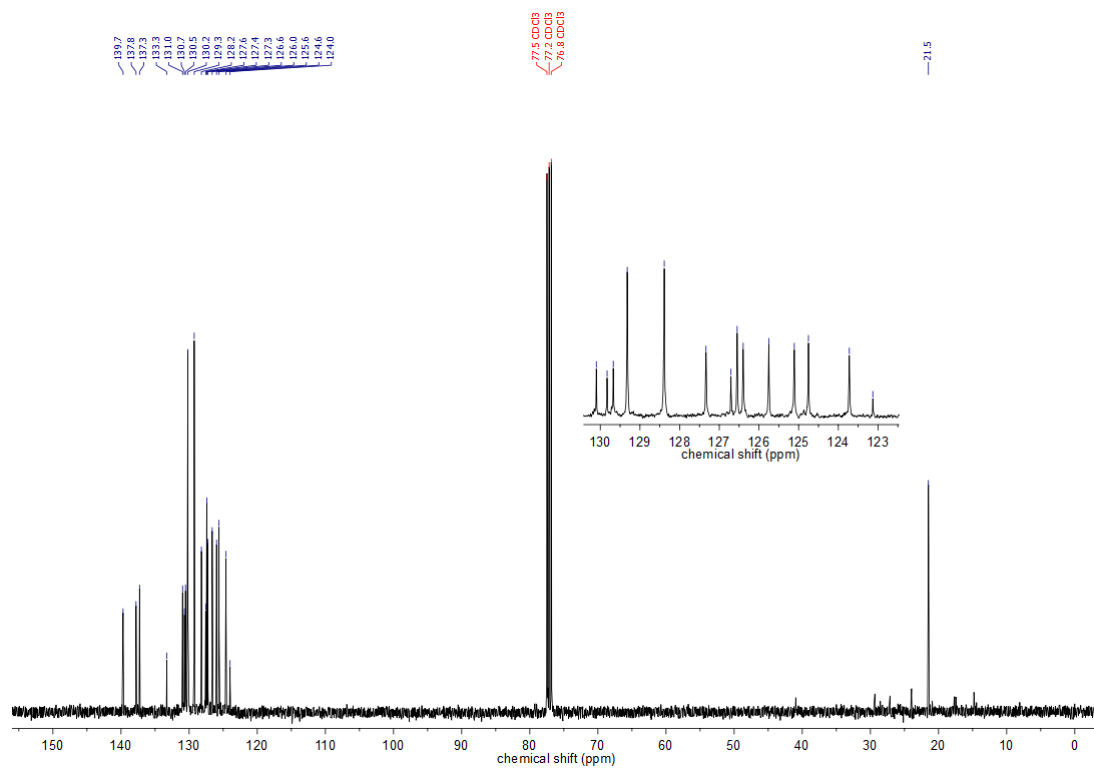
Assignments for compound *E*-**190ab**:
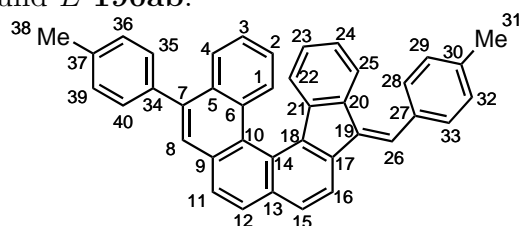
Atom	δ (ppm)	Correlations		
		COSY	HMBC	NOESY
1 C	130,834		3	
1 H	8,581 2	3, 5, 10	2, 25	
2 C	125,746		4	
2 H	7,053	1, 3	4, 6	1, 3
3 C	125,864		1	
3 H	7,24	2, 4	1, 5	4, 2
4 C	126,138		2	
4 H	8,226	3	2, 6, 7	35, 40, 3
5 C	130,914		1, 8, 3	
6 C	131,15		4, 2	
7 C	140,06		4, 35, 40	
8 C	126,718		11	
8 H	7,854		34, 5, 10, 11, 9	11, 35, 40
9 C	131,992		8, 12	
10 C	126,291		1, 8, 11	
11 C	126,488		8	
11 H	7,658	12	8, 10, 13	8, 12
12 C	128,118		15	
12 H	7,82	11	9, 14, 15	11
13 C	134,735		16, 11	
14 C	124,256		12, 15	
15 C	127,221		16, 12	
15 H	7,796	16	12, 14, 17	16
16 C	118,755			
16 H	7,937	15	13, 18, 19, 15	15
17 C	140,341		26, 15	
18 C	136,771		16, 25	
19 C	136,896		22, 16	
20 C	136,652		26, 25, 23	
21 C	142,758		22, 24	

Continued on next page

| Atom | δ (ppm) | | Correlations | |
		COSY	HMBC	NOESY
22 C	123,483		24	
22 H	7,973	23	21, 24, 19	28, 23, 32
23 C	125,685		25	
23 H	6,777	22, 24	20, 25	22, 24
24 C	126,896		22	
24 H	6,646	23, 25	21, 22	25, 23
25 C	125,137		23	
25 H	6,818	24	18, 20, 23	1, 24
26 C	127,944		28, 32	
26 H	7,803		28, 32, 20, 17	28, 32
27 C	134,221		29, 33	
28 C	129,702		26, 32	
28 H	7,54	29	30, 32, 26	22, 26, 29
29 C	129,205		31, 33	
29 H	7,041	28	27, 33, 31	28, 31
30 C	137,841		31, 28, 32	
31 C	20,886		29, 33	
31 H(3)	2,15		29, 30, 33	29, 33
32 C	129,702		26, 28	
32 H	7,54	33	26, 28, 30	22, 26, 33
33 C	129,205		31, 29	
33 H	7,041	32	27, 29, 31	32, 31
34 C	137,871		8, 36, 39	
35 C	130,177		40	
35 H	7,516		7, 37, 40	4, 8, 36
36 C	129,061		38, 39	
36 H	7,16		38, 39, 34	35, 38
37 C	136,847		38, 35, 40	
38 C	20,993		36, 39	
38 H(3)	2,256		37, 36, 39	36, 39
39 C	129,061		38, 36	
39 H	7,16	40	38, 36, 34	40, 38
40 C	130,178		35	
40 H	7,516	39	7, 37, 35	4, 8, 39

Table A.3: Assignment of NMR signals for **190ab**. Spectrometer: Bruker AV600; Solvent: C_6D_6.
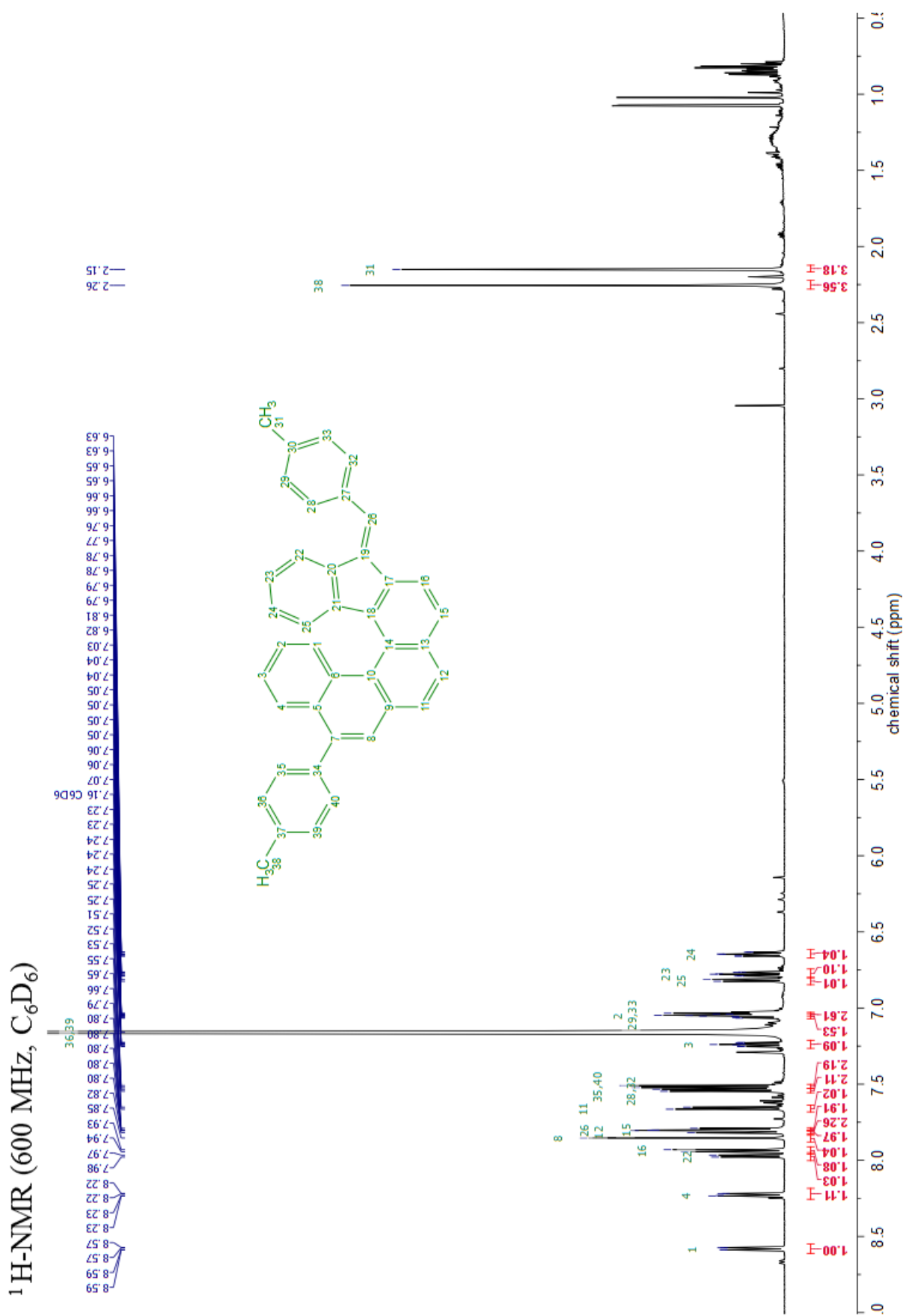
^{1}H-NMR (600 MHz, C$_6$D$_6$)

^{13} C-NMR (151 MHz, C$_6$D$_6$)

HSQC

HMBC

COSY

NOESY
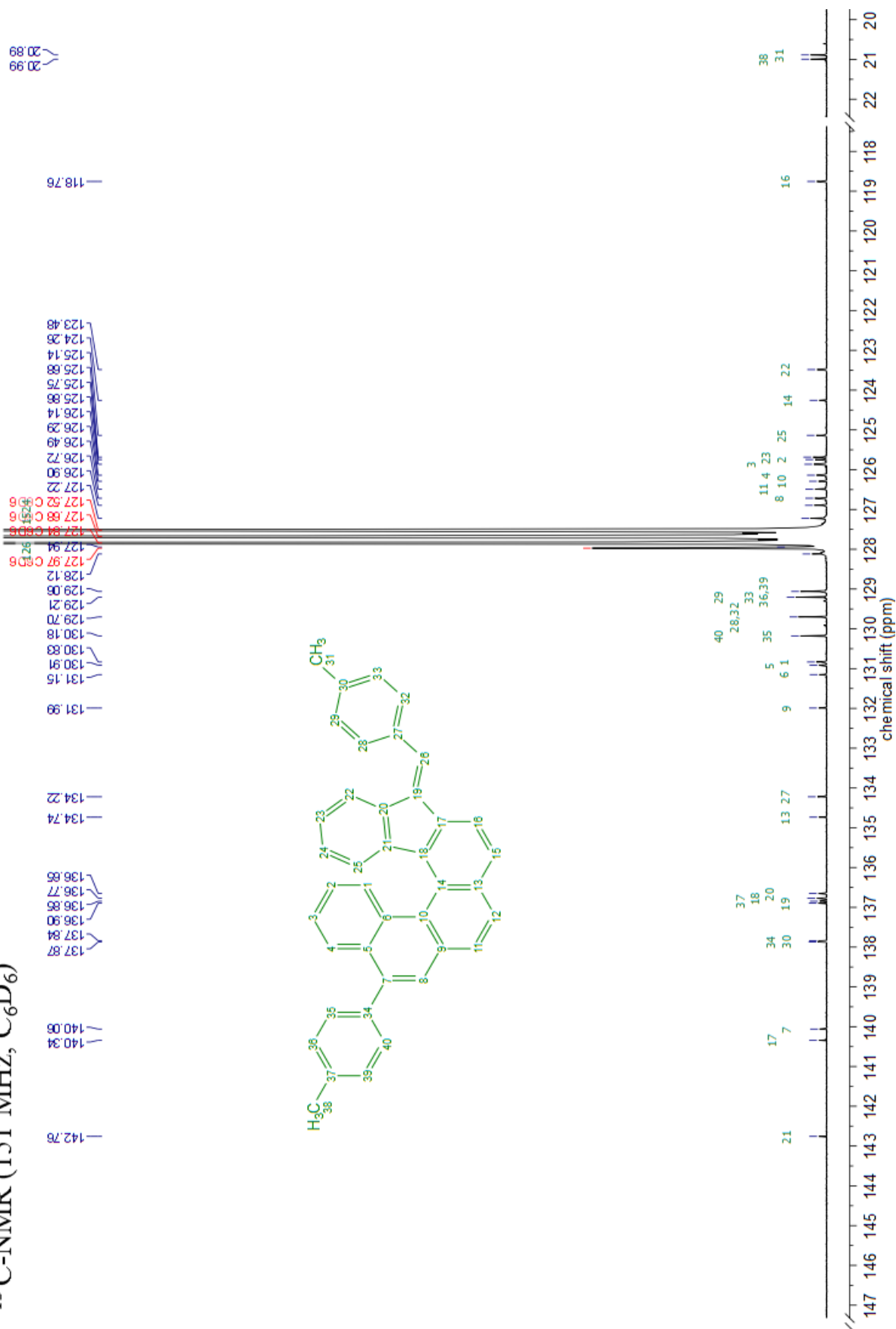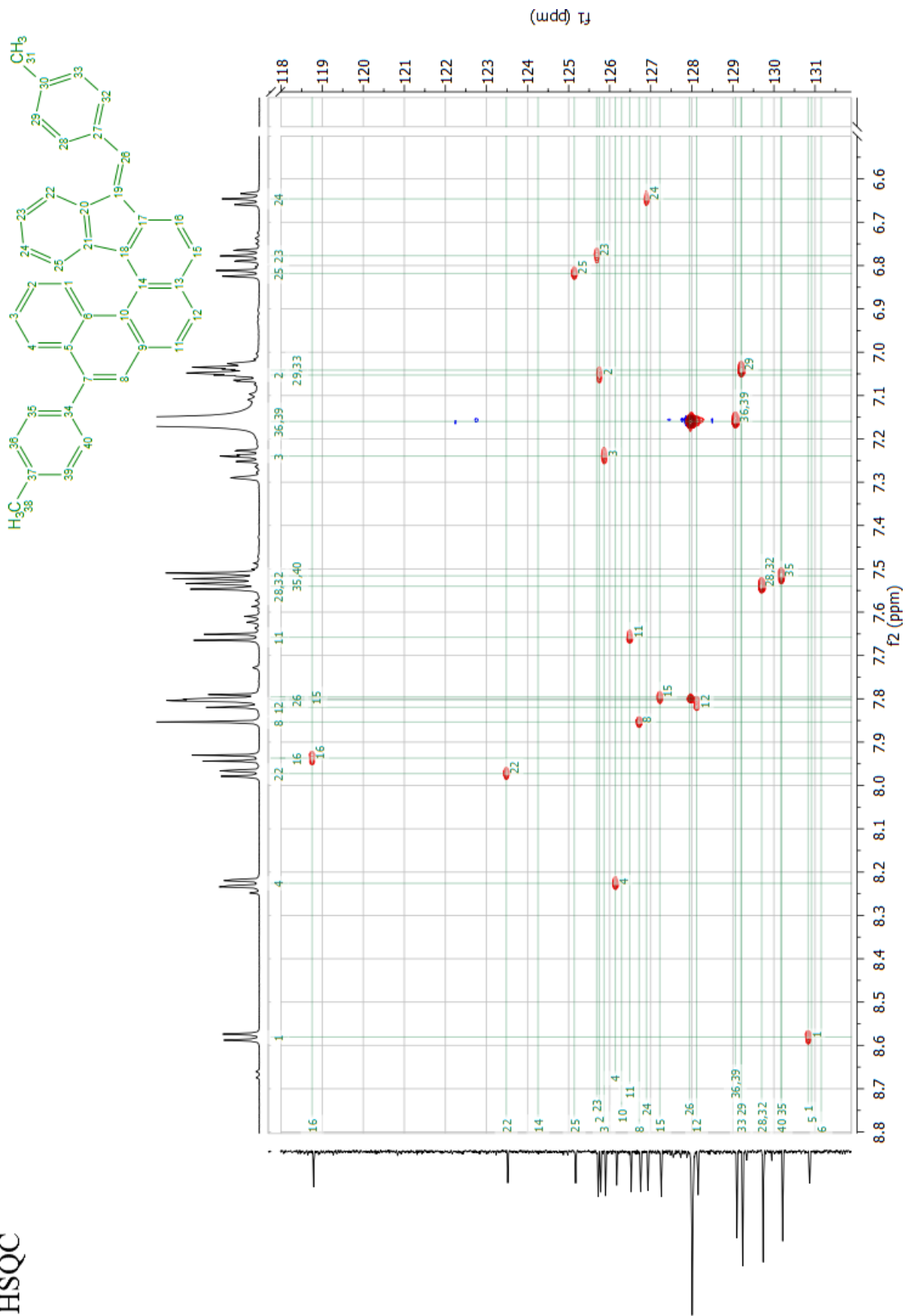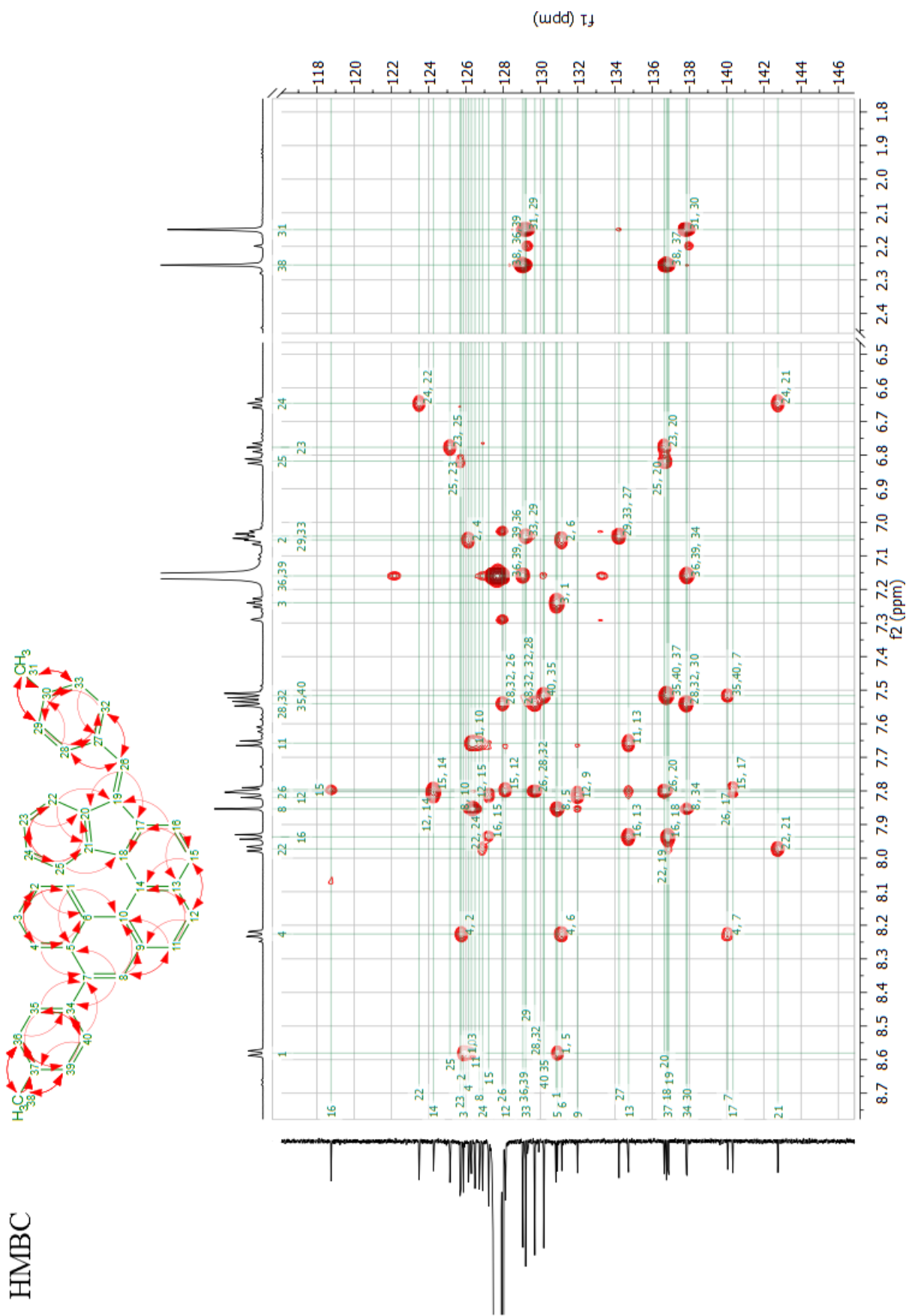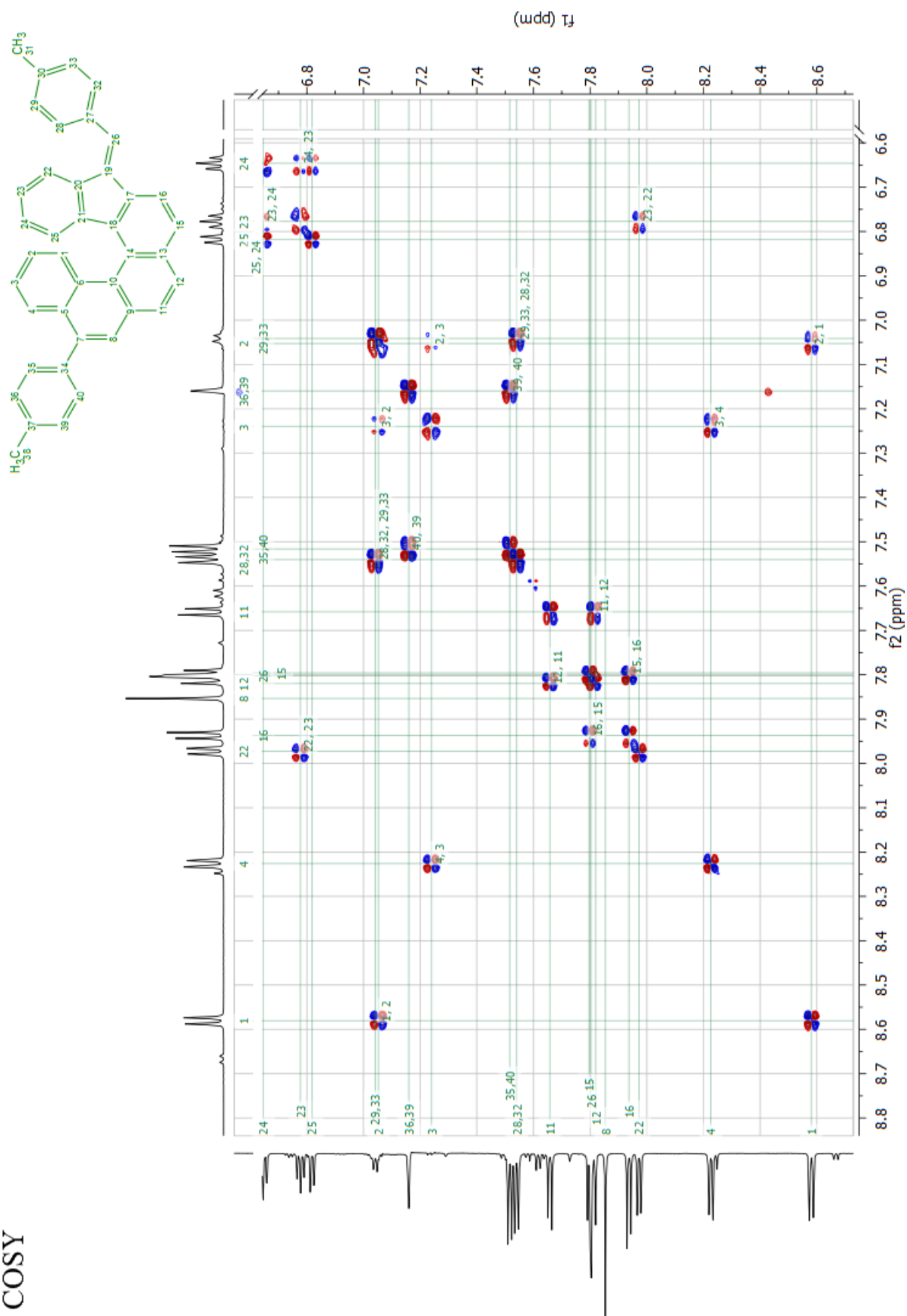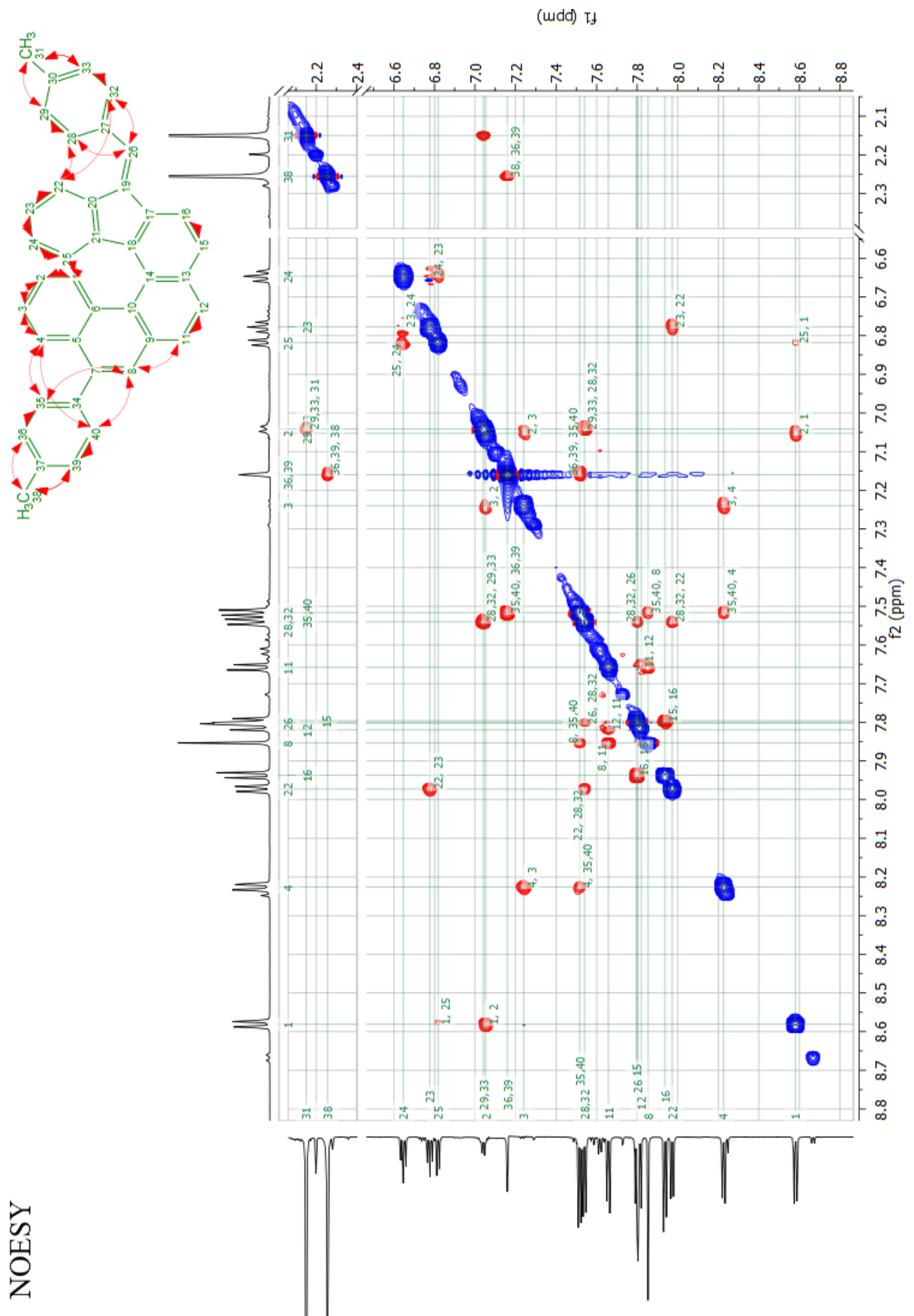
^{1}H-NMR(400 MHz, CDCl$_3$) **200ab**
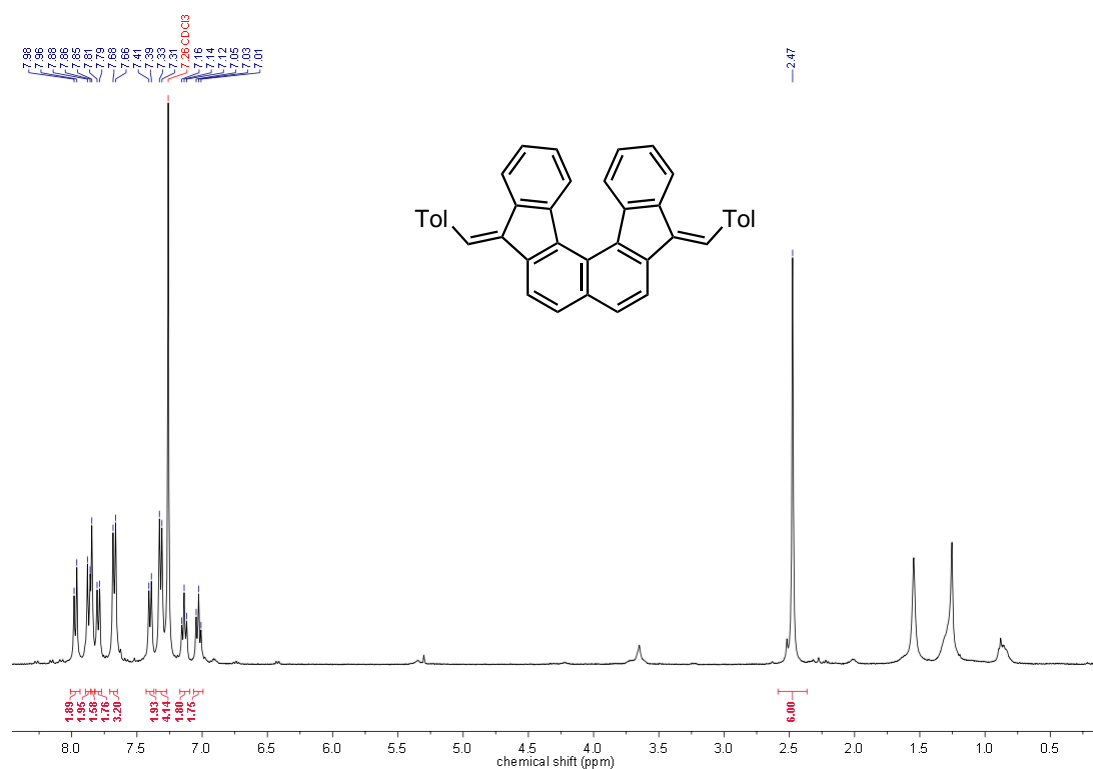
^{13}C-NMR(101 MHz, CDCl$_3$) **200ab**
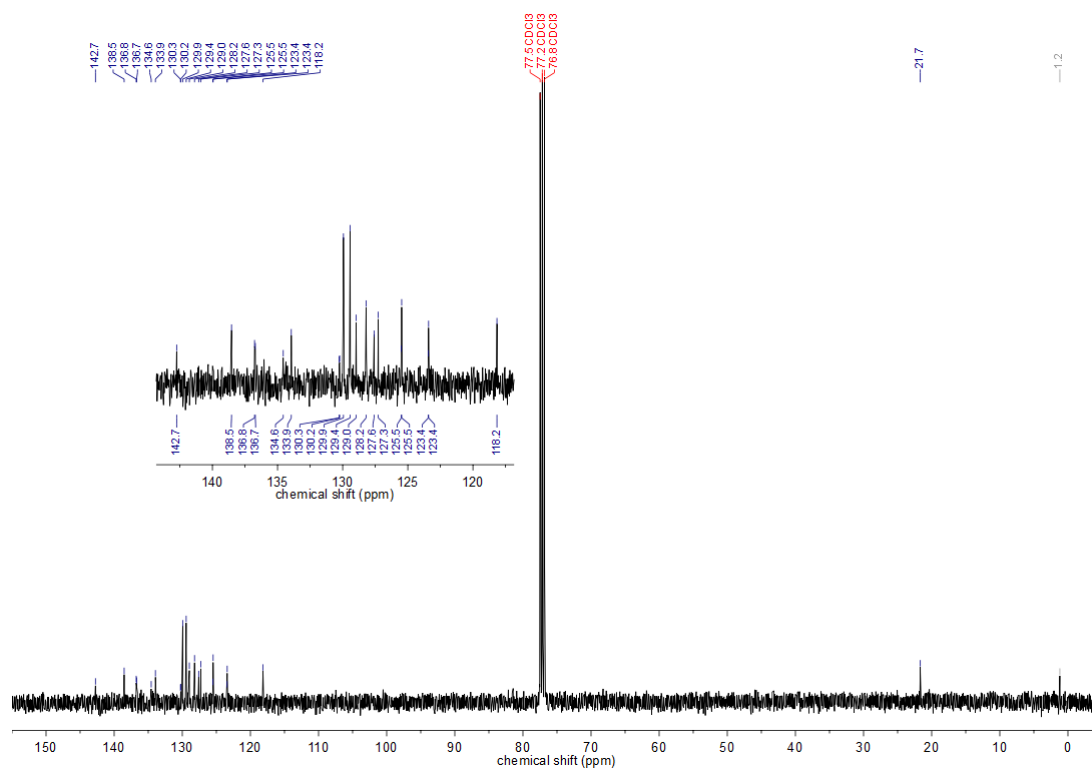
^{1}H-NMR(500 MHz, CDCl$_3$) **26ac**
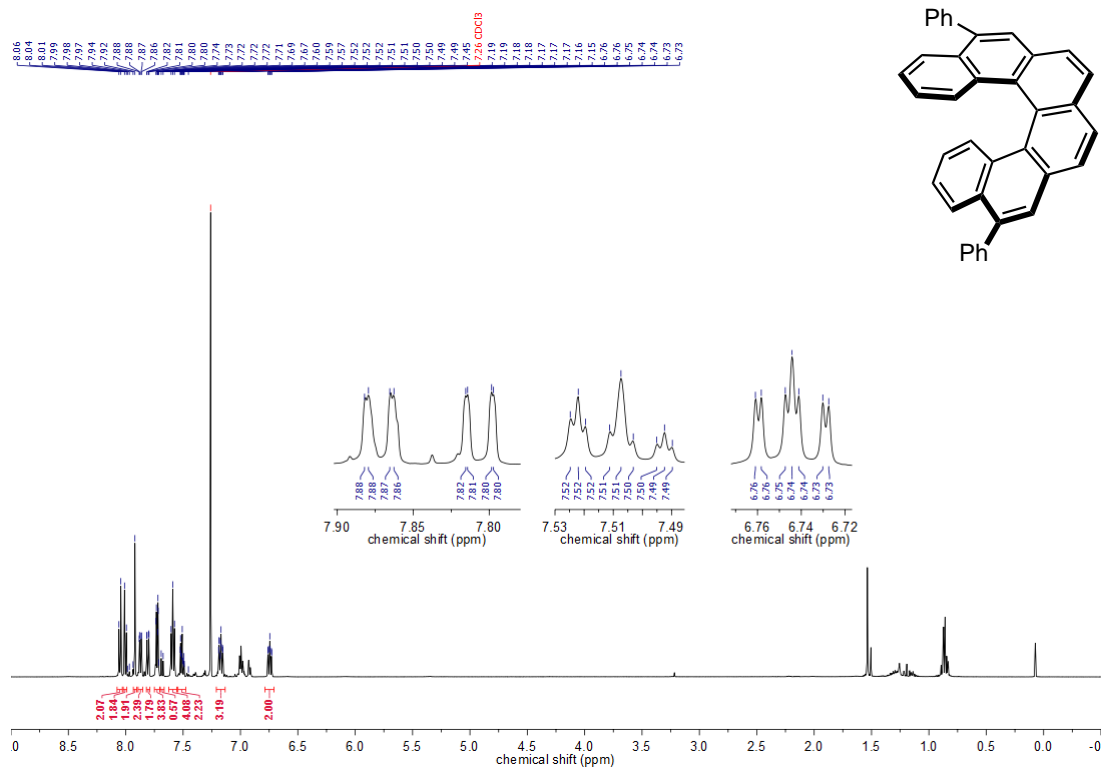
^{13}C-NMR(126 MHz, CDCl$_3$) **26ac**
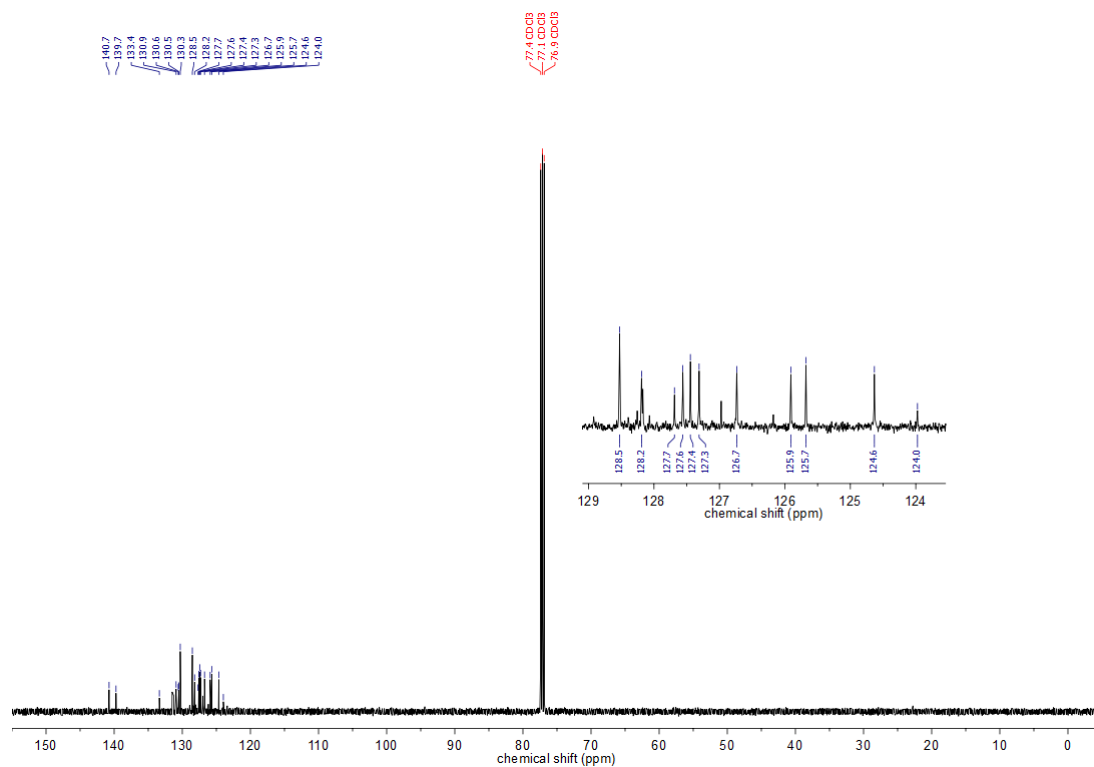
^{1}H-NMR(400 MHz, CDCl$_3$) **26ba**
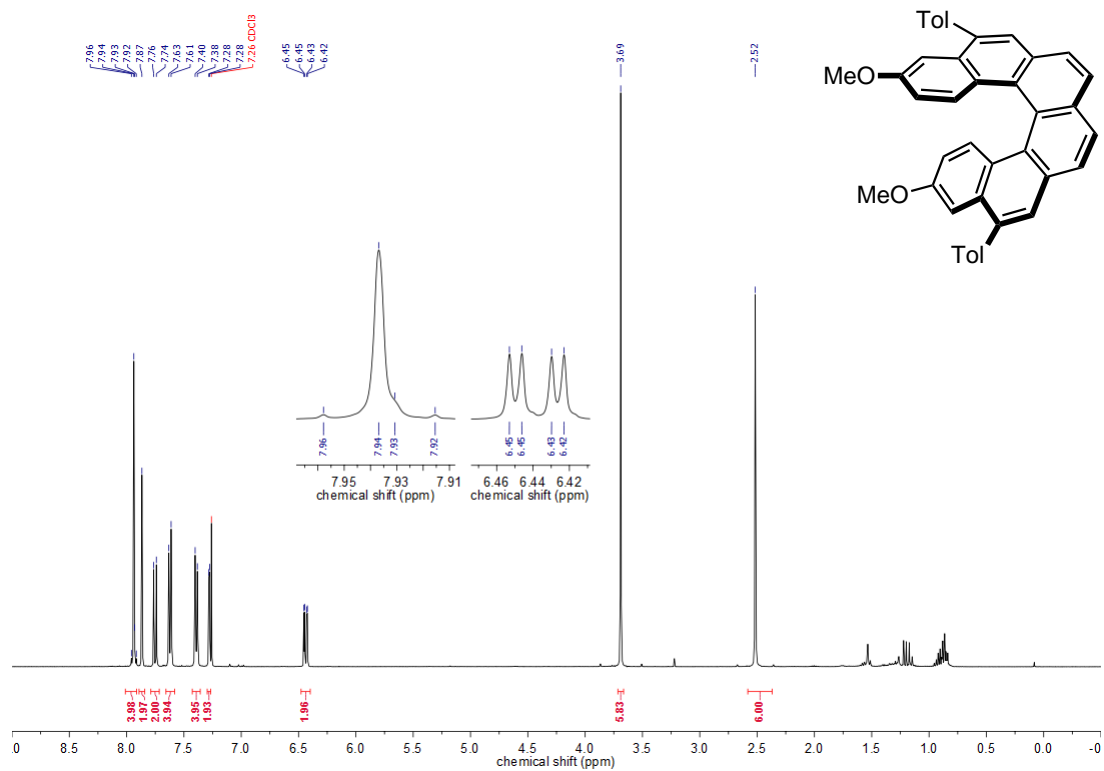
^{13}C-NMR(101 MHz, CDCl$_3$) **26ba**
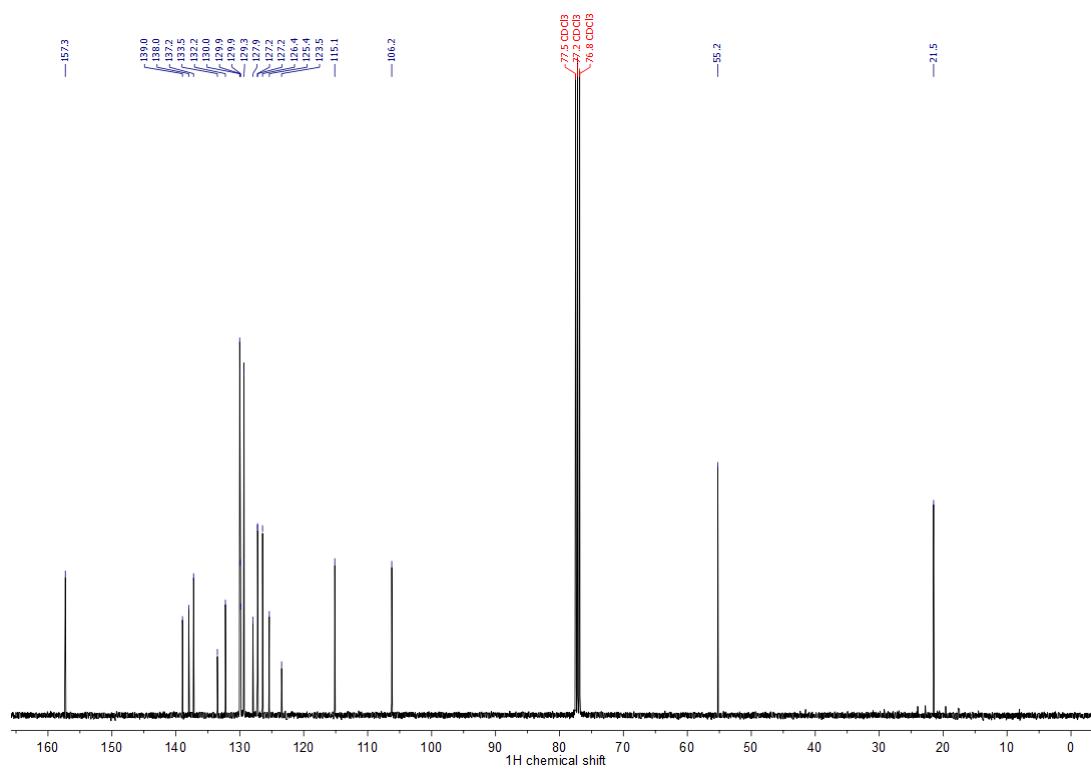
^{1}H-NMR(400 MHz, CDCl$_3$) **205a**
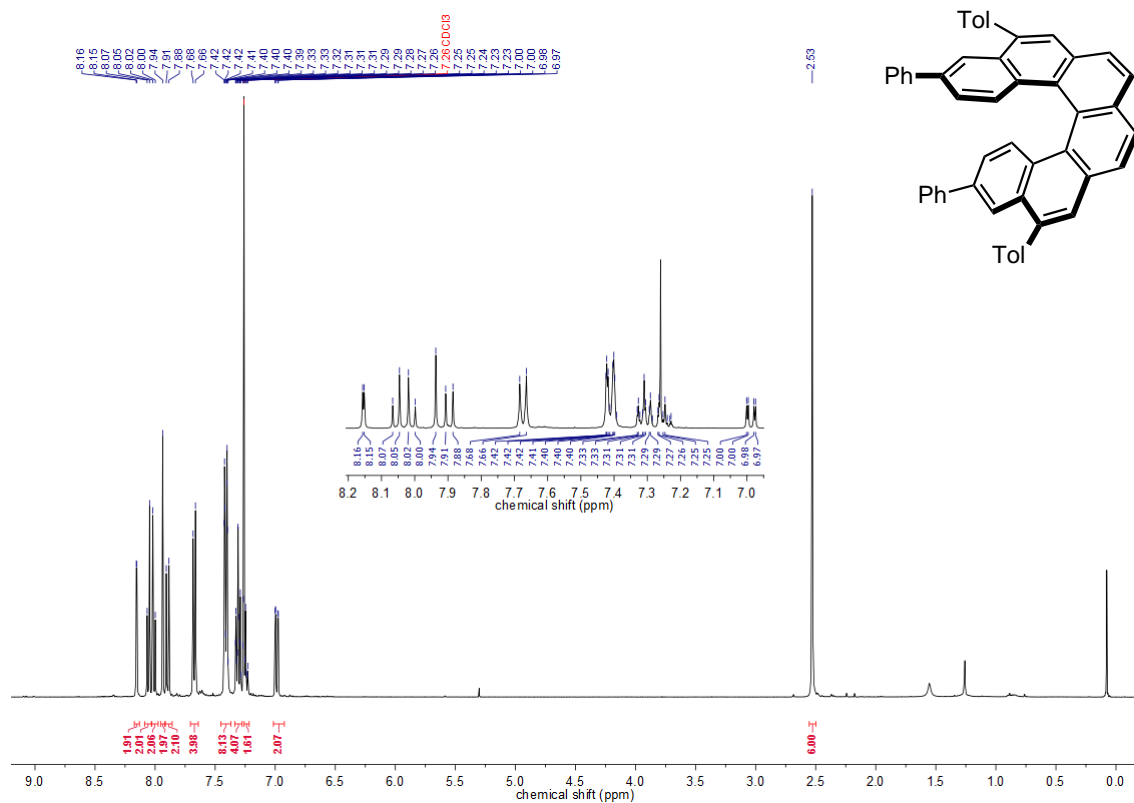
^{13}C-NMR(101 MHz, CDCl$_3$) **205a**
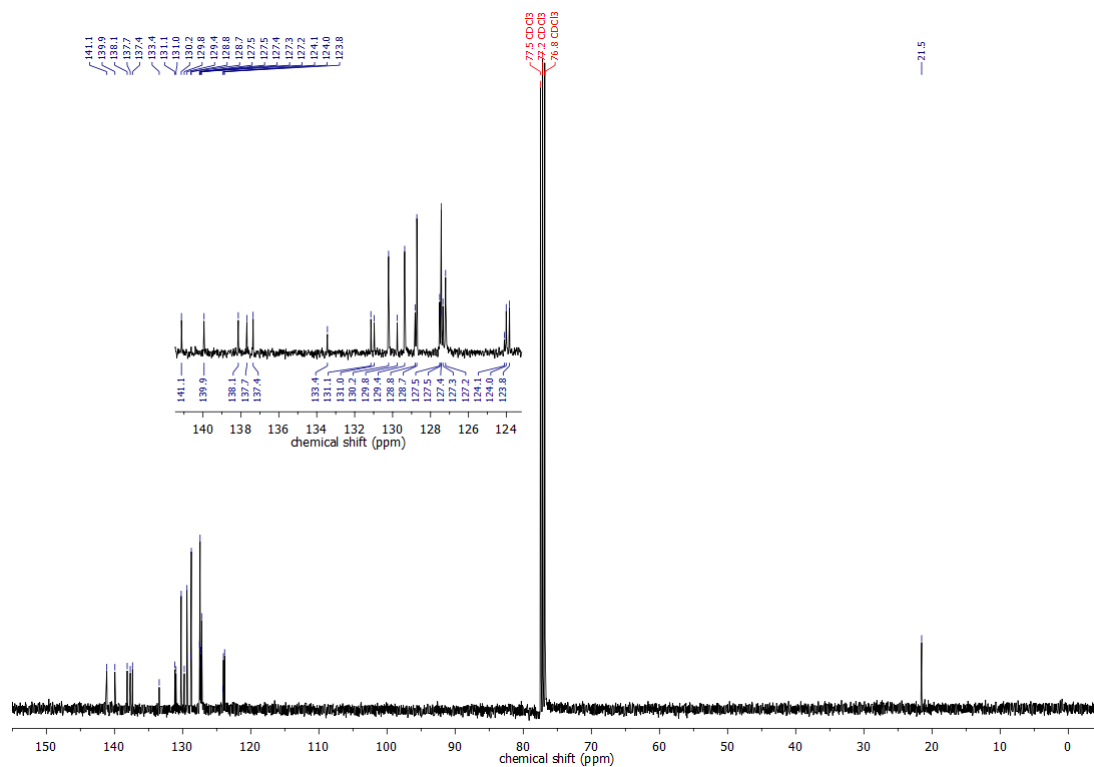
Assignments for compound **192aa**:
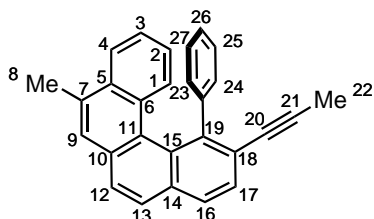
Atom	δ (ppm)		Correlations	
		COSY	HMBC	NOESY
1 C	130.734			
1 H	7.960	2	5, 11, 3	
2 C	124.251		4	
2 H	6.989	3, 1	6, 4	
3 C	124.946		1	
3 H	7.240	4, 2		5
4 C	122.268		2	
4 H	7.793	3	2, 6, 7	8
5 C	130.973		3, 9, 8, 1	
6 C	129.481		2, 4	
7 C	133.903		8, 4	
8 C	19.682		9	
8 H(3)	2.737		9, 5, 7	9, 4
9 C	125.920		12, 8	
9 H	7.593		5, 10, 11, 8	12, 8
10 C	132.084		12, 9, 13	
11 C	126.438		12, 9, 1	
12 C	126.725			
12 H	7.728	13	9, 10, 11, 14	9
13 C	126.802		16	
13 H	7.807	12	10, 15, 16, 14	16
14 C	133.816		12, 13, 17, 16	
15 C	128.694		13, 16	
16 C	127.315		13, 17	
16 H	7.885	17	15, 18, 13, 17, 14	13
17 C	130.395		22, 16	
17 H	7.762	16	14, 20, 19, 16	
18 C	122.781		22, 16	

Continued on next page

Atom	δ (ppm)	Correlations		
---	---	COSY	HMBC	NOESY
19 C	142.065		22, 17	
20 C	80.673		22, 17	
21 C	90.368		22	
22 C	4.898			
22 H(3)	1.992		18, 19, 17, 21, 20	
23 C	141.497			
24 C	132.621		26	
24 H	8.369	25		28
25 C	126.950			
25 H	7.362	26, 24		27
26 C	126.303			
26 H	6.899	27, 25	24, 28	
27 C	126.950			
27 H	6.505	28, 26		25
28 C	130.302		26	
28 H	5.943	27		24

Table A.4: Assignment of NMR signals for **192aa**. Spectrometer: Bruker AV600; Solvent: CDCl$_3$.

¹H-NMR (600 MHz, CDCl₃)

HSQC
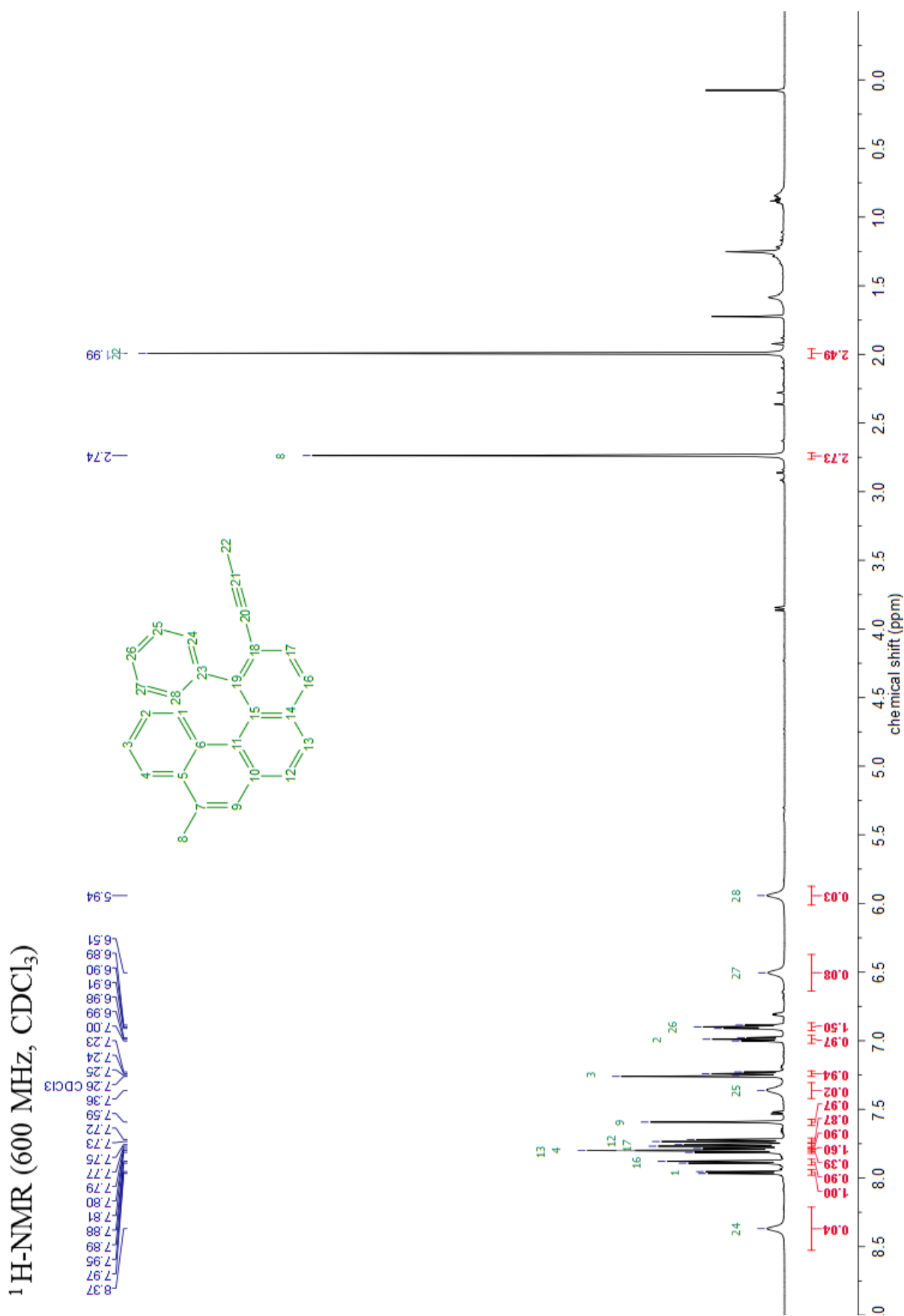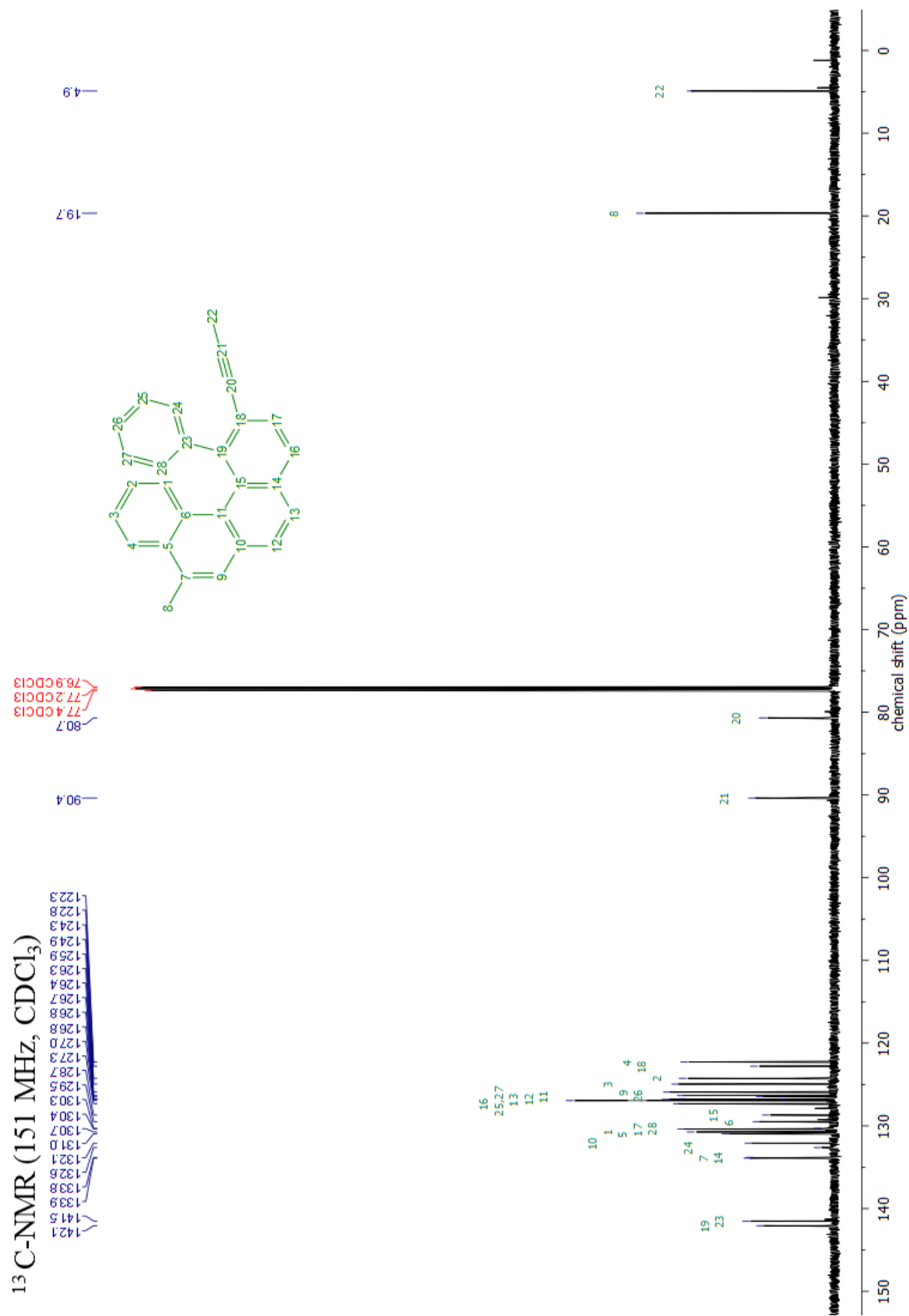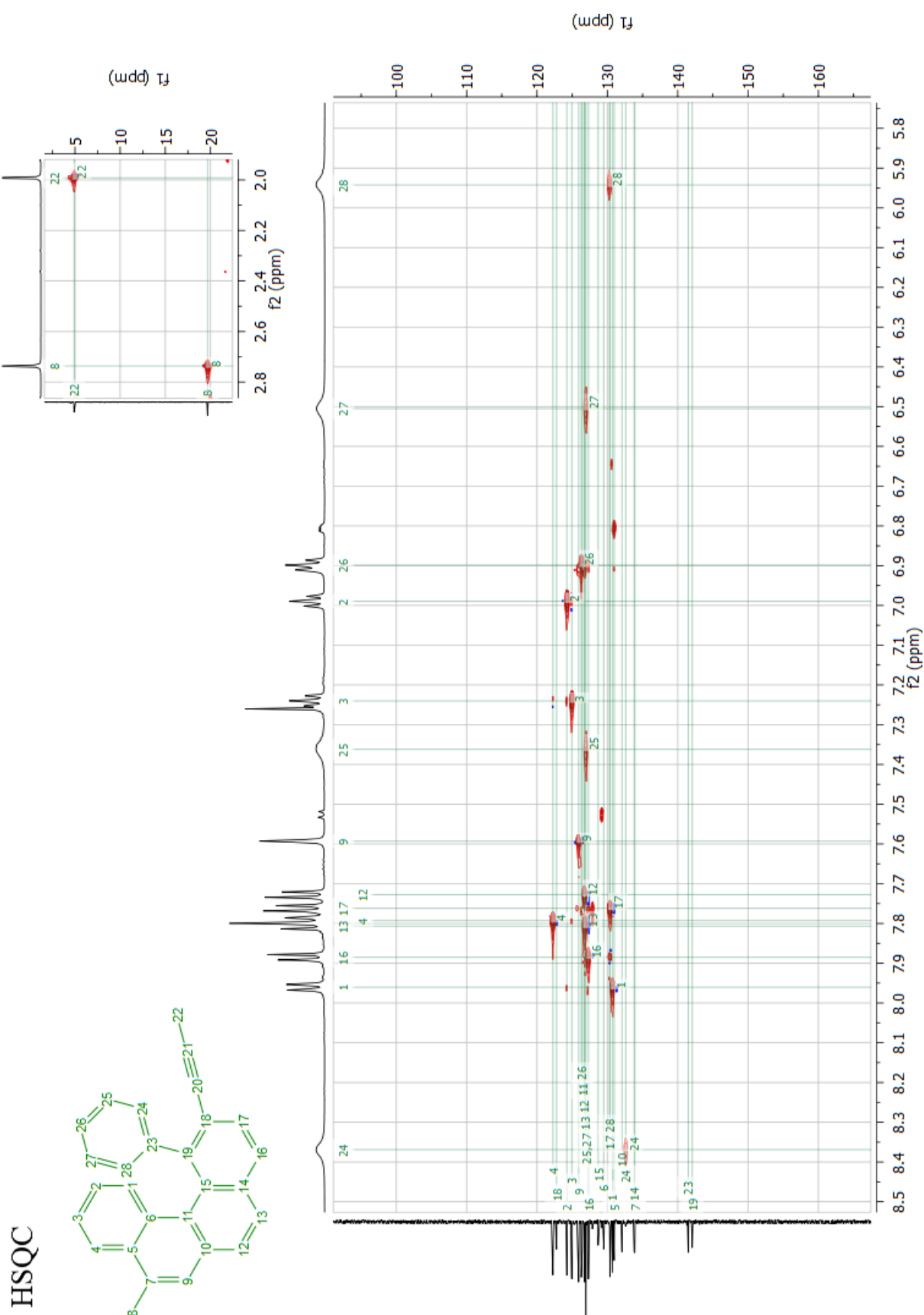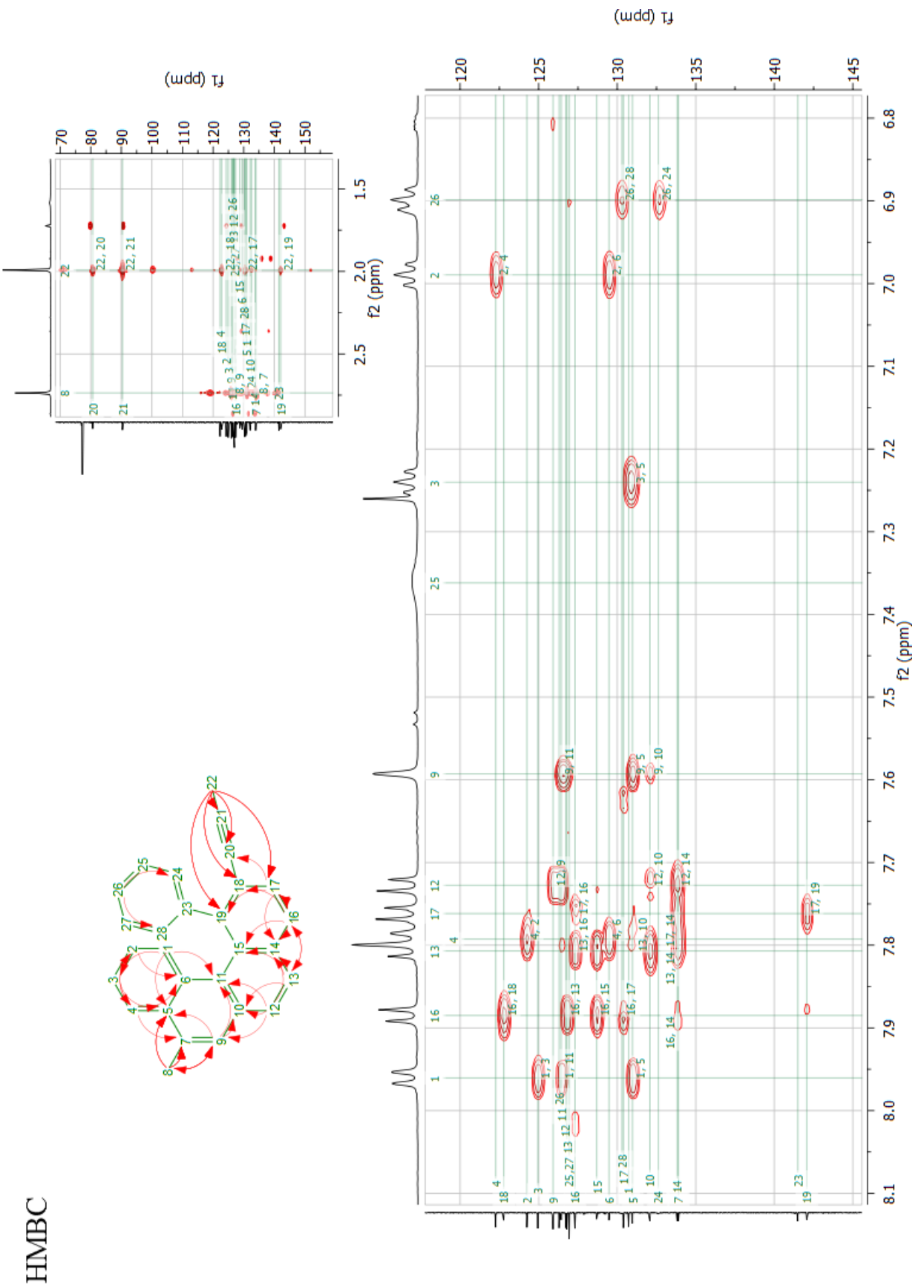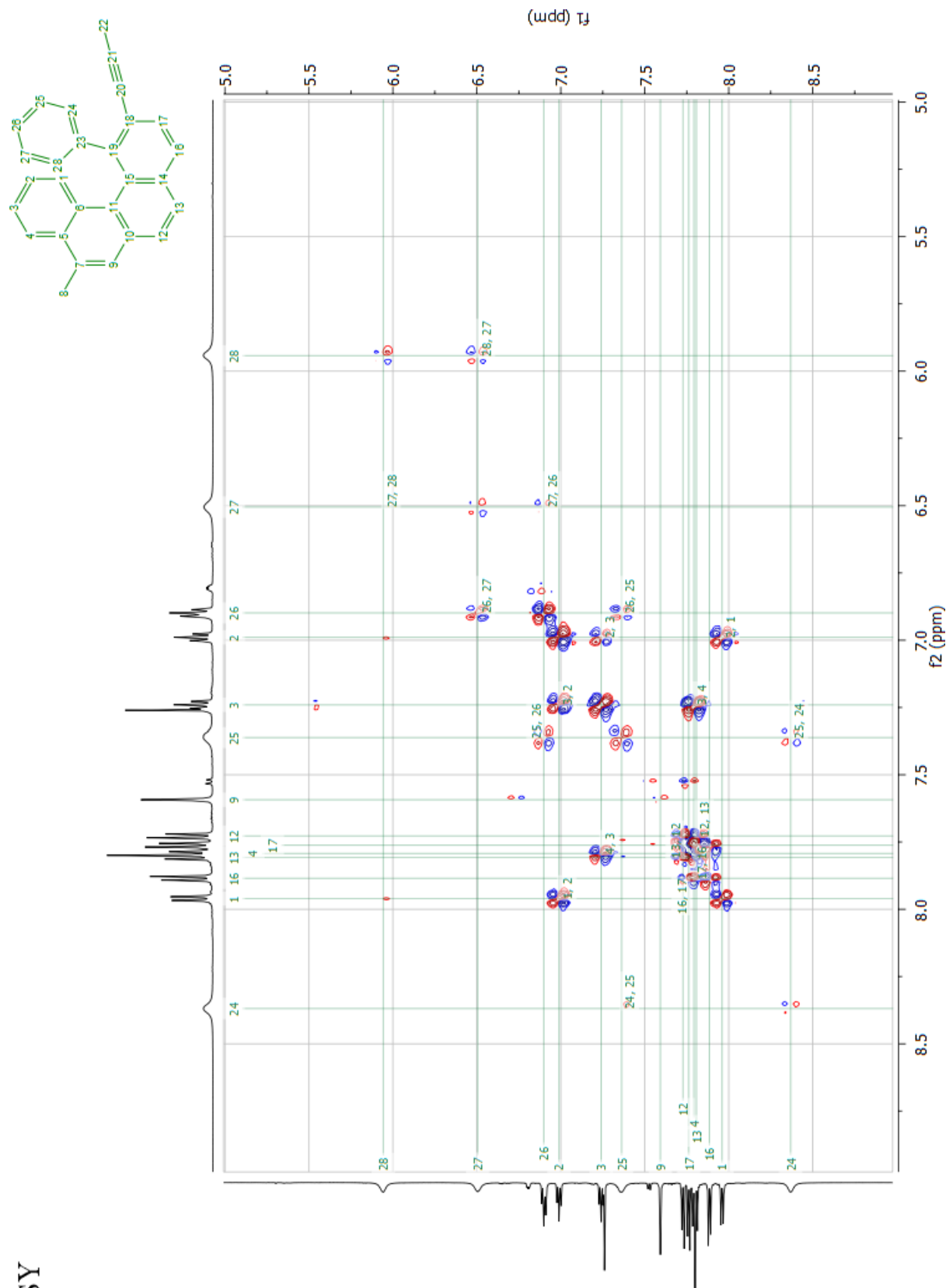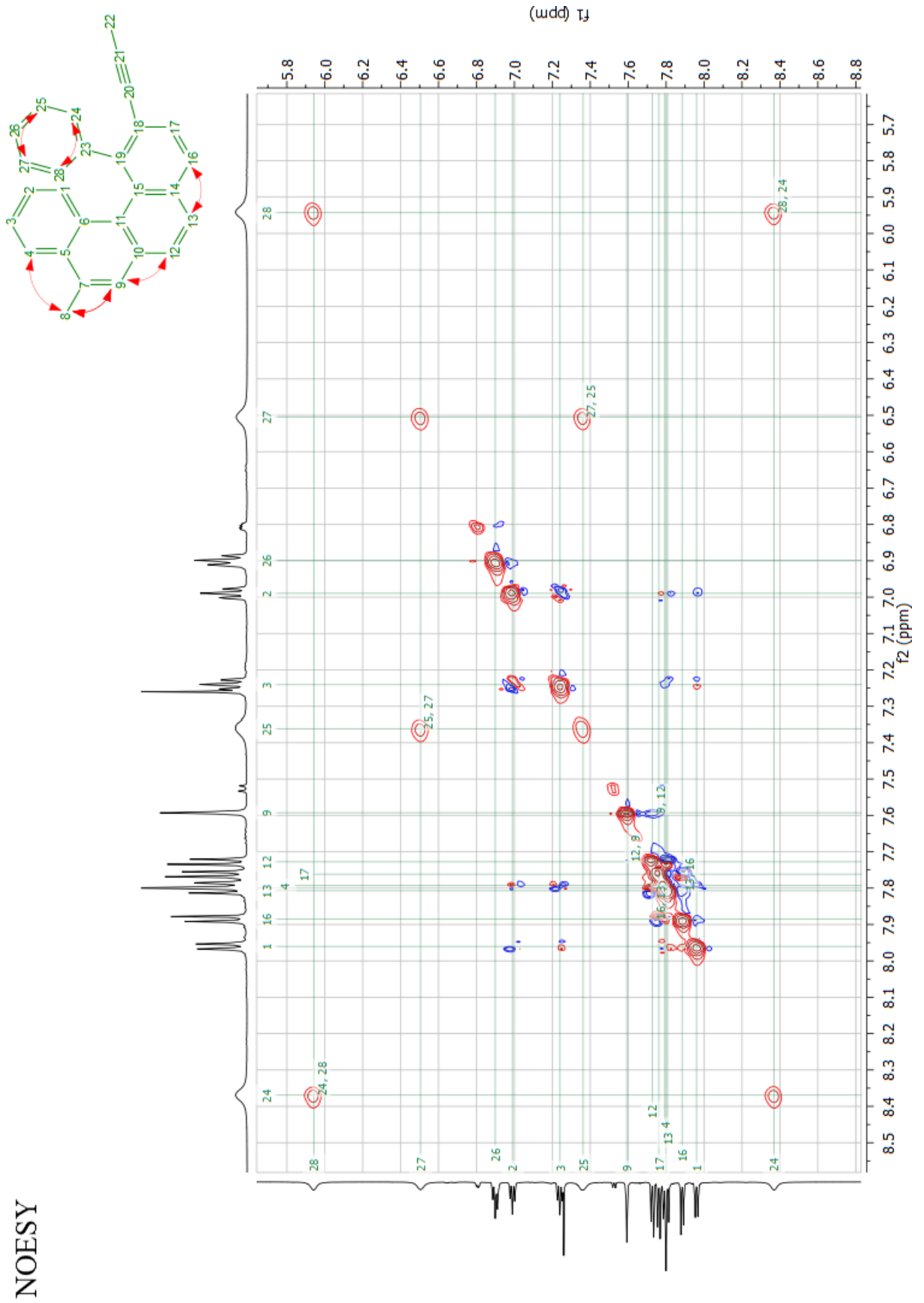
HMBC

COSY

NOESY

Assignments for compound **192bb**:
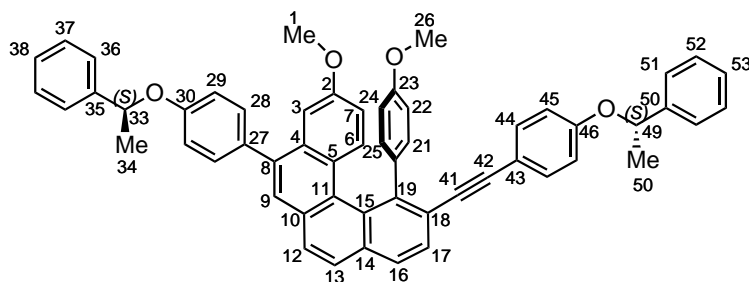
Atom	δ (ppm)			Correlations		
	333 K	233 K	predicted	COSY	HMBC	NOESY
1 C	54,674	53.94, 53.99	55,54			
1 H(3)	3,256	3.09, 3.12	3,87		2	7, 3
2 C	157,775	157,21	155,61		6, 1	
3 C	127,783	104,08	129,06			
3 H	105,558	7.28, 7.3	104,95		5, 7, 8	1, 28
4 C	132,642	132.00, 132.09	137,13		6, 9	
5 C	125,7	125,3	124,26		7, 3	
6 C	132,905	132,8	127,24			
6 H	8,009	8.10, 8.13	8,71	7	2, 4, 11	7
7 C	115,48	115,84	114,97		3	
7 H	6,706	6.85, 6.87	7,34	6	5	1, 6
8 C	139,302	138.91, 138.99	134,2		3, 28	
9 C	126,989	126.74, 126.83	132,32		12	
9 H	7,556	7.56, 7.64	8,45		27, 4, 11	28
10 C	131,19	130,84	129,94		13	
11 C	127,979	127,57	125,59		6, 12, 9	
12 C	127,526	127.45, 127.46	128,84			
12 H	7,565	7,62	8,15		14, 11, 9	
13 C	126,349	126,2	127,77		16	
13 H	7,565	7,58	8,08		10, 16, 15	16
14 C	135,111	134.76, 134.77	134,04		17, 12	
15 C	129,27	128,81	134,52		13, 16	
16 C	127,346	127,34	128,33		13	
16 H	7,645	7,61	8,19	16	15, 18, 13	13, 17
17 C	130,58	130.24, 130.26	133,18			
17 H	7,866	8,01	8,14	16	19, 14, 41	16
18 C	123,289	122,98	125,56		16	

Continued on next page

Atom	δ (ppm)			Correlations		
	333 K	233 K	predicted	COSY	HMBC	NOESY
19 C	142,92	142.68, 142.70	153,1		17	
20 C	134,697	134,07	130,29			
21 C	br	131,97	130,6			25
21 H	br	6.10, 6.11	7,6	22	23, 19, 25	
22 C	br	111.70, 111.77	113,58	24		
22 H	br	5.89, 5.93	6,96	21	24, 20	
23 C	159,149	158,37	161,98		26, 25, 21	
24 C	br	113,06	113,58		22	
24 H	br	6.82, 6.94	6,96	25	22, 20	
25 C	br	134,24	130,6		21	
25 H	br	8.29, 8.33	7,6	24	21, 19, 23	
26 C	54,656	53.97, 53.99	55,15			
26 H(3)	3,156	2.96, 2.98	3,8		23	
27 C	133,824	132.94, 132.97	135,56		29, 9	
28 C	131,358	131,23	129,78			
28 H	7,361	7,41	7,25	29	8, 30	9, 3, 29
29 C	116,464	115,74	116,02			
29 H	6,963	7,02	7,29	28	27	34, 33, 28
30 C	158,246	157.63, 157.65	159,34		28, 33	
33 C	76,615	75.56, 75.63	74,64		36	
33 H	5,138	4,99	5,12		30	29, 34
34 C	24,497	25.03, 25.07	19,21			
34 H(3)	1,524	1,53	1,7		35	29, 36, 33
35 C	143,458	143.44, 143.48	141,76		37, 34	
36 C	125,983	125.53, 125.58	126,63		38	
36 H	7,268	7,22	7,63	37	38, 33	34
37 C	128,917	128,8	128,26			
37 H	7,12	7,08	7,36	36, 38	35	
38 C	127,712	127,53	128,24		36	
38 H	7,03	7,01	7,31	37	36	
41 C	90,75	90.41, 90.43	82,37		17	
42 C	94,236	93.79, 93.81	87,46		44	
43 C	117,043	116,15	115,51		45	
44 C	133,06	132.89, 132.91	132,74			
44 H	7,29	7,41	7,1	45	46, 42	45
45 C	116,464	115,88	116,92			

Atom	δ (ppm)			Correlations		
	333 K	233 K	predicted	COSY	HMBC	NOESY
45 H	6,7	6,71	7,18	44	43	50, 49, 44
46 C	158,616	158.01, 158.05	158,2		49, 44	
49 C	76,468	75.39, 75.47	74,64			
49 H	4,971	4,800	5,05		46, 51	45, 50
50 C	24,277	24.71, 24.82	19,21			
50 H(3)	1,418	1,41	1,67		56	51, 45, 49
51 C	125,825	125,41	126,63		49, 53	
51 H	7,152	7,08	7,59	52	53	50
52 C	128,917	128,83	128,26			
52 H	7,13	7,13	7,36	51, 53	56	
53 C	127,675	127,54	128,24		51	
53 H	7,033	7,04	7,31	52	51	
56 C	143,887	142.97, 143.04	141,76		50, 52	

Table A.5: Assignment of NMR signals for **192bb**. Spectrometer: Bruker AV500; Solvent d_8-toluene.

Not all the signals are visible at 333K, therefore the assignment at 233 K is also presented. However at 233 K the hindered rotation generates splitting (both chemical shifts are displayed on the table) in several signals, complicating the analysis of the multiplicity.

^{1}H-NMR (500 MHz, 333 K, d$_8$-toluene)

¹H-NMR (500 MHz, 233 K, d₈-toluene)
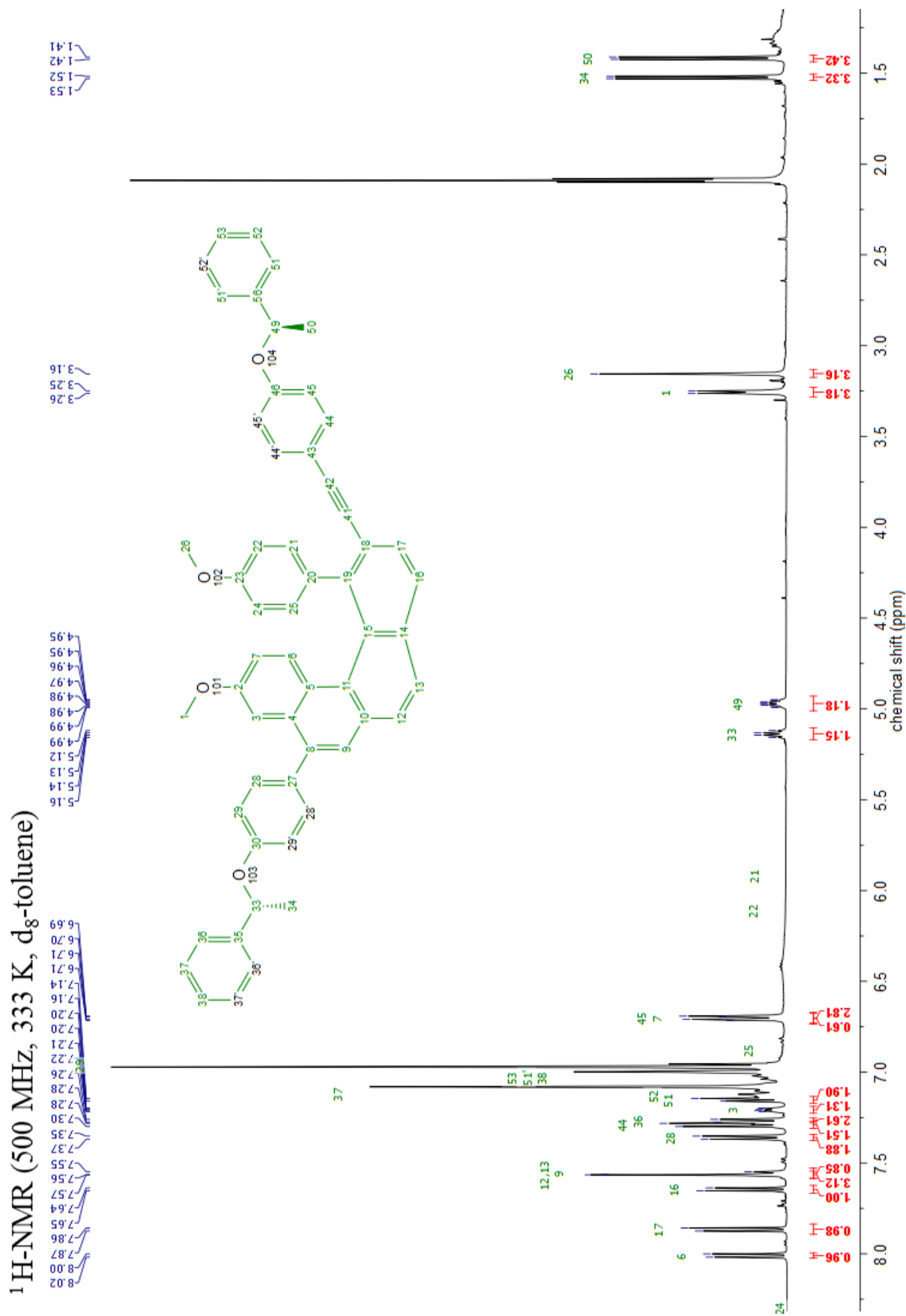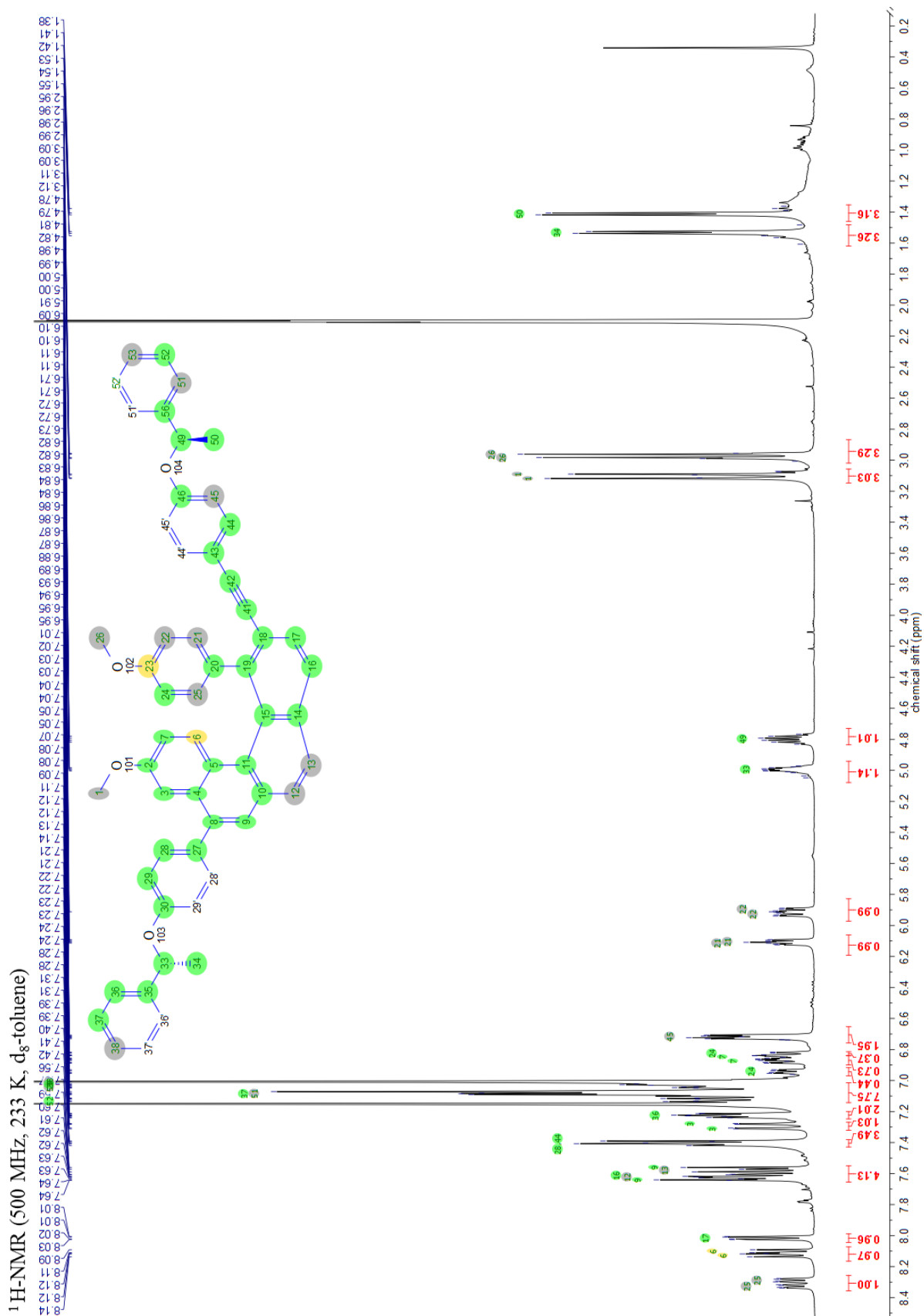
^{13}C-NMR (126 MHz, 333 K, d$_8$-toluene)

HMBC

COSY
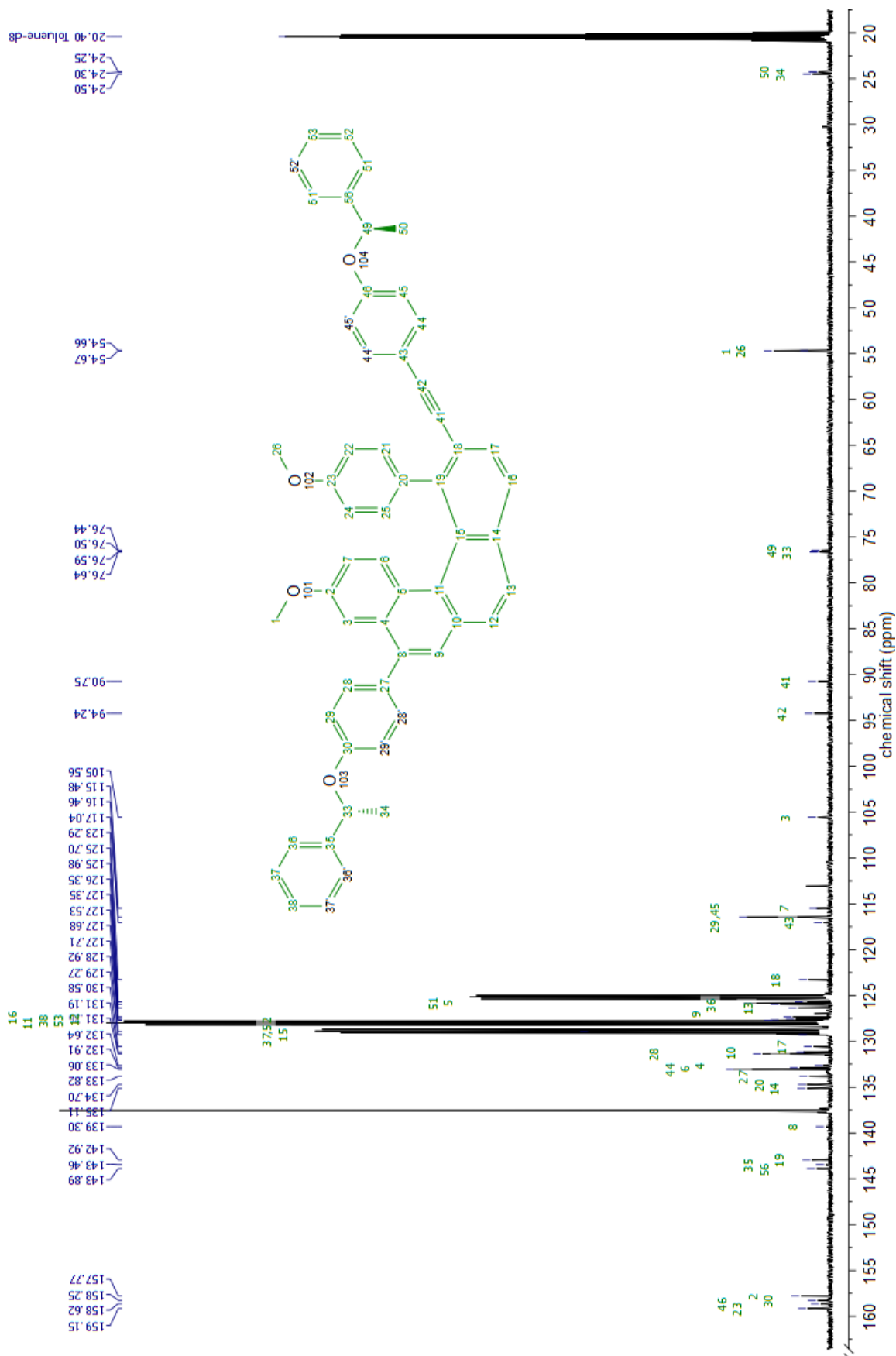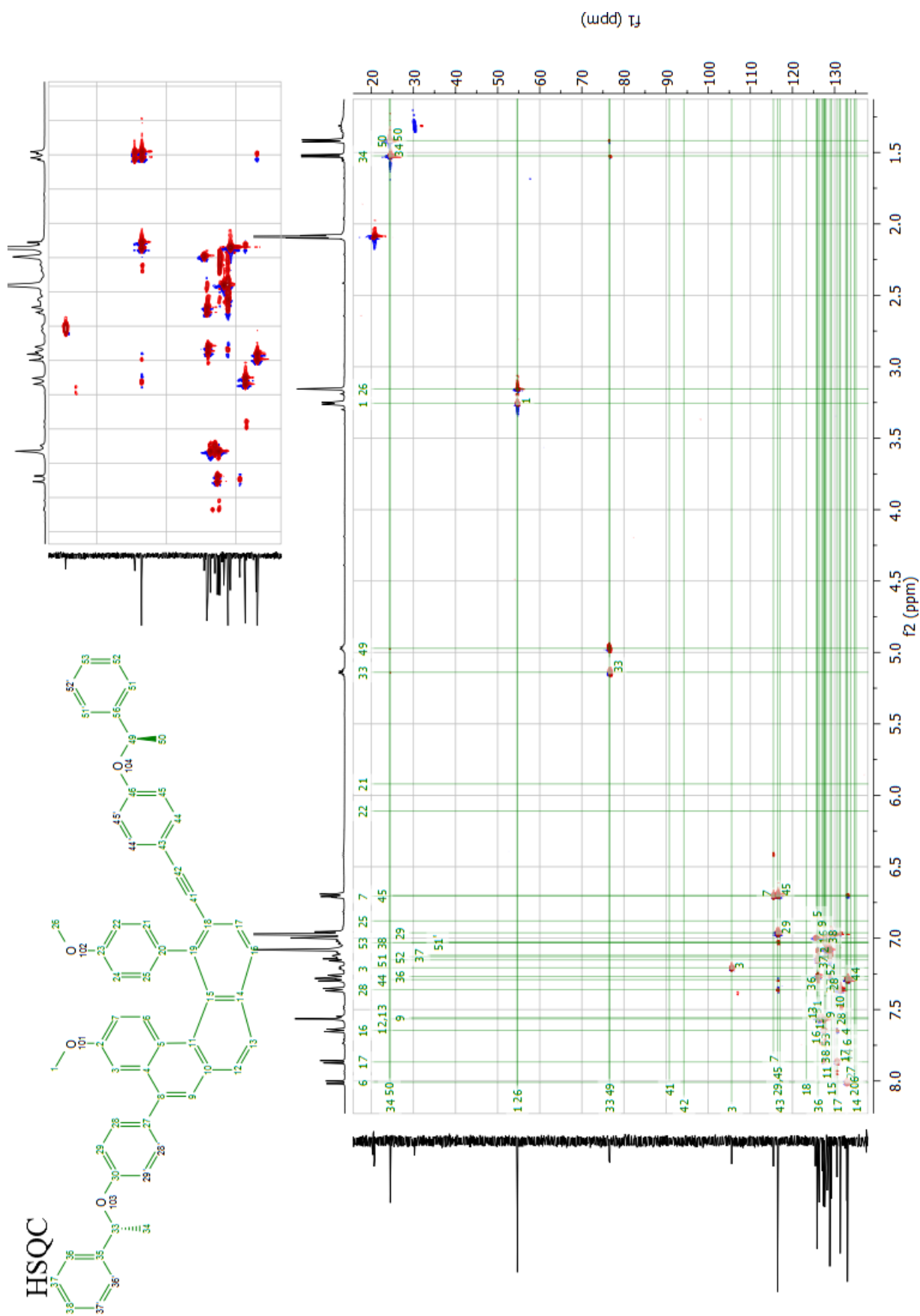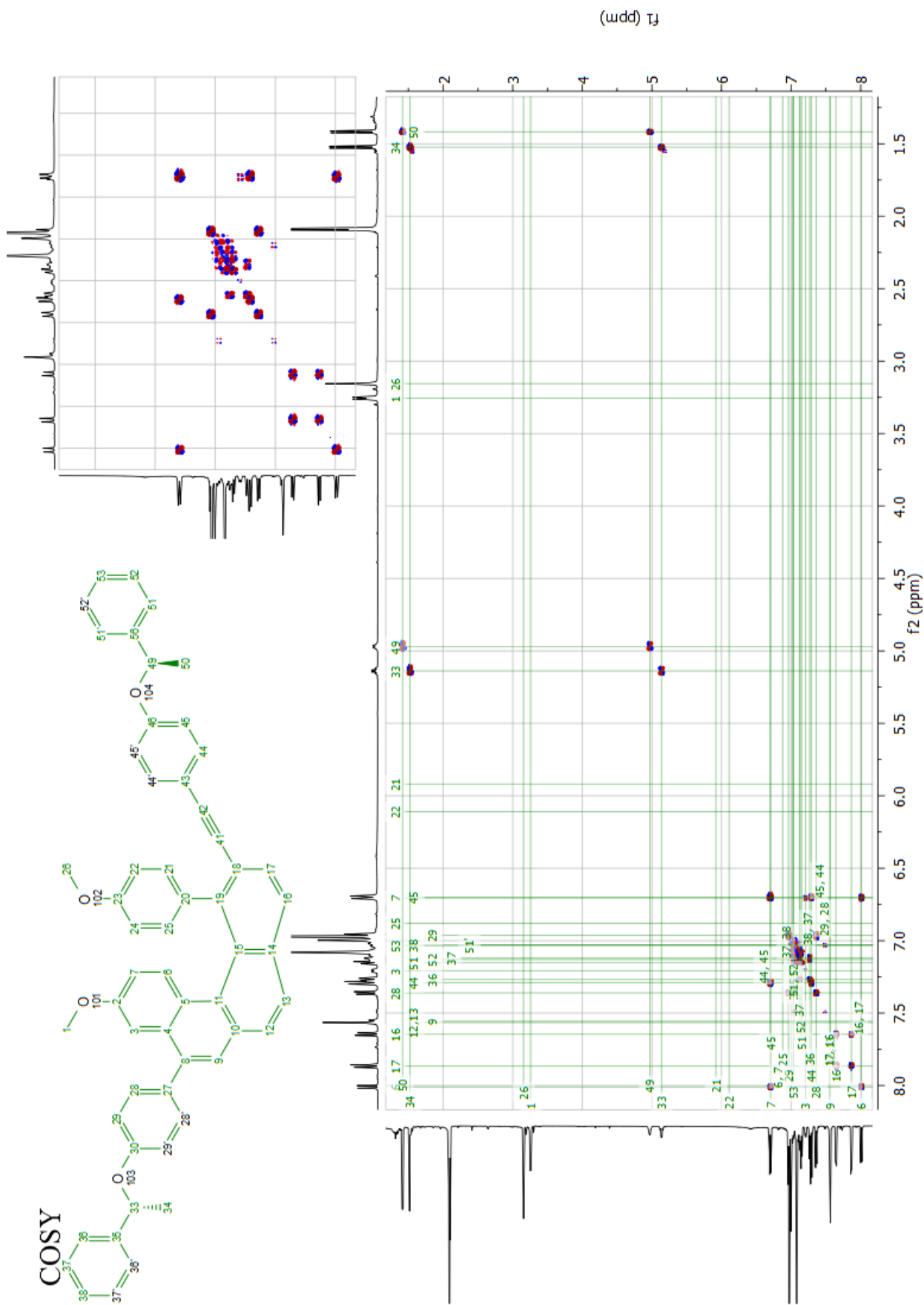
NOESY
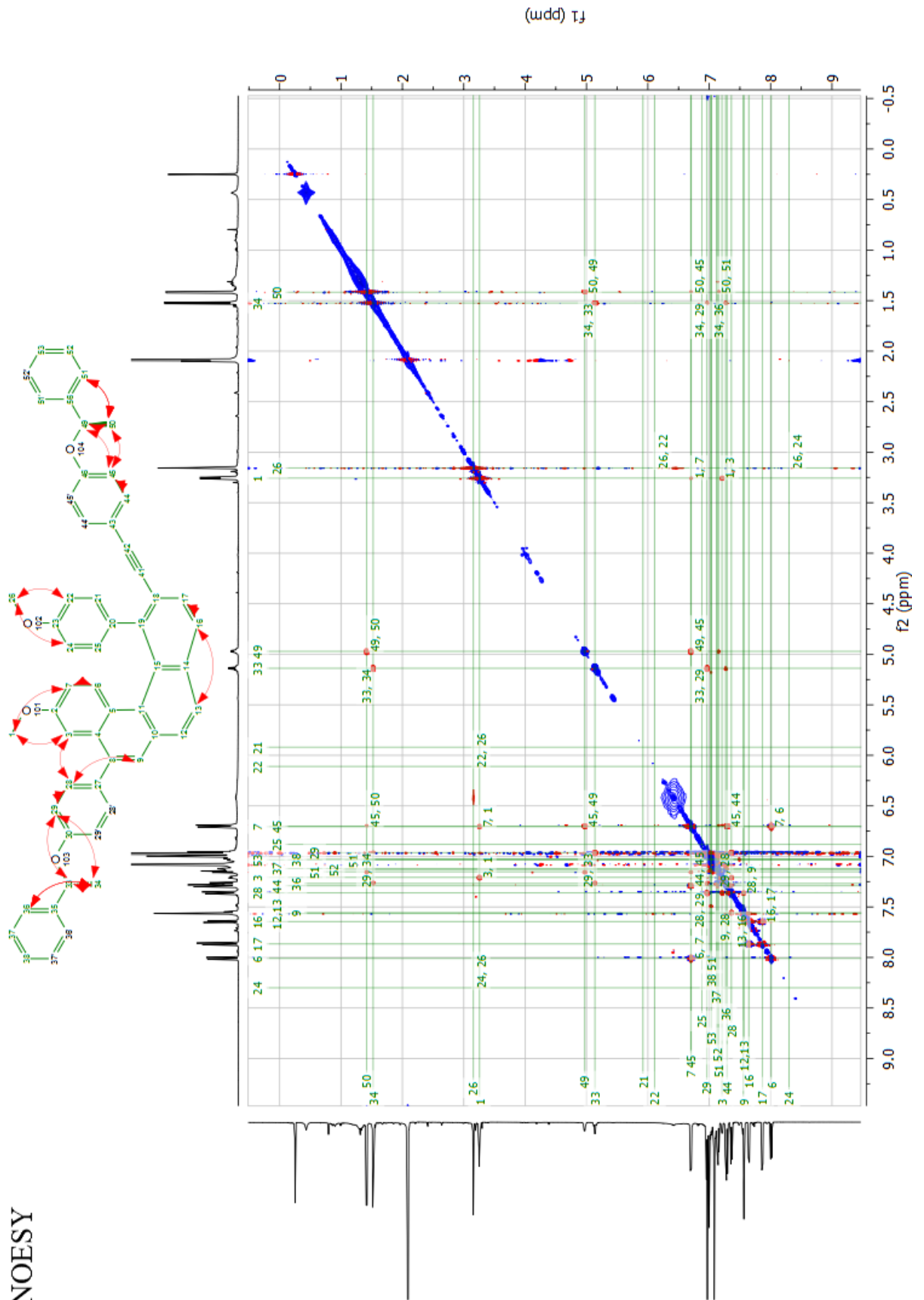
B.   X-Ray structures

Compound 81e:
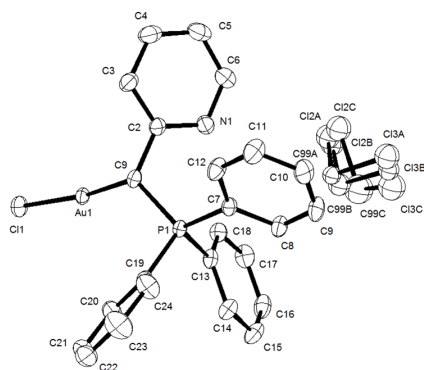
Empirical formula	$C_{25}H_{22}AuCl_3NP$
Colour	colourless
Formula weight	670.72 g mol^{-1}
Temperature	150 K
Wavelength	0.71073 Å
Crystal system	MONOCLINIC
Space group	$C2/c$, (no. 15)
Unit cell dimensions	a = 24.4111(6) Å $\alpha = 93.067(5)°$.
	b = 8.577(2) Å $\beta = 90°$.
	c = 23.0774(16) Å $\gamma = 90°$.
Volume	6725(5) Å^3
Z	8
Density (calculated)	1.847 Mg m^{-1}
Absorption coefficient	6.511 mm^{-1}
F(000)	2592 e
Crystal size	0.30 x 0.12 x 0.07 mm
Θ range for data collection	3.05 to 33.10°.
Index ranges	$-37 \leq h \leq 37, -13 \leq k \leq 13, -35 \leq l \leq 35$
Reflections collected	67463
Independent reflections	9159 [$R_{int} = 0.0532$]
Reflections with $I > 2\sigma(I)$	7901
Completeness to $\Theta = 27.5°$	99.9 %
Absorption correction	Gaussian
Max. and min. transmission	0.81 and 0.39
Refinement method	Full-matrix least-squares on F^2
Data / restraints / parameters	9159 / 0 / 289
Goodness-of-fit on F^2	1.086
Final R indices [$I > 2\sigma(I)$]	$R_1 = 0.0288$ $wR_2 = 0.0665$
R indices (all data)	$R_1 = 0.0378$ $wR_2 = 0.0704$
Largest diff. peak and hole	1.327 and -2.047 eÅ^{-3}

Compound 80a :
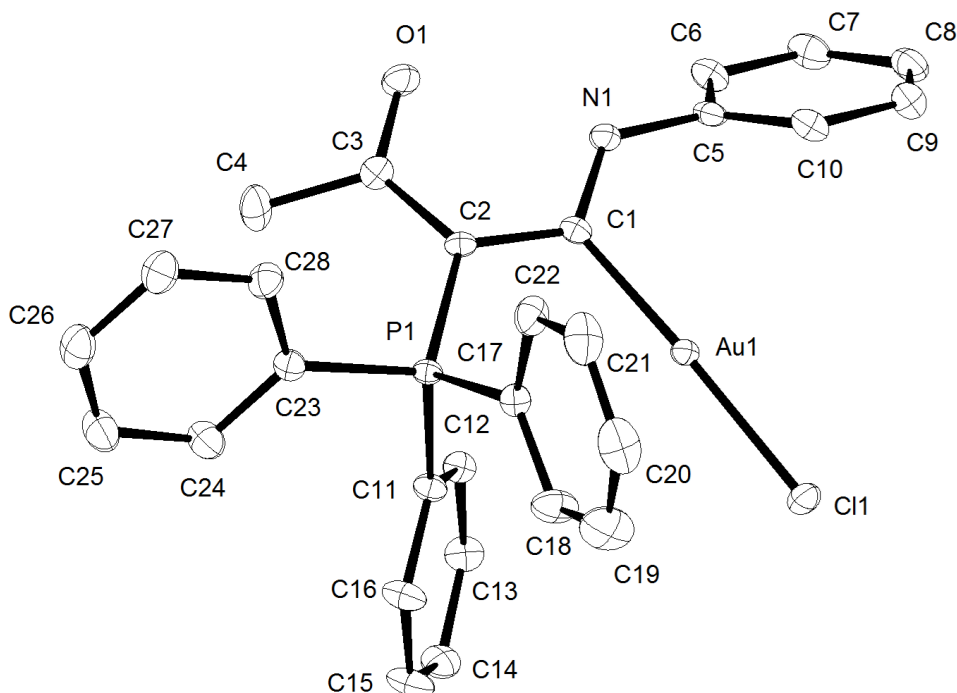
Empirical formula	$C_{28}H_{24}AuClNOP$
Colour	colourless
Formula weight	$681.92\ \mathrm{g\,mol^{-1}}$
Temperature	100 K
Wavelength	0.71073 Å
Crystal system	MONOCLINIC
Space group	$P2_1/c$, (no. 14)
Unit cell dimensions	a = 14.7905(9) Å $\alpha = 90°$.
	b = 11.9586(10) Å $\beta = 115.796(4)°$.
	c = 15.2551(7) Å $\gamma = 90°$.
Volume	2429.3(3) Å
Z	4
Density (calculated)	$1.788\ \mathrm{Mg\,m^{-1}}$
Absorption coefficient	$6.253\ \mathrm{mm^{-1}}$
F(000)	1272 e
Crystal size	0.27 x 0.21 x 0.10 mm
Θ range for data collection	2.68 to 37.00°.
Index ranges	$-24 \leq h \leq 25, -20 \leq k \leq 20, -25 \leq l \leq 25$
Reflections collected	60767
Independent reflections	12321 $[R_{int} = 0.0518]$
Reflections with $I > 2\sigma(I)$	9429
Completeness to $\Theta = 37.00\ °$	99.8 %
Absorption correction	Gaussian
Max. and min. transmission	0.55184 and 0.21375
Refinement method	Full-matrix least-squares on F^2
Data / restraints / parameters	12321 / 0 / 299
Goodness-of-fit on F^2	1.037
Final R indices $[I > 2\sigma(I)]$	$R_1 = 0.0329$ $wR_2 = 0.0548$
R indices (all data)	$R_1 = 0.058$ $wR_2 = 0.0605$
Largest diff. peak and hole	1.425 and -2.498 eÅ^{-3}

Compound 80d :

Empirical formula	$C_{28}H_{21}AuCl_3N_2P$
Colour	colourless
Formula weight	716.75 g mol^{-1}
Temperature	100 K
Wavelength	0.71073 Å
Crystal system	MONOCLINIC
Space group	$P2_1/n$, (no. 14)
Unit cell dimensions	a = 13.6094(12) Å $\alpha = 90°$.
	b = 8.9800(8) Å $\beta = 97.8470(10)°$.
	c = 22.0590(19) Å $\gamma = 90°$.
Volume	2670.6(4) Å
Z	4
Density (calculated)	1.790 Mg m^{-1}
Absorption coefficient	5.889 mm^{-1}
F(000)	1392 e
Crystal size	0.20 x 0.19 x 0.05 mm
Θ range for data collection	1.66 to 27.50 °.
Index ranges	$-17 \leq h \leq 17, -11 \leq k \leq 11, -28 \leq l \leq 28$
Reflections collected	59399
Independent reflections	6137 $[R_{int} = 0.0246]$
Reflections with $I > 2\sigma(I)$	5982
Completeness to $\Theta = 21.50°$	100.0 %
Absorption correction	Gaussian
Max. and min. transmission	0.76 and 0.25
Refinement method	Full-matrix least-squares on F^2
Data / restraints / parameters	6137 / 0 / 313
Goodness-of-fit on F^2	1.057
Final R indices $[I > 2\sigma(I)]$	$R_1 = 0.0184$ $wR_2 = 0.0434$
R indices (all data)	$R_1 = 0.0191$ $wR_2 = 0.0440$
Largest diff. peak and hole	1.173 and -2.018 eÅ^{-3}

Compound 80e :

Empirical formula	$C_{31}H_{25}AuClN_2P \cdot CH_2Cl_2$
Colour	yellow
Formula weight	$731.38 \text{ g mol}^{-1}$
Temperature	100 K
Wavelength	0.71073 Å
Crystal system	MONOCLINIC
Space group	$P2_1/c$, (no. 14)
Unit cell dimensions	a = 8.7003(3) Å $\alpha = 90°$.
	b = 19.0210(12) Å $\beta = 90.348(4)°$.
	c = 17.8177(14) Å $\gamma = 90°$.
Volume	2948.6(3) Å
Z	4
Density (calculated)	1.648 Mg m^{-1}
Absorption coefficient	5.248 mm^{-1}
F(000)	1428 e
Crystal size	0.17 x 0.10 x 0.09 mm
Θ range for data collection	3.17 to 34.94°.
Index ranges	$-14 \leq h \leq 13, -28 \leq k \leq 30, -28 \leq l \leq 28$
Reflections collected	95323
Independent reflections	12890 [$R_{int} = 0.0388$]
Reflections with $I > 2\sigma(I)$	11231
Completeness to $\Theta = 27.5°$	99.8 %
Absorption correction	Gaussian
Max. and min. transmission	0.66 and 0.49
Refinement method	Full-matrix least-squares on F^2
Data / restraints / parameters	12890 / 0 / 345
Goodness-of-fit on F^2	1.091
Final R indices [$I > 2\sigma(I)$]	$R_1 = 0.0244$ $wR_2 = 0.0570$
R indices (all data)	$R_1 = 0.0326$ $wR_2 = 0.0605$
Largest diff. peak and hole	2.411 and -1.792 eÅ^{-3}

Compound 80f :

Empirical formula	$C_{33}H_{28}AuCl_3NP$
Colour	colourless
Formula weight	772.85 $g\,mol^{-1}$
Temperature	100 K
Wavelength	0.71073 Å
Crystal system	TRICLINIC
Space group	$P\bar{1}$, (no. 2)
Unit cell dimensions	a = 9.3905(9) Å $\quad$ $\alpha = 93.296(2)°$.
	b = 12.0001(12) Å $\quad$ $\beta = 102.318(2)°$.
	c = 14.4938(14) Å $\quad$ $\gamma = 105.550(2)°$.
Volume	1525.8(3) Å
Z	2
Density (calculated)	1.682 $Mg\,m^{-1}$
Absorption coefficient	5.159 mm^{-1}
F(000)	756 e
Crystal size	0.14 x 0.10 x 0.05 mm
Θ range for data collection	2.15 to 33.14°.
Index ranges	$-14 \le h \le 14, -18 \le k \le 18, -22 \le l \le 22$
Reflections collected	95467
Independent reflections	11634 [$R_{int} = 0.0478$]
Reflections with $I > 2\sigma(I)$	11286
Completeness to $\Theta = 27.5°$	100.0 %
Absorption correction	Gaussian
Max. and min. transmission	0.64 and 0.29
Refinement method	Full-matrix least-squares on F^2
Data / restraints / parameters	11634 / 0 / 365
Goodness-of-fit on F^2	1.044
Final R indices [$I > 2\sigma(I)$]	$R_1 = 0.0232$ $\quad$ $wR_2 = 0.0602$
R indices (all data)	$R_1 = 0.0240$ $\quad$ $wR_2 = 0.0609$
Largest diff. peak and hole	3.1 and -2.0 $e\text{Å}^{-3}$

Compound 80g :

Empirical formula	$C_{30}H_{28}AuClNOP$
Colour	colourless
Formula weight	$681.92 \ \mathrm{g \, mol^{-1}}$
Temperature	100 K
Wavelength	0.71073 Å
Crystal system	MONOCLINIC
Space group	$P2_1/c$, (no. 14)

Unit cell dimensions		
	a = 15.1375(13) Å	$\alpha = 90°$.
	b = 11.9784(8) Å	$\beta = 90.471(5)°$.
	c = 14.0468(5) Å	$\gamma = 90°$.

Volume	2546.9(3) Å
Z	4
Density (calculated)	$1.778 \ \mathrm{Mg \, m^{-1}}$
Absorption coefficient	$5.968 \ \mathrm{mm^{-1}}$
F(000)	1336 e
Crystal size	0.28 x 0.22 x 0.18 mm
Θ range for data collection	3.18 to 35.01°.
Index ranges	$-24 \leq h \leq 24, -19 \leq k \leq 19, -22 \leq l \leq 22$
Reflections collected	71224
Independent reflections	11208 $[R_{int} = 0.0380]$
Reflections with $I > 2\sigma(I)$	10170
Completeness to $\Theta = 35.01°$	99.8 %
Absorption correction	Gaussian
Max. and min. transmission	0.40098 and 0.24727
Refinement method	Full-matrix least-squares on F^2
Data / restraints / parameters	11208 / 0 / 319
Goodness-of-fit on F^2	1.071
Final R indices $[I > 2\sigma(I)]$	$R_1 = 0.0209 \qquad wR_2 = 0.0503$
R indices (all data)	$R_1 = 0.0260 \qquad wR_2 = 0.0529$
Largest diff. peak and hole	1.551 and -3.258 eÅ^{-3}

Compound 80i :
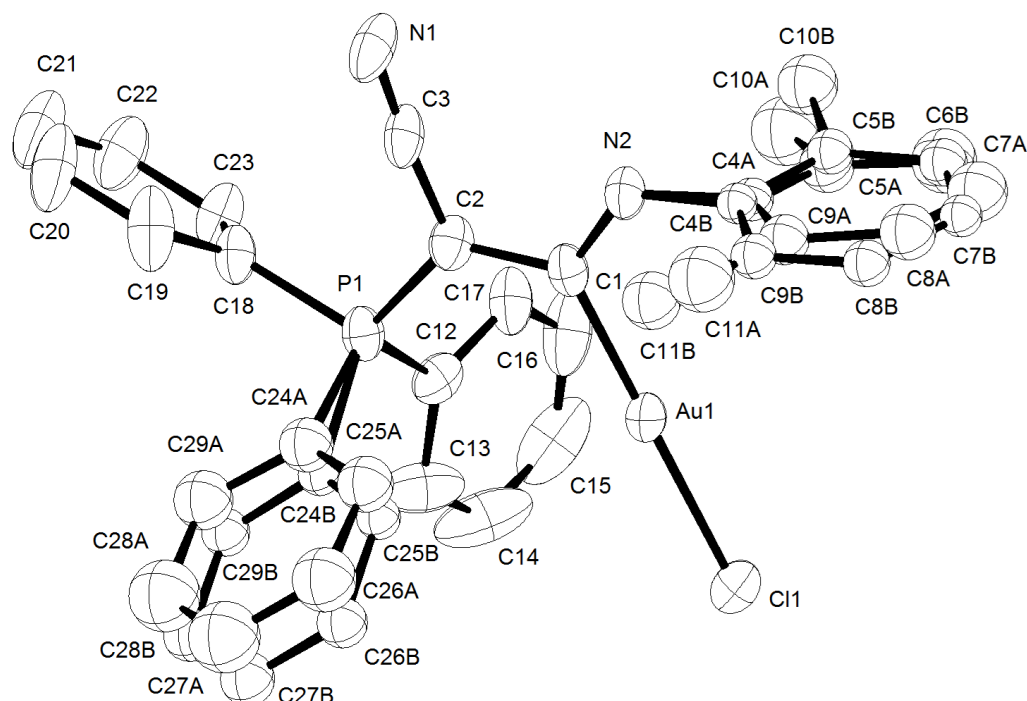
Empirical formula	$C_{29}H_{25}AuClN_2P$
Colour	colourless
Formula weight	664.90 $g\,mol^{-1}$
Temperature	100 K
Wavelength	1.54178 Å
Crystal system	MONOCLINIC
Space group	$C2/c$, (no. 15)
Unit cell dimensions	a = 22.3581(6) Å $\alpha = 90°$.
	b = 13.3395(4) Å $\beta = 106.3180(10)°$.
	c = 20.7109(5) Å $\gamma = 90°$.
Volume	5928.1(3) Å
Z	8
Density (calculated)	1.490 $Mg\,m^{-1}$
Absorption coefficient	10.795 mm^{-1}
F(000)	2592 e
Crystal size	0.18 x 0.10 x 0.06 mm
Θ range for data collection	3.90 to 67.31°.
Index ranges	$-24 \leq h \leq 26, -15 \leq k \leq 15, -24 \leq l \leq 24$
Reflections collected	66300
Independent reflections	5255 [$R_{int} = 0.0630$]
Reflections with $I > 2\sigma(I)$	4802
Completeness to $\Theta = 67.31°$	98.6 %
Absorption correction	Gaussian
Max. and min. transmission	0.56 and 0.20
Refinement method	Full-matrix least-squares on F^2
Data / restraints / parameters	5255 / 0 / 297
Goodness-of-fit on F^2	1.053
Final R indices [$I > 2\sigma(I)$]	$R_1 = 0.0295$ $wR_2 = 0.0691$
R indices (all data)	$R_1 = 0.0331$ $wR_2 = 0.0713$
Largest diff. peak and hole	1.042 and -0.981 e$Å^{-3}$

Compound 80j :
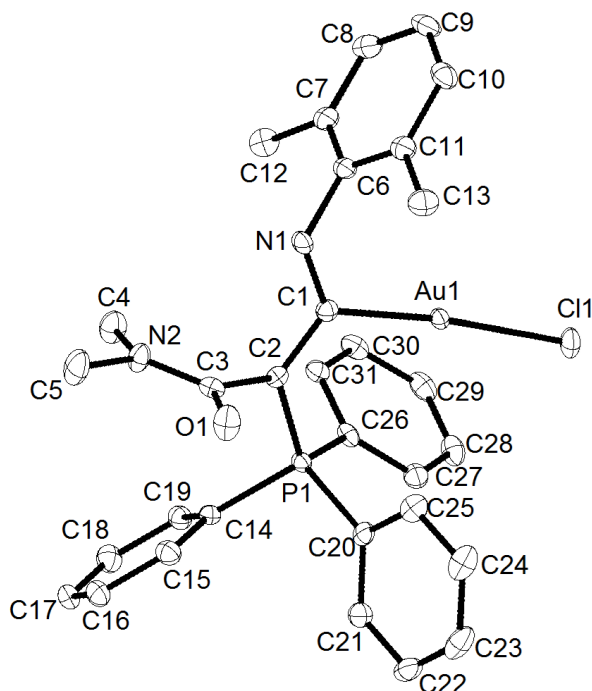
Empirical formula	$C_{31}H_{31}AuClN_2OP$
Colour	colourless
Formula weight	$710.96 \ \mathrm{g \, mol^{-1}}$
Temperature	100 K
Wavelength	1.54178 Å
Crystal system	MONOCLINIC
Space group	$P2_1/c$, (no. 14)
Unit cell dimensions	a = 16.8854(7) Å $\quad \alpha = 90°$.
	b = 10.9240(5) Å $\quad \beta = 111.3890(10)°$.
	c = 16.4234(7) Å $\quad \gamma = 90°$.
Volume	2820.7(2) Å
Z	4
Density (calculated)	$1.674 \ \mathrm{Mg \, m^{-1}}$
Absorption coefficient	$11.412 \ \mathrm{mm^{-1}}$
F(000)	1400 e
Crystal size	0.14 x 0.13 x 0.10 mm
Θ range for data collection	2.81 to 67.16°.
Index ranges	$-18 \leq h \leq 20, -12 \leq k \leq 13, -19 \leq l \leq 19$
Reflections collected	67770
Independent reflections	4988 [$R_{int} = 0.0481$]
Reflections with $I > 2\sigma(I)$	4859
Completeness to $\Theta = 67.16°$	99.2 %
Absorption correction	Gaussian
Max. and min. transmission	0.54295 and 0.22715
Refinement method	Full-matrix least-squares on F^2
Data / restraints / parameters	4988 / 0 / 338
Goodness-of-fit on F^2	1.123
Final R indices [$I > 2\sigma(I)$]	$R_1 = 0.0183 \qquad wR_2 = 0.0442$
R indices (all data)	$R_1 = 0.0193 \qquad wR_2 = 0.0445$
Largest diff. peak and hole	0.496 and -0.717 e$\mathrm{\AA}^{-3}$

Compound 80k :
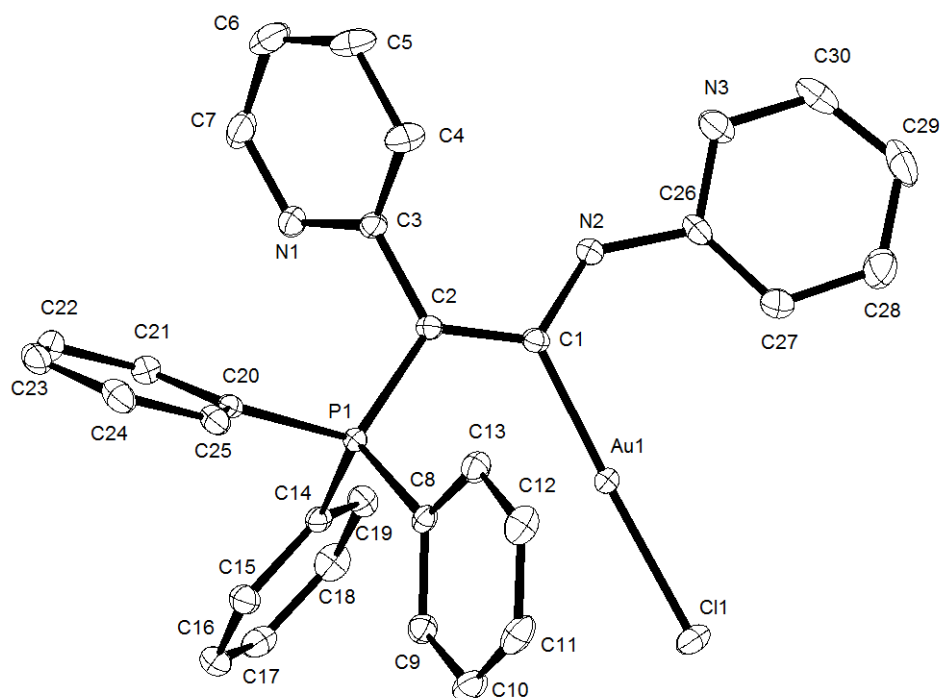
Empirical formula	$C_{30}H_{24}AuClN_3P$
Colour	colourless
Formula weight	$689.91 \text{ g mol}^{-1}$
Temperature	100 K
Wavelength	0.71073 Å
Crystal system	MONOCLINIC
Space group	$P2_1/n$, (no. 14)
Unit cell dimensions	a = 7.8814(13) Å $\alpha = 90°$.
	b = 21.271(3) Å $\beta = 92.434(3)°$.
	c = 15.328(3) Å $\gamma = 90°$.
Volume	2567.4(7) Å
Z	4
Density (calculated)	1.785 Mg m^{-1}
Absorption coefficient	5.921 mm^{-1}
F(000)	1344 e
Crystal size	0.22 x 0.05 x 0.04 mm
Θ range for data collection	1.64 to 30.99°.
Index ranges	$-11 \le h \le 11, -30 \le k \le 30, -22 \le l \le 22$
Reflections collected	116078
Independent reflections	8169 $[R_{int} = 0.0441]$
Reflections with $I > 2\sigma(I)$	7346
Completeness to $\Theta = 30.99°$	99.9 %
Absorption correction	Gaussian
Max. and min. transmission	0.80 and 0.37
Refinement method	Full-matrix least-squares on F^2
Data / restraints / parameters	8169 / 0 / 329
Goodness-of-fit on F^2	1.078
Final R indices $[I > 2\sigma(I)]$	$R_1 = 0.0186$ $wR_2 = 0.0365$
R indices (all data)	$R_1 = 0.0235$ $wR_2 = 0.0376$
Largest diff. peak and hole	0.9 and -0.9 eÅ^{-3}

Compound 84 :
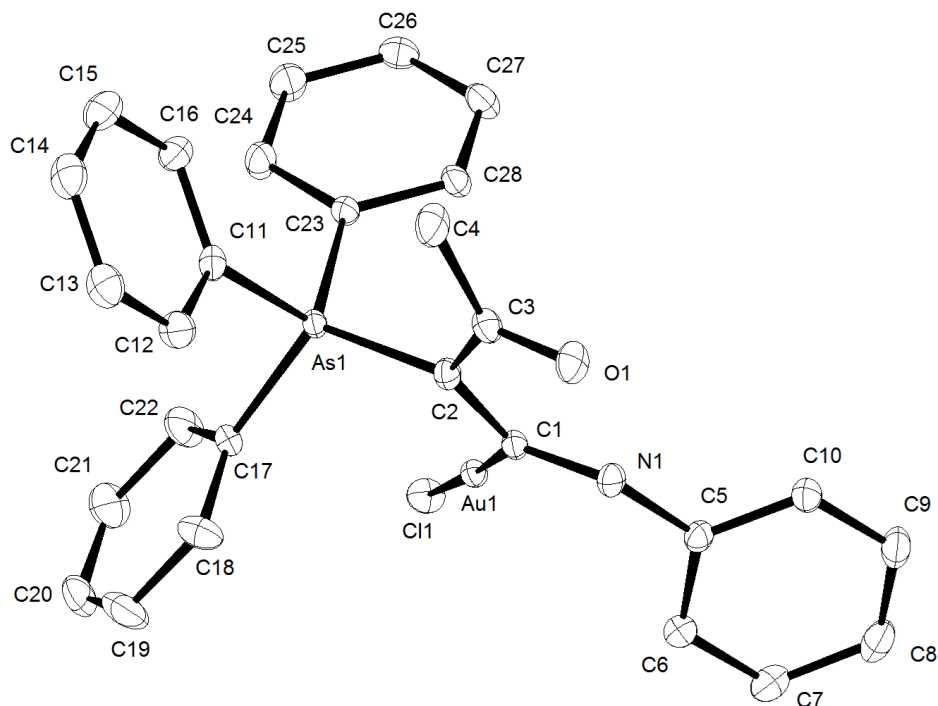
Empirical formula	$C_{28}H_{24}AsAuClNO$
Colour	colourless
Formula weight	$697.82 \mathrm{\,g\,mol^{-1}}$
Temperature	100 K
Wavelength	0.71073 Å
Crystal system	MONOCLINIC
Space group	$P2_1/n$, (no. 14)
Unit cell dimensions	a = 14.9063(15) Å $\alpha = 90°$.
	b = 12.0478(12) Å $\beta = 115.743(3)°$.
	c = 15.3302(3) Å $\gamma = 90°$.
Volume	2479.9(4) Å
Z	4
Density (calculated)	$1.869 \mathrm{\,Mg\,m^{-1}}$
Absorption coefficient	$7.385 \mathrm{\,mm^{-1}}$
F(000)	1344 e
Crystal size	0.20 x 0.17 x 0.07 mm
Θ range for data collection	2.67 to 36.00°.
Index ranges	$-24 \leq h \leq 24, -19 \leq k \leq 19, -25 \leq l \leq 25$
Reflections collected	62465
Independent reflections	11702 $[R_{int} = 0.0491]$
Reflections with $I > 2\sigma(I)$	10436
Completeness to $\Theta = 27.50°$	99.8 %
Absorption correction	Gaussian
Max. and min. transmission	0.62 and 0.27
Refinement method	Full-matrix least-squares on F^2
Data / restraints / parameters	11702 / 0 / 299
Goodness-of-fit on F^2	1.094
Final R indices $[I > 2\sigma(I)]$	$R_1 = 0.0294$ $wR_2 = 0.0693$
R indices (all data)	$R_1 = 0.0357$ $wR_2 = 0.0723$
Largest diff. peak and hole	1.897 and -4.624 e$\mathrm{\AA}^{-3}$

Compound 87 :
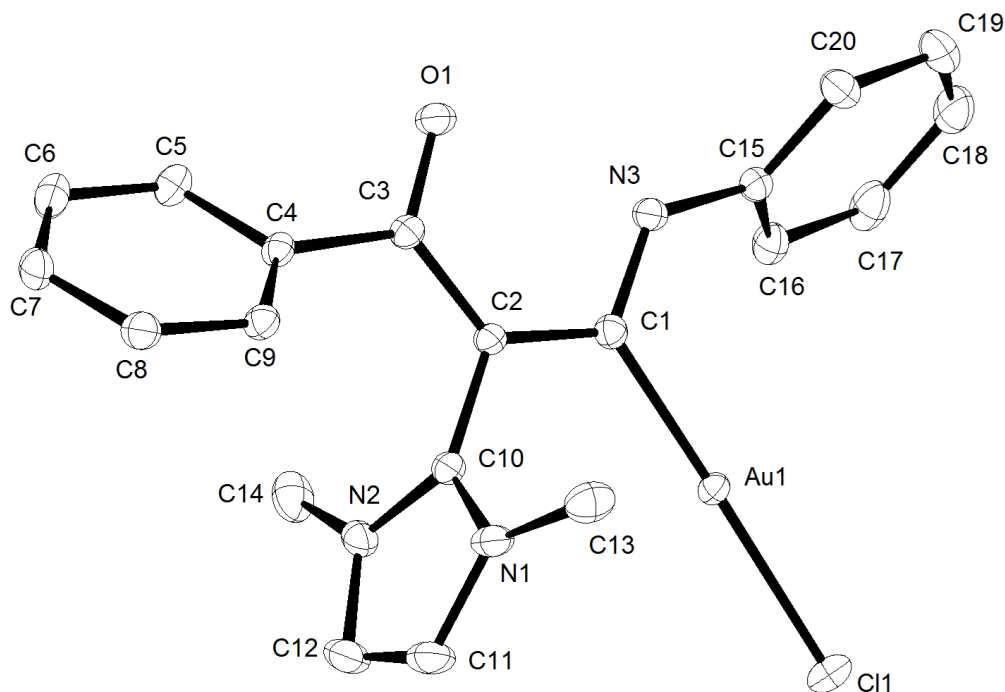
Empirical formula	$C_{20}H_{19}AuClN_3O$
Colour	yellow
Formula weight	697.82 $g\,mol^{-1}$
Temperature	100 K
Wavelength	0.71073 Å
Crystal system	MONOCLINIC
Space group	$P2_1/n$, (no. 14)
Unit cell dimensions	a = 12.3447(8) Å $\quad\alpha = 90°$.
	b = 11.9732(8) Å $\quad\beta = 110.926(5)°$.
	c = 13.8197(9) Å $\quad\gamma = 90°$.
Volume	1907.9(2) Å
Z	4
Density (calculated)	1.914 $Mg\,m^{-1}$
Absorption coefficient	7.864 mm^{-1}
F(000)	1056 e
Crystal size	0.27 x 0.26 x 0.05 mm
Θ range for data collection	2.76 to 34.99°.
Index ranges	$-19 \leq h \leq 19, -19 \leq k \leq 19, -22 \leq l \leq 22$
Reflections collected	55520
Independent reflections	8346 [$R_{int} = 0.0311$]
Reflections with $I > 2\sigma(I)$	7679
Completeness to $\Theta = 34.99°$	99.4 %
Absorption correction	Gaussian
Max. and min. transmission	0.69 and 0.14
Refinement method	Full-matrix least-squares on F^2
Data / restraints / parameters	8346 / 0 / 237
Goodness-of-fit on F^2	1.172
Final R indices [$I > 2\sigma(I)$]	$R_1 = 0.0157 \qquad wR_2 = 0.0432$
R indices (all data)	$R_1 = 0.0192 \qquad wR_2 = 0.0450$
Largest diff. peak and hole	0.668 and -1.638 $e\mathring{A}^{-3}$

Compound 88 :
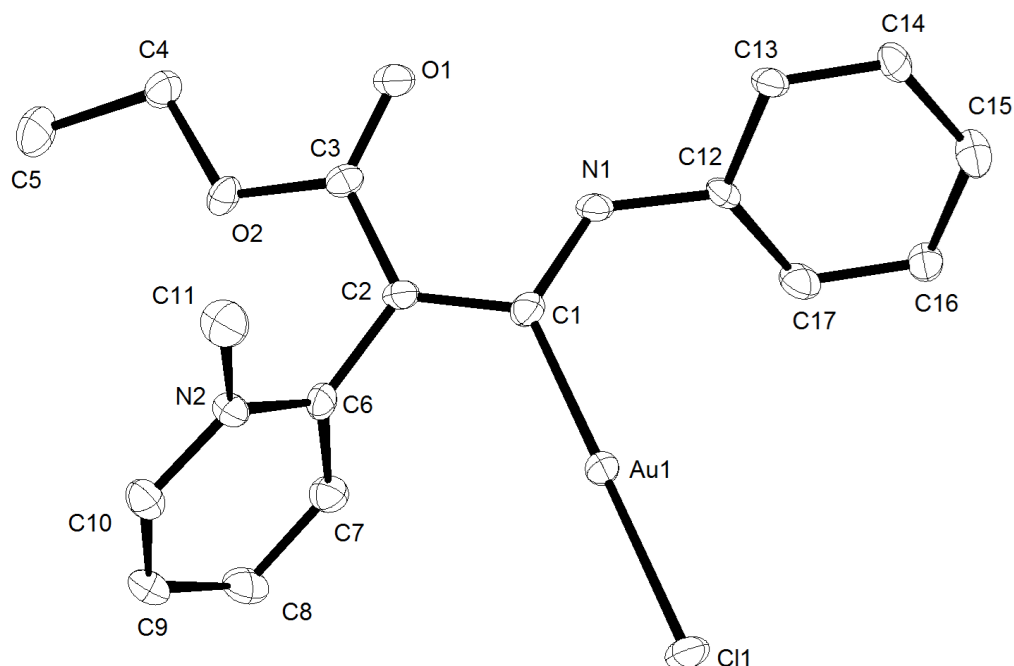
Empirical formula	$C_{17}H_{18}AuClN_2O_2$
Colour	yellow
Formula weight	514.75 $g\,mol^{-1}$
Temperature	100 K
Wavelength	0.71073 Å
Crystal system	MONOCLINIC
Space group	$P2_1/n$, (no. 14)
Unit cell dimensions	a = 15.6583(16) Å $\quad$ $\alpha = 90°$.
	b = 13.6797(13) Å $\quad$ $\beta = 96.433(9)°$.
	c = 8.2938(9) Å $\quad$ $\gamma = 90°$.
Volume	1765.4(3) Å
Z	4
Density (calculated)	1.937 $Mg\,m^{-1}$
Absorption coefficient	8.494 mm^{-1}
F(000)	984 e
Crystal size	0.38 x 0.05 x 0.04 mm
Θ range for data collection	2.618 to 33.127°.
Index ranges	$-24 \leq h \leq 24, -21 \leq k \leq 20, -12 \leq l \leq 12$
Reflections collected	35129
Independent reflections	6706 [$R_{int} = 0.0514$]
Reflections with $I > 2\sigma(I)$	5171
Completeness to $\Theta = 25.242°$	99.9 %
Absorption correction	Gaussian
Max. and min. transmission	0.72 and 0.24
Refinement method	Full-matrix least-squares on F^2
Data / restraints / parameters	6706 / 0 / 210
Goodness-of-fit on F^2	1.457
Final R indices [$I > 2\sigma(I)$]	$R_1 = 0.0474$ $\quad$ $wR_2 = 0.1972$
R indices (all data)	$R_1 = 0.0660$ $\quad$ $wR_2 = 0.2080$
Largest diff. peak and hole	1.9 and -2.7 $e\text{Å}^{-3}$

Compound 90 :
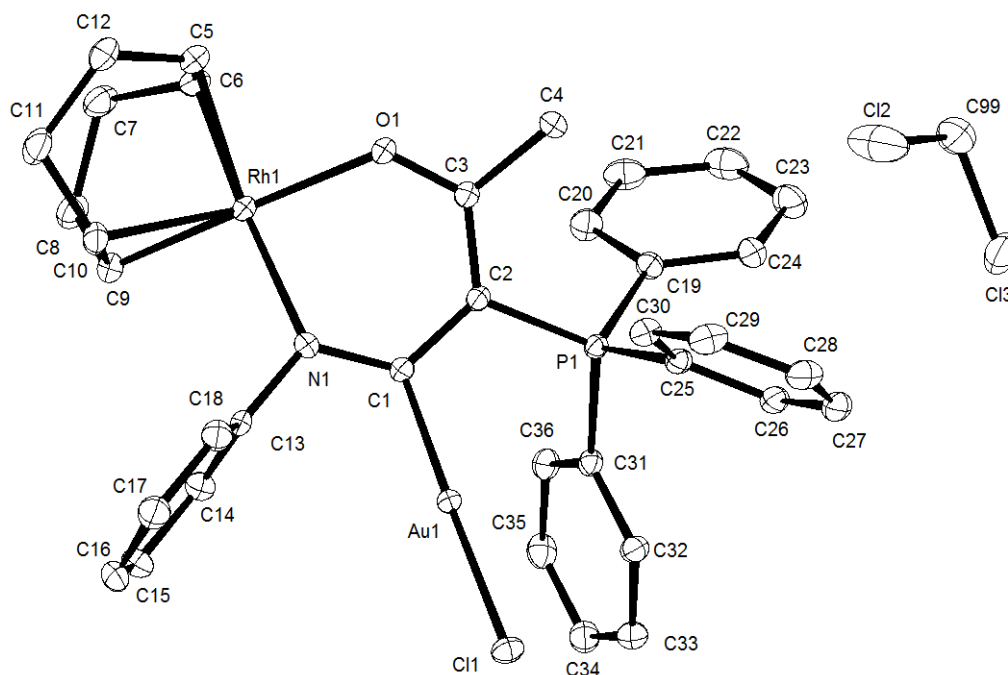
Empirical formula	$C_{37}H_{37}AuCl_3NOPRh$
Colour	orange
Formula weight	$948.87\ \text{g\,mol}^{-1}$
Temperature	100 K
Wavelength	0.71073 Å
Crystal system	MONOCLINIC
Space group	$P2_1/n$, (no. 14)
Unit cell dimensions	a = 15.2528(12) Å $\qquad \alpha = 90°$.
	b = 12.7151(19) Å $\qquad \beta = 101.855(11)°$.
	c = 17.885(4) Å $\qquad \gamma = 90°$.
Volume	3394.7(10) Å
Z	4
Density (calculated)	$1.857\ \text{Mg\,m}^{-1}$
Absorption coefficient	$5.118\ \text{mm}^{-1}$
F(000)	1856 e
Crystal size	0.14 x 0.12 x 0.06 mm
Θ range for data collection	2.729 to 33.218°.
Index ranges	$-23 \le h \le 23, -19 \le k \le 19, -25 \le l \le 27$
Reflections collected	58509
Independent reflections	12950 $[R_{int} = 0.0360]$
Reflections with $I > 2\sigma(I)$	11849
Completeness to $\Theta = 25.242°$	99.8 %
Absorption correction	Gaussian
Max. and min. transmission	0.75 and 0.51
Refinement method	Full-matrix least-squares on F^2
Data / restraints / parameters	12950 / 0 / 407
Goodness-of-fit on F^2	1.096
Final R indices $[I > 2\sigma(I)]$	$R_1 = 0.0294 \qquad wR_2 = 0.0676$
R indices (all data)	$R_1 = 0.0342 \qquad wR_2 = 0.0698$
Largest diff. peak and hole	1.7 and -3.4 eÅ^{-3}

Compound 93 :
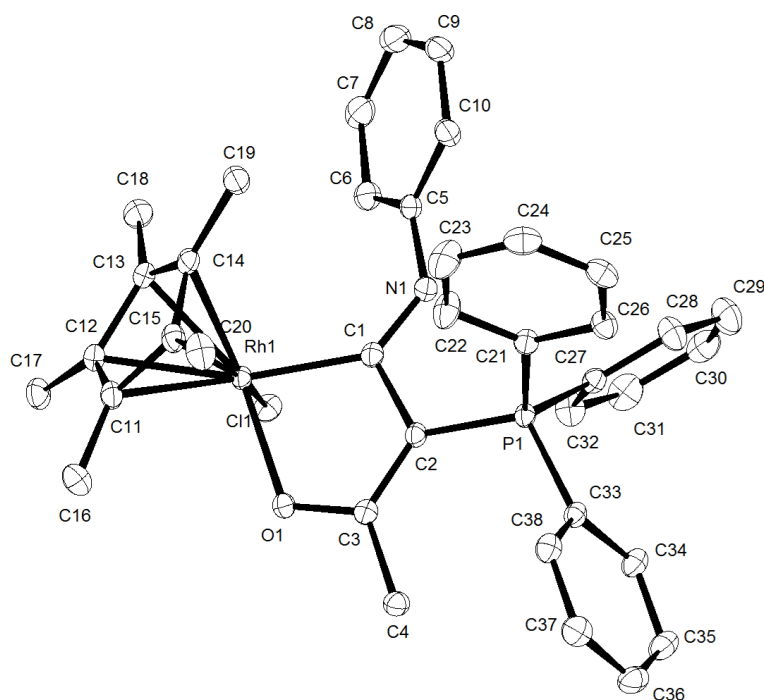
Empirical formula	$C_{38}H_{38}ClNOPRh$
Colour	orange
Formula weight	$694.02 \text{ g mol}^{-1}$
Temperature	100 K
Wavelength	0.71073 Å
Crystal system	MONOCLINIC
Space group	$P2_1/n$, (no. 14)

Unit cell dimensions	a = 10.7983(10) Å	$\alpha = 90°$.
	b = 13.1084(12) Å	$\beta = 100.263(2)°$.
	c = 23.391(2) Å	$\gamma = 90°$.

Volume	3394.7(10) Å
Z	4
Density (calculated)	1.415 Mg m^{-1}
Absorption coefficient	0.686 mm^{-1}
F(000)	1432 e
Crystal size	0.15 x 0.12 x 0.08 mm
Θ range for data collection	1.77 to 33.31°.
Index ranges	$-16 \leq h \leq 16, -20 \leq k \leq 20, -35 \leq l \leq 36$
Reflections collected	107131
Independent reflections	12543 $[R_{int} = 0.0424]$
Reflections with $I > 2\sigma(I)$	10641
Completeness to $\Theta = 27.50°$	100.0 %
Absorption correction	Gaussian
Max. and min. transmission	0.77 and 0.54
Refinement method	Full-matrix least-squares on F^2
Data / restraints / parameters	12543 / 0 / 394
Goodness-of-fit on F^2	1.114
Final R indices $[I > 2\sigma(I)]$	$R_1 = 0.0233$ $wR_2 = 0.0596$
R indices (all data)	$R_1 = 0.0333$ $wR_2 = 0.0684$
Largest diff. peak and hole	0.535 and -0.498 eÅ^{-3}

Compound 94 :

Empirical formula	$C_{38}H_{37}ClNOPRu$
Colour	orange
Formula weight	$691.17 \text{ g mol}^{-1}$
Temperature	100 K
Wavelength	1.54178 Å
Crystal system	TRICLINIC
Space group	$P\bar{1}$, (no. 2)
Unit cell dimensions	a = 12.0706(9) Å $\quad \alpha = 103.223(2)°.$
	b = 14.0017(10) Å $\quad \beta = 104.078(2)°.$
	c = 22.6559(16) Å $\quad \gamma = 96.295(2)°.$
Volume	3559.7(4) Å
Z	4
Density (calculated)	1.290 Mg m^{-1}
Absorption coefficient	4.892 mm^{-1}
F(000)	1424 e
Crystal size	0.47 x 0.34 x 0.31 mm
Θ range for data collection	2.085 to 67.024°.
Index ranges	$-14 \leq h \leq 14, -16 \leq k \leq 16, -26 \leq l \leq 26$
Reflections collected	80389
Independent reflections	12196 [$R_{int} = 0.0436$]
Reflections with $I > 2\sigma(I)$	10736
Completeness to $\Theta = 67.679°$	94.6 %
Absorption correction	Gaussian
Max. and min. transmission	0.38 and 0.12
Refinement method	Full-matrix least-squares on F^2
Data / restraints / parameters	12196 / 0 / 783
Goodness-of-fit on F^2	1.046
Final R indices [$I > 2\sigma(I)$]	$R_1 = 0.0427 \quad wR_2 = 0.1023$
R indices (all data)	$R_1 = 0.0463 \quad wR_2 = 0.1041$
Largest diff. peak and hole	1.502 and -0.864 $e\text{Å}^{-3}$

Compound 97 :

Empirical formula	$C_{35}H_{31}AuClF_3N_3O_3PS$
Colour	yellow-green
Formula weight	$894.07 \text{ g mol}^{-1}$
Temperature	100 K
Wavelength	0.71073 Å
Crystal system	MONOCLINIC
Space group	$P2_1/n$, (no. 14)
Unit cell dimensions	a = 11.9333(9) Å $\qquad \alpha = 90°$.
	b = 23.477(3) Å $\qquad \beta = 93.473(4)°$.
	c = 12.4237(7) Å $\qquad \gamma = 90°$.
Volume	3474.1(5) Å
Z	4
Density (calculated)	1.709 Mg m^{-1}
Absorption coefficient	4.473 mm^{-1}
F(000)	1760 e
Crystal size	0.12 x 0.09 x 0.04 mm
Θ range for data collection	3.11 to 28.02°.
Index ranges	$-15 \leq h \leq 15, -31 \leq k \leq 31, -16 \leq l \leq 16$
Reflections collected	68346
Independent reflections	8367 [$R_{int} = 0.0994$]
Reflections with $I > 2\sigma(I)$	5791
Completeness to $\Theta = 27.50°$	99.8 %
Absorption correction	Gaussian
Max. and min. transmission	0.84 and 0.50
Refinement method	Full-matrix least-squares on F^2
Data / restraints / parameters	8367 / 0 / 435
Goodness-of-fit on F^2	1.122
Final R indices [$I > 2\sigma(I)$]	$R_1 = 0.0351 \qquad wR_2 = 0.0546$
R indices (all data)	$R_1 = 0.0844 \qquad wR_2 = 0.0687$
Largest diff. peak and hole	2.2 and -1.6 eÅ^{-3}

Compound 164e :
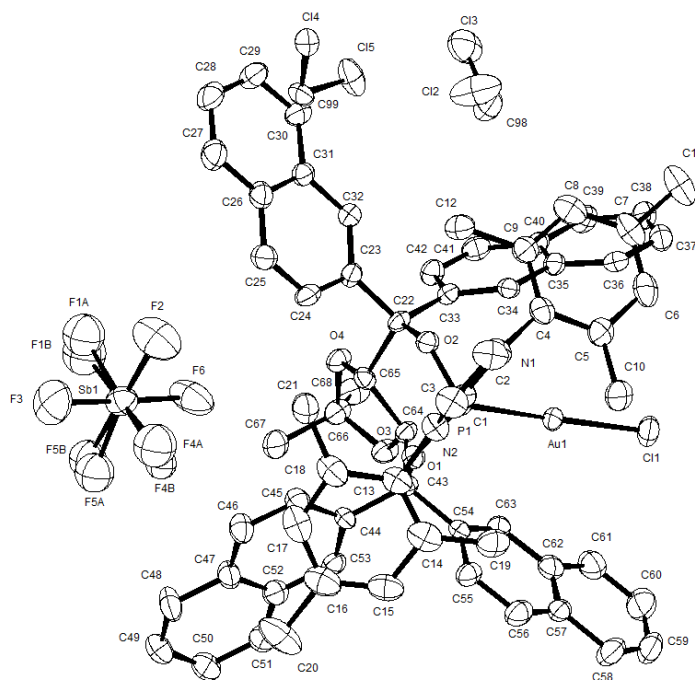
Empirical formula	$C_{69.50}H_{63}AuCl_4F_6N_2O_4PSb$
Colour	colourless
Formula weight	1595.70 g mol^{-1}
Temperature	100 K
Wavelength	0.71073 Å
Crystal system	ORTHORHOMBIC
Space group	$P2_12_12_1$, (no. 19)
Unit cell dimensions	a = 10.750(4) Å $\qquad \alpha = 90°$.
	b = 24.403(14) Å $\qquad \beta = 90°$.
	c = 25.635(6) Å $\qquad \gamma = 90°$.
Volume	6725(5) Å
Z	4
Density (calculated)	1.576 Mg m^{-1}
Absorption coefficient	2.829 mm^{-1}
F(000)	3172 e
Crystal size	0.12 x 0.04 x 0.02 mm
Θ range for data collection	2.610 to 32.104°.
Index ranges	$-16 \leq h \leq 16, -36 \leq k \leq 36, -38 \leq l \leq 37$
Reflections collected	112554
Independent reflections	23459 [$R_{int} = 0.1238$]
Reflections with $I > 2\sigma(I)$	16974
Completeness to $\Theta = 26.000°$	99.8 %
Absorption correction	Gaussian
Max. and min. transmission	0.95 and 0.78
Refinement method	Full-matrix least-squares on F^2
Data / restraints / parameters	23459 / 0 / 816
Goodness-of-fit on F^2	1.054
Final R indices [$I > 2\sigma(I)$]	$R_1 = 0.0681 \qquad wR_2 = 0.1573$
R indices (all data)	$R_1 = 0.1087 \qquad wR_2 = 0.1859$
Absolute structure parameter	-0.020(5)
Largest diff. peak and hole	2.3 and -2.4 eÅ^{-3}

Compound 164f :
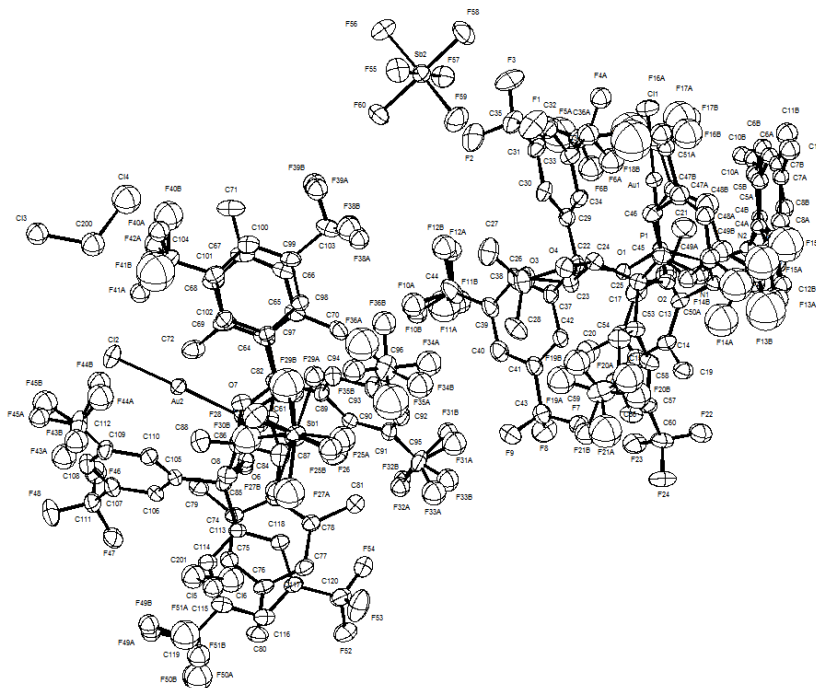
Empirical formula	$C_{60.50}H_{45}AuCl_2F_{30}N_2O_4PSb$
Colour	colourless
Formula weight	1854.57 $\mathrm{g\,mol^{-1}}$
Temperature	100 K
Wavelength	0.71073 Å
Crystal system	MONOCLINIC
Space group	$P2_1$, (no. 4)
Unit cell dimensions	a = 13.253(2) Å $\qquad \alpha = 90°$.
	b = 25.560(6) Å $\qquad \beta = 90.730(12)°$.
	c = 20.336(3) Å $\qquad \gamma = 90°$.
Volume	6888(2) Å
Z	4
Density (calculated)	1.788 $\mathrm{Mg\,m^{-1}}$
Absorption coefficient	2.748 $\mathrm{mm^{-1}}$
F(000)	3612 e
Crystal size	0.14 x 0.10 x 0.03 mm
Θ range for data collection	2.663 to 32.576°.
Index ranges	$-20 \leq h \leq 20, -38 \leq k \leq 38, -30 \leq l \leq 30$
Reflections collected	141512
Independent reflections	50013 [$R_{int} = 0.0705$]
Reflections with $I > 2\sigma(I)$	43675
Completeness to $\Theta = 25.242°$	99.8 %
Absorption correction	Gaussian
Max. and min. transmission	0.93 and 0.71
Refinement method	Full-matrix least-squares on F^2
Data / restraints / parameters	50013 / 1 / 1792
Goodness-of-fit on F^2	1.026
Final R indices [$I > 2\sigma(I)$]	$R_1 = 0.0613 \qquad wR_2 = 0.1582$
R indices (all data)	$R_1 = 0.0722 \qquad wR_2 = 0.1685$
Absolute structure parameter	0.015(4)
Largest diff. peak and hole	1.8 and -2.4 $\mathrm{e\AA^{-3}}$

Compound 165d :
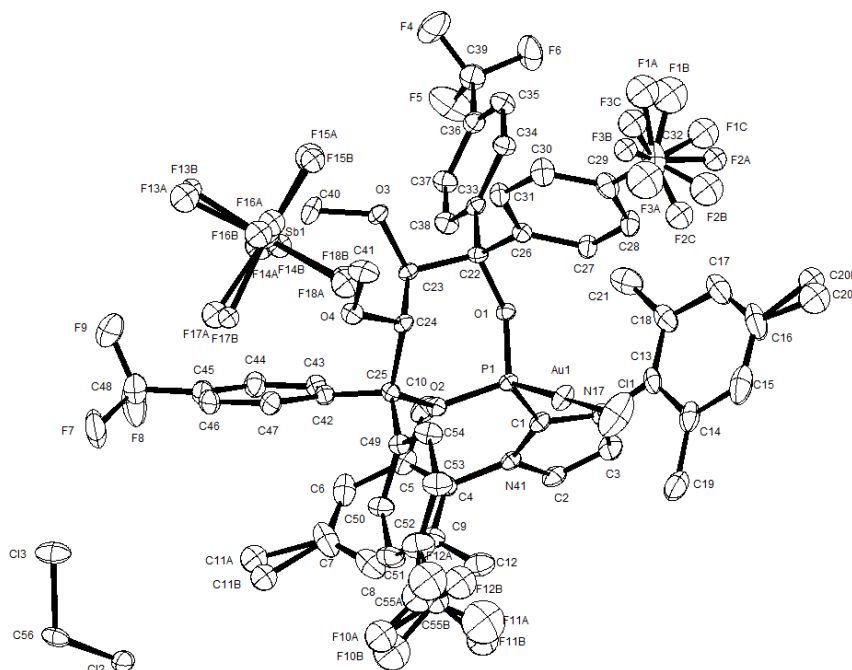
Empirical formula	$C_{55.50}H_{49}AuCl_2F_{18}N_2O_4PSb$
Colour	colourless
Formula weight	1570.55 $g\,mol^{-1}$
Temperature	100 K
Wavelength	0.71073 Å
Crystal system	TRICLINIC
Space group	$P1$, (no. 1)
Unit cell dimensions	a = 10.9830(12) Å $\alpha = 66.668(2)°$.
	b = 11.4243(12) Å $\beta = 83.965(2)°$.
	c = 13.3626(14) Å $\gamma = 88.252(2)°$.
Volume	1530.9(3) Å
Z	1
Density (calculated)	1.704 $Mg\,m^{-1}$
Absorption coefficient	3.047 mm^{-1}
F(000)	769 e
Crystal size	0.108 x 0.092 x 0.062 mm
Θ range for data collection	2.676 to 33.446°.
Index ranges	$-16 \le h \le 16, -17 \le k \le 17, -20 \le l \le 20$
Reflections collected	44170
Independent reflections	21832 [$R_{int} = 0.0366$]
Reflections with $I > 2\sigma(I)$	19047
Completeness to $\Theta = 25.242°$	99.7 %
Absorption correction	Gaussian
Max. and min. transmission	0.7465 and 0.6607
Refinement method	Full-matrix least-squares on F^2
Data / restraints / parameters	21832 / 3 / 782
Goodness-of-fit on F^2	1.016
Final R indices[$I > 2\sigma(I)$]	$R_1 = 0.0470$ $wR_2 = 0.1046$
R indices (all data)	$R_1 = 0.0598$ $wR_2 = 0.1113$
Absolute structure parameter	-0.002(2)
Largest diff. peak and hole	4.005 and -2.354 e$Å^{-3}$

Compound 170:
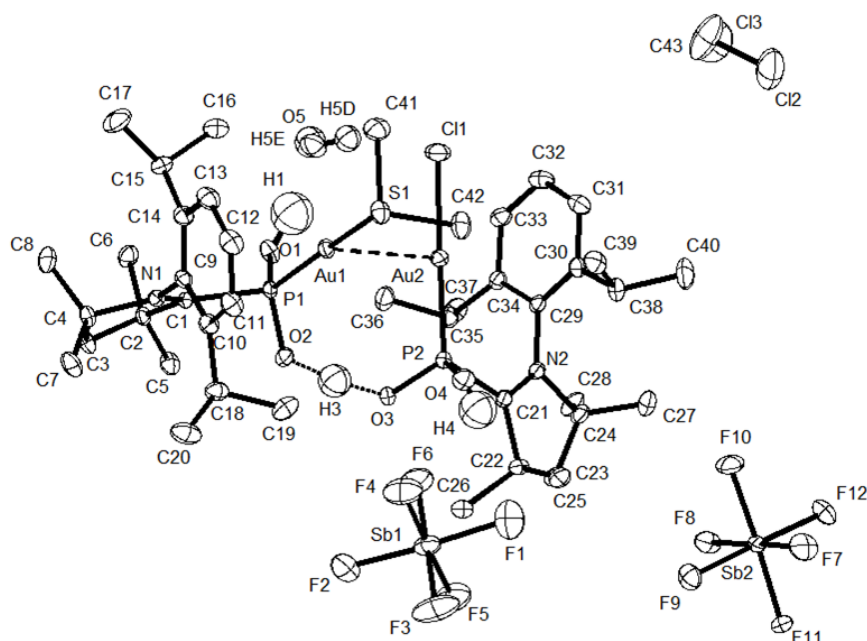
Empirical formula	$C_{85}H_{148}Au_4Cl_4F_{24}N_4O_{10}P_4S_2Sb_4$
Colour	colourless
Formula weight	3446.73 g mol^{-1}
Temperature	100 K
Wavelength	0.71073 Å
Crystal system	TRICLINIC
Space group	$P\bar{1}$, (no. 2)
Unit cell dimensions	a = 14.1224(13) Å $\quad$ $\alpha = 111.050(6)°$.
	b = 14.3201(6) Å $\quad$ $\beta = 108.050(8)°$.
	c = 16.3265(14) Å $\quad$ $\gamma = 90.835(5)°$.
Volume	2900.2(4) Å
Z	1
Density (calculated)	1.973 Mg m^{-1}
Absorption coefficient	6.227 mm^{-1}
F(000)	1662 e
Crystal size	0.22 x 0.10 x 0.02 mm
Θ range for data collection	2.663 to 35.037°.
Index ranges	$-22 \leq h \leq 22, -23 \leq k \leq 23, -26 \leq l \leq 26$
Reflections collected	95474
Independent reflections	25528 [$R_{int} = 0.0389$]
Reflections with $I > 2\sigma(I)$	22839
Completeness to Θ = 25.242°	99.8 %
Absorption correction	Gaussian
Max. and min. transmission	0.88424 and 0.30172
Refinement method	Full-matrix least-squares on F^2
Data / restraints / parameters	25528 / 0 / 687
Goodness-of-fit on F^2	0.970
Final R indices [$I > 2\sigma(I)$]	$R_1 = 0.0301$ $\quad$ $wR_2 = 0.1143$
R indices (all data)	$R_1 = 0.0359$ $\quad$ $wR_2 = 0.1211$
Extinction coefficient	0
Largest diff. peak and hole	2.934 and -3.424 eÅ^{-3}

Compound 169:
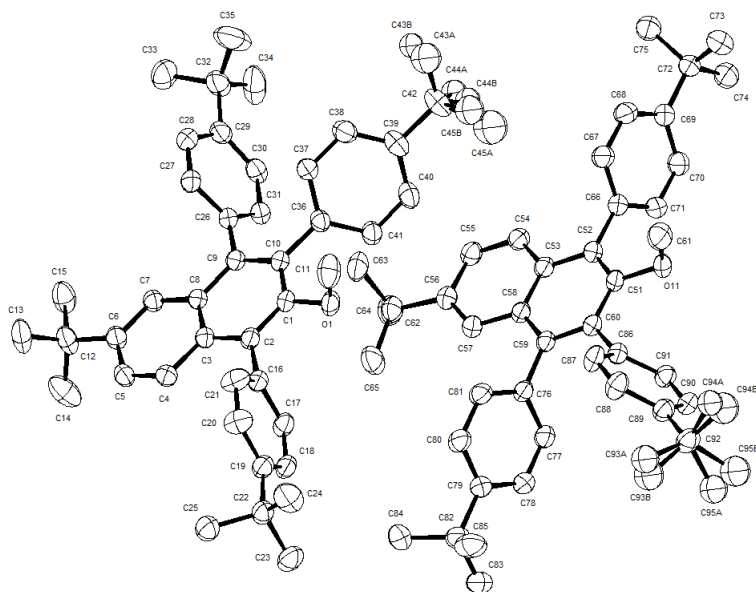
Empirical formula	$C_{45}H_{54}O$
Colour	colourless
Formula weight	610.88 $g\,mol^{-1}$
Temperature	100 K
Wavelength	1.54178 Å
Crystal system	TRICLINIC
Space group	$P\bar{1}$, (no. 2)
Unit cell dimensions	a = 13.0480(3) Å $\quad \alpha = 69.8393(12)°$.
	b = 15.9745(4) Å $\quad \beta = 74.7061(11)°$.
	c = 20.3351(5) Å $\quad \gamma = 79.3386(11)°$.
Volume	3817.17(16) Å
Z	4
Density (calculated)	1.063 $Mg\,m^{-1}$
Absorption coefficient	0.459 mm^{-1}
F(000)	1328 e
Crystal size	0.28 x 0.10 x 0.06 mm
Θ range for data collection	2.371 to 67.693°.
Index ranges	$-15 \leq h \leq 15, -19 \leq k \leq 19, -23 \leq l \leq 20$
Reflections collected	90751
Independent reflections	13297 [$R_{int} = 0.0903$]
Reflections with $I > 2\sigma(I)$	8599
Completeness to $\Theta = 67.679°$	96.2 %
Absorption correction	Gaussian
Max. and min. transmission	0.97 and 0.90
Refinement method	Full-matrix least-squares on F^2
Data / restraints / parameters	13297 / 0 / 856
Goodness-of-fit on F^2	1.024
Final R indices [$I > 2\sigma(I)$]	$R_1 = 0.0701 \qquad wR_2 = 0.1753$
R indices (all data)	$R_1 = 0.1128 \qquad wR_2 = 0.2119$
Extinction coefficient	0.0038(3)
Largest diff. peak and hole	0.5 and -0.4 $e\text{Å}^{-3}$

Compound 189a :
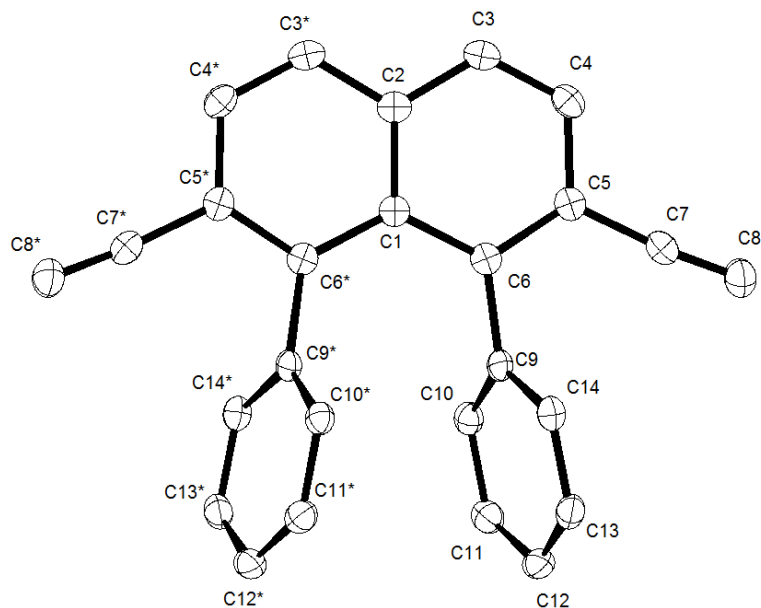
Empirical formula	$C_{26}H_{16}$
Colour	colourless
Formula weight	328.39 $\mathrm{g\,mol^{-1}}$
Temperature	100 K
Wavelength	1.54178 Å
Crystal system	MONOCLINIC
Space group	C2/c, (no. 15)
Unit cell dimensions	a = 16.9802(8) Å $\alpha = 90°$.
	b = 14.1991(7) Å $\beta = 104.4357(9)°$.
	c = 7.2267(3) Å $\gamma = 90°$.
Volume	1687.37(13) Å
Z	4
Density (calculated)	1.293 $\mathrm{Mg\,m^{-1}}$
Absorption coefficient	0.557 $\mathrm{mm^{-1}}$
F(000)	688 e
Crystal size	0.40 x 0.23 x 0.20 mm
Θ range for data collection	4.113 to 67.934°.
Index ranges	$-20 \leq h \leq 20, -16 \leq k \leq 16, -8 \leq l \leq 8$
Reflections collected	37427
Independent reflections	1523 [$R_{int} = 0.0300$]
Reflections with $I > 2\sigma(I)$	1514
Completeness to $\Theta = 67.679°$	99.2 %
Absorption correction	Gaussian
Max. and min. transmission	0.91 and 0.84
Refinement method	Full-matrix least-squares on F^2
Data / restraints / parameters	1523 / 0 / 120
Goodness-of-fit on F^2	1.067
Final R indices [$I > 2\sigma(I)$]	$R_1 = 0.0361$ $wR_2 = 0.0929$
R indices (all data)	$R_1 = 0.0363$ $wR_2 = 0.0930$
Extinction coefficient	0.0033(3)
Largest diff. peak and hole	0.3 and -0.1 $\mathrm{e\AA^{-3}}$

Compound 27aa:

Empirical formula	$C_{28}H_{20}$	
Colour	colourless	
Formula weight	$356.44 \text{ g mol}^{-1}$	
Temperature	100 K	
Wavelength	1.54178 Å	
Crystal system	MONOCLINIC	
Space group	C2/c, (no. 15)	
Unit cell dimensions	a = 18.4625(9) Å	$\alpha = 90°$.
	b = 14.2040(7) Å	$\beta = 108.6516(18)°$.
	c = 7.6031(4) Å	$\gamma = 90°$.
Volume	1889.13(17) Å	
Z	4	
Density (calculated)	1.253 Mg m^{-1}	
Absorption coefficient	0.536 mm^{-1}	
F(000)	752 e	
Crystal size	0.18 x 0.12 x 0.10 mm	
Θ range for data collection	4.009 to 67.779°.	
Index ranges	$-21 \le h \le 22, -16 \le k \le 16, -9 \le l \le 8$	
Reflections collected	20805	
Independent reflections	1686 [$R_{int} = 0.0468$]	
Reflections with $I > 2\sigma(I)$	1472	
Completeness to $\Theta = 67.679°$	98.5 %	
Absorption correction	Gaussian	
Max. and min. transmission	0.96 and 0.92	
Refinement method	Full-matrix least-squares on F^2	
Data / restraints / parameters	1686 / 0 / 130	
Goodness-of-fit on F^2	1.123	
Final R indices [$I > 2\sigma(I)$]	$R_1 = 0.0406$	$wR_2 = 0.1082$
R indices (all data)	$R_1 = 0.0502$	$wR_2 = 0.1204$
Extinction coefficient	0.0018(3)	
Largest diff. peak and hole	0.2 and -0.2 $e\text{Å}^{-3}$	

Compound 27ac:
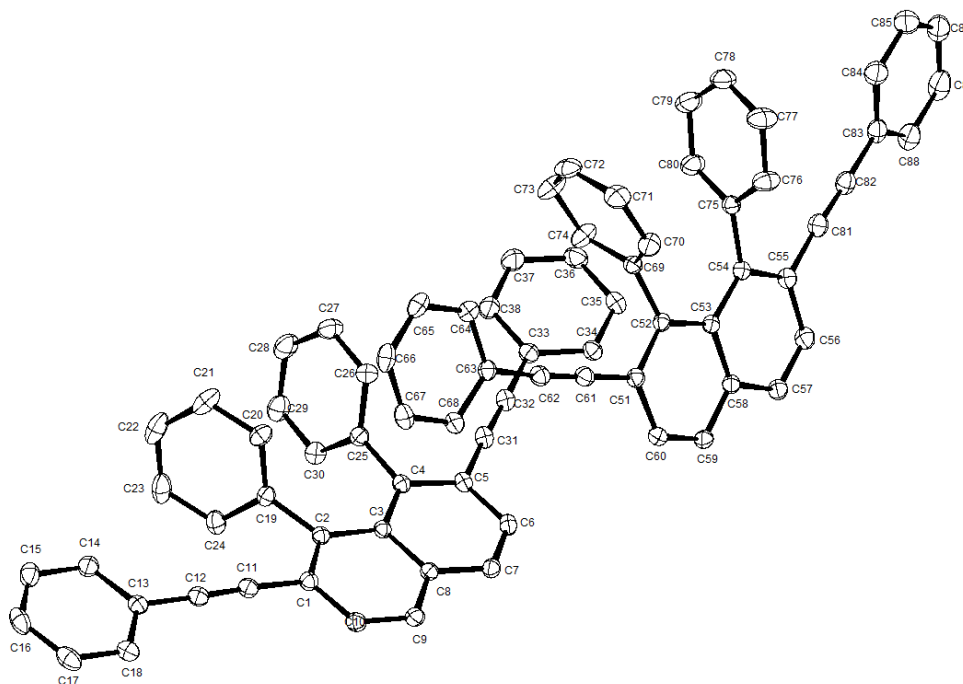
Empirical formula	$C_{38}H_{24}$
Colour	colourless
Formula weight	$480.57 \text{ g mol}^{-1}$
Temperature	100 K
Wavelength	0.71073 Å
Crystal system	TRICLINIC
Space group	$P\bar{1}$, (no. 2)
Unit cell dimensions	a = 10.2480(6) Å $\alpha = 85.397(5)°$.
	b = 15.0433(8) Å $\beta = 82.509(5)°$.
	c = 16.9963(8) Å $\gamma = 87.759(6)°$.
Volume	2588.4(2) Å
Z	4
Density (calculated)	1.233 Mg m^{-1}
Absorption coefficient	0.070 mm^{-1}
F(000)	1008 e
Crystal size	0.19 x 0.10 x 0.04 mm
Θ range for data collection	2.688 to 33.136°.
Index ranges	$-15 \leq h \leq 15, -23 \leq k \leq 23, -26 \leq l \leq 26$
Reflections collected	107452
Independent reflections	19635 $[R_{int} = 0.0458]$
Reflections with $I > 2\sigma(I)$	14852
Completeness to $\Theta = 25.242°$	99.3 %
Absorption correction	Gaussian
Max. and min. transmission	0.99725 and 0.98649
Refinement method	Full-matrix least-squares on F^2
Data / restraints / parameters	19635 / 0 / 685
Goodness-of-fit on F^2	1.087
Final R indices $[I > 2\sigma(I)]$	$R_1 = 0.0514$ $wR_2 = 0.1265$
R indices (all data)	$R_1 = 0.0749$ $wR_2 = 0.1416$
Extinction coefficient	n/a
Largest diff. peak and hole	0.407 and -0.261 eÅ^{-3}

Compound 26aa:

Empirical formula	$C_{28}H_{20}$
Colour	colourless
Formula weight	356.44 g mol^{-1}
Temperature	100 K
Wavelength	0.71073 Å
Crystal system	MONOCLINIC
Space group	$P2_1/c$, (no. 14)
Unit cell dimensions	a = 8.5356(11) Å $\qquad \alpha = 90°.$
	b = 15.5623(19) Å $\qquad \beta = 98.380(3)°.$
	c = 13.6640(17) Å $\qquad \gamma = 90°.$
Volume	1795.7(4) Å
Z	4
Density (calculated)	1.318 Mg m^{-1}
Absorption coefficient	0.075 mm^{-1}
F(000)	752 e
Crystal size	0.17 x 0.12 x 0.02 mm
Θ range for data collection	2.957 to 30.675°.
Index ranges	$-12 \leq h \leq 12, -22 \leq k \leq 22, -19 \leq l \leq 18$
Reflections collected	51392
Independent reflections	5540 [$R_{int} = 0.0658$]
Reflections with $I > 2\sigma(I)$	4161
Completeness to $\Theta = 25.242°$	99.9 %
Absorption correction	Gaussian
Max. and min. transmission	1.00 and 0.99
Refinement method	Full-matrix least-squares on F^2
Data / restraints / parameters	5540 / 0 / 255
Goodness-of-fit on F^2	1.025
Final R indices [$I > 2\sigma(I)$]	$R_1 = 0.0471 \qquad wR_2 = 0.1181$
R indices (all data)	$R_1 = 0.0700 \qquad wR_2 = 0.1320$
Largest diff. peak and hole	0.4 and -0.2 eÅ^{-3}

Compound 26ac:
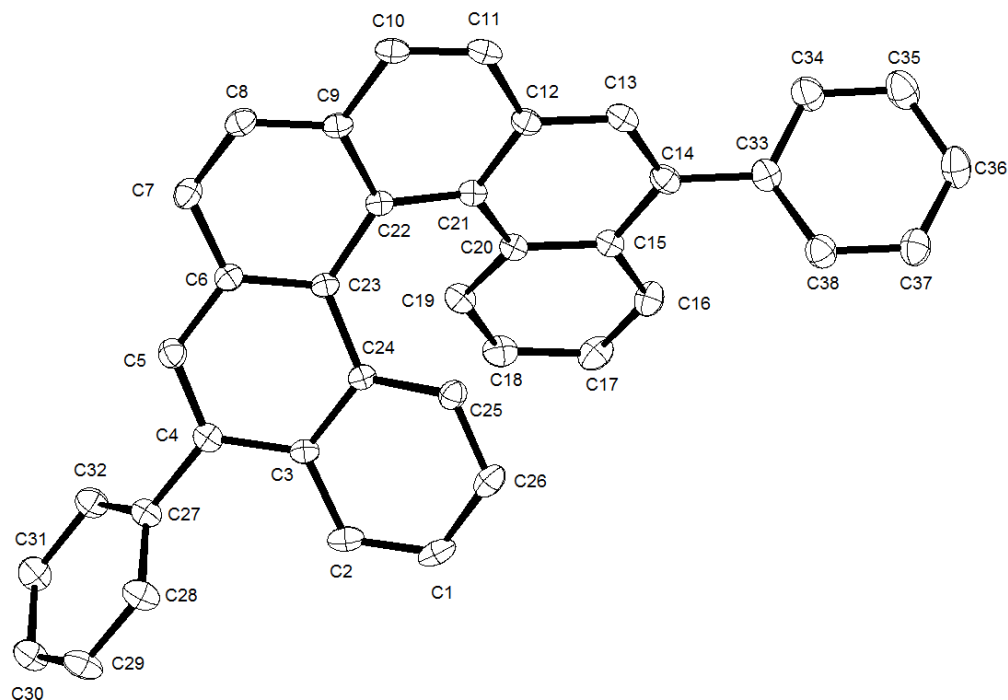
Empirical formula	$C_{38}H_{24}$
Color	yellow
Formula weight	480.57 g mol^{-1}
Temperature	100 K
Wavelength	0.71073Å
Crystal system	TRICLINIC
Space group	$P\bar{1}$, (no. 2)
Unit cell dimensions	a = 9.6273(14) Å $\quad \alpha = 106.794(2)°$.
	b = 9.6571(14) Å $\quad \beta = 91.195(3)°$.
	c = 14.569(2) Å $\quad \gamma = 104.193(2)°$.
Volume	1251.0(3) Å
Z	2
Density (calculated)	1.276 Mg m^{-1}
Absorption coefficient	0.072 mm^{-1}
F(000)	504 e
Crystal size	0.19 x 0.16 x 0.14 mm
Θ range for data collection	2.309 to 31.050°.
Index ranges	$-13 \leq h \leq 13, -13 \leq k \leq 13, -21 \leq l \leq 21$
Reflections collected	37030
Independent reflections	7946 [$R_{int} = 0.0248$]
Reflections with $I > 2\sigma(I)$	6749
Completeness to $\Theta = 25.242°$	99.8 %
Absorption correction	Gaussian
Max. and min. transmission	0.99264 and 0.98765
Refinement method	Full-matrix least-squares on F^2
Data / restraints / parameters	7946 / 0 / 343
Goodness-of-fit on F^2	1.020
Final R indices [$I > 2\sigma(I)$]	$R_1 = 0.0604 \qquad wR_2 = 0.1637$
R indices (all data)	$R_1 = 0.0697 \qquad wR_2 = 0.1728$
Extinction coefficient	n/a
Largest diff. peak and hole	0.840 and -0.369 eÅ^{-3}

Compound 200ab:
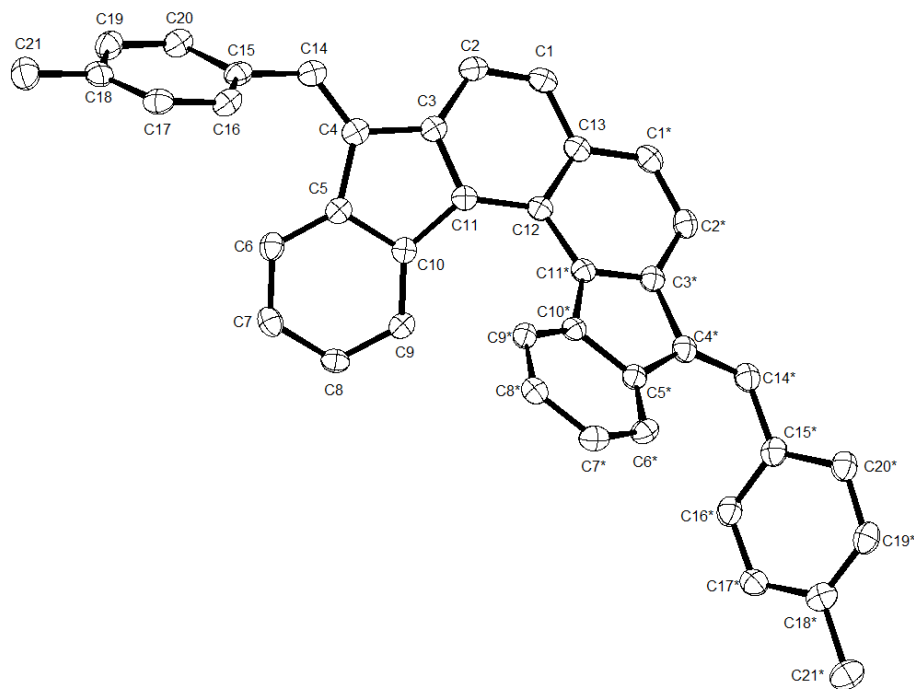
Empirical formula	$C_{40}H_{28}$
Colour	yellow
Formula weight	508.62 g mol^{-1}
Temperature	100 K
Wavelength	1.54178 Å
Crystal system	MONOCLINIC
Space group	C 2/c, (no. 15)
Unit cell dimensions	a = 24.6931(12) Å $\alpha = 90°$.
	b = 9.8945(5) Å $\beta = 107.0020(10)°$.
	c = 11.3008(5) Å $\gamma = 90°$.
Volume	2640.4(2) Å
Z	4
Density (calculated)	1.279 Mg m^{-1}
Absorption coefficient	0.548 mm^{-1}
F(000)	1072 e
Crystal size	0.29 x 0.21 x 0.12 mm
Θ range for data collection	3.744 to 67.386°.
Index ranges	$-29 \leq h \leq 29, -10 \leq k \leq 11, -13 \leq l \leq 13$
Reflections collected	30429
Independent reflections	2358 [$R_{int} = 0.0328$]
Reflections with $I > 2\sigma(I)$	2276
Completeness to $\Theta = 67.386°$	99.7 %
Absorption correction	Gaussian
Max. and min. transmission	0.94245 and 0.88133
Refinement method	Full-matrix least-squares on F^2
Data / restraints / parameters	2358 / 0 / 183
Goodness-of-fit on F^2	1.064
Final R indices [$I > 2\sigma(I)$]	$R_1 = 0.0399$ $wR_2 = 0.0947$
R indices (all data)	$R_1 = 0.0407$ $wR_2 = 0.0952$
Extinction coefficient	n/a
Largest diff. peak and hole	0.290 and -0.178 eÅ^{-3}

C. HPLC chromatograms

26aa achiral sample:

Sample Info   : 0.2 µL GON-GC-218-02 (400/400 µL Acetonitril)
                  achiral:
                  50 mm Eclipse Plus C18 1.8 µm, 3.0 mm i.D.; USDEA01836
                  Acetonitril / Wasser = 90:10
                  0.5 mL/min, 11.1 MPa, 308 K
                  UV, 254 nm
                  chiral:
                  150 mm Chiralpak IC-3R, 4.6 mm i.D., Säule 2
                  Acetonitril
                  1.0 mL/min, 6.9 MPa, 298 K
                  UV, 254 nm

Additional Info : Peak(s) manually integrated
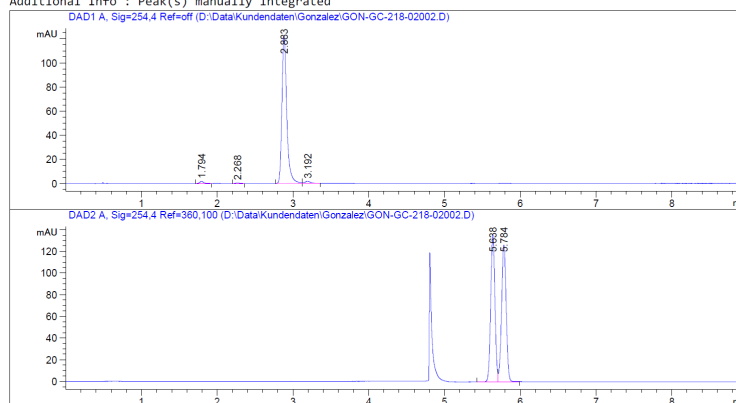
===
                      Area Percent Report
===

Sorted By   :   Signal
Multiplier   :   1.0000
Dilution   :   1.0000
Do not use Multiplier & Dilution Factor with ISTDs

Signal 1: DAD1 A, Sig=254,4 Ref=off

Peak RetTime Type Width   Area   Height   Area
 #   [min]   [min]   [mAU*s]   [mAU]   %
----|-------|----|-------|----------|----------|--------|
  1   1.794 BB   0.0550   6.70311   1.73841   1.1993
  2   2.268 BB   0.0459   1.97039 5.42311e-1 0.3525
  3   2.883 BV   0.0671 541.06586 122.31776 96.8019
  4   3.192 VB   0.0813   9.20210   1.61821   1.6463

Totals :   558.94145 126.21670

Signal 2: DAD2 A, Sig=254,4 Ref=360,100

Peak RetTime Type Width   Area   Height   Area
 #   [min]   [min]   [mAU*s]   [mAU]   %
----|-------|----|-------|----------|----------|--------|
  1   5.638 BV   0.0608 529.95276 136.35725 49.8674
  2   5.784 VB   0.0663 532.77179 126.01279 50.1326

Totals :   1062.72455 262.37005

===
                      *** End of Report ***

Helicene 26aa synthesised by enantioselective gold(I)-catalysis:

```
Sample Info      : 0.2 µL GON-GC-627-01 (1.06 mg in 1 mL ACN +200 µL MTBE + 200 µL Ch2Cl2)
                   achiral:
                   50 mm Eclipse Plus C18 1.8 µm, 4.6 mm i.D.
                   USDEA01836
                   Acetonitril/Wasser = 95:5
                   0.5 mL/min, 19.1 MPa, 308 K
                   UV, 254 nm
                   chiral:
                   150 mm Chiralpak IC-3R, 4.6 mm i.D., Säule 2
                   Acetonitril/Methanol = 100:0
                   1.0 mL/min, 7.6 MPa, 298 K
                   UV, 254 nm

Additional Info : Peak(s) manually integrated
```



```
================================================================
                     Area Percent Report
================================================================

Sorted By             :      Signal
Multiplier            :      1.0000
Dilution              :      1.0000
Do not use Multiplier & Dilution Factor with ISTDs


Signal 1: DAD1 A, Sig=254,4 Ref=off                           achiral

Peak RetTime Type  Width     Area      Height     Area
 #   [min]        [min]   [mAU*s]     [mAU]       %
----|-------|----|-------|----------|----------|-------|
   1   1.290 VV    0.0315   20.86531    9.93832   1.2385
   2   1.946 VV    0.0417    3.72124    1.34682   0.2209
   3   2.019 VB    0.0460    2.96692 9.48027e-1   0.1761
   4   2.244 VB    0.0551   39.75180   10.77052   2.3595
   5   2.614 BV    0.0591   41.37236   10.70621   2.4557
   6   2.852 VV    0.0642 1558.45947  365.72205  92.5039  helicene
   7   3.153 VB    0.0853   17.61299    2.92324   1.0454

Totals :                  1684.75010  402.35518


Signal 2: DAD2 A, Sig=254,4 Ref=360,100                       chiral

Peak RetTime Type  Width     Area      Height     Area
 #   [min]        [min]   [mAU*s]     [mAU]       %
----|-------|----|-------|----------|----------|-------|
   1   5.649 BV    0.0764 2252.72192  470.12610  81.2610  1. enantiomer
   2   5.794 VV    0.0806  519.48334  101.61444  18.7390  2. enantiomer     ee = 62.5 %

Totals :                  2772.20526  571.74054


================================================================
                     *** End of Report ***
```

Helicene 26ab racemic sample:

- Achiral separation:

Injection Volume : 1 uL
Data File Name : gon-gc-463-01-test01.lcd
Method File Name : Gonzalez.lcm

1 μL GON-GC-463 (100 μL of solution in 400μL Acetonitrile, prepared from 0.41 mg in 1ml MTBE + 0.4 ml DCM)
50mm Eclipse Plus C18 1.8μm, 4.6mm i. D., USUXG12018
Acetonitrile:Water = 95:5
1 ml/min, 6.0 MPa, 308 K
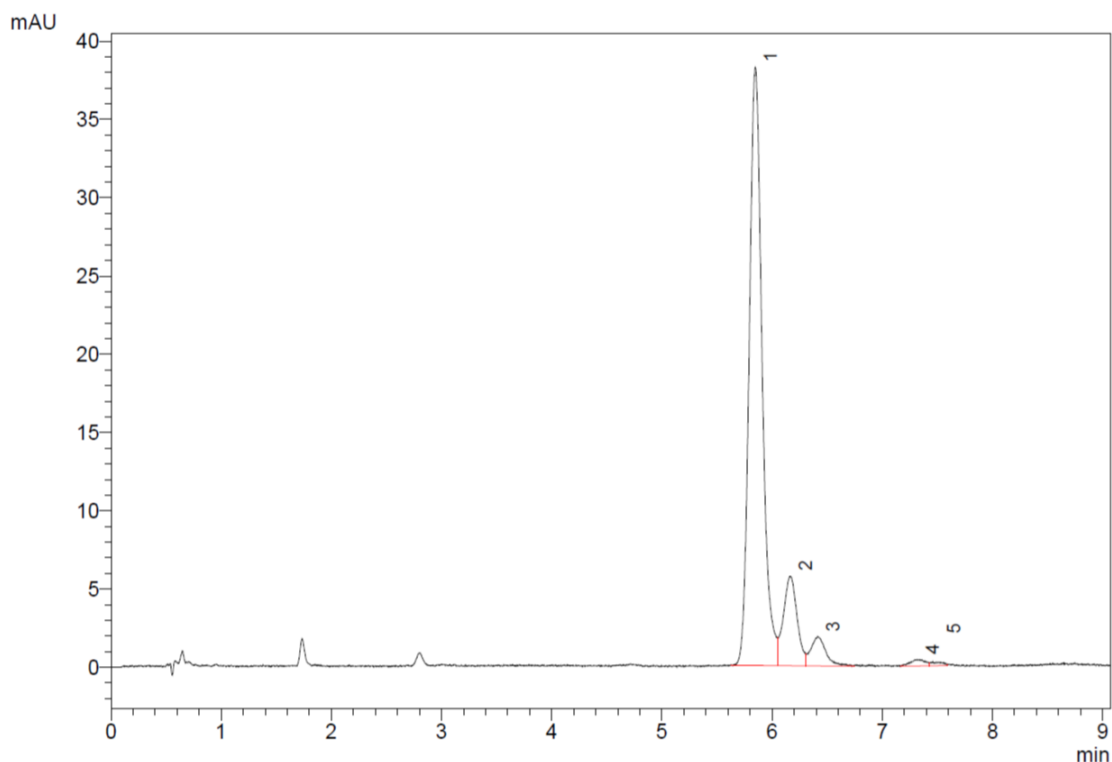
1   254nm,4nm

PDA Ch1 254nm

Peak #	Ret. Time	Area %	Name
1	5.85	80.82	helicene
2	6.17	13.04	isomer
3	6.41	4.66	
4	7.32	1.00	
5	7.51	0.49	
Total		100.00	

- Chiral separation:


```
Sample Info     : 1 µL GON-GC-463-01 (100/400 µL ACN)
                  achiral:                                    Racemat
                  50 mm Eclipse Plus C18 1.8 µm, 3.0 mm i.D.
                  USDEA01836
                  Acetonitril/Wasser = 95:5 (ACN aus Port D)
                  0.5 mL/min, 11.6 MPa, 308 K
                  UV, 254 nm
                  chiral:
                  150 mm Chiralpak IC3, 4.6 mm i.D. Säule 2
                  Acetonitril/Methanol = 95:5
                  1.0 mL/min, 5.9 MPa, 298 K
                  DAD 254 nm

Additional Info : Peak(s) manually integrated
```
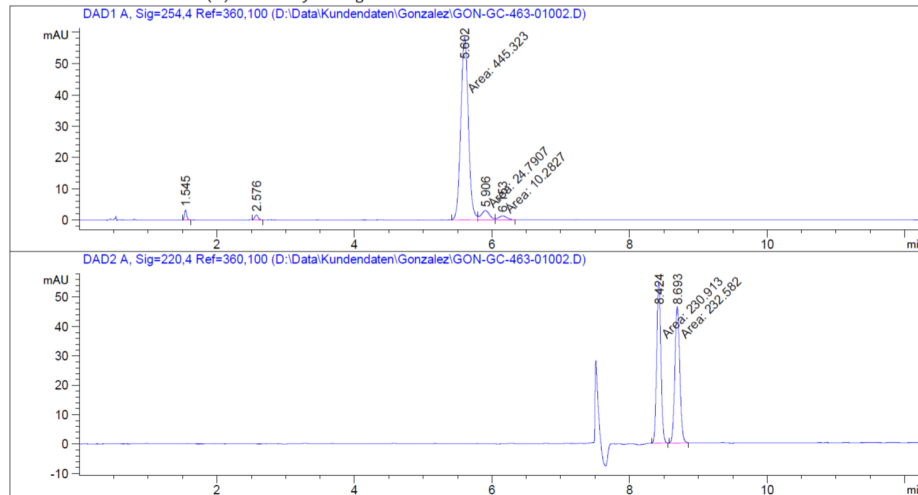
```
=====================================================================
                       Area Percent Report
=====================================================================

Sorted By          :     Signal
Multiplier         :     1.0000
Dilution           :     1.0000
Do not use Multiplier & Dilution Factor with ISTDs


Signal 1: DAD1 A, Sig=254,4 Ref=360,100

Peak RetTime Type  Width     Area       Height    Area
  #   [min]        [min]   [mAU*s]      [mAU]      %
----|-------|----|-------|----------|----------|--------|
  1   1.545 BB    0.0340    7.07563    3.17249   1.4353
  2   2.576 BB    0.0537    5.51091    1.57975   1.1179
  3   5.602 MF    0.1270  445.32257   58.43129  90.3323
  4   5.906 MF    0.1393   24.79068    2.96525   5.0287
  5   6.153 FM    0.1378   10.28270    1.24386   2.0858

Totals :                  492.98249   67.39264


Signal 2: DAD2 A, Sig=220,4 Ref=360,100

Peak RetTime Type  Width     Area       Height    Area
  #   [min]        [min]   [mAU*s]      [mAU]      %
----|-------|----|-------|----------|----------|--------|
  1   8.424 MM    0.0704  230.91316   54.67726  49.8200
  2   8.693 MM    0.0835  232.58185   46.43721  50.1800

Totals :                  463.49501  101.11446


=====================================================================
                       *** End of Report ***
```

Helicene 26ab synthesised by enantioselective gold(I)-catalysis:

- Achiral separation:

Injection Volume   : 2 uL
Data File Name   : GON-GC-589-01-01.lcd
Method File Name   : Gonzalez.lcm

2 μL GON-GC-589-01 (100 μL of solution in 400 μL Acetonitrile, prepared with 0.60 mg in 1ml MTBE and 0.4 ml DCM)
50mm Eclipse Plus C18 1.8μm, 4.6mm i. D., USUXG12018
Acetonitrile:Water = 90:10
1 ml/min, 6.7 MPa, 308 K
254 nm
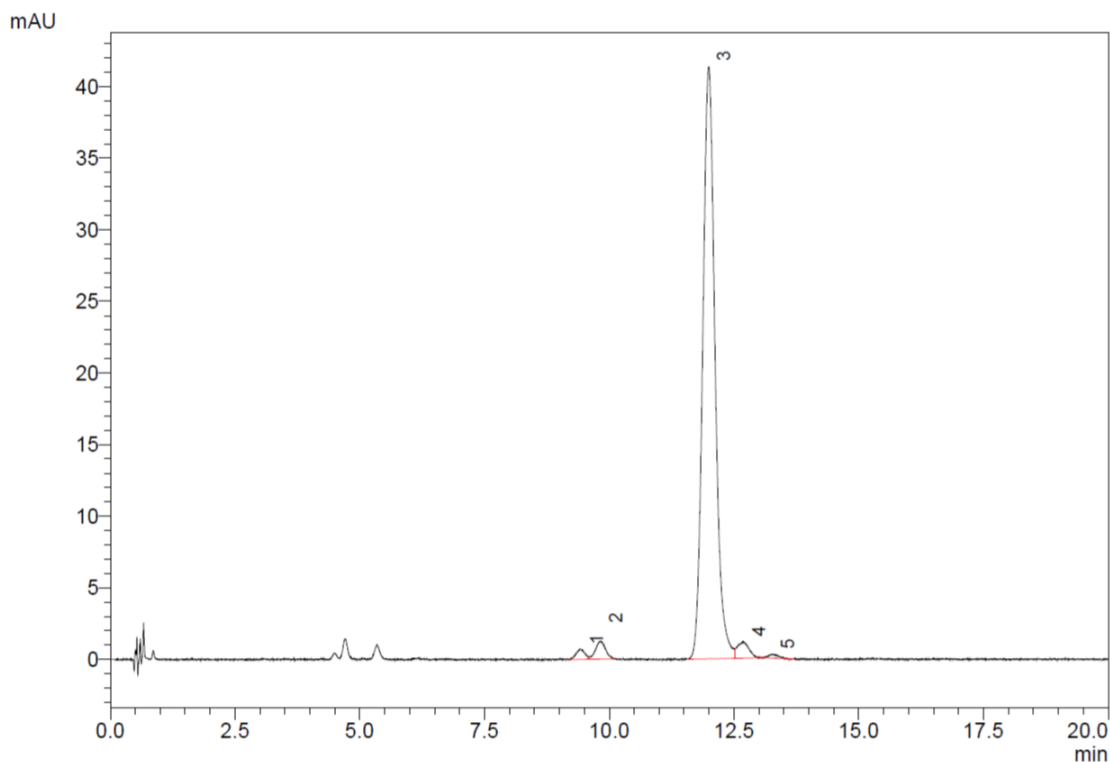
1   254nm,4nm

PDA Ch1 254nm

Peak #	Ret. Time	Area %	Name
1	9.44	1.17	Intermediate
2	9.83	2.31	Starting Material
3	11.99	93.58	Helicene
4	12.69	2.49	Isomer
5	13.27	0.45	
Total		100.00	

- Chiral separation:

```
Sample Info    : 5 µL GON-GC-589-01
                 achiral:
                 50 mm Eclipse Plus C18 1.8 µm, 3.0 mm i.D.
                 USDEA01836
                 Acetonitril/Wasser = 95:5
                 0.5 mL/min, 11.3 MPa, 308 K
                 UV, 254 nm
                 chiral:
                 150 mm Chiralpak IC-3R, 4.6 mm i.D. Säule 2
                 Acetonitril / Methanol = 95:5
                 1.0 mL/min, 6.9 MPa, 298 K
                 DAD 220 nm

Additional Info : Peak(s) manually integrated
```



```
================================================================
                    Area Percent Report
================================================================

Sorted By            :       Signal
Multiplier           :       1.0000
Dilution             :       1.0000
Do not use Multiplier & Dilution Factor with ISTDs
 Signal 1: DAD1 A, Sig=254,4 Ref=360,100

Peak RetTime Type  Width     Area        Height      Area
 #   [min]        [min]    [mAU*s]      [mAU]        %
----|-------|----|-------|----------|----------|--------|
  1   0.478 VV     0.0124    2.93500     3.29905   0.1230
  2   0.516 VV     0.0139   20.98230    21.41684   0.8792
  3   0.623 VV     0.0428    9.18219     3.41802   0.3848
  4   2.367 BV     0.0667    4.56337     1.08127   0.1912
  5   2.508 VB     0.0690   35.05524     8.02421   1.4690
  6   2.814 BB     0.0734   21.54573     4.58099   0.9029
  7   4.266 BV     0.1025   16.01632     2.36461   0.6711
  8   5.448 BV     0.1267 2244.37695   275.16666  94.0485  helicene
  9   5.729 VV     0.1071   23.31223     3.23432   0.9769
 10   5.986 VB     0.1198    8.43510 9.47959e-1   0.3535

Totals :                  2386.40443   323.53391


 Signal 2: DAD2 A, Sig=220,4 Ref=360,100

Peak RetTime Type  Width     Area        Height      Area
 #   [min]        [min]    [mAU*s]      [mAU]        %
----|-------|----|-------|----------|----------|--------|
  1   8.261 BB     0.0695 2378.53247   533.77728  95.3651   1. Enantiomer
  2   8.546 BB     0.0840  115.60075    21.41953   4.6349   2. Enantiomer   ee = 90.7 %

Totals :                  2494.13322   555.19681


================================================================
                    *** End of Report ***
```

Helicene 26ac racemic sample:

```
Sample Info      : 1 µL GON-GC-441-02 (100/400 µL ACN)
                   achiral:                                      Racemat
                   50 mm Eclipse Plus C18 1.8 µm, 3.0 mm i.D.
                   USDEA01836
                   Acetonitril/Wasser = 90:10 (ACN aus Port D)
                   0.5 mL/min, 12.6 MPa, 308 K
                   UV, 254 nm
                   chiral:
                   150 mm Chiralpak IC3, 4.6 mm i.D. Säule 2
                   Acetonitril/Methanol = 95:5
                   1.0 mL/min, 5.9 MPa, 298 K
                   DAD 254 nm

Additional Info : Peak(s) manually integrated
```
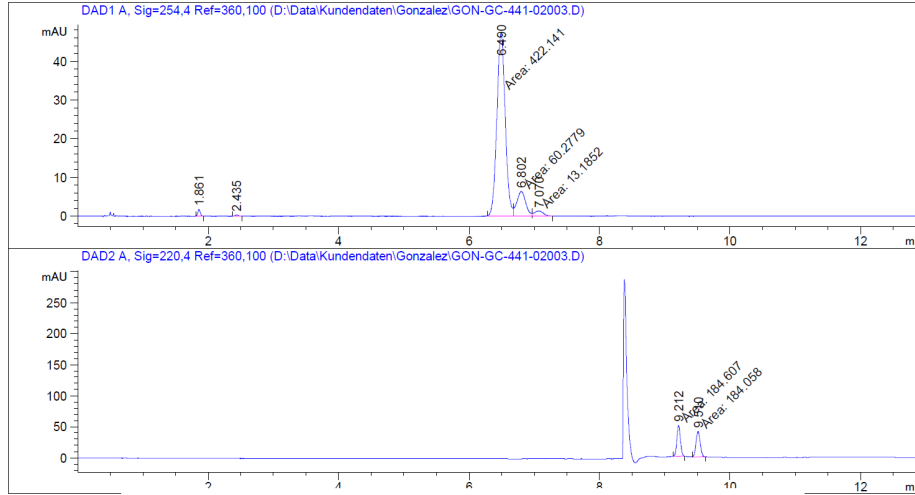


```
====================================================================
                        Area Percent Report
====================================================================

Sorted By            :      Signal
Multiplier           :      1.0000
Dilution             :      1.0000
Do not use Multiplier & Dilution Factor with ISTDs


Signal 1: DAD1 A, Sig=254,4 Ref=360,100

Peak RetTime Type  Width     Area      Height     Area
  #   [min]        [min]   [mAU*s]     [mAU]       %
----|-------|----|-------|----------|----------|-------|
  1   1.861 BB    0.0406    4.64928   1.77348    0.9272
  2   2.435 BB    0.0411    1.18134 3.52563e-1   0.2356
  3   6.490 MF    0.1493  422.14056  47.13905   84.1866
  4   6.802 MF    0.1569   60.27790   6.40201   12.0211
  5   7.070 FM    0.1614   13.18516   1.36150    2.6295

Totals :                  501.43426  57.02859


Signal 2: DAD2 A, Sig=220,4 Ref=360,100

Peak RetTime Type  Width     Area      Height     Area
  #   [min]        [min]   [mAU*s]     [mAU]       %
----|-------|----|-------|----------|----------|-------|
  1   9.212 MM    0.0615  184.60684  50.06533   50.0744
  2   9.510 MM    0.0744  184.05846  41.24463   49.9256

Totals :                  368.66530  91.30996


====================================================================
                      *** End of Report ***
```

Helicene 26ac synthesised by enantioselective gold(I)-catalysis:

- Achiral separation:

Injection Volume : 2 uL
Data File Name : GON-GC-603-02-01.lcd
Method File Name : Gonzalez.lcm

2 μL GON-GC-603-02 (100 μL of solution in 400 μL Acetonitrile, prepared from 0.57mg in 1 ml MTBE + 0.4 ml DCM)
50 mm Eclipse Plus C18 1.8 μm, 4.6 mm i. D., USUXG08325
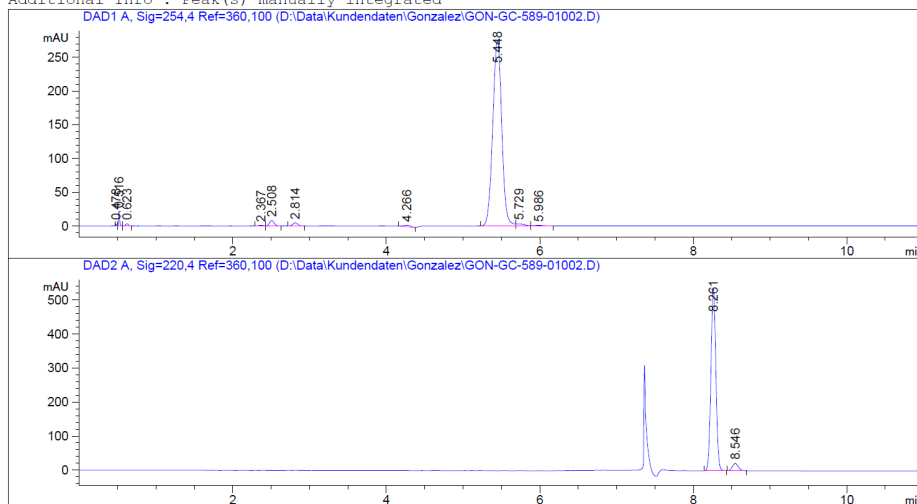Acetonitrile/Water =90:10
1 ml/min, 6.4 MPa, 308 K
254 nm
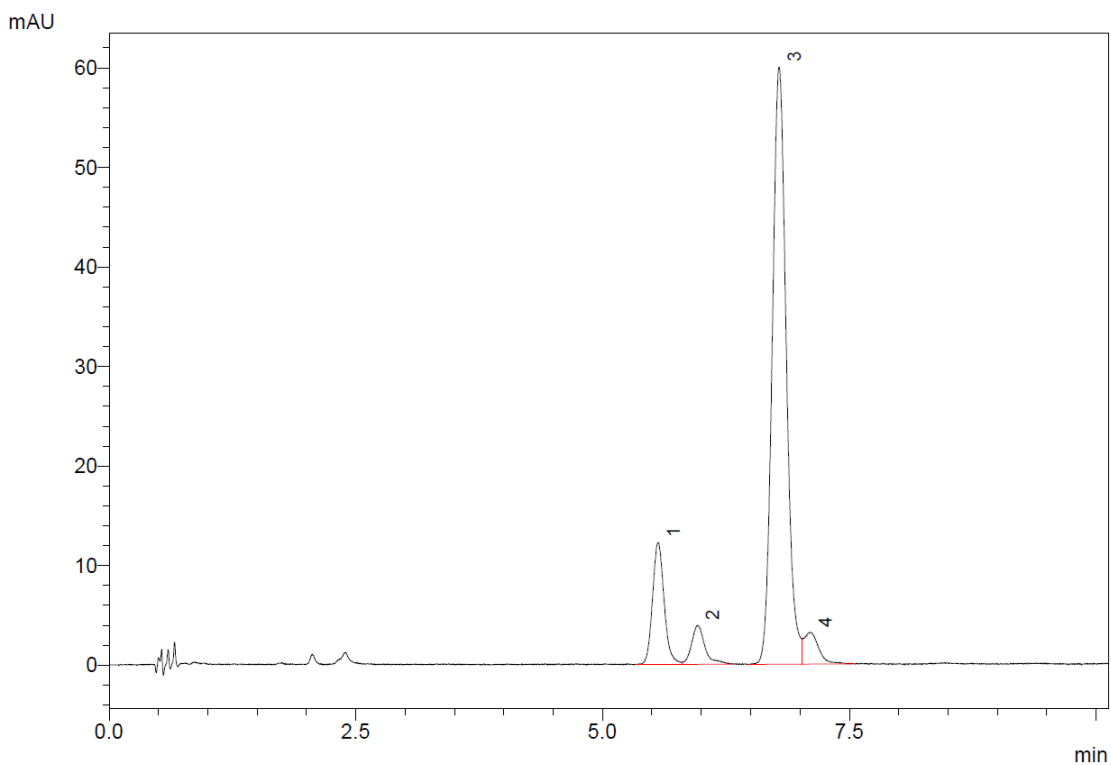
1   254nm,4nm

PDA Ch1 254nm

Peak #	Ret. Time	Area %	Name
1	5.56	13.12	Intermediate
2	5.96	4.79	Starting Material
3	6.79	77.72	Helicene
4	7.10	4.37	Isomer
Total		100.00	

- Chiral separation:

```
Sample Info      : 2.0 µL GON-GC-603-02
                   achiral:
                   50 mm Eclipse Plus C18 1.8 µm, 3.0 mm i.D.
                   USDEA01836
                   Acetonitril/Wasser = 90:10
                   0.5 mL/min, 12.1 MPa, 308 K
                   UV, 275 nm
                   chiral:
                   150 mm Chiralpak IC-3R, 4.6 mm i.D. Säule 2
                   Acetonitril / Methanol = 95:5
                   1.0 mL/min, 6.8 MPa, 298 K
                   DAD 275 nm

Additional Info : Peak(s) manually integrated
```



```
=================================================================
                    Area Percent Report
=================================================================

Sorted By            :       Signal
Multiplier           :       1.0000
Dilution             :       1.0000
Do not use Multiplier & Dilution Factor with ISTDs


Signal 1: DAD1 A, Sig=275,4 Ref=off                            achiral

Peak RetTime Type  Width     Area       Height     Area
 #   [min]        [min]   [mAU*s]      [mAU]       %
----|-------|----|-------|----------|----------|--------|
   1   1.826 BB    0.0419    3.39216    1.20392   0.2623
   2   2.082 BB    0.0481    5.52829    1.76387   0.4275
   3   5.173 BV    0.1101  150.68985   21.28709  11.6521 Intermediate
   4   5.561 VB    0.1227  126.44702   15.82058   9.7775 starting material
   5   6.344 BV    0.1335  967.23322  112.31601  74.7914 Helicene
   6   6.644 VB    0.1332   39.95022    4.47314   3.0892 Isomer

Totals :                   1293.24076  156.86461


Signal 2: DAD2 A, Sig=275,4 Ref=360,100

Peak RetTime Type  Width     Area       Height     Area              chiral
 #   [min]        [min]   [mAU*s]      [mAU]       %
----|-------|----|-------|----------|----------|--------|
   1   9.069 BV    0.0635 1033.49146  251.37321  95.8597 1. enantiomer
   2   9.377 VB    0.0798   44.63802    8.56763   4.1403 2. enantiomer  ee = 91.7 %

Totals :                   1078.12947  259.94084


=================================================================
                    *** End of Report ***
```
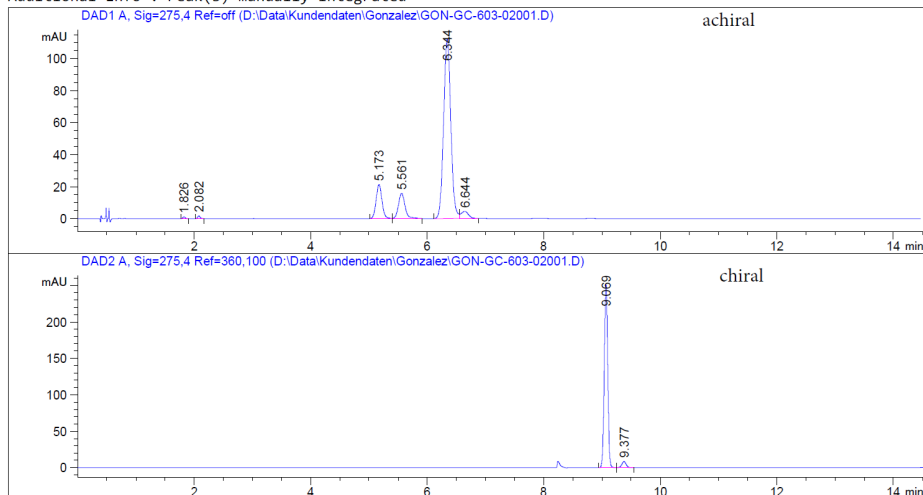
Helicene 26ba racemic sample:

- Achiral separation:

Injection Volume   : 2 uL
Data File Name   : GON-GC-586-01-05.lcd
Method File Name   : Gonzalez.lcm

2 µL GON-GC-587-01 (100 µL of solution in 400 µL Acetonitrile, prepared with 0.56 mg in 1ml MTBE and 0.4 ml DCM)
50mm Eclipse Plus C18 1.8µm, 4.6mm i. D., USUXG12018
Methanol:Water = 93:7
1 ml/min, 11.9 MPa, 308 K
254 nm
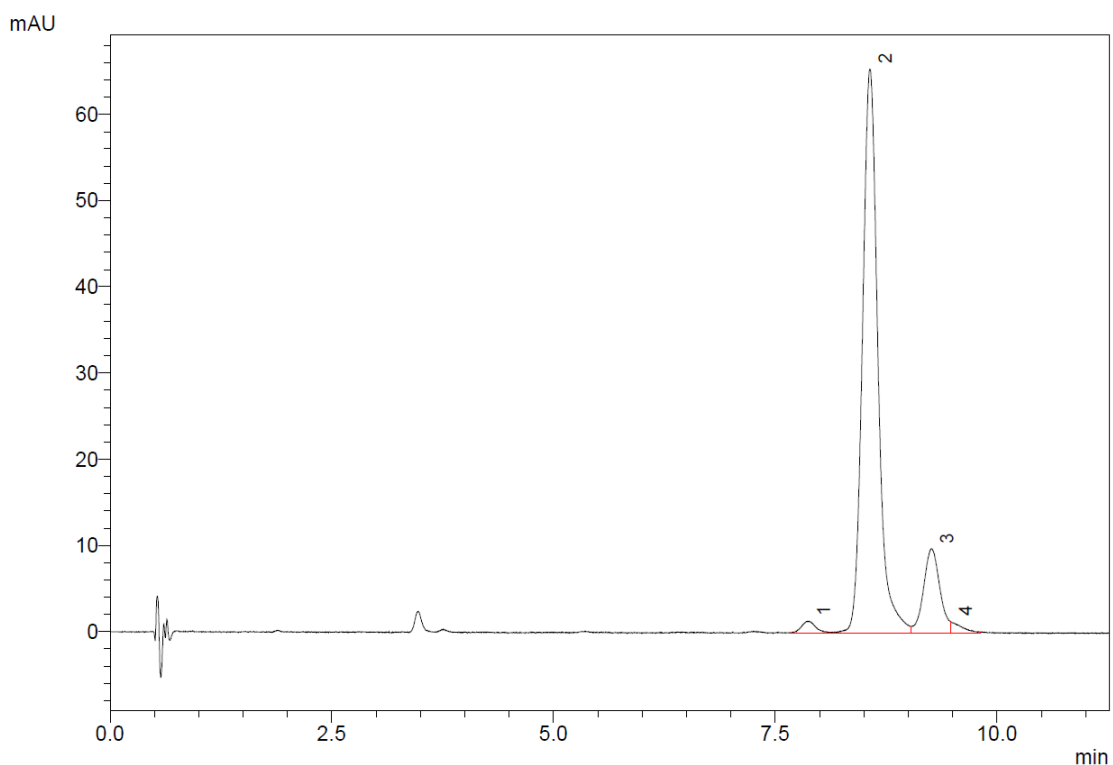
1   254nm,4nm

PDA Ch1 254nm

Peak #	Ret. Time	Area %	Name
1	7.88	1.60	
2	8.57	84.01	Helicene
3	9.26	13.19	isomer
4	9.47	1.20	
Total		100.00	

- Chiral separation:

```
Sample Info      : 2 µL GON-GC-586-01
                   achiral:
                   50 mm Eclipse Plus C18 1.8 µm, 3.0 mm i.D.
                   USDEA01836
                   Acetonitril/Wasser = 90:10
                   0.5 mL/min, 12.2 MPa, 308 K
                   UV, 254 nm
                   chiral:
                   150 mm Chiralpak IC-3R, 4.6 mm i.D. Säule 2
                   Acetonitril / Methanol = 95:5
                   1.0 mL/min, 6.8 MPa, 298 K
                   DAD 254 nm

Additional Info : Peak(s) manually integrated
```



```
===================================================================
                      Area Percent Report
===================================================================

Sorted By             :      Signal
Multiplier            :      1.0000
Dilution              :      1.0000
Do not use Multiplier & Dilution Factor with ISTDs


Signal 1: DAD1 A, Sig=254,4 Ref=off                          achiral

Peak RetTime Type  Width     Area       Height     Area
  #   [min]        [min]   [mAU*s]      [mAU]        %
----|-------|----|-------|----------|----------|--------|
   1   1.832 VB   0.0399    1.41715 4.80180e-1   0.0798
   2   3.301 BV   0.0701   24.51821    5.33544   1.3807
   3   3.482 VB   0.0911    4.50533 6.39988e-1   0.2537
   4   8.236 VV   0.1454   26.04914    2.37603   1.4669
   5   8.767 VV   0.1856 1438.27258  119.80643  80.9910  helicene
   6   9.318 VB   0.2619  281.08038   16.82176  15.8280  isomer

Totals :                1775.84280  145.45983



Signal 2: DAD2 A, Sig=254,4 Ref=360,100

Peak RetTime Type  Width     Area       Height     Area
  #   [min]        [min]   [mAU*s]      [mAU]        %         chiral
----|-------|----|-------|----------|----------|--------|
   1  11.614 VV   0.0764  488.18875   99.18675  50.0392  1. enantiomer helicene
   2  11.970 VB   0.0977  487.42462   77.20412  49.9608  2. enantiomer helicene

Totals :                 975.61337  176.39087


===================================================================
                      *** End of Report ***
```
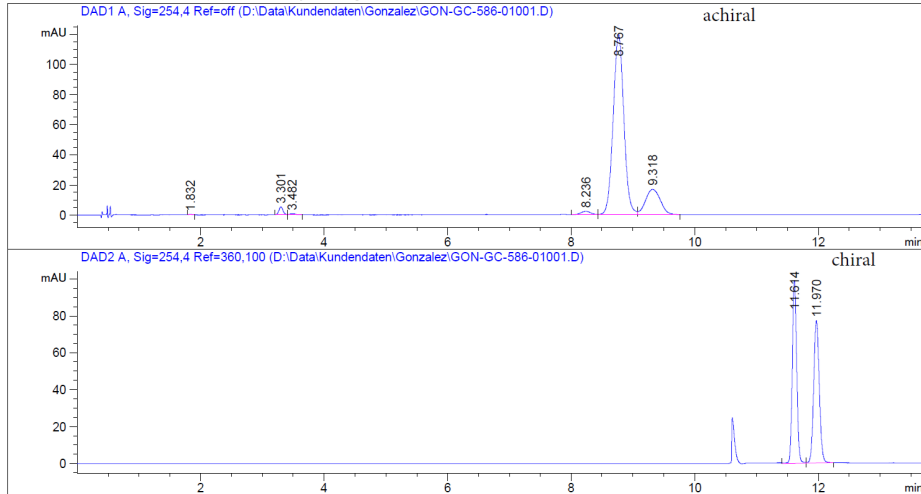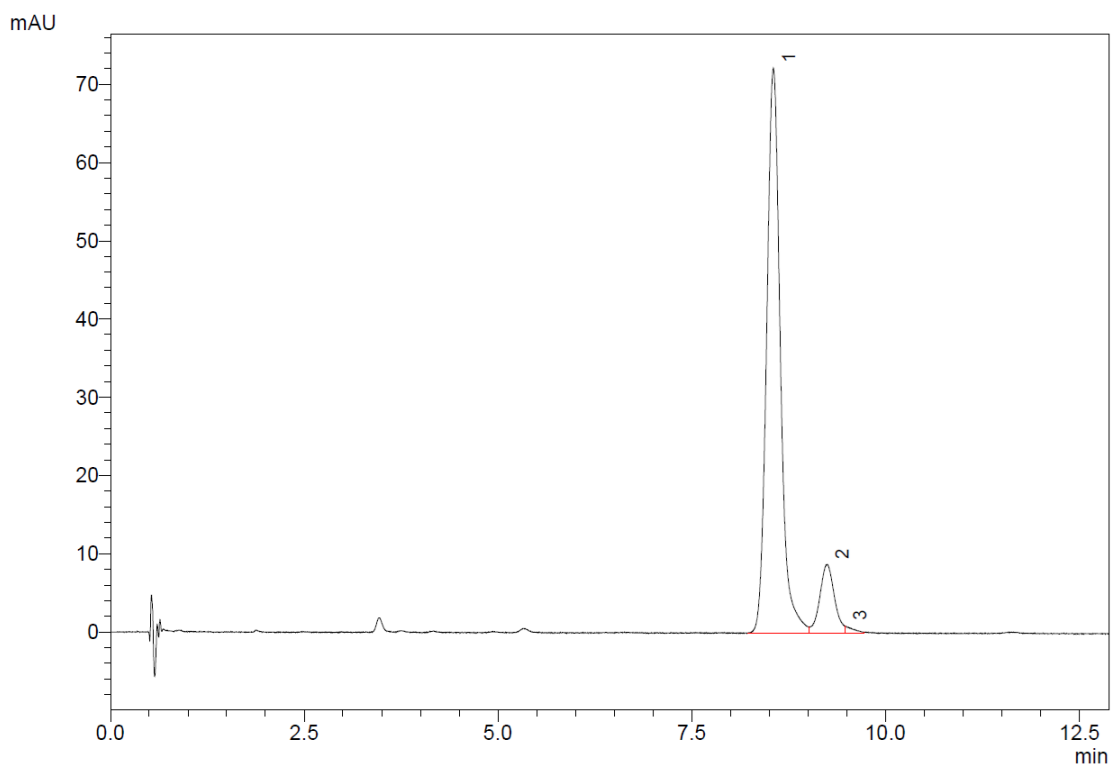
Helicene 26ba synthesised by enantioselective gold(I)-catalysis:

- Achiral separation:

Injection Volume   : 2 uL
Data File Name   : GON-GC-601-02-01.lcd
Method File Name   : Gonzalez.lcm

2 µL GON-GC-601-02 (100 µL of solution in 400 µL Acetonitrile, prepared from 0.50 mg in 1 ml MTBE + 0.4 ml DCM)
50 mm Eclipse Plus C18 1.8 µm, 4.6 mm i. D., USUXG08325
Methanol/Water = 93:7
1 ml/min, 11.3 MPa, 308 K
254 nm

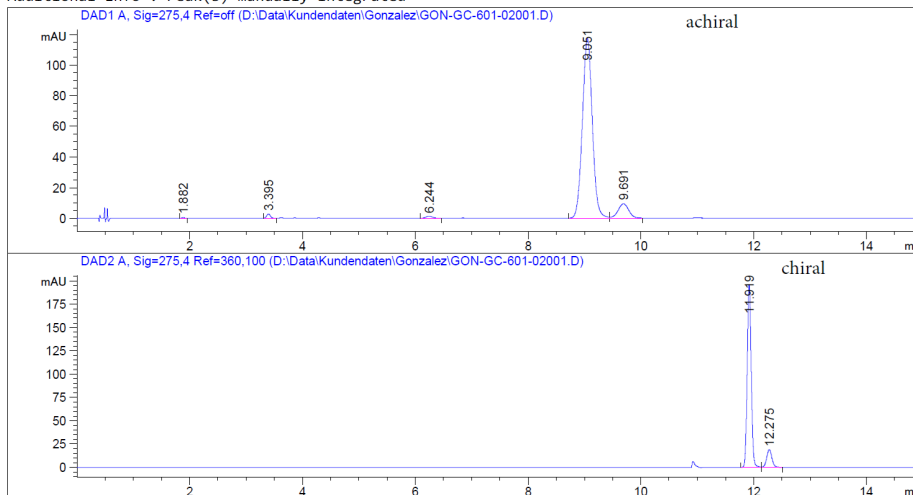

1   254nm,4nm

PDA Ch1 254nm

Peak #	Ret. Time	Area %	Name
1	8.55	87.99	Helicene
2	9.24	11.36	Isomer
3	9.47	0.65	
Total		100.00	

- Chiral separation:

```
Sample Info    : 2.0 µL GON-GC-601-02
                 achiral:
                 50 mm Eclipse Plus C18 1.8 µm, 3.0 mm i.D.
                 USDEA01836
                 Acetonitril/Wasser = 90:10
                 0.5 mL/min, 12.1 MPa, 308 K
                 UV, 275 nm
                 chiral:
                 150 mm Chiralpak IC-3R, 4.6 mm i.D. Säule 2
                 Acetonitril / Methanol = 95:5
                 1.0 mL/min, 6.8 MPa, 298 K
                 DAD 275 nm

Additional Info : Peak(s) manually integrated
```



```
=================================================================
                    Area Percent Report
=================================================================

Sorted By           :      Signal
Multiplier          :      1.0000
Dilution            :      1.0000
Do not use Multiplier & Dilution Factor with ISTDs


Signal 1: DAD1 A, Sig=275,4 Ref=off
```
achiral
```
Peak RetTime Type  Width     Area       Height     Area
  #   [min]        [min]    [mAU*s]      [mAU]       %
----|-------|----|-------|----------|----------|--------|
  1   1.882 BB    0.0449    1.80667 6.20980e-1   0.1135
  2   3.395 BB    0.0742   14.01032    2.93290    0.8802
  3   6.244 BB    0.1216   12.07131    1.42130    0.7584
  4   9.051 BV    0.1899 1436.79272  117.27880   90.2681  helicene
  5   9.691 VB    0.1977  127.01376    9.51972    7.9798   isomer

Totals :                 1591.69478  131.77371
```

```
Signal 2: DAD2 A, Sig=275,4 Ref=360,100
```
chiral
```
Peak RetTime Type  Width     Area       Height     Area
  #   [min]        [min]    [mAU*s]      [mAU]       %
----|-------|----|-------|----------|----------|--------|
  1  11.919 BV    0.0773  972.27704  196.27148   88.8957  1. enantiomer
  2  12.275 VB    0.0985  121.45080   19.03104   11.1043  2. enantiomer

Totals :                 1093.72784  215.30252
```
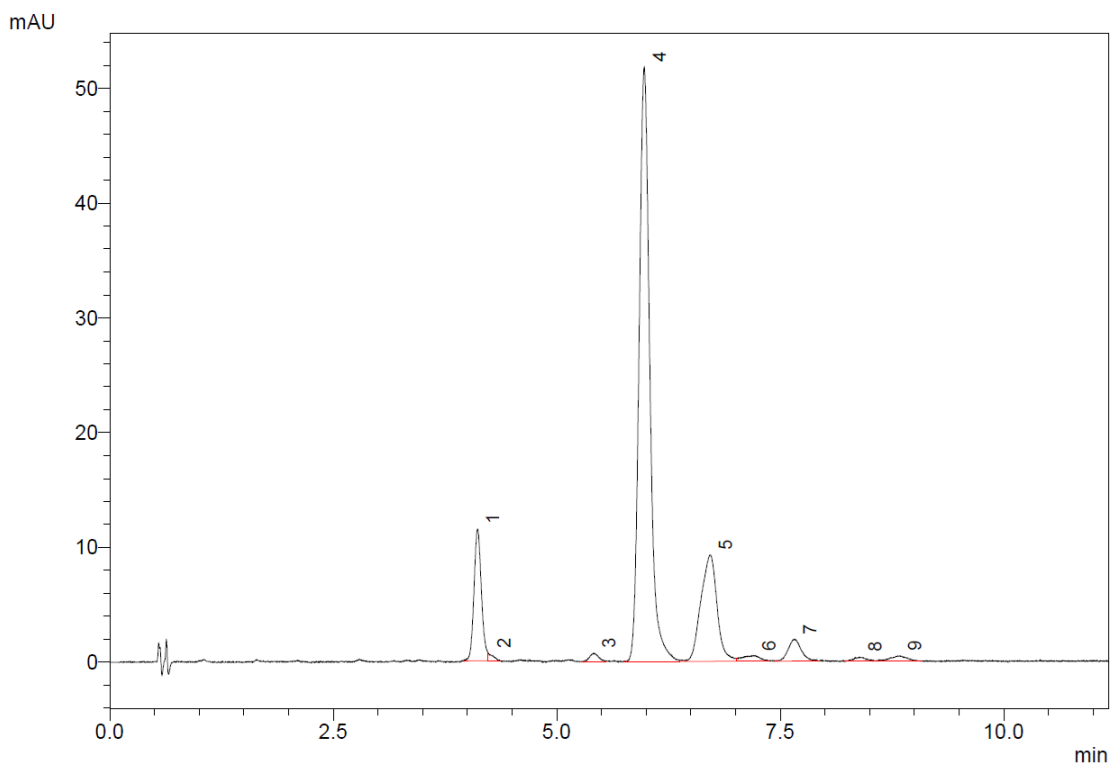ee = 77.8 %

```
=================================================================
                    *** End of Report ***
```

Helicene 26c racemic sample:

- Achiral separation:

Injection Volume   : 2 uL
Data File Name   : GON-GC-584-01-04.lcd
Method File Name   : Gonzalez.lcm

2 μL GON-GC-584-01 (100 μL of solution in 400 μL Acetonitrile, prepared with 0.54 mg in 1ml MTBE and 0.4 ml DCM)
50mm Eclipse Plus C18 1.8μm, 4.6mm i. D., USUXG12018
Acetonitrile:Water = 100:00
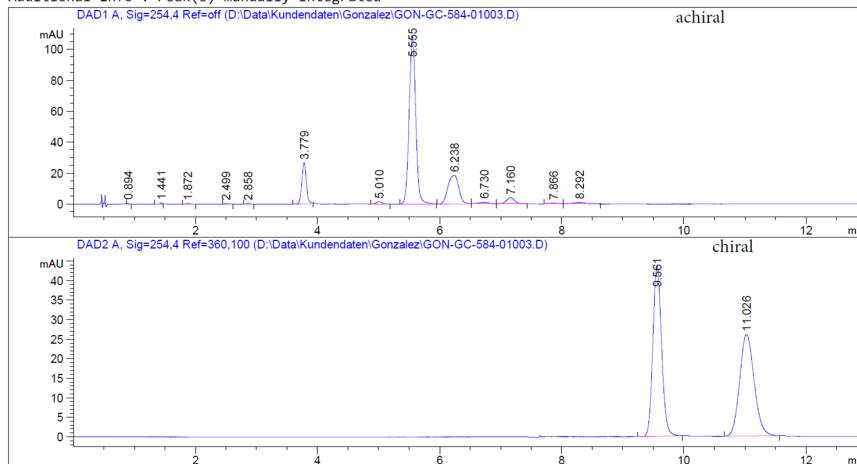1 ml/min, 5.8 MPa, 308 K
254 nm

1   254nm,4nm

PDA Ch1 254nm

Peak #	Ret. Time	Area %	Name
1	4.12	10.13	Starting Material
2	4.24	0.38	
3	5.41	0.76	
4	5.98	65.52	Helicene
5	6.72	17.76	isomers
6	7.21	1.01	
7	7.66	2.93	
8	8.39	0.55	
9	8.84	0.96	
Total		100.00	

- Chiral separation:

```
Sample Info     : 2 µL GON-GC-584-01
                  achiral:
                  50 mm Eclipse Plus C18 1.8 µm, 3.0 mm i.D.
                  USDEA01836
                  Acetonitril/Wasser = 100:0
                  0.5 mL/min, 10.5 MPa, 308 K
                  UV, 254 nm
                  chiral:
                  150 mm Chiralpak IC-3R, 4.6 mm i.D. Säule 2
                  Acetonitril / Methanol = 95:5
                  1.0 mL/min, 6.8 MPa, 298 K
                  DAD 254 nm

Additional Info : Peak(s) manually integrated
```



```
================================================================
                      Area Percent Report
================================================================

Sorted By            :     Signal
Multiplier           :     1.0000
Dilution             :     1.0000
Do not use Multiplier & Dilution Factor with ISTDs


Signal 1: DAD1 A, Sig=254,4 Ref=off
```
                                                              achiral
```
Peak RetTime Type  Width     Area      Height    Area
  #   [min]        [min]   [mAU*s]     [mAU]      %
----|-------|----|-------|----------|----------|--------|
   1   0.894 VB   0.0284   1.38835 7.38514e-1   0.1094
   2   1.441 BV   0.0385   2.06690 8.04583e-1   0.1629
   3   1.872 BB   0.0589   1.93823 3.93833e-1   0.1528
   4   2.499 BB   0.0560   1.88996 4.12423e-1   0.1490
   5   2.858 BB   0.0483   2.04156 5.25690e-1   0.1609
   6   3.779 BB   0.0803 137.77840   26.64352  10.8598  starting material
   7   5.010 VB   0.0986   9.97907    1.51018   0.7866
   8   5.555 BB   0.1158 810.30573  108.24127  63.8691  helicene
   9   6.238 BV   0.1992 227.94876   18.57402  17.9671  isomers
  10   6.730 VV   0.1411  13.40383    1.15777   1.0565
  11   7.160 VB   0.1426  38.50250    4.09675   3.0348
  12   7.866 BV   0.1165   5.94469 6.11172e-1   0.4686
  13   8.292 VB   0.1680  15.50954    1.10979   1.2225

Totals :                1268.69750  164.81951




Signal 2: DAD2 A, Sig=254,4 Ref=360,100
```
                                                              chiral
```
Peak RetTime Type  Width     Area      Height    Area
  #   [min]        [min]   [mAU*s]     [mAU]      %
----|-------|----|-------|----------|----------|--------|
   1   9.561 BB   0.1525 432.71271   43.50992  50.1687  1. enantiomer helicene
   2  11.026 BB   0.2253 429.80255   26.01134  49.8313  2. enantiomer helicene

Totals :                 862.51526   69.52126


================================================================
                    *** End of Report ***
```

375

Helicene 26c synthesised by enantioselective gold(I)-catalysis:

- Achiral separation:

Injection Volume : 2 uL
Data File Name : GON-GC-599-02-01.lcd
Method File Name : Gonzalez.lcm

2 µL GON-GC-599-02 (100 µL of solution in 400 µL Acetonitrile, prepared from 0.57mg in 1 ml MTBE + 0.4 ml DCM)
50 mm Eclipse Plus C18 1.8 µm, 4.6 mm i. D., USUXG08325
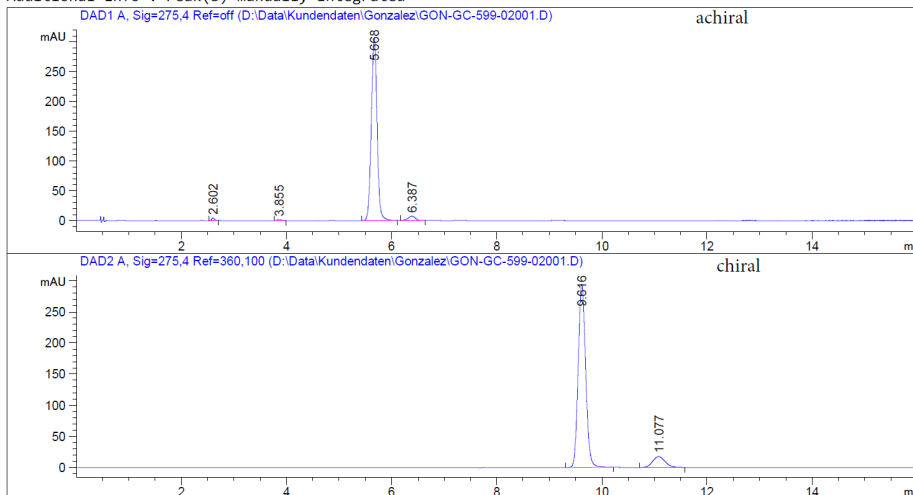Acetonitrile/Water =100:0
1 ml/min, 5.6 MPa, 308 K
275 nm
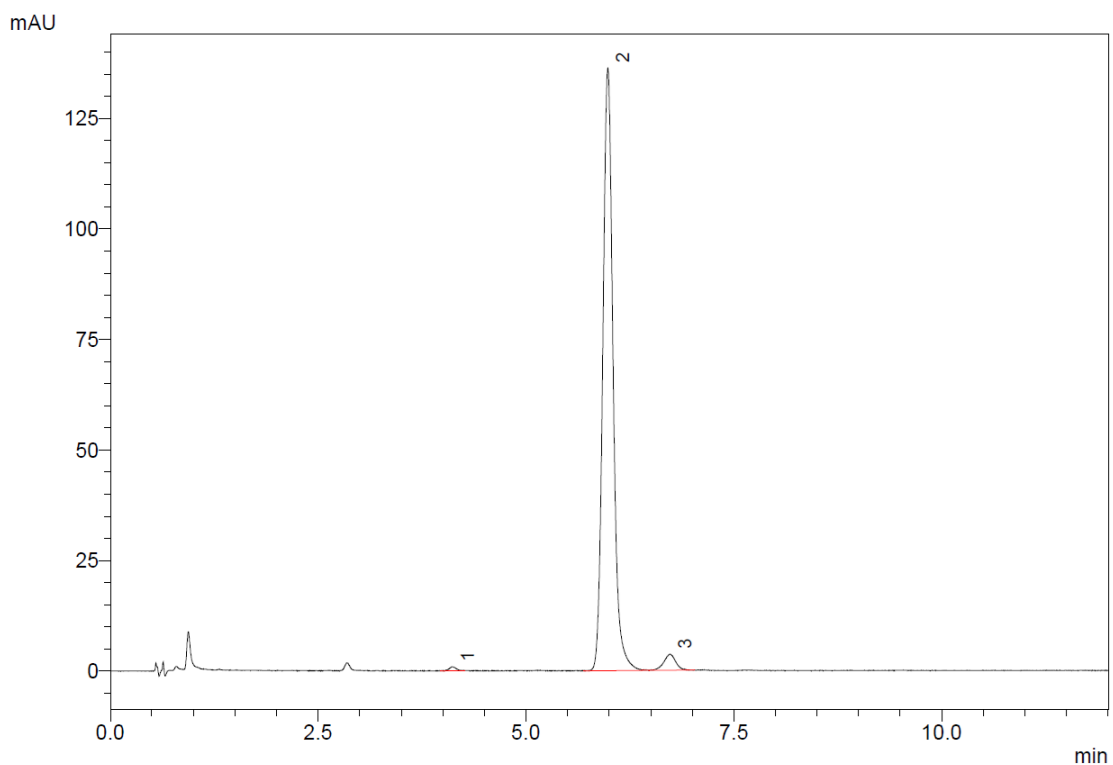
1   275nm,4nm

PDA Ch1 275nm

Peak #	Ret. Time	Area %	Name
1	4.11	0.45	Starting Material
2	5.98	96.55	Helicene
3	6.73	3.00	Isomer
Total		100.00	

- Chiral separation:

```
Sample Info    : 2.0 µL GON-GC-599-02
                 achiral:
                 50 mm Eclipse Plus C18 1.8 µm, 3.0 mm i.D.
                 USDEA01836
                 Acetonitril/Wasser = 100:0
                 0.5 mL/min, 10.5 MPa, 308 K
                 UV, 275 nm
                 chiral:
                 150 mm Chiralpak IC-3R, 4.6 mm i.D. Säule 2
                 Acetonitril / Methanol = 95:5
                 1.0 mL/min, 6.8 MPa, 298 K
                 DAD 275 nm

Additional Info : Peak(s) manually integrated
```



```
================================================================
                    Area Percent Report
================================================================

Sorted By            :      Signal
Multiplier           :      1.0000
Dilution             :      1.0000
Do not use Multiplier & Dilution Factor with ISTDs
```

achiral

```
Signal 1: DAD1 A, Sig=275,4 Ref=off

Peak RetTime Type  Width     Area       Height     Area
  #   [min]        [min]   [mAU*s]      [mAU]       %
----|-------|----|-------|----------|----------|--------|
   1   2.602 BB   0.0554   15.54418    4.38389   0.6427
   2   3.855 BB   0.0792   10.09586    1.97338   0.4174 starting material
   3   5.668 BB   0.1156 2317.76050  305.15555  95.8255 helicene
   4   6.387 BB   0.1431   75.33035    7.77030   3.1145 isomer

Totals :                 2418.73088  319.28312
```

```
Signal 2: DAD2 A, Sig=275,4 Ref=360,100

Peak RetTime Type  Width     Area       Height     Area      chiral
  #   [min]        [min]   [mAU*s]      [mAU]       %
----|-------|----|-------|----------|----------|--------|
   1   9.616 BB   0.1527 2902.84399  293.89188  90.9543  1. enantiomer   ee = 81.9 %
   2  11.077 BB   0.1976  288.69565   17.48572   9.0457  2. enantiomer

Totals :                 3191.53964  311.37760
```

```
================================================================
                    *** End of Report ***
```

List of Abbreviations

α	specific rotation	CPL	Circulary Polarised Light
Å	Angstrom	Cy	cyclohexyl
a.u.	atomic units	cym	*para*-cymene
AAYC	acyclic (amino)-(ylide)carbene	δ	chemical shift
Ac	acetyl	ΔE_{S-T}	singlet-triplet gap
Ad	adamantyl	$\Delta H^{\ddagger}$	enthalpy of activation
ADC	acyclic (diamino)carbene	$\Delta G^{\ddagger}$	Gibbs energy of activation
APPI	Atmospheric Pressure Photoionization	$\Delta S^{\ddagger}$	entropy of activation
		d	doublet (NMR)
aq.	aqueous media	D-	dextrorotatory
Ar	aromatic substituent	dba	dibenzylideneacetone
atm	atmosphere	DCM	dichloromethane
AYC	(amino)-(ylide)carbene	DCE	dichloroethane
BINAP	2,2'-bis(diphenylphosphino)-1,1'-binaphthalene	dd	doublet of doublets (NMR)
		ddd	doublet of doublets of doublets (NMR)
BINOL	1,1'-bi-2-naphthol		
BIPHEP	(biphenyl-2,2'-diyl)bis-(diphenylphosphine)	DDQ	2,3-Dichloro-5,6-dicyano-*p*-benzoquinone
Bn	benzyl	decomp.	decomposition
br	broad NMR signal	DFT	Density Functional Theory
BSA	*N,O*-bis(trimethylsilyl) acetonide	DIPA	diisopropylamine
		Dipp	2,6-Diisopropylphenyl
Bu	butyl	DMF	*N,N*-Dimethylformamide
°C	degree Celsius	DNA	deoxyribonucleic acid
c	concentration	DNMR	Dynamic Nuclear Magnetic Resonance
CAAC	cyclic (alkyl)-(amino)carbene		
cat.	catalytic amount	dq	doublet of quartets (NMR)
Cbz	carboxybenzyl	dt	doublet of triplets (NMR)
CD	Circular Dichroism	e^-	electron
cm	centimetres	E_2	bimolecular elimination reaction
cod	cyclooctadiene		
comp.mix.	complex mixture	*e.g.*	*exempli gratia*
Cond.	conditions	*ee*	enantiomeric excess
COSY	correlation spectroscopy	EI	Electron Ionization
Cp	cyclopentadienyl	equiv.	equivalents
Cp*	1,2,3,4,5-pentamethylcyclopentadienyl	ESI	Electrospray Ionization
		Et	ethyl

et al.	*et alii*		M	Molar
eV	electronvolt		Me	methyl
fum	fumarate		Me-DuPhos	(-)-1,2-Bis(2,5-dimethyl-phospholano)benzene
g	gram			
GC	gass chromatography		Mes	mesityl
h	hour		min	minute
h	Planck constant		ml	millilitre
hν	light irradiation		Mol.sieves	molecular sieves
HMDS	hexamethyldisilazane		MOM	methoxymethyl
HMBC	Heteronuclear Multiple-Bond Correlation spectroscopy		MOP	2-(Diphenylphosphino)-2'-methoxy-1,1'-binaphthyl
HOMO	Highest Occupied Molecular Orbital		MS	Mass Spectroscopy
			MTBE	methyl-*tert*-buthylether
HPLC	High Pressure Liquid Chromatography		MW	microwave
			$\tilde{\nu}$	wave numbers
HRMS	High Resolution Mass Spectroscopy		$\tilde{\nu}_{CO}(\text{av})$	average of symmetric and asymmetric CO stretching frequencies
HSQC	Heteronuclear Single-Quantum Correlation spectroscopy		*n*	linear
			n.d.	not determined
Hz	Herz		n.r.	no reaction
η	hapticity			
IMes	1,3-bis(2,4,6-trimethyl-phenyl)imidazol-2-ylidene		NAPHEP	(2-(2-methoxynaphthalen-1-yl)phenyl)diphenylphosphine
i	*iso-*		NBS	*N*-bromosuccinimide
IPr	1,3-bis(2,6-diisopropyl-phenyl)imidazol-2-ylidene		NHC	N-heterocyclic carbene
IR	infrarred spectroscopy		NMR	Nuclear Magnetic Resonance
IUPAC	International Union of Pure and Applied Chemistry		NOESY	Nuclear Overhauser Effect Spectroscopy
J	coupling constant		Nu	generic nucleophile
K	Kelvin		*o*	*ortho-*
k	exchange rate		oct	octet (NMR)
k_B	Boltzmann constant		OLED	Organic Light-Emitting Diode
kcal	kilocalorie			
kJ	kilojoule		*p*	*para-*
λ	wavelength		Pa	Pascal
L	generic ligand		PCC	pyridinium chlorochromate
L-	levorotatory		PG	protecting group
L*	generic chiral ligand		Ph	phenyl
LUMO	Lowest Unoccupied Molecular Orbital		PMB	4-methoxybenzyl ether
			Pr	propyl
m	multiplet (NMR)		ppm	parts per million
m	*meta−*		PVA-SIL	polyvinyl alcohol-silica
m/z	mass-to-charge ratio		pyr	pyridine
			q	quartet (NMR)

qd	quartet of doublets (NMR)	t_R	retention time
QUINAP	1-(2-Diphenylphosphino-1-naphthyl)isoquinoline	T	temperature
		T_c	coalescence temperature
R	gas constant	TADDOL	$\alpha,\alpha,\alpha',\alpha'$-tetraaryl-2,2-disubstituted 1,3-dioxolane-4,5-dimethanol
R	generic substituent		
R^+	generic cationic substituent		
r_{vdW}	van der Waals radii	TAPA	2-[2,4,5,7-tetranitro-9-fluorenylidene-aminooxy]propionic acid
rac	racemic		
rt	room temperature		
s	second	TBS	*tert*-butyldimethylsilyl
s	singlet (NMR)	TEP	Tolman Electronic Parameter
SCF	Self-Consistent Field		
SEGPHOS	5,5'-Bis(diphenylphosphino)-4,4'-bi-1,3-benzodioxole	TES	triethylsilyl
		Tf	triflate
		THF	tetrahydrofurane
sept	septet (NMR)	TIPS	tri-*iso*-propylsilyl
sext	sextuplet (NMR)	TLC	Thin Layer Chromatography
SPhos	2-Dicyclohexylphosphino-2',6'-dimethoxybiphenyl	TMS	trimethylsilyl
		Tol	tolyl
SPINOL	2,2',3,3'-tetrahydro-1,1'-spirobi[indene]-7,7'-diol	Ts	tosyl
		tt	triplet of triplets (NMR)
STM	Scanning Tunneling Microscope	v/v	volume/volume
		V_{bur}	buried volume
t	time	vs	*versus*
t	triplet (NMR)	X	generic halogen
t	*tert*-	xyl	xylyl
$t_{1/2}$	half-life time	Y	general heteroatom

List of Schemes

List of Figures

List of Tables

Bibliography

[1] J. H. Teles, S. Brode, M. Chabanas, *Angew. Chem. Int. Ed.* **1998**, *37*(10), 1415–1418; *Angew. Chem.* **1998**, *110*, 1475-1478.

[2] E. Mizushima, K. Sato, T. Hayashi, M. Tanaka, *Angew. Chem. Int. Ed.* **2002**, *41*(23), 4563–4565; *Angew. Chem.* **2002**, *114*, 4745–4747.

[3] a) A. Fürstner, P. Davies, *Angew. Chem. Int. Ed.* **2007**, *46*(19), 3410–3449; *Angew. Chem.* **2007**, *119*, 3478–3519; b) D. Toste, V. Michelet (Eds.), *Gold Catalysis: An Homogeneous Approach*, Imperial College Press, **2014**; c) M. S. LeGrande (Ed.), *Homogeneous Gold Catalysis*, Springer, **2014**; d) R. Dorel, A. M. Echavarren, *Chem. Rev.* **2015**, *115*(17), 9028–9072.

[4] a) P. Schwerdtfeger, M. Lein, „Theoretical Chemistry of Gold – From Atoms to Molecules, Clusters, Surfaces and the Solid State“ in *Gold Chemistry: Applications and Future Directions in the Life Sciences* (Ed. F. Mohr), Wiley-VCH Verlag, **2009**, p. 183–247; b) P. Pyykkö, *Angew. Chem. Int. Ed.* **2004**, *43*(34), 4412–4456; *Angew. Chem.* **2004**, *116*, 4512–4557; c) D. J. Gorin, F. D. Toste, *Nature* **2007**, *446*(22), 395–403; d) A. Leyva-Pérez, A. Corma, *Angew. Chem. Int. Ed.* **2012**, *51*(3), 614–635; *Angew. Chem.* **2012**, *124*, 636–658.

[5] P. Pyykkö, J. P. Desclaux, *Acc. Chem. Res.* **1979**, *12*(8), 276–281.

[6] J. Desclaux, P. Pyykk *Chem. Phys. Lett.* **1976**, *39*(2), 300 – 303.

[7] J. J. Kennedy-Smith, S. T. Staben, F. D. Toste, *J. Am. Chem. Soc.* **2004**, *126*(14), 4526–4527.

[8] a) M. C. Gimeno, „The Chemistry of Gold“ in *Modern Supramolecular Gold Chemistry: Gold-Metal Interactions and Applications* (Ed. A. Laguna), Wiley-VCH Verlag, **2009**, p. 1–63; b) P. Schwerdtfeger, P. D. W. Boyd, A. K. Burrell, W. T. Robinson, M. J. Taylor, *Inorg. Chem.* **1990**, *29*(18), 3593–3607; c) P. Schwerdtfeger, H. L. Hermann, H. Schmidbaur, *Inorg. Chem.* **2003**, *42*(4), 1334–1342.

[9] F. A. Cotton, G. Wilkinson, *Advanced Inorganic Chemistry*, 3. Ed., Wiley-VCH Verlag, **1972**.

[10] D. Benitez, N. D. Shapiro, E. Tkatchouk, Y. Wang, W. A. Goddard-III, F. D. Toste, *Nat. Chem.* **2009**, *1*(6), 482–486.

[11] C. Obradors, A. M. Echavarren, *Chem. Commun.* **2014**, *50*, 16–28.

[12] a) H. Schmidbaur, A. Schier, *Organometallics* **2010**, *29*(1), 2–23; b) H. G. Raubenheimer, H. Schmidbaur, *S. Afr. J. Sci.* **2011**, *107*(3/4), 1–13; c) D.-A. Roşca, J. A. Wright, M. Bochmann, *Dalton Trans.* **2015**, *44*(48), 20785–20807.

[13] a) M. Dewar, *Bull. Soc. Chim. Fr.* **1951**, *18*, C71–C79; b) J. Chatt, L. A. Duncanson, *J. Chem. Soc.* **1953**, 2939–2947; c) J. Chatt, L. A. Duncanson, L. M. Venanzi, *J. Chem. Soc.* **1955**, 4456–4460.

[14] a) R. H. Hertwig, W. Koch, D. Schröder, H. Schwarz, J. Hrušák, P. Schwerdtfeger, *J. Phys. Chem.* **1996**, *100*(30), 12253–12260; b) M. S. Nechaev, V. M. Rayón, G. Frenking, *J. Phys. Chem. A* **2004**, *108*(15), 3134–3142.

[15] S. Flügge, A. Anoop, R. Goddard, W. Thiel, A. Fürstner, *Chem. Eur. J.* **2009**, *15*(34), 8558–8565.

[16] a) N. Salvi, L. Belpassi, F. Tarantelli, *Chem. Eur. J.* **2010**, *16*(24), 7231–7240; b) G. Bistoni, L. Belpassi, F. Tarantelli, *Angew. Chem. Int. Ed.* **2013**, *52*(44), 11599–11602; *Angew. Chem.* **2013**, *125*, 11813–11816.

[17] W. Wang, G. B. Hammond, , B. Xu, *J. Am. Chem. Soc.* **2012**, *134*(12), 5697–5705.

[18] C. A. Gaggioli, G. Ciancaleoni, D. Zuccaccia, G. Bistoni, L. Belpassi, F. Tarantelli, P. Belanzoni, *Organometallics* **2016**, *35*(13), 2275–2285.

[19] a) D. J. Gorin, B. D. Sherry, F. D. Toste, *Chem. Rev.* **2008**, *108*(8), 3351–3378; b) Y. Wang, M. E. Muratore, A. M. Echavarren, *Chem. Eur. J.* **2015**, *21*(20), 7332–7339.

[20] a) P. Mauleón, R. M. Zeldin, A. Z. González, F. D. Toste, *J. Am. Chem. Soc.* **2009**, *131*(18), 6348–6349; b) D. Benítez, E. Tkatchouk, A. Z. González, W. A. Goddard-III, F. D. Toste, *Org. Lett.* **2009**, *11*(21), 4798–4801; c) I. Alonso, B. Trillo, F. López, S. Montserrat, G. Ujaque, L. Castedo, A. Lledós, J. L. Mascareñas, *J. Am. Chem. Soc.* **2009**, *131*(36), 13020–13030; d) M. Alcarazo, T. Stork, A. Anoop, W. Thiel, A. Fürstner, *Angew. Chem. Int. Ed.* **2010**, *49*(14), 2542–2546; *Angew. Chem.* **2010**, *122*, 2596-2600.

[21] a) A. Fürstner, *Chem. Soc. Rev.* **2009**, *38*, 3208–3221; b) M. Rudolph, A. S. K. Hashmi, *Chem. Soc. Rev.* **2012**, *41*, 2448–2462; c) Y. Zhang, T. Luo, Z. Yang, *Nat. Prod. Rep.* **2014**, *31*, 489–503.

[22] B. M. Trost, D. Guangbin, *Nature* **2008**, *456*, 485–488.

[23] M. P. Muñoz, J. Adrio, J. C. Carretero, A. M. Echavarren, *Organometallics* **2005**, *24*(6), 1293–1300.

[24] a) R. Widenhoefer, *Chem. Eur. J.* **2008**, *14*(18), 5382–5391; b) S. Sengupta, X. Shi, *ChemCatChem* **2010**, *2*(6), 609–619; c) A. Pradal, P. Y. Toullec, V. Michelet, *Synthesis* **2011**; d) F. López, J. L. Mascareñas, *Beilstein J. Org. Chem.* **2013**, *9*, 2250–2264; e) W. Zi, F. Dean Toste, *Chem. Soc. Rev.* **2016**, *45*, 4567–4589.

[25] a) H. Teller, S. Flügge, R. Goddard, A. Fürstner, *Angew. Chem. Int. Ed.* **2010**, *49*, 1949–1953; *Angew. Chem.* **2010**, *122*, 1993-1997; b) H. Teller, A. Fürstner, *Chem. Eur. J.* **2011**, *17*, 7764–7767; c) H. Teller, M. Corbet, L. Mantilli, G. Gopakumar, R. Goddard, W. Thiel, A. Fürstner, *J. Am. Chem. Soc.* **2012**, *134*(37), 15331–15342.

[26] a) J. Petuškova, M. Patil, S. Holle, C. W. Lehmann, W. Thiel, M. Alcarazo, *J. Am. Chem. Soc.* **2011**, *133*(51), 20758–20760; b) J. Petuškova, H. Bruns, M. Alcarazo, *Angew. Chem. Int. Ed.* **2011**, *50*(16), 3799–3802; *Angew. Chem.* **2011**, *123*, 3883-3886; c) H. Tinnermann, C. Wille, M. Alcarazo, *Angew. Chem. Int. Ed.* **2014**, *53*(33), 8732–8736; *Angew. Chem.* **2014**, *126*, 8877-8881; d) M. Alcarazo, *Chem. Eur. J.* **2014**, *20*(26), 7868–7877; e) E. Haldon, A. Kozma, H. Tinnermann, L. Gu, R. Goddard, M. Alcarazo, *Dalton Trans.* **2016**, *45*, 1872–1876.

[27] a) J. Carreras, M. Patil, W. Thiel, M. Alcarazo, *J. Am. Chem. Soc* **2012**, *134*(40), 16753–16758; b) Á. Kozma, T. Deden, J. Carreras, C. Wille, J. Petuškova, J. Rust, M. Alcarazo, *Chem. Eur. J.* **2014**, *20*(8), 2208–2214.

[28] J. Carreras, G. Gopakumar, L. Gu, A. Gimeno, P. Linowski, J. Petuškova, W. Thiel, M. Alcarazo, *J. Am. Chem. Soc* **2013**, *135*(50), 18815–18823.

[29] a) R. H. Martin, *Angew. Chem. Int. Ed.* **1974**, *13*(10), 649–660; b) T. J. Katz, *Angew. Chem. Int. Ed.* **2000**, *39*(11), 1921–1923; *Angew. Chem.* **2000**, *112*, 1997-1999; c) A. Urbano, *Angew. Chem. Int. Ed.* **2003**, *42*(34), 3986–3989; *Angew. Chem.* **2003**, *115*, 4116–4119; d) Y. Shen, C.-F. Chen, *Chem. Rev.* **2012**, *112*(3), 1463–1535; e) M. Gingras, *Chem. Soc. Rev.* **2013**, *42*(3), 968–1006.

[30] M. Gingras, *Chem. Soc. Rev.* **2013**, *42*(3), 1051–1095.

[31] A. Geuther, *Liebigs Ann. Chem.* **1862**, *123*(1), 121–122.

[32] a) H. Staudinger, O. Kupfer, *Ber. Deut. Chem. Ges.* **1911**, *44*(3), 2194–2197; b) H. Meerwein, H. Rathjen, H. Werner, *Ber. Deut. Chem. Ges.* **1942**, *75*(12), 1610–1622; c) W. V. E. Doering, L. H. Knox, *J. Am. Chem. Soc.* **1950**, *72*(5), 2305–2306; d) G. F. Hennion, D. E. Maloney, *J. Am. Chem. Soc.* **1951**, *73*(10), 4735–4737; e) W. H. Urry, J. R. Eiszner, *J. Am. Chem. Soc.* **1951**, *73*(6), 2977–2977; f) W. von E. Doering, L. H. Knox, *J. Am. Chem. Soc.* **1953**, *75*(2), 297–303.

[33] E. O. Fischer, A. Maasböl, *Angew. Chem. Int. Ed.* **1964**, *3*(8), 580–581; *Angew. Chem.* **1964**, *76*, 645-645.

[34] K. Öfele, *J. Organomet. Chem.* **1968**, *12*(3), P42 – P43.

[35] H. W. Wanzlick, H. J. Schönherr, *Angew. Chem. Int. Ed.* **1968**, *7*(2), 141–142; *Angew. Chem.* **1968**, *80*, 154.

[36] R. R. Schrock, *J. Am. Chem. Soc.* **1974**, *96*(21), 6796–6797.

[37] a) A. Igau, H. Grutzmacher, A. Baceiredo, G. Bertrand, *J. Am. Chem. Soc.* **1988**, *110*(19), 6463–6466; b) T. Kato, H. Gornitzka, A. Baceiredo, A. Savin, G. Bertrand, *J. Am. Chem. Soc.* **2000**, *122*(5), 998–999.

[38] A. J. Arduengo-III, R. L. Harlow, M. Kline, *J. Am. Chem. Soc.* **1991**, *113*(1), 361–363.

[39] a) D. Bourissou, O. Guerret, F. P. Gabbaï, , G. Bertrand, *Chem. Rev.* **2000**, *100*(1), 39–92; b) K. Hirai, T. Itoh, H. Tomioka, *Chem. Rev.* **2009**, *109*(8), 3275–3332.

[40] R. Hoffmann, G. D. Zeiss, G. W. VanDine, *J. Am. Chem. Soc.* **1968**, *90*(6), 1485–1499.

[41] a) R. Gerhardt, T. Gerlbig, J. Buschamann, P. Luger, K. Seppelt, *Angew. Chem. Int. Ed.* **1988**, *27*(11), 1534–1536; b) G. R. Gillette, A. Baceiredo, G. Bertrand, *Angew. Chem. Int. Ed.* **1990**, *29*(12), 1429–1431; *Angew. Chem.* **1990**, *102*, 1486-1488; c) M. Soleilhavoup, A. Baceiredo, O. Treutler, R. Ahlrichs, M. Nieger, G. Bertrand, *J. Am. Chem. Soc.* **1992**, *114*(27), 10959–10961; d) P. Dyer, A. Baceiredo, G. Bertrand, *Inorg. Chem.* **1996**, *35*(1), 46–50.

[42] a) F. Hahn, M. Jahnke, *Angew. Chem. Int. Ed.* **2008**, *47*(17), 3122–3172; *Angew. Chem.* **2008**, *120*, 3166-3216; b) M. N. Hopkinson, C. Richter, M. Schedler, F. Glorius, *Nature* **2014**, *510*, 485–496; c) N. Kuhn, A. Al-Sheikh, *Coord. Chem. Rev.* **2005**, *249*(7–8), 829 – 857; d) D. Enders, O. Niemeier, A. Henseler, *Chem. Rev.* **2007**, *107*(12), 5606–5655; e) D. M. Flanigan, F. Romanov-Michailidis, N. A. White, T. Rovis, *Chem. Rev.* **2015**, *115*(17), 9307–9387; f) M. Soleilhavoup, G. Bertrand, *Acc. Chem. Res.* **2015**, *48*(2), 256–266; g) S. Roy, K. C. Mondal, H. W. Roesky, *Acc. Chem. Res.* **2016**, *49*(3), 357–369.

[43] A. V. Zhukhovitskiy, M. J. MacLeod, J. A. Johnson, *Chem. Rev.* **2015**, *115*(20), 11503–11532.

[44] a) L. Mercs, M. Albrecht, *Chem. Soc. Rev.* **2010**, *39*, 1903–1912; b) R. Visbal, M. C. Gimeno, *Chem. Soc. Rev.* **2014**, *43*, 3551–3574; c) C. I. Ezugwu, N. A. Kabir, M. Yusubov, F. Verpoort, *Coord. Chem. Rev.* **2016**, *307 (Part 2)*, 188 – 210.

[45] K. M. Hindi, M. J. Panzner, C. A. Tessier, C. L. Cannon, W. J. Youngs, *Chem. Rev.* **2009**, *109*(8), 3859–3884.

[46] a) C. S. J. Cazin (Ed.), *N-Heterocyclic Carbenes in Transition Metal Catalysis and Organocatalysis*, Springer, **2011**; b) W. A. Herrmann, *Angew. Chem. Int. Ed.* **2002**, *41*(8), 1290–1309; *Angew. Chem.* **2002**, *114*, 1342–1363; c) S. Díez-González, N. Marion, S. P. Nolan, *Chem. Rev.* **2009**, *109*(8), 3612–3676; d) F. Wang, L. jun Liu, W. Wang, S. Li, M. Shi, *Coord. Chem. Rev.* **2012**, *256*(9–10), 804 – 853; e) N. Marion, S. P. Nolan, *Chem. Soc. Rev.* **2008**, *37*, 1776–1782; f) E. Kantchev, C. O'Brien, M. Organ, *Angew. Chem. Int. Ed.* **2007**, *46*(16), 2768–2813; *Angew. Chem.* **2007**, *119*, 2824-2870; g) N. Marion, S. P. Nolan, *Acc. Chem. Res.* **2008**, *41*(11), 1440–1449; h) S. Würtz, F. Glorius, *Acc. Chem. Res.* **2008**, *41*(11), 1523–1533; i) G. C. Fortman, S. P. Nolan, *Chem. Soc. Rev.* **2011**, *40*, 5151–5169; j) C. Valente, S. Çalimsiz, K. H. Hoi, D. Mallik, M. Sayah, M. G. Organ, *Angew. Chem. Int. Ed.* **2012**, *51*(14), 3314–3332; *Angew. Chem.* **2012**, *124*, 3370-3388;

k) C. Samojłowicz, M. Bieniek, K. Grela; l) G. C. Vougioukalakis, R. H. Grubbs, *Chem. Rev.* **2010**, *110*(3), 1746–1787.

[47] H. Jacobsen, A. Correa, A. Poater, C. Costabile, L. Cavallo, *Coord. Chem. Rev.* **2009**, *253*(5–6), 687 – 703.

[48] a) R. H. Crabtree, *J. Organomet. Chem.* **2005**, *690*(24–25), 5451 – 5457; b) R. Tonner, G. Heydenrych, G. Frenking, *Chem. Asian J.* **2007**, *2*(12), 1555–1567.

[49] H. Jacobsen, A. Correa, C. Costabile, L. Cavallo, *J. Organomet. Chem.* **2006**, *691*(21), 4350 – 4358.

[50] D. Nemcsok, K. Wichmann, G. Frenking, *Organometallics* **2004**, *23*(15), 3640–3646.

[51] a) R. Dorta, E. D. Stevens, S. P. Nolan, *J. Am. Chem. Soc.* **2004**, *126*(16), 5054–5055; b) N. M. Scott, R. Dorta, E. D. Stevens, A. Correa, L. Cavallo, S. P. Nolan, *J. Am. Chem. Soc.* **2005**, *127*(10), 3516–3526.

[52] a) X. Hu, Y. Tang, P. Gantzel, K. Meyer, *Organometallics* **2003**, *22*(4), 612–614; b) X. Hu, I. Castro-Rodríguez, K. Olsen, K. Meyer, *Organometallics* **2004**, *23*(4), 755–764.

[53] a) D. J. Nelson, S. P. Nolan, *Chem. Soc. Rev.* **2013**, *42*, 6723–6753; b) L. Falivene, A. Poater, L. Cavallo, „Tuning and Quantifying Steric and Electronic Effects of N-Heterocyclic Carbenes" in *N-Heterocyclic Carbenes: Effective Tools for Organometallic Synthesis* (Ed. S. P. Nolan), Wiley-VCH Verlag GmbH, **2014**, p. 25–38.

[54] C. A. Tolman, *J. Am. Chem. Soc.* **1970**, *92*(10), 2953–2956.

[55] R. H. Carbtree (Ed.), *The organometallic chemistry of the transition metals*, 4. Ed., John Wiley and Sons, **2005**.

[56] A. C. Hillier, W. J. Sommer, B. S. Yong, J. L. Petersen, L. Cavallo, S. P. Nolan, *Organometallics* **2003**, *22*(21), 4322–4326.

[57] R. A. Kelly-III, H. Clavier, S. Giudice, N. M. Scott, E. D. Stevens, J. Bordner, I. Samardjiev, C. D. Hoff, L. Cavallo, S. P. Nolan, *Organometallics* **2008**, *27*(2), 202–210.

[58] S. Leuthäußer, D. Schwarz, H. Plenio, *Chem. Eur. J.* **2007**, *13*(25), 7195–7203.

[59] a) A. J. Arduengo-III, H. V. R. Dias, R. L. Harlow, M. Kline, *J. Am. Chem. Soc.* **1992**, *114*(14), 5530–5534; b) A. J. Arduengo-III., J. R. Goerlich, W. J. Marshall, *J. Am. Chem. Soc.* **1995**, *117*(44), 11027–11028.

[60] M. Iglesias, D. J. Beetstra, J. C. Knight, L.-L. Ooi, A. Stasch, S. Coles, L. Male, M. B. Hursthouse, K. J. Cavell, A. Dervisi, I. A. Fallis, *Organometallics* **2008**, *27*(13), 3279–3289.

[61] W. Y. Lu, K. J. Cavell, J. S. Wixey, B. Kariuki, *Organometallics* **2011**, *30*(21), 5649–5655.

[62] E. Despagnet-Ayoub, R. H. Grubbs, *J. Am. Chem. Soc.* **2004**, *126*(33), 10198–10199.

[63] V. Lavallo, Y. Canac, B. Donnadieu, W. W. Schoeller, G. Bertrand, *Science* **2006**, *312*(5774), 722–724.

[64] E. L. Rosen, M. D. Sanderson, S. Saravanakumar, C. W. Bielawski, *Organometallics* **2007**, *26*(24), 5774–5777.

[65] a) P. Bazinet, G. P. A. Yap, , D. S. Richeson, *J. Am. Chem. Soc.* **2003**, *125*(44), 13314–13315; b) M. Mayr, K. Wurst, K.-H. Ongania, M. R. Buchmeiser, *Chem. Eur. J.* **2004**, *10*(5), 1256–1266; c) M. Iglesias, D. J. Beetstra, A. Stasch, P. N. Horton, M. B. Hursthouse, S. J. Coles, K. J. Cavell, A. Dervisi, I. A. Fallis, *Organometallics* **2007**, *26*(19), 4800–4809; d) J. J. Dunsford, K. J. Cavell, B. M. Kariuki, *Organometallics* **2012**, *31*(11), 4118–4121; e) J. J. Dunsford, D. S. Tromp, K. J. Cavell, C. J. Elsevier, B. M. Kariuki, *Dalton Trans.* **2013**, *42*, 7318–7329; f) N. Phillips, T. Dodson, R. Tirfoin, J. I. Bates, S. Aldridge, *Chem. Eur. J.* **2014**, *20*(50), 16721–16731.

[66] a) O. Back, M. Henry-Ellinger, C. D. Martin, D. Martin, G. Bertrand, *Angew. Chem. Int. Ed.* **2013**, *52*(10), 2939–2943; *Angew. Chem.* **2013**, *125*, 3011-3015; b) D. Martin, Y. Canac, V. Lavallo, G. Bertrand, *J. Am. Chem. Soc.* **2014**, *136*(13), 5023–5030.

[67] B. Maji, M. Breugst, H. Mayr, *Angew. Chem. Int. Ed.* **2011**, *50*(30), 6915–6919; *Angew. Chem.* **2011**, *123*, 7047–7052.

[68] a) K. E. Krahulic, G. D. Enright, M. Parvez, R. Roesler, *J. Am. Chem. Soc.* **2005**, *127*(12), 4142–4143; b) C. Präsang, B. Donnadieu, G. Bertrand, *J. Am. Chem. Soc.* **2005**, *127*(29), 10182–10183; c) A. Kausamo, H. M. Tuononen, K. E. Krahulic, R. Roesler, *Inorg. Chem.* **2008**, *47*(3), 1145–1154.

[69] a) J. Vignolle, X. Cattoën, D. Bourissou, *Chem. Rev.* **2009**, *109*(8), 3333–3384; b) L. M. Slaughter, *ACS Cat.* **2012**, *2*(8), 1802–1816; c) V. P. Boyarskiy, K. V. Luzyanin, V. Y. Kukushkin, *Coord. Chem. Rev.* **2012**, *256*(17–18), 2029 – 2056; d) L. M. Slaughter, „Catalysis with Acyclic Aminocarbene Ligands: Alternatives to NHCs with Distinct Steric and Electronic Properties" in *N-Heterocyclic Carbenes: Effective Tools for Organometallic Synthesis* (Ed. S. P. Nolan), Wiley-VCH Verlag GmbH, **2014**, p. 499–524.

[70] a) M. Tamm, F. E. Hahn, *Coord. Chem. Rev.* **1999**, *182*(1), 175 – 209; b) R. A. Michelin, A. J. Pombeiro, M. F. C. Guedes-daSilva, *Coord. Chem. Rev.* **2001**, *218*, 75 – 112; c) A. S. K. Hashmi, C. Lothschütz, K. Graf, T. Häffner, A. Schuster, F. Rominger, *Adv. Synth. Cat.* **2011**, *353*(9), 1407–1412; d) A. S. K. Hashmi, C. Lothschütz, C. Böhling, F. Rominger, *Organometallics* **2011**, *30*(8), 2411–2417; e) V. P. Boyarskiy, N. A. Bokach, K. V. Luzyanin, V. Y. Kukushkin, *Chem.*

Rev. **2015**, *115*(7), 2698–2779; f) A. Zeiler, M. Rudolph, F. Rominger, A. S. K. Hashmi, *Chem. Eur. J.* **2015**, *21*(31), 11065–11071; g) T. Wurm, F. Mulks, C. R. N. Böhling, D. Riedel, P. Zargaran, M. Rudolph, F. Rominger, A. S. K. Hashmi, *Organometallics* **2016**, *35*(8), 1070–1078.

[71] J. Ruiz, B. F. Perandones, *Organometallics* **2009**, *28*(3), 830–836.

[72] I. Yu, C. J. Wallis, B. O. Patrick, P. L. Diaconescu, P. Mehrkhodavandi, *Organometallics* **2010**, *29*(22), 6065–6076.

[73] a) F. Bonati, G. Minghetti, *J. Organomet. Chem.* **1973**, *59*, 403 – 410; b) A. S. K. Hashmi, C. Lothschütz, C. Böhling, T. Hengst, C. Hubbert, F. Rominger, *Adv. Synth. Cat.* **2010**, *352*(17), 3001–3012.

[74] a) M. O. Owusu, S. Handa, L. M. Slaughter, *App. Organomet. Chem.* **2012**, *26*(12), 712–717; b) M. A. Kinzhalov, K. V. Luzyanin, V. P. Boyarskiy, M. Haukka, V. Y. Kukushkin, *Organometallics* **2013**, *32*(18), 5212–5223; c) E. A. Valishina, M. F. C. G. da Silva, M. A. Kinzhalov, S. A. Timofeeva, T. M. Buslaeva, M. Haukka, A. J. Pombeiro, V. P. Boyarskiy, V. Y. Kukushkin, K. V. Luzyanin, *J. Mol. Cat. A* **2014**, *395*, 162 – 171; d) S. A. Timofeeva, M. A. Kinzhalov, E. A. Valishina, K. V. Luzyanin, V. P. Boyarskiy, T. M. Buslaeva, M. Haukka, V. Y. Kukushkin, *J. Cat.* **2015**, *329*, 449 – 456; e) M. Knorn, E. Lutsker, O. Reiser, *Organometallics* **2015**, *34*(18), 4515–4520; f) V. N. Mikhaylov, V. N. Sorokoumov, K. A. Korvinson, A. S. Novikov, I. A. Balova, *Organometallics* **2016**, *35*(11), 1684–1697.

[75] a) C. Bartolomé, Z. Ramiro, P. Pérez-Galán, C. Bour, M. Raducan, A. M. Echavarren, P. Espinet, *Inorg. Chem.* **2008**, *47*(23), 11391–11397; b) C. Bartolomé, Z. Ramiro, D. García-Cuadrado, P. Pérez-Galán, M. Raducan, C. Bour, A. M. Echavarren, P. Espinet, *Organometallics* **2010**, *29*(4), 951–956; c) A. S. Hashmi, T. Hengst, C. Lothschütz, F. Rominger, *Adv. Synth. Cat.* **2010**, *352*(8), 1315–1337; d) C. Bartolomé, D. García-Cuadrado, Z. Ramiro, P. Espinet, *Organometallics* **2010**, *29*(16), 3589–3592; e) M. C. Blanco-Jaimes, C. R. N. Böhling, J. M. Serrano-Becerra, A. S. K. Hashmi, *Angew. Chem. Int. Ed.* **2013**, *52*(31), 7963–7966; *Angew. Chem.* **2013**, *125*, 8121-8124.

[76] a) Y.-M. Wang, C. N. Kuzniewski, V. Rauniyar, C. Hoong, F. D. Toste, *J. Am. Chem. Soc.* **2011**, *133*(33), 12972–12975; b) S. Handa, L. M. Slaughter, *Angew. Chem. Int. Ed.* **2012**, *51*(12), 2912–2915; *Angew. Chem.* **2012**, *124*, 2966-2969.

[77] C. Urbina-Blanco, X. Bantreil, H. Clavier, A. M. Z. Slawin, S. P. Nolan, *Beilstein J. Org. Chem.* **2010**, *6*, 1120–1126.

[78] a) M. Braun, W. Frank, G. J. Reiss, C. Ganter, *Organometallics* **2010**, *29*(20), 4418–4420; b) M. G. Hobbs, T. D. Forster, J. Borau-Garcia, C. J. Knapp, H. M. Tuononen, R. Roesler, *New J. Chem.* **2010**, *34*, 1295–1308.

[79] Y. Zhang, V. César, G. Storch, N. Lugan, G. Lavigne, *Angew. Chem. Int. Ed.* **2014**, *53*(25), 6482–6486; *Angew. Chem.* **2014**, *126*, 6600–6604.

[80] M. Melaimi, M. Soleilhavoup, G. Bertrand, *Angew. Chem. Int. Ed.* **2010**, *49*(47), 8810–8849; *Angew. Chem.* **2010**, *122*, 1521-3757.

[81] V. Lavallo, Y. Canac, C. Präsang, B. Donnadieu, G. Bertrand, *Angew. Chem. Int. Ed.* **2005**, *44*(35), 5705–5709; *Angew. Chem.* **2005**, *117*, 5851-5855.

[82] O. Schuster, L. Yang, H. G. Raubenheimer, M. Albrecht, *Chem. Rev.* **2009**, *109*(8), 3445–3478.

[83] S. Gómez-Bujedo, M. Alcarazo, C. Pichon, E. Álvarez, R. Fernández, J. M. Lassaletta, *Chem. Commun.* **2007**, 1180–1182.

[84] A. J. Arduengo, J. R. Goerlich, W. J. Marshall, *Liebigs Ann.* **1997**, *1997*(2), 365–374.

[85] R. W. Alder, C. P. Butts, A. G. Orpen, *J. Am. Chem. Soc.* **1998**, *120*(44), 11526–11527.

[86] G. D. Frey, M. Song, J.-B. Bourg, B. Donnadieu, M. Soleilhavoup, G. Bertrand, *Chem. Commun.* **2008**, 4711–4713.

[87] M. Z. Kassaee, F. A. Shakib, M. R. Momeni, M. Ghambarian, S. M. Musavi, *J. Org. Chem.* **2010**, *75*(8), 2539–2545.

[88] H. V. Huynh, G. Frison, *J. Org. Chem.* **2013**, *78*(2), 328–338.

[89] a) M. Z. Kassaee, F. A. Shakib, M. R. Momeni, M. Ghambarian, S. M. Musavi, *J. Org. Chem.* **2010**, *75*(8), 2539–2545.

[90] a) G. Facchin, R. Campostrini, R. A. Michelin, *J. Organomet. Chem.* **1985**, *294*(2), c21 – c25; b) R. A. Michelin, G. Facchin, D. Braga, P. Sabatino, *Organometallics* **1986**, *5*(11), 2265–2274; c) R. A. Michelin, M. Mozzon, G. Facchin, D. Braga, P. Sabatino, *J. Chem. Soc., Dalton Trans.* **1988**, 1803–1811.

[91] a) S.-y. Nakafuji, J. Kobayashi, T. Kawashima, *Angew. Chem. Int. Ed.* **2008**, *47*(6), 1141–1144; *Angew. Chem.* **2008**, *120*, 1157–1160; b) M. Asay, B. Donnadieu, A. Baceiredo, M. Soleilhavoup, G. Bertrand, *Inorg. Chem.* **2008**, *47*(10), 3949–3951; c) J. Kobayashi, S.-y. Nakafuji, A. Yatabe, T. Kawashima, *Chem. Commun.* **2008**, 6233–6235; d) A. Fürstner, M. Alcarazo, K. Radkowski, C. Lehmann, *Angew. Chem. Int. Ed.* **2008**, *47*(43), 8302–8306; *Angew. Chem.* **2008**, *120*, 8426–8430.

[92] a) K. Bartel, W. P. Fehlhammer, *Angew. Chem. Int. Ed.* **1974**, *13*(9), 599–600; b) R. Ishii, T. Kaharu, N. Pirio, S.-W. Zhang, S. Takahashi, *J. Chem. Soc., Chem. Commun.* **1995**, 1215–1216; c) S.-W. Zhang, R. Ishii, , S. Takahashi, *Organometallics* **1997**, *16*(1), 20–26.

[93] O. I. Kolodiazhnyi (Ed.), *Phosphorus Ylides: Chemistry and Application in Organic Synthesis*, Wiley-VCH Verlag GmbH, **2008**.

[94] a) H. Schmidbaur, *Angew. Chem. Int. Ed.* **1983**, *22*(12), 907–927; *Angew. Chem.* **1983**, *95*, 980–1000; b) E. P. Urriolabeitia, „Ylide Ligands" in *Transition Metal Complexes of Neutral η^1-Carbon Ligands* (Eds. R. Chauvin, Y. Canac), Springer Berlin Heidelberg, **2010**, p. 15–48.

[95] a) J. Vicente, M. T. Chicote, J. A. Cayuelas, J. Fernández-Baeza, P. G. Jones, G. M. Sheldrick, P. Espinet, *J. Chem. Soc., Dalton Trans.* **1985**, 1163–1168; b) R. Usón, A. Laguna, M. Laguna, A. Usón, M. Gimeno, *Inorg. Chim. Acta* **1986**, *114*(1), 91 – 94; c) J. Vicente, M. T. Chicote, M. C. Lagunas, *Inorg. Chem.* **1993**, *32*(17), 3748–3754.

[96] K. Coetzee, C. Strasser, S. Cronje, H. G. Raubenheimer, *Z. Naturforsch. B Chem. Sci.* **2014**, *64*(11-12), 1449–1457.

[97] A. Bondi, *J. Phys. Chem.* **1964**, *68*(3), 441–451.

[98] a) M. P. Guy, J. T. Guy, D. W. Bennett, *J. Mol. Struc. THEOCHEM* **1985**, *122*(1), 95 – 99; b) R. F. Johnston, J. C. Cooper, *J. Mol. Struc. THEOCHEM* **1991**, *236*(3), 297 – 307.

[99] A. S. K. Hashmi, D. Riedel, M. Rudolph, F. Rominger, T. Oeser, *Chem. Eur. J.* **2012**, *18*(13), 3827–3830.

[100] a) Y.-Z. Huang, Y.-C. Shen, *Adv. Organomet. Chem.* **1982**, *20*, 115–157; b) H. S. He, C. W. Y. Chung, T. Y. S. But, P. H. Toy, *Tetrahedron* **2005**, *61*(6), 1385 – 1405.

[101] G. Facchin, L. Zanotto, R. Bertani, L. Canovese, P. Uguagliati, *J. Chem. Soc., Dalton Trans.* **1993**, 2871–2874.

[102] A. Fürstner, M. Alcarazo, R. Goddard, C. Lehmann, *Angew. Chem. Int. Ed.* **2008**, *47*(17), 3210–3214; *Angew. Chem.* **2008**, *120*, 3254–3258.

[103] F. H. Allen, O. Kennard, D. G. Watson, L. Brammer, A. G. Orpen, R. Taylor, *J. Chem. Soc., Perkin Trans. 2* **1987**, S1–S19.

[104] P. deFrémont, N. M. Scott, E. D. Stevens, S. P. Nolan, *Organometallics* **2005**, *24*(10), 2411–2418.

[105] a) A. Poater, B. Cosenza, A. Correa, S. Giudice, F. Ragone, V. Scarano, L. Cavallo, *Eur. J. Inorg. Chem.* **2009**, *2009*(13), 1759–1766; b) L. Cavallo, „SambVca - A tool to calculate the buried volume of ligands.", **2008**, https://www.molnac.unisa.it/OMtools/sambvca2.0/index.html.

[106] a) M. H. Pérez-Temprano, J. A. Casares, P. Espinet, *Chem. Eur. J.* **2012**, *18*(7), 1864–1884; b) J. Park, S. Hong, *Chem. Soc. Rev.* **2012**, *41*, 6931–6943; c) E. Bodio, M. Picquet, P. Le Gendre, „"Early–Late" Heterobimetallic Catalysis and Beyond" in *Homo- and Heterobimetallic Complexes in Catalysis: Cooperative Catalysis* (Ed. P. Kalck), Springer International Publishing, **2016**, p. 139–186.

[107] a) A. Labande, J.-C. Daran, N. J. Long, A. J. P. White, R. Poli, *New J. Chem.* **2011**, *35*, 2162–2168; b) F. Aznarez, P. J. S. Miguel, T. T. Y. Tan, F. E. Hahn, *Organometallics* **2016**, *35*(3), 410–419.

[108] Y. Shi, S. A. Blum, *Organometallics* **2011**, *30*(7), 1776–1779.

[109] A. S. K. Hashmi, L. Molinari, *Organometallics* **2011**, *30*(13), 3457–3460.

[110] S.-T. Liu, C.-I. Lee, C.-F. Fu, C.-H. Chen, Y.-H. Liu, C. J. Elsevier, S.-M. Peng, J.-T. Chen, *Organometallics* **2009**, *28*(24), 6957–6962.

[111] a) O. Guerret, S. Solé, H. Gornitzka, G. Trinquier, G. Bertrand, *J. Organomet. Chem.* **2000**, *600*(1–2), 112 – 117; b) A. Chaumonnot, B. Donnadieu, S. Sabo-Etienne, B. Chaudret, C. B. G. Bertrand, P. Metivier, *Organometallics* **2001**, *20*(26), 5614–5618; c) C. Buron, L. Stelzig, O. Guerret, H. Gornitzka, V. Romanenko, G. Bertrand, *J. Organomet. Chem.* **2002**, *664*(1–2), 70 – 76; d) D. Khramov, E. Rosen, V. Lynch, C. Bielawski, *Angew. Chem. Int. Ed.* **2008**, *47*(12), 2267–2270; *Angew. Chem.* **2008**, *120*, 2299–2302; e) B. Hildebrandt, S. Raub, W. Frank, C. Ganter, *Chem. Eur. J.* **2012**, *18*(21), 6670–6678; f) K. Verlinden, C. Ganter, *J. Organomet. Chem.* **2014**, *750*, 23 – 29; g) H. Valdés, M. Poyatos, E. Peris, *Organometallics* **2014**, *33*(1), 394–401.

[112] L.-A. Schaper, S. J. Hock, W. A. Herrmann, F. E. Kühn, *Angew. Chem. Int. Ed.* **2013**, *52*(1), 270–289; *Angew. Chem.* **2013**, *125*, 284–304.

[113] M. S. Newman, D. Lednicer, *J. Am. Chem. Soc.* **1956**, *78*(18), 4765–4770.

[114] J. Maisenheimer, K. Witte, *Chem. Ber.* **1903**, *36*(4), 4153–4164.

[115] a) E. Harnik, F. H. Herbstein, G. M. J. Schmidt, F. L. Hirshfeld, *J. Chem. Soc.* **1954**, 3288–3294; b) F. H. Herbstein, G. M. J. Schmidt, *J. Chem. Soc.* **1954**, 3302–3313.

[116] a) M. S. Newman, R. M. Wise, *J. Am. Chem. Soc.* **1956**, *78*(2), 450–454; b) F. Bell, D. H. Waring, *J. Chem. Soc.* **1949**, 2689–2693.

[117] M. S. Newman, W. B. Lutz, D. Lednicer, *J. Am. Chem. Soc.* **1955**, *77*(12), 3420–3421.

[118] a) J. Borkent, W. Laarhoven, *Tetrahedron* **1978**, *34*(16), 2565 – 2567; b) H. Scherübl, U. Fritzsche, A. Mannschreck, *Chem. Ber.* **1984**, *117*(1), 336–343; c) R. Fritsch, E. Hartmann, D. Andert, A. Mannschreck, *Chem. Ber.* **1992**, *125*(4), 849–855; d) R. H. Janke, G. Haufe, E.-U. Würthwein, J. H. Borkent, *J. Am. Chem. Soc.* **1996**, *118*(25), 6031–6035.

[119] a) R. H. Martin, M. J. Marchant, *Tetrahedron Lett.* **1972**, *13*(35), 3707–3708; b) R. H. Martin, M. J. Marchant, *Tetrahedron* **1974**, *30*(2), 347–349.

[120] a) J. M. Schulman, R. L. Disch, *J. Phys. Chem. A* **1999**, *103*(33), 6669–6672; b) G. Portella, J. Poater, J. M. Bofill, P. Alemany, M. Solà, *J. Org. Chem.* **2005**, *70*(7), 2509–2521.

[121] Y.-H. Tian, G. Park, M. Kertesz, *Chem. Mater.* **2008**, *20*(10), 3266–3277.

[122] a) Y. Yang, R. C. da Costa, M. J. Fuchter, A. J. Campbell, *Nat. Photon.* **2013**, *7*(8), 634–638; b) J. Storch, J. Zadny, T. Strasak, M. Kubala, J. Sykora, M. Dusek, V. Cirkva, P. Matejka, M. Krbal, J. Vacek, *Chem. Eur. J.* **2015**, *21*(6), 2343–2347.

[123] a) S. Sahasithiwat, T. Mophuang, L. Menbangpung, S. Kamtonwong, T. Sooksimuang, *Synth. Met.* **2010**, *160*(11-12), 1148 – 1152; b) L. Shi, Z. Liu, G. Dong, L. Duan, Y. Qiu, J. Jia, W. Guo, D. Zhao, D. Cui, X. Tao, *Chem. Eur. J.* **2012**, *18*(26), 8092–8099.

[124] a) Y. Ooyama, A. Ishii, Y. Kagawa, I. Imae, Y. Harima, *New J. Chem.* **2007**, *31*, 2076–2082; b) Y. Ooyama, Y. Shimada, Y. Kagawa, I. Imae, Y. Harima, *Org. Biomol. Chem.* **2007**, *5*, 2046–2054.

[125] a) F. Furche, R. Ahlrichs, C. Wachsmann, E. Weber, A. Sobanski, F. Vögtle, S. Grimme, *J. Am. Chem. Soc.* **2000**, *122*(8), 1717–1724; b) E. Botek, B. Champagne, *J. Chem. Phys.* **2007**, *127*(20), 204101; c) Y. Nakai, T. Mori, Y. Inoue, *J. Phys. Chem. A* **2012**, *116*(27), 7372–7385.

[126] H. Isla, J. Crassous, *C. R. Chimie* **2016**, *19*(1–2), 39 – 49.

[127] D. Schweinfurth, M. Zalibera, M. Kathan, C. Shen, M. Mazzolini, N. Trapp, J. Crassous, G. Gescheidt, F. Diederich, *J. Am. Chem. Soc.* **2014**, *136*(37), 13045–13052.

[128] a) B. L. Feringa, R. A. van Delden, N. Koumura, E. M. Geertsema, *Chem. Rev.* **2000**, *100*(5), 1789–1816; b) Z. Dai, J. Lee, W. Zhang, *Molecules* **2012**, *17*(2), 1247.

[129] M. T. Reetz, S. Sostmann, *Tetrahedron* **2001**, *57*(13), 2515 – 2520.

[130] a) K. Tanaka, H. Osuga, H. Suzuki, Y. Shogase, Y. Kitahara, *J. Chem. Soc., Perkin Trans. 1* **1998**, 935–940; b) Y. Xu, Y. X. Zhang, H. Sugiyama, T. Umano, H. Osuga, K. Tanaka, *J. Am. Chem. Soc.* **2004**, *126*(21), 6566–6567.

[131] a) K. Tanaka, H. Osuga, Y. Kitahara, *J. Org. Chem.* **2002**, *67*(6), 1795–1801; b) K. ichi Shinohara, Y. Sannohe, S. Kaieda, K. ichi Tanaka, H. Osuga, H. Tahara, Y. Xu, T. Kawase, T. Bando, H. Sugiyama, *J. Am. Chem. Soc.* **2010**, *132*(11), 3778–3782.

[132] S. Honzawa, H. Okubo, S. Anzai, M. Yamaguchi, K. Tsumoto, I. Kumagai, *Bioorg. Med. Chem.* **2002**, *10*(10), 3213 – 3218.

[133] N. Saleh, C. Shen, J. Crassous, *Chem. Sci.* **2014**, *5*, 3680–3694.

[134] a) M. T. Reetz, E. W. Beuttenmüller, R. Goddard, *Tetrahedron Lett.* **1997**, *38*(18), 3211 – 3214; b) M. T. Reetz, S. Sostmann, *J. Organomet. Chem.* **2000**, *603*(1), 105 – 109.

[135] a) S. D. Dreher, T. J. Katz, K.-C. Lam, A. L. Rheingold, *J. Org. Chem.* **2000**, *65*(3), 815–822; b) D. Nakano, M. Yamaguchi, *Tetrahedron Lett.* **2003**, *44*(27), 4969 – 4971.

[136] Z. Krausová, P. Sehnal, B. P. Bondzic, S. Chercheja, P. Eilbracht, I. G. Stará, D. Šaman, I. Starý, *Eur. J. Org. Chem.* **2011**, *2011*(20-21), 3849–3857.

[137] a) K. Yavari, P. Retailleau, A. Voituriez, A. Marinetti, *Chem. Eur. J.* **2013**, *19*(30), 9939–9947; b) K. Yavari, P. Aillard, Y. Zhang, F. Nuter, P. Retailleau, A. Voituriez, A. Marinetti, *Angew. Chem. Int. Ed.* **2014**, *53*(3), 861–865; *Angew. Chem.* **2014**, *126*, 880–884; c) P. Aillard, P. Retailleau, A. Voituriez, A. Marinetti, *Chem. Eur. J.* **2015**, *21*(34), 11989–11993.

[138] a) B. Ye, N. Cramer, *J. Am. Chem. Soc.* **2013**, *135*(2), 636–639; b) M. Dieckmann, Y.-S. Jang, N. Cramer, *Angew. Chem. Int. Ed.* **2015**, *54*(41), 12149–12152; *Angew. Chem.* **2015**, *127*, 12317–12320.

[139] a) B. Ben Hassine, M. Gorsane, F. Geerts-Evrard, J. Pecher, R. H. Martin, D. Castelet, *Bull. Soc. Chim. Belg.* **1986**, *95*(7), 547–556; b) ; c) I. Sato, R. Yamashima, K. Kadowaki, J. Yamamoto, T. Shibata, K. Soai, *Angew. Chem. Int. Ed.* **2001**, *40*(6), 1096–1098.

[140] a) B. Ben Hassine, M. Gorsane, J. Pecher, R. H. Martin, *Bull. Soc. Chim. Belg.* **1985**, *94*(8), 597–603; b) B. Ben Hassine, M. Gorsane, J. Pecher, R. H. Martin, *Bull. Soc. Chim. Belg.* **1987**, *96*(10), 801–808.

[141] a) N. Takenaka, R. S. Sarangthem, B. Captain, *Angew. Chem. Int. Ed.* **2008**, *47*(50), 9708–9710; *Angew. Chem.* **2008**, *120*, 9854–9856; b) J. Chen, N. Takenaka, *Chem. Eur. J.* **2009**, *15*(30), 7268–7276; c) J. Chen, B. Captain, N. Takenaka, *Org. Lett.* **2011**, *13*(7), 1654–1657; d) M. R. Crittall, H. S. Rzepa, D. R. Carbery, *Org. Lett.* **2011**, *13*(5), 1250–1253.

[142] a) R. Martin, M. Flammang-Barbieux, J. Cosyn, M. Gelbcke, *Tetrahedron Lett.* **1968**, *9*(31), 3507 – 3510; b) H. Wynberg, M. B. Groen, H. Schadenberg, *J. Org. Chem.* **1971**, *36*(19), 2797–2809; c) R. Martin, M. Marchant, *Tetrahedron* **1974**, *30*(2), 343 – 345.

[143] C. Nuckolls, T. J. Katz, L. Castellanos, *J. Am. Chem. Soc.* **1996**, *118*(15), 3767–3768.

[144] a) A. J. Lovinger, C. Nuckolls, T. J. Katz, *J. Am. Chem. Soc.* **1998**, *120*(2), 264–268; b) C. Nuckolls, T. J. Katz, G. Katz, P. J. Collings, L. Castellanos, *J. Am. Chem. Soc.* **1999**, *121*(1), 79–88.

[145] a) C. Nuckolls, T. J. Katz, T. Verbiest, S. V. Elshocht, H.-G. Kuball, S. Kiesewalter, A. J. Lovinger, A. Persoons, *J. Am. Chem. Soc.* **1998**, *120*(34), 8656–8660; b) T. Verbiest, S. V. Elshocht, M. Kauranen, L. Hellemans, J. Snauwaert, C. Nuckolls, T. J. Katz, A. Persoons, *Science* **1998**, *282*(5390), 913–915; c) T. Verbiest, S. van Elshocht, A. Persoons, C. Nuckolls, K. E. Phillips, T. J. Katz, *Langmuir* **2001**, *17*(16), 4685–4687.

[146] a) C. Nuckolls, , T. J. Katz, *J. Am. Chem. Soc.* **1998**, *120*(37), 9541–9544; b) C. Nuckolls, R. Shao, W.-G. Jang, N. A. Clark, D. M. Walba¡, T. J. Katz, *Chem. Mater.* **2002**, *14*(2), 773–776; c) T. Verbiest, S. Sioncke, A. Persoons, L. Vyklický, T. J. Katz, *Angew. Chem. Int. Ed.* **2002**, *41*(20), 1521–3773; *Angew. Chem.* **2002**, *114*, 4038-4040.

[147] a) J. M. Fox, T. J. Katz, S. V. Elshocht, T. Verbiest, M. Kauranen, A. Persoons, T. Thongpanchang, T. Krauss, L. Brus, *J. Am. Chem. Soc.* **1999**, *121*(14), 3453–3459; b) E. Murguly, R. McDonald, N. R. Branda, *Org. Lett.* **2000**, *2*(20), 3169–3172; c) K. E. S. Phillips, T. J. Katz, S. Jockusch, A. J. Lovinger, N. J. Turro, *J. Am. Chem. Soc.* **2001**, *123*(48), 11899–11907; d) R. Amemiya, M. Yamaguchi, *Org. Biomol. Chem.* **2008**, *6*, 26–35; e) M. Shcherbina, X.-b. Zeng, T. Tadjiev, G. Ungar, S. Eichhorn, K. Phillips, T. Katz, *Angew. Chem. Int. Ed.* **2009**, *48*(42), 7837–7840; *Angew. Chem.* **2009**, *121*, 7977-7980; f) T. Kaseyama, S. Furumi, X. Zhang, K. Tanaka, M. Takeuchi, *Angew. Chem. Int. Ed.* **2011**, *50*(16), 3684–3687; *Angew. Chem.* **2011**, *123*, 3768-3771.

[148] a) M. Taniguchi, H. Nakagawa, A. Yamagishi, K. Yamada, *J. Mol. Cat. A* **2003**, *199*(1–2), 65 – 71; b) P. Rahe, M. Nimmrich, A. Greuling, J. Schütte, I. G. Stará, J. Rybáček, G. Huerta-Angeles, I. Starý, M. Rohlfing, A. Kühnle, *J. Phys. Chem. C* **2010**, *114*(3), 1547–1552; c) J. Rybáček, G. Huerta-Angeles, A. Kollárovič, I. G. Stará, I. Starý, P. Rahe, M. Nimmrich, A. Kühnle, *Eur. J. Org. Chem.* **2011**, *2011*(5), 853–860; d) A. Shchyrba, M.-T. Nguyen, C. Wäckerlin, S. Martens, S. Nowakowska, T. Ivas, J. Roose, T. Nijs, S. Boz, M. Schär, M. Stöhr, C. A. Pignedoli, C. Thilgen, F. Diederich, D. Passerone, T. A. Jung, *J. Am. Chem. Soc.* **2013**, *135*(41), 15270–15273; e) B. Hoff, M. Gingras, R. Peresutti, C. R. Henry, A. S. Foster, C. Barth, *J. Phys. Chem. C* **2014**, *118*(26), 14569–14578.

[149] a) K.-H. Ernst, M. Neuber, M. Grunze, U. Ellerbeck, *J Am. Chem. Soc.* **2001**, *123*(3), 493–495; b) K.-H. Ernst, *Phys. Status Solidi B* **2012**, *249*(11), 2057–2088.

[150] a) K.-H. Ernst, Y. Kuster, R. Fasel, M. Müller, U. Ellerbeck, *Chirality* **2001**, *13*(10), 675–678; b) R. Fasel, M. Parschau, K.-H. Ernst, *Angew. Chem. Int. Ed.* **2003**, *42*(42), 5178–5181; *Angew. Chem.* **2003**, *115*, 5336-5339; c) T. Balandina, M. W. van der Meijden, O. Ivasenko, D. Cornil, J. Cornil, R. Lazzaroni, R. M. Kellogg, S. De Feyter, *Chem. Commun.* **2013**, *49*, 2207–2209; d) H. Ascolani, M. W. van der Meijden, L. J. Cristina, J. E. Gayone, R. M. Kellogg, J. D. Fuhr, M. Lingenfelder, *Chem. Commun.* **2014**, *50*, 13907–13909.

[151] R. Fasel, M. Parschau, K.-H. Ernst, *Nature* **2006**, *439*(7075), 449–452.

[152] a) M. Stöhr, S. Boz, M. Schär, M.-T. Nguyen, C. A. Pignedoli, D. Passerone, W. B. Schweizer, C. Thilgen, T. A. Jung, F. Diederich, *Angew. Chem. Int. Ed.* **2011**, *50*(42), 9982–9986; *Angew. Chem.* **2011**, *123*, 10158-10162; b) J. Seibel, O. Allemann, J. S. Siegel, K.-H. Ernst, *J. Am. Chem. Soc.* **2013**, *135*(20), 7434–7437.

[153] R. Amemiya, M. Yamaguchi, *Chem. Rec.* **2008**, *8*(2), 116–127.

[154] a) Z. Y. Wang, Y. Qi, T. P. Bender, J. P. Gao, *Macromolecules* **1997**, *30*(4), 764–769; b) T. P. Bender, Y. Qi, J. P. Gao, Z. Y. Wang, *Macromolecules* **1997**, *30*(20), 6001–6006; c) T. P. Bender, Z. Y. Wang, *J. Polym. Sci. A Polym. Chem.* **1998**, *36*(9), 1349–1353; d) T. P. Bender, S. M. MacKinnon, Z. Y. Wang, *J. Polym. Sci. A Polym. Chem.* **2000**, *38*(4), 758–763.

[155] a) T. Iwasaki, K. Katayose, Y. Kohinata, H. Nishide, *Polym. J.* **2005**, *37*(8), 592–598; b) T. Iwasaki, Y. Kohinata, H. Nishide, *Org. Lett.* **2005**, *7*(5), 755–758; c) I. Takemura, R. Sone, H. Nishide, *Polym. Adv. Technol.* **2008**, *19*(8), 1092–1096.

[156] Z. Y. Wang, J. E. Douglas, *Macromolecules* **1997**, *30*(25), 8091–8093.

[157] a) Y. Saiki, K. Nakamura, Y. Nigorikawa, M. Yamaguchi, *Angew. Chem. Int. Ed.* **2003**, *42*(42), 5190–5192; *Angew. Chem.* **2003**, *115*, 5348-5350; b) Y. Saiki, H. Sugiura, K. Nakamura, M. Yamaguchi, T. Hoshi, J. ichi Anzai, *J. Am. Chem. Soc.* **2003**, *125*(31), 9268–9269; c) H. Sugiura, Y. Nigorikawa, Y. Saiki, K. Nakamura, M. Yamaguchi, *J. Am. Chem. Soc.* **2004**, *126*(45), 14858–14864.

[158] T. J. Katz, A. Sudhakar, M. F. Teasley, A. M. Gilbert, W. E. Geiger, M. P. Robben, M. Wuensch, M. D. Ward, *J. Am. Chem. Soc.* **1993**, *115*(8), 3182–3198.

[159] a) J. M. Fox, D. Lin, Y. Itagaki, , T. Fujita, *J. Org. Chem.* **1998**, *63*(6), 2031–2038; b) Y. Dai, T. J. Katz, D. A. Nichols, *Angew. Chem. Int. Ed.* **1996**, *35*(18), 2109–2111; *Angew. Chem.* **1996**, *108*, 2230-2232.

[160] M. Gingras, G. Félix, R. Peresutti, *Chem. Soc. Rev.* **2013**, *42*(3), 1007–1050.

[161] K. B. Jørgensen, *Molecules* **2010**, *15*(6), 4334–4358.

[162] M. Scholz, M. M *Tetrahedron Lett.* **1967**, *8*(7), 665–668.

[163] M. Flammang-Barbieux, J. Nasielski, R. Martin, *Tetrahedron Lett.* **1967**, *8*(8), 743–744.

[164] N. Hoffmann, *J. Photochem. Photobiol. C* **2014**, *19*, 1 – 19.

[165] K. Mori, T. Murase, M. Fujita, *Angew. Chem. Int. Ed.* **2015**, *54*(23), 6847–6851; *Angew. Chem.* **2015**, *127*, 6951–6955.

[166] H. Kagan, A. Moradpour, J. F. Nicoud, G. Balavoine, G. Tsoucaris, *J. Am. Chem. Soc.* **1971**, *93*(9), 2353–2354.

[167] a) W. J. Bernstein, M. Calvin, O. Buchardt, *J. Am. Chem. Soc.* **1972**, *94*(2), 494–498; b) W. J. Bernstein, M. Calvin, O. Buchardt, *Tetrahedron Lett.* **1972**, *13*(22), 2195 – 2198; c) W. J. Bernstein, M. Calvin, O. Buchardt, *J. Am. Chem. Soc.* **1973**, *95*(2), 527–532.

[168] H. Kagan, A. Moradpour, J. Nicoud, G. Balavoine, R. Martin, J. Cosyn, *Tetrahedron Lett.* **1971**, *12*(27), 2479 – 2482.

[169] a) J. Tribout, R. Martin, M. Doyle, H. Wynberg, *Tetrahedron Lett.* **1972**, *13*(28), 2839 – 2842; b) R. El Abed, B. Ben Hassine, J.-P. Genêt, M. Gorsane, J. Madec, L. Ricard, A. Marinetti, *Synthesis* **2004**, (15), 2513–2516; c) M. S. M. Pearson, D. R. Carbery, *J. Org. Chem.* **2009**, *74*(15), 5320–5325.

[170] a) R. H. Martin, V. Libert, *J. Chem. Res., Synop.* **1980**, 130–131; b) R. H. Martin, V. Libert, *J. Chem. Res., Miniprint.* **1980**, 1940–1950.

[171] L. Liu, T. J. Katz, *Tetrahedron Lett.* **1990**, *31*(28), 3983 – 3986.

[172] N. D. Willmore, L. Liu, T. J. Katz, *Angew. Chem. Int. Ed.* **1992**, *31*(8), 1093–1095; *Angew. Chem.* **1992**, *104*, 1081-1082.

[173] a) M. C. Carreño, R. Hernández-Sánchez, J. Mahugo, A. Urbano, *J. Org. Chem.* **1999**, *64*(4), 1387–1390; b) M. C. Carreño, S. García-Cerrada, A. Urbano, *J. Am. Chem. Soc.* **2001**, *123*(32), 7929–7930.

[174] a) M. C. Carreño, S. García-Cerrada, M. J. Sanz-Cuesta, A. Urbano, *Chem. Commun.* **2001**, 1452–1453; b) M. C. Carreño, S. García-Cerrada, A. Urbano, *Chem. Eur. J.* **2003**, *9*(17), 4118–4131; c) M. C. Carreño, M. Gónzalez-López, A. Urbano, *Chem. Commun.* **2005**, 611–613; d) A. Latorre, A. Urbano, M. C. Carreño, *Chem. Commun.* **2009**, 6652–6654; e) A. Urbano, M. C. Carreño, *Org. Biomol. Chem.* **2013**, *11*, 699–708.

[175] a) M. Yamaguchi, H. Okubo, M. Hirama, *Chem. Commun.* **1996**, 1771–1772; b) J. Ichikawa, M. Yokota, T. Kudo, S. Umezaki, *Angew. Chem. Int. Ed.* **2008**, *47*(26), 4870–4873; *Angew. Chem.* **2008**, *120*, 4948–4951; c) G. Pieters, A. Gaucher, D. Prim, J. Marrot, *Chem. Commun.* **2009**, 4827–4828; d) K. Fuchibe, H. Jyono, M. Fujiwara, T. Kudo, M. Yokota, J. Ichikawa, *Chem. Eur. J.* **2011**, *17*(43), 12175–12185.

[176] a) D. C. Harrowven, M. I. Nunn, D. R. Fenwick, *Tetrahedron Letters* **2002**, *43*(17), 3189 – 3191; b) D. C. Harrowven, I. L. Guy, L. Nanson, *Angew. Chem. Int. Ed.* **2006**, *45*(14), 2242–2245; *Angew. Chem.* **2006**, *118*, 2300–2303.

[177] a) F. Dubois, M. Gingras, *Tetrahedron Lett.* **1998**, *39*(28), 5039 – 5040; b) M. Gingras, F. Dubois, *Tetrahedron Lett.* **1999**, *40*(7), 1309 – 1312; c) S. Goretta, C. Tasciotti, S. Mathieu, M. Smet, W. Maes, Y. M. Chabre, W. Dehaen, R. Giasson, J.-M. Raimundo, C. R. Henry, C. Barth, M. Gingras, *Org. Lett.* **2009**, *11*(17), 3846–3849.

[178] a) I. G. Stará, I. Starý, A. Kollároviă, F. Teplý, D. Šaman, M. Tichý, *J. Org. Chem.* **1998**, *63*(12), 4046–4050; b) I. G. Stará, I. Starý, A. Kollároviă, F. Teplý, Štěpán Vyskočil, D. Šaman, *Tetrahedron Lett.* **1999**, *40*(10), 1993–1996.

[179] B. Heller, M. Hapke, C. Fischer, A. Andronova, I. Starý, I. G. Stará, *J. Organomet. Chem.* **2013**, *723*, 98 – 102.

[180] F. Teplý, I. G. Stará, I. Starý, A. Kollároviă, D. Šaman, L. Rulíšek, P. Fiedler, *J. Am. Chem. Soc.* **2002**, *124*(31), 9175–9180.

[181] a) F. Teplý, I. G. Stará, I. Starý, A. Kollároviӑ, D. Šaman, Štěpán Vyskočil, P. Fiedler, *J. Org. Chem.* **2003**, *68*(13), 5193–5197; b) F. Teplý, I. G. Stará, I. Starý, A. Kollárovic, D. Luštinec, Z. Krausová, D. Šaman, P. Fiedler, *Eur. J. Org. Chem.* **2007**, *2007*(25), 4244–4250; c) L. Adriaenssens, L. Severa, T. Šálová, I. Císařová, R. Pohl, D. Šaman, S. Rocha, N. Finney, L. Pospíšil, P. Slavíček, F. Teplý, *Chem. Eur. J.* **2009**, *15*(5), 1072–1076; d) O. Songis, J. Míšek, M. B. Schmid, A. Kollároviӑ, I. G. Stará, D. Šaman, I. Císařová, I. Starý, *J. Org. Chem.* **2010**, *75*(20), 6889–6899; e) S. Chercheja, J. Klívar, A. Jančařík, J. Rybáček, S. Salzl, J. Tarábek, L. Pospíšil, J. Chocholoušová, J. Vacek, R. Pohl, I. Císařová, I. Starý, I. G. Stará, *Chem. Eur. J.* **2014**, *20*(27), 8477–8482.

[182] P. Sehnal, I. G. Stará, D. Šaman, M. Tichý, J. Míšek, J. Cvačka, L. Rulíšek, J. Chocholoušová, J. Vacek, G. Goryl, M. Szymonski, I. Císařová, I. Starý, *Proc. Natl. Acad. Sci.* **2009**, *106*(32), 13169–13174.

[183] J. Žádný, A. Jančařík, A. Andronova, M. Šámal, J. Chocholoušová, J. Vacek, R. Pohl, D. Šaman, I. Císařová, I. G. Stará, I. Starý, *Angew. Chem. Int. Ed.* **2012**, *51*(24), 5857–5861; *Angew. Chem.* **2012**, *124*, 5959-5963.

[184] a) I. G. Stará, Z. Alexandrová, F. Teplý, P. Sehnal, I. Starý, D. Šaman, M. Buděšínský, J. Cvačka, *Organic Lett.* **2005**, *7*(13), 2547–2550; b) P. Sehnal, Z. Krausová, F. Teplý, I. G. Stará, I. Starý, L. Rulíšek, D. Šaman, I. Císařová, *J. Org. Chem.* **2008**, *73*(6), 2074–2082; c) M. R. Crittall, N. W. G. Fairhurst, D. R. Carbery, *Chem. Commun.* **2012**, *48*, 11181–11183.

[185] A. Jančařík, J. Rybáček, K. Cocq, J. Chocholoušová, J. Vacek, R. Pohl, L. Bednárová, P. Fiedler, I. Císařová, I. G. Stará, I. Starý, *Angew. Chem. Int. Ed.* **2013**, *52*(38), 9970–9975; *Angew. Chem.* **2013**, *125*, 10154-10159.

[186] a) K. Tanaka, A. Kamisawa, T. Suda, K. Noguchi, M. Hirano, *J. Am. Chem. Soc.* **2007**, *129*(40), 12078–12079; b) Y. Kimura, N. Fukawa, Y. Miyauchi, K. Noguchi, K. Tanaka, *Angew. Chem. Int. Ed.* **2014**, *53*(32), 8480–8483; *Angew. Chem.* **2014**, *126*, 8620-8623.

[187] a) K. Tanaka, N. Fukawa, T. Suda, K. Noguchi, *Angew. Chem. Int. Ed.* **2009**, *48*(30), 5470–5473; *Angew. Chem.* **2009**, *121*, 5578-5581; b) N. Fukawa, T. Osaka, K. Noguchi, K. Tanaka, *Org. Lett.* **2010**, *12*(6), 1324–1327.

[188] a) Y. Sawada, S. Furumi, A. Takai, M. Takeuchi, K. Noguchi, K. Tanaka, *J. Am. Chem. Soc.* **2012**, *134*(9), 4080–4083; b) K. Murayama, Y. Oike, S. Furumi, M. Takeuchi, K. Noguchi, K. Tanaka, *Eur. J. Org. Chem.* **2015**, *2015*(7), 1409–1414.

[189] J. Caeiro, D. Peña, A. Cobas, D. Pérez, E. Guitián, *Adv. Synth. Cat.* **2006**, *348*(16-17), 2466–2474.

[190] T. Shibata, T. Uchiyama, Y. Yoshinami, S. Takayasu, K. Tsuchikama, K. Endo, *Chem. Commun.* **2012**, *48*, 1311–1313.

[191] S. K. Collins, A. Grandbois, M. P. Vachon, J. Côté, *Angew. Chem. Int. Ed.* **2006**, *45*(18), 2923–2926; *Angew. Chem.* **2006**, *118*, 2989-2992.

[192] A. Grandbois, S. Collins, *Chem. Eur. J.* **2008**, *14*(30), 9323–9329.

[193] a) A. Fürstner, , V. Mamane, *J. Org. Chem.* **2002**, *67*(17), 6264–6267; b) A. Fürstner, V. Mamane, *Chem. Commun.* **2003**, 2112–2113; c) V. Mamane, P. Hannen, A. Fürstner, *Chem. Eur. J.* **2004**, *10*(18), 4556–4575.

[194] E. Soriano, J. Marco-Contelles, *Organometallics* **2006**, *25*(19), 4542–4553.

[195] a) J. Storch, J. Sýkora, J. Čermák, J. Karban, I. Císařová, A. Ružička, *J. Org. Chem.* **2009**, *74*(8), 3090–3093; b) P. F. Thomson, D. Parrish, P. Pradhan, M. K. Lakshman, *J. Org. Chem.* **2015**, *80*(15), 7435–7446.

[196] a) J. Storch, J. Čermák, J. Karban, I. Císařová, J. Sýkora, *J. Org. Chem.* **2010**, *75*(9), 3137–3140; b) M. Weimar, R. C. da Costa, F.-H. Lee, M. J. Fuchter, *Org. Lett.* **2013**, *15*(7), 1706–1709; c) H. Oyama, K. Nakano, T. Harada, R. Kuroda, M. Naito, K. Nobusawa, K. Nozaki, *Org. Lett.* **2013**, *15*(9), 2104–2107.

[197] J. Storch, M. Bernard, J. Sýkora, J. Karban, J. Čermák, *Eur. J. Org. Chem.* **2013**, *2013*(2), 260–263.

[198] a) G. Bringmann, A. J. Price Mortimer, P. A. Keller, M. J. Gresser, J. Garner, M. Breuning, *Angew. Chem. Int. Ed.* **2005**, *44*(34), 5384–5427; b) J. Wencel-Delord, A. Panossian, F. R. Leroux, F. Colobert, *Chem. Soc. Rev.* **2015**, *44*, 3418–3430.

[199] K. Nakamura, S. Furumi, M. Takeuchi, T. Shibuya, K. Tanaka, *J. Am. Chem. Soc.* **2014**, *136*(15), 5555–5558.

[200] a) R. L. LaLonde, B. D. Sherry, E. J. Kang, F. D. Toste, *J. Am. Chem. Soc.* **2007**, *129*(9), 2452–2453; b) G. Zhou, F. Liu, J. Zhang, *Chem. Eur. J.* **2011**, *17*(11), 3101–3104; c) A. D. Melhado, G. W. Amarante, Z. J. Wang, M. Luparia, F. D. Toste, *J. Am. Chem. Soc.* **2011**, *133*(10), 3517–3527; d) M. Kojima, K. Mikami, *Chem. Eur. J.* **2011**, *17*(50), 13950–13953; e) M. Martín-Rodríguez, C. Nájera, J. M. Sansano, A. deCózar, F. P. Cossío, *Chem. Eur. J.* **2011**, *17*(50), 14224–14233; f) S. A. Gawade, S. Bhunia, R.-S. Liu, *Angew. Chem. Int. Ed.* **2012**, *51*(31), 7835–7838; *Angew. Chem.* **2012**, *124*, 7955-7958; g) J. F. Briones, H. M. L. Davies, *J. Am. Chem. Soc.* **2012**, *134*(29), 11916–11919; h) M. Bandini, A. Bottoni, M. Chiarucci, G. Cera, G. P. Miscione, *J. Am. Chem. Soc.* **2012**, *134*(51), 20690–20700; i) D. H. Miles, M. Veguillas, F. D. Toste, *Chem. Sci.* **2013**, *4*, 3427–3431; j) W. Zi, F. D. Toste, *J. Am. Chem. Soc.* **2013**, *135*(34), 12600–12603; k) J. F. Briones, H. M. L. Davies, *J. Am. Chem. Soc.* **2013**, *135*(36), 13314–13317; l) H. Wu, W. Zi, G. Li, H. Lu, F. D. Toste, *Angew. Chem. Int. Ed.* **2015**, *54*(29), 8529–8532; *Angew. Chem.* **2015**, *127*, 8649-8652.

[201] a) A. Z. González, F. D. Toste, *Org. Lett.* **2010**, *12*(1), 200–203; b) A. Z. González, D. Benitez, E. Tkatchouk, W. A. Goddard-III, F. D. Toste, *J. Am. Chem. Soc.*

2011, *133*(14), 5500–5507; c) B. Liu, K.-N. Li, S.-W. Luo, J.-Z. Huang, H. Pang, L.-Z. Gong, *J. Am. Chem. Soc.* **2013**, *135*(9), 3323–3326; d) F. Liu, Y. Wang, W. Ye, J. Zhang, *Org. Chem. Front.* **2015**, *2*, 221–225; e) Z.-Q. Shen, X.-X. Li, J.-W. Shi, B.-L. Chen, Z. Chen, *Tetrahedron Lett.* **2015**, *56*(27), 4080 – 4083; f) Y. Wang, P. Zhang, Y. Liu, F. Xia, J. Zhang, *Chem. Sci.* **2015**, *6*, 5564–5570; g) S. Klimczyk, A. Misale, X. Huang, N. Maulide, *Angew. Chem. Int. Ed.* **2015**, *54*(35), 10365–10369; *Angew. Chem.* **2015**, *127*, 10507-10511; h) Z. Wu, K. Isaac, P. Retailleau, J.-F. Betzer, A. Voituriez, A. Marinetti, *Chem. Eur. J.* **2016**, *22*(10), 3278–3281.

[202] C. Maaliki, C. Lepetit, Y. Canac, C. Bijani, C. Duhayon, R. Chauvin, *Chem. Eur. J.* **2012**, *18*(25), 7705–7714.

[203] D. Seebach, A. K. Beck, A. Heckel, *Angew. Chem. Int. Ed.* **2001**, *40*(1), 92–138; *Angew. Chem.* **2001**, *113*, 96-142.

[204] J. Teichert, B. Feringa, *Angew. Chem. Int. Ed.* **2010**, *49*(14), 2486–2528; *Angew. Chem.* **2010**, *122*, 2538-2582.

[205] D. Seebach, P. B. Rheiner, A. K. Beck, F. N. M. Kühnle, B. Jaun, *Polish J. Chem.* **1994**, *68*(11), 2397–2413.

[206] A. M. Butterfield, B. Gilomen, J. S. Siegel, *Org. Process Res. Dev.* **2012**, *16*(4), 664–676.

[207] H. Larkem, A. Larkem, D. Messadi, *Egypt. J. Chem.* **2004**, *47*(4), 413–426.

[208] T. E. Barder, S. D. Walker, J. R. Martinelli, S. L. Buchwald, *J. Am. Chem. Soc.* **2005**, *127*(13), 4685–4696.

[209] a) R. L. Clough, J. D. Roberts, *J. Am. Chem. Soc.* **1976**, *98*(4), 1018–1020; b) F. Cozzi, M. Cinquini, R. Annuziata, J. S. Siegel, *J. Am. Chem. Soc.* **1993**, *115*(12), 5330–5331; c) G. Pieters, V. Terrasson, A. Gaucher, D. Prim, J. Marrot, *Eur. J. Org. Chem.* **2010**, *2010*(30), 5800–5806; d) D. K. Judge, P. Haycock, R. D. Richardson, M. J. Fuchter, *Synlett* **2013**, *24*(18), 2365–2369; e) H. Ghosh, R. Vavilala, A. M. Szpilman, *Tetrahedron Asymm.* **2015**, *26*(2–3), 79 – 84.

[210] R. Martin, N. Defay, H. Figeys, M. Flammang-Barbieux, J. Cosyn, M. Gelbcke, J. Schurter, *Tetrahedron* **1969**, *25*(20), 4985 – 4998.

[211] W. H. Laarhoven, W. J. C. Prinsen, „Carbohelicenes and heterohelicenes" in *Stereochemistry* (Eds. F. Vögtle, E. Weber), Springer Berlin Heidelberg, **1984**, p. 63–130.

[212] F. Aloui, R. E. Abed, T. Guerfel, B. B. Hassine, *Synth. Commun.* **2006**, *36*(11), 1557–1567.

[213] W. Laarhoven, W. Peters, A. Tinnemans, *Tetrahedron* **1978**, *34*(6), 769 – 777.

[214] a) A. D. Bain, *Prog. Nucl. Magn. Reson. Spectrosc.* **2003**, *43*(3–4), 63 – 103; b) C. Wolf, „Analytical Methods" in *Dynamic Stereochemistry of Chiral Compounds: Principles and Applications*, The Royal Society of Chemistry, **2008**, p. 136–179.

[215] L. Lunazzi, M. Mancinelli, A. Mazzanti, S. Lepri, R. Ruzziconi, M. Schlosser, *Org. Biomol. Chem.* **2012**, *10*, 1847–1855.

[216] C. Wolf, „Racemization, Enantiomerization and Diastereomerization" in *Dynamic Stereochemistry of Chiral Compounds: Principles and Applications*, The Royal Society of Chemistry, **2008**, p. 29–135.

[217] W. L. F. Armarego, C. L. L. Chai, *Purification of laboratory chemicals*, 5. Ed., El Servier, **2003**.

[218] W. P. Weber, G. W. Gokel, *Tetrahedron Lett.* **1972**, *13*(17), 1637 – 1640.

[219] J. Vicente, M. T. Chicote, M. C. Lagunas, P. G. Jones, *J. Chem. Soc., Dalton Trans.* **1991**, 2579–2583.

[220] J. Vicente, J. A. Abad, R. Bergs, P. G. Jones, D. Bautista, *J. Chem. Soc., Dalton Trans.* **1995**, 3093–3095.

[221] A. A. Skatova, I. L. Fedushkin, O. V. Maslova, M. Hummert, H. Schumann, *Russ. Chem. Bull. Int. Ed.* **2007**, *56*, 2284–2289.

[222] J. A. Teagle, J. L. Burmeister, *Inorg. Chim. Acta* **1986**, *118*(1), 65 – 72.

[223] X. Gao, J. Han, L. Wang, *Org. Lett.* **2015**, *17*(18), 4596–4599.

[224] S. Allmendinger, H. Kinuta, B. Breit, *Adv. Synth. Catal.* **2015**, *357*, 41–45.

[225] A. K. Beck, B. Bastani, D. A. Plattner, W. Petter, D. Seebach, H. Braunschweiger, P. Gysi, L. L. Vecchia, *Chimia* **1991**, *45*(7/8), 238–244.

[226] H. Teller, PhD thesis, Technische Universität Dortmund, **2012**.

[227] P. Tang, W. Wang, T. Ritter, *J. Am. Chem. Soc.* **2011**, *133*(30), 11482–11484.

[228] X. Bantreil, S. P. Nolan, *Nat. Protoc.* **2010**, *6*(1), 69–77.

[229] P. Gallant, L. Dhaenens, M. Vandewalle, *Synth. Commun.* **1984**, *14*(2), 155–161.

[230] H. Jullien, D. Brissy, R. Sylvain, P. Retailleau, J.-V. Naubron, S. Gladiali, A. Marinetti, *Adv. Synth. Catal.* **2011**, *353*(7), 1109–1124.

[231] M. B. Andrus, M. A. Christiansen, E. J. Hicken, M. J. Gainer, D. K. Bedke, K. C. Harper, S. R. Mikkelson, D. S. Dodson, , D. T. Harris, *Org. Lett.* **2007**, *9*(23), 4865–4868.

[232] A. Granzhan, E. Largy, N. Saettel, M.-P. Teulade-Fichou, *Chem. Eur. J.* **2010**, *16*(3), 878–889.

Ω

Curriculum Vitae

Personal Data

Name	Elisa González Fernández
Date of birth	23.04.1988
Place of Birth	Terrassa, Spain
Nationality	Spanish
Gender	Female
E-mail	e.gonzalezfernande@stud.uni-goettingen.de
Current adress	Dohne 87, 45468, Mülheim an der Ruhr, Germany
Tel.	+49208 88377329
	+491748536263 (mobile)

Academic Education

2015-present	PhD student at Georg-August-Universität Götingen (Götingen, Germany) Supervisor: Prof. Manuel Alcarazo Dissertation: Towards an effective control of the electronic properties in Au(I)-complexes. From basic principles to asymmetric catalysis.
2012-2015	PhD student at Max-Plack Institut für Kohlenforschung (Mülheim an der Ruhr, Germany) Supervisor: Prof. Dr. Manuel Alcarazo Dissertation: Towards an effective control of the electronic properties in Au(I)-complexes. From basic principles to asymmetric catalysis.
2011-2014	"Grado de Salamanca" in Universidad de Salamanca (Salamanca, Spain) Supervisor: Prof. Dr. David Díez Martín Thesis: Nueva Metodología de Síntesis de Indolizidinas a partir de Nitronas (New Methodology of Synthesis of Indolizidines starting from Nitrones). Awarded with "Grado de Salamanca" prize.

| 2006-2012 | Licenciatura en Química (5 years degree in Chemistry) at Universidad de Salamanca (Salamanca, Spain) |

Publications

- **Elisa González-Fernández**, Jörg Rust and Manuel Alcarazo, Synthesis and Reactivity of Metal Complexes with Acyclic (Amino)-(Ylide)Carbene Ligands, *Angew. Chem. Int. Ed.* **2013**, *52*, 11392-11395 (English version); *Angew. Chem.* **2013**, *125*, 11603-11606 (German version).

- **Elisa González-Fernández**, Leo D. M. Nicholls[‡], Lukas Schaaf, Christophe Fàres, Christian W. Lehmann and Manuel Alcarazo, Enantioselective Synthesis of [6]Carbohelicenes, submitted to *J. Am. Chem. Soc.*